Regulatory roles of photoreceptors and non-coding RNA in *Fusarium fujikuroi*

Memoria elaborada por Javier Pardo Medina para optar al grado de Doctor en Biología

This work has been carried out in the Department of Genetics of the Faculty of Biology of the University of Seville

under the direction of

Dr. Francisco Javier Avalos Cordero

and Dr. María del Carmen Limón Mirón.

Seville, 2021

Francisco Javier Avalos Cordero

María del Carmen Limón Mirón

Javier Pardo Medina

Agradecimientos

Esta tesis ha supuesto posiblemente la etapa más determinante, tanto a nivel formativo como de crecimiento personal, por la que he pasado. Desde que entré al departamento, siendo un estudiante de Grado despistado que no tenía absolutamente ni idea de lo que era *Fusarium*, he pasado por momentos geniales y regulares, hemos luchado batallas científicas en las que a veces ganamos y otras veces no, pero al final, han dado sus frutos. Durante el camino me llevo amigos, conocimientos, experiencias y herramientas que valoro profundamente. Tengo mucho que por lo que dar gracias

Me gustaría agradecer en primer lugar a mis directores de tesis, Javier y Carmen, por su apoyo constante durante la tesis, sus consejos y su guía. Creyeron en mí desde el principio y sólo espero haber cumplido al menos parte sus expectativas. Han sido un ejemplo de dedicación, constancia y buen hacer que creo que es lo más valioso que he aprendido durante esta tesis. Si llego algún día a ser una décima parte de lo buenos científicos, docentes y mentores que han sido para mí, me daré por satisfecho.

A mis padres, por haberme animado desde el principio a hacer la tesis, sin saber dónde me metía yo y, por mi culpa, se metían ellos. Su apoyo incondicional ha hecho también posible este trabajo. Su ejemplo de esfuerzo y constancia ha sido mi motivación para intentar superar las adversidades inherentes al trabajo científico. Espero que os podáis sentir casi tan orgullosos como yo de haberla terminado, porque sin vosotros hubiera sido imposible A mis hermanos por su interés y su cariño.

A mis compañeros del L9, luego L1, y finalmente L10 (¡Tres mudanzas me he comido en el laboratorio!), antiguos y presentes, que me han enseñado y a los que he enseñado, aprendiendo a su vez en el proceso, con los que he compartido fatigas, alegrías y decepciones en este trabajo, a veces de Sísifo, que es la ciencia. Me gustaría mencionar especialmente a tres, las cuales de alguna manera determinaron el pasado, presente y futuro de mi tesis, enseñándome a perseverar, y al mismo tiempo, a tomarme las cosas con filosofía. A Macarena, por darme su amistad incondicional nada más entrar y enseñarme, entre otras cosas, que el laboratorio, se puede convertir en parte en un hogar. Ella fue la culpable inicial de que acabara enredado hasta las 12 de la noche, todavía recuerdo la primera de muchas veces, de tal que forma que, al pasar las horas, los experimentos degeneraban en confidencias y confianzas. Sin ella nada hubiera sido lo mismo. A Duli, su alegría, su sinceridad, su organización y su decisión. Ella me ha enseñado que quien persevera alcanza, y que las dudas son necesarias, pero no te pueden paralizar. Sin ella no habría conseguido ni la mitad de lo que aquí cuento (¡y de lo que no!). Y a Julia, de cuya futura tesis supongo soy en parte culpable por animarla a tirarse a la piscina. Es lo malo de los doctorandos, que vamos pasando el virus. Ella me ha dado tantísimo durante estos últimos años, que no hay palabras suficientes para agradecerle lo que hace. Su ejemplo frente a los malos momentos (¡Lucha, lucha, lucha!) me ha ayudado a superar los míos. Nos veremos en tu defensa (Hazme caso y ve escribiendo).

A todos mis compañeros de departamento, doctorandos, profesores y técnicos, por ayuda durante los experimentos, sin los cuales puede que se me hubiera hecho mucho más difícil terminar esta tesis. Especialmente me gustaría agradecer a Gabi, su inestimable ayuda durante los análisis transcriptómicos. A Ángela por haber sido mi compañera de fatigas y filosofías durante estos años, por sus convicciones y por su cariño. A Sara, por su trabajo incansable, por su curiosidad y, por supuesto, por ser mi "novia de los congresos".

A mi segundo grupo de Barcelona, a Miguel, Vicky y Salva, con quienes pasé una corta estancia, pero me llevé una amistad para toda la vida.

A Alfred Batschauer, Stephan Kiontke y mis compañeros de Marburg por enseñarme y ayudarme durante mi estancia en Alemania.

A todos mis amigos. Podría hacer una tesis igual de larga que ésta agradeciéndoos vuestro apoyo e interés, os nombre o no, también la habéis hecho posible. A Miriam, Fofi, Dédalo e Irene. A Rodri, Alejandra y Quique. A mis compañeros de biología, a Rosa, a Amanda y a Tere. A Miguel, Marina, Paula y Quique. A Paz, Cris, Marta, Merce, Pedro y Cristina. A todos, muchísimas gracias.

Finalmente, a Sandi, por su apoyo constante e infinito durante la escritura.

Gracias

INDEX

ABREVIATIONS

A	Adenine
Ago	Argonaute
asRNA	anti-sense RNA
BBH	Best bidirectional hit
bdH_2O	Bi-distilled H_2O
BLUF	Blue light using FAD
bp	Base pair
BSA	Bovine serum albumin
C	Cytosine
cAMP	Cyclic adenosine monophosphate
cDNA	Complementary DNA
CDS	Coding sequence
CPD	Cyclobutane pyrimidine dimer
cry-DASH	DASH-cryptochrome
Ct	Threshold-cycle of amplification
CX	X=number of carbon atoms
DEG	Differentially expressed genes
DET	Differentially expressed transcripts
DIG	Digoxigenin
DMAPP	Dimethylalyl pyrophosphate
DMSO	Dimethyl sulfoxide
DNA	Deoxyribonucleic acid
dNTP	Deoxynucleoside triphosphate
dsRNA	double-strand RNA
esRNA	Endogenous sRNA
Ex-siRNA	Exon derived small interfering RNAs
FAD	Flavin adenine dinucleotide
FC	Fold-change
Fig	Figure
FMN	Flavin mononucleotide
Fph	Fungal phytochrome
FPKM	Fragments Per Kilobase of transcript per Million mapped reads
FPP	Farnesyl pyrophosphate
G	Guanine
GGPP	Geranylgeranyl pyrophosphate
GO	Gene Ontology
GPP	Geranyl pyrophosphate
GTP	Guanosine-5'-triphosphate
H314ac	Acetylation of histone H3
H3K9me3	Lysine 9 in histoneH3 trimethylation
HMG-CoA	Hydroxymethyl glutaryl coenzyme A
IPP	Isopentyl pyrophosphate

IPTG	Isopropyl β-D-1-thiogalactopyranoside
Kb	Kilobase
LB	Bertani's Lysogenic Broth
lncRNA	long non-coding RNA
LOV	Light Oxygen Voltage
milRNA	miRNA-like RNA
min	Minute
miRNA	Micro RNA
mRNA	Messenger RNA
MSUD	Meiotic Silencing by Unpaired DNA
MTHF	5,10-methenyltetrahydrofolate
NCBI	National Center for Biotechnology Information
ncRNA	Non-coding RNA
NG	N-metil-N'-nitro-N-nitrosoguanidine
NRPS	Non-ribosomal peptide synthetase
nt	Nucleotide
NX	Neurosporaxanthin
OD	Optical density
ORF	Open reading frame
PAS	Per-Arnt-Sim domain
PCA	Principal component analysis
PCR	Polymerase chain reaction
PEG	Polyethylene glycol
PHR	Photolyase
PKS	Polyketide synthase
PS	PCR Primer set
qiRNA	QDE-2 interacting sRNA
RALDH	Retinaldehyde dehydrogenase
rDNA	Ribosomal DNA
RIN	RNA integrity number in *F. fujikuroi*
RISC	RNA-induced silencing complex
RNA	Ribonucleic acid
RNAi	RNA interference
RNA-seq	RNA sequencing
ROS	Reactive oxygen species
RPM	Reads per million
rpm	Revolutions per minute
rRNA	Ribosomal RNA
RsRP	RNA dependent RNA polymerase
RT-PCR	Reverse Transcription Polymerase chain reaction
RTPS	RT-qPCR Primer set
RT-qPCR	Reverse Transcription Quantitative Polymerase Chain Reaction
SDS	Sodium dodecyl sulfate
siRNA	Small-interfering RNA

SM	Secondary metabolite/metabolism
sRNA	small RNA
ssRNA	Single-strand RNA
T	Thymine
TC	Terpene cyclases
T-DNA	Transfer DNA
TPM	Transcripts per million
tRNA	Transferent RNA
UV	Ultraviolet radiation
Vol	Volume
WCC	White-collar complex
WT	Wild type
X-Gal	5-bromo-4-chloro-3-indolyl-β-D-galactopyranoside
Zn	Zinc

SUMMARY

The genus *Fusarium* comprises hundreds of species of pathogenic and saprophytic fungi, usually characterized by a complex secondary metabolism. This includes the production of carotenoids, terpenoid pigments that give a characteristic orange color to their colonies. All the biosynthetic genes have been identified, and two of them are grouped in a coregulated cluster. Light plays a major role in promoting their synthesis by activating their transcription, but their effects on fungal biology are much wider. Light is presumably perceived by *F. fujikuroi* by a battery of photoreceptors, including members of the White-Collar complex, cryptochromes and photolyases, rhodopsins, and phytochromes. The main photoresponses in fungi are normally dependent on the White-collar complex, and carotenoid biosynthesis in *Fusarium* mainly depends on it, with WcoA as the light-absorbing component. Another photoreceptor, the DASH cryptochrome CryD, also affects the response of carotenogenesis to light, although the available information suggests its participation in a post-transcriptional regulation. Carotenogenesis is downregulated by a protein of the RING Finger family, called CarS, whose mutation results in a carotenoid overproduction phenotype. The *carS* gene is preceded by a 4 kb sequence with no known genes, in which the presence of two putative genes for microRNA like small RNAs precursors had previously been suggested.

In this Thesis, a massive sequencing specific for small RNAs has been carried out in *F. fujikuroi*, which confirmed their occurrence in this fungus. The result was consistent with the existence of a functional RNA interference system, supported by the identification of all the predicted enzymatic components encoded in the genome. This system seems to play a role in the biology of the fungus, as suggests the association between some sRNAs and the sequences of some transposons, indicating their role in silencing of these mobile elements. Deletion of one of the components, the gene for a Dicer protein predictably involved in their generation, showed no phenotype under laboratory conditions, suggesting other roles of the produced sRNAs in processes related with other stages of its life cycle, such as pathogenesis or sexual reproduction.

The global sRNA analysis failed to identify possible sRNA elements upstream of *carS*, contradicting the former hypothesis on the participation of microRNAS in *carS* regulation. However, a new 1.2 kb transcript, that was denominated *carP*, was identified in *carS* upstream region. Its sequence lacks relevant open reading frames and the few that exist do not coincide in the equivalent sequence of the close relative *Fusarium oxysporum*, indicating that the transcript is a long non-coding RNA (lncRNA). The results showed that *carP* is independently transcribed from *carS*, and its deletion produces an albino phenotype due to a drop in transcription of the structural *car* genes, probably as a result of the higher transcription of *carS* gene. This phenotype was only complemented by reintegration of the *carP* gene in the native *locus*, while its ectopic integration did not allow to recover carotenoid production in the recipient *carP* mutant, indicating a *cis*-acting regulatory mechanism for *carP* on *carS* expression. Global transcriptomic data showed that *carP* deletion affects the expression of many genes, most of them predictably through its effect on CarS. However, some of the differentially expressed genes are hardly affected by the *carS* mutation, pointing to specific regulatory effects

of *carP* on other target genes.

Global transcriptomic data after different illumination times revealed a diversity of kinetics patterns in mRNA accumulation in the wild strain. Photoinduced genes exhibited fast, intermediate and late responses, while only intermediate and late responses were found for light-repressed genes. A vast majority of these photoresponses were lost in the *wcoA* mutant, indicating that WcoA is the main photoreceptor responsible for light regulation in *F. fujikuroi.* Outstandingly, the *wcoA* mutation brought about massive changes in the transcriptome, affecting about 20% of the genes. Most of these effects were produced regardless of illumination, indicating that WcoA plays a more general light-independent regulatory role in *F. fujikuroi*. Outstandingly, many of the genes influenced by WcoA were related to secondary metabolism biosynthetic clusters, raising a biotechnological interest for this protein. Parallel analysis of the effect of light on a *cryD* deletion mutant revealed less severe transcriptomic effects. However, it resulted in changes in the degrees of photoinduction or photorepression of many genes, suggesting an accessory function of CryD in *Fusarium* photobiology.

The summarized results constitute a significant contribution to the knowledge of the regulation of carotenogenesis in *F. fujikuroi* and its photobiology and provide further evidence on its molecular complexity.

Introduction

FILAMENTOUS FUNGI IN RESEARCH AND THE GENUS *FUSARIUM*

Filamentous fungi form a heterogeneous group of microorganisms that have been widely used as research model to study multiple biological processes such as gene regulation, environmental sensing, production of secondary metabolites or circadian rhythm, among others. Some of their advantages are their capacity to grow under defined conditions in the laboratory, their easy maintenance and propagation, and their short and predominantly haploid life cycles. Several species stand out for their relevance as model organisms. *Neurospora crassa* constitutes a paradigmatic example since their use by Beadle and Tatum to formulate, test and prove their "one gene one enzyme" hypothesis that was later awarded with a Nobel prize. *N. crassa* was also a pioneer organism in the study of other processes like light sensing and circadian rhythm or generation of small RNAs and their functions (Davis, 2000; Perkins and Davis, 2000). *Aspergillus nidulans* is another model organism essential for studies of cell biology and gene regulation, in which the initial work on the genetics of tubulin and microtubules was done. It has contributed to our understanding of genetic transmission, recombination, and to unraveling metabolic pathways and its regulations (Brandl and Andersen, 2017; Oakley, 2017).

Basic research is not the only field in which filamentous fungi can be relevant. Besides their ecological importance in nature, filamentous fungi are interesting because of the impact they can have on humans. Their outstanding metabolic diversity is the source of not only valuable compounds for the chemical or food industries (Adrio and Demain, 2003; Gmoser et al., 2017; Lin and Xu, 2020), but also of toxic metabolites called mycotoxins (Janik et al., 2020). Furthermore, their adaptability and resilience make them efficient pathogens, affecting animal and plant biodiversity, causing epidemics in staple and commodity crops and even affecting human health, as infection-causing organisms or as a result of mycotoxin production (Fisher et al., 2020). The mechanisms that control the production of diverse potentially beneficial or harmful compounds or their pathogenicity are important fields of research, in which the fungi belonging to *Fusarium* genus stand out, constituting a model of great interest in their study. For all these reasons, *Fusarium* species are very interesting organisms to study in the laboratory, using molecular biology techniques to answer some of the biological questions they pose.

Fusarium genus comprises a large and heterogeneous group of ascomycetes (class *Sordariomycetes*, order *Hypocreale*s, family *Nectriaceae*) widely distributed in nature. The genus includes numerous species of which the best known are important plant pathogens, with great impacts on crops and as producers of mycotoxins, but others are non-pathogenic, saprophytic or parasitic species of other organisms (Leslie and Summerell, 2006; Moss and Smith, 1982). *Fusarium* was defined as a genus by Link in 1809 (Booth, 1971), which brings together numerous imperfect fungi characterized by the production of spindle-shaped non-septate conidia. *Fusarium* represents one of the most important groups of phytopathogenic fungi, affecting

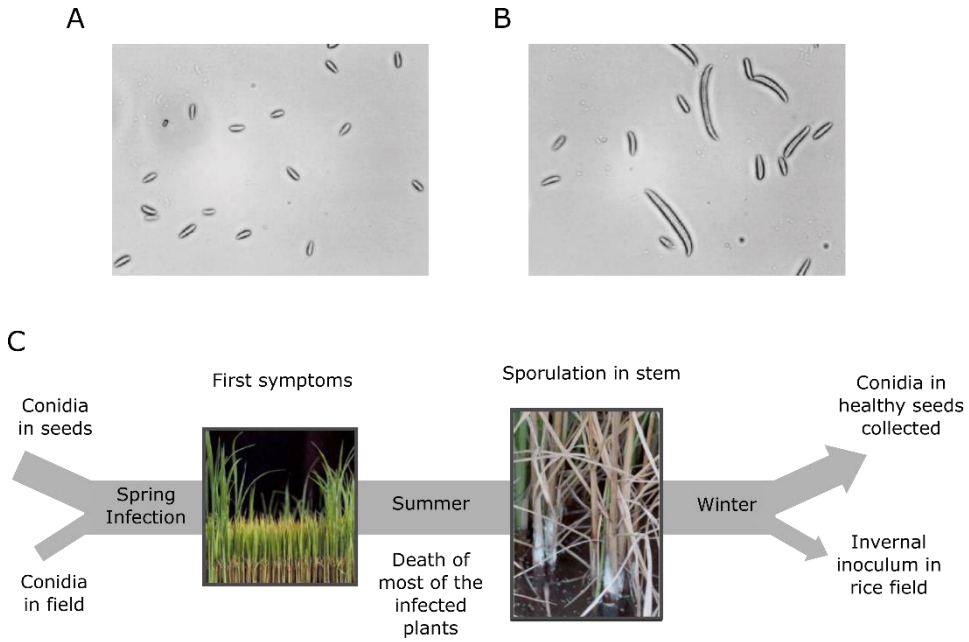

Figure I.1. Some relevant stages of the life cycle of *F. fujikuroi*. A) Microconidia from the wild strain IMI58289. B) Macroconidia and microconidia from the wild strain FKMC1995. C) Stages of the infective cycle of *F. fujikuroi* in rice plants. Modified from (Castrillo, 2014).

practically all cultivable plant species (Summerell, 2019). Its global distribution is due both to its metabolic diversity, which broadens its accessibility to very diverse potential substrates, and to its efficient dispersal mechanism based on different types of conidia (Leslie and Summerell, 2006). Although most *Fusarium* species present only asexual reproduction, at least in the laboratory, there are exceptions. The classification of the genus *Fusarium* into species has been historically hampered by this absence of sexual cycle and the scarcity of easily observable morphological traits (Leslie and Summerell, 2006). The nomenclature of species changed over the years once their sexual cycle, teleomorph or perfect state, was observed under laboratory conditions, transferring those which had it to the genus *Gibberella*. This was the case of *Fusarium moniliforme*, whose teleomorph was called *Gibberella fujikuroi* (Nelson et al., 1983). Years later, different strains forming independent crossing groups were gathered in a larger group known as *G. fujikuroi* "species complex". The strains of each crossing group are generally heterothallic, with separate sexes determined by a sexual locus with two alleles, *MAT-1* and *MAT-2* (Steenkamp et al., 2000) that define the sexual type of each fungus (+ or -). The complex comprises at least 11 crossing groups (A-K), each corresponding to a different species. More recent DNA-based phylogenetic analyses resolved *Fusarium* species into a monophyletic lineage consisting of 20 species complexes that include almost 300 phylogenetically distinct species (Geiser et al., 2013). The *Fusarium fujikuroi* species complex (FFC) includes at least 50 distinct species that group into three clades: the American, African, and Asian clades (Niehaus et al., 2016; O'Donnell et al., 1998). FFC species infect a wide range of plants and vary in host specificity.

F. fujikuroi, which belongs to the Asian cereal pathogen clade of the FFC (Kvas et al., 2009; Leslie and Summerell, 2006), and which would correspond to the crossing group C of the

G. fujikuroi complex, is mostly known for being the pathogen that causes the *bakanae* disease in *Oryza sativa*, the rice plant. Infected rice plants grow inordinately long, developing unusually tall, thin and brittle stems, a characteristic alteration attributed to the action of excreted growth-inducing hormones, gibberellins, by the fungus (Avalos et al., 2007). In the later stages of infection, sick plants produce abnormal rice grains, show symptoms of wilting and eventually fall off and die, generating important economic losses (Fig. I.1C) (Spadaro, 2017).

F. fujikuroi uses asexual reproduction through the formation of spindle-shaped spores, called conidia. This fungus produces two types of conidia: the small and uninucleated ones, named microconidia (Fig. I.1A), and the more elongated, half-moon shaped, septated and multinucleated ones, called macroconidia (Fig. I.1B) (Kuhlman, 1982; Leslie and Summerell, 2006). Macroconidia are abundantly formed by many *Fusarium* species but are less frequent in *F. fujikuroi*. The predominant production of uninucleate microconidia and its haploid nature facilitates laboratory isolation of strains with recessive mutations in this species (Avalos et al., 1985). When the environmental conditions are favorable, the conidia germinate forming hyphae that develop and branch forming a dense mycelium. During the infective life cycle (Fig. I.1C), hyphae can penetrate through small lesions in the rice roots and develop inside the plant until its severe weakening and deterioration, when the mycelia come out and sporulates, dispersing the conidia and starting the cycle again (Ou, 1985). *F. fujikuroi* sexual cycle is rarely observed in nature but it can be induced under laboratory conditions. The addition of (-) mating type conidia to a (+) mating type mycelia incubated in a plant-based substrate, as carrot extract medium, with 12-hour photoperiods of white light and near ultraviolet radiation alternating with darkness (Leslie et al., 2005), can trigger perithecia formation, which contain the ascospores forming disordered tetrads.

SECONDARY METABOLISM IN *FUSARIUM*

One of the most striking characteristics of the *Fusarium* species is their ability to produce a wide variety of secondary metabolites, some with toxic effects in humans or domestic animals and others innocuous or with biotechnological interest. Secondary metabolites are not essential for the survival of the fungus, but their prevalence in many species strongly indicate that they provide adaptive advantages in their natural habitats or in the interactions with other organisms. Their production is usually subject to appropriate environmental conditions or specific stages of development. They are derived from central metabolic pathways and primary metabolite pools, as acyl-CoA is the initial molecule for the synthesis of polyketides, terpenes, or amino acids for the synthesis of non-ribosomal peptides, three classes of secondary metabolites present in *Fusarium* (Calvo et al., 2002; Keller, 2019). In contrast to primary metabolism, normally the genes encoding the enzymatic activities to produce secondary metabolites are arranged in biosynthetic gene clusters (Hoogendoorn et al., 2018).

Unlike other *Fusarium* species, whose research interest has mainly focused on their pathogenicity or development, *F. fujikuroi* has exceled as a model in the study of secondary metabolism regulation. *F. fujikuroi* can synthetize a wide array of compounds from different metabolic origins (Fig. I.2). Among them are apicidin F, beauvericin, ferricrocin, ferrichrome. and

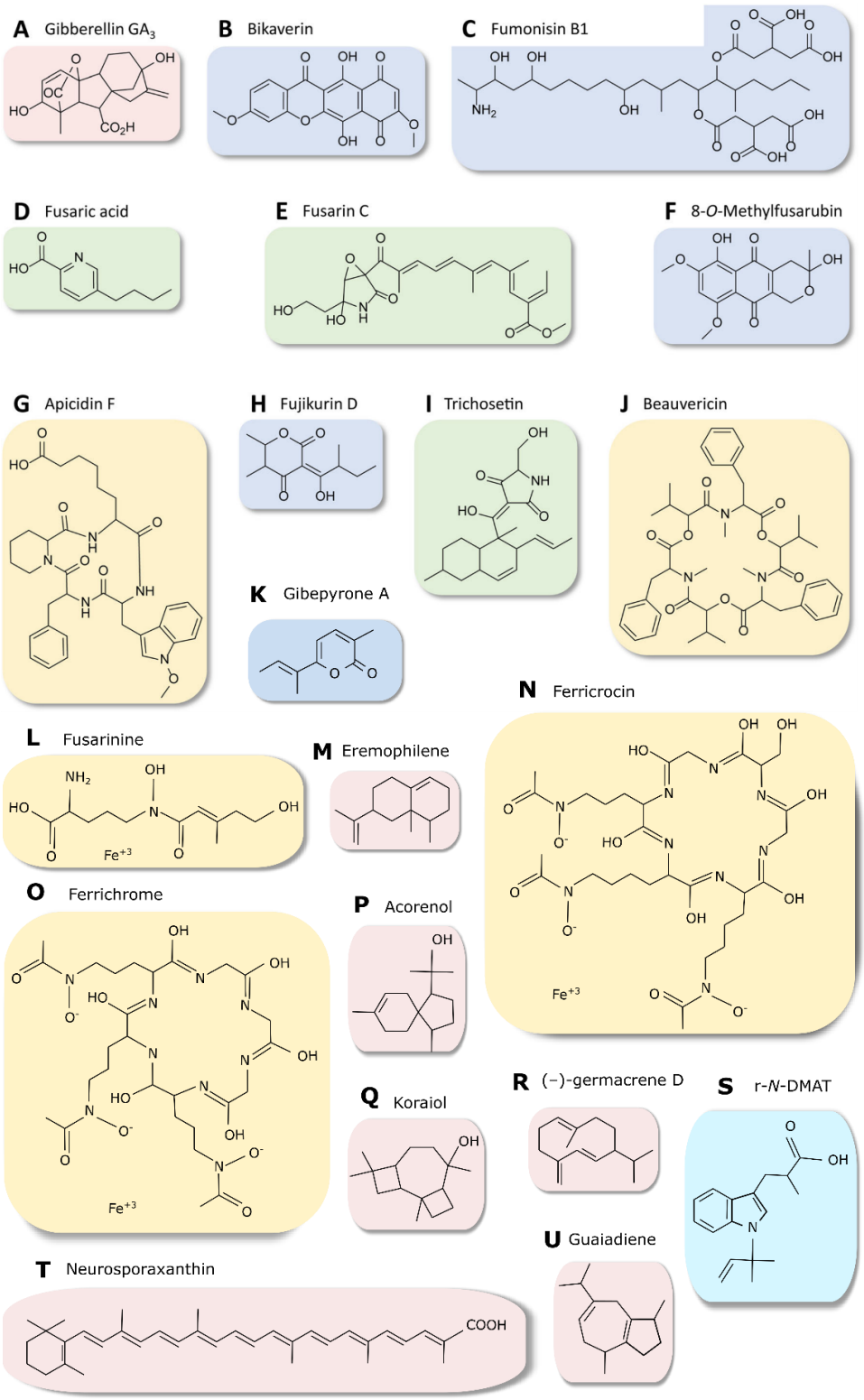

Figure I.2. Chemical structures of *F. fujikuroi* secondary metabolites. Metabolites produced by terpene cyclases are highlighted in pink (A, M, P, Q, R, T, U), metabolites, highlighted in blue (B, C, F, H and K) are polyketide synthase (PKS) products, those highlighted in yellow (G, J, I, N and O) are non-ribosomal peptide synthetase (NRPS)-derived, metabolites shown in green (D, E and I) are PKS-NRPS products and the compound shown in cyan is the product of a dimethylallyltryptophan synthase. Modified from (Janevska and Tudzynski, 2018).

fusarinine, derived from non-ribosomal peptide synthetases (NRPS); bikaverin, fumonisins, fusarubins, fujikurins and gibepyrone, produced by polyketide synthases (PKS); fusarins, trichotesin and fusaric acid, synthesized by hybrid PKS-NRPS enzymes; r-N-DMAT, synthesized by a dimethylallyltryptophan synthase; and gibberellins, germacrene D, koraiol, eremophilene, acorenol, guaiadiene and carotenoids are produced by terpene cyclases (TC). Although the most characteristic enzymatic activities are indicated, other enzymes participate in the syntheses of these compounds, frequently with complex biosynthetic pathways involving very diverse chemical reactions. The list of metabolites mentioned above is not exhaustive, since several identified biosynthetic clusters or key secondary metabolite enzymes still lack an associated metabolite (Avalos et al., 2007; Janevska and Tudzynski, 2018; Wiemann et al., 2013).

Special attention has been paid to the potential applications of some *F. fujikuroi* polyketides, including bikaverin (Limón et al., 2010), and to two families of terpenoids, the carotenoids and the gibberellins, with considerable biotechnological interest. Terpenoids are a highly diverse family of chemicals that have in common their origin from isopentenyl pyrophosphate. Terpenoids include compounds essential for life, such as sterols, vital to preserve the integrity of cell membranes (Kodedová and Sychrová, 2015), as well as the mentioned secondary metabolites. Gibberellins are plant hormones that regulate different processes of their development, such as stem elongation, induction of hydrolytic enzymes during germination, flowering stimulation or fruit formation (Hernández-García et al., 2020; Tudzynski et al., 2016; Yamaguchi, 2008). The growth stimulating properties of gibberellins result in numerous applications in agriculture (Hedden and Sponsel, 2015). Beside plants, they are synthesized by very few microorganisms, among which *F. fujikuroi* stands out due to its high biosynthetic capacity. In fact, the industrial production of gibberellins is based on the use of *F. fujikuroi* cultures. The seven genes of the gibberellin biosynthetic pathway are grouped in a coregulated cluster (Tudzynski et al., 2016). In their regulation plays a prominent role AreA, a transcription factor that mediates the use of alternative nitrogen sources, but other regulatory proteins are also implicated (Janevska and Tudzynski, 2018; Tudzynski, 2014). Carotenoids, on the other hand, are pigments with health promoting properties, widely used as food additives, and biotechnologically obtained from different sources, including some fungi (Avalos et al., 2017a).

CAROTENOIDS

Carotenoids are tetraterpenoid pigments derived from the fusion of two molecules of geranylgeranyl pyrophosphate (GGPP), present in all photosynthetic organisms, but also produced by many others (Britton et al., 1998). They are linear hydrocarbon molecules of variable length, with double conjugated bonds, which usually have closed rings at the ends of the chain. According to the substitutions they present, they are classified as carotenes, with only carbon and hydrogen, or xanthophylls, which also contain oxygen. Conjugated double bonds give them the ability to absorb radiation of the visible spectrum and are responsible for their characteristic color, usually in the range of red to yellow. The color of each carotenoid depends

both on the number of conjugated double bonds, and on the presence of rings in the molecule (Meléndez-Martínez et al., 2007).

In plants and other photosynthetic organisms, carotenoids are essential, since they are involved in the photosystem assembly, light reception, photoprotection, quenching against singlet oxygen and photomorphogenesis (Sun et al., 2018). They act as photoreceptor pigments, absorbing light and transferring its energy to the reaction centers of photosynthesis (Hashimoto et al., 2016). Carotenoids also provide striking colors to flowers and fruits, facilitating the attraction of animals and, consequently, the pollination or seed dispersal. The biosynthetic pathways of carotenoids are also present in many non-photosynthetic organisms, such as fungi (Sandmann and Misawa, 2002). In animals, carotenoids are important as a source of retinoids, that include retinal, as the chromophore of visual opsins, and retinoic acid, a critical regulatory signal involved in morphogenesis (Dawson, 2000; von Lintig, 2010). Carotenoids also provide pigmentation in different species, in some cases related with the ethology of sexual attraction (Whitehead et al., 2012). In general, animals obtain these pigments through their diet because they are unable to produce them *de novo*, but it was exceptionally found that some arthropods acquired the biosynthetic enzymes genes by horizontal transfer (Moran and Jarvik, 2010). Due to their chemical properties, carotenoids affect the fluency of cell membranes and they have antioxidant properties that allow them to neutralize singlet oxygen molecules and radicals generated in the lipid peroxidation (Sandmann, 2019). Their cooperation with other vitamins as photooxidation protectors (Stahl and Sies, 2002) positively links carotenoid consumption to protection against aging, cancer or an improved immunological response (Eggersdorfer and Wyss, 2018; Rao and Rao, 2007). Given their benefits on human health, carotenoids have important commercial applications, and they are widely used in cosmetics and as food additives. Carotenoids can be obtained by the chemical industry, but current preferences for the use of natural sources have favored their biotechnological production, and some fungi are among the organisms used for their industrial production (Avalos et al., 2017a).

FUNGAL CAROTENOIDS: FUNCTION AND SYNTHESIS

The role of carotenoids in fungi is not as clear as in other organisms, although their main role seems to be protection against oxidative stress (Avalos and Limón, 2015; Gessler et al., 2002). Evidence for this protective role has been found in different organisms. E.g., in the yeast *Xanthophyllomyces dendrorhous*, singlet oxygen stimulates carotenogenesis in the dark (Schroeder and Johnson, 1995). In *N. crassa*, the mutants of the genes involved in the defense against oxidative stress, *sod-1* (Yoshida and Hasunuma, 2004) and *cat-3* (Michán et al., 2003), accumulate higher amounts of carotenoids than the wild strain under illumination. It is not surprising that carotenogenesis is a frequent photoresponse in fungi, since light increases oxidative stress (Avalos et al., 1993; Corrochano, 2019). A relationship between carotenoid pigmentation and survival under UV light irradiation has also been described (Moliné et al., 2010; Morris and Subden, 1974). Reactive oxygen species (ROS) generated by normal cell metabolism include hydrogen peroxide. Addition of this compound increases carotenoid accumulation in different fungi, such as *N. crassa* (Iigusa et al., 2005) and *Fusarium*

aquaeductuum (Bindl et al., 1970), among others. All these observations suggest a protective role of carotenoids against oxidative stress. In addition, carotenoids may have other functions. In certain zygomycetes, such as *Blakeslea trispora* or *Phycomyces blakesleeanus*, they are the source of the trisporic acids, that derive from chemical modifications of cleavage carotene products and exert function as sex hormones (Austin et al., 1970; Polaino et al., 2010). For this reason, mutants blocked in the carotenoids biosynthetic pathway are sexually incompetent (Sutter, 1975). In fungi, carotenoids may be also to produce retinal by the oxidative cleavage of β-carotene, as evidenced in *Ustilago maydis* (Estrada et al., 2009) and *F. fujikuroi* (Prado-Cabrero et al., 2007a). The retinal is the chromophore that many rhodopsins need to be functionally photoactive. The photosensory roles of fungal rhodopsins are still to be determined, although a relationship with germination and virulence in *F. fujikuroi* has been suggested (Adam et al., 2018).

Many fungi synthesize carotenoids, and both the enzymology of the pathways and their regulation have been the object of extensive studies in some of them, especially in *N. crassa*, *P. blakesleeanus*, *Mucor circinelloides,* and *F. fujikuroi* (Avalos et al., 2014; Sandmann and Misawa, 2002). Comparison of their biosynthetic pathways shows that they are similar in the first steps, but they subsequently diversify to produce in carotenes or xanthophylls, depending on the species. Among the main carotenoids produced by fungi are β-carotene, with two end β rings, astaxanthin, which carries hydroxyl and keto radicals in its β rings, and neurosporaxanthin (NX), an apocarotenoid with 35 carbon atoms (C35) and an end carboxyl group, chemically defined as β-apo-4'-carotenoic acid (Aasen and Jensen, 1965). Although, NX is not common in fungi, it is produced by *Neurospora* and *Fusarium* species, two well-known models in the investigation of carotenogenesis in fungi.

The carotenoid biosynthetic route begins with isopentyl pyrophosphate (IPP), the first compound in the synthesis of terpenoids. IPP can be synthesized from hydroxymethyl glutaryl coenzyme A (HMG-CoA) (mevalonate pathway) or from D-1-deoxyxylulose 1-phosphate, generated by condensation of pyruvate and 3-phosphate glyceraldehyde (non-mevalonate pathway). Although an alternative route has been described from valine and leucine in some organisms (Goodwin, 1980), in the fungi investigated the synthesis is achieved from mevalonate, which is converted to IPP by two phosphorylation reactions and a decarboxylation. IPP is condensed with an IPP isomer, dimethylalyl pyrophosphate (DMAPP), to produce geranyl pyrophosphate (GPP, C10). Two new condensation reactions give rise to farnesyl pyrophosphate (FPP, C15) and geranylgeranyl pyrophosphate (GGPP, C20). Subsequently, two GGPP molecules are condensed to produce phytoene, the first 40-carbon molecule with the typical structure of carotenes. Phytoene is colorless, but a desaturase successively introduces double conjugated bonds that provide carotenoids the ability to absorb light, and therefore, their characteristic colors. Phytoene has a central axis of symmetry and desaturations are performed in pairs on each side of it. On the partially desaturated ends, a cyclic end group can be introduced. Several types of cyclases exist depending on the type of ring they introduce, but the most common in the studied fungi are the β type. Lastly, in some cases, oxygenated radicals can be incorporated to produce xanthophylls (Avalos et al., 2014).

In fungi, the phytoene synthase and cyclase activities reside in a single bifunctional enzyme, initially discovered in *P. blakesleeanus* by genetic methods (Ootaki et al., 1973; Roncero and Cerdá-Olmedo, 1982; Torres-Martínez et al., 1980), and later confirmed at the molecular level in this and other fungi (Arrach et al., 2001; Verdoes et al., 1999a). Cyclization of one end of lycopene produces γ-carotene and cyclization of the second end produces β-carotene. These four desaturations and two β-cyclizations are known as the Porter and Lincoln pathway (Porter and Lincoln, 1950), present in various zygomycetes, such as *P. blakesleeanus* (Cerdá-Olmedo, 1987), *M. circinelloides* (Fraser et al., 1996), or *B. trispora* (Mehta et al., 2003), the latter used in the production of β-carotene at industrial scale (Avalos and Cerdá-Olmedo, 2004; Avalos et al., 2017a). Other examples of carotenogenesis studied in some non-zygomycete fungi do not follow the Porter and Lincoln pathway, producing in many cases xanthophylls. The basidiomycete yeast *X. dendrorhous* accumulates astaxanthin, which results from the introduction of keto and carboxyl groups in the terminal rings of β-carotene. All the genes responsible for its synthesis have been cloned and characterized: *crtI* (encoding a desaturase), *crtYB* (a phytoene synthase/cyclase and a desaturase) and *ast* (required for the conversion of β-carotene to astaxanthin) (Ojima et al., 2006; Verdoes et al., 1999b, 1999a). *X. dendrorhous*, formerly known as *Phaffia rhodozyma*, is one of the organisms used for the industrial production of astaxanthin (Avalos et al., 2017a; Johnson and Schroeder, 1996).

N. crassa, an extensively studied genetic model, produces NX. The easy genetic analysis in this organism allowed the identification of the first carotenogenesis genes in fungi: *al-1,* which encodes a desaturase (Schmidhauser et al., 1990), *al-2* which encodes a phytoene synthase/cyclase (Arrach et al., 2002; Schmidhauser et al., 1994), and *al-3*, which encodes GGPP synthase (Sandmann, 1993). These genes are not clustered in the genome. The genes *cao-2* (Saelices et al., 2007) and *ylo-1* (Estrada et al., 2008a) encode the enzymes for the final steps of the synthesis of NX, whose reactions are the same as those of the *Fusarium* pathway.

CAROTENOGENESIS IN *FUSARIUM*

The *Fusarium* main carotenoid, NX, is responsible for its typical orange pigmentation. The presence of NX was initially detected in *F. aquaeductuum* together with other neutral carotenoid precursors, such as ζ-carotene, neurosporene, lycopene, γ-carotene, and torulene (Bindl et al., 1970). Later studies in *F. fujikuroi* showed a similar carotenoid composition, except that β-zeacarotene was detected instead of lycopene. This indicates that cyclization can be achieved through neurosporene or lycopene depending on the species. In *F. fujikuroi*, β-carotene is also detected, showing that the cyclase is also able to recognize γ-carotene as a substrate (Avalos and Cerdà-Olmedo, 1987). Due to its carboxylic group, NX can be esterified, as occurs in a marine species of *Fusarium*, where a NX portion is converted to glycosyl-ester (Sakaki et al., 2002). Carotenoid biosynthesis in *Fusarium* has been the subject of a recent review (Avalos et al., 2017b) and the pathway is shown in Fig. I.3.

The first carotenogenesis gene identified in *Fusarium* was *carB* of *F. fujikuroi* (Fernández-Martín et al., 2000), based on its sequence similarity to *al-1* of *N. crassa* (Schmidhauser et al., 1990). CarB enzyme is responsible for the five desaturation steps in the NX biosynthesis

pathway, as indicated the identification of a mutant allele specifically affected in the fifth desaturation (Prado-Cabrero et al., 2009). Due to its proximity to *carB*, the next discovered gene was *carRA*, ortholog of the *al-2* gene that encodes the phytoene synthase of *N. crassa* (Schmidhauser et al., 1994). The phytoene synthase activity or *carRA* of *F. fujikuroi* was consistent with the albino phenotype of its mutants (Linnemannstöns et al., 2002). In both species, a carboxylic domain with similarity to carotene cyclases precedes the phytoene synthase domain. No mutants affecting this domain have been described in *Fusarium*, although mutants of the cyclase domain of the *N. crassa* gene *al-2* are defective in the cyclization steps (Arrach et al., 2002; Díaz-Sánchez et al., 2011a), suggesting a similar function for the *Fusarium* CarRA domain. From phytoene, CarB performs three consecutive desaturations that originate phytofluene, ζ-carotene and neurosporene. The cyclase activity of CarRA then introduces a β ring at one end to produce β-zeacarotene. This compound is subjected to two new desaturations by CarB, successively giving rise to γ-carotene and torulene.

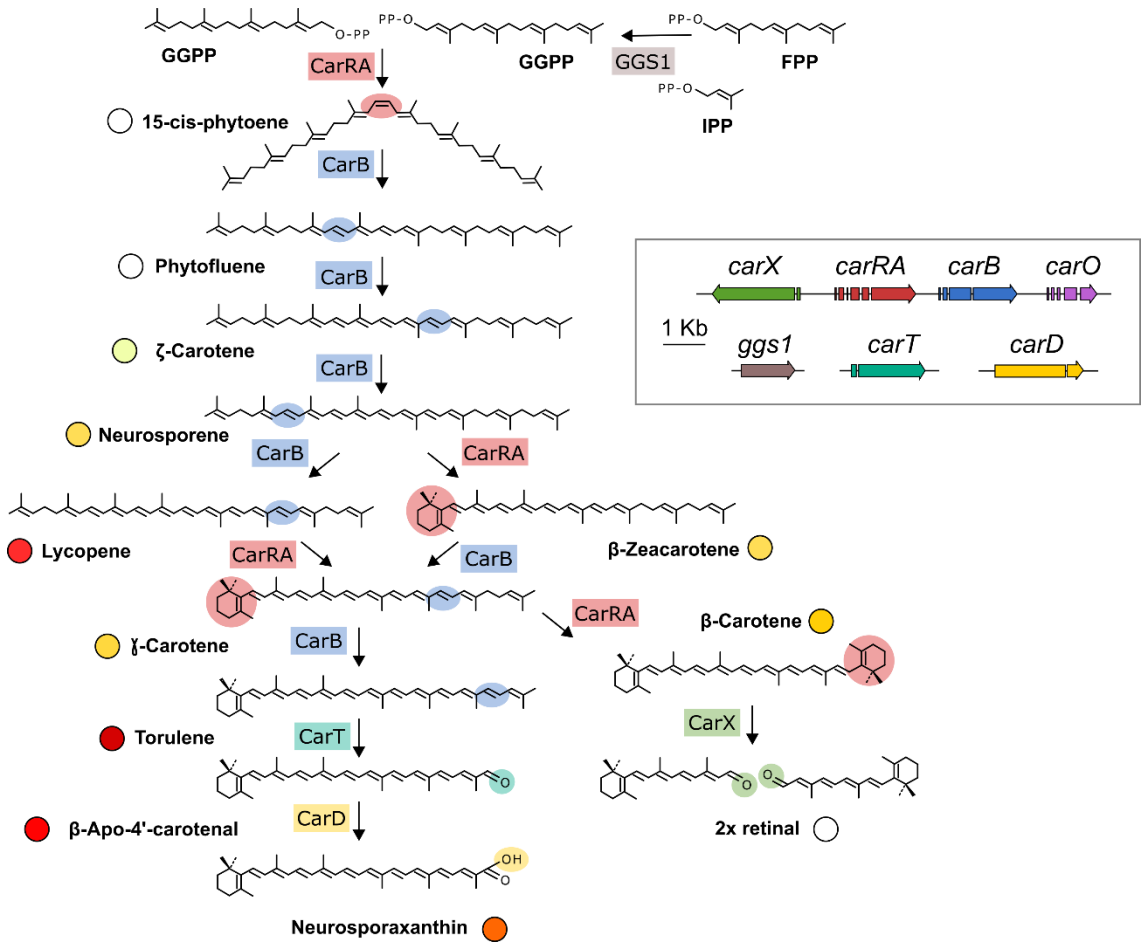

Figure I.3. Carotenoid biosynthesis pathway in *Fusarium*. Gene products responsible for the biosynthetic steps are indicated close to each arrow. The colors of the carotenoids are indidicated in the side dots. Genomic organization of the genes responsible for carotenogenesis in *Fusarium* is shown in the inserted box. The structural genes, *carX*, *carRA*, *carB* and *carO* are clustered while *ggs1*, *carT,* and *carD* are not. Gaps in the genes represent introns. The sites where the different enzymatic reactions have occurred are highlighted with different colors. Modified from (Avalos et al., 2017b).

CarX is a carotenoid oxygenase (Sui et al., 2013), initially suspected to be the enzyme that cleaves torulene to produce NX. *carX* gene is located next to the *carRA* and is transcribed divergently, but its targeted mutation did not prevent the synthesis of NX (Thewes et al., 2005). The study of the enzymatic activity of CarX revealed that it symmetrically cleaves β-carotene to produce two retinal molecules (Prado-Cabrero et al., 2007a). Next to the *carX/carRA/carB* genes it is *carO* gene, that encodes a rhodopsin, and that shares their regulation (Avalos et al., 2017b). Rhodopsins usually bind retinal as a prosthetic group that absorbs light. This fact provides biological coherence to the *car* cluster, which contains all the genes to produce retinal, which is presumably used by CarO, along with a second rhodopsin, encoded by the *opsA* gene (Estrada and Avalos, 2009). Interestingly, the *Fusarium* genomes contain a gene for an aldehyde dehydrogenase with high similarity to RALDH enzymes, which convert retinal to retinoic acid. This enzyme, CarY, was investigated in *F. verticilloides* and its enzymatic activity *in vitro* was demonstrated (Díaz-Sánchez et al., 2016). Although *carY* mutation in *F. verticilloides* had no effect on carotenogenesis, it caused various developmental alterations (Díaz-Sánchez, 2013). Nevertheless, retinoic acid has not been detected in *Fusarium* mycelium and the biological function of CarY has not been firmly determined (Avalos et al., 2017b).

The search for other putative carotenoid oxygenase genes allowed to identify gene *carT*, whose function was revealed thanks to a torulene-accumulating mutant (Prado-Cabrero et al., 2007b). Purified CarT enzyme expressed in *E. coli* cleaved *in vitro* torulene and produced β-apo-4'carotenal. The targeted mutation of *N. crassa* ortholog *cao-2* causes the blockage in NX production and torulene accumulation (Saelices et al., 2007). Similar results confirmed its presence in *Gibberella zeae*, teleomorph of *Fusarium graminearum* (Jin et al., 2010). The β-apo-4'carotenal requires oxidation to produce NX. The gene responsible for this step was first discovered in *N. crassa* thanks to the study of a yellow mutant that did not synthesize NX (Goldie and Subden, 1973; Sandmann, 1993). This mutant was affected in *ylo-1* gene, that encodes an aldehyde dehydrogenase that mediates the last step of NX biosynthesis. This was demonstrated with the complementation of the *ylo-1* mutation and with the purification of YLO-1 protein, that converts β-apo-4'carotenal to NX *in vitro* (Estrada et al., 2008a). The orthologous gene in *F. fujikuroi* was called *carD* (Díaz-Sánchez et al., 2011b). Its function was confirmed through targeted mutation, which resulted in the loss of NX and an unusual accumulation of carotenoids, interpreted as derivatives of β-apo-4'carotenal. The gene required for torulene cleavage, *carT*, and the gene needed for its final oxidation to NX, *carD*, are not in the *car* cluster. This genomic organization is conserved in the available genomes of other *Fusarium* species (Avalos et al., 2017b).

Although most of the work has been done in *F. fujikuroi*, both the *car* genes and their regulation are highly conserved in other *Fusarium* species investigated, such as *F. verticillioides* (Díaz-Sánchez, 2013) and *F. oxysporum* (Rodríguez-Ortiz, 2012). It is worth highlighting the similarities between the genes of the carotenogenesis pathway in *N. crassa* and *F. fujikuroi*. However, despite the apparent similarities, both fungi differ in some aspects of their biochemistry and pathway regulation. In *N. crassa* the order in which the reactions occur may

differ depending on the culture conditions although the final product of the route is the same (Estrada et al., 2008b).

The expression of carotenogenesis structural genes in fungi, including those of *Fusarium*, can be regulated by different environmental cues, such as light, stress, or certain chemical agents (Avalos et al., 2014). Of all of them, the regulatory factor that has received the most attention by researchers is light. Carotenoid biosynthesis is stimulated by light in many organisms, including filamentous fungi such as *P. blakesleeanus*, *M. circinelloides*, *B. trispora*, *F. fujikuroi* and *N. crassa* (Avalos and Cerdà-Olmedo, 1987; Bejarano et al., 1991; Morelli et al., 1993; Navarro et al., 1995; Quiles-Rosillo et al., 2005). However, the effect of light on the biology of filamentous fungi is broader than its effect on carotenogenesis.

LIGHT AND PHOTORECEPTION IN FUNGI

Light controls important physiological and morphological responses in fungi, including circadian rhythms, morphogenesis, tropism, and synthesis of pigments among others (Fischer et al., 2017). The integration of external signals helps organisms to improve their competitiveness in their environment and constitutes a major driving force for evolution and adaptation (Tisch and Schmoll, 2010). Therefore, most organisms, included fungi, have developed systems to detect light and adapt their activity accordingly. Even after 50 years of study of fungal light responses, the application of new experimental techniques, especially those grouped under the term “omics”, and the subsequent availability of hundreds of fungal genome sequences have provided novel insights into fungal light sensing and signaling pathways (Yu and Fischer, 2019). From a transcriptomic point of view, light regulates the expression of a large proportion of the genome in several fungi (Chen et al., 2009; Ruger-Herreros et al., 2011, 2019; Tisch and Schmoll, 2013). The responses to light frequently include the modulation of some characteristic fungal processes, such as sporulation, or production of secondary metabolites and hydrolytic enzymes.

The proteins responsible for light detection and signal transmission are known as photoreceptors. These proteins bind to small molecules called chromophores, which absorb light and cause a conformational change of the proteins themselves. This initiates the signal transduction pathway leading to the cellular response (Beattie et al., 2018). Depending on the nature of their chromophore, the photoreceptors can detect light or radiation of a specific wavelength range. Thus, UV, blue/UV light, green light or red-light photoreceptors can be distinguished. Retinal, tetrapyrroles, and flavins are the typical fungal chromophores (Yu and Fischer, 2019). Most studied responses to light in fungi are due to the detection of blue light, although responses to other wavelengths are also known (Corrochano, 2019; Purschwitz et al., 2008; Schumacher, 2017; Yu and Fischer, 2019).

White-collar complex (WCC) was the first photoreceptor system investigated in fungi. It was first discovered in *N. crassa* because of its requirement for the light induction of carotenogenesis (Harding and Turner, 1981). The WCC is composed of two proteins, called WC-1 and WC-2 (Ballario et al., 1996; Linden and Macino, 1997). The *wc-1* gene was initially identified in mutants with a deregulated pattern of carotenogenesis (Degli-Innocenti and Russo,

1984). Normally, carotenogenesis in the mycelium is light dependent while in the conidium is light independent. The mutants present pigmented aerial hyphae whereas in the base of the cultures a ring of albino mycelium is observed, hence its name. This feature makes them easily distinguishable from altered albino mutants in the structural genes of the biosynthetic pathway, in which both the mycelia and the conidia are albino. Genetic analysis of the white-collar mutants allowed to discover a second gene, *wc-2*, whose mutation produces the same phenotype. The WCC centralizes all the known photoresponses of *N. crassa,* including light-regulated conidiation, circadian rhythm, or light orientation of their perithecial beaks (Ballario et al., 1996; Degli-Innocenti and Russo, 1984). White Collar-1 type photoreceptor proteins are characterized by having a LOV domain (from Light, Oxygen and Voltage), which is a variant of the PAS domain of interaction between proteins, and a kinase domain, necessary for its activity (Briggs, 2007; Taylor and Zhulin, 1999). LOV-type photoreceptors regulate most responses to light in fungi (Corrochano, 2019; Yu and Fischer, 2019), using flavin-type chromophores (van der Horst and Hellingwerf, 2004). In fact, experiments with flavin analogs, for example, supported the proposal that a flavin acts as a chromophore for phototropism in *P. blakesleeanus* (Bergman et al., 1973), which would later be linked to the function of a white-collar protein. Within the LOV domain there is a flavin noncovalently bound through hydrogen bonds, Van der Waals bonds, and electrostatic interactions. The excitation by light of flavins, flavin mononucleotide (FMN) or flavin dinucleotide (FAD), produces a transient covalent bond with a conserved cysteine of the LOV domain (Crosson and Moffat, 2002; Pfeifer et al., 2009). The formation of this link modifies the structure of WC-1 allowing its kinase activity and thus initiating a cascade of signals in response to light. When light excitation stops, this link slowly breaks, restoring the initial fully oxidized state of the protein. White collar-2 type proteins lack LOV domains, so they cannot act as photoreceptors on their own, but they have PAS and zinc finger domains. In *N. crassa*, these complexes, together with the FREQUENCY (FRQ) protein, are part of the central oscillator of the circadian clock (Cheng et al., 2002; Schafmeier and Diernfellner, 2011).

The mechanism by which the WCC controls the transcription of the target genes in response to light conditions in *N. crassa* is very complex and new elements with a role at the different stages of the process are still being described (Figure I.4) (reviewed in Corrochano, 2019; Yu and Fischer, 2019). In its basal state in the dark, WCC is bound to specific DNA elements, mostly located in the promoters of light-regulated genes (Sancar et al., 2015; Wu et al., 2014). Light promotes the interaction of two WC-1 proteins through their LOV domains, forming a dimer of WCCs (Malzahn et al., 2010). The binding of WC-1 and WCC mediate chromatin remodeling, facilitating the accessibility of RNA polymerase and the initiation of transcription. Thus, is known that WC-1 mediates the acetylation of histone H3 (H3K14ac) by histone acetyltransferase NGF-1 (Brenna et al., 2012; Grimaldi et al., 2006) and the nucleosomes are displaced after the binding of the transcription factor Sub-1 and WCC (Sancar et al., 2015). Activation of WC-1 by light (Káldi et al., 2006) leads to the phosphorylation of WC-1 and WC-2 (Schwerdtfeger and Linden, 2000). WC-1 phosphorylation promotes its partial degradation while reducing its DNA-binding capabilities (He and Liu, 2005; Schafmeier et al., 2005). WCC activity and stability are determined by the protein FREQUENCY and the interactions with kinases and phosphatases such as the Protein Kinase C (PKC) (Dunlap and Loros, 2017; Franchi et al., 2005).

The enhanced transcription of light-activated genes is transient, and after an extended illumination their mRNA decrease or even return to basal dark levels, a phenomenon known as photoadaptation (Schwerdtfeger and Linden, 2001). This is mainly due to the participation of the photoreceptor VVD (VIVID), that exerts a negative effect on the light-dependent interactions of the WCC to DNA. VVD is a small protein with a LOV domain and a 70 amino acid N-terminal extension involved in its dimerization (Zoltowski and Crane, 2008). The role of VVD in photoadaptation is evidenced by the increased accumulation of light-regulated mRNAs in the *vvd* mutants, including those for the enzymes needed for carotenoid biosynthesis, that leads to a deeper orange color of the mutant mycelia, hence its name (Corrochano, 2019; Schwerdtfeger and Linden, 2003). Upon illumination, transcription of the *vvd* gene is stimulated by the WCC and the VVD protein is accumulated (Schwerdtfeger and Linden, 2003). The newly formed VVD protein represses the WCC by forming WCC-VVD heterodimers and regulating their phosphorylation (Hunt et al., 2010).

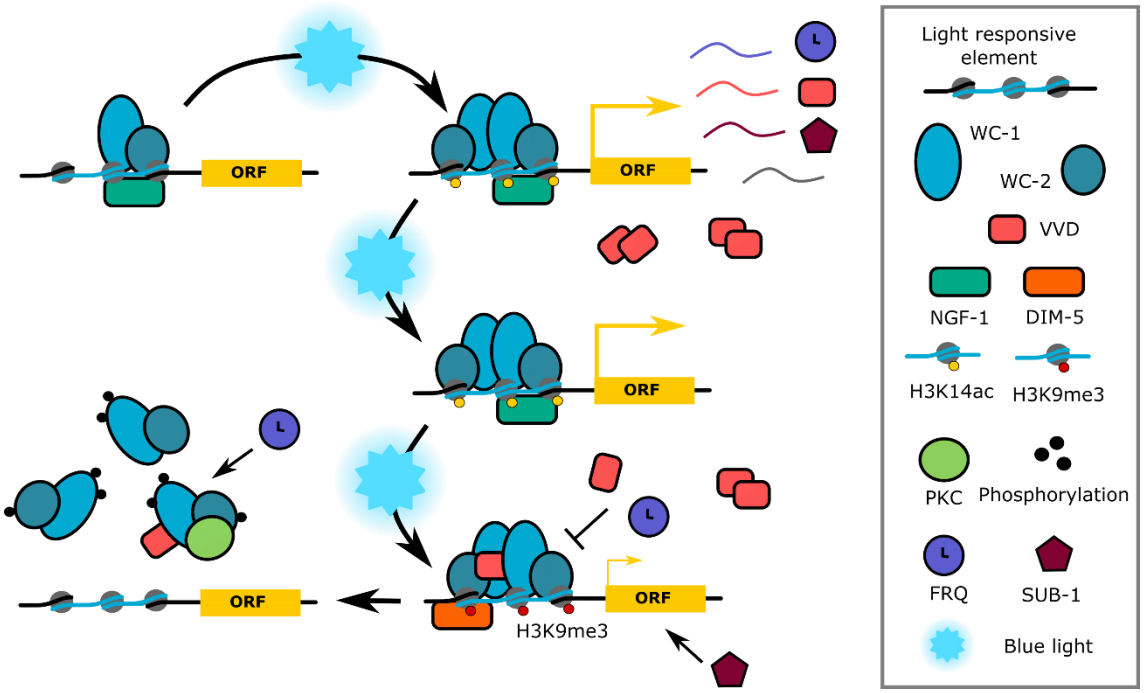

Figure I.4. Mode of action of the White-collar complex. The WCC binds to the promoters in the dark. Upon blue light reception, WC-1 forms WCCs dimers which activate transcription through chromatin modifications (H3K14ac) by the histone acetyltransferase NGF-1. Transcription of many genes is stimulated, including *vvd*, *frq,* and *sub-1*. VVD protein accumulates forming dimers and interacting with WC-1. FRQ also promotes the destabilization of WCCs dimers while factor SUB-1 promotes transcription. Modification of histones (H3K9me3) by DIM-5 further contributes to WCC dissociation from the promoters. The transient phosphorylation of WCCs and the partial degradation of WC-1 probably occur through the activity of PKC, other proteins like FRQ, and phosphatases. Modified from Corrochano 2019 and Yu and Fischer 2019.

The mechanism of action of VVD has been investigated in detail. VVD can unstably dimerize itself and with the WCC complex dependent on illumination. A cysteine of VVD forms a covalent bond with a flavin, inducing a conformational change in its N-terminal domain which appears to be essential for its repressor function (Chen et al., 2010). VVD heterodimerization with the WCC via the WC-1 LOV domain, disrupts WCCs dimers and reduces the transcriptional

response, leading to photoadaptation (Malzahn et al., 2010). VVD-WC-1 interactions protect WC-1 from degradation but also keeps it inactive (Malzahn et al., 2010). The *vvd* gene itself is also subject of tight regulation, as the repressor complex formed by RCO-1 and RCM-1 proteins, and alterations of either transcription or protein structure impact deeply the photoadaptation process (Dasgupta et al., 2015; Ruger-Herreros et al., 2014). During it, chromatin modifications also take place. DIM-5 mediates lysine 9 in histoneH3 trimethylation (H3K9me3), for example in *frq* promoter after long light exposures, and its mutation supports the role of H3K9me3 in WCC eviction, as *frq* accumulates faster and more WC-2 bind to its promoter (Ruesch et al., 2014). Through all this, *N. crassa* can dampen the transcriptional response to light and prevent the accumulation of light-regulated mRNAs in constant light.

There are proteins like VVD in other fungi. In *Trichoderma reesei*, the VVD ortholog ENVOY (Env1) has also been thoroughly studied. Env1 has an important role since its loss causes poor growth in light (Schmoll et al., 2005), unlike *N. crassa vvd* mutants, and affects cellulase production (Schmoll et al., 2004). Both *env1* and *vvd* mutants have certain light-dependent responses affected, as well as their ability to maintain the photoinduction of the genes (Castellanos et al., 2010). In the case of ENV1, it has emerged as a central checkpoint for integration of nutrient sensing, light response and development in *Trichoderma* (Schmoll, 2018).

Subsequent analyses in other fungi have shown the presence of WC-1 and WC-2 type proteins in numerous species. The wide distribution of these photoreceptors in fungi suggests an early onset in evolution to regulate responses to light (Idnurm et al., 2010). WC orthologs have been described in zygomycetes, such as *M. circinelloides* or *P. blakesleeanus* (Sanz et al., 2009; Silva et al., 2006); in basidiomycetes, such as *Cryptococcus neoformans* (Idnurm and Heitman, 2005), *U. maydis* (Brych et al., 2016) or *Pleurotus ostreatus* (Qi et al., 2020); and in ascomycetes, such as *T. reesei* (Castellanos et al., 2010), *B. cinerea* (Canessa et al., 2013) or *A. nidulans* (Purschwitz et al., 2008). In general, fungal genomes possess a single copy of the type gene *wc1*, although it has been lost in some species (Idnurm et al., 2010). A special case is found in some zygomycetes, which present several copies of the *wc* genes (Corrochano and Garre, 2010). Their functions have been studied in detail in *M. circinelloides*, where they have different specialized functions, possibly as a result of the loss of other photoreceptors (Corrochano, 2019). Thus, *mcwc-1a* regulates phototropism, *mcwc-1b* participates in a regulatory mechanism of carotene synthesis independent of light by an ubiquitylation mechanism through the CrgA protein (discussed below) (Silva et al., 2008), and *mcwc-1c* regulates the light-dependent expression of carotenogenic genes (Silva et al., 2006). In recent years, the *wc* mutants of *N. crassa* have shown phenotypes related to processes not regulated by light (Sancar et al., 2015).

Besides the WCC, which seems to be the main photoregulatory system in fungi (Corrochano, 2019), another important family of fungal photoreceptors is the cryptochrome-photolyase family. It is present in all major taxa and is divided into 10 subfamilies (Ozturk, 2017). Five subfamilies correspond to photolyases (PHR): class 0 (previously called DASH-cryptochromes) or ssDNA photolyases, class I, class II and class III photolyases, that repair cyclobutane pyrimidine dimers (CPD), and (6-4) photolyases, that repair (6–4) photoproducts

consisting in 6–4 pyrimidine-pyrimidone or 6-4 pyrimidine–pyrimidinone. On the other hand, there are five cryptochromes (CRY) subfamilies: one of plant cryptochromes; and the rest, type 0, type 1, type 2, and type 4 cryptochromes, that are usually found in animals.

From the point of view of function, cryptochromes can be divided into two subtypes, both using the same UV-A/blue spectral range: those acting as light-driven DNA-repair enzymes, the photolyases (Sancar, 2004), and those functioning as photoreceptors involved in signal transduction, the cryptochromes. This type includes the DASH-cryptochromes (DASH as an acronym of *Drosophila*, *Arabidopsis*, *Synechocystis* and *Homo sapiens*), sharing both functions (Kiontke et al., 2020). Cryptochromes consist of an N-terminal region typical of a photolyase (PHR), to which two chromophores, FAD and 5,10-methenyltetrahydrofolate (MTHF) bind (Sancar, 2004). The photolyase region is followed by a carboxyl terminal domain of variable length, involved in signal transduction functions. In general, CRY-DASH family binds to single-stranded DNA, with some exceptions that bind to double-stranded DNA (Navarro et al., 2020) to perform repair functions typical of photolyases (Kiontke et al., 2020). Cryptochromes belonging to the plant type and to the DASH-cryptochromes groups are usually found in fungi, which also contain canonical CPD and 6–4 CPD photolyases exerting repair functions. In some zygomycetes, nevertheless, which lack photolyases, the repair function is carried out by DASH-cryptochromes (Navarro et al., 2020; Tagua et al., 2015). Compared to other taxonomic groups, there is not much information about fungal cryptochromes and their signaling mechanisms (Yu and Fischer, 2019), although several mutants have been described. CryA in *A. nidulans* groups with CPD photolyases, as it also has repair functions (Bayram et al., 2008a) and represses sexual development in the presence of light. In *N. crassa*, the Cry-DASH protein CRY participates in the regulation of circadian rhythm and binds to DNA and single- and double-stranded RNA but shows no evidence of photolyase activity *in vivo* (Froehlich et al., 2010; Olmedo et al., 2010). *B. cinerea* has two members of the family with segregated functions, BcCRY1, a CPD photolyase, and BcCRY2, a Cry-DASH protein dispensable for photorepair but playing a role as a conidiation repressor (Cohrs and Schumacher, 2017). Fungal Cry-DASH proteins in other species, as *F. fujikuroi*, *Sclerotinia sclerotum* and *Cordyceps miliatiris,* have been shown to regulate very different processes, including morphology, development, or secondary metabolite production (Castrillo et al., 2013; Veluchamy and Rollins, 2008; Wang et al., 2017a). Other type of blue-light photoreceptors, the BLUF proteins (sensors of blue-light using FAD), have been found in several fungi, but their functions have not yet been studied (Brych et al., 2016).

Green light can be sensed in fungi by retinal-binding proteins, known as opsins. Rhodopsins are integral membrane proteins with a highly conserved three-dimensional structure, consisting of seven transmembrane helices that bind a retinal molecule as a chromophore by a covalent bond with a lysine residue. Rhodopsins, initially discovered in archaea, allow translocation of protons across membranes. Three different classes of opsins are distinguished: the first class has a slow photocycle with low proton-pumping activity, as NOP-1 in *N. crassa* (Wang et al., 2018), the second class is characterized by strong green-light-dependent proton-pumping activity, as CarO in *F. fujikuroi* (García-Martínez et al., 2015), and the third class lacks the retinal binding residue (Yu and Fischer, 2019). The genomes of many

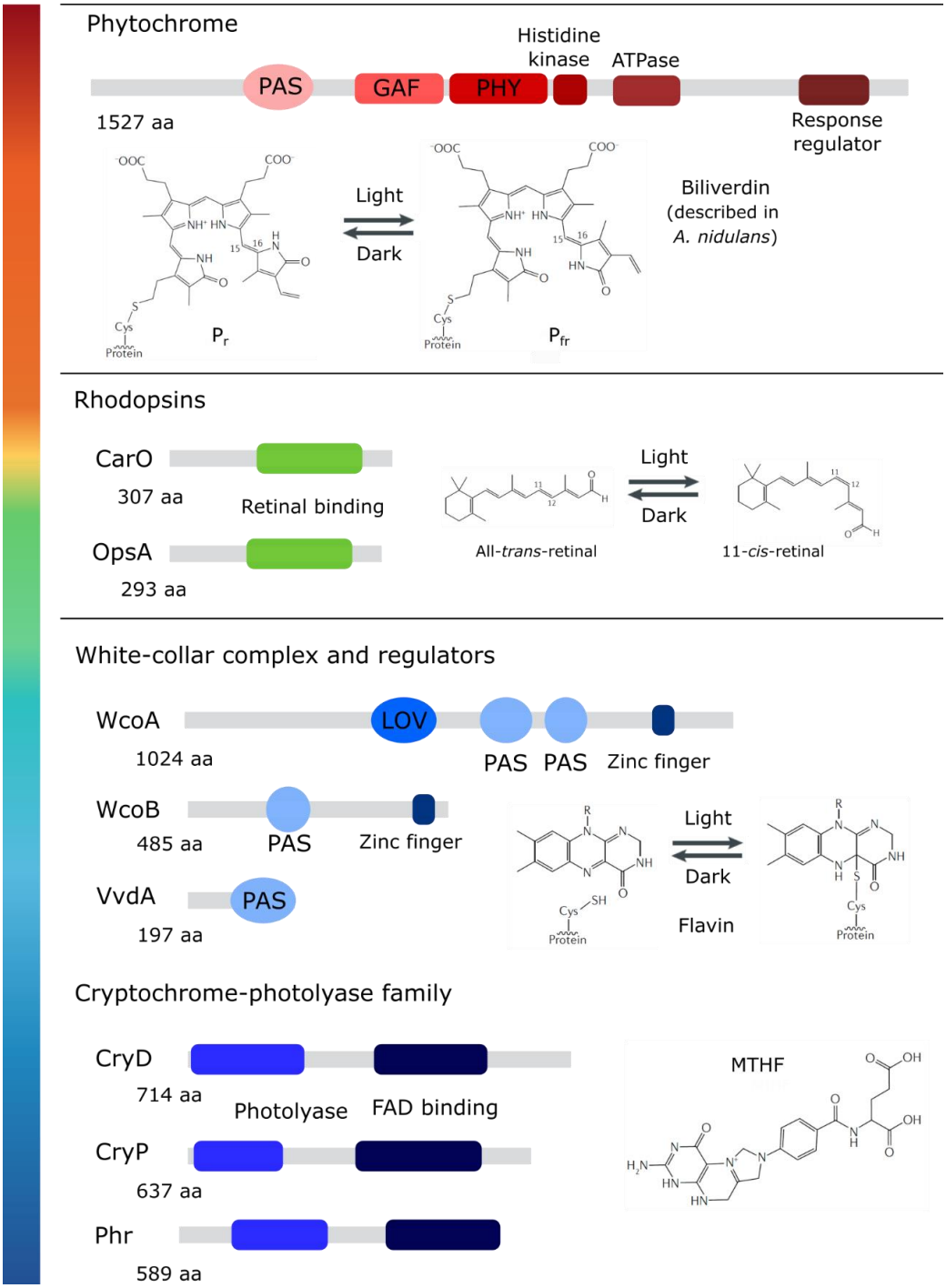

Figure I.5. Structure of *F. fujikuroi* photoreceptors and their chromophores. *F. fujikuroi* phytochrome (*FFUJ_05887*) was identified due to its sequence homology with the described *F. graminearum* FgFph (*FGSG_08608*) (Kim et al., 2015). *F. fujikuroi* opsins (CarO encoded by *FFUJ_11804*, OpsA encoded by *FFUJ_02352*) are transmembrane proteins with retinal as chromophore (Adam et al., 2018). The White-collar proteins (WcoA encoded by *FFUJ_13691*, WcoB encoded by *FUJ_00530*) and Vivid (VvdA encoded by *FFUJ_06055*) contain LOV domains where an FAD is covalently bound to a cysteine upon illumination (Castrillo and Avalos, 2014; Estrada and Avalos, 2008). The WcoA protein, as WC-1 in *N. crassa*, contains two PAS domains and a zinc-finger domain for DNA binding. The cryptochrome/photolyase proteins (CryD encoded by *FFUJ_05732*, CryP encoded by *FFUJ_03105*, Phr encoded by *FFUJ_00436*) contain a flavin and a methyltetrahydrofolate (MTHF (Castrillo et al., 2015). The size of the photoreceptors is indicated in amino acids. Modified from (Yu and Fischer, 2019)

fungi encode further opsin-related proteins lacking the lysine residue for chromophore binding whose functions are still enigmatic (Rodriguez-Romero et al., 2010). NOP-1 in *N. crassa* is involved in the regulation of developmental processes, possibly through the control of the oxidative state of the cell (Wang et al., 2018) while the CarO-type rhodopsin has been found only in plant-associated fungi and has a role in germination and infection in *F. fujikuroi* (Adam et al., 2018). The signal transduction pathway for fungal green light receptors is still unknown. The presence of genes for rhodopsins in fungal genomes is very variable and phylogenetic studies suggest horizontal transfer events followed by duplications and losses, theoretically leading to functional diversifications (Wang et al., 2018).

Red light and far-red light are sensed in fungi by phytochromes. Their photodetection mechanism depends on a linear tetrapyrrole (bilin), autocatalytically bound to the apoprotein via a conserved cysteine residue (Rensing et al., 2016). Initially described in plants, in fungi this photoreceptor type was first discovered in *A. nidulans* and *N. crassa* (Blumenstein et al., 2005; Froehlich et al., 2005). Fungal phytochromes (Fph) have a photosensor module at the amino end that consists of a PAS domain, present only in fungal and bacterial phytochromes, a GAF domain (cGMP phosphodiesterase/Adenylate cyclase/FhIA) with bilin lyase activity, which includes the conserved cysteine residue that binds the chromophore, a PHY, exclusive of this class of photoreceptors, and a regulatory module at its highly variable carboxyl terminal end depending on the species, but which always contains a domain related to the histidine kinases or HKRD (Rensing et al., 2016). The nature of the bilin derivative chromophore of fungal phytochromes has not yet been determined, although it was shown that FphA from *A. nidulans* uses biliverdin (Blumenstein et al., 2005; Froehlich et al., 2005). Phytochrome genes are common in ascomycetes (Schumacher and Gorbushina, 2020) and basidiomycetes (Corrochano, 2019), but have not been described in zygomycetes. Phytochromes regulate in *A. nidulans* the balance between asexual and sexual development and the germination process, as well as the biosynthesis of secondary metabolites (Blumenstein et al., 2005; Röhrig et al., 2013). They are also involved in the modulation of the activity of the WCC and in the transcription of some of their genes in several fungi, as *N. crassa* (Corrochano, 2019; Olmedo et al., 2010; Purschwitz et al., 2008; Yu and Fischer, 2019).

PHOTORECEPTORS AND PHOTORESPONSES IN *FUSARIUM*

The *Fusarium* genomes contain genes for all the photoreceptors displayed in Fig. I.4 and some of them have been studied by targeted deletion in in several *Fusarium* species, particularly in *F. fujikuroi*. These include the ortholog for *wc-1* of *N. crassa,* whose mutant phenotypes differ greatly between both genera. There are also differences in their regulations: while the expression of *wc-1* is photoinducible in *N. crassa*, *F. fujikuroi wcoA* is hardly affected by light (Estrada and Avalos, 2008). Secondary metabolism is deeply impacted in *F. fujikuroi wcoA* mutants, which are affected in the production of gibberellins, bikaverin, and fusarins, while trichotecenes and aurofusarin syntheses were affected in *F. graminearum* (Kim et al., 2014). *F. fujikuroi wcoA* mutants produced lower amounts of conidia either on agar or in liquid cultures with standard nitrogen concentration (Estrada and Avalos, 2008). Moreover, the mycelium of

this mutant was less hydrophobic than the one of the wild type, a phenotype that was also found in *F. oxysporum wc1* mutant (Ruiz-Roldán et al., 2008). Photoreactivation after UV treatment was impaired too, as there was not transcriptional activation of the *phr1* under illumination in the *wc1* mutant in *F. oxysporum* (Ruiz-Roldán et al., 2008) and *F. graminearum* (Kim et al., 2015). Even pathogenesis was affected, mutation of *wc1* impaired the virulence of *F. oxysporum* in immune-depressed mice. Although no effect on plants was reported, recent experiments with *F. asiaticum Fawc1* mutant showed a decrease of virulence on wheat, as well as defects on perithecia and ascospore formation (Tang et al., 2020). This also happened in *F. graminearum* (Kim et al., 2015). The *wcoA* mutation also affects carotenogenesis, but this effect will be discussed later. Interestingly, many of these alterations were light independent. Differential phenotypes have been described for *Fawc1* depending on the LOV and the Zn-finger domains of the protein. This could explain a differential role of WC-1 orthologs, working as a light-dependent/photoreceptor transcription factor for some processes while working as a standard one in others.

Orthologs of the *N. crassa wc-2* have also been deleted in *F. graminearum* and *F. asiaticum* (Kim et al., 2015; Tang et al., 2020), where impairment of sexual reproduction, photoreactivation, and secondary metabolism phenotypes were described. Nevertheless, the virulence seems to be *Fawc1*-dependent in *F. asiaticum*. The ortholog of *N. crassa vvd*, another member of the WCC, has also been studied in *F. fujikuroi* (Castrillo and Avalos, 2014). Its expression depends on illumination and on the WcoA protein. In contrast to its ortholog in *N. crassa*, the targeted mutation of *vvdA* causes a pale pigmentation due to lower accumulation of carotenoids than in the wild strain. Mutants of this genes also show other phenotypic alterations under illumination, such as a lower production of conidia and differences in the morphology of the mycelial colonies (Castrillo and Avalos, 2014).

Fusarium genomes usually have two genes for cryptochromes: a plant-type cryptochrome and a DASH-cryptochrome. Cryptochrome-DASH CryD in *F. fujikuroi* has received special attention. Gene expression of *cryD* was strongly stimulated by light through WcoA and its targeted mutation produced different phenotypic alterations under illumination but not in the dark (Castrillo et al., 2013), which are described in the introduction of chapter 3. Moreover, CryD seems to be responsible for a long-term photoinduction of carotenogenesis (Castrillo and Avalos 2015). No information is available on the function of the other *Fusarium* cryptochrome, but it is known from RNA-seq studies that its expression is also photoinduced (Ruger-Herreros et al., 2019). As it has been mentioned, the photoreactivation of UV damage is mainly performed in *Fusarium* by the photolyase, whose expression is also light dependent (Alejandre-Durán et al., 2003; Castrillo et al., 2015). Moreover, it was highly expressed at early stages of germination (Milo-Cochavi et al., 2019).

Fusarium has two rhodopsins, and both have been studied in *F. fujikuroi*. The gene for the rhodopsin CarO is linked to the *carRA*, *carB* and *carX* genes in the *car* gene cluster (Prado et al., 2004) and its transcription is induced by light. The CarO protein is an efficient proton pump in response to green light and its activity is enhanced in the presence of the plant hormone indole-3-acetic acid (Adam et al., 2018; García-Martínez et al., 2015). Despite the lack of

apparent phenotypic changes in a targeted mutant of the *carO* gene (Prado et al., 2004), a slight alteration in the germination speed was found in the conidia of the mutant in certain culture conditions. Germination analyses of conidia from *carO* mutant showed a faster development of light-exposed germlings than the control strain. Additionally, YFP labeling of CarO showed its presence in conidia from illuminated mycelia. Orthologs of this rhodopsin have been found in many plant-associated fungi, suggesting a possible role in plant infection. In fact, rice plants infected with the *carO* mutant showed more severe *bakanae* symptoms, indicating a potential role of the CarO rhodopsin in the regulation of plant infection.

Fusarium genome includes a gene for a second rhodopsin, *opsA*, which is the ortholog for the *N. crassa* gene *nop-1*. Its mutation did not reveal a new phenotype, except for a moderate decrease in mRNA levels of the *car* genes that did not affect to the carotenoid content (Estrada and Avalos, 2009). The *carO* and *opsA* genes were differentially expressed during sexual reproduction in perithecia. The transcript levels of *carO* increased along perithecia maturation in *F. graminerarum* (Wang et al., 2018). In *N. crassa*, the Δ*nop-1* mutant initiated sexual development earlier than the wild type *nop-1.* Moreover, comparative transcriptomics showed that *nop-1* mutant abundantly expressed genes involved in oxidative stress response (Wang et al., 2018). It was concluded that the *nop-1* gene could play a role in regulating asexual–sexual development in response to different environmental signals including light and ROS. *Fusarium* presents a third gene of the rhodopsin family, *hspO*, which most probably is an opsin-related protein presumably not photoactive, since it lacks the retinal binding lysine (Estrada and Avalos, 2009).

The role of the only phytochrome (Fph) found in *Fusarium* genomes (Avalos and Estrada, 2010) has been analyzed in *F. graminearum* (Kim et al., 2015). Although *fgfph* deletion showed no phenotype in the studied processes, *in vivo* protein-protein interaction assays using split luciferase complementation found that FgFph interacts with FgWc-1 as well as with the members of the Velvet complex, FgVeA and FgLaeA, linking light reception with sexual reproduction. The Velvet complex has been described as the coordinator between light perception and development and secondary metabolism in many fungi (Bayram et al., 2008b). Moreover, Illumination of the mycelium of *F. fujikuroi* with red light appreciably induces the expression of several genes, including *carRA* (Castrillo and Avalos, 2015). As carotenoids photoinduction is mainly dependent on WcoA, this observation suggests the involvement of a phytochrome in the photosensory system that regulates this response.

Different reports have shown stimulatory effects of visible and near-UV light on conidiation in various *Fusarium* species (Avalos and Estrada, 2010). Nevertheless, results are species dependent. Even for *F. fujikuroi* two strains have been found that differ greatly: FKMC1995 exhibits high conidia production in the dark (Costa et al., 2020), while conidiation by IMI58289 is induced under illumination (Avalos and Estrada, 2010). There are also reports on the differential fitness towards light in conidia produced at different wavelengths (Costa et al., 2020). Sexual reproduction, characterized by perithecia formation, normally requires specific light conditions. This has been investigated in *F. graminearum* (Kim et al., 2015; Tschanz et al., 1976). In this species, perithecia are not formed in the dark, but 4 h of daily light are enough for

their optimal production. Moreover, reduction of UV exposure lowers the number of perithecia. Ascospore release is also stimulated by light in this fungus (Trail et al., 2002).

Regarding secondary metabolism, light modulates the production of many metabolites, in addition to carotenoids. Gibberellin biosynthesis is stimulated by light in some *F. fujikuroi* strains (Avalos and Estrada, 2010; Castrillo et al., 2013), although its effect is minor compared to the one caused by nitrogen availability. The effect of light has also been investigated in the synthesis of enniatins, cyclohexadepsipeptide antibiotics produced by different *Fusarium* species. Enniatin production was enhanced by light in *F. sambucinum* compared to dark-grown cultures (Audhya and Russell, 1974). In fact, light was known to influence the expression of fungal SMs through the fungal-specific regulator velvet complex VelB/VeA/LaeA (Gerke and Braus, 2014) and its impact on secondary metabolism have also been studied in *Fusarium*. Disruption of this complex almost totally abolished biosynthesis of gibberellins, fumonisin, fusarins, and fusaric acid in *F. fujikuroi* (Niehaus et al., 2018; Wiemann et al., 2010), as well as conidiation. The FgVeA or FgVe1 deletion mutants of *F. graminearum* exhibited reduced aerial hyphal formation as well as reduced aurofusarin and deoxynivalenol biosynthesis (Jiang et al., 2011; Merhej et al., 2012). The participation of the Velvet complex in both conidiation and secondary metabolism regulation and its documented interdependency in other fungi with the WCC (Calvo, 2008) suggests a possible explanation for the *wcoA* mutant phenotypes in *F. fujikuroi*. Moreover, the light-regulated repressor of macroconidia formation and regulator of secondary metabolism Ltf1 in *B. cinerea,* ortholog to *F. fujikuroi* Csm1, have been shown to regulate conidiation, as its deletion resulted in elevated microconidia formation and secondary metabolism, deregulating bikaverin and fusarubins production under otherwise repressing conditions. This protein has also been described to restore the conidiation impairment phenotype in *F. fujikuroi vel1* mutant.

The impact of light on *Fusarium* transcriptome has been recently addressed in the group (Ruger-Herreros et al., 2019). Up to 8% of the genome is positively or negatively affected by light in *F. fujikuroi* and *F. oxysporum*. A strong tendency towards the activation of genes has been observed in 60-min illuminated cultures of both fungi, indicating a more relevant up-regulating role for light in *Fusarium*. Strongly upregulated genes included several photoreceptors, as *vvdA*, *cryD* and the putative photolyase *phr1*, others related with stress response, especially genes for catalases with putative functions towards oxidative stress protection, and genes associated to carotenoids metabolism. The synthesis of carotenoids, which will be discussed in more detail in the next section, is one the best described responses to light in *Fusarium*.

PHOTOCAROTENOGENESIS IN *FUSARIUM*

Photocarotenogenesis is the best characterized light-regulated process in *Fusarium* (Avalos et al., 2017b). Early studies on the effect of light on carotenogenesis were carried out in *F. aquaeductuum*, whose response showed a gradual accumulation of carotenoids under illumination, with a peak at 12 hours (Rau, 1967). Reaction of carotenogenesis to light is independent of temperature in the range of 5-25 °C but depends on oxygenation and requires active protein synthesis (Rau, 1971). The effect of light can be partially replaced by the addition

of oxidizing reagents (Rau, 1967; Rau et al., 1967), suggesting that the oxidation of the -SH groups plays a role in the light detection system. Consequently, the photoinduction disappears when reducing agents are added (Theimer and Rau, 1970). However, while a short light exposure is sufficient to sustain photoinduction, the oxidizing agents must remain to maintain its stimulating effect, and such stimulation is additive with that of light (Theimer and Rau, 1972) which indicates different mechanisms of action. Nevertheless, oxidizing agent p-hydroxymercuribenzoate had no effect in other *Fusarium* species (Ávalos and Cerdá-Olmedo, 1986).

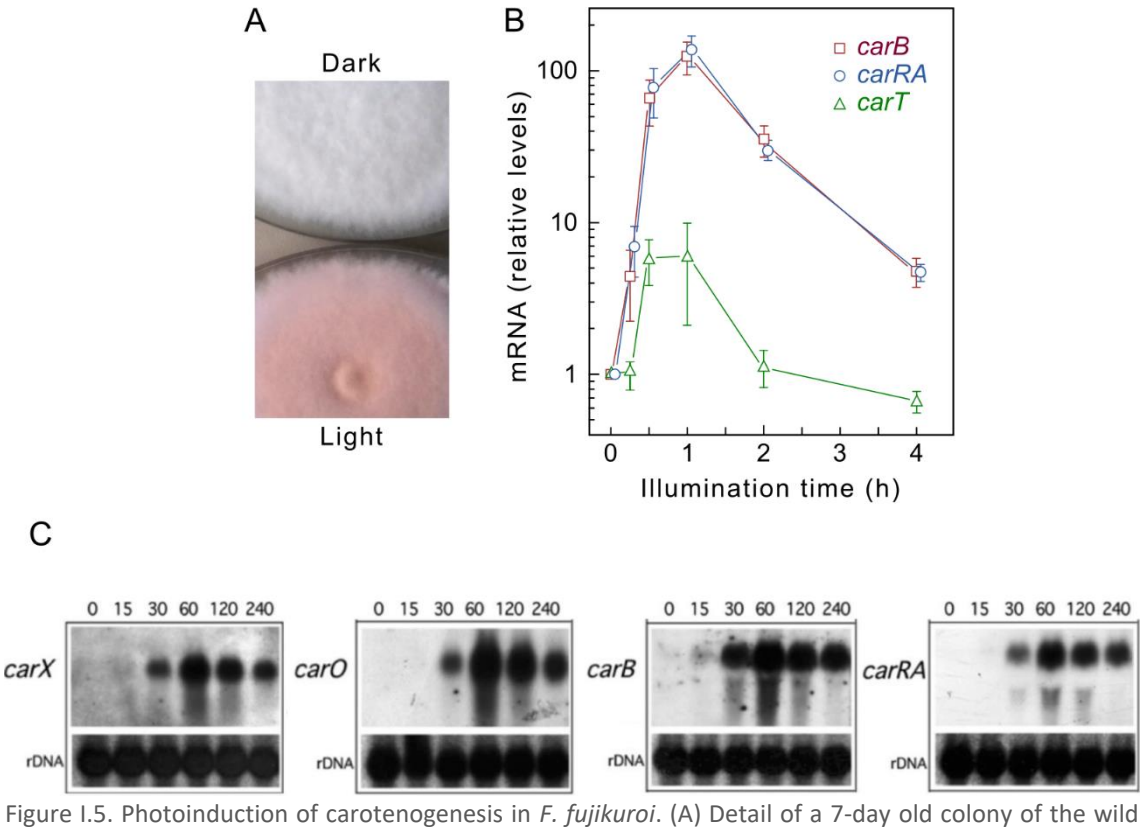

Figure I.5. Photoinduction of carotenogenesis in *F. fujikuroi*. (A) Detail of a 7-day old colony of the wild strain IMI58289 grown on minimal medium in the dark or under continuous illumination. (B and C) Effect of light on the kinetics of mRNA accumulation for some of the genes of the carotenogenesis pathway. Transcript levels were determined by (B) RT-qPCR (real time quantitative PCR) and referred to those of β-tubulin gene (levels in the dark for each gene were taken as 1) and by (C) Northern-blot hybridization. The numbers on the lanes of each Northern indicate illumination time in minutes. Shown below is one of the ribosomal RNA bands used as load control. Modified from (Avalos et al., 2017b) and (Avalos and Estrada, 2010).

Photoinduction of carotenogenesis in *Fusarium* is externally manifested within the first hour after illumination onset by a rapid increase in levels of transcripts of most structural genes, followed by an accumulation of carotenoids in the subsequent hours, providing an orange pigmentation to the mycelium. Northern blot experiments in *F. fujikuroi* showed similar induction kinetics of the four genes of the *car* cluster, *carRA*, *carB*, *carO,* and *carX*, as well as *carT* (Avalos et al., 2017b), as can be seen in Fig. I.5. This photoinduction pattern has been confirmed by RT-qPCR approaches, and similar results have been obtained in *F. oxysporum* (Rodríguez-Ortiz et al., 2012) and *F. verticillioides* (Adám et al., 2011). Previously underestimated

(Mende et al., 1997), recent RNA-seq data have revealed also a significant photoinduction of *ggs1* (Ruger-Herreros et al., 2019). A minor photoresponse was exhibited by *carD* in *F. fujikuroi* (Díaz-Sánchez et al., 2011b), corroborated by the RNA-seq data (Avalos et al., 2017b). Therefore, in *F. fujikuroi*, the whole NX biosynthetic pathway is regulated by light.

In *N. crassa*, a fungus with a similar action spectrum for light-induced carotenogenesis (De Fabo et al., 1976), photoinduction is entirely dependent on the WCC (Yu and Fischer, 2019). However, *wcoA* mutants in *F. fujikuroi* (Estrada and Avalos, 2008) and its ortholog, *wc1*, in *F. oxysporum* (Ruiz-Roldán et al., 2008) and in *F. asiaticum* (Tang et al., 2020) maintain, with different degrees of efficiency, the production of carotenoids in continuous light. Targeted mutations of *wc-1* and *wc-2* ortholog genes of *F. graminearum*, *fgwc-1* and *fgwc-2*, caused pale pigmentation of the surface of colonies under light (Kim et al., 2014). Recently, it was shown that *fawc2* deletion in *F. asiaticum* also caused a major drop in carotenoid biosynthesis under constant illumination, but it did not abolish it (Tang et al., 2020). Analysis of carotenoid revealed two responses in *F. fujikuroi*, first, a rapid response dependent on WcoA and a second phase of slower carotenoid accumulation which depended on the cryptochrome DASH CryD (Castrillo and Avalos, 2015). The participation of CryD as a second photoreceptor could explain the maintenance of carotenoid accumulation in *wcoA* mutants in continuous illumination.

The photoinduction of the structural genes for carotenogenesis in the mutants for *wcoA* and *cryD* was consistent with different mechanisms of action for the encoded photoreceptors (Castrillo and Avalos, 2015). After illumination, the *wcoA* mutants exhibited photoinduction of carotenogenesis, but they accumulate carotenoids more slowly and their total levels do not reach those of the wild type. However, both the carotenoid content and the mRNA levels of the structural *car* genes were much lower in the dark in the *wcoA* mutants than in the wild strain. Even more, the transcriptional photoinduction of the *car* genes was basically absent in the *wcoA* mutants, with mRNA levels after illumination lower than those of the wild strain in the dark. Therefore, the induction of carotenogenesis by the alternative photoreceptor, presumably CryD, must be carried out through a transcription-independent mechanism that remains to be elucidated.

In contrast to *N. crassa*, where the mutation of the VVD photoreceptor prevents the decay of mRNA levels after photoinduction and therefore results in higher carotenoid content under illumination, the mutation of *vvdA* in *F. fujikuroi* caused a lower carotenoid accumulation (Castrillo and Avalos, 2014). The kinetics of carotenogenesis in the *vvdA* mutants showed a faster carotenoid accumulation immediately after light exposure, consistent with an attenuating function of VvdA on the photoactivated WcoA, but a slower accumulation after more prolonged growth under light, suggesting an up-regulating role during the second stage of carotenoid photoinduction (Castrillo and Avalos, 2015). The effects in carotenogenesis of these mutants are represented in Figure I.6.

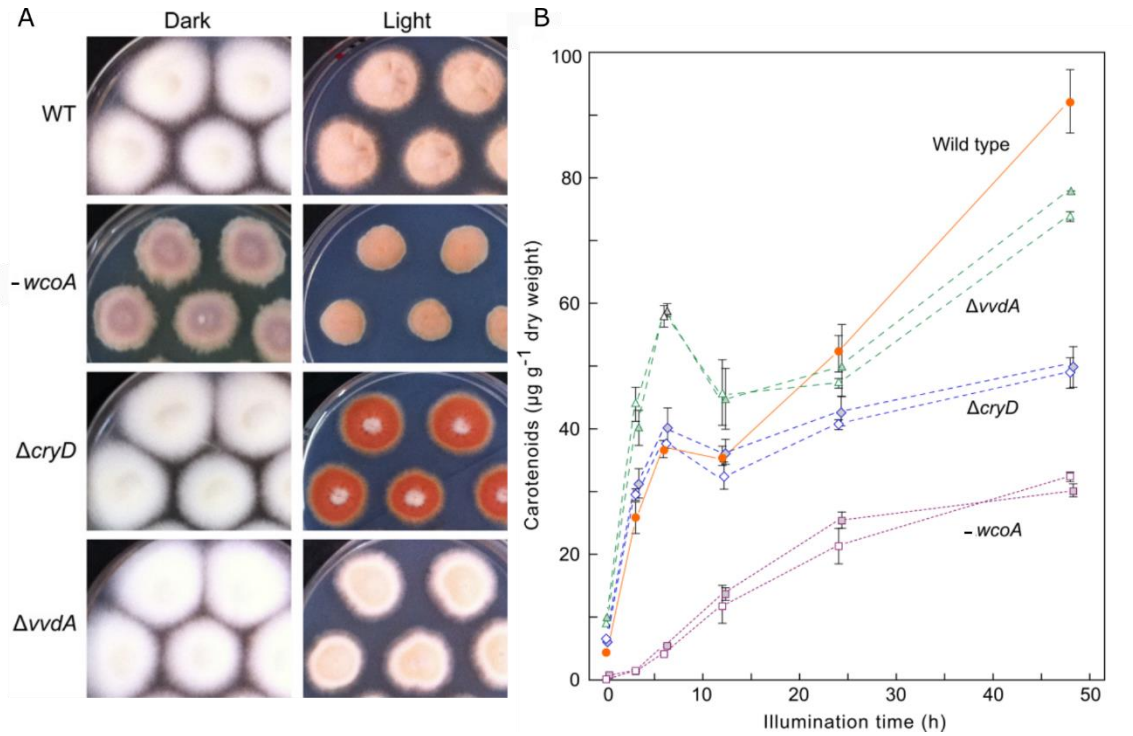

Figure I.6. *F. fujikuroi* photoreceptor mutants. (A) Colonies of the wild strain (WT) and *wcoA*, *cryD* and *vvdA* mutants grown for 7 days at 30°C in the dark or under continuous illumination. The brownish color of the *wcoA* mutants in the dark and the reddish color of the *cryD* mutants in the light are due to the production of secondary metabolite pigments unrelated to carotenoids, such as bikaverin and other polyketides. (B) Kinetics of carotenoid accumulation after illumination of the wild type and *wcoA*, *cryD,* and *vvdA* mutants. Modified from (Castrillo and Avalos, 2015).

Other proteins related with the light signal transduction pathway may also be involved in carotenogenesis. Fflae1, a member of the velvet complex in *F. fujikuroi* with two proteins of the velvet family, FfVel1 and FfVel2 (Wiemann et al., 2010), is a transcriptome master regulator whose deletion generally causes decreased SM production levels, altered asexual and sexual development, and reduced virulence for pathogenic fungi (Jain and Keller, 2013). In *F. fujikuroi,* it regulates the production of several secondary metabolites synthetases. Among others, *carRA* is upregulated in the *fflae1* mutant, indicating a repressor activity for the protein (Niehaus et al., 2018).

REGULATION OF CAROTENOGENESIS BY LIGHT-INDEPENDENT FACTORS IN *FUSARIUM*

Nitrogen availability controls the production of different secondary metabolites in *Fusarium*, with gibberellins as a paradigmatic example (Tudzynski, 2014). Nitrogen also affects carotenogenesis: experiments with immobilized mycelia of *F. fujikuroi* revealed a higher synthesis of carotenoids under nitrogen starvation (Garbayo et al., 2003). The negative effect of nitrogen was confirmed by experiments in which carotenoid synthesis was enhanced or reduced depending on the transference to low or high nitrogen conditions, respectively, indicating that the repressing effect is reversible. The effect of nitrogen was studied in shake cultures of wild-type and carotenoid overproducing strains, showing that the production was higher in a medium with a low nitrogen/carbon ratio than with high N/C ratio in either of the tested strains

(Rodríguez-Ortiz et al., 2009). A different set of experiments, in which cultures grown under an excess of nitrogen were transferred to a nitrogen-free solution, showed an increase of transcript levels of the structural genes *carRA* and *carB* after the transfer, which was accompanied by an enhanced accumulation of carotenoids. As found for photoinduction, the transcriptional increase was transitory. The stimulatory effect of nitrogen starvation on *F. fujikuroi* carotenogenesis, either at mRNA or carotenoids levels, was additive with the one produced by light (Rodríguez-Ortiz et al., 2009), indicating different activating mechanisms. The regulation of carotenogenesis by nitrogen has been also described in *N. crassa* (Sokolovsky et al., 1992). The regulation by nitrogen might involve control of expression at the level of chromatin structure, as indicated by the differences in histone methylation found for the genes of the *car* cluster in a mutant of the methyltransferase KMT6 in *F. graminearum* (Connolly et al., 2013).

Other regulatory circuits may also influence carotenoid biosynthesis. A major regulatory pathway is the one involving cyclic adenosine monophosphate (cAMP), produced by adenylate cyclase under the stimulation of a G unit from a heterotrimeric G protein. cAMP affects other proteins, including protein kinases that phosphorylate target proteins to module their activity. The mutation of the adenylate cyclase gene *acyA* in *F. fujikuroi* resulted in higher levels of carotenoids in the dark but in a reduced photoinduction after exposure to light (García-Martínez et al., 2012). The mutation affected also the growth pattern and the production of other secondary metabolites. Carotenogenesis may also have a regulatory connection with sexual development, as suggested by the lower carotenoid photoinduction of the mutants of the MAT1-2-1 mating-type gene of *F. verticillioides* (Adám et al., 2011).

In *N. crassa*, besides the regulation by light, the synthesis of carotenoids is coupled to conidiation in a light-independent manner (Avalos and Corrochano, 2013). In fact, conidiation is stimulated by light and aerial growth in this fungus, leading to a massive conidia production that provides a typical orange pigmentation in slant cultures. Conidiation is less abundant in *Fusarium* and the conidia formed by the wild strain in the dark contained low amounts of carotenoids, indicating lack of a developmental induction as that described in *N. crassa* (Avalos et al., 2017b).

The cellular location of carotenoid biosynthesis is a regulatory aspect that has received little attention. Because of their hydrophobic nature, the carotenoids are assumed to interact with membranes, but their subcellular distribution in *Fusarium* is unknown. A biochemical approach based on the specific labeling of different terpenoids from ^{14}C-labeled mevalonate stablished that the carotenoids are produced in cell compartments different from those where the gibberellins and the sterols are synthesized (Domenech et al., 1996). Recent experiments have used the intrinsic property of carotenoids to emit fluorescence (500-550 nm) after laser excitation (488 nm) (D'Andrea et al., 2014) to visualize carotenoid accumulation in several *F. fujikuroi* strains. Results suggested that carotenoids were stored as droplets or vesicles along the hyphae, but more experiments must be performed to analyze the nature of these structures (Pardo-Medina, unpublished data, Fig. I.7).

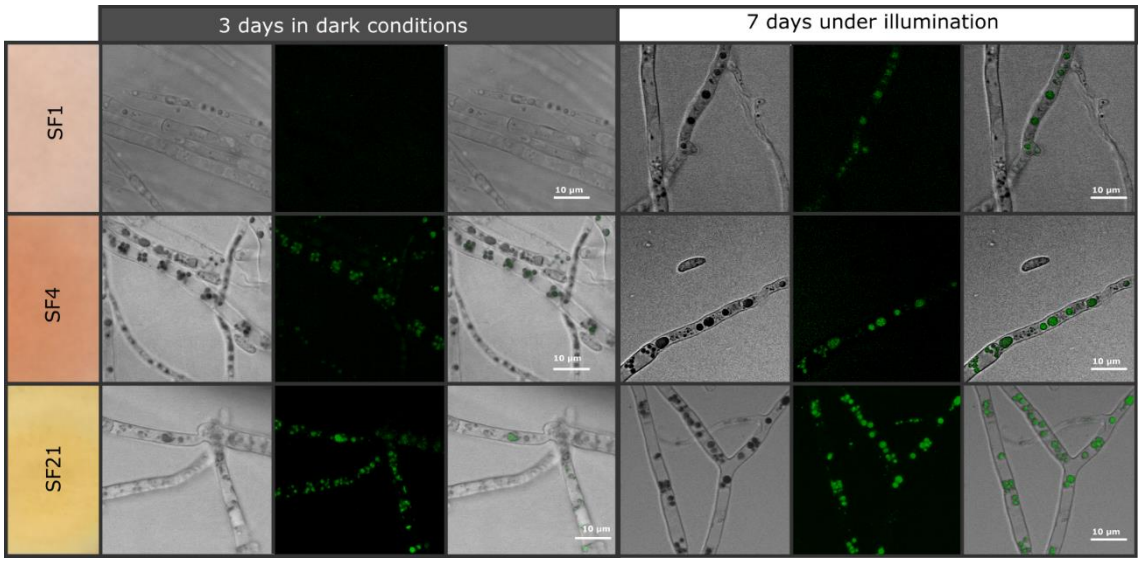

Figure I.7. Carotenoid accumulation in *F. fujikuroi*. The physical location of the carotenoids in *Fusarium* cells is unknown. Taking advantage of the high carotenoid content of the overproducing strains, we have studied their subcellular location through Confocal Laser Scanning Microscopy. Three mutants with the genetic background of the wild strain FKMC1995 were used: a nitrate utilizing mutant with normal carotenogenesis (SF1, *niaD*), a NX overproducer (SF4, *niaD carS*), and a SF4 derived strain overproducing γ-carotene and β-carotene (SF21, *niaD carS carB*)* (Prado-Cabrero et al., 2009). Strains were grown for a week in Petri dishes in the dark or under illumination. Confocal microscopy was performed with a Leica TCS SP5 confocal laser-scanning microscope using excitation at 488 nm and collecting emitted light from 500 to 550 nm (D'Andrea et al., 2014). Accumulation of different types of carotenoids was identified in intracellular vesicles in the hyphae, but their biochemical nature remains to be determined.

REGULATION OF CAROTENOGENESIS BY CARS PROTEIN

The development of mutagenesis protocols allowed the identification of *Fusarium* mutants affected in carotenoid biosynthesis, easily distinguishable by the changes in their pigmentation. Mutants can be albino in the light due to mutations in the genes for the enzymes of the first steps of the pathway or in a regulatory gene. Other mutants may have an orange pigmentation in the dark, and in this case, they are necessarily regulatory mutants (Avalos et al., 2017b).

Mutants strongly pigmented in the dark have been described in *F. fujikuroi* (Avalos and Cerdà-Olmedo, 1987) and *F. oxysporum* (Rodríguez-Ortiz et al., 2012), where they are generically called *carS* mutants (Figure I.8). These strains accumulate increasing amounts of carotenoids as the culture ages (Avalos and Cerdá-Olmedo, 1986) and contain large amounts of mRNA for the structural genes, from *carRA* to *carD* (Díaz-Sánchez et al., 2011b; Prado et al., 2004; Prado-Cabrero et al., 2007a; Thewes et al., 2005). Although the effect of light is less evident due to their high carotenoid content, photoinduction of structural gene transcripts still occurs in the *carS* mutants of *F. fujikuroi* (Prado et al., 2004) and *F. oxysporum* (Rodríguez-Ortiz et al., 2012), as also confirmed by transcriptomic analyses (Ruger-Herreros et al., 2019). The qualitative composition of the carotenoids accumulated by *carS* mutants in *F. fujikuroi* is like the one of the wild strain under illumination (Avalos et al., 2017b). Due to their intense pigmentation, *carS* strains have been used as tools to detect mutants with changes in the proportions of carotenoid

intermediates, revealed by their color alterations (Avalos and Cerdà-Olmedo, 1987; Prado-Cabrero et al., 2009), or to verify the effect of possible inhibitors of *Fusarium* carotenogenesis (Ávalos and Cerdá-Olmedo, 1986).

The gene responsible for the *carS* phenotype was identified thanks to the study of orange mutants of *F. oxysporum* obtained by random insertion of *Agrobacterium tumefaciens* T-DNA. Details on the process that led to the discovery of the gene which would be known as *carS* are described in the introduction to Chapter 1. Once the sequence was known, the mutations of this gene were verified in all known *carS* mutants. Moreover, its directed mutation caused the same *carS* phenotype (Rodríguez-Ortiz et al., 2012) and complementation of this mutation in *F. fujikuroi* restored the wild phenotype (Rodríguez-Ortiz et al., 2013). The *carS* gene of *F. fujikuroi* is also capable of restoring the basal production of carotenoids if introduced into *carS* mutants of *F. oxysporum*, indicating that its function is conserved in both species (Rodríguez-Ortiz et al., 2012). Interestingly, *carS* mutants have not been described in other *Fusarium* species.

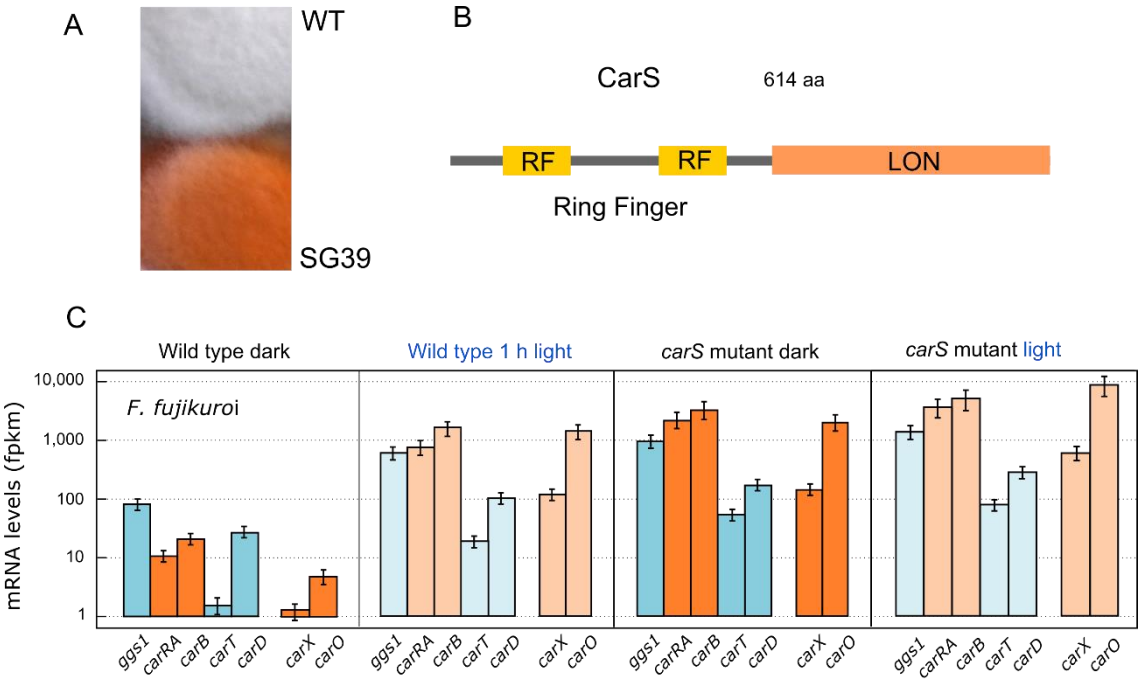

Figure I.8. Effect of *carS* mutation in *F. fujikuroi*. (A) Detail of a 7-day old colony of the wild strain IMI58289 (WT) and the *carS* mutant SG39 grown on minimal medium in the dark. (B) Structure of *F. fujikuroi* CarS protein. (C) Effect of light and *carS* mutation on the mRNA levels for the *F. fujikuroi* genes involved in carotenoid metabolism. The genes are grouped according to their functions: *ggs1*, *carRA*, *carB*, *carT*, and *carD* involved in biosynthesis of NX, and *carX* and *carO* in the synthesis of functional CarO rhodopsin (Avalos et al., 2017b). Orange colors correspond to the clustered *car* genes and blue color to genes unlinked in the genome. Dark colors indicate cultures incubated in the dark and pale colors indicate cultures illuminated for one hour. Wild-type strain IMI58289 and its *carS* mutant SG39 are represented. Modified from (Avalos et al., 2017b).

The *carS* gene encodes a protein of the "RING finger" (RF) family with sequence similarities to the CrgA protein of *M. circinelloides*, whose mutation also causes overproduction

of carotenoids (Lorca-Pascual et al., 2004; Navarro et al., 2001). The degree of similarity between the CarS and CrgA proteins is not very high, which was not surprising as they belong to two taxonomically distant fungi, but both proteins share the most relevant domains. These include two RF domains in the amino terminal region, one of them initially ignored in CarS because of the wrong assignment of an intron in the annotation of the *F. fujikuroi* genome (Ruger-Herreros, 2016), and a LON protease domain (Navarro et al., 2000). CrgA also has two glutamine-rich regions and an isoprenylation site near the carboxyl terminus, not conserved in CarS. The RF domains interact with ubiquitin ligase type 3 (E3) enzymes, that mediate the ubiquitination of target proteins, often as a label for their degradation. The CrgA function of *M. circinelloides* has received considerable attention and may provide clues to the possible mechanism of action of CarS in *Fusarium*. At least one of the RF domains of CrgA is essential for its regulatory role in carotenogenesis, suggesting that it could function as a type-3 ubiquitin ligase (Lorca-Pascual et al., 2004). However, CrgA interacts with one of the three proteins of the WC complex of *M. circinelloides*, MCWC-1b, to trigger its degradation through a mechanism independent of ubiquitination (Silva et al., 2008). There are other similarities in function between CrgA and CarS. First, as observed in *Fusarium carS* mutants, *M. circinelloides crgA* mutants maintain the photoinduction of carotenoid biosynthesis (Navarro et al., 2001). Second, both proteins are involved in other processes besides carotenogenesis, indicating broader regulatory functions. This conclusion is based on alterations of growth and sporulation in the *crgA* mutants of *M. circinelloides* (Murcia-Flores et al., 2007; Quiles-Rosillo et al., 2003) and in the production of bikaverin and gibberellins in the *carS* mutants of *F. fujikuroi* (Candau et al., 1991; Rodríguez-Ortiz et al., 2009). Orthologs of CrgA have been found in other *Mucorales*. *P. blakesleeanus* presents four putative orthologs, CrgA-D, but only CrgD could complement the absence of CrgA in *M. circinelloides* (Tagua et al., 2020).

Function of CarS as a general transcriptomic regulator, with other roles beyond the control of carotenogenesis, was later supported by transcriptomic data of *F. fujikuroi* and *F. oxysporum* (Ruger-Herreros et al., 2019). The impact of the mutation of the *carS* gene on transcriptome was quantitatively not very different from that of light, predominantly having activating effects, with about 10% of the genes affected (Figure I.9). The number of genes influenced by light decreased drastically in the *carS* mutant, indicating that CarS modulates the expression of many light-regulated genes. Approximately 27% of genes activated at least two-fold by light overlapped with those activated by the *carS* mutation, raising this percentage to 40% for higher activation thresholds. The large overlap between the two sets of genes confirmed regulatory connections between the control of gene expression by light and the CarS protein, which seems to play a role by keeping the mRNA levels of many light-inducible genes low in the dark. Besides carotenogenesis genes, other common regulatory targets were proteins with putative connections with stress responses, including several genes with catalase domains, which is consistent with roles of light and CarS protein in the control of oxidative stress. Nevertheless, the fact that the high photoinduction of secondary receptors as CryD or VvdA was not affected by *carS* mutation suggested that CarS either plays a role downstream of the light-transduction pathway or as an independent regulator (although *carS* gene itself is regulated by light).

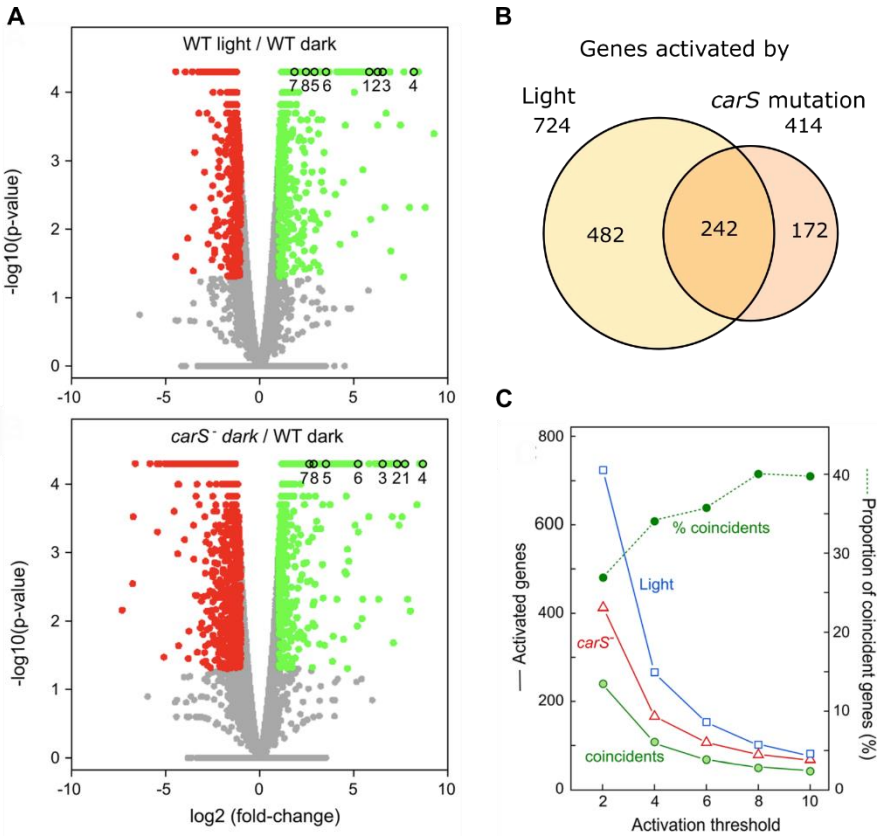

Figure I.9. Transcriptomic effect of illumination and *carS* mutation in *F. fujikuroi* transcriptome. (A) Volcano plot representations of global expression data in the comparisons between the wild strain (WT) kept in the dark and after one hour of illumination and between WT and the SG39 *carS* mutant, both kept in the dark. The empty circles indicate the positions of carotenogenesis related genes (*carRA, carB, carX, carO, ggs1, carT, carD, and carS*). (B) Venn diagram of the genes activated by light or by the *carS* mutation, showing the overlap between both effects in the transcriptome. The surfaces of the circles are proportional to the numbers of genes. Overlapping areas of the circles correspond to genes that coincide in the conditions compared. (C) Effect of the threshold for expression change in the number of genes activated by light and by the *carS* mutation. The graph represents the genes activated by any of the two conditions and the coinciding ones. Percentages of coinciding genes are also represented (dotted line). Modified from (Ruger-Herreros et al., 2019).

Aims

AIMS

The aim of this Thesis is to deepen in the knowledge of how light and ncRNAs affect *F. fujikuroi* biology, with especial attention to their participation in the control of the carotenoid biosynthetic pathway through protein CarS. For this purpose, based on the former findings in this fungus, the following specific objectives have been addressed:

● To analyze the existence of small interfering RNAs in *F. fujikuroi* and their putative regulatory impact on its biology through the mutation of relevant genes of its machinery.

● To investigate the participation of non-coding RNA species linked to the *carS* gene in the control of carotenoid synthesis.

● To study the functions of the white-collar protein WcoA and the DASH cryptochrome CryD in *F. fujikuroi* through the effects of the deletions of their genes on the transcriptome.

Chapter 1

Small interfering RNA in *F. fujikuroi*

CHAPTER 1: SMALL INTERFERING RNA IN *F. FUJIKUROI*

INTRODUCTION

A collection of *F. oxysporum* T-DNA insertion mutants generated by *Agrobacterium*-mediated transformation was screened for carotenoid overproducers by a member of our group (Rodríguez-Ortiz et al., 2012). The aim of the screening was to identify regulators of the carotenoid biosynthetic genes. In that work, three orange transformants, 20B12, 93C9 and 107E6, were selected and two of them, 93C9 and 107E6, contained T-DNA integrated in nearby regions. The gene *FOXG_09307*, which is ortholog to *Mucor crgA,* was near these insertions. This fact led to sequence alleles of this gene to check if they were affected in *F. oxysporum* SX1 and SX2 overproducer mutants, obtained by chemical mutagenesis. Both strains contained mutations in *FOXG_09307*. The ortholog *FFUJ_08714* gene was also analyzed in other similar *F. fujikuroi* mutants, which also showed mutations in its coding region. Moreover, transformant 20B12, abbreviated as T1, apparently lacked a T-DNA insertion in this genomic region but it contained a 5-bp insertion in the coding sequence of FOXG_09307, presumably due to a molecular event associated to the T-DNA insertion process. Taken together, all the data pointed to *FOXG_09307* and *FFUJ_08714* are the genes responsible for the carotenoid accumulation phenotype or *carS* gene in *F. oxysporum* and *F. fujikuroi*, respectively. This conclusion was genetically confirmed by targeted mutation in *F. oxysporum* (Rodríguez-Ortiz et al., 2012), and by complementation SG39 overproducer mutant in *F. fujikuroi* (Rodríguez-Ortiz et al., 2013). The CarS protein, reviewed in the general introduction, constitutes a negative regulator of *Fusarium* carotenogenesis, although it also affects other cellular processes (Ruger-Herreros et al., 2019), possibly through an ubiquitylation process of target proteins, as in other fungi (Navarro et al., 2001).

Transformants 93C9 (abbreviated as T2) and 107E6 (T3) did not have any mutation in their *carS* alleles, which suggested that their T-DNA insertions could be the cause for their phenotype. A detailed analysis found DNA alterations produced by the T-DNA insertions in the 4.5-kb intergenic region in both transformants between the *carS* (*FOXG_09307*) and *carF* (*FOXG_09306*) genes (Parra-Rivero, 2018). Additionally, T3 also had a T-DNA integration between the *FOXG_09304* and *FOXG_09305* genes (Fig. C1.1). The intergenic region upstream to *carS* has no annotated ORFs, neither in *F. oxysporum* nor in *F. fujikuroi*, as judged by the annotation derived from the publication of their genomes.

A previous study proposed the possible participation of small RNAs in the regulation of carotenogenesis in *F. oxysporum* (Rodríguez-Ortiz, 2012). This was based in the bioinformatic prediction of two putative microRNA-like precursor sequences in the intergenic region between *FOXG_09307* (*carS*) and *FOXG_09306* (*carF*) (Fig. C1.1). These putative miRNA precursor genes were named *fox-mir1* and *fox-mir2*. Similar putative *ffu-mir* precursor sequences were found also in *F. fujikuroi*, although their location did not match exactly with those in *F. oxysporum*. Although *fox-mir2* and *ffu-mir2* partially overlapped, *ffu-mir1* was closer to *carF* compared to *fox-mir1* (Pardo-Medina, 2014). The T-DNA insertions in T2 and T3 did not directly affect the *fox-*

mir1 and *fox-mir2* sequences but it was proposed that they could have altered their expression, resulting in a carotenoid overproduction phenotype. However, these transformants were later shown to have a strong reduction in the transcription of a long genomic region around the gene *carS* (Parra-Rivero, 2018). Although canonical miRNAs characteristic of plants and animals have not been described in fungi, the miRNA-like RNAs (milRNAs) share several similarities with them (Lee et al., 2010; Nicolás et al., 2020).

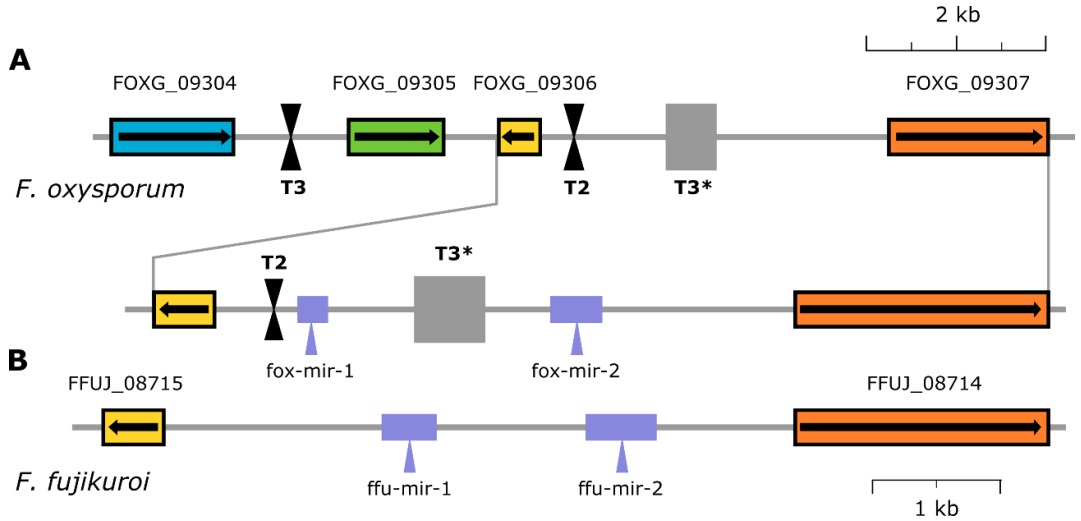

Figure C1.1. Map of the genomic region affected in *carS* mutants showing putative genes for microRNA precursors. (A). Map of the genomic region under study between the *FOXG_09304* and *FOXG_09307* genes of *F. oxysporum*. Approximate insertion sites are indicated by black triangles and a second affected region is represented as a gray box (T3 *). (B). Location of two genes for putative *fox-mir1* and *fox-mir2* microRNA precursors in the intergenic sequence between *FOXG_09306* and *FOXG_09307* (*carS*) in *F. oxysporum* genome and the genes for *ffu-mir1* and *ffu-mir2* between *FFUJ_08715* and *FFUJ_08714* (*carS*) in *F. fujikuroi* genome.

The milRNAs constitute a subfamily of the small interfering RNAs with a conserved eukaryotic regulatory mechanism (Carthew and Sontheimer, 2009) that suppresses gene expression through sequence-specific messenger RNA degradation, translational repression, or transcriptional inhibition (Torres-Martínez and Ruiz-Vázquez, 2017). Although initially described in plants, *N. crassa* was one of the first organisms in which this regulatory mechanism was discovered and investigated (Cogoni and Macino, 1997). Gene and meiotic silencing caused by unpaired DNA are two RNAi-related phenomena in *Neurospora* and its characterization has significantly contributed to understand the mechanism of action of sRNAs in eukaryotes (Li et al., 2010). *M. circinelloides* is another model organism with decisive contributions to understand RNAi in fungi (Torres-Martínez and Ruiz-Vázquez, 2016). Fungal RNAi pathways are as plastic and diverse as its kingdom and has evolved to regulate cell activities as different as a protection mechanism against potentially harmful exogenous DNA, genome integrity, development, sexual reproduction, adaptability to environment, or virulence (Lax et al., 2020).

Several RNAi pathways have been described in fungi (Nicolás et al., 2020; Villalobos-Escobedo et al., 2016), but in most cases, they share the core components, which are conserved with other kingdoms. At a biogenesis level, all sRNAs derive from double-strand RNA precursors which are recognized and processed by the RNAse III protein Dicer. These duplexes of sRNA,

typically around 20-25 nt and whose denomination depends on function, features, and origin, are later incorporated to the Argonaute (Ago) protein. Ago functions as an sRNA-guided endonuclease, recognizing the target mRNA or DNA *loci* by sequence complementarity to the incorporated sRNA, normally resulting in either transcriptional or post-transcriptional gene silencing (Villalobos-Escobedo et al., 2016). In some cases, an RNA dependent RNA polymerase (RdRP) generates dsRNA from single-strand RNA (ssRNA) by *de novo* primer-independent second-strand synthesis using sRNAs as primers to synthesize RNA molecules complementary to the target mRNAs, which then act as inducers or amplifiers of the sRNA signal (Torres-Martínez and Ruiz-Vázquez, 2017). These core components of the pathway are present in almost all the phyla of the fungal kingdom, with some relevant exceptions such as the subphylum *Saccharomycotina*, among others (Billmyre et al., 2013).

A recent revision proposed that fungal small RNAs can be divided into two big subclasses according to their biological role: protective sRNAs and sRNAs that regulate gene expression (Nicolás et al., 2020). The first group of sRNAs are involved in genome defense and constitutes the original evolutive function of RNAi. Among these sRNAs are the first ones described in a RNAi process in fungi, those involved in quelling in *N. crassa*, that silences highly homologous repetitive elements of the genome in its vegetative state (Catalanotto et al., 2002; Cogoni and Macino, 1997). The repetitive elements, either exogenous, such as transgenes, or endogenous, such as fungal transposable elements arrays and ribosomal genes (rDNA), cause potential genome instability. The post-transcriptional gene silencing of the target genes is caused by the binding of the double-stranded small-interfering RNAs (siRNAs) to an Ago protein forming the RNA-induced silencing complex (RISC) which then target mRNAs(Pickford and Cogoni, 2003; Treiber et al., 2019). These types of defense responses also take place specifically during the sexual cycle, as the Meiotic Silencing by Unpaired DNA (MSUD) in *N. crassa* (Shiu and Metzenberg, 2002) or the sex induced silencing (SIS), described in *Cryptococcus neoformans* (Wang et al., 2010). Another type of defense sRNAs are antiviral that functions as an innate immune system in fungi, among which outstands those studied in *Cryphonectria parasitica*, also found in *F. graminearum* (Yu et al. 2018). The last group proposed in this category is a special group of sRNAs, the primal sRNAs, discovered in *Schizosaccharomyces pombe,* which governs the establishment of heterochromatin formation in the regional centromeres and seem to play an essential function in centromere evolution (Halic and Moazed, 2010).

The second group of sRNAs, the endogenous sRNAs (esRNAs), composes a vast regulatory network in plants and animals which plays a fundamental role on gene expression (Carthew and Sontheimer, 2009). It was unknown in fungi until the discovery of molecules like miRNAs and regulatory esRNAs in *N. crassa* (Lee et al., 2010) and *M. circinelloides* (Nicolas et al., 2010). Those milRNAs are subdivided in four classes depending on the RNAi components that are required for their biogenesis (Nicolás et al., 2020) and they are characterized by their genesis from single-strand RNA precursors that form a typical hairpin structure. Their dsRNA region is processed to generate two complementary sRNAs, one of them predominantly preserved while the other is degraded. Also, they normally present a strong bias for uracil bases at the 5’ termini of the milRNA (Lee et al., 2010). Nevertheless, unlike plant and animals, fungal milRNAs are not

very conserved and their precursors have some differences in origin and processing (Carthew and Sontheimer, 2009; Yang et al., 2013). Fungal milRNAs have been described in a wide variety of fungi. Noteworthily, no milRNAs have been identified in *M. circinelloides* and other related fungi. However, they accumulate a large variety of esRNA molecules that are generated by canonical and noncanonical RNAi pathways. The esRNAs genesis can be Dicer-dependent, most of them derived from exons (ex-siRNAs), or Dicer-independent, in which case they are rdrp-dependent degraded RNAs (rdRNAs), which correspond to non-random degradation products of specific mRNA molecules able to control mRNA levels (Torres-Martínez and Ruiz-Vázquez, 2017; Trieu et al., 2017).

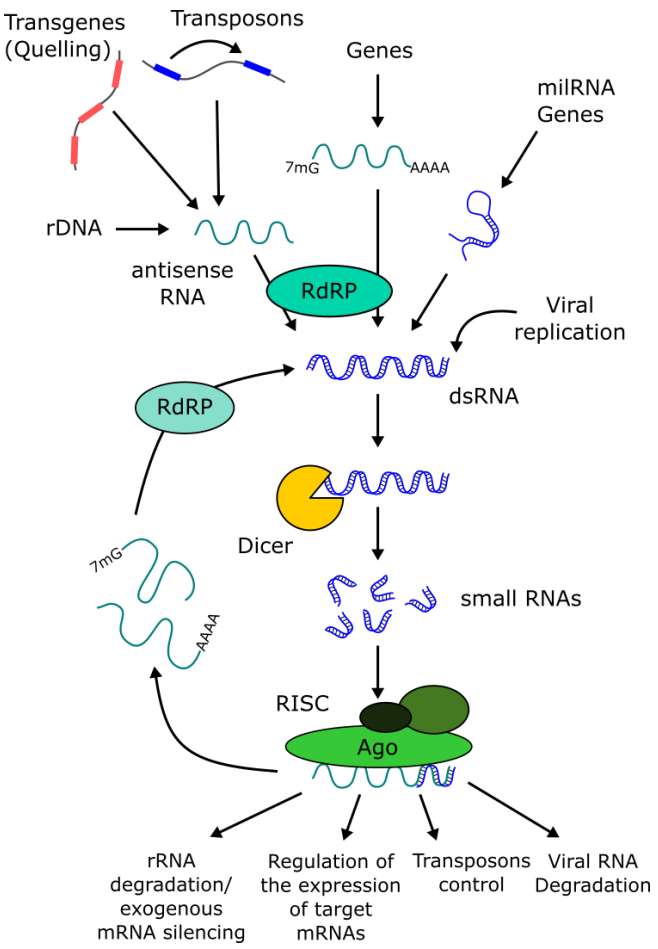

Figure C1.2. A simplified model for RNAi pathways in fungi. Core components of the pathways are depicted, as well as some examples of the processes in which sRNAs can participate. Modified from (Nicolás et al., 2020)

Examples of both esRNAs, milRNAs and ex-siRNAs, are found in *Fusarium* or close species. *Trichoderma atroviride*, a fungus widely used for both industrial and agronomic applications, is one of the few examples (along with *M. circinelloides*) in which alterations of core components of the RNAi pathway show clear phenotypes. The deletion of the different genes encoding Ago, Dicer and RdRP in this fungus produces aberrant conidia and vegetative growth (Carreras-Villaseñor et al., 2013). Different components of the RNAi machinery are also involved in formation of sexual spores after sexual interaction in *F. graminearum* (Son et al., 2017), as well as conidiation, virulence and deoxynivalenol production (Gaffar et al., 2019). In *F. oxysporum,* one of the Ago proteins have been described to be involved in virulence (Jo et al., 2018). Similar milRNAs to those discovered in *N. crassa* have been described in *T. reesei* (Kang et al., 2013), *F. oxysporum* (Chen et al. 2014), and *F. graminerarum,* where a specific milRNA regulates biotin synthesis (Guo et al., 2019). However, no candidate of milRNA was found in the upstream region of *carS* in *F. oxysporum*.

The transcription of the two putative milRNA precursor sequences upstream to *carS* in *F. oxysporum*, mentioned above, has been recently analyzed (Parra-Rivero, 2018). The RNA levels of these precursors increase under illumination in the wild strain and decrease in the

transformants T2 and T3, which suggest a deregulation caused by the T-DNA insertions. These putative milRNA precursors would be regulated like the *carS* gene: photoinduced in the wild strain and downregulated in the transformants T2 and T3, since they are included in the silenced genomic segment. Deletions of *fox-mir1* and *fox-mir2* were done by replacing them with an hygromycin resistance cassette. The resulting strains, Δ*mir1* and Δ*mir2,* presented an albino phenotype, which was unexpected, as it was opposite to the pigmented phenotype of T2 and T3. Their lack of carotenoids correlated with a decrease in mRNA levels of the *car* cluster genes. Carotenoid quantifications revealed 10- and 100-fold drop in carotenoid content in Δ*fox-mir1* and Δ*fox-mir2* mutants, respectively.

This chapter aims to study the possible participation of these putative miRNA precursors in the regulation of carotenogenesis in *F. fujikuroi.* Moreover, a more general approach is addressed based on the analysis of small non-coding RNAs in *F. fujikuroi* and *F. oxysporum* transcriptome, and on the study of the elimination of key pieces of the machinery involved in miRNAs processing, which was expected to provide valuable information on the processes in which these types of small regulatory RNAs participate in *Fusarium*.

RESULTS

ANALYSIS OF SMALL RNA PRODUCTION IN THE UPSTREAM REGION TO *CARS*

Experiments similar to those described for *F. oxysporum* were performed in *F. fujikuroi* to analyze the transcription of the putative sRNA precursor sequences in the *carS* upstream region in different illumination conditions. RT-qPCR experiments detected RNA for several parts of this upstream region, which were higher after light exposure, in a similar way to the neighbor *carS* gene (Fig. C1.2). The *carB* and *carRA* genes, two of the structural genes of the carotenogenesis pathway, were used as photoinduced controls in this experiment and along the Thesis.

These experiments only tested RNA levels, therefore another approach was needed to demonstrate sRNA production. To search the potential production of sRNAs from the *ffu-mir1* and *ffu-mir2* precursor genes, small RNAs were blotted and hybridized with specific probes (see Materials and methods). Three fragments were amplified by PCR from *ffu-mir1*, *ffu-mir2,* and a region between both (primer sets PSC1.1, PSC1.2, and PSC1.3, located in table A.2, Material and Methods) and were cloned into the pGEM-T Easy vector (Promega) in both orientations under the control of T7 promoter. The cloned fragments were sequenced and used as templates to radioactively label six riboprobes. Subsequently, RNA was isolated from wild-type cultures kept in the dark or exposed to light. The RNA samples were enriched in small RNA, subjected to denaturing polyacrylamide gel electrophoresis and transferred to a membrane, which was hybridized with the six riboprobes. As a result, no signal was obtained in any of the northern-blot hybridizations. This result was not conclusive, since the transcription of the putative sRNAs

could be too low to be detected with this method, or the protocol was not optimized for *F. fujikuroi.* Therefore, *a*n alternative approach was used.

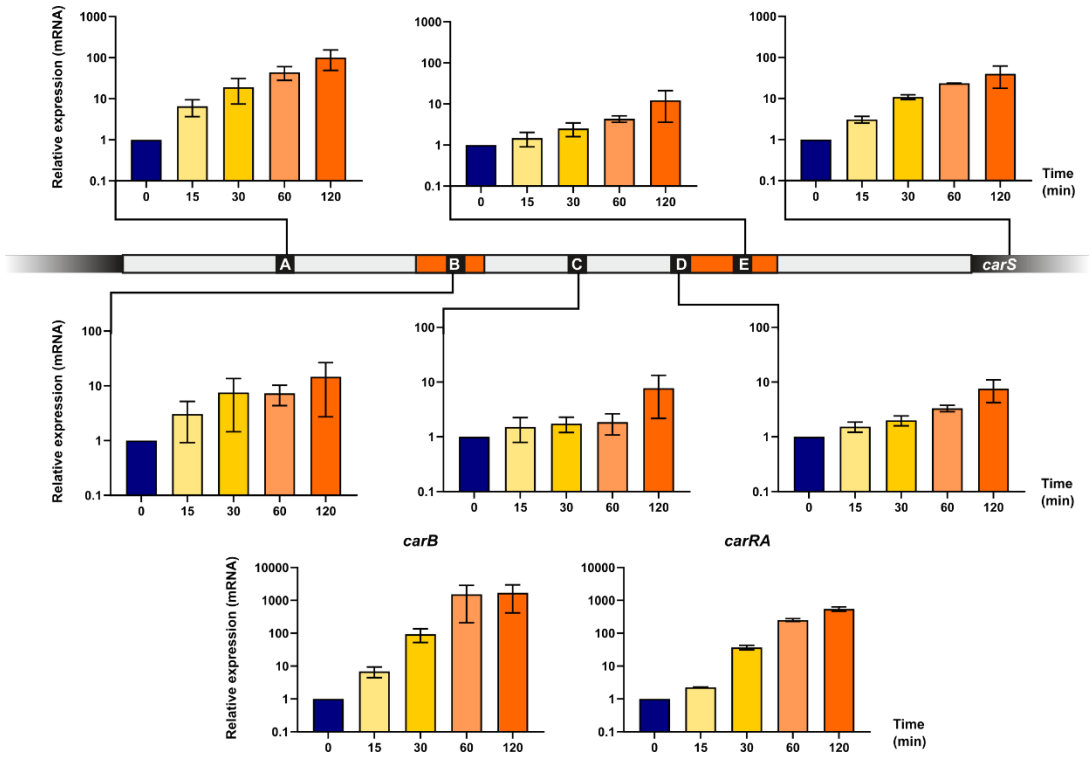

Figure C1.2. RT-qPCR data showing the effect of time illumination on transcript levels for several locations in the intergenic region upstream *carS*, covering the two putative miRNA precursor sequences. RTPS primer used for the experiment were: A, RTPS.1.1; B, RTPS1.2; C, RTPS1.3; D, RTPS1.4; and E, RTPS1.5. *carRA* (RTPS.6) and *carB* genes (RTPS.4) were used as photoinduction controls. Transcript levels were normalized against the β-tubulin gene *FFUJ_04397* (RTPS.5). Strains were grown in DGasn broth for 3 days in the dark and exposed for several times to light. RT-qPCR data show the mean and standard error of RT-qPCR data from two independent experiments. Relative RNA levels are referred to the RNA content of the wild strain in darkness. RTPS primer sets are located in table A.3, Material and Methods

A transcriptomic study on the effect of light and *carS* mutation in *Fusarium* (Ruger-Herreros et al., 2019) revealed the production of a transcript in the upstream intergenic region of *carS*. However, as the library for RNA-seq was prepared with polyadenylated RNA, no information was provided about the existence of sRNAs in this region. To test this hypothesis, a new sequencing was proposed focused on the sRNA fraction of the previously sequenced samples. The main advantage of this experimental approach was that it allows a general study of the sRNA transcriptome in *F. oxysporum* and *F. fujikuroi*. In the case of *F. fujikuroi*, no works have been published on this subject. This opportunity was also used to explore the influence of light on the regulation of sRNA production.

SEQUENCING OF SRNA

Total RNA samples of *F. fujikuroi* and *F. oxysporum* wild strains from that previous transcriptomic analysis, grown in dark conditions and after one hour of illumination, were used for the search of sRNA. The culture conditions used to obtain the biological samples, stated in

the original work (Ruger-Herreros et al, 2019), resembled those used for our expression analyses (described in Materials and Methods). RNA extraction and quality parameters of the samples followed the same protocol described in this Thesis (Material and methods). The protocol for sRNA sequencing included a new step of size cutoff. RNAs with a size below 150 nt, covering the sRNAs and their precursors, of two samples from each condition were used to construct the small RNA libraries. They were sequenced on Illumina's Hiseq platform in mode 50 bp single read. Raw reads for all samples were trimmed, filtered and quality controlled with AfterQC. The readings obtained and their basic characteristics are described in Table C1.1.

Table C1.1. Summary of the sequencing characteristics of each RNA-seq sample.

Sample name	Number of trimmed sequences	Average length	Average quality	Sequences 18-25 nt (%)
Ffuj_dark_R1	47609550	38.84	39.41	11.97
Ffuj_dark_R2	26679687	35.57	39.33	19.09
Ffuj_light_R1	52755629	35.6	39.31	18.96
Ffuj_light_R2	26219382	39.8	39.4	7.68
Foxy_dark_R1	32247420	35.17	39.32	19.07
Foxy_dark_R2	46332088	33.8	39.33	21.10
Foxy_light_R1	47081719	37.98	39.39	10.33
Foxy_light_R2	47548893	39.45	39.3	7.30

The analysis of the sRNA sequences was performed in collaboration with Dr. Tim Dahlman and Dr. Minou Nowrussian from the University of Bochum (Germany). Data from both fungi were processed in a uniform manner.

MAPPING AND CHARACTERIZATION OF THE SRNA SEQUENCING

The mapping of sRNA reads was done using Bowtie v1.1.1, designed to map short Illumina reads of ~35 nt, or Bowtie2 v2.2.9 for longer reads. To find all miRNA-like RNAs, total reads of both growing conditions were merged to a single file. The sRNAs were mapped to the genome so that reads that occurred several times within the dataset were collapsed to a single entry and their read count was added to the fasta header, decreasing file size without losing information. The alignment results of collapsed reads are shown in Table C1.2.

A further benefit of using collapsed reads is that the overvaluation of overrepresented reads, such as those originated form tRNAs and rRNAs, is decreased (see Table C1.3). While redundant reads showed only a small proportion in the merged reads of *F. fujikuroi* (8.5 %), they were dominant in *F. oxysporum* (82.5 %). This probably indicates an overrepresented amount of rRNAs and tRNAs that was incorporated during *F. oxysporum* library preparation. To proof this, reads of *F. fujikuroi* and *F. oxysporum* were mapped to tRNA and rRNA sequences. The

corresponding tRNA sequences were extracted from the annotation files and putative rRNA-producing *loci* (rDNAs) were predicted with RNAmmer v1.2 for both fungi. The higher number of reads discarded by bowtie due to multiple alignments (-m 5) in *F. oxysporum* might correlate with the higher number of rDNAs. However, it is very unlikely that biological effects caused the increased number of discarded reads. It is more probable that rDNAs were not considered during *F. fujikuroi* genome assembly. To test this hypothesis, the collapsed reads were mapped to the predicted rDNAs of *F. oxysporum* and the total read count was calculated.

Table C1.2. Mapping results of sequencing of sRNA.

Organism		Total reads	Mapped reads	Unmapped reads	Reads discarded by -m 5
F. fujikuroi	All reads	153,264,248	115,369,397 (75.3 %)	24,828,229 (16.2 %)	13,066,622 (8.5 %)
	Collapsed reads	6,612,908	4,447,147 (67.3 %)	2,105,318 (31.8 %)	60,443 (0.91 %)
	Collapsed reads (x≥10)	272,776	195,387 (71.6 %)	67,398 (24.7 %)	9,991 (3.7 %)
F. oxysporum	All reads	173,210,120	18,021,169 (10.4 %)	12,125,747 (7.0 %)	143,063,204 (82.6 %)
	Collapsed reads	7,034,397	3,920,202 (55.7 %)	2,096,047 (29.8 %)	1,018,148 (14.5 %)
	Collapsed reads (x≥10)	305,475	76,281 (25.0 %)	51,981 (17.0 %)	177,213 (58.0 %)

As hypothesized, most of total reads within the *F. oxysporum* data set could be mapped to rDNAs (73.6 %). Although the dataset looked rather diverse, the proportion of mapped collapsed reads (Table C1.1) was only slightly different between *F. fujikuroi* (67.3 %) and *F. oxysporum* (55.7 %). Thus, rDNA from *F. oxysporum* was used for a second analysis with the total reads of *F. fujikuroi* and 70.3 % of the reads mapped to the *Fusarium* rDNA.

Dicer-like RNases III process many fungal sRNAs, like siRNAs and the majority of milRNAs. It was demonstrated that sRNAs processed by Dicer-like endonucleases show a strong preference for a size of 19 to 22 nt and a 5' uracil (Dahlmann and Kück, 2015; Lee et al., 2010; Zhou et al., 2012). Thus, analyses of size distribution and 5’ nucleotide preference of the mapped total and mapped collapsed sRNA reads were performed (Fig. C1.3A and 3B). To elucidate the existence of ‘true’ sRNAs, the proportion of the four nucleotides at the first position was analyzed for the collapsed reads (Fig. C1.3C). The results showed an increased proportion of 5’ uracil in the RNA samples of the expected sizes in both species.

Table C1.3. Reads mapping to predicted ribosomal DNA.

Organism		Total reads	Reads mapping to rDNA	Unmapped reads
F. fujikuroi	Total reads	153,264,248	25,029,046 (16.3 %)	128,235,202 (83.7 %)
	Collapsed reads	6,612,908	251,425 (3.8 %)	6,361,483 (96.2 %)
F. oxysporum	Total reads	173,210,120	127,479,642 (73.6 %)	45,730,478 (26.4 %)
	Collapsed reads	7,034,397	866,926 (12.3 %)	6,167,471 (87.7 %)
F. fujikuroi (incl. rDNA from *F. oxysporum*)	Total reads	153,264,248	107,751,205 (70.3 %)	45,513,043 (29.7 %)
	Collapsed reads	6,612,908	740,534 (11.2 %)	5,872,374 (88.8 %)

ORIGIN OF SRNAS IN *FUSARIUM* SPECIES

The increased amount of sRNAs starting with uracil is consistent with the presence of small interfering RNAs (siRNAs). A functional RNAi-machinery was described in *F. graminearum* (Chen et al., 2015), therefore we predict it should be also present in *F. fujikuroi* and *F. oxysporum*. If sRNA originates from double-stranded RNAs, which are produced by RNA-dependent RNA polymerases as counter reaction to retrotransposons or from other endogenous transcripts, we should be able to identify transcribed loci that produce sRNAs from both DNA strands. The gff annotation files from both fungi were used to extract fasta files, containing coding, intronic, and intergenic sequences. The extraction was done after creating the corresponding features with the genome browser Artemis 16.0.0.

The amounts of sRNAs mapping to different features were very similar in *F. fujikuroi* and *F. oxysporum* (Fig. C1.4). Only the numbers of collapsed reads (x≥10) mapping on the sense and antisense strand at CDS (marked by red color in Table C1.4) varied strongly in the data sets. Interestingly, in *F. fujikuroi* the number of collapsed reads (x≥10) mapping to CDS *loci* was significantly higher compared to those from *F. oxysporum*. This was in accordance with the findings from the length and nucleotide distribution of the collapsed reads (Fig. C1.3). It must be noted that the high number of collapsed reads mapping to CDS *loci* in both fungi might be caused by non-specific mRNA-degradation.

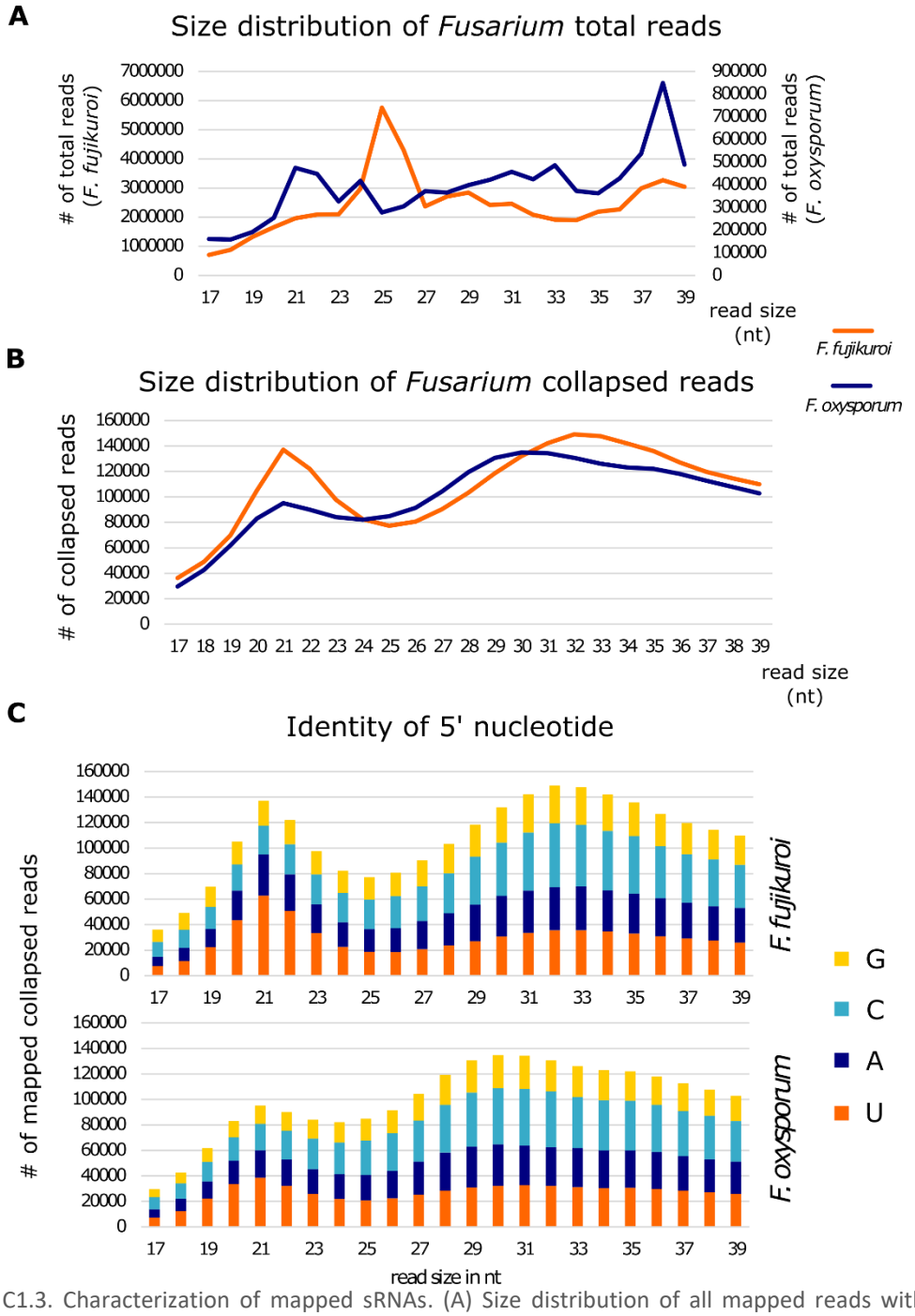

Figure C1.3. Characterization of mapped sRNAs. (A) Size distribution of all mapped reads within the merged datasets of *F. fujikuroi* and *F. oxysporum*. (B) Size distribution of all mapped and collapsed reads within the merged datasets of both fungi. A peak at 19-22 nt was observed in *F. fujikuroi*, while a second peak was present between 28 and 35 nt in both fungi. The peak at 19-22 nt is typical for Dicer-processed small RNAs. (C) Size distribution and 5'-nucleotide preference of sRNAs in *F. fujikuroi* and *F. oxysporum.* sRNAs with a size of 19 to 23 nt predominantly started with a 5'-uracil (up to 45.8 % in *F. fujikuroi* and 40.5 % in *F. oxysporum*), while sRNAs with other sizes showed balanced proportions for each of the four nucleotides. In comparison to *F. fujikuroi,* the peak between 19 and 23 nt was not so prevalent in *F. oxysporum*.

Table C1.4. Origin of sRNAs in *Fusarium*. Relevant data are marked in color. Predicted rDNAs of both *Fusarium* species were used for calculation of rRNA-mapping reads in *F. fujikuroi* and *F. oxysporum.*

		F. fujikuroi			*F. oxysporum*		
Feature		Total reads	Collapsed reads	Collapsed reads (x≥10)	Total reads	Collapsed reads	Collapsed reads (x≥10)
rRNA	Sense	107,441,729	734,758	137,200	132,061,732	894,041	162,931
	Antisense	1,438,898	53,471	7,023	2,495,057	25,796	3,250
tRNA	Sense	10,061,987	42,861	6,378	8,668,518	49,186	7,132
	Antisense	70,482	3,372	34	100,435	3,192	17
CDS	Sense	5,911,950	2,759,531	251,402	5,763,287	2,504,352	11,297
	Antisense	7,978,889	243,429	14,888	2,563,605	182,700	1,322
Intron	Sense	2,719,506	104,448	6,982	2,555,759	122,882	7,165
	Antisense	7,712,652	39,037	2,584	4,649,363	94,585	9,982
Intergenic	Both	111,807,186	1,633,420	155,047	153,725,629	2,493,370	234,515

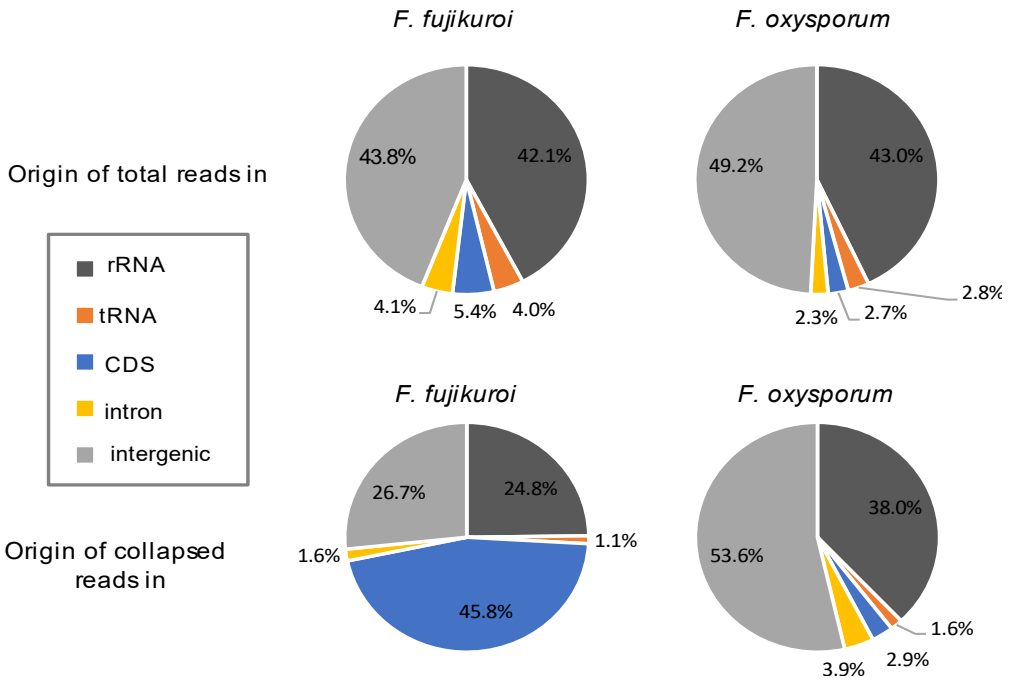

Figure C1.4. Origin of total and collapsed reads (x≥10) in *F. Fujikuroi* and *F. oxysporum.*

Table C1.5. Putative transposable elements detected in the *F. Fujikuroi* and *F. oxysporum* genomes.

Transposable element	*F. fujikuroi*			*F. oxysporum*		
	Gene ID	Identity (%)	e-value	gene ID	Identity (%)	e-value
HobS	*FFUJ_04535*	100	0.0	*FOXG_15494*	39.09	9e-142
	FFUJ_02576	100	0.0	*FOXG_12541*	25.94	6e-065
	FFUJ_04521	96.24	0.0	*FOXG_15105*	26.89	4e-057
	FFUJ_05678	96.24	0.0	*FOXG_06872*	43.48	8e-049
	FFUJ_05881	100	0.0	*FOXG_16138*	43.48	1e-048
Impala	*FFUJ_07491*	87.35	0.0	unpredicted_chr14: 1236756-1237727	89.56	0.0
	unpredicted_chrV: 2117840-2118331	29.09	7e-013	unpredicted_chr14: 1117562-1116699	87.84	0.0
	-	-	-	unpredicted_chr14: 121747-121423	87.80	1e-103
	-	-	-	unpredicted_chr1: 6134797-6136077	82.54	0.0
	-	-	-	unpredicted_chr15: 1546451-1545171	82.54	0.0
Ty1/Copia	*FFUJ_08062*	31.08	7e-066	unpredicted_chr3: 342220-343926	98.42	0.0
	FFUJ_13355	31.08	7e-066	unpredicted_chr3: 415150-416856	98.42	0.0
	FFUJ_00408	31.08	1e-065	unpredicted_chr3: 982302-984008	98.42	0.0
	FFUJ_14407	30.59	3e-065	unpredicted_chr3: 3405691-3403985	98.42	0.0
	-	-	-	*FOXG_14142*	43.42	6e-062
Skippy	unpredicted_chrIV: 3140654-3142846	53.08	0.0	unpredicted_chr5: 4489311-4493195	97.99	0.0
	unpredicted_chrVI: 3662701-3660476	52.96	0.0	unpredicted_DS231747: 67362-63478	97.99	0.0
	unpredicted_chrIII: 4890426-4892675	49.47	0.0	unpredicted_chr14: 1418859-1422395	97.71	0.0
	unpredicted_chrX: 887601-889802	52.04	0.0	*FOXG_17761*	36.73	2e-137
	FFUJ_00160	25.77	6e-068	*FOXG_17760*	40.37	9e-133
MAGGY	unpredicted_chrX: 4392-6848	37.61	4e-134	*FOXG_17760*	68.33	0.0
	FFUJ_00160	26.67	3e-078	*FOXG_17761*	66.33	0.0

Transposable elements are often post-transcriptionally silenced. Both *Fusarium* species contain transposable elements in their genomes, but this does not mean that they are active. BLAST analyses of sequences from the transposable elements skippy, Ty1/copia, and impala from *F. oxysporum*, HobS from *F. fujikuroi*, and MAGGY from *Magnaporthe grisea* were used to identify siRNAs that could be generated in response to these mobile genetic elements. Therefore, the annotated proteins and the genomic sequences were used for blastp and tblastx analyses.

F. fujikuroi carries at least one transcriptionally expressed copy of a Ty1/copia-like element. In all four *loci* sRNAs were present in their sense and antisense DNA strands, a clear indication for an active siRNA-based RNAi-pathway. In *F. oxysporum,* only skippy-like elements seemed to be slightly expressed and might be silenced by RNAi.

To find sense and antisense transcripts that may be differentially synthesized during growth in darkness and after illumination, each sample was aligned separately to the reference genome. The read counts for each dataset were calculated with the R script summarizeOverlaps, which is part of the Bioconductor GenomicAlignments package. After normalization, features that showed differential formation of small RNAs were calculated with DESeq2 (adjusted *p*-value < 0.1). The sense strand was used as control for the impact of the altered conditions on gene expression.

In the comparison of dark *vs*. light samples in *F. fujikuroi*, 18 genes were found to form sRNAs differentially under both conditions. Due to the absence of antisense sRNAs, these strand-specific sRNAs were very likely originated by 'unspecific' mRNA degradation from the single-stranded mRNA. In fact, these genes were among the most light-induced ones in the original mRNA data (Ruger-Herreros et al., 2019) (Table C1.6). Using the same analysis of sRNAs that originate from the antisense strand, either by transcription of the antisense *loci* or by formation of double-stranded RNAs by RNA-dependent RNA-polymerases, no sRNA-producing *loci* were found showing differential sRNA-expression under the tested conditions. Plots of the log-fold change (FC) of genes from *F. fujikuroi* and their sRNA mean expression are displayed in Fig. C1.5.

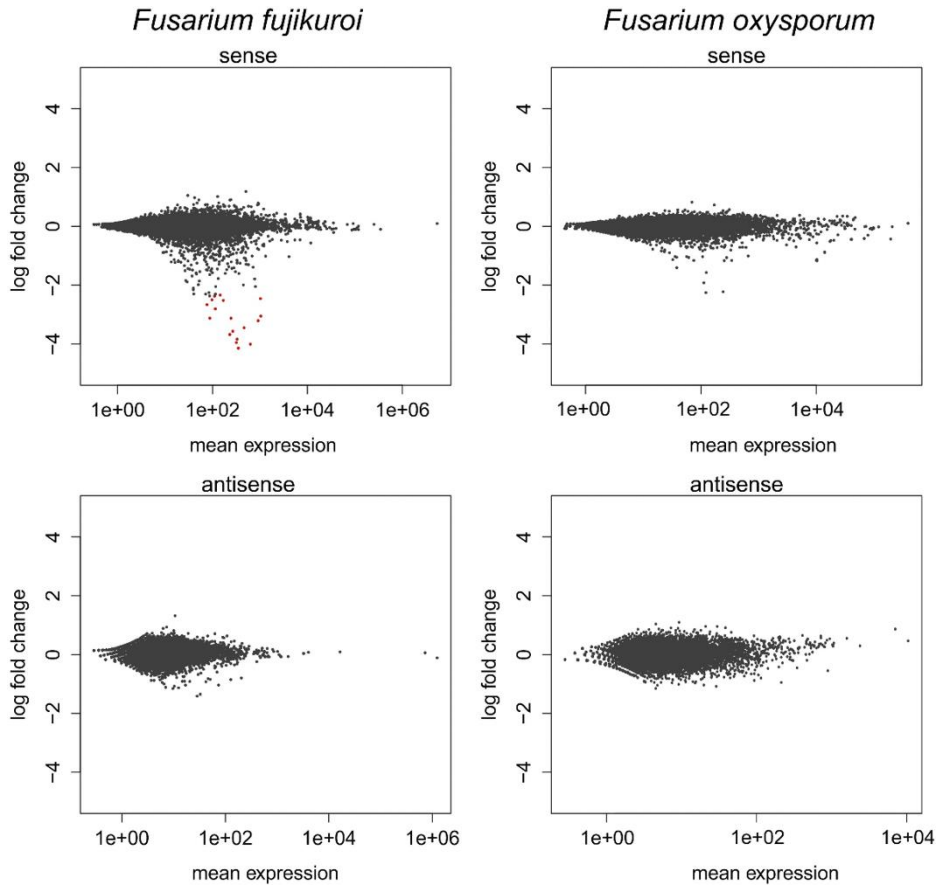

Figure C1.5. Log-fold change and sRNA mean expression of sRNA-producing protein-coding genes of *F. fujikuroi* and *F. oxysporum* in sense and antisense orientation to the corresponding genomic feature. Genes that show differential formation of sRNAs in dark *vs*. light are indicated by red dots.

Table C1.6. Formation of small RNAs within genomic features in sense orientation (dark *vs*. light). The listed genes show a downregulation of log2 < -1 and an adjusted *p*-value < 0.1. Some genes that show light-dependent expression in *Fusarium* and other fungi are indicated in red and *car* genes are highlighted in orange color.

ID	Functional annotation	baseMean	log2FC	lfcSE	stat	*P*-value	padj
FFUJ_08272	uncharacterized protein	349.39	-4.14	0.37	8.39	4.94E-17	1.76E-13
FFUJ_11803	*carB*	626.88	-4.01	0.37	8.19	2.58E-16	4.60E-13
FFUJ_11804	*carO*	318.30	-3.95	0.38	7.75	9.21E-15	1.09E-11
FFUJ_01292	uncharacterized protein	329.32	-3.84	0.37	7.57	3.87E-14	3.44E-11
FFUJ_09320	related to Rds1 protein	230.73	-3.68	0.38	7.02	2.22E-12	1.58E-09
FFUJ_06055	*vvdA*	267.11	-3.57	0.38	6.79	1.11E-11	6.57E-09
FFUJ_13896	related to TGF beta induced protein ig-h3 precursor	461.74	-3.45	0.37	6.63	3.32E-11	1.69E-08
FFUJ_01088	related to short-chain alcohol dehydrogenase	913.82	-3.21	0.38	5.85	4.99E-09	2.22E-06
FFUJ_11802	*carRA*	245.30	-3.12	0.37	5.67	1.39E-08	4.97E-06
FFUJ_12435	uncharacterized protein	87.71	-3.12	0.40	5.35	9.01E-08	2.92E-05
FFUJ_04335	uncharacterized protein	1042.24	-3.05	0.36	5.68	1.38E-08	4.97E-06
FFUJ_09119	related to flavin-containing amine oxidasedehydrogenase	114.61	-2.80	0.39	4.58	4.61E-06	1.37E-03
FFUJ_11801	*carX*	76.47	-2.66	0.40	4.18	2.94E-05	8.04E-03
FFUJ_05732	*cryD*	169.08	-2.52	0.39	3.92	9.03E-05	2.14E-02
FFUJ_08014	related to formaldehyde dehydrogenase	97.23	-2.50	0.39	3.83	1.27E-04	2.83E-02
FFUJ_05515	probable ATP-binding multidrug cassette transport protein	1024.56	-2.46	0.36	4.09	4.28E-05	1.09E-02
FFUJ_00295	*con10*	110.77	-2.37	0.39	3.51	4.53E-04	9.39E-02
FFUJ_07515	related to arabinose 5-phosphate isomerase	145.09	-2.34	0.38	3.49	4.74E-04	9.39E-02

The same calculation was also performed for *F. oxysporum*. No differential expressed sRNA-producing *loci* were found on the sense or antisense strand matching the criteria of log2 ± 1 and adjusted *p* value < 0.1. Plots of the log2 fold change of genes from *F. oxysporum* and their sRNA mean expression are shown in Fig. C1.5.

Table C1.7. *De novo* predicted miRNA-like RNAs in the merged sRNA dataset of *F. fujikuroi*.

F. fujikuroi		Read count						
ID	Score	Total	Mature	Loop	Star	*p*-value	Mature sequence	Precursor sequence
VII_86570	1.3e+1	34	33	0	1	no	ugggacgaggacaaggcugaa	ugggacgaggacaaggcugaaugggguuuaugguggaaggauuguuggcgcucgcau
VII_90055	3.8	14	12	0	2	no	ucaccguuagaccauuacag	uauugggaugggcgguugagcgggguugaacgccuucaccguuagaccauuacag
VII_98350	2.7	5	4	0	1	yes	guccuggaggcacuuga	cgaguauacuuuggugccugaucaaguuuacccaaggcagguccuggaggcacuuga
III_209346	2.3	2	1	0	1	yes	ggcgcgagaagagaucgaggauc	ccggcagaucucgucgacgggcgaccggcgcgagaagagaucgaggauc
II_193099	2.1	3	2	0	1	yes	agcccaauccuugugccacu	agcccaauccuugugccacucacuaugacacugguggcauccucucccgggguugugaggacagggaugaaccu
I_289987	1.9	3	2	0	1	yes	agaggaaucgacgaugugacu	agaggaaucgacgaugugacuuuggcgucaaagguugguagguuggcgucaaaaugcguugucguaccugagga
III_235482	1.5	68	42	26	0	yes	ugcagagcuuauucuauccc	ugcagagcuuauucuaucccuuuaggccucccgcuuuccugcacuggauuggguuuagaggcuaagguaagcucccucuu
X_17800	1.5	330	330	0	0	yes	uuaggguuaggguuaggguua	gccucuuaccuucccgauuaaacgaaaaucuugcguuuugccuuaggguuaggguuagggguua
VII_89770	1.4	2	1	0	1	yes	uccgagcgccauggguugaugaga	ucuugaccguggcuuuggggguaugguuucuuuccgagcgccaugguugaugaga
II_198003	0.6	25	25	0	0	yes	uuccacuaccuauggucguau	uuccacuaccuauggucguauguaccuauugacuaugggaagaggauaa
IV_60042	0	5	4	0	1	no	ucgacaaccucgucugccuc	ucgacaaccucgucugccuccaugacaagggacuccuggguuaccuucagacagaggagaucgggguagagcc

Analysis of miRDeep2

To carry out the miRDeep2 analysis, white spaces from the genome fasta files and collapsed reads shorter than 17 nt were eliminated. The analysis was done without any additional information on *Fusarium* milRNAs, other fungal milRNAs, or known *Fusarium* precursors. No score cutoff was used, and all precursors were analyzed. As a result, very few miRDeep2 the novo predicted putative miRNA-like RNAs were detected, most of them with either a low miRDeep2 score (< 5) or not showing the characteristic precursor formation, known from fungal milRNAs. In comparison with previous studies in fungi, only few predicted milRNAs

seemed "true" products of microRNA-like Dicer-dependent processing. Putative milRNAs from *F. fujikuroi* are described in Table C1.7, while those from *F. oxysporum* are shown in Table S1.1 in Annex. the annex.

Given the low score of almost all the predicted milRNAs detected with mir2Deep, these results should be viewed with caution. Moreover, none of these predicted milRNAs or sequenced sRNAs either in *F. fujikuroi* or *F. oxysporum* were located in the intergenic region upstream of the gene *carS*. Regarding possible regulatory roles of sRNAs in carotenoid metabolism or other light-regulated processes, none of them were produced from genes related with carotenogenesis or photoregulation. As a relevant conclusion, the sRNA-seq do not support the existence of the genes for putative milRNA precursors *ff-mir1* or *ff-mir2*, as formerly suggested.

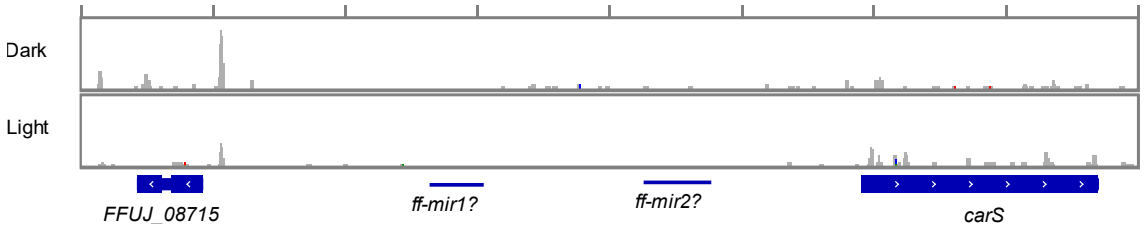

Figure C1.6. Reads of sRNA transcripts corresponding to the merged samples of the wild strain grown in the dark and after 1-hour illumination. The putative location of the milRNA precursors is shown. The reads were represented with the IGV program. Y-axis is limited to 25 reads for each sample.

ANALYSIS OF THE SMALL RNA MACHINERY IN *F. FUJIKUROI*

In parallel to the small RNA sequencing analysis, another approach was used to study the biological relevance of small regulatory RNAs in *F. fujikuroi*. At the starting point of this work, very little information was available on the functioning of RNAi systems in *Fusarium*. The only one was a study carried out in *Gibberella zeae* (Son et al., 2011) describing a meiotic silencing system very similar to the MSUD of *N. crassa.* The taxonomic proximity of *F. fujikuroi* to *G. zeae* (teleomorph of *F. graminearum*) strongly suggests that it contains an equivalent RNAi enzymatic machinery. The ortholog genes for the corresponding proteins described in *N. crassa* were searched in the genome of *F. fujikuroi*.

The *N. crassa* genes *qde-2* (Cogoni and Macino 1997; Catalanotto et al. 2002), a member of the Argonaute family, *dcl-1* and *dcl-2*, members of the RNAse III family, and *qde-1*, an RNA-dependent RNA polymerase, were used as input to perform a BLAST search for orthologs in the *F. fujikuroi* genome. As a result, 10 genes were found: three genes belonging to the Argonaute family, *FFUJ_00855, FFUJ_06303,* and *FFUJ_06580*, denominated *ago1, ago2* and, *ago3*; two RNAse III genes, *FFUJ_08936* and *FFUJ_09877,* called *dcl1* and *dcl2;* and five genes corresponding to RdRPs, *FFUJ_01792, FFUJ_03509, FFUJ_03638, FFUJ_07230,* and *FFUJ_14261*. Their sequences were subsequently analyzed using the PFAM protein domain database (Finn et al., 2014) and the results are represented in Fig. C1.6. The three Ago proteins from *F. fujikuroi* have all the known domains of the Argonaute proteins (DUF1785, PAZ and Piwi). The two Dicer

proteins present also the typical characteristics of the RNAse III family. The five putative RdRPs have their characteristic domain; noteworthily, *FFUJ_03638* also presents an ATPase domain.

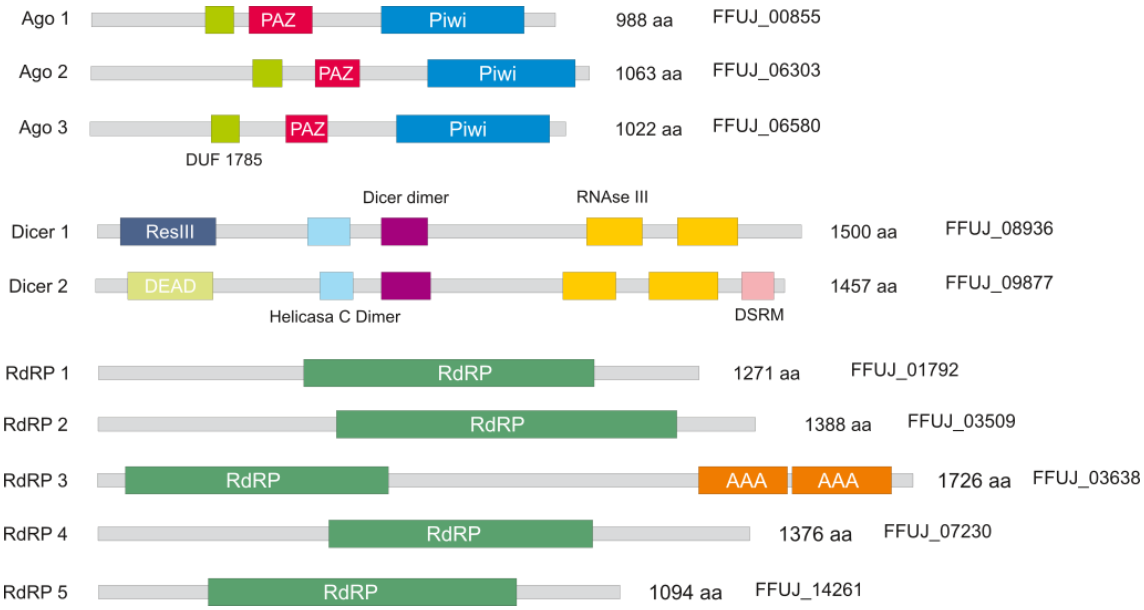

Figure C1.7. Protein domains found in the potential components of the RNAi machinery in *F. fujikuroi.* The gray bars correspond to the complete sequence of the predicted protein and expected numbers of amino acids (aa) are indicated on the right. Domains represented as colored boxes are: DUF1785 (green, domain of unknown function); PAZ (red, Piwi/Argonaute /Zwille); PIWI (blue); ResIII (dark blue, type III restriction enzyme res subunits); HelC (clear blue, conserved C-terminal helicase domain); Dicer dimer (purple, Dicer dimerization domain); RNAse III (yellow, ribonuclease domain III); DEAD (pale green, domain of the DEAD-like helicase superfamily); DSRM (pink, double-stranded RNA binding motif); RdRP (green, RNA-dependent RNA polymerase); AAA (orange, AAA domain, from ATPase associated with various cellular activities).

The effect of light and *carS* mutation on the mRNA levels for the genes corresponding to the Argonaute and Dicer proteins was analyzed in the available RNA-seq datasets already mentioned. In general, transcript levels for these genes were not much affected by light and CarS, particularly in the case of *dcl1* and *dcl2*. The results for two of the *ago* genes exhibited more variability, but in the case of *ago3*, the mRNA values decreased in the *carS* mutant SG39. However, the wild-type levels were not recovered after complementation with the functional *carS* allele. Since SG39 was obtained by chemical mutagenesis, this effect could be due to a random point mutation in this strain. On the other hand, *ago2* mRNA exhibited a slight photoinduction in the three strains.

As a fist attempt to understand the biological relevance of this presumed sRNA machinery, experiments were done to delete the *dcl1* and *dcl2* genes. It is expected that the loss of Dicer proteins would prevent generation of sRNA.

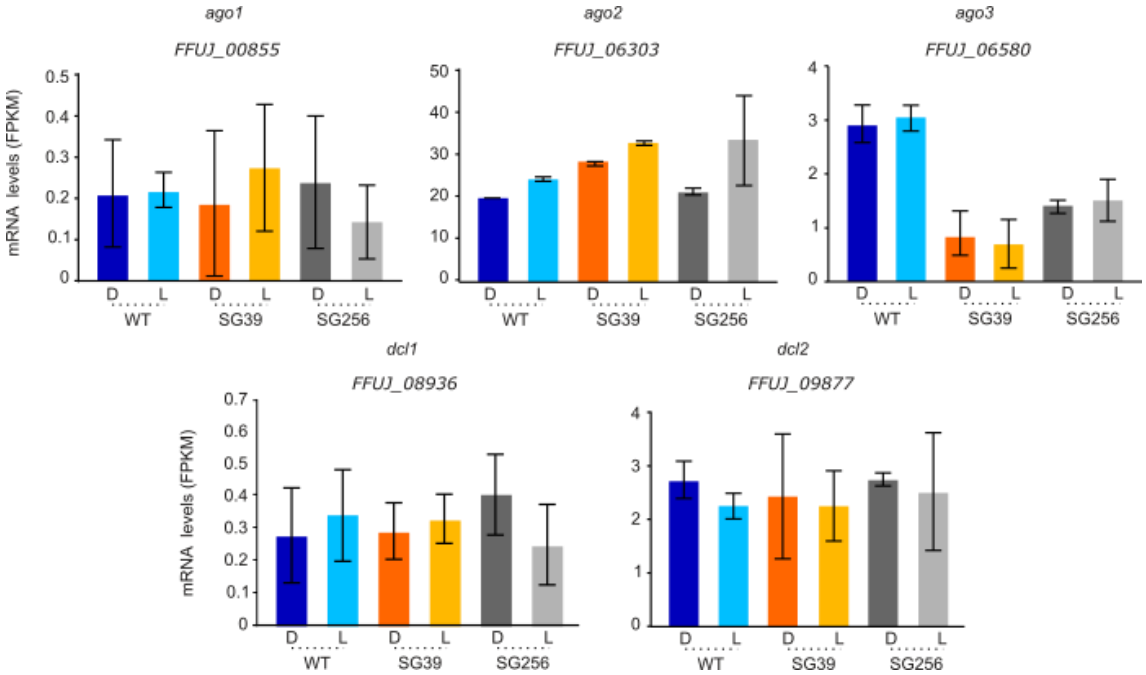

Figure C1.8. Levels of mRNA of the genes coding for the Argonaute and Dicer proteins in *F. fujikuroi* wild type, SG39 *carS* mutant, and its complementant SG256. Strains were cultured in the dark (D) or illuminated for one hour (L). Levels of RNA were the means from two samples measured in FPKM (Fragments Per Kilobase of transcript per Million mapped reads). Bars represent ± standard deviations.

GENERATION OF *DCL2* AND *DCL1* DELETION MUTANTS

Experiments were carried out to replace the *dcl2* and *dcl1* ORFs by homologous recombination with cassettes containing a selection marker. The first step in the process was to obtain the deletion constructs.

The replacement cassette to substitute the *dcl2* gene for an hygromycin resistance gene was constructed by homologous recombination in *S. cerevisiae* (Colot et al., 2006). The sequences adjacent to *dcl2* ORF were amplified by PCR with primers PS1.4 and PS1.5, and fragments of approximately 1.5 kb flanking the sequence to be replaced were obtained. These fragments corresponded to 5' and 3' regions out of the coding sequence of the target gene and possessed specific tails with homology to sequences from plasmid pRS426 and Hyg^R cassette. The Hyg^R cassette from plasmid pCSN44 was also amplified using PS1.6 primer set. All the fragments along with the linear plasmid pRS426 were incubated with competent *S. cerevisiae* cells. The construction to replace the *dcl2* sequence was used to transform wild-type protoplasts, which were then selected for regeneration and growth on an hygromycin-containing medium. As a result, four transformants were obtained and purified by selection of uninucleated spores in successive steps. All of them were then subjected to a molecular analysis to determine if *dcl2* had been substituted as expected. Several combinations of primers, detailed in Fig. C1.9, were used to check the deletion of the native *dcl2* and the presence of the *hph* gene.

Genomic DNA of transformants #3 and #4 did not contain the native *dcl2* gene and gave by PCR the expected band using primers specific for 5' *carP* sequence and *hph* gene. As an additional verification step, a Southern-blot hybridization with a radioactively labeled probe was performed. The results confirmed that the Hyg^{R} cassette had effectively replaced the *dcl2* gene in transformants #3 and #4.

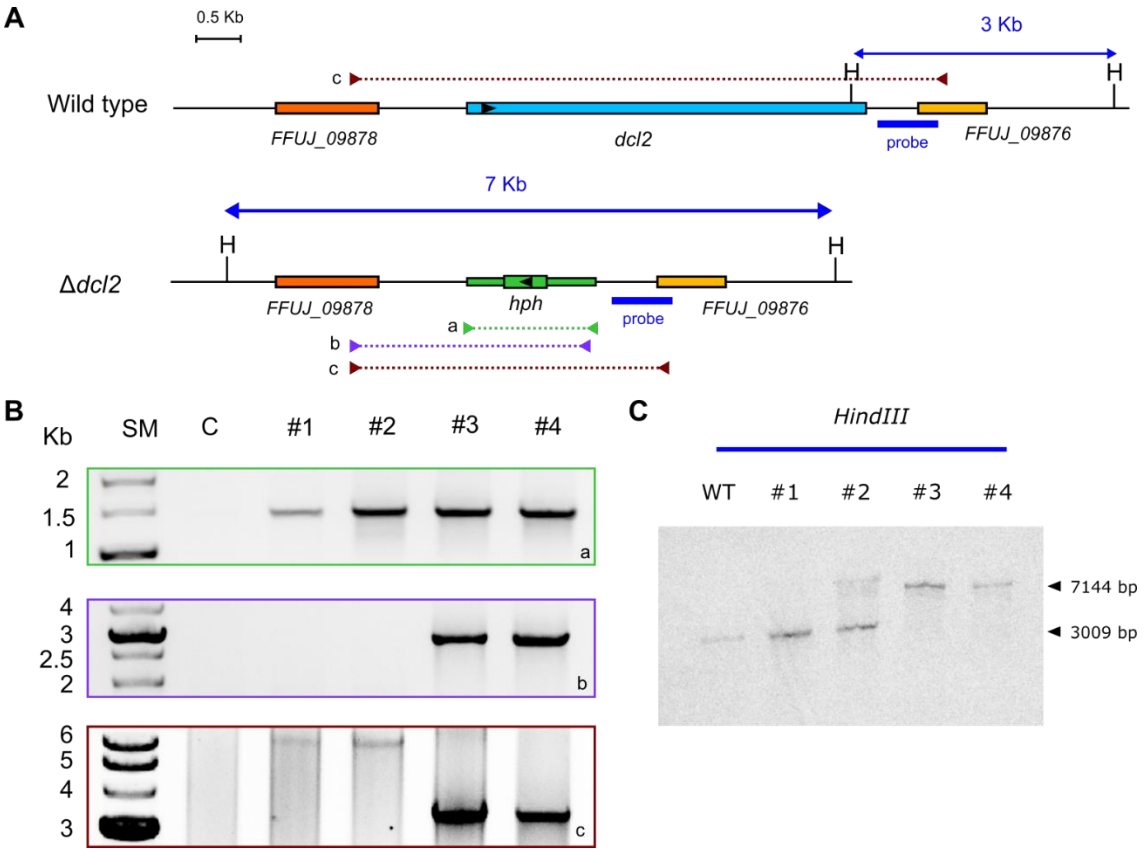

Figure C1.9. Molecular analysis of the deletion of the *dcl2* gene in the *F. fujikuroi* wild strain. (A) Genomic map covering the area for the wild strain (WT) and the Δ*dcl2* mutants showing the replacement with *hph* gene. (B) PCR amplifications of transformants #1, #2, #3, and #4 to select candidates with the correct replacement of *dcl2*. Primer sets (PS) used to amplify relevant regions are indicated on the map with colored arrowheads and their corresponding products are indicated with colored dotted lines. Expected band sizes in positive transformants for the different PCRs are 1,432 bp for amplicon a (in green) using PS1.6 primer set, 2,781 bp for amplicon b (purple) using PS1.7 primer set, and 3,660 bp for reaction c (red) using PS2.8 primer set. In the wild strain no amplification was expected for reactions a (green) and b (purple), while a band of 6,842 bp was expected for reaction c (red). (C) Southern blot of transformants #1, #2, #3, and #4 to test the correct integration. SM: Size markers. C: DNA-free control. HindIII restriction sites are indicated as H. Hybridization probe is indicated in the upper map as a blue bar and the expected hybridization products as blue lines, including the expected sizes of the bands in the Southern blot. The 769-pb probe was amplified with PS1.9 primer set.

A similar protocol was used to substitute the *dcl1* gene for a neomycin resistance cassette (Neo^{R}). In this case, due to technical problems with the construction of the replacement plasmid by recombination in *S. cerevisiae*, a different approach was carried out. The gene *dcl1*, including approximately 1.3 kb upstream and downstream its ORF, was obtained by PCR using

PS1.10 primer set and cloned in the vector pSparkI (Canvax). The resultant plasmid, pSdcl1, was used as template for an inverse PCR using PS1.11 primers that contained *Asc*I restriction sites and amplified the whole vector from the *dcl1*-5' end to the *dcl1*-3' end, leaving the *dcl1* ORF out. The Neo^R cassette was amplified with PS1.12 primers which also contained *Asc*I restriction sites and cloned into the pGEM-T Easy vector (Promega), resulting in plasmid pGneo2P. After that it was sequenced to confirm that no mutations had affected to the integrity of the resistance cassette. Plasmid PGneo2P was digested with *Asc*I and the fragment containing the Neo^R cassette was ligated with the inverse PCR product amplified from PSparkdcl1 plasmid previously digested with *Asc*I enzyme. Ligation products were checked until a plasmid which contained *dcl1* 5' and 3' adjacent sequences surrounding the Neo^R cassette was constructed, which was named pdcl1neo. This plasmid was used to transform wild-type and Δ*dcl2* strain protoplasts to obtain simple and double mutants for the dicer genes. The transformed protoplasts were selected in a G418-containing media. After 10 transformation experiments, 137 candidates for Δ*dcl1* and Δ*dcl1*/Δ*dcl2* were purified and analyzed. However, none of the transformants had the *dcl1* gene replaced by the Neo^R cassette. The reasons why these mutants could not be generated under our experimental conditions are considered in the discussion.

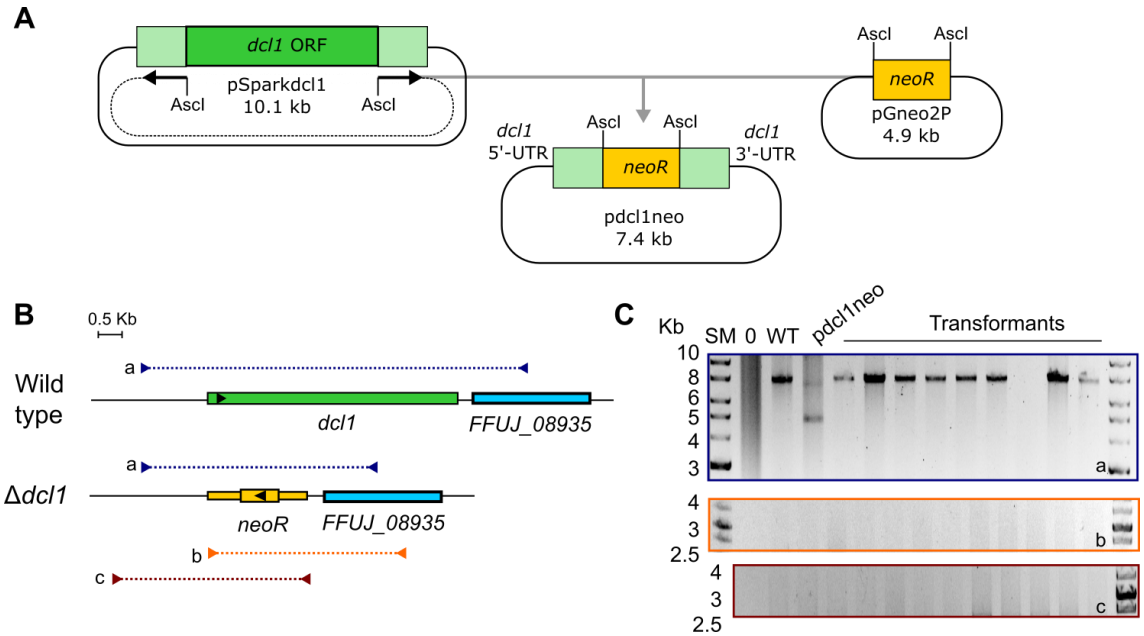

Figure C1.10. Molecular analysis of the expected deletion of the *dcl1* gene in the *F. fujikuroi* wild strain by replacement with a neomycin resistance cassette (*neoR*). (A) Strategy to construct pdcl1neo plasmid to replace the *dcl1* gene. (B) Genomic map of the wild strain (Wild type) and the expected Δ*dcl1* mutant. Primer sets (PS) used to amplify relevant regions are indicated in the map with colored arrowheads. The blue arrowheads correspond to PS1.10 primers, the orange ones to PS1.13 primers and the red ones to PS1.14 primers. The PCR products obtained are indicated with dotted lines of the same color as the corresponding primer sets. (C) Analysis of the putative *dcl1* replacement by PCR in a selection of candidates transformants. Expected amplicon sizes with PS1.10 primers (blue) were 7.1 kb in the wild strain (WT) and 4.36 kb in the Δ*dcl1* mutant. The expected sizes od PCR products were 3.4 kb and 3.6 kb with PS1.13 and PS2.14 primers, respectively. SM: Size marker. 0: DNA-free control.

The phenotype of the two positive transformants with a *dcl2* deletion was analyzed in different culture media, liquid or solid, with different sources and amounts of nitrogen, and a different pH. The experiment was done at two temperatures, 22°C and 30°C, in darkness or under constant illumination. No differences between the wild strain and the *dcl2* mutants were observed, including growing rate, mycelial development, morphology or pigmentation, under any of the conditions tested. An example of the results obtained is shown in Fig. C1.10A. Their conidiation capacities were also assessed but no significant differences were found between the strains (Fig. C1.10B).

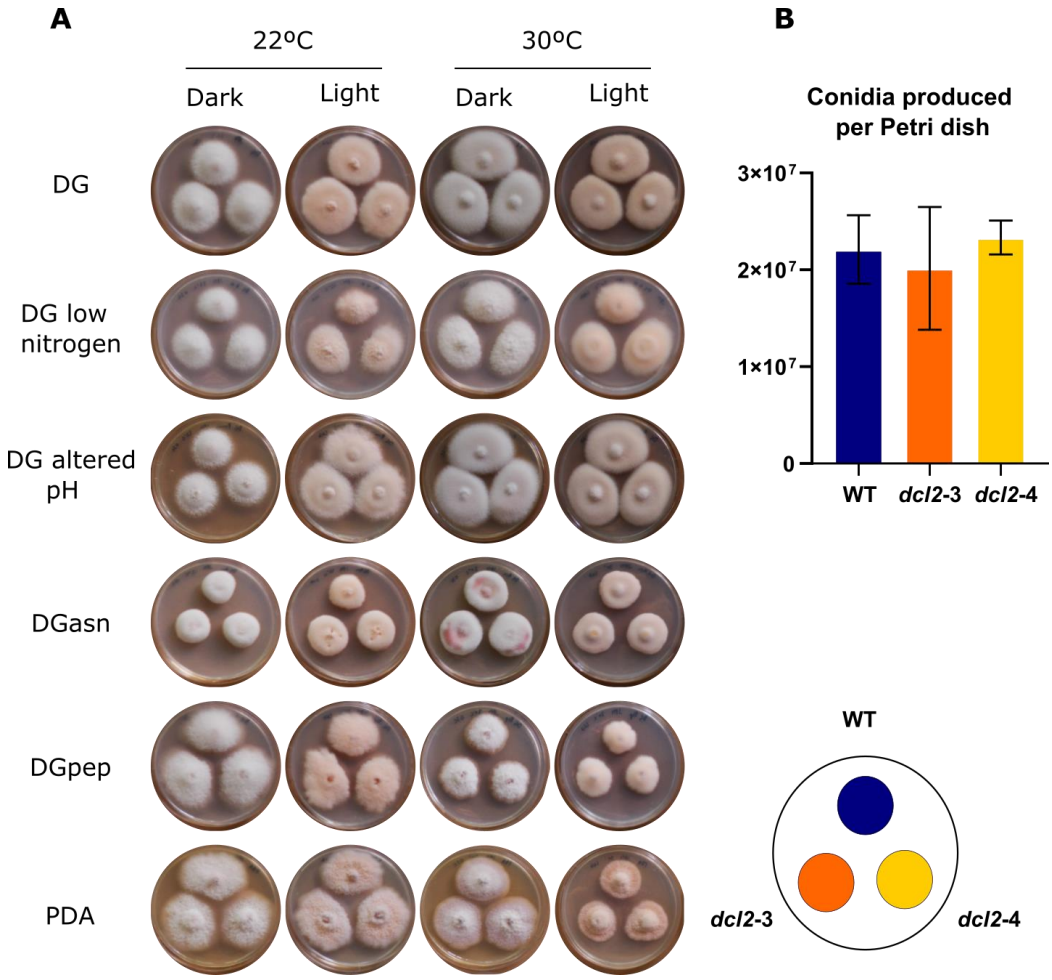

Figure C1.11. Phenotypic characterization of Δ*dcl2* transformants. (A) Growth and pigmentation of wild strain and Δ*dcl2* mutants *dcl2*-3 and *dcl2*-4 in the following media: DG: minimal medium, DG low nitrogen: DG with 0.3 g l^{-1} $NaNO_3$, DG with altered pH: DG with HK_2PO_4 (neutral pH) instead of H_2KPO_4 (acidic pH), DGasn: DG with asparagine instead of nitrate, DGpep: DG supplemented with 2 g l^{-1} peptone, PDA. potato dextrose agar. All strains were cultured per triplicate in each medium for one week at 22 °C or 30 °C, in the dark and under continuous illumination. Disposition of the three strains in the Petri dishes in the medium screening is shown on the right. (B) Conidia production of the wild strain and the two Δ*dcl2* mutants in EG medium. The values are the average of four independent determinations. The bar represents ± standard error.

RNA-SEQ OF THE *DCL2* MUTANT

Given the lack of biological differences observed under laboratory conditions in mutants lacking the *dcl2* gene in *F. fujikuroi*, in order to discover potentially altered processes the effect of *dcl2* deletion in the transcriptome was investigated. The wild-type and *dcl2*-4 strains were chosen for a RNA-seq experiment. Culture conditions followed those described in in chapter 3, consisting in three-day incubation in liquid cultures of liquid DG minimal medium in the dark, followed by 4 hours of adaptation to static culture in Petri dishes. The cultures of the two strains were incubated in parallel, with three independent biological replicas, resulting in 6 analyzed samples. RNA from each sample was extracted using the TRIzol reagent protocol, treated with DNAse I and purified by passing through a commercial kit column (detailed process described in Material and methods). The quality and integrity of the RNA samples was evaluated by spectrophotometry (A260/A280>1.8 and A260/A230>1.5) and agarose gel visualization, and the samples were sent for mass sequencing to the company LifeSequencing S. L. (Valencia, Spain). RIN values were above 8.5 in all the samples. Sequencing was carried out using the Illumina platform (Metzker 2010). Samples were sequenced on Illumina's NextSeq platform in 75 bp single read mode. The readings obtained and their basic characteristics are described in Table C1.8.

Table C1.8. Basic characteristics of the sequenced samples and yield of the readings.

Sample	Number of sequences	Average length	Average quality	G+C(%)	Mapping rate (%)
WT.0.R2	24235008	75.35	36.28	52	98.48
WT.0.R3	34924904	75.37	36.31	52	98.68
WT.0.R4	47559597	75.35	36.29	52	98.70
dcl2.4.0.R2	20277079	75.29	36.28	52	98.61
dcl2.4.0.R3	39929806	75.29	36.26	52	98.51
dcl2.4.0.R4	21674473	75.40	36.32	52	98.68

Sequences were mapped with STAR (Dobin et al., 2013). Quantitation was performed merging transcripts and counting reads over exons and percentile normalized. The representation of expression data corrected for each gene and expressed as RPM (Reads Per Million mapped reads) in a bean plot graph (Fig. C1.12.C) showed a high parallelism between all the samples. The data store similarity tree (Fig. C1.12.B) showed some experimental dispersion in the case of replicate 2.

Deseq2 tool (Love, Huber, and Anders 2014), implemented in SeqMonk, which needs raw counts for quantitation, was used to compare among conditions. The differentially expressed genes were selected based on criteria combining a log2 fold change of 1 and a *p*-value of 0.05. Under this algorithm, only 4 genes were considered deregulated among the two strains: *FFUJ_09878*, *FFUJ_09877*, *FFUJ_09875,* and *FFUJ_14259*. The gene *FFUJ_09877* corresponds to

the *dcl2* gene, while *FFUJ_09878* and *FFUJ_09875* are adjacent to the deletion, so its overexpression in the mutant can be considered a side effect of the Hyg^R cassette in the *dcl2* locus. *FFUJ_14259* encodes a putative GTP cyclohydrolase I and it was the only overexpressed gene in the mutant independent of the deletion *locus* (log2 FC = 3.7). When an alternative algorithm like EdgeR was used, another gene falled into the activated category, *FFUJ_14373* (log2 FC = 5.6), coding for an uncharacterized protein.

Provided the role that sRNAs may have in the silencing of transposable elements, as deduced from the data of small RNA massive sequencing, the expression of the previously identified transposons was checked in the wild strain and Δ*dcl2* mutant in the new RNA-seq data. However, no differences were observed among both strains.

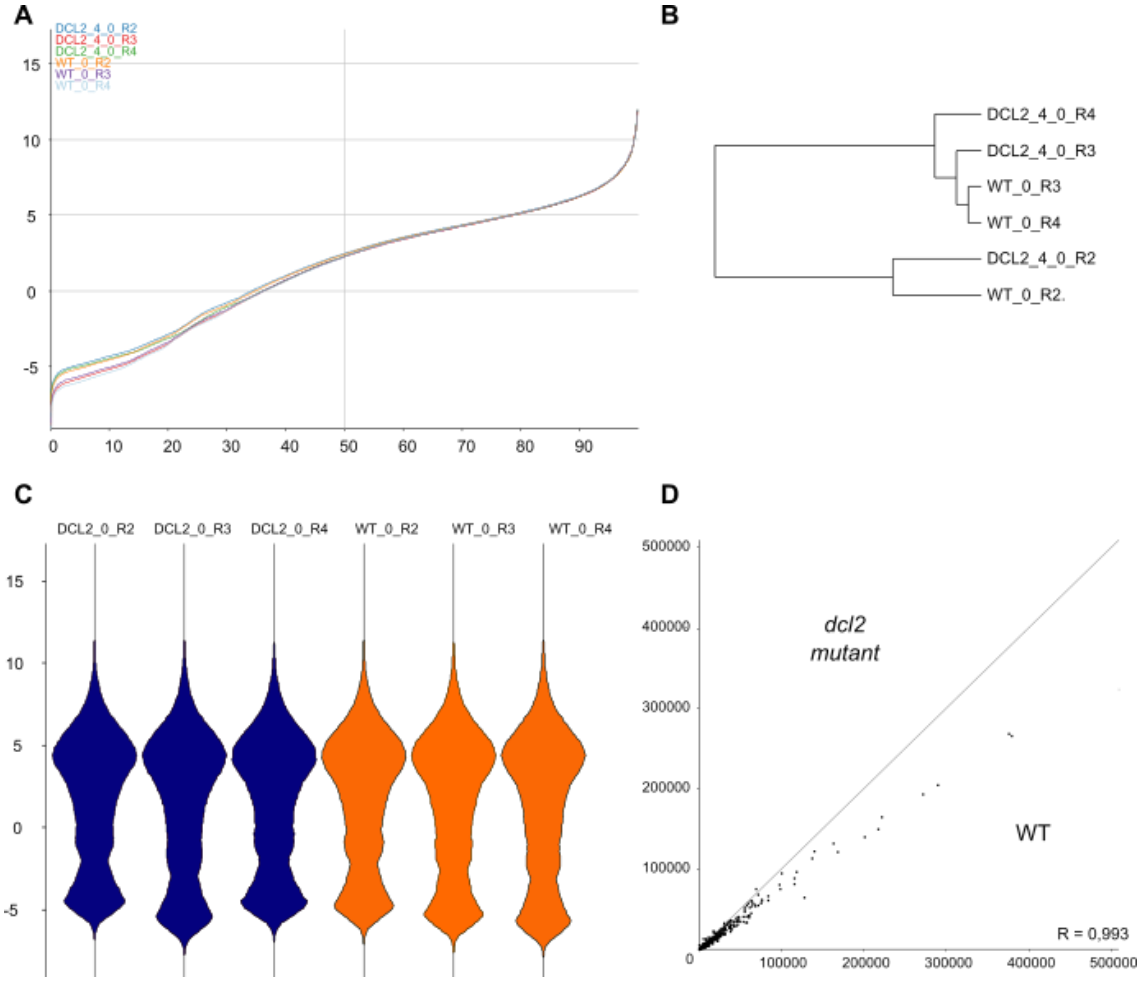

Figure C1.12. Dispersion and distribution graphs of RNA-seq samples from the wild strain and *dcl2* mutant. (A) Cumulative distribution plot after percentile normalization. (B) Datastore Tree Graph. (C) Bean distribution plots. (D) Scatter plot comparing the transcriptomes of the wild strain (WT) and the Δ*dcl2* mutant.

DISCUSSION

The discovery of sRNAs and RNA-mediated gene silencing brought a change of paradigm in our way to understand RNA as a regulatory molecule. Since then, RNAi has been intensively studied in many groups of organisms, proving to play a critical regulatory role in many biological processes, and the components of the RNAi pathway are conserved in a wide range of eukaryotic genomes. Among filamentous fungi they were shown to regulate genome integrity preservation, gene expression, phenotypic plasticity or the ability to interact with other organisms (Nicolás et al., 2020), but the biological function of RNAi and its molecular components can vary widely among different fungi. The role or presence of RNAi across them, adapting to meet the needs of each fungal species, possibly has played a very significant role in their evolutionary success both as a kingdom and as individual organisms (Lax et al., 2020). With the revolution of "omic" techniques, the knowledge on their RNAi metabolism and pathways are rapidly increasing. In *Fusarium* sp., there is evidence in the head blight pathogen *F. graminearum* on how RNAi may be crucial for processes like sexual and asexual reproduction, secondary metabolism production, and virulence (Gaffar et al., 2019), and in *F. oxysporum* for milRNAs production (Chen et al., 2014) and virulence (Jo et al., 2018), both species with great agricultural impact.

Our initial interest in the potential link between sRNA regulation and *Fusarium* comes from the hypothesis that the existence and alteration of some putative precursors of milRNAs in the region upstream to *carS* could be the cause for the carotenoid overproducing phenotype of transformants T2 and T3 (Rodríguez-Ortiz, 2012), as mentioned in the introduction of this chapter. The *carS* mutants accumulate neurosporaxanthin, a carotenoid with interesting antioxidant properties (Parra-Rivero et al., 2020a). The relationship between some milRNAs and the production of compounds with industrial applications as antibiotics have been shown in *Penicillium chrysogenum* (Dahlmann and Kück, 2015). Nevertheless, taking together several findings, such as the already described silencing of a whole region neighbor to T-DNA insertions in both transformants, which covered also *carS* (Parra-Rivero, 2018), the lack of detection of sRNAs described in this chapter by northern-blot and sRNA sequencing, and the results described in the next chapter on the discovery of a lncRNA in the same region (Parra-Rivero et al., 2020b), make very unlikely the participation of sRNA in *carS* regulation.

This work, however, constitutes the first approach to a sRNA profiling in *F. fujikuroi*, and it can serve as a starting point to understand the impact RNAi could have in this organism, joining to the information available in *F. oxysporum* (Chen et al., 2014) and *F. graminearum* (Chen et al. 2015). We provide strong evidence for a functioning RNAi pathway in *F. fujikuroi*. In the small RNA massive sequence data, the preference for a 5-prime uracil found for sRNAs within the size-range of 20 to 22 nt in *F. fujikuroi* and the slight enrichment of these sRNAs in *F. oxysporum*, are strong indications for Dicer-processed sRNAs. The sRNAs originated in both species from diverse genomic *loci*, with a notable proportion of rRNA. This fact matches former results in *F. oxysporum*, suggesting that qiRNAs, a class of DNA damage-induced and rDNA locus derived sRNAs, might be also present in both fungi (Chen et al., 2014; Lee et al., 2009). A further hint to Dicer-dependent siRNAs is the large number of antisense reads to transposable elements.

Quelling-like RNAi pathways and their role in limiting transposon and retrotransposon activity, maintaining genome integrity during vegetative growth, has been confirmed in fungal models such as *A. nidulans* (Hammond and Keller, 2005), *T. atroviride* (Carreras-Villaseñor et al., 2013) and *F. graminearum* (Chen et al., 2015), among many others. To investigate if sRNAs occur in response to selfish-genetic elements like transposons, BLAST analysis of *Fusarium* transposable elements was performed to identify those *loci*. Interestingly, Ty1/copia elements showed a strong accumulation of sRNAs in their sequences on the antisense orientation *in F. fujikuroi*. In *F. oxysporum* this might be also the case for skippy-like elements. Although evidence for a working RNAi mechanism in *F. oxysporum* was provided before (Hu et al., 2015), it might be interesting to further analyze if there is downregulation of the transcriptional active transposable elements.

One of the characteristics of this study that could add something new to the vast amount of information about how sRNAs participate in the regulation of many biological processes, is the comparison of samples obtained in the dark or after one hour of illumination. To our knowledge, the effect of light has not been addressed in any small RNA-seq study carried out in ascomycetes. However, the relationship between various phenotypes, especially those related to conidiation, and light has been demonstrated in mutants of the RNAi pathway. In *T. atroviride* it was shown that light-dependent asexual reproduction was affected in mutants of the RNAi pathway. The authors suggested that it was not due to light perception genes, but to those that are involved directly in the morphogenetic changes necessary to produce conidia, which were directly targeted by Dicer2 dependent sRNAs produced under illumination (Carreras-Villaseñor et al., 2013). Similarly, *dicer* and *ago* mutants of *Metarhizium robertsii* show reduced abilities to produce conidia in the light (Meng et al., 2017). Even within the genus *Fusarium*, there has been recent evidence of involvement of RNAi in conidiation in *F. graminerarum*, but it was only detectable under low light intensity (Gaffar et al., 2019), so it is possible that there might be some sRNAs involved in the photoregulation of conidiation. Therefore, the study of differential sRNA-formation in dark *vs*. light samples carried out in in *F. fujikuroi* and *F. oxysporum* in this chapter is a novel contribution in this field. Using sRNA-seq data to calculate differential expressed *loci* is always difficult: the use of all mapped reads results in a higher coverage but does not consider that reads might originate from a single *locus*, while using the subset of reads mapping uniquely to the genome results in a too low coverage to predict differential expressed *loci* correctly. In our case, manual checking of some sequences, for a more detailed analysis, seemed more useful than increasing their accuracy although it means missing regions due to small coverage. In *F. fujikuroi,* 18 genes were found that showed formation of sRNAs in sense orientation, but no corresponding antisense region showed differential sRNA formation. However, in *F. oxysporum* regions matching these criteria were not found either on the sense or on the antisense DNA strand. Within the identified 18 genes, most are known to be upregulated by light (Ruger-Herreros et al., 2019). Although it cannot be discarded that these sRNAs could belong to a similar group as the ex-siRNAs (Nicolas et al., 2010), their profiles do not point to specific sequences but to random locations along highly expressed genes. Thus, it is very likely that these sRNAs originate from mRNA processing and/or fragmentation.

Prediction of milRNAs in both fungi using miRDeep2 did not provide consistent results. Although several putative milRNAs were obtained, their prediction scores were very low, and both the read count and the precursor structure suggested that they might be false positives. More evidence by other methods, like northern-blot analysis or small RNA qRT-PCR, must be gathered before trying to identify putative target sites. However, sequence origin of putative *F. fujikuroi* milRNAs was checked in the genome and one of them, whose precursor sequence matched an intron from the gene *FFUJ_08631*, caught our attention. This gene corresponded to a hydrolase protein which might be secreted due to the presence of a signal peptide. Nevertheless, this sequence of this putative milRNA also matched the rice genes Os07t0685700-01, encoding a transcription factor linked to the response to ethylene stimulus and wound signaling, and Os09t0504400-01, encoding a cyclin. *F. fujikuroi* specifically colonizes rice plants as a pathogen. It has been shown that certain fungi, like *B. cinerea*, can transfer siRNAs during the infection to the plant host hijacking components of the plant RNAi pathway to suppress the expression of host immunity genes (Wang et al., 2017b). Those sRNAs have also been found in extracellular vesicles which work as cross-species vehicles of sRNA exchange (Cai et al., 2019). Moreover, in *F. graminearum*, the Fg-sRNA1 can suppress wheat defense response by targeting and silencing a resistance-related gene (TaCEBiP) (Jian and Liang, 2019). It is a very tempting hypothesis that one of the functions of the sRNA forming machinery of *F. fujikuroi* is to interfere with the expression of some critical rice genes during the infection process. This may explain the lack of phenotype of the Δ*dcl2* mutant under the laboratory conditions used in our culture screenings.

Several members of the RNAi pathway were searched in the *F. fujikuroi* genome, leading to the discovery of genes for two Dicer proteins, as usually found in ascomycetes, five RdRPs, as described in *F. graminearum* (Gaffar et al., 2019), and three Ago proteins, one more than in the mentioned species. Their transcript levels were not importantly influenced by light or *carS* mutation, using information retrieved from a former RNA-seq study (Ruger-Herreros et al., 2019). A minor photoinduction could be appreciated in the case of *ago2*, but because of the minor differences observed, this would require to be confirmed by new experiments. The possible photoinduction of *ago2* led us to reconsider the potential link between RNAi and light. However, the photoinduction levels were too low to think that they could have regulatory relevance. On the other hand, the lack of photoinduction of the genes of this system does not imply that the machinery cannot perform regulatory functions associated with light. In fact, the gene for WcoA photoreceptor gene is not regulated by light, whereas, as will be seen in chapter 3, it is responsible for basically all photoresponses in *F. fujikuroi*. Nevertheless, it should be noted that none of the putative candidates found in the sequencing study of small RNAS provided any clue on a possible relation with light.

A major goal of this chapter was to check the effect of the lack of RNAi pathway in *F. fujikuroi*. For this objective we chose to delete the *dcl* genes because of the lower number of gene deletions needed to be done than in the case of the *ago* genes. On the other hand, *dicer* mutants of *T. atroviride,* a species taxonomically close to *F. fujikuroi*, were described to show phenotypic alterations (Carreras-Villaseñor et al., 2013). Unfortunately, we could not achieve

our goal due to the impossibility to delete *dcl1* under our experimental conditions. An evident explanation for the lack of *dcl1* deletion is that it is an essential gene. However, the low number of small RNAs detected under the same experimental conditions, and the fact that none of the deletions of genes for Dicer proteins described in fungi were lethal, make the hypothesis of an essential function for *dcl1* improbable. Another explanation could be a lower chance to get the homologous recombination due to the low transcription of *dcl1* (around one tenth of *dcl2*), which suggests that this genomic region might be less accessible to the recombination machinery, possibly because in the investigated culture conditions chromatin in the *dcl1* region is in a condensed state. As a third possibility, *dcl1* is very close to a gene for a putative ubiquitin thiolesterase. The proximity of the Neo^R cassette to this gene after the replacement could interfere with its transcription, as observed for the overexpression of the genes neighboring the Hyg^R cassette in the Δ*dcl1* mutant. It does not seem likely that a change in the expression of a ubiquitin thiolesterase gene could have a so deleterious effect, but the possibility cannot be ruled out.

New approaches should be done to determine the reason for the lack of Δ*dcl1* mutants in the transformation experiments despite the large number of transformants that have been analyzed. As already mentioned, Δ*cl1* and Δ*dcl2* mutants have been described in *F. graminearum*, making very unlikely an essential role in *F. fujikuroi*. In that species both mutants were affected in conidiation (in liquid media and under special light conditions), ascospore discharge and aurofusarin and deoxynivalenol synthesis, and in the case of *Fgdcl1* mutant, also in wheat spikes infection (Gaffar et al., 2019). No effect was observed for conidiation in the Δ*dcl2* mutant under our experimental conditions, on solid medium under constant illumination. However, dimmed light should be used in new experiments to test the *F. graminearum* phenotype in *F. fujikuroi*. Unfortunately, *F. fujikuroi* IMI 52829 does not conidiate in liquid media. The experiments on sexual reproduction in *F. fujikuroi* have also remained elusive, making difficult to confirm whether ascospore discharge could be affected in *F. fujikuroi* Δ*dcl2* mutant. Moreover, *F. fujikuroi* does not have the genes necessary for tricothecenes (Chen et al., 2019; Tokai et al., 2005) or aurofusarin syntheses, which are reddish pigments. In any case, a change in the production of similarly colored metabolites, as bikaverin, would have been visible in the transformant. Therefore, at least referred to the production of conidia and visually detected secondary metabolites, the results indicate differences in Dcl2 functions between *F. fujikuroi* and *F. graminearum*.

In conclusion, this chapter constitutes the first approximation in the study of RNAi production in *F. fujikuroi* and their putative functions, at least in some cases probably related to silencing mechanisms of transposable elements. As previously stated, other findings in close species suggest that this mechanism could also play regulatory roles in *F. fujikuroi*. More efforts should be done to find phenotypes that may have been overlooked in our analysis of *dcl2* mutant, e.g., in relation to rice pathogenesis, and alternative strategies should be considered to delete *dcl1*.

Chapter 2

Characterization of the *carp* gene, a putative lncRNA regulator of carotenogenesis

CHAPTER 2: CHARACTERIZATION OF THE *CARP* GENE, A PUTATIVE LNCRNA REGULATOR OF CAROTENOGENESIS

INTRODUCTION

As shown in the previous chapter, a transcriptomics study from mycelial samples of *F. fujikuroi* and *F. oxysporum*, grown either in the dark or after illumination, failed to detect small RNAs in the upstream *carS* intergenic region (Fig. C1.1). However, an RNA-seq analysis on the effect of light and *carS* mutations of polyadenylated transcripts (Ruger-Herreros et al., 2019) revealed a non-annotated transcript located upstream to the gene *carS* in both species, which overlaps with the previously mentioned *fox-mir* and *ffu-mir* sequences. This transcript, which according to the transcriptomic data, appeared to be differentially expressed between the wild strains and the *carS* mutants, or between dark or illuminated samples, exhibited features consistent with a long noncoding RNA (lncRNA), which will be detailed in this chapter.

Massive sequencing studies have revealed that most of the genome, from baker yeast (Nagalakshmi et al., 2008) to mammals, as humans (Djebali et al., 2012) or mouse (Carninci et al., 2005) are transcribed. Pervasive transcription is considered a common evolutionary feature in eukaryotes. Genome-wide transcription produces a complex population of transcripts in which coding and noncoding transcripts are "interwoven in a rich tapestry" (Ponting et al., 2009). Protein-coding transcripts seem to be a minority among the transcription products, even though they are frequently expressed at high levels, whereas larger numbers of non-coding *loci* are expressed at lower levels, possibly representing cryptic signals that offer higher control complexity (Mattick and Makunin, 2006). Although most of transcripts are still presumably associated with known protein-coding genes (Van Bakel et al., 2010), there is a vast world of non-coding RNAs consisting of housekeeping noncoding RNAs, which include ribosomal, transfer, small nuclear and small nucleolar RNAs, usually expressed constitutively, and regulatory noncoding RNAs, among which we find microRNAs, small interfering RNAs and Piwi-associated RNAs. Nevertheless, most of the non-coding total sequences are associated to lncRNAs (Mattick and Makunin, 2006).

LncRNAs can be subclassified depending on their genomic location and context (Djebali et al., 2012, 2012; Mercer and Mattick, 2013): (i) sense lncRNAs, overlapping with one or more exons of a transcript on the same strand, (ii) antisense lncRNAs, overlapping with one or more exons of a transcript on the opposite strand, (iii) intronic lncRNAs, derived from an intron within another transcript, and (iv) intergenic lncRNAs, occurring in the interval between two genes on the same DNA strand (Ma et al., 2013; Quan et al., 2015; Smith et al., 2019) (Fig. C2.2).

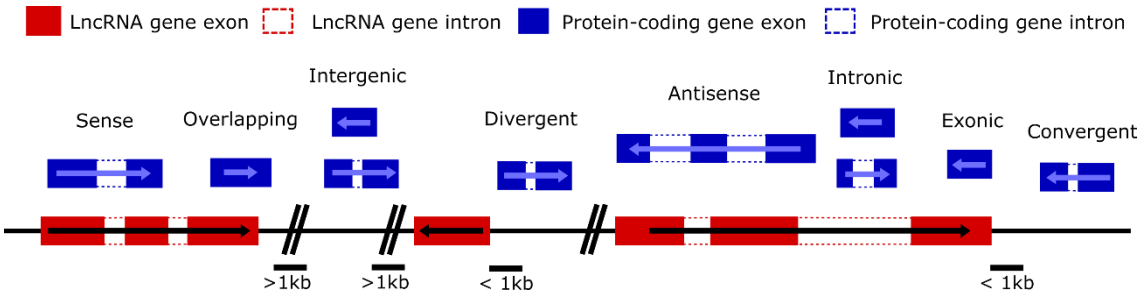

Figure C2.1 Overview of lncRNA subtypes and genomic origin. LncRNAs can be originated from proximal, distal or overlapping protein genes. Divergent/convergent and intergenic lncRNAs are arbitrarily distinguished based on the distance from the nearest protein coding gene (modified from Smith et al. 2019).

LncRNAs modulate the expression of target genes through a wide variety of mechanisms. The most common is the physical interference with the transcription of adjacent or overlapping sense or antisense-oriented target genes in *cis*, but they can also affect nucleosome repositioning, histone modifications or the recruitment of chromatin remodeling factors. Less common are *trans* interactions with proteins, DNA or other RNAs and even in some cases they can provide a scaffold for the attachment of multiple factors (Ponting et al., 2009).

LncRNAs are involved in many important biological processes. They were first described in mammals and some of the best-known examples belong to this group, like *HOTAIR*, a *trans* regulator of the Hox cluster widely involved in gene silencing (Rinn et al., 2007) or *Xist*, the central factor for X chromosomal inactivation (Brockdorff et al., 2020). However, they are found in all groups of eukaryotes, including invertebrates, plants, and fungi.

LncRNAs have been less studied in fungi than in other taxonomic groups (Till et al., 2018a), although there are cases investigated in detail, especially in *S. cerevisiae* (Niederer et al., 2017) and *S. pombe* (Yamashita et al., 2016). In most cases, yeast lncRNAs function in a transcription interfering manner. Transcriptional interference happens when transcription from a promoter, regardless of the produced transcript, interferes with transcription from another nearby promoter (Shearwin et al., 2005). Interfering mechanisms include block of the transcription machinery, nucleosome repositioning or histone modification, leading to binding or dissociation of regulatory proteins, like transcription factors. Well known examples of this phenomenon are found in both yeasts. *Nc-tgp1*, *prt* and *prt2* are sense directed lncRNAs which exert a repressing effect in neighboring genes in *S. pombe*, whose interconnected transcription and repressions regulate the expression of the gene *pho1* (Garg et al., 2018). *SRG1* is a lncRNA in *S. cerevisiae* that negatively interferes with the expression of the *SER3* gene under serine-rich conditions (Niederer et al., 2017), and *ICR1* and *PWR1*, also found in this organism, regulate the expression of their adjacent gene *FLO11* (Bumgarner et al., 2009). Nevertheless, there are some lncRNAs that function on their own, in a *cis* or *trans* manner. This is the case of the *cis*-acting CDC28 antisense lncRNA, which is produced after the osmostress-induced binding of Hog1 at the 3' end of *CDC28*; this results in a curvature of the genomic region to form a genetic loop that distributes Hog1 to both the 3' and 5' ends of gene *CDC28,* subsequently promoting chromatin remodeling and increasing its expression (Nadal-Ribelles et al., 2014). *GAL10* lncRNA promotes

deacetylation in neighboring genes, but for exerting correctly its function it requires its decapping, constituting an example of a lncRNA function by its own (Geisler et al., 2012). Trans acting lncRNAs are less common, but there are examples of some of them, as the antisense lncRNA of *PHO84* (initially described as *cis* acting), which triggers silencing of its sense gene in aged *S. cerevisiae* cells via the Set1 histone methyltransferase (Camblong et al., 2009), or SPNCRNA.1164, a regulator of *atf1* expression in response to oxidative stress in *S. pombe* (Leong et al., 2014).

Functionally characterized lncRNAs in filamentous fungi are rather scarce. Different transcriptomic experiments have provided plenty of putative noncoding transcripts in several fungi, like the model organism *N. crassa*, in which a study revealed 939 lncRNAs (Arthanari et al., 2014), adding up to about 20% of non-coding transcripts associated to RNA polymerase II (Cemel et al., 2017), or *Fusarium graminearum*, with 2,574 lncRNAs, of which 1,040 were antisense transcripts (Kim et al., 2018). Nevertheless, there are two long non-coding RNAs that have been studied in detail. The firs one is *qrf*, the antisense transcript of *frequency*, whose transcriptional interference is an essential feature of its circadian regulation (Xue et al., 2014). The second one is *HAX1*, a lncRNA identified as a trans-activator of cellulase expression in *T. reesei* (Till et al., 2018b). *HAX1* mechanism of action has been recently reported: it forms an RNA-protein complex with the activator Xyr1, interfering with its negative feedback regulatory loop (Till et al., 2020). *F. oxysporum* plant infection induces changes in the formation of plant lncRNAs during the process as a defense mechanism (Li et al., 2017; Zhu et al., 2014), but lncRNA production in the fungus was not analyzed. This is also the case of *F. fujikuroi*, in which no lncRNAs have been identified so far.

In the last years, lncRNAs are emerging as new epigenetic or transcriptional regulatory factors with a large diversity of possible action mechanisms (summarized in Fig C2.2) in filamentous fungi, suggesting the possibility that the *carP* transcript is a lncRNA with a regulatory role associated to the *carS* gene. This chapter describes the characterization of this transcript in *F. fujikuroi*. The experiments were done in parallel with those of the equivalent sequence in *F. oxysporum*, whose results have been described in the Thesis of Obdulia Parra (Parra-Rivero, 2018), and in a publication combined with data described in this chapter (Parra-Rivero et al., 2020b).

Figure C2.2. Fungal lncRNAs involved in transcriptional regulation. (A) Transcriptional interference: upstream sense lncRNA. The lncRNA transcription results in deposition of nucleosomes or repressive histone modifications which impede the binding of the transcription factor (TF) necessary for mRNA transcription. If the lncRNA is not transcribed, the chromatin remains in an open state, allowing mRNA transcription. (B) Transcriptional interference: downstream antisense (as) lncRNA. Transcription of the as-lncRNA interferes with mRNA transcription, repressing it. (C) Transcriptional activation via gene looping. An environmental stimulus promotes TF recruitment to the promoter of a downstream as-lncRNA. lncRNA transcription and recruitment of looping factors result in gene looping, stimulating recruitment of the transcription factor to the mRNA promoter and mRNA transcription. (D) After transcribed, an as-lncRNA can promote repressive histone modification, recruiting histone modifiers, at the mRNA promoter. Due to decapping, the lncRNA gradually disappears, although the turnover is outweighed by active

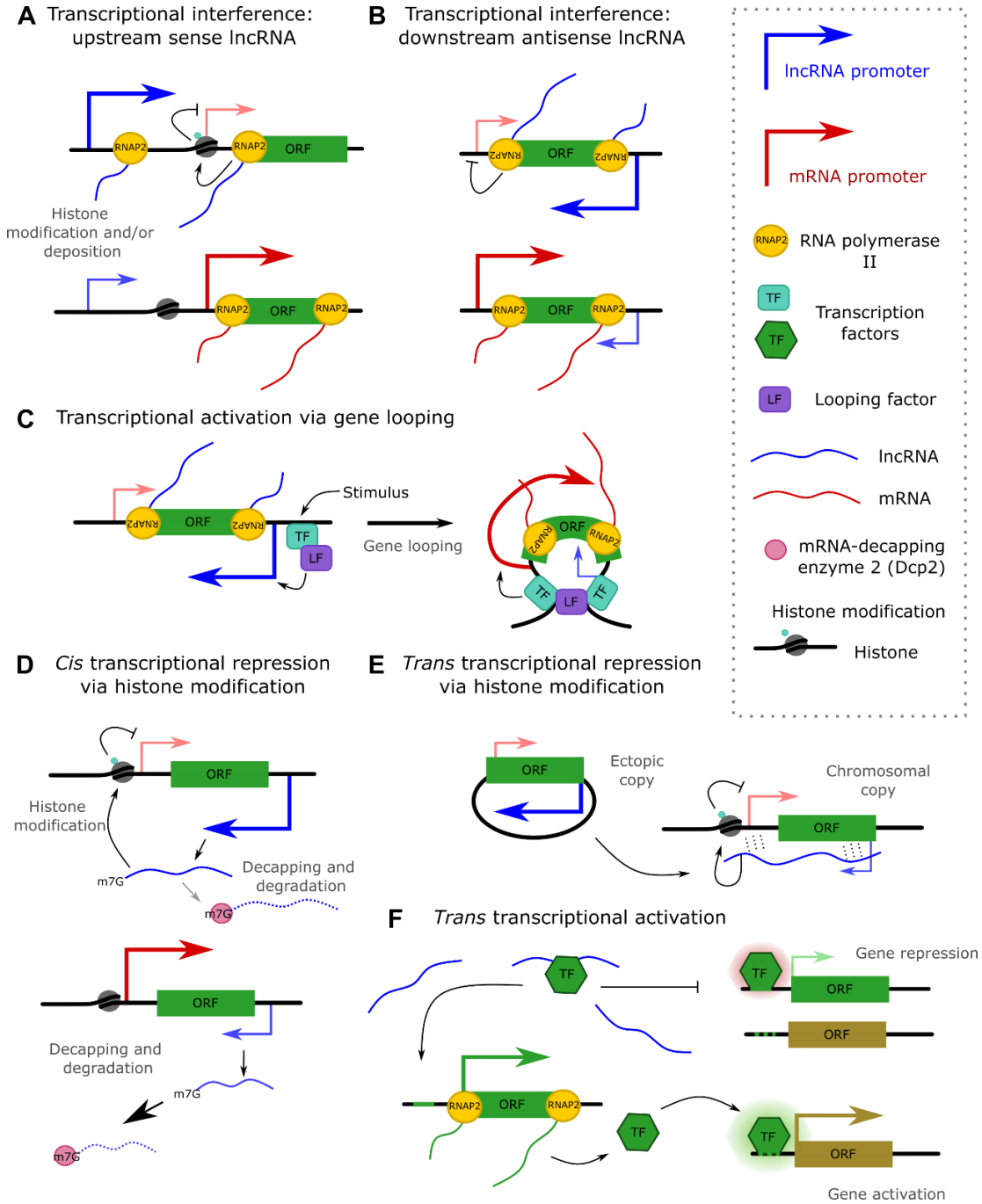

transcription. When lncRNA transcription is downregulated, decapping-dependent degradation clears the smaller amount of lncRNA present, allowing mRNA transcription. (E) Trans transcriptional repression via histone modification. In some cases, an ectopically expressed as--lncRNA can repress transcription from the endogenous chromosomal *locus* via histone modification. Homology between the upstream and downstream sequences of the gene and the lncRNA is necessary for this repression in *trans*. (F) *Trans* transcriptional activation. There are very few described activating lncRNAs. A lncRNA can bind a TF which regulates its own transcription in a negative feedback loop. The TF preferentially binds a sequence in the promoter of its own gene, repressing its transcription, while it also binds other sequences with less affinity in other genes, with activating functions. lncRNA-TF interaction promotes transcription and synthesis of the TF, therefore activating the transcription of those other genes (Modified from Niederer et al. 2017 and Till et al. 2020).

RESULTS

IDENTIFICATION AND CHARACTERIZATION OF THE *CARP* TRANSCRIPT

Transcriptomic data on small RNAs, already mentioned in chapter 1, did not find microRNAs in the 4-kb upstream sequence of *carS* in *F. oxysporum* or *F. fujikuroi*. The RNA-seq analysis describing the effect of light and carS mutation (Ruger-Herreros et al., 2019) revealed a transcript in both species, called *carP,* which overlaps with the previous putative sequence of *fox-mir-2* and *ffu-mir-2* in *F. oxysporum* and *F. fujikuroi* (Fig. C2.3). Samples included in these analyses corresponded to the wild strain IMI58289, the *carS* mutant SG39 (generated by chemical mutagenesis, and containing a point mutation in the coding sequence) and the complementing strain SG256, in which a wild-type allele of *carS* was reintroduced. SG256 was the real SG39 control, since it must contain other random mutations independent to *carS* present in SG39. In this study two experimental conditions were analyzed: mycelia collected in darkness or after one hour of illumination. No annotation could be found for *carP* in the available databases for the IMI59289 genome (NCBI or Ensembl Fungi), indicating the lack of characteristics for a protein coding gene.

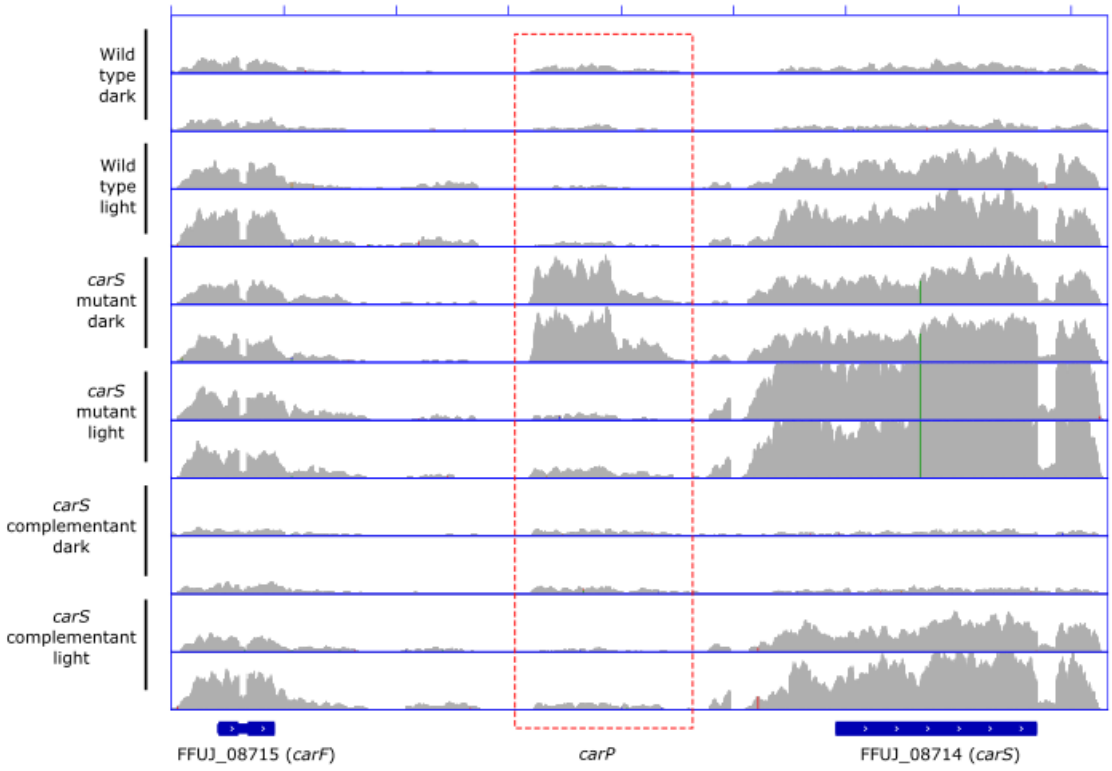

Figure C2.3. Effect of light (one-hour illumination) and *carS* mutation on transcript readings according to RNA-seq data in the genomic region between *FFUJ_08715* and *FFUJ_08714* (*carS*) genes in the wild type, SG39 and SG256 strains of *F. fujikuroi*. The green line represents the point mutation in the SG39 *carS* allele. Profiles of two biological replicates are shown for each condition. The space between the graduation marks on the top corresponds to 1 kb. The reads were represented with the IGV program. Y-axis is limited to 110 reads for each sample.

The *F. fujikuroi carP* transcript (mentioned as *Ff-carP* when required to be distinguished from the *F. oxysporum* version, *Fo-carP*), has a length of 1,357 bp, considering as initial and final nucleotides their occurrence in at least two reads among the different conditions and strains in the transcriptomic data. Due to the characteristics of the RNA-seq methodology, the *carP* transcript is expected to be polyadenylated and, therefore, to be transcribed by RNA polymerase II. Lecture quantities indicated that, under the culture conditions tested in the RNA-seq study, *carP* RNA levels were very low except in the *carS* mutant in the dark, and no detectable post-transcriptional splicing was observed within its sequence.

Transcription orientation is important to understand the potential regulatory function of *carP*. As the sequencing was not strand specific, the RNA-seq results did not provide information about *carP* orientation. To address this question, an experimental strategy was used based on the retrotranscription of each strand of cDNA with strand-specific primers and its subsequent detection by PCR. Two independent mixtures of primers were prepared, one containing three "forward" (F) primers (primer set PS2.1, located in table A.2, Material and Methods) at several locations of *carP* and three "reverse" (R) primers (PS2.2), taking the orientation of the *carS* gene as a reference for each strand sense. They were used to retrotranscribe *carP* specifically from RNA isolated from wild-type mycelia of *F. fujikuroi* incubated for three days in darkness. Retrotranscription from a complete *carP* sequence would only be produced by the transcript mix able to bind to the transcript. In other words, the F-mix would bind the antisense RNA, referenced to *carS*, and the R-mix would bind to the sense RNA.

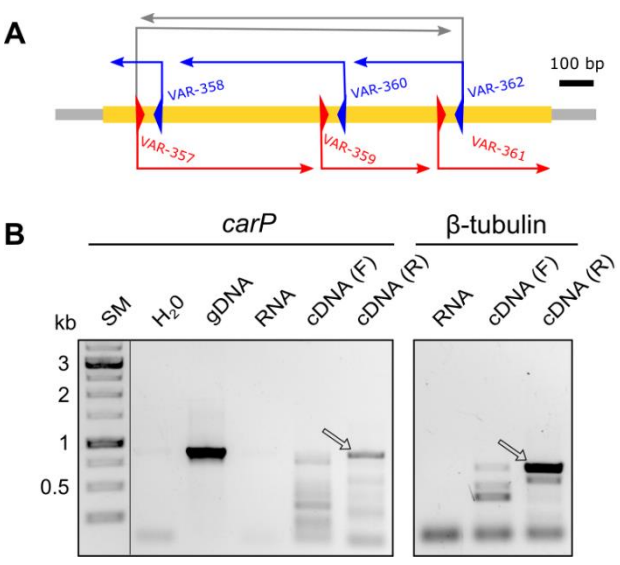

Figure C2.4. PCR analysis of *carP* transcription orientation. (A) Location of the primers used to determine the orientation of the *carP* transcript. The primers indicated in red are forward and the primers indicated in blue are reverse. The first and last primers were used in the final PCR to detect *carP* (amplification products in grey). (B) Determination of the orientation of the transcription of *carP* through the amplification from cDNA. SM: size markers. gDNA: *carP* amplification using genomic DNA of the wild strain as template; RNA: lack of amplification using total RNA as template (negative PCR control and DNA contamination control). cDNA (F): lack of amplification of *carP* from ssDNA obtained from retrotranscription of total RNA with a mixture of forward *carP* primers. cDNA (R): amplification of *carP* from ssDNA obtained from retrotranscription of total RNA with a mixture of reverse *carP* primers. Results are also shown for amplification of the β-tubulin gene as a control with a known transcriptional orientation. The sizes of the expected PCR products were 910 bp for *carP* and 693 bp for β-tubulin gene.

To test the orientation of *carP* transcription, the resulting specific complementary single stranded DNA samples (ssDNA) were used as a template to amplify *carP* in a PCR assay with the pair of external primers (primer set PS2.3). As a positive control, the same protocol was used to

determine the orientation of the β-tubulin gene *FFUJ_04397* (primer sets PS2.4 and PS2.5 for retrotranscription and PS2.6 for standard PCR). The results showed that *carP* is transcribed from the same strand as the neighboring *carS* gene (Fig. C2.5).

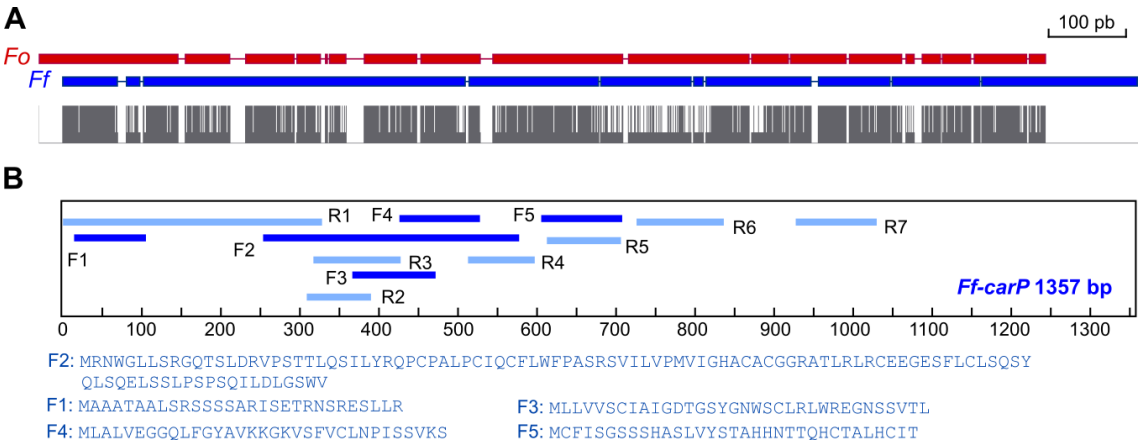

Figure C2.5. (A) Schematic representation of the clustal alignment between *Fo-carP* (red) and *Ff-carP* (blue). Gaps resulting from the alignment are indicated. The matching bases are shown below as long grey lines. (B) Positions of the ORFs in *Ff-carP* (F: forward, in dark color; R: reverse, in pale color) and residues encoded by the forward ORFs.

Although *carP* was not annotated as a gene in the *F. fujikuroi* genome, its identification as a transcript required to examine the function of the putative coded protein. A Clustal alignment between the *carP* sequences of *F. fujikuroi* and *F. oxysporum* (*Fo-carP*) revealed low divergence, with 929 identical nucleotides along 1,165 bp in *Fo-carP* and 1,238 bp in *Ff-carP*. However, as already indicated the different covered DNA segments, the alignment revealed numerous small gaps (Fig C2.5). Potential protein products were searched for in *Ff-carP*. Its Open Reading Frames (ORFs) were determined using the ORFfinder tool (NCBI Insights) in both chains for a minimum of 25 consecutive amino acids. Results showed 12 ORFs, of which 5 are in the forward direction (Fig. C2.5)(Parra-Rivero, 2018). Potential homologies between these putative proteins and those in protein Data Bases did not provide any match, with no significant similarity to any known conserved protein domain. The predicted ORFs were different to those in *Fo-carP* (Parra-Rivero, 2018), reinforcing the hypothesis of a non-coding role for *carP*.

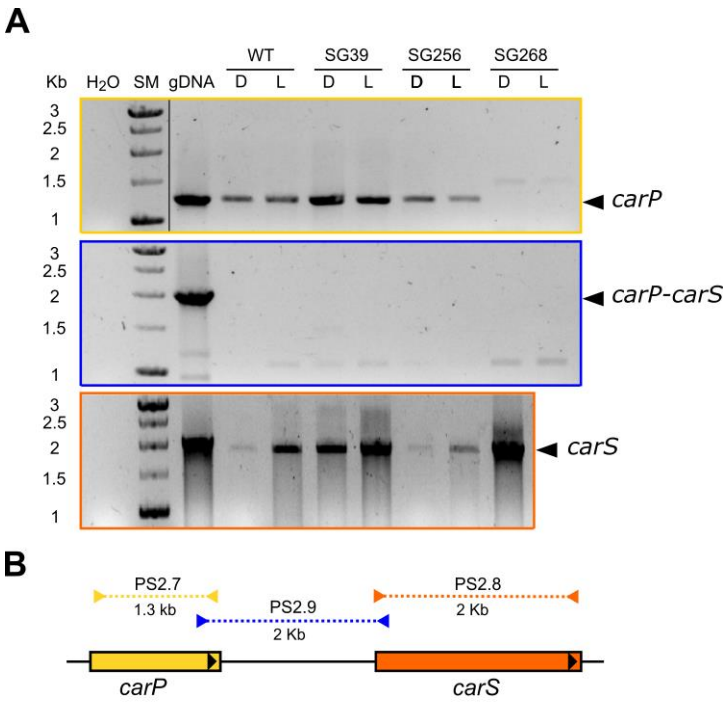

Figure C2. 6. PCR amplification to test if *carP* and *carS* are independently transcribed. SM: size markers. H_2O: Negative control without DNA template. gDNA: amplification from genomic DNA from the wild strain (positive control), WT: Wild strain. SG39: *carS* mutant. SG256: SG39 complemented with wild *carS* allele. SG268: mutant lacking the *carP* sequence (*ΔcarP*) as an additional negative control (see section "Deletion of the gene *carP*"). (B) Map showing locations and sizes of PCR products. Expected amplicon sizes were 1,245 bp with PS2.7 primers (in yellow), 2,002 bp with PS2.9 primers (in blue), and 2,029 bp with PS2.8 primers (in orange).

GENOMIC ORGANIZATION OF *CARP* IN RELATION TO *CARS*

Transcription of *carP* on the same strand as *carS* and the short distance between both genes suggest a possible functional connection. As we can see in Fig. C2.7, when the *carS* transcripts are sufficiently abundant, some reads were detected very close to the 3' end of *carP*. Therefore, we may hypothesize that *carP* is the result from the transcription of *carS* from a 5' distant site, resulting in a long *carP*-containing 5'-UTR. Several combinations of PCR reactions were used to test this hypothesis using as templates cDNA retrotranscribed from different strains and illumination conditions. Internal amplifications corresponding to *carP* (primer set PS2.7) and *carS* (primer set PS2.8) transcripts are expected according to the reading pattern in the RNA-seq analysis. However, amplification from an internal forward primer located in *carP* sequence and a reverse primer close to *carS* ATG codon (primer set PS2.9) would only be expected if both genes are found in a single common transcript.

The results showed that amplification between the *carS* and *carP* genes was possible from genomic DNA, but no amplification could be obtained from cDNA of any of the strains and conditions tested (Fig. C2.6). However, the internal *carP* and *carS* sequences were detected in most of the samples. These results strongly suggest that *carP* and *carS* derive from separate transcription events, thus providing further support to a role of *carP* as an independent lncRNA.

TRANSCRIPTION OF *CARP*

RNA-seq results suggested that *carP* expression responds to environmental and genetic factors. *carP* RNA was detected in higher amounts in the absence of a functional CarS protein in the dark. The levels of *carP* RNA descended abruptly after one hour of illumination in the SG39

carS mutant, but due to the low transcription observed in the wild strain in the dark it was difficult to determine if such decrease did also occur in this genetic background. To determine the regulation of *carP* transcription, its RNA levels were determined in different conditions and strains by RT-qPCR. As a well-known light-regulated control, the gene *carB* was also analyzed in these experiments in comparison to *carP*. Several primer sets, whose location on the *carP* sequence or its upstream region is shown in Fig. C2.7, were used in this study.

The results showed that the relative *carP* RNA levels were hardly affected by light in the wild strain (Fig. C2.7). However, as found in the RNA-seq data, the *carS* mutation in SG39 lead to a strong upregulation of *carP*, which returned to wild type-like levels in the *carS* complementing strain SG256. The amount of *carP* RNA was reduced after one-hour illumination in the *carS* mutant, although it remained at higher levels than in the *carS*$^{+}$ strains. A different result was observed for a sequence between the genes *carP* and *FFUJ_08715* (Parra-Rivero, 2018). According to the RNA-seq data, this sequence was transcribed at very low levels, but it exhibited a strong relative photoinduction, and it was enhanced in the *carS* mutant, where however the photoinduction was not apparent.

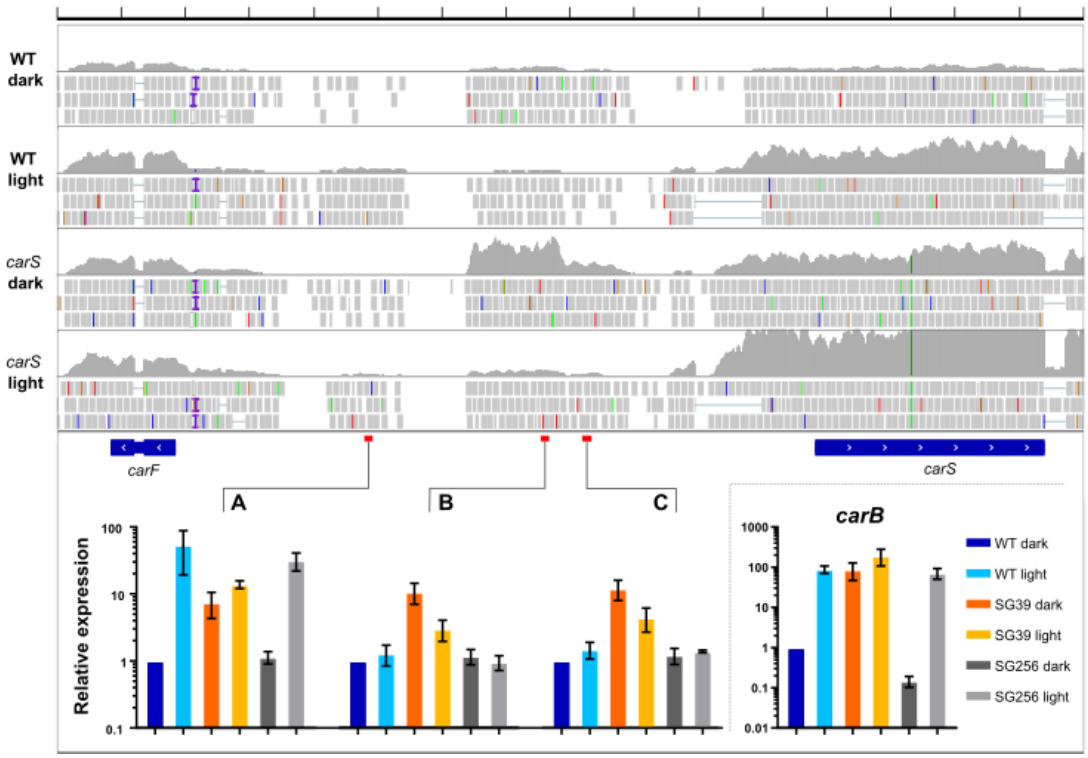

Figure C2.7. Transcripts reads corresponding to the merged samples of wild strain and SG39 *carS* mutant before and after 1-hour illumination. Below, RT-qPCR data showing the effect of light (1-hour illumination) or *carS* mutation (SG39) and *carS* complementation (SG256) on the transcript levels for *carP* or an adjacent sequence (RTPS primer sets, from left to right: A-RTPS.1, B-RTPS.2 and C-RTPS.3) and *carB* genes (RTPS.4). Transcript levels were normalized against the β-tubulin gene *FFUJ_04397* (RTPS.5). Strains were grown in DGasn liquid culture for 3 days in the dark and exposed for 1 h to light. RT-qPCR data show the mean and standard error of RT-qPCR data from three independent experiments. Relative RNA levels are referred to the RNA content of the wild strain in darkness. RTPS primer sets are located in table A.3, Material and Methods.

DELETION OF *CARP*

To determine the function of the *carP* gene in *F. fujikuroi*, deletion mutants were generated in the wild strain by replacing their *carP* sequence with a hygromycin resistance cassette (Hyg^R). The vector pCarPhyg, in which the *carP* sequence was replaced by the Hyg^R cassette from plasmid pCSN44, was constructed through homologous recombination in *S. cerevisiae*. Primer combinations used to amplify the different fragments that gave rise to the plasmid were PS2.10, PS2.11 and PS2.12. The deletion cassette was then used to transform wild type protoplasts. After selection on hygromycin B containing media, 25 transformants were obtained. Twelve transformants were genetically purified by growth of uninucleated microconidia in three successive steps. A subset of them was then subjected to a genetic analysis to confirm the expected *carP* replacement (Fig. C2.8).

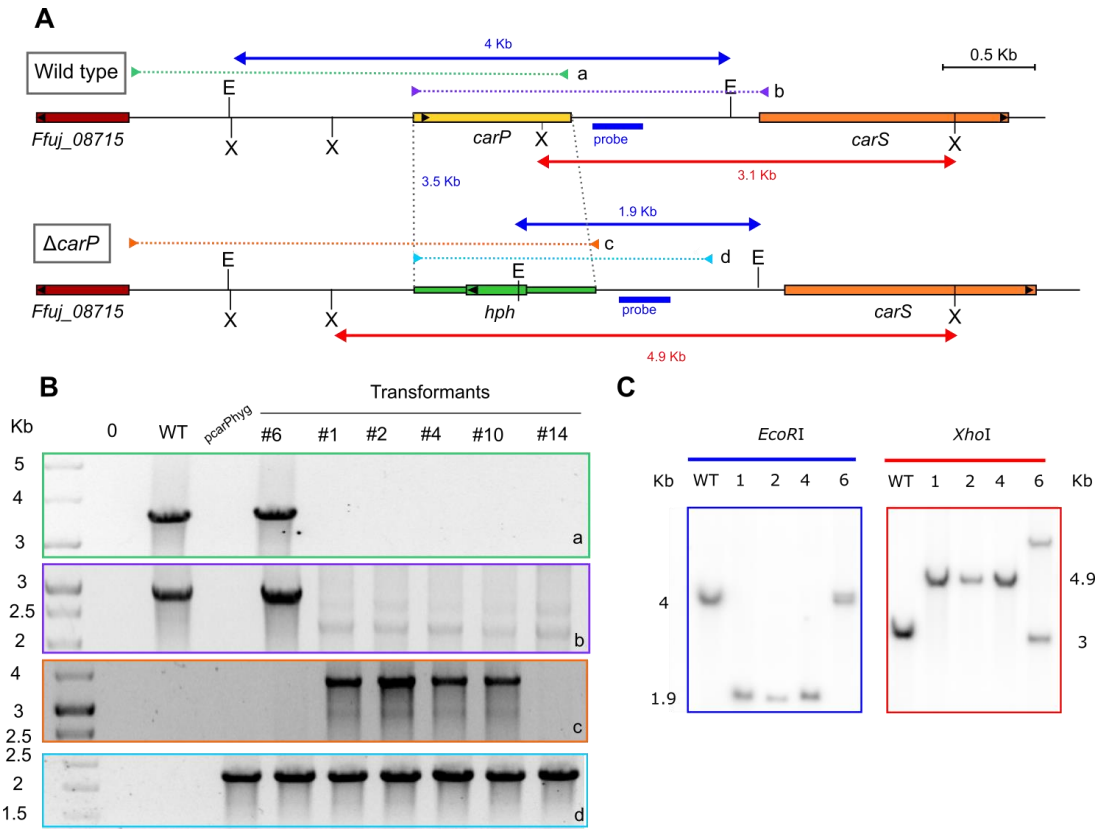

Figure C2.8. Molecular analysis of deletion of the *carP* sequence in the *F. fujikuroi* wild strain by replacement with a Hyg^R cassette (*hph* gene). (A) A genomic map of the wild type strain and the expected Δ*carP* mutants covering the relevant DNA segments. (B) PCR results to check the correct *carP* replacement of six candidate transformants. DNA from the wild strain (WT) and plasmid pcarPhyg, or lack of DNA (0), were used as controls. (C) Southern blot of the wild strain (WT) and four candidate transformants. Primer sets (PS) used to amplify relevant regions are indicated on the upper map with colored arrowheads at the extremes of the corresponding products, which are indicated in colored dotted lines. Primers, amplicons and electrophoresis gels are in the same color. Expected sizes of amplicons, a: 3,705 bp with for PS2.14 primers, b: 2,223 bp with PS2.15 primers, c: 3,496 bp with PS2.16 primers, and d: 1,245 bp with PS2.17 primers. SM: Size markers. C: DNA-free control. P: plasmid pcarPhyg. *Eco*RI and *Xho*I restriction sites are indicated as E and X. Hybridization probe is indicated as a blue bar on the upper map and expected hybridization bands as blue lines, including the expected sizes. The 412-bp probe was amplified by PCR using the PS2.18 primer set.

Several combinations of primers, external to the homologous region used for the integration of the Hyg^R cassette by homologous recombination, were used to check by PCR the presence of the native *carP* gene or its replacement by the cassette (Fig. C2.8A). Amplification from genomic DNA of transformants 1, 2, 4, and 10 gave the expected PCR products using primers located upstream of *carP* and at ends of the sequences of the Hyg^R cassette (Fig. C2.8A and 8B), while no amplification was detected (PCRs a and b) using primers that bind *carP* (Fig. C2.8B). As an additional verification step, genomic DNA samples from the wild strain and transformants 1, 2, 4, as well as number 6 as a control of ectopic integration, were digested using two independent restriction enzymes to perform a Southern-blot hybridization with a radioactively labeled probe (Fig. C2.8C). The hybridization results confirmed that the *carP* gene was effectively replaced by the Hyg^R cassette in transformants 1, 2, and 4. These transformants were subsequently named SG268, SG269, and SG270.

PHENOTYPIC CHARACTERIZATION OF THE Δ*CARP* MUTANTS

During the genetic purification process, the transformants could be divided into two distinct classes according to their color: some of them maintained the wild-type pigmentation while others exhibited an albino phenotype. The molecular analysis of the transformants showed a correspondence between the conservation of *carP* and wild-type aspect, and the absence of *carP* and albino phenotype.

Growth and morphology of the colonies of the three Δ*carP* strains were similar to those of the wild strain but lacked the characteristic orange pigmentation in the light. To confirm this phenotype, the carotenoid content of the wild strain and the Δ*carP* mutants SG268, SG269, and SG270, grown in darkness or under continuous illumination, was determined (Fig. C2.9). As expected, Δ*carP* mutants exhibited a drastic decrease in the carotenoid content in both light and dark, with only trace amounts. Under these conditions, the wild strain contained about 10 µg carotenoids/g dry weight in the dark, and this amount increased ten-fold in the light. However, the low carotenoid content of the wild strain was insufficient to provide pigmentation, but it was clearly above the levels in the transformants, that were hardly detectable by this analytical method. To deepen in the molecular basis of this carotenoid decrease, the mRNA levels of different genes related to carotenoid production were checked in the mutants.

RNA was extracted from wild-type and the Δ*carP* mycelia (see material and methods) grown in the dark or exposed to light for one hour, and it was retrotranscribed to cDNA for RT-qPCR determinations. In addition to the structural genes *carRA* and *carB*, the *carS* gene was included in the measurements (Fig C2.9C). The results showed that mRNA levels for the *carRA* and *carB* genes decreased about 100-fold in Δ*carP* mutants, explaining the lack of detectable carotenoid production. Interestingly, the mutants still maintained a photoinduction for the *car* genes comparable to that of the wild strain, indicating that *carP* does not participate in light regulation. Regarding the gene *carS,* the Δ*carP* mutants exhibited a modest increase on its mRNA levels in the dark, which was not apparent after illumination. The increased amount of *carS* transcript could be related with a lower expression of the *car* genes in the dark, but not under light, in which there were similar *carS* mRNA levels.

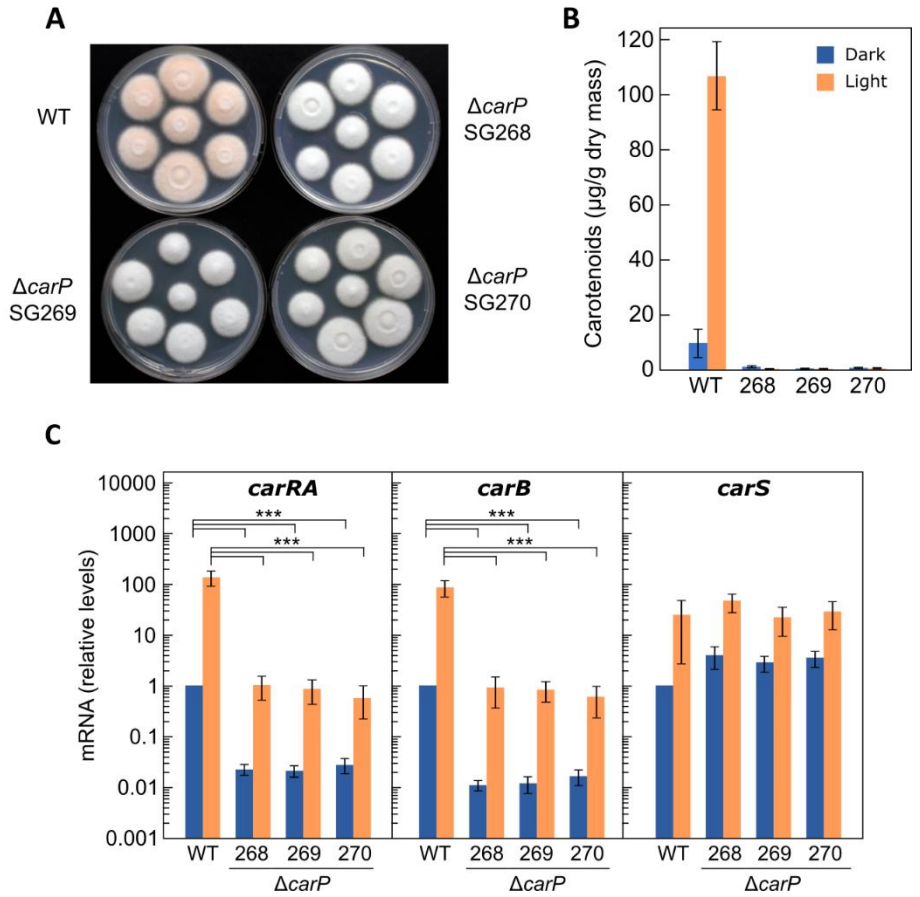

Figure C2.9. Effect of *carP* deletion in *F. fujikuroi*. (A) Aspect of colonies of the wild strain and three Δ*carP* mutants, SG268, SG269, and SG270, grown on minimal agar medium for 1 week under light. (B) Carotenoid content in the wild strain and the *ΔcarP* mutants grown for 1 week in the dark or under light. (C) Transcript levels for the *carRA*, *carB*, and *carS* genes in the four strains grown for 3 days in liquid culture in the dark or exposed for 1 hour to light. RT-qPCR data show the mean and standard error of three independent experiments. Primer sets used to measure the mRNA levels of the genes were RTPS6 for *carRA*, RTPS.4 for *carB* and RTPS7 for *carS*. Transcript levels were normalized against the β-tubulin *FFUJ_04397* (RTPS.5). Relative mRNA levels refer to the mRNA content of the wild strain in darkness. Differences found to be significant according to the t tests are indicated (P-values, *$p < 0.033$; **$p < 0.002$; ***$p < 0.001$).

EFFECT OF *CARP* DELETION ON THE EXPRESSION OF PHOTORECEPTOR GENES.

The induction of carotenogenesis by light in *F. fujikuroi* relies mainly on the WcoA protein, presumably working as a complex with its WC-2 partner WcoB, currently under investigation in the same group. However, at least two other photoreceptors seem to be involved in the control by light of this process, the DASH-Cryptochrome CryD and the small Vivid photoreceptor VvdA (Castrillo and Avalos, 2015). Moreover, WcoA is needed for carotenoid production also in the dark, while the possible participation of CryD and VvdA under these conditions is unknown. For that reason, we wondered whether the reduced expression of *car* structural genes caused by the absence of *carP* was due to changes in the expression of the genes *wcoA*, *cryD*, or *vvdA*. Therefore, their mRNA levels were determined through RT-qPCR in

the *ΔcarP* mutants in comparison to the wild strain. The transcript levels of *wcoA* did not change in response to illumination, as earlier described for the wild strain (Estrada and Avalos, 2008), and those of *cryD* and *vvdA* genes were strongly photoinduced, but this photoinduction was maintained in the Δ*carP* mutants. Moreover, the results showed the same expression patterns for the three genes in the four strains, indicating that the *carP* phenotype is not related to the expression of the genes for these photoreceptors.

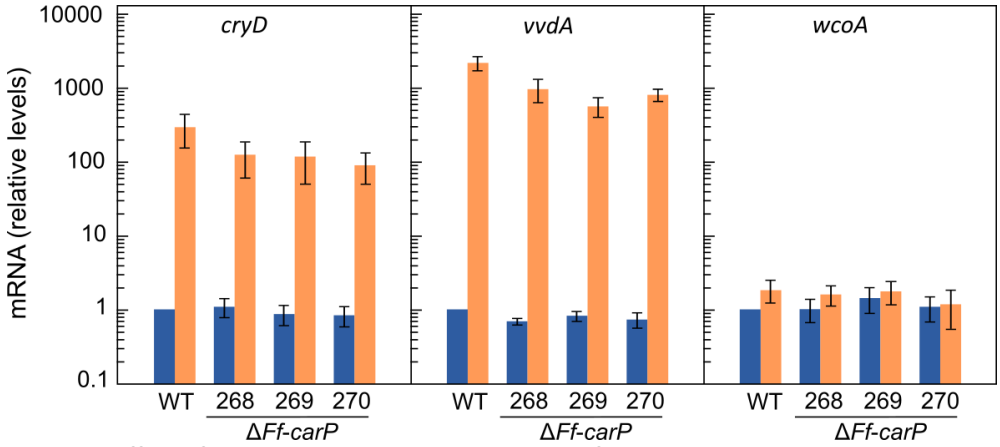

Figure C2.10. Effect of *carP* deletion on transcript levels of photoreceptor genes *wcoA*, *cryD* and *vvdA* in *F. fujikuroi* grown in the dark (blue bars) or exposed for one hour to light (orange bars). Primer sets used to measure the gene mRNA levels were RTPS8 for *wcoA*, RTPS9 for *cryD* and RTPS10 for *vvdA*. The results show mean and standard error of RT-qPCR data from three independent experiments. Transcript levels were normalized against the β-tubulin gene (RTPS.5). Relative RNA levels are referred to the RNA content of the wild strain in darkness.

REINTEGRATION OF THE *CARP* SEQUENCE IN THE Δ*CARP* MUTANT SG268

After characterizing the phenotype of the Δ*carP* mutants, to confirm that the albino phenotype was due to the lack of *carP*, we reintroduced the wild *carP* allele in the Δ*carP* mutant SG268. In transformation experiments, plasmids containing homologous sequences are typically integrated in the genome either by homologous recombination in the native site, or by heterologous recombination at random locations in the genome. Since the mechanism of action of *carP* is unknown, the analysis of both types of transformants can provide valuable information on whether *carP* RNA acts in *cis* or *trans*. Therefore, transformation plasmid pRS246carPneo, containing the native *carP* sequence (including its presumptive promoter and terminator) and the G418 resistance cassette (Neo^R) from plasmid pNTP1, was constructed through homologous recombination in *S. cerevisiae*. The primer combinations used to amplify by PCR the *carP* and Neo^R fragments were PS2.19 and PS2.20, and the resulting plasmid was sequenced to ensure *carP* integrity. Only a change was detected, the loss of a cytidine close to a C-rich segment, 166 bp upstream the *carP* transcript (marked in Fig. C2.11), which was not expected to affect *carP* function.

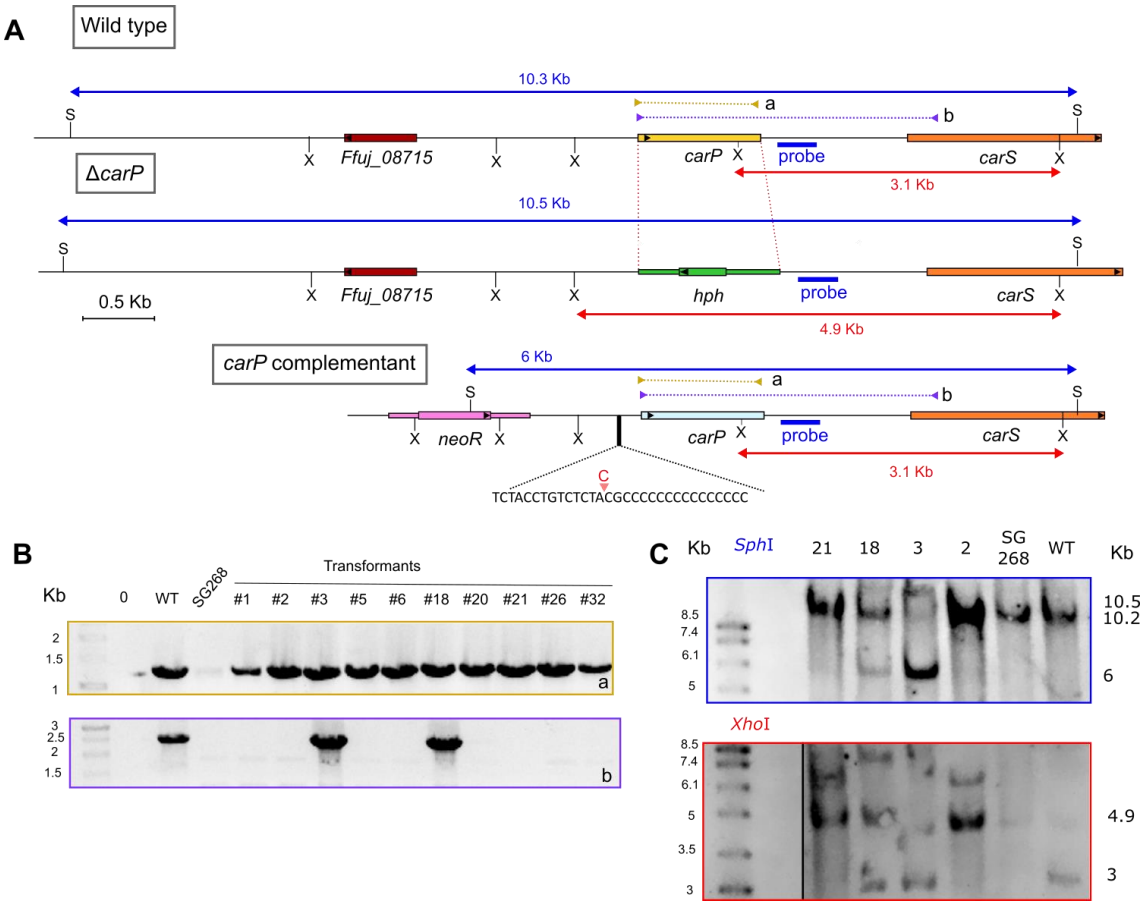

Figure C2.11. Molecular analysis of the reintegration of the *carP* sequence in SG268 by replacement with a G418^R cassette (*neoR* gene). (A) Genomic maps covering the area are shown for the wild strain, the Δ*carP* mutant SG268 and the *carP* reintegrated strains. Deleted cytosine is featured in red in the *carP* reintegration map. (B) Gel electrophoresis of PCRs of candidate transformants to check the insertion of the cassette. DNA from the wild strain (WT) and SG268 Δ*carP* mutant, or lack of DNA (0), were used as controls. (C) Southern blot of the wild strain (WT), SG268 and four candidate transformants. Primer sets (PS) used to amplify relevant regions are indicated on the upper map with colored arrowheads at the extremes of the corresponding products, indicated as colored dotted lines. Expected PCR sizes are 1,245 bp for PS2.7, and 2,194 bp for PS2.21. SM: Size markers. C: DNA-free control. *Sph*I and *Xho*I restriction sites are indicated as S and X. Hybridization probe is indicated on the upper map as a blue bar and expected hybridization fragments with blue and red lines when DNA was digested with *Sph*I and *Xho*I, respectively. A 412-bp probe was obtained by PCR using primer set PS2.18.

Plasmid pRS246carPneo was linearized by digestion with *Hin*dIII and used to transform SG268 protoplasts. Neomycin resistant colonies were selected in G418 containing media, and 32 presumptive transformants were obtained. Ten of them were genetically purified by growing uninucleated microconidia in two successive steps. The ten transformants were analyzed by PCR with different primer combinations to check the presence of the *carP* gene in its original location (Fig C2.11). Although all the G418 resistant transformants contained the pRS246carPneo plasmid, only two of them had its sequence integrated in the native *carP* locus. To confirm this result, the integration was analyzed using two independent restriction enzymes by Southern-blot hybridization and with the same probe used to test the Δ*carP* mutants, labeled with digoxigenin. In the Southern blot, the bands corresponding to wild *carP* in its locus appeared in transformants 3 and 18, indicating a correct reintroduction of the gene, but they also showed

other hybridizing bands, suggesting the occurrence of additional ectopic plasmid integrations. Transformants T3 and T18, along with T2 and T21, used as controls for ectopic *carP* integration, were used to perform phenotypic analyses of carotenoid production.

PHENOTYPIC CHARACTERIZATION OF TRANSFORMANTS OBTAINED IN THE COMPLEMENTATION OF Δ*CARP* MUTANT

Transformants T3 and T18 exhibited a phenotype distinguishable from that of the other transformants, represented by T2 and T21 as examples. The latter conserved the characteristic albino phenotype of SG268, but T3 and T8 recovered the ability to accumulate carotenoids and exhibited an orange pigmentation (Fig. C2.12A). Therefore, the capacity to produce carotenoids was only recovered when *carP* was integrated in its own genomic location. The fact that *carP* must be located upstream from *carS* to exert its regulatory role on carotenogenesis suggests that this lncRNA is a *cis*-acting regulatory element.

No differences in growth or morphology were noticeable between the colonies of the transformants and the parental strain, apart from pigmentation in the case of T3 and T18. Carotenoid analyses confirmed the visual phenotype of the mycelia. However, there were differences in the carotenoid content between T3 and T18 (Fig. C2.12B). While carotenoid production of T3 resembled that of the wild strain in darkness, it only accumulated one third of the wild-type carotenoid content under light. In contrast, T18 exhibited a different pattern of carotenoid accumulation: its levels were like those of the wild strain under light, but they were much higher in the dark, resembling those by the same strain under illumination.

The mRNA levels of the structural gene *carB*, and the regulatory genes *carS* and *carP*, were analyzed in the wild strains and the four transformants described above. As expected from the integration of plasmid pRS246carPneo, *carP* expression was restored in the four transformants, regardless of the genomic location. However, all the strains contained a higher *carP* RNA content, suggesting the presence of more than one integrated copy. This was consistent with the additional bands observed in the Southern blot (Fig. C2.11C). The *carP* transcript levels were appreciably higher in the dark than after illumination in all the strains, especially in T2.

The mRNA levels of gene *carS* exhibited a 5- to 10-fold increase after illumination compared to dark controls in all the strains tested, a result consistent with former observations for *carS* regulation (Ruger-Herreros, 2016). Irrespective of the effect of light, the amount of *carS* mRNA was markedly higher in all the transformants, including the *carP* mutant SG268, compared to those of the wild strain. Lower *carS* levels seemed apparent in the transformants T3 and T18 compared to T2, T21, and SG268, in the dark, although the amounts were still clearly above those of the wild strain. The higher *carS* levels in T18 in the dark in relation to the wild strain was an unexpected result considering its high carotenoid content.

The *carB* mRNA levels matched the carotenoid content of the different strains. Thus, *carB* transcript was found in lower amounts in the transformants T2 and T21 than in the wild

strain, and the levels were similar as those found in the original SG268 strain (Fig. C2.12C). In T3 and T18 the *carB* mRNA levels were as high after illumination as those of the wild strain and, in the case of T18, even higher in the dark, correlating with the high carotenoid content under these conditions.

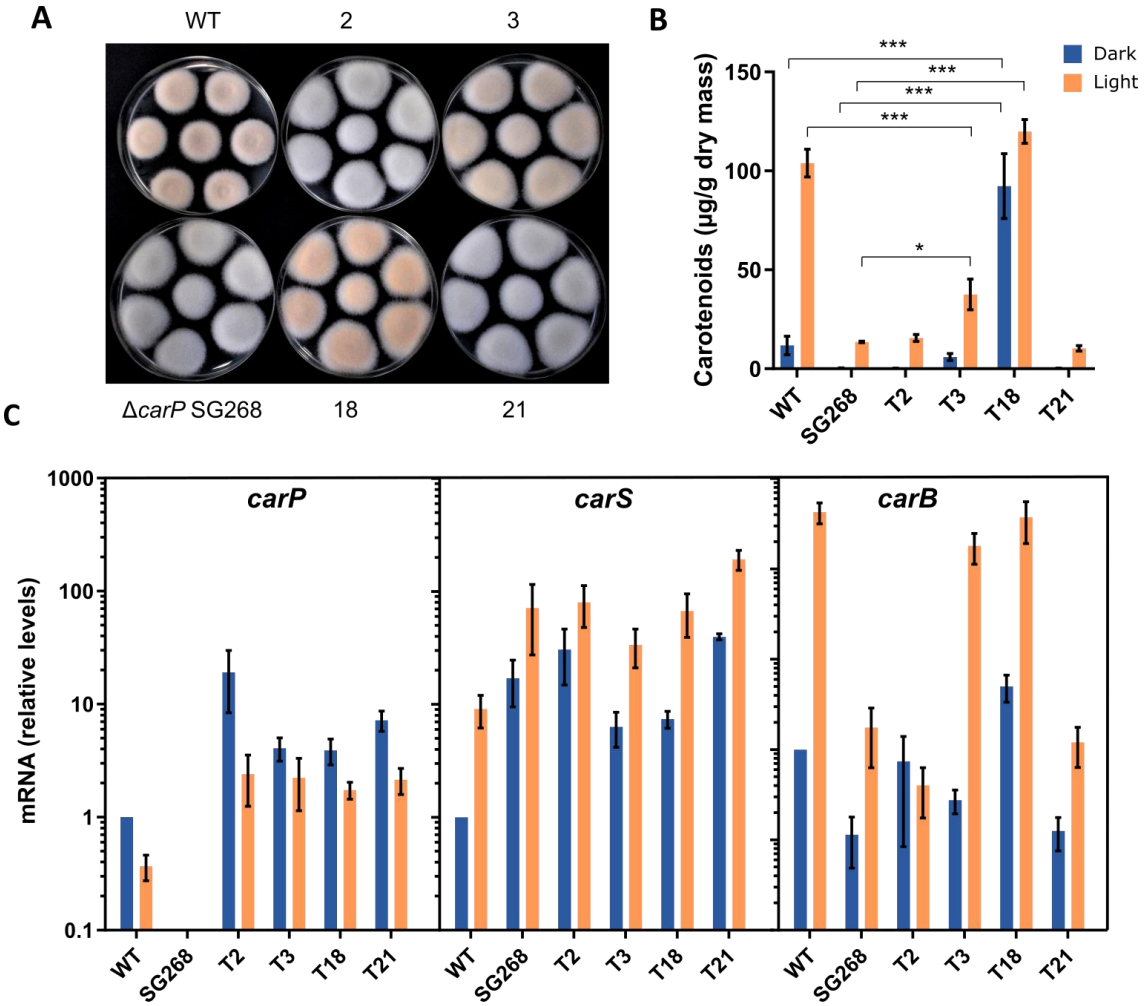

Figure C2.12. Effect of *carP* reintegration in the *ΔcarP* mutant SG268. (A) Aspect of colonies of the wild strain (WT), SG268, and four putative complemented strains grown on minimal agar medium for 1 week under light. (B) Carotenoid content in the same strains grown for 1 week in the dark or under light. Data are the average and standard error from three independent experiments. (C) Transcript levels for the *carP*, *carS*, and *carB* genes in the same strains grown for 3 days in liquid culture in the dark or exposed for 1 hour to light. RT-qPCR data show the mean and standard error of three independent experiments. Primer sets used to measure the expression of the genes were RTPS6 for *carRA*, RTPS.4 for *carB,* and RTPS.7 for *carS*. Transcript levels were normalized against the β-tubulin gene *FFUJ_04397* (RTPS.5) and GPDH gene *FFUJ_13490* (RTPS.11). Relative mRNA levels are referred to the mRNA content of the wild strain in darkness.

TRANSCRIPTOMIC ANALYSIS OF SG268 Δ*CARP* MUTANT

The results described above showed the dramatic effect that the deletion of *carP* has on the regulation of carotenogenesis in *F. fujikuroi*. However, even though there are not apparent differences in other phenotypic aspects, as colony morphology or growth between the wild strain and the Δ*carP* mutants, it is not known if *carP* absence could be affecting other processes in *Fusarium*. Therefore, we decided to investigate the effect of *carP* deletion at the global level in the transcriptome, and its relationship with light regulation.

The wild strain and SG268, already characterized in this chapter, were analyzed by RNA-seq. The culture conditions are described thoroughly in the next chapter and in Material and methods. Briefly, they consisted of a three-day incubation in the dark in liquid DG minimal medium, followed by 4 hours of adaptation to static culture in Petri dishes and then one hour of light exposure. The cultures of the two strains were carried out in parallel, with three independent biological replicates. In total 12 samples were analyzed. Extraction and purification conditions were as those used for the Δ*dcl2* RNA-seq experiment. Quality and integrity of the RNA samples were evaluated by spectrophotometry, with a RIN value above 8.5 for all samples (see Table. A.1 Material and methods). The readings obtained and their basic characteristics are described in Table C2.1.

Table C.1. Basic characteristics of the sequenced samples and yields of the readings.

Sample	Number of sequences	Average length	Average quality	G+C%	Mapping rate (%)
WT.0.R2	24235008	75.35	36.28	52	98.48
WT.0.R3	34924904	75.37	36.31	52	98.68
WT.0.R4	47559597	75.35	36.29	52	98.70
WT.60.R2	21365331	75.49	36.34	52	98.70
WT.60.R3	27473677	75.46	36.35	52	98.83
WT.60.R4	25832762	75.44	36.33	52	98.54
SG268.0.R2	22575455	75.18	36.2	52	98.24
SG268.0.R3	20962725	75.22	36.25	52	98.77
SG268.0.R4	25106589	75.21	36.25	52	98.47
SG268.60.R2	21636775	75.09	36.19	52	98.43
SG268.60.R3	20589649	75.44	36.33	52	98.77
SG268.60.R4	36335822	75.29	36.25	52	98.39

Sequences were mapped with STAR (Dobin et al., 2013). Quantitation was performed merging transcripts and counting reads over exons and percentile normalized. Deseq2 tool

(Love, Huber, and Anders 2014), implemented in SeqMonk, which needs raw counts for quantitation, was used to compare among conditions. The representation of expression data corrected for each gene and expressed as RPM in a bean plot graph (Fig. C2.13D) showed a high parallelism between the distribution of all the samples. The correlation matrix (Fig. C2.13.B), which calculates a Pearson correlation for all pairs of data stores, showed that the dataset owes its main source of divergence to the dark/light condition (with some experimental dispersion in the case of replicate 3), with the illuminated samples of the wild strain clearly separated from the rest, also confirmed in the PCA plot (Fig. C2.13C). The differentially expressed genes were selected based on criteria combining a log2 fold change of 1 and a *p*-value of 0.05. The numbers of differentially expressed genes resulting from of each relevant comparison are represented in Table C2.1.

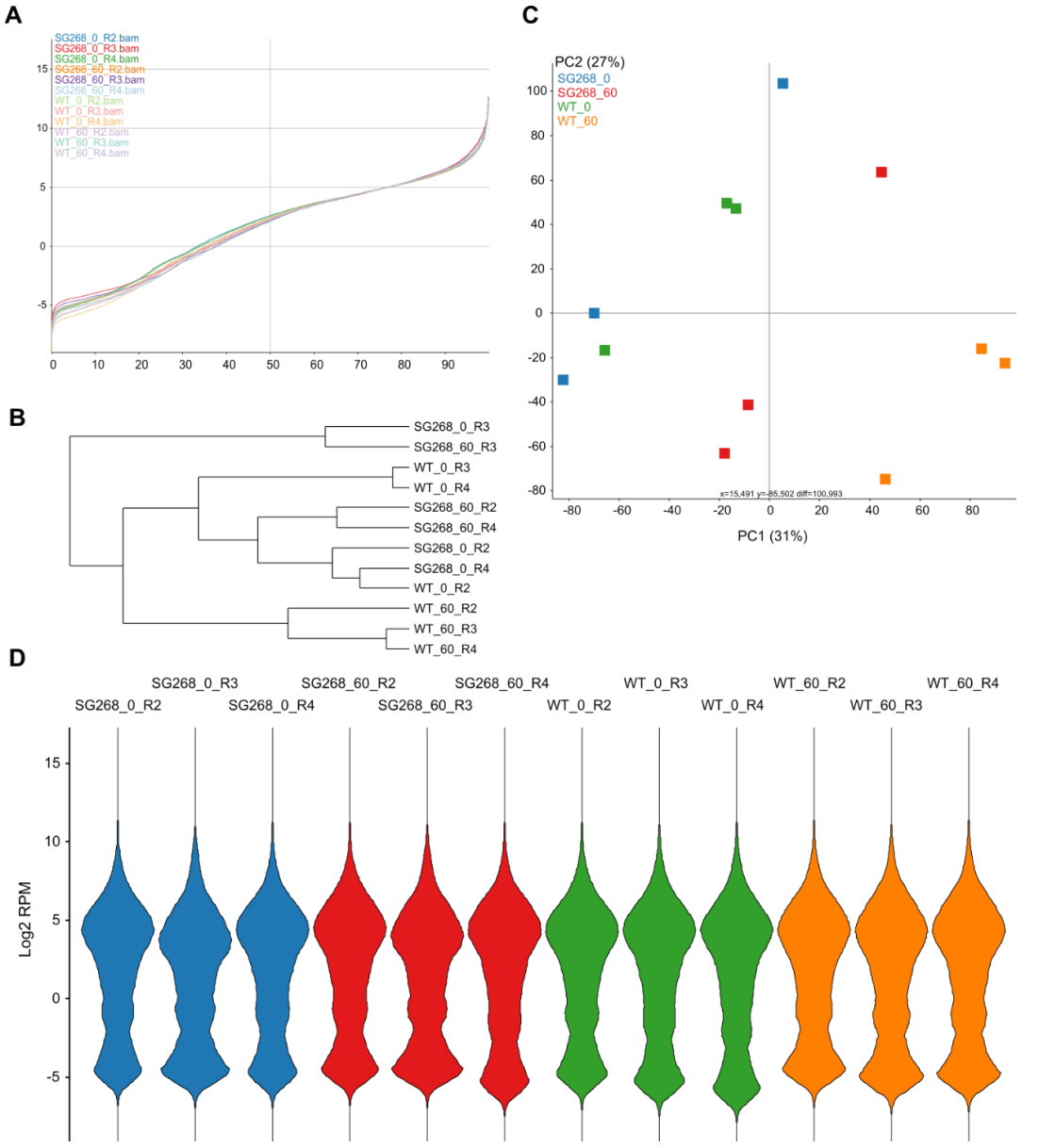

Figure C2.13. Dispersion and distribution graphs of the wild strain and SG268 mutant RNA-seq samples. (A) Cumulative distribution plot after percentile normalization. (B) Datastore Tree Graph. (C) PCA plot. (D) Bean graph.

Table C2.1. Number of genes whose expression changes more than two-fold above (upregulated) or below (downregulated) in the first strain or condition in relation with the reference strain or condition. [1] Illumination for 60 min. [2] Percentage referred to the total number of genes annotated in the genome (15,097).

Differentially expressed genes	Activated	%[2]	Repressed	%[2]
Light [1] *vs* dark in wild strain	970	6.4	860	5.7
Light[1] *vs* dark in *ΔcarP* mutant	270	1.8	192	1.3
Δ*carP* mutant *vs* wild strain in the dark	71	0.4	40	0.2
Δ*carP* mutant *vs* wild strain after light[1]	148	1.0	405	2.7

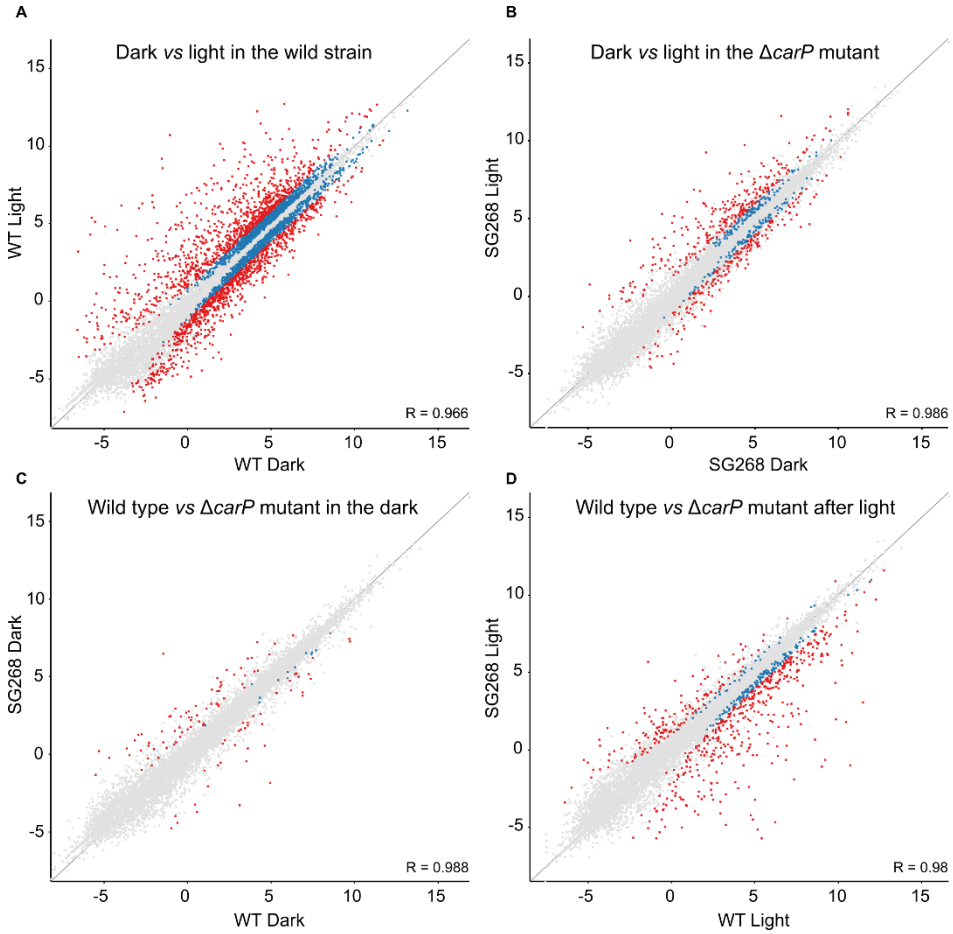

Figure C2.14. Scatter plot representations on the effect of light and *carP* deletion on the *F. fujikuroi* transcriptome. Genes differentially expressed according to the Deseq analysis of the Seqmonk program are indicated in blue. Genes exceeding the log2 values of ±1 are indicated in red.

The data revealed a total of 1,830 genes regulated by light in the wild strain, a result consistent with previous analyses under similar experimental conditions for the same strain (Ruger-Herreros et al., 2019). The number of genes influenced by light was appreciably shortened in the Δ*carP* mutant, with reductions of 3.5-fold for upregulated genes and 4.5-fold

for downregulated genes. In other words, about 75% of the transcripts that were upregulated by light in the wild strain, and about 81% of those that were downregulated, lost a significant photoregulation in the Δ*carP* mutant. Comparison of transcript levels between *ΔcarP* mutant and wild strain showed higher numbers of differentially expressed genes after illumination than in the dark, with a higher abundance of genes downregulated in the mutant.

The differences are seen with more clarity in scatter plots representations (Fig. C2.14). Despite similar numbers of genes were upregulated and downregulated by light, greatest changes in mRNA levels were mainly observed among the photoinducible genes. However, the bigger effects disappeared in the Δ*carP* mutant (compare graphs A and B in Figure C2.14), specially for photoinduced genes. On the other hand, comparisons between transcripts sets of wild strain and Δ*carP* mutant under the same conditions showed a higher impact of the *carP* mutation after illumination than in the dark (graphs C and D in Fig. C2.14).

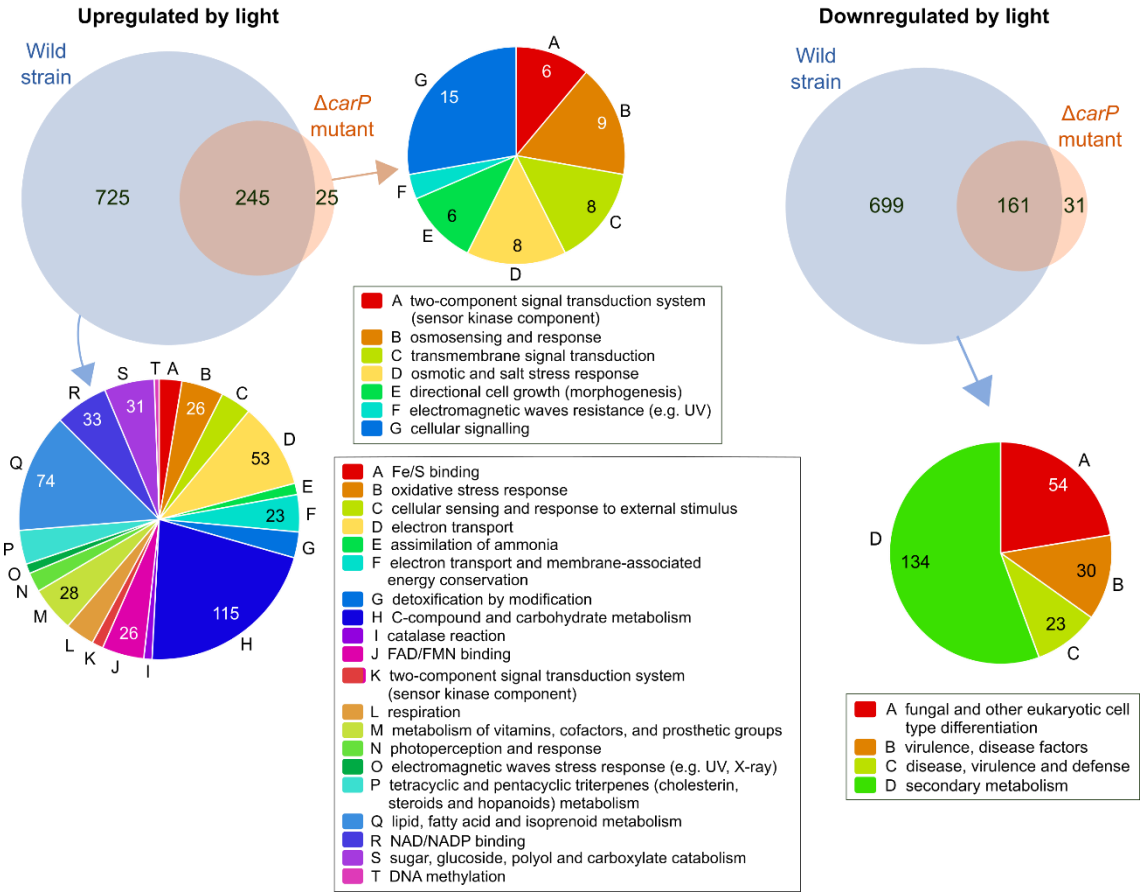

Figure C2.15. Effect of light in the transcriptomes of the wild strain and the *ΔcarP* mutant. Venn diagrams show the proportion of coincident genes between those upregulated (left) or downregulated (right) by light in both transcriptomes. Enriched GO categories for the total subset of differentially expressed genes in the wild strain and the *carP* mutant are shown for the three transcript sets for which significant categories were found.

GENES AFFECTED BY LIGHT IN THE WILD STRAIN AND IN THE *ΔCARP* MUTANT

Comparison of the lists of genes affected by light in the two strains showed that about 90% of the genes photoinduced in the *ΔcarP* mutant was also photoinduced in the wild strain (Fig. C2.15), a proportion that was also very high (ca. 83%) for the photorepressed genes. As expected, there was a large diversity of functions in the genes induced by light in the wild strain, many of them involved in a large diversity of metabolic processes, some related with stress. However, functional categories found to be relevant in the genes that exhibited photoinduction in the Δ*carP* mutant were enriched in functions related to signaling pathways. Functional assignations were less clear among the photorepressed genes in the wild strain, some of them related to cell differentiation, virulence and secondary metabolism, but no significant functional groups were identified among the photorepressed genes in the Δ*carP* mutant.

GENES DIFFERENTIALLY EXPRESSED IN THE *ΔCARP* MUTANT COMPARED TO THE WILD STRAIN

As mentioned above, illumination brought about an increase in the numbers of differentially expressed genes in the Δ*carP* mutant. More than half of the genes upregulated or downregulated in the mutant in darkness were also upregulated or downregulated after illumination (Fig. C2.16). Interestingly, a high proportion of the genes downregulated in the Δ*carP* mutant under light were upregulated in the wild strain under the same conditions, indicating that *carP* is needed for proper photoinduction of a large collection of genes.

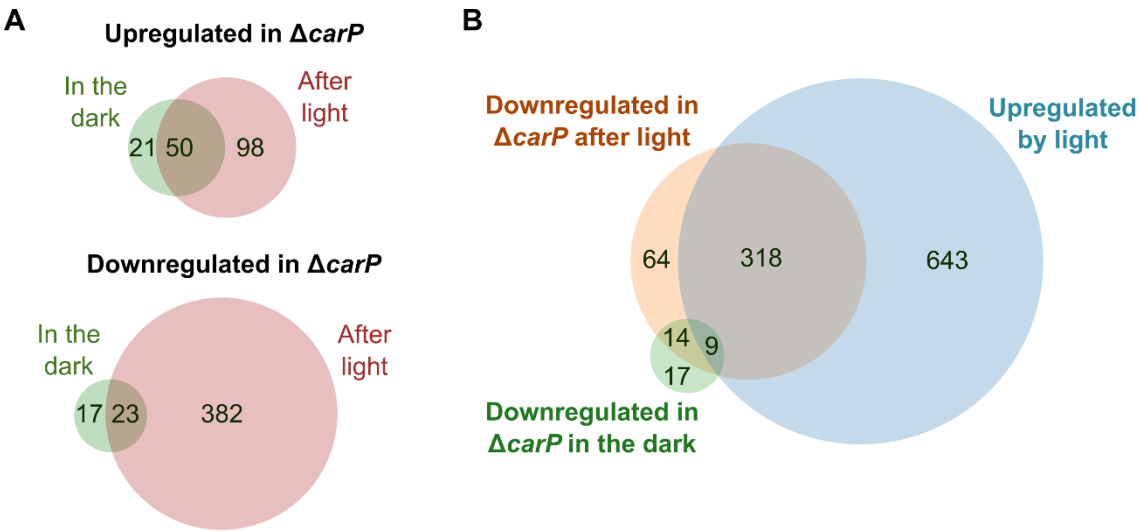

Figure C2.16. Effect of the Δ*carP* mutation in the dark or after oner hour illumination. (A) Venn diagrams show the proportion of coincident genes between those upregulated (above) or downregulated (below) in the Δ*carP* mutant in the dark or after one hour in the light. (B) Venn diagram that visualizes the coincidences between genes upregulated by light in the wild strain and those downregulated in the Δ*carP* mutant.

The get information of the possible functions of the genes influenced by *carP*, we carried out a hierarchical heatmap according to the mRNA levels of the 591 genes that exhibited a change compared to the wild strain in at least one of the two conditions tested (Fig. C2.17). The tree separates into two main branches, which correspond to genes that are upregulated or

downregulated in the Δ*carP* mutant compared to the wild strain. For more detailed analysis, we arbitrarily chose a discrimination threshold (red dotted line in the figure) that distinguish five cluster groups, two corresponding to upregulated genes (I-II) and three to those downregulated (III-V).

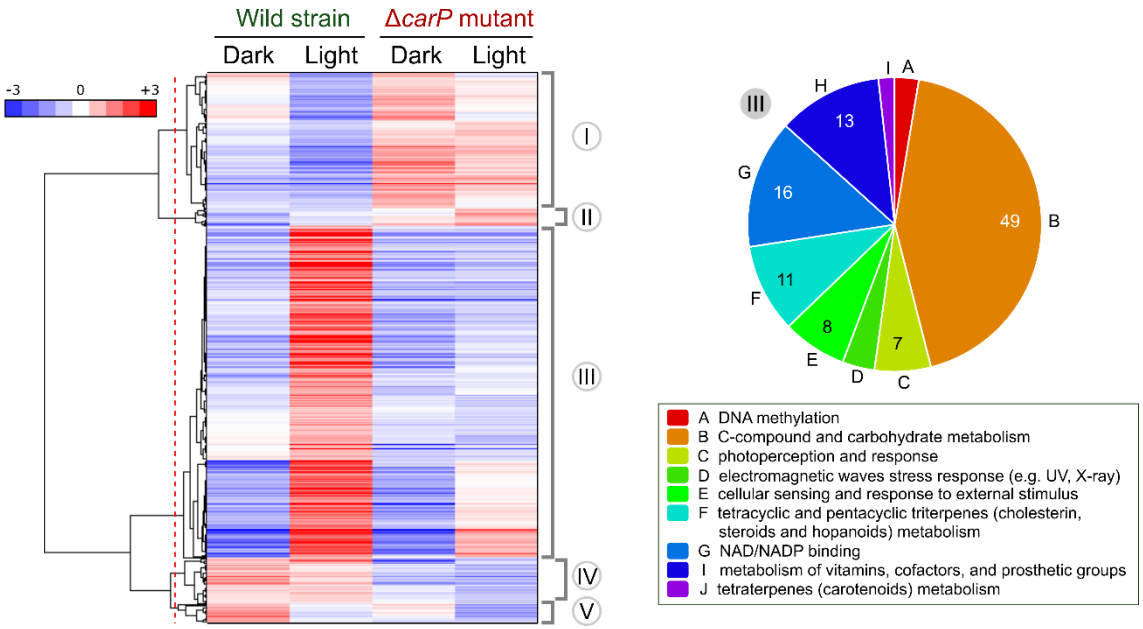

Figure C2.17. Hierarchical heatmap for genes influenced by *carP* in the transcriptomes of the wild strain and the Δ*carP* mutant. The red line indicates an arbitrary separation of five cluster groups. Significant GO enriched categories found in cluster III are shown on the right.

Cluster I consisted of 145 genes that in most cases were downregulated in the wild strain. Although their patterns are quite diverse, all of them exhibited higher transcript levels in the Δ*carP* mutant either in the dark or after illumination, in many cases maintaining photorepression. The GO enrichment analysis in FunCat only found as significant 26 genes belonging to the category "C-compound and carbohydrate metabolism". On the other hand, Cluster II included only 19 genes with a predominance of photoinduction in the wild strain, which, as those of cluster I, were upregulated in the Δ*carP* mutant. Six of the genes were found to be involved in "sugar, glucoside, polyol and carboxylate anabolism". Thus, all genes of clusters I and II with significant associations to FunCat categories are related with metabolism.

Cluster III was the major class, covering 357 genes induced by light in the wild strain and downregulated in the Δ*carP* mutant. This category included genes associated to nine GO categories (Fig. C2.17), corresponding to very diverse functions. The genes for carotenoid biosynthesis, already shown to be repressed in the Δ*carP* mutant, and other genes regulated by CarS (Ruger-Herreros et al., 2019) are included in this set.

Clusters IV and V included genes that were downregulated in the Δ*carP* mutant, but in this case in the wild strain they were only moderately affected (cluster 4) or clearly downregulated (cluster 5) by light. No significant GO categories were found in the 49 genes of cluster 4, that included the genes for the nitrate reductase NiaD (*FFUJ_12277*, repressed about

10-fold in the Δ*carP* mutant) and the probable nitrate transport protein CrnA (*FFUJ_00934*, repressed about 5-fold). On the other hand, 5 out of the 20 genes included in cluster V were associated to polysaccharide metabolism.

RELATION OF THE EFFECTS OF *CARP* AND *CARS* MUTATIONS

The finding in the *carP* complementation experiments that the carotenoid producing phenotype is only recovered when the wild-type *carP* gene is integrated at the same genomic location suggests that *carP* modulates *carS* expression by a *cis*-acting mechanism. As already mentioned, a recent study of the effect of the *carS* mutation on the transcriptome showed that CarS influences the expression of a large set of genes (Ruger-Herreros et al., 2019). This arises the hypothesis that the effects of *carP* deletion in the transcriptome could be due to its influence on *carS* expression. To check this hypothesis, we compared the sets of genes affected by both mutations using the same 2X threshold of differential expression. The numbers of affected genes differed appreciably in both cases: loss of *carS* function resulted in the upregulation of 424 genes, compared to 170 in the case of the loss of *carP*, and the downregulation of 330, compared to 423 in the case of *carP*. Interestingly, the numbers of genes upregulated in the *carS* mutant (424) and downregulated in the *carP* mutant (423) were very similar, and about half of them were coincident. However, the proportion of coincidences was much lower in the opposite combination (upregulated in Δ*carP* and downregulated in *carS*$^-$). In contrast, overlapping between affected genes in both strains was basically inexistent if the effects of the mutation were the same (lower Venn diagrams in Fig. C2.18).

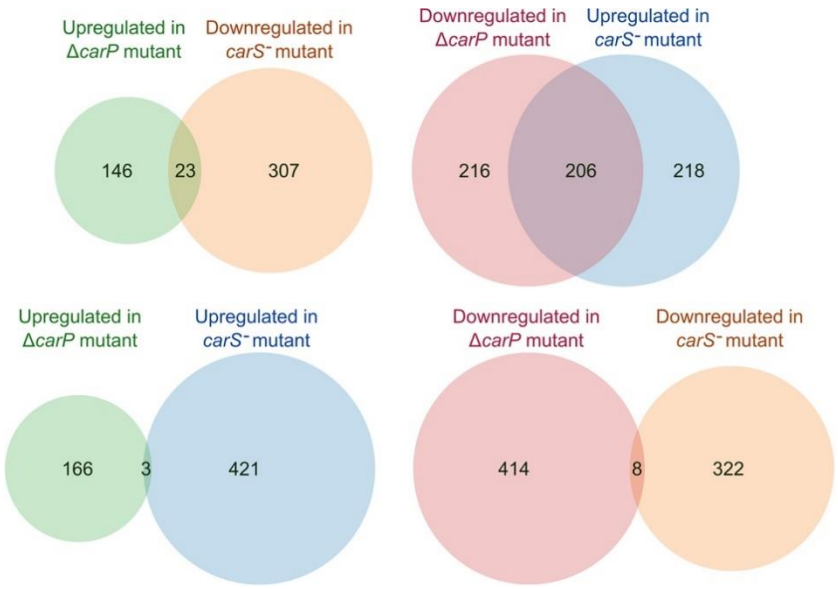

Figure C2.18**.** Relation between the genes affected by the Δ*carP* or the *carS*$^-$ mutations. Venn diagrams show the proportion of coincident genes between those upregulated or downregulated in any of the combinations between the tested mutants. Data for *carS* mutant taken from RNA-seq analyses of the effect of the *carS* mutation (Ruger-Herreros et al., 2019).

The product of the gene *carS* downregulates the expression of all the genes involved in NX and retinal biosynthesis in *F. fujikuroi* (Fig. C19A). All these genes are also upregulated by light (enzymes indicated in red in the pathway in the same figure). The comparison of the effects of *carS* and *carP* mutations showed opposite effects in these genes, with a clear upregulation for all of them in the absence of *carP*. Such effect was particularly strong for the genes of the *car* cluster, which includes the gene for the CarO rhodopsin. Only mild effects were appreciated for the genes corresponding to the early steps in terpenoid biosynthesis, from HMG-CoA to FPP, shared with the synthesis of sterols. Interestingly, the gene *carY* exhibited the opposite pattern, but the effect was less pronounced, and its significance is doubtful.

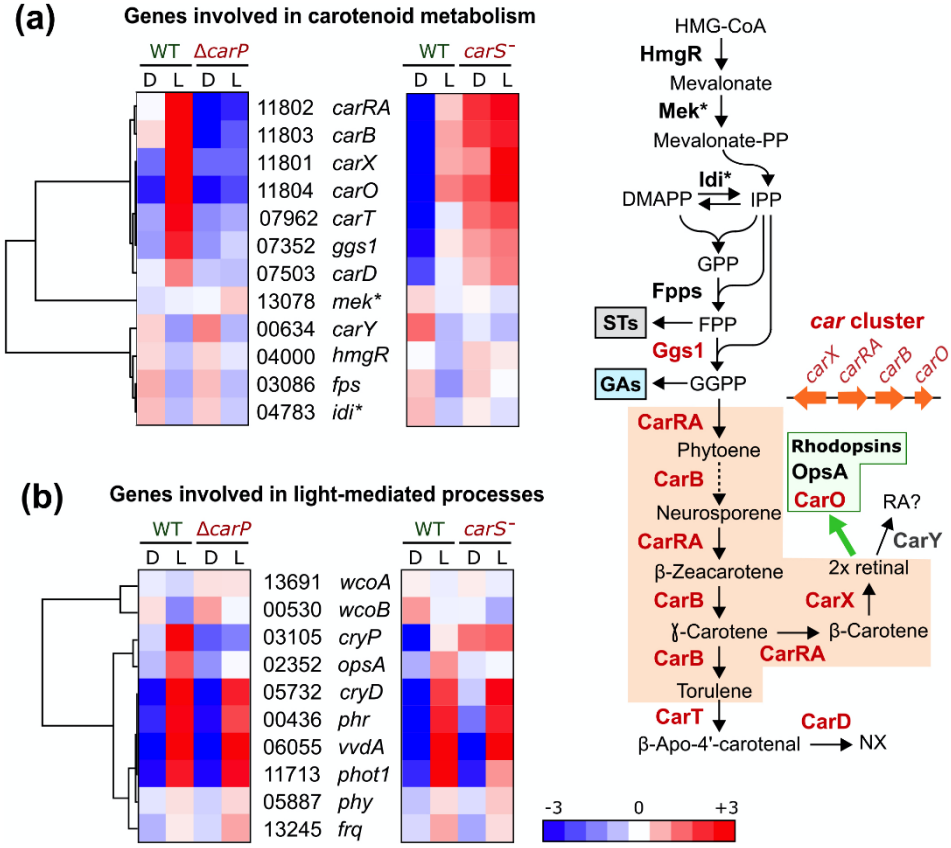

Figure C2.19. Relation between the effects of the Δ*carP* or the *carS*⁻ mutations on the expression of the genes related with carotenoid metabolism or with regulation by light. (a) Hierarchical maps of the relative transcript levels for the genes involved in carotenoid metabolism. Reactions carried out by each encoded enzyme are depicted on the right panel. Enzymes whose genes are regulated by light are indicated in red. The orange box indicates reactions encoded by genes from the *car* cluster. The green box highlights the rhodopsins OpsA and CarO as presumed users of retinal as prosthetic group. The dotted lines indicate more than one reaction. HMG-CoA: hydroxymethyl glutaryl coenzyme A; DMAPP, dimethyl allyl diphosphate; IPP, isopentenyl diphosphate; GPP, geranyl diphosphate. FPP, farnesyl diphosphate; GGPP, geranylgeranyl diphosphate; STs, sterols; Gas, gibberellins; RA?, possible formation of retinoic acid. (b) Hierarchical maps of the relative transcript levels for the genes involved in light regulation. In (a) and (b) the numbers correspond to the *FFUJ_* codes in the genome.

Because of the relation of *carP* with light regulation, the effects of the *carS* and *carP* mutations on the mRNAs for the genes encoding photoreceptors were also investigated and compared to the equivalent data from the RNA-seq analyses of the *carS* mutant (Fig. C2.19). The

gene for the protein homologous to Frq of *N. crassa*, involved in circadian rhythmicity, was also included in this analysis. The heatmaps showed that the genes encoding the DASH cryptochrome CryD, the photolyase Phr, the flavoprotein VvdA and the phototropin Phot1 (mentioned in chapter 3) were strongly induced by light, but such induction was not affected by the *carP* lncRNA, as was not basically affected either by CarS. However, the gene for the other cryptochrome CryP, and to a lesser extent also the gene for the rhodopsin OpsA, were downregulated in the *carP* mutant. The *carS* mutation produced the opposite effect in *cryP* mRNA levels, but not in the case of *opsA*, for which a similar downregulation was also observed in the *carS* mutant. No clear changing patterns were found in the other genes investigated, those for the White-collar proteins WcoA and WcoB, the phytochrome Phy, and the protein Frq.

Interestingly, the comparison of our RNA-seq data with those previously available on the influence of the *carS* mutation on the transcriptome shows the existence of genes that were clearly affected by the *carP* deletion but on which the *carS* mutation had no important influence. Examples were mostly found in the case of genes upregulated in the Δ*carP* mutant, and some outstanding ones are displayed in Figure C2.20.

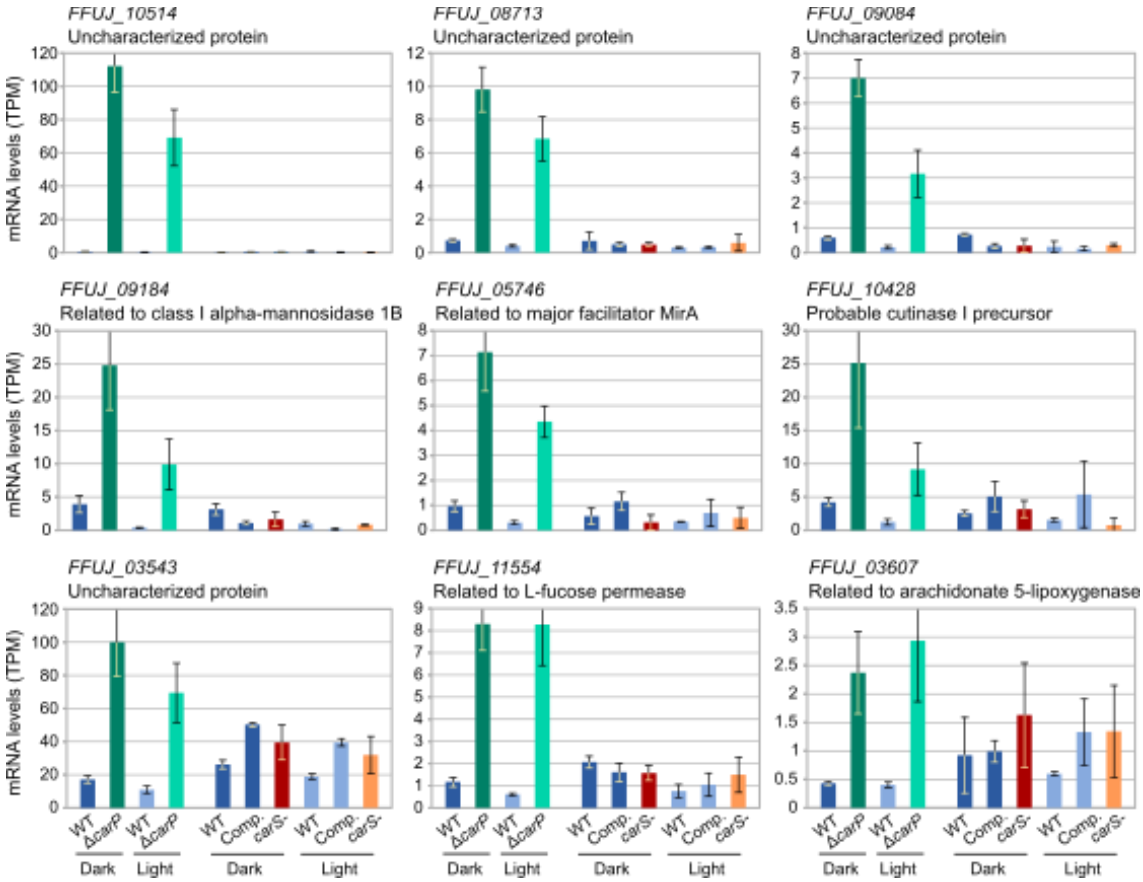

Figure C2.20. Examples of genes differentially expressed in the *carP* mutant that were not affected by *carS* mutation. Expression is represented in TPM. Transcriptomic datasets from which the data were extracted are the RNA-seq analyzed in this chapter and those from the work described in Ruger-Herreros et al. 2019.

DISCUSSION

The emergence of massive sequencing techniques has changed our perspectives on the coding capacity of the genomes. Being the pervasive transcription a conserved characteristic of eukaryotes, the discovery of non-coding transcripts which may play regulatory roles is becoming more and more frequent in every studied organism (Ponting et al., 2009). Although most of the described efforts in understanding lncRNAs correspond to other taxonomic groups, including well characterized examples in yeast already mentioned in the introduction of this chapter (Yamashita et al., 2016), filamentous fungi are not an exception in terms of the presence of these regulatory elements.

The existence of non-coding transcripts has been described in several filamentous fungi, including the model organism *N. crassa*, which was the first one in which it was reported (Arthanari et al., 2014). A massive RNA sequencing revealed 939 lncRNAs, more than half of them antisense of annotated genes. Among them stands out for the attention it has received *qrf*, the antisense transcript of the *frq* gene, a key element of the molecular clock (Xue et al., 2014). Regarding the genus *Fusarium*, 2,574 lncRNAs were identified *in F. graminerarum*, including 1,040 antisense transcripts, of which 547 exhibited differential expression associated to the formation of fruiting bodies (Kim et al., 2018). Recent examples of lncRNAs in other fungi are *Metharrizium robertsii* (Wang et al., 2019b), in which lncRNAs involved in the heat stress response were identified, or *Cordyceps militaris* (Wang et al., 2019a). The only example of a fully characterized lncRNA in filamentous fungi is HAX1 from *T. reesei* (Till et al., 2018b), which plays a regulatory role in the expression of cellulases. HAX1 was identified thanks to the study of phenotypic alterations exhibited by insertional mutants (interestingly, a similar situation to the origin of the discovery of *carP* in our study), and targeted mutation and overexpression confirmed its role. Hax1 exerts its function forming an RNA-protein complex with the activator Xyr1, interfering with its negative feedback regulatory loop (Till et al., 2020).

The combined studies in *F. oxysporum* (Parra-Rivero, 2018) and *F. fujikuroi* (this thesis), lead to the discovery for the first time of the participation of a *Fusarium* lncRNA, denominated *carP*, in a specific metabolic function (Parra-Rivero et al., 2020b). Although it is difficult to affirm the lack of translation of a lncRNA, the divergence between the predicted ORFs in the *carP* sequence in both *Fusaria*, while their deletions produce similar phenotypes, supports the absence of a conserved protein involved in the regulatory function of *carP*. *Fo-carP* and *Ff-carP* alignment showed that the lack of correlation between their sequences is basically due to the occurrence of gains or losses of few bases. Therefore, the function was maintained during evolution regardless the ORFs. Incidentally, one of the ORFs of *F. oxysporum* was previously annotated as a hypothetical protein in *F. oxysporum f.sp. vasinfectum* and *pisi*, but it was not annotated in other *Fusarium* genomes. Several bioinformatic tools were used to check the coding capacity of *carP* and none of them found any indication of protein coding functions either in *Fo-carP* or *Ff-carP* (Parra-Rivero et al., 2020b), including analyses based on 3-base periodicity, codon usage, or tools as the Coding Potential Calculator and RNAcode. Our findings strongly indicate that *carP* plays a role as a lncRNA.

The *carP* sequence is specific to *Fusarium* among the fungi and is not found outside the fungal kingdom. Even within the *Fusarium* genus, the *carP* sequence is widespread but not universal, being absent in one third of the species. However, when it was present, it exhibited a high sequence conservation, even though orthologous lncRNAs tend to show weak sequence similarity between organisms (Pang et al., 2006), while retaining their function. A possible consensus secondary structure has been described for *carP* suggesting the possibility of a structure-based function, while lacks matching sequences in the predictable target genes seem to discard the modulation of the translation or stability of mRNAs involved in carotenogenesis (Parra-Rivero et al., 2020b). A partial deletion of *Fo-carP*, only affecting the 3' segment, resulted in a phenotype very similar to the elimination of the entire *carP*. This could be interpreted as that the 3' end region of *carP* plays an essential role in its function, but it does exclude the possibility of an overall RNA structure-depending function of the molecule (Parra-Rivero 2018).

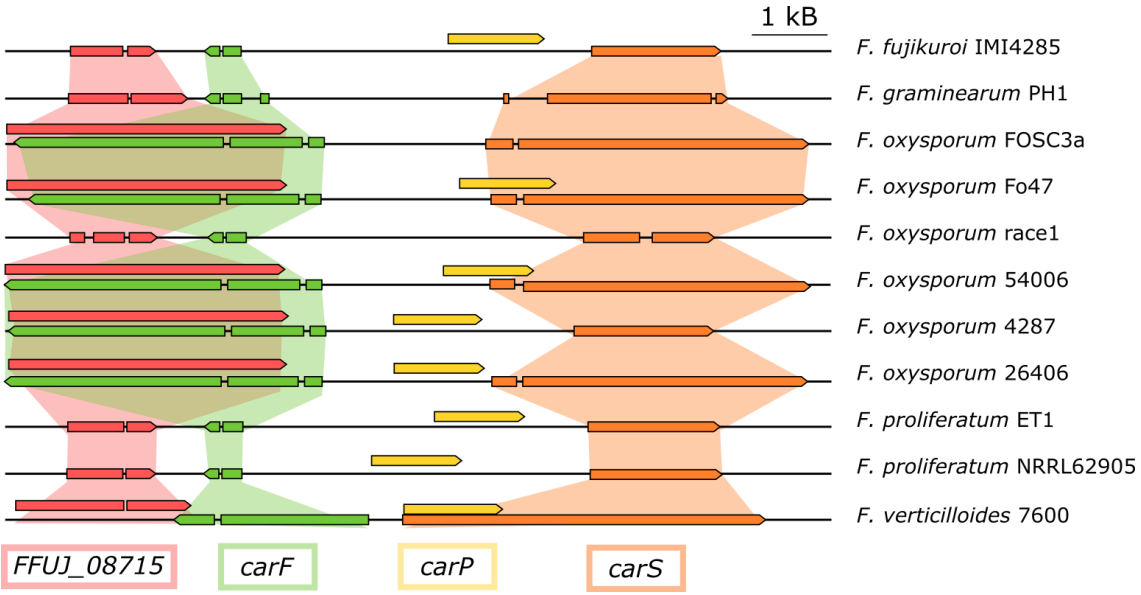

Figure C2.21. Transcripts associated to protein-coding genes in the *carS* region of several *Fusarium* species. Data correspond to syntenic sequences referred to *F. oxysporum* f. sp. *lycopersici* 4287, as shown in the Browser FungiDB with the available *Fusarium* genomes. Sequences of *carP* are shown as a yellow arrow in the species in which it could be identified (Modified from Parra-Rivero et al. 2020).

The results on the synthesis of *carP* and *carS* as independent transcripts in *F. fujikuroi* and *F. oxysporum* does not rule out their potential linkage in other species (Fig. C2.21). In fact, in the *Fusarium* species in which *carP* is present, there is a high variability in the 5'-UTR of *carS* gene (Parra-Rivero et al., 2020b). In some cases, the 5' end of the *carS* transcript extended to the 4-kb upstream region, and at least in the case of *F. verticillioides*, it overlapped with the homologous *carP* sequence, being the length of this 5'-UTR very exceptional compared to usual 5'-UTR lengths (Leppek et al., 2018). This suggests an evolutionary origin for *carP* from a long 5'-UTR region of the *carS* gene, that later developed its own function as an independent regulatory transcript. This also makes sense in terms of the differences in transcript levels observed for *carP* and *carS*.

RNA-seq readings of *carP* are scarce in the wild strain under the studied conditions, indicating a low transcription or a very short life for this lncRNA. However, the levels rise in the *carS* mutant, suggesting a putative regulatory loop between both genes. RT-qPCR results later confirmed the photorepresion of *Ff-carP*, an opposite behavior to the photoinduction of the transcript in *F. oxysporum*, which already suggests regulatory differences between both organisms, despite their similar *carP* deletion phenotypes.

Δ*Ff-carP* mutants are significantly affected in carotenoid synthesis in both light and in darkness. Nevertheless, the fungus still maintains the photoinduction of the transcript levels for the structural genes of carotenogenesis, the albino phenotype being due to the nearly 100-fold decrease in transcript levels in the two conditions studied. This differs from the results obtained in *F. oxysporum*, in which photoinduction of the *car* genes in the *ΔFo-carP* mutant was less apparent. On the other hand, the lack of effect of *carP* deletion on the expression of the photoreceptor genes is consistent with a downstream effect in carotenogenesis regulation.

The reintroduction of the *carP* sequence in the *ΔFf-carP* mutant has provided valuable information about its mechanism of action. Even though the two carotenoid-producing complementing transformants exhibited phenotypic variability, they support *carP* as a *cis*-regulatory element, as the rest of the transformants, although being able to transcribe *carP*, are still albino. These results rule out a mechanism of action like the one described for HAX1, as a transactivator of carotenogenesis. Although the three-dimensional conformation of *carP* could interfere with the function of a putative regulatory protein, e.g. binding CarS and blocking its carotenogenesis repressor function (which would be consistent with the accumulation of *carP* transcript in the absence of a functional CarS polypeptide), it seems not likely due to the position-dependent function of the *carP* transcript.

The *carP* reintegration experiment allowed to confirm the photorepression of *carP* under illumination, something that in previous analyses was not sufficiently clear. That was possible since transcription of *carP* was apparently higher (until 10-fold increase in RNA levels) in some of the transformants, as T2 and T21. It also confirmed that even a relative overexpression of *carP* RNA was not sufficient to revert the albino phenotype if it is not on its native locus.

The phenotypic differences between the two complementing strains which recovered the ability to produce carotenoids are puzzling. The increased *carS* transcript levels could explain the lower transcription of *carB* in SG268, T2 and T21, being sensibly higher than the wild strain in both conditions. They could even be the cause of T3 intermediate phenotype, in which the carotenoids accumulation exists but not as strongly as in the wild strain, coinciding with an intermediate transcription of *carS* between albino and wild strains. Nevertheless, T18, whose *carS* mRNA levels are comparable to those in T3, presented much higher mRNA levels of *carB* and therefore, accumulated more carotenoids. The molecular reasons that cause the phenotypic disparity between the wild strain and the transformants T3 and T18, and even between these two, remain unknown. Both *carS* and *carP* sequences in the two transformants were sequenced to check if they had mutations that could explain their different behavior. No mutations were

detected excepting the already mentioned C deletion in the unstranscribed upstream *carP* sequence, but even if this change affected the regulation of the *carP-carS* system, it was present in both strains.

With the available data, considering the most noticeable effect of *carP* deletion was the loss of pigmentation due to a drastic reduction in the synthesis of carotenoids and in the transcription of the genes of its biosynthetic pathway, the potential regulatory linkage between *carP* and *carS* remains the most likely explanation for this phenotype, at least in the case of carotenogenesis. An evident hypothesis is that the expression of the *carP* gene exerts a negative action on the function of the downstream *carS* gene, which encodes a repressor protein for carotenogenesis. Recently it has been shown that *carS* expression is finely regulated to allow an adequate response of carotenoid synthesis in response to light, since the increase of the wild-type level of *carS* transcription leads to an albino phenotype (Marente et al., 2021), and its loss of function produces an overproducing phenotype. Previous RNA-seq studies performed with a *carS* mutant demonstrated that the CarS protein influences the expression of an extensive battery of genes. If the hypothesis of the regulatory role of *carP* on *carS* is true, it is expected in the Δ*carP* mutant cascade effects reminding those produced by the *carS* mutation. Our analyses of the effect of the Δ*carP* mutation on the transcriptome confirmed this result, but only for genes whose expression is decreased in the mutant, including those for carotenogenesis. As the Venn diagrams from Fig. S2.18 show, this was much less evident for the case of genes upregulated in the absence of *carP*.

Previous data on the influence of CarS on the *F. fujikuroi* transcriptome showed a high coincidence between the genes influenced by this protein and those affected by light. Our results with the *carP* mutant are reminiscent of this association between light and CarS, but in a different way: a high proportion of the genes regulated by light lose this regulation in the absence of a *carP* transcript. Photocarotenogenesis, as other photoresponses in this organism, is mediated by the WcoA protein, presumably in coordination with the WcoB protein forming a complex. However, the loss of *carP* does not noticeably affect the expression levels of WcoA or WcoB, nor does it affect those of the genes of other photoreceptors that also participate in the regulation of carotenogenesis by light, such as CryD and VvdA (Castrillo and Avalos, 2015).

According to the hypothesis of the action of *carP* as a regulatory element of *carS*, the lack of coincidence between the downregulated genes in the *carS* mutant and the genes affected both positively and negatively by the *carP* mutation suggest that *carP* can exert repressive actions on other genes without mediation of the CarS protein. The detailed analysis of the expression data of these genes, and their comparison with the effects produced by the *carS* mutation, showed the existence of genes strongly affected by *carP*, without changing significantly in the *carS* mutant. This was especially clear for genes upregulated in the *carP* mutant. Among them there were several genes of unknown function with a sharp rise in their mRNA levels in the absence of *carP* either in the dark or after illumination, while there was no apparent change in the *carS* mutants. Although with not so strong effects, a similar result was obtained for some photorepressed genes, as those for a protein related to a class I-alpha-mannosidase 1B (*FFUJ_09184*), major facilitator MirA (*FFUJ_05746*), or a cutinase I precursor

(*FFUJ_10428*). These examples of genes strongly upregulated in the Δ*carP* mutant but hardly affected by the *carS* mutation suggest that the lncRNA *carP* exert regulatory functions without the mediation of *carP*. The genes found to be affected by *carP* in a *carS*-independent may be the result of direct *carP* effects, or secondary effects resulting from the control by *carP* of expression or activity of other regulatory proteins.

The mechanism of action of *carP* is still a subject for debate, and there are different possibilities. *CarP* might act as a scaffold to facilitate the assembly of histone modification enzymes and alter the expression of target genes. An example of a *cis*-acting lncRNA of this type is the *GAL10* lncRNA in *S. cerevisiae*. Under glucose-caused repressing conditions, *GAL10* ncRNA is produced and mediates di- and trimethylation of K4 and dimethylation of K36 on histone 3 by Set2. These are repressive chromatin marks which are bound by Eaf3, which recruits the histone deacetylase Rpd3S, thus resulting in broad deacetylation and silencing of the whole *GAL* locus (Houseley et al., 2008). *TERRA*, on the other hand, acts in *trans* as a scaffold for telomeric DNAs and chromatin-modifying enzymes during telomere synthesis (Luke and Lingner, 2009). Nevertheless, the most common described mechanism for lncRNAs in yeast is transcriptional interference, in which lncRNAs transcription results in the downregulation of a downstream neighbor gene due to alterations in the start of such gene transcription. This is the case of *SRG1* also in yeast, which regulates in this way the *SER3* gene (Niederer et al., 2017). This hypothesis could suit better the case of the *carP* gene, whose transcription could interfere negatively with the transcription of *carS*. However, the transformants T3 and T18, which express *carP* at higher levels, also present more *carS* mRNA compared to the wild strain, and so they do not support this model. It must be noted that lncRNAs may act not only modulating the transcription of the target gene, but also altering the stability of target transcripts, as the case of SUT169 (Huber et al., 2016). In summary, although some progress has been made in the understanding of its mechanism of action, the way in which *carP* exerts its control over carotenogenesis is still unknown, and it will be the focus of future work.

This work constitutes one of the very few efforts done in the characterization of filamentous fungi lncRNAs, which for sure will exponentially increase in the near future. The available information points to the lncRNA *carP* as a *cis*-regulator element for *carS*, either transcriptionally or post-transcriptionally, but the transcriptomic results also point to possible effects of *carP* that could not be related directly with CarS function. After the efforts spent on the characterization of the deletion mutants in two *Fusarium* species, future studies should be addressed to understand the biochemical mechanism by which *carP* exerts it function, with transcriptional interference, direct interaction with CarS protein or other regulator, or posttranscriptional modifications of *carS* mRNA, as the more likely hypotheses.

Chapter 3

Impact of the white-collar photoreceptor WcoA and the DASH-cryptochrome CryD on the *F. fujikuroi* transcriptome

CHAPTER 3: IMPACT OF THE WHITE COLLAR PHOTORECEPTOR WCOA AND THE DASH-CRYPTOCHROME CRYD ON THE *F. FUJIKUROI* TRANSCRIPTOME

INTRODUCTION

Light is not only a primary source of energy (photosynthesis), sunlight properties such as intensity, duration, polarization, and spectral composition are used as sources of information (Casas-Flores and Herrera-Estrella, 2016). The integration of light as external signal helps organisms to improve their survival, their fitness, and their ability to compete in their environment (Tisch and Schmoll, 2010). Filamentous fungi are no exception, and electromagnetic radiation, ranging from UV to infrared wavelengths, can trigger several metabolic and genetic responses to regulate a wide diversity of biological processes, affecting many aspects of fungal life. Except for some yeast species, e.g. *S. cerevisiae* and *S. pombe,* and some dermatophytid pathogenic species, all studied fungi present some type of photoreceptor (Fischer et al. 2017).

The life cycle of fungi is strongly affected by light. At a developmental level, it plays a determinant role in morphological and physiological processes, including phototropism, conidial germination, hyphal branching and sexual and asexual development (Corrochano, 2019; Dasgupta et al., 2016; Fischer et al., 2017) (see general introduction). Light can also have metabolic effects, as reprogramming of primary metabolic pathways or alteration of secondary metabolites or hydrolytic enzymes production (Schmoll, 2011). Fungal photoresponses modulate also pathogenicity, as shows the effect of light on the timing of infection in *Botrytis cinerea* (Hevia et al., 2015). Visible light perception can also serve to warn the mycelia about the environmental stresses associated with light, including genotoxic UV exposure, oxidative stress, increased temperature, or desiccation (Fuller, Loros, and Dunlap 2015). *Fusarium*, as other ascomycetes, presents a wide variety of photoresponses, of which photocarotenogenesis has been the one described in more detail. Secondary metabolism is not usually influenced by light in *Fusarium*; however, light is a major regulatory signal in the control of carotenogenesis (Avalos and Estrada, 2010). *F. aquaeductuum, F. oxysporum* and *F. fujikuroi* have been used as models to study photocarotenogenesis (Avalos and Estrada, 2010; Avalos et al., 2017b). Another process that is frequently influenced by light in *Fusarium* is conidiation (Avalos and Estrada, 2010), but the diversity of strains, experimental approaches and culture conditions makes the response diverse. Perithecia formation and ascospore release are stimulated by light in *F. graminearum* (Trail et al., 2002). An excess of light reduces germination in conidia of *F. fujikuroi* (García-Martínez et al., 2015). Even pathogenicity may be affected by photoreceptors in *F. oxysporum* (Ruiz-Roldán et al., 2008).

Light is also an important input in circadian rhythmicity, and in *N. crassa* and other fungi, the light-sensing and circadian clock systems share the main blue light photoreceptor, the White-Collar complex (Yu and Fischer, 2019). The White-Collar complex (WCC) is composed of

WC-1 and WC-2 proteins and is essential for light sensing in *N. crassa* (Dasgupta et al., 2016; Fuller et al., 2016). Molecular features of the complex and its mechanism of action in *N. crassa* have been already detailed in the general introduction. White collar proteins contain a Zn finger domain that allows binding to specific target sequences in DNA, and WC-1 has in addition a LOV domain, which induces a conformational change in the protein when it absorbs light (Fischer et al., 2017). Both allow the WCC to operate as a transcription factor with a light-regulated activity (He et al., 2002).

Fungal genomes frequently contain orthologs for *wc-1* and *wc-2* genes, and this is the case of *Fusarium* (Corrochano, 2019). Although due to their taxonomical proximity to *N. crassa* and the occurrence of photoinduced NX accumulation, an albino phenotype was predictable, null mutants of the *wc-1* orthologous genes of *F. fujikuroi, wcoA*, exhibited carotenoid accumulation under illumination, suggesting the participation of at least an additional photoreceptor (Estrada and Avalos, 2008). As already stated in the general introduction, similar results have been reported for the *wc-1* orthologs in *F. oxysporum* (*wc1*) and *F. asiaticum* (*Fawc1*) (Ruiz-Roldán et al., 2008; Tang et al., 2020) However, WcoA was found to be the major transcriptional activator of the genes of the carotenoid pathway in *F. fujikuroi*, as indicated the drastic reduction of mRNA levels for the *carRA* and *carB* genes in the absence of this protein, either in the dark or following illumination (Estrada and Avalos 2008; Castrillo and Avalos 2015). Moreover, the synthesis of other metabolites, such as bikaverin, gibberellins or fusarins, were also altered in the *wcoA* mutants, pointing to a wider regulatory role in SM production (Estrada and Avalos 2008). In other *Fusarium* species secondary metabolism, as aurofusarin and tricothecene synthesis in *F. graminearum* (Kim et al., 2014), are also affected. Interestingly, the mutation caused phenotypic effects not only in light but also in the dark, affecting other biological processes. The colonies of the *wcoA* mutant have an aberrant morphology, they present a reduced surface hydrophobicity as well as altered conidiation patterns when grown on media with different amounts of nitrogen (Estrada and Avalos 2008), indicating that WcoA can control the transcription of many genes in the absence of its alleged regulatory signal. In fact, different phenotypes were linked to the different domains of the protein in *F. asiaticum* (Tang et al., 2020). Among Fusaria, the White-collar 1 protein is also involved in processes as relevant as sexual reproduction (Kim et al., 2015; Tang et al., 2020) and virulence, both on plants (Tang et al., 2020) and animals (Ruiz-Roldán et al., 2008).

As already indicated, *F. fujikuroi* has other photoreceptors in addition to the WCC: two rhodopsins (Adam et al., 2018), one phytochrome and three proteins of the cryptochrome/photolyase family (Chaves et al., 2011). One of them is the DASH cryptochrome CryD. In other fungi, cry-DASH proteins are involved in different light-dependent processes such as development of sexual structures in *Sclerotinia sclerotium* (Veluchamy and Rollins, 2008), conidiation, which is repressed by light in *B. cinerea* (Cohrs and Schumacher, 2017), fruiting body development and secondary metabolism, both regulated by light in *Cordyceps militaris* (Wang et al., 2017a), and circadian rhythm, which is slightly altered in the cry-DASH mutant of *N. crassa* (Froehlich et al., 2010). Previous work on *F. fujikuroi* showed that the mutant lacking the *cryD* gene had phenotypic alterations only under illumination. The *cryD* mutants produced

macronidia in medium with low nitrogen, unlike the wild strain, and showed differences on morphology and pigmentation of the colonies, especially at high temperature (Castrillo et al., 2013). Secondary metabolism was also affected, producing higher levels of bikaverin and lower amounts of gibberellins than the control strain. These changes in the production of secondary metabolites were different from those shown by the *wcoA* mutants, indicating a complex regulatory role for CryD, which is at least partially independent of WcoA (Castrillo et al., 2013). Moreover, mRNA levels for the biosynthetic genes for bikaverin and gibberellins did not correlate with the amounts of the metabolites, suggesting a post-transcriptional regulatory mechanism for CryD, possibly associated with mRNA translation or stability (Castrillo et al., 2013). The photochemical properties of the CryD protein have been investigated (Castrillo and Avalos, 2015). The protein showed binding of the two characteristic cofactors of cryptochromes, FAD and MTHF, and its ability to repair thymine dimers in single strand DNA. However, DNA lesion repair is probably not a major role for CryD in *F. fujikuroi* since no differences in sensitivity to UV were observed between wild type and the *cryD* mutant conidia. The most interesting finding was the presence of RNAs bound to purified CryD protein and its effect on the protein behavior. RNAs present in the preparations accelerated the photoreduction from FADox to FADH- and affected the catalytic turnover of the repair of thymine dimers. RNA also competes with DNA probes for binding to CryD, with the possibility of forming tripartite RNA-CryD-DNA complexes due to the presence of two nucleic acid binding sites. It was proposed that CryD may post-transcriptionally modulate the gene expression through direct binding to specific RNA targets.

To gain information on the functions in *Fusarium* of the widespread WC-1-like fungal photoreceptor WcoA and the presumed accessory photoreceptor CryD, we described here the effect of the mutations of both genes on the transcriptome of *F. fujikuroi*, either in the dark or after several times of illumination. The results of the impact of WcoA on the *F. fujikuroi* transcriptome have been recently published (Pardo-Medina et al., 2021).

RESULTS

EXPERIMENTAL DESIGN

The study of the effect of the *wcoA* mutation and the *cryD* deletion on the transcriptome of *F. fujikuroi* was addressed with the RNA-seq methodology. For this objective, we used the mutants available for these genes in *F. fujikuroi*, *wcoA* (Estrada and Avalos 2008) and *cryD* (Castrillo et al., 2013), which have been obtained from the wild strain FKMC1995, different from the strain IMI58289 used in the first two chapters. Two *wcoA* mutants, SF226 and SF229, were generated by interruption of the *wcoA* coding region with a Hyg^R resistance cassette, and two *cryD* mutants, SF236 and SF237, in which the *cryD* gene was replaced by a Hyg^R resistance cassette, were selected to perform the experiments in comparison to the control wild strain FKMC1995.

In order to deepen in the study of the effect of light on the *Fusarium* transcriptome, in this chapter different illumination times were used. In a recent study (Ruger-Herreros et al., 2019), already mentioned, the effect of white light in the transcriptome of *Fusarium* was analyzed in parallel in *F. fujikuroi* IMI58289 and *F. oxysporum* f. sp *lycopersici* 4287 comparing total RNA samples from mycelia grown in the dark or after one hour of illumination. This time of light exposure was chosen regarding previous RT-PCR data on expression of structural genes of carotenogenesis, selecting the time when their mRNA levels were higher (Avalos and Estrada, 2010). The experiment also included the transfer of cultures grown in a flask in dynamic conditions to static Petri dishes under red safelight, where the light exposure is more homogeneous. This process entails major changes in the culture conditions, especially in aeration. So, to have a clearer idea of the short-medium term effects of this modification, the levels of mRNAs of the *car* genes were checked as a reference for light-induced expression in a new experiment. After transferring the culture to the Petri dishes, samples were taken at increasing times of incubation (from 1 to 24 hours) in darkness and RNA was extracted from the mycelia. This change in culture conditions led to a decrease in the relative mRNA levels of the genes *carRA* and *carB* during the first four hours, which then slowly stabilized (Fig. C3.1B). Taking samples at different times of illumination immediately after the transfer to the Petri dishes would overestimate the level of induction of genes like the ones tested. So, for a better comparison of different light exposures, illumination was carried out in this study after 4 h of adaptation of the culture to the static conditions in the Petri dish in the dark.

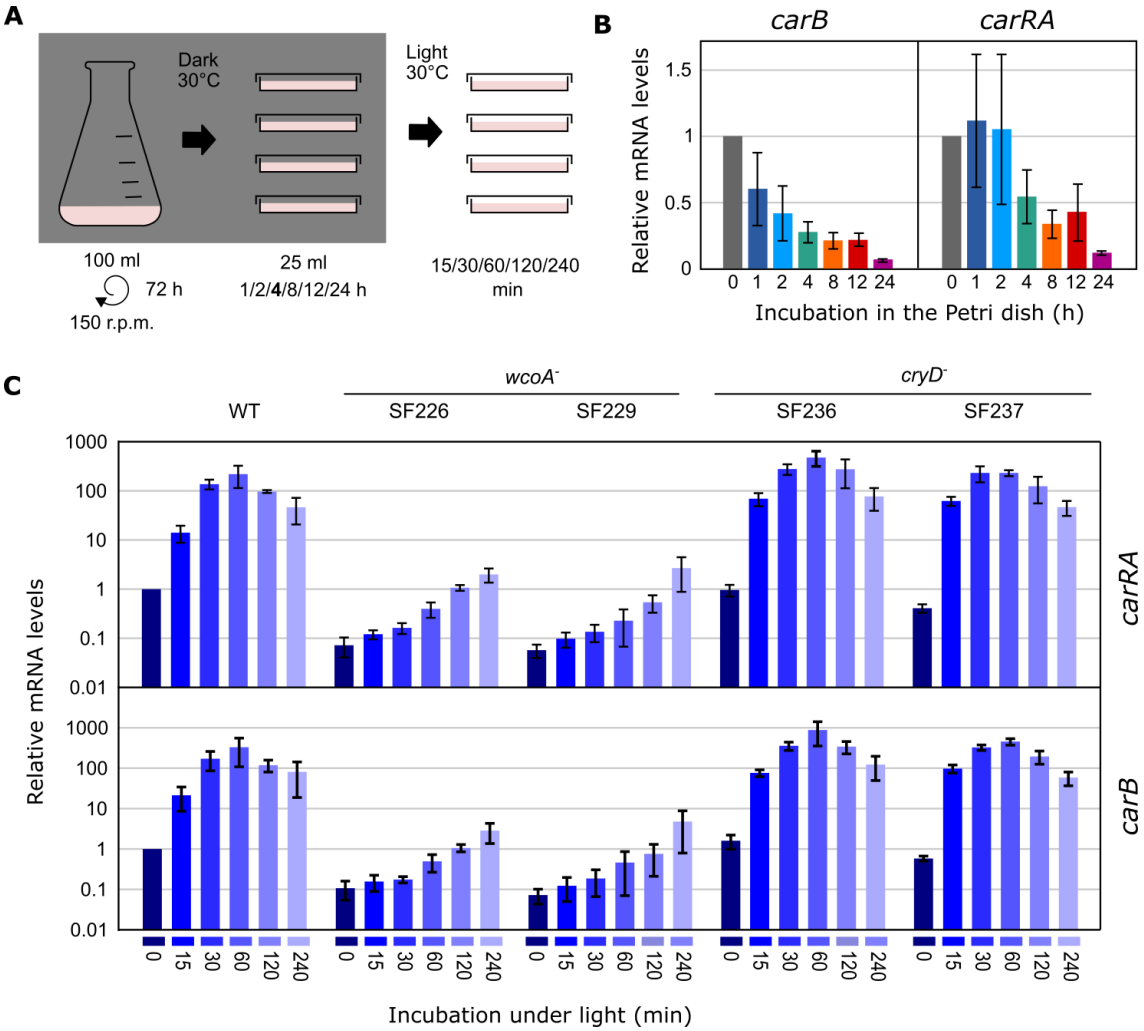

Figure C3.1. Experimental design and mRNA levels of the *carRA* and *carB* genes. (A) Schematic representation of the experimental conditions used for illumination. The cultures were transferred to Petri dishes for more homogeneous illumination. Final conditions chosen for the transcriptomic experiment are highlighted. (B) Effect of the incubation of the mycelia of the wild strain in the Petri dish in the dark on mRNA levels of the *carRA* and *carB* genes. The times correspond to the hours after the transfer from the flasks. Primer sets used to measure the expression of the genes were RTPS6 for *carRA* and RTPS.4 for *carB*. Transcript levels were normalized against the β-tubulin with primers RTPS.5. Relative mRNA levels refer to the mRNA content of the wild strain in darkness. (C) Effect of illumination on the mRNA levels of the *carRA* and *carB* genes after 4 h of incubation in the dark. RTPS primer sets are located in table A.3, Material and Methods

Once fixed the conditions to carry out the experiment, mycelial samples were taken after the three days of flask dynamic incubation, 4 hours of adaptation in Petri dishes and the corresponding times of subsequent exposure to white light (experimental conditions described in detail in the Materials and methods section). Prior to the RNA-seq study, relative mRNA levels for the *car* genes were determined in the control sample in the dark and after 15 min, 30 min, 60 min, 120 min and 240 min of illumination for the wild strain and the *wcoA* and *cryD* mutants (Fig. C3.1C) As expected from previous works (Castrillo and Avalos, 2015), the mRNA content of the *car* genes increased rapidly upon illumination and reached maximal values after one hour, to slowly decrease afterwards. The RNA samples from the cultures of the *wcoA* mutant, done in

parallel, revealed a drastic decrease in the levels of those genes. However, they still exhibited a noticeable increase upon illumination which did not reach a peak after 60 min of illumination. On the other hand, the expression of the *car* genes in the *cryD* mutant increased slightly compared to the wild strain. This contrasts with a former report, in which a small reduction was described in the mutant (Castrillo and Avalos, 2015), although in that case there was not a 4-h adaptation in the dark in the Petri dish before light exposure.

To ensure statistical reliability three independent biological replicates were used per each experimental condition. However, the use of 5 different light exposure times and 3 strains, added to the control conditions in the dark, resulted in an excessive number of samples. Therefore, 15, 60 and 240 min were chosen as light exposure times for the wild strain and the *wcoA* mutant in order to perform a sufficiently detailed description of the general photoresponse in *Fusarium*, similar to other works done with *N. crassa* (Wu et al., 2014). In the case of the *cryD* mutant, which is expected to have lower transcriptomic effects, the analysis was limited to samples grown in the dark and after one hour of illumination. Moreover, as the behavior between mutant strains was very similar, only one of them was used for each gene.

Table C3.1 Summary of the conditions and strains whose RNA was subjected in triplicate to RNA-seq analyses. These abbreviations will be used to mention the investigated samples throughout the chapter.

Samples (x3)		Light exposure time (min)			
		0	15	60	240
Strains	WT (FKMC1995)	WT0	WT15	WT60	WT240
	SF226 (*wcoA*-)	WC0	WC15	WC60	WC240
	SF237 (Δ*cryD*)	CRY0		CRY60	

In summary, to investigate the role of the WcoA and CryD photoreceptors at the global transcriptomic level, we performed RNA-seq analyses with three replicates of mycelia of the wild strain and the mutant SF226 (*wcoA*$^{-}$) incubated either in the dark or exposed to 15 min, 60 min, and 240 min of illumination; and three replicates of mycelia of the mutant SF237 (Δ*cryD*) incubated in the dark and after 60 min of illumination. Final data used for this experiment are summarized in Table C3.1.

EXTRACTION, QUALITY CONTROL AND SEQUENCING OF THE SAMPLES

RNA-seq technology generates a large amount of information that, as a previous step to its analysis, must undergo an evaluation of the quality of the RNA samples and their corresponding sequencing data (Conesa et al., 2016; Zhou et al., 2013). Total RNA from each sample was obtained using the TRIzol reagent extraction protocol, treated with DNAse I, and purified by passing through a commercial kit column. The quality and integrity of the RNA samples was evaluated by spectrophotometry (A260/A280>1.8 and A260/A230>1.5) and agarose gel visualization and the samples were sent for mass sequencing to LifeSequencing S. L. (Valencia). The RNA Integrity Number (RIN) was also quantified, and their values ranged between 9.5 and 10 (Table A1, Methods), being recommended a minimum value of 8 to proceed with the sequencing protocol (Schroeder et al., 2006). No evidence of degradation was observed, and 18S and 20S ribosomal RNAs were detected in a correct relationship.

Sequencing was carried out using the Illumina platform (Metzker, 2010). Samples were sequenced on Illumina's NextSeq platform in 75 mode bp single read. 'Bcl2fastq2' version 2.19.1 provided by Illumina was used for the conversion of 'bcl' files into 'fastq' sequence files, program which also removes the sequencing adapters. Raw reads for all samples were trimmed, filtered, and quality controlled with AfterQC (Chen et al., 2017). The readings obtained and their basic characteristics are described in Table C3.2.

ANALYSIS OF THE EFFECT OF SHORT-, MEDIUM- AND LONG-TERM LIGHT EXPOSURES IN THE WILD STRAIN AND THE *wcoA* MUTANT

The complexity of the total amount of RNA-seq data led us to independently analyze by separate the effects of the mutation of each photoreceptor, beginning with the effect of the different light exposures on the wild-type and *wcoA* mutant transcriptomes. Sequences were mapped with TopHat 2.1.1 (Trapnell et al., 2009). A meta-assembly of the transcriptome with the Cufflinks-Cuffmerge protocol (Roberts et al., 2011) was generated to improve the level of annotation of the analyzed strain. 16,888 transcripts were annotated, while the reference genome annotation presents 15,095 genes. Quantification was performed using the RNA-seq quantitation pipeline with the improved mRNA annotation generated by Cuffmerge, merging transcripts and counting reads over exons. The representation of expression data corrected for each gene and expressed as RPM (Reads Per Million mapped reads) in a bean plot graph (Fig. C3.2D) showed a high parallelism between all the samples. A Pearson correlation matrix for all pairs of data stores (Fig. C3.2C), showed that the dataset owed its main source of divergence to the strain genotype, compared to the light exposure condition, which played a less influential role.

Table C3.2 Basic characteristics of the sequenced samples and yield of the readings.

Sample name	Number of reads	Average length	Average quality	G+C%	Mapping rate (%)
CRY0_R1	1.92E+07	75.53	33.66	54	68.2
CRY0_R2	2.27E+07	75.53	33.69	54	60.5
CRY0_R3	2.12E+07	75.53	33.65	54	67
CRY60_R1	2.41E+07	75.54	33.64	54	67.8
CRY60_R2	2.11E+07	75.52	33.64	54	67.4
CRY60_R3	2.36E+07	75.51	33.76	54	66.8
WT0_R1	2.96E+07	75.52	33.65	54	66
WT0_R2	2.60E+07	75.52	33.67	54	66.1
WT0_R3	2.31E+07	75.51	33.45	54	67.5
WT15_R1	2.19E+07	75.52	33.68	54	67.3
WT15_R2	2.14E+07	75.52	33.7	54	66.9
WT15_R3	1.54E+07	75.52	33.62	54	67.8
WT60_R1	2.05E+07	75.51	33.62	54	67.4
WT60_R2	1.90E+07	75.52	33.65	54	66.6
WT60_R3	2.41E+07	75.53	33.67	54	67.3
WT240_R1	2.25E+07	75.49	33.68	54	66.1
WT240_R2	2.32E+07	75.5	33.55	54	66.3
WT240_R3	2.12E+07	75.52	33.67	54	67.7
WC0_R1	1.79E+07	75.53	33.65	54	71.9
WC0_R2	1.93E+07	75.53	33.64	54	70.9
WC0_R3	1.79E+07	75.52	33.64	54	71.2
WC15_R1	1.98E+07	75.53	33.52	54	71.5
WC15_R2	2.21E+07	75.53	33.59	54	71.8
WC15_R3	1.85E+07	75.53	33.62	54	68.2
WC60_R1	2.01E+07	75.53	33.61	54	71.3
WC60_R2	1.87E+07	75.53	33.61	54	70.6
WC60_R3	1.72E+07	75.53	33.6	54	70.7
WC240_R1	2.35E+07	75.51	33.54	54	70.4
WC240_R2	1.94E+07	75.52	33.63	54	70.8
WC240_R3	2.43E+07	75.53	33.56	54	67.8

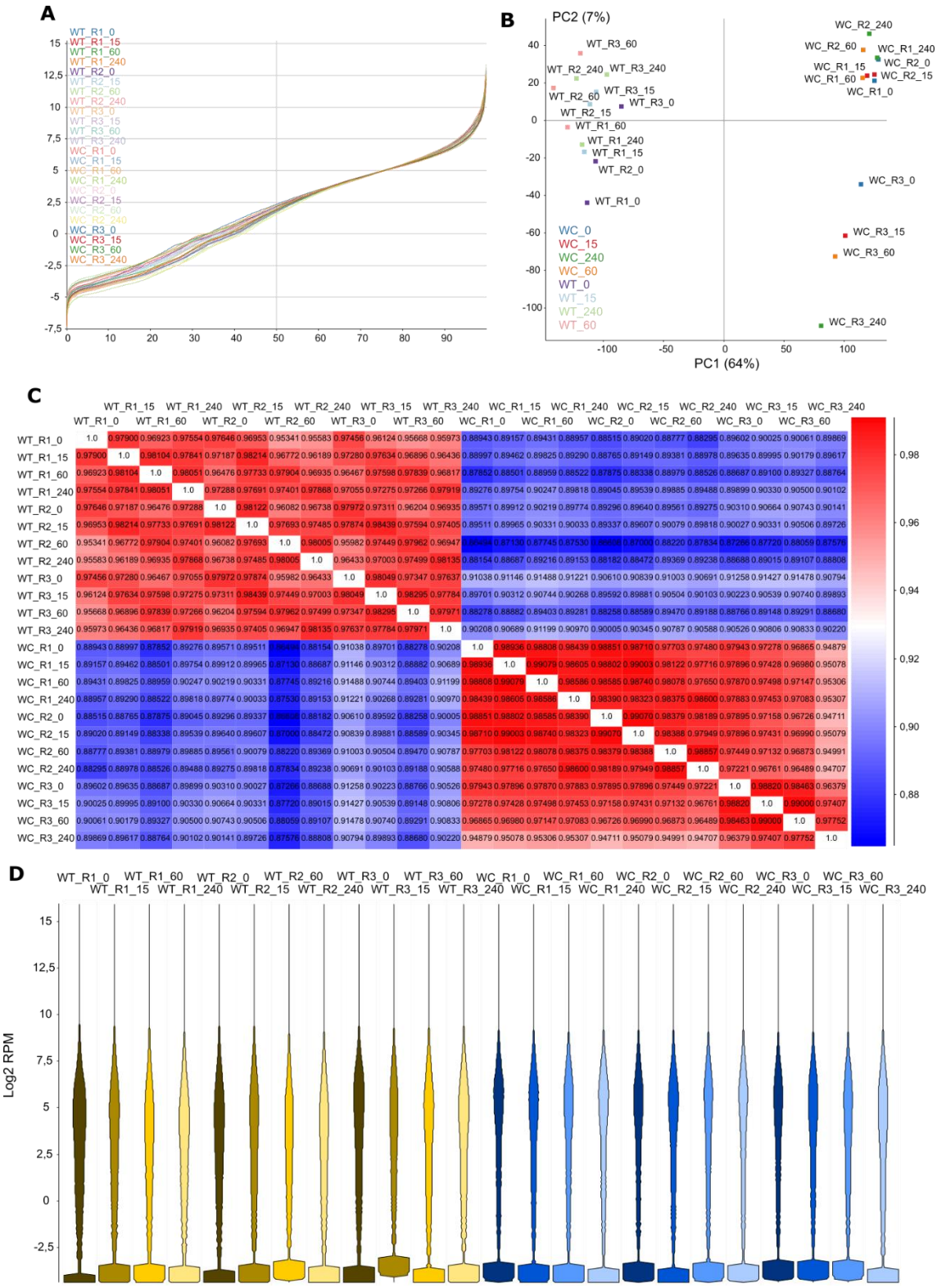

Figure C3.2. Dispersion and distribution graphs of the wild strain and *wcoA* mutant RNA-seq samples. (A) Cumulative distribution plot after percentile normalization. (B) PCA plot. (C) Pearson's correlation matrix. (D) Bean distribution plot.

Deseq2 tool (Love et al., 2014), implemented in SeqMonk, which needs raw counts for quantitation, was used to compare transcript levels between conditions. As the number of affected genes, especially as a result of the *wcoA* mutation, was unexpectedly high, a relatively high threshold was used to focus on the most relevant regulatory effects. The differentially expressed genes were selected based on criteria combining a log2 fold change of 2 and a *p*-value of 0.05. Those genes whose fold-change was higher than this threshold, were considered as activated, and those with a value below the threshold, were considered as repressed. Based on the mentioned criteria, the number of genes activated and repressed because of light or the *wcoA* mutation are shown in Table C3.3.

Table C3.3. Number of genes whose expression changed more than four-fold (log2 = 2) above (activated) or below (repressed) the controls, under the indicated conditions. The percentage refers to the total number of genes annotated in the reference genome (15,095). New transcripts not formerly annotated are indicated in parenthesis.

	Activated	%	Repressed	%
Effect of 15 min light in the wild strain	67 (+4)	0.44	5 (+1)	0.03
Effect of 60 min light in the wild strain	226 (+15)	1.50	84 (+12)	0.56
Effect of 240 min light in the wild strain	116 (+4)	0.77	80 (+10)	0.53
Effect of 15 min light in the *wcoA* mutant	1	< 0.01	0	-
Effect of 60 min light in the *wcoA* mutant	3 (+1)	0.02	0	-
Effect of 240 min light in the *wcoA* mutant	21 (+5)	0.14	22	0.15
Effect of *wcoA* mutation in the dark [a]	1,877 (+253)	12.43	588 (+86)	3.90
Effect of *wcoA* mutation after 15 min light [a]	1,567 (+220)	10.38	750 (+116)	4.97
Effect of *wcoA* mutation after 60 min light [a]	1,870 (+205)	12.39	708 (+102)	4.69
Effect of *wcoA* mutation after 240 min light [a]	1,530 (+164)	10.14	560 (+101)	3.71

[a] Comparisons between wild strain and *wcoA* mutant.

Effect of illumination time in the wild strain transcriptome

Analysis of the data showed a very high number of genes affected by light with a four-fold activation, around 1.5% of the total number of genes in the genome, while the proportion of repressed genes was appreciably lower. Among those influenced by light, the analyses revealed also new transcripts that did not correspond to genes formerly identified in the genome annotation (indicated in parenthesis in Table C3.3). Total numbers of differentially expressed transcripts (DET) after different illumination times are represented in Fig. C3.3C. As expected, the major effect of light was observed after one hour of illumination, resulting in changes in expression of 337 transcripts. Induction was predominant over repression (*ca.* 71% *vs* 29%), being the impact on the activated genes also higher than on the repressed ones (Fig.

C3.3.A). Seventeen transcripts exhibited more than 64-fold increase (log2 = 6) after 60 min of illumination compared to the control in the dark, while the highest repression was of log2 = -5.8 (Fig. C3.3B). The 15-min and 240-min illumination exposures had less impact on *F. fujikuroi* transcriptome, as shown in the corresponding scatter plots (Fig. C3.3D). Transcripts that met the parameters of being differentially expressed more than log2 = 2 were 77 and 210 respectively (Fig. C3.3C). Mostly, light had a short-term induction effect, as it only repressed 4 transcripts of the total ones affected after 15 min (92% vs. 4 %), but this proportion falled gradually till reaching almost a balance between induction and repression after 240 min (57% vs. 43%). This shift in the tendency of the transcriptomic response probably reflects secondary transcriptional effects.

Overall, 298 transcripts were induced by light under any of the illumination conditions tested. Nevertheless, their induction was not homogeneous among conditions. In fact, they exhibited considerable variation in induction patterns, as shown in a Venn diagram (Fig. C3.3E). There was only partial overlapping between the transcripts induced after 60 min and those responding to 15 min and 240 min, being the shared ones also different between these two groups. Only 25 transcripts were induced more than 4-fold at the three illumination times. Among those genes we can find those belonging to the *car* cluster, which were used as a previous illumination control prior to the sequencing of the samples (Fig. C3.3G). Of the 241 transcripts induced after 60 min of light, 132 were not induced at the other exposure times, and just a few were induced exclusively after 15 min (18), or after 240 min (39). On the other hand, the transcripts repressed by light showed less variability, increasing its number after longer light exposures (Fig. C3.3C), stabilizing around 90 transcripts. In fact, transcripts with a sharp reduction in the first 15 min of illumination were essentially absent. However, the overlap between the 4-fold repressed transcripts after 60 and 240 min was only of 27, a third of the originally repressed ones on each of the illumination times (Fig. C3.3F).

Figure C3.3. Effect of illumination time on the wild strain transcriptome. (A) Box-plot representations of the log2RPM of the DET with a FC> ±log2(2) by 60 min of light exposure in the WT0 and WT60 transcriptomes. (B) Individual values of the log2(FC) of the previously mentioned DET upregulated (green) or downregulated (red) comparing dark *vs*. 60 min of illumination. (C) Numbers of genes upregulated (green) or downregulated (red) after 15, 60, or 240 min of illumination. (D) Scatter plot representations of the effect of 15, 60 and 240 min of illumination in the wild strain. Genes differentially expressed according to the Deseq analysis are indicated in blue. Genes exceeding the log2 values of ± 2 are indicated in red. (E) Venn diagrams of the overlap between the genes induced after the illumination times indicated. (F) Effect of 15, 60, and 240 min of illumination on the transcript readings according to RNA-seq data in the genomic region corresponding to the *car* cluster (*carX*: *FFC1_12355*, *carRA*: *FFC1_12354, carB*: *FFC1_12353*, and *carO*: *FFC1_12352*). In each condition, the profiles are the result of merging the three independent biological samples. The readings (0-2000) were represented with IGV program. (G) Venn diagrams of the overlap between the genes repressed after the illumination times indicated. (H) Venn diagrams of the overlap between the induced and repressed genes after 60 min of illumination according to CuffDiff analysis in *F. fujikuroi* IMI58289 and FKMC1995 (in this case only genes with a BBC with the IMI58289 were considered) strains. (I) Individual values of the log2(FC) of the previously mentioned DEG upregulated (green) or downregulated (red) comparing dark *vs*. 60 min of illumination dividing them into common genes for IMI58289 and FKMC1995 strains or specific ones. Common genes are represented with different FC for each transcriptome.

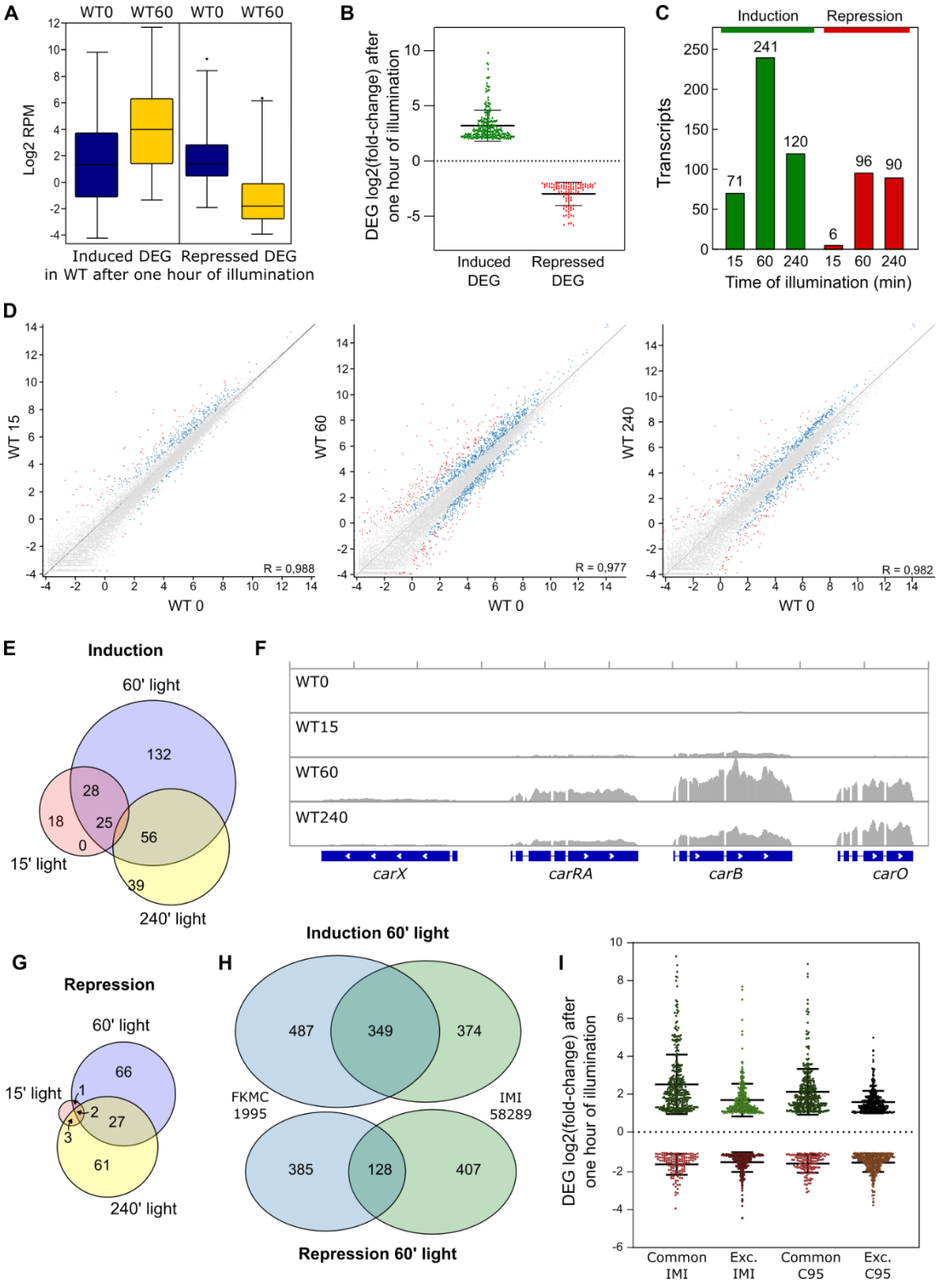
A
WT0 WT60 WT0 WT60
Log2 RPM
Induced DEG Repressed DEG
in WT after one hour of illumination
B
DEG log2(fold-change) after one hour of illumination
Induced DEG
Repressed DEG
C
Induction
Repression
Transcripts
71
241
120
6
96
90
15 60 240 15 60 240
Time of illumination (min)
D
WT 15
WT 60
WT 240
WT 0
R = 0,988
R = 0,977
R = 0,982
E
Induction
60' light
15' light
240' light
132
28
18
25
0
56
39
F
WT0
WT15
WT60
WT240
carX
carRA
carB
carO
G
Repression
60' light
15' light
240' light
66
1
2
27
3
61
H
Induction 60' light
487
349
374
FKMC 1995
IMI 58289
385
128
407
Repression 60' light
I
DEG log2(fold-change) after one hour of illumination
Common IMI
Exc. IMI
Common C95
Exc. C95

The effect of 60 min of illumination has already been studied in another work with a different wild strain (Ruger-Herreros et al., 2019). The results with FKMC1995 are comparable to those obtained with the wild strain IMI58289, in which log2 = 1 was applied as the threshold for induction or repression. Those data were analyzed with the Cufflinks protocol instead of the one from Seqmonk. The application of the Cufflinks method to our not-illuminated and 60-min illuminated samples in the wild strain FKMC1995, considering a log2 = 1 threshold, yielded 920 up-regulated and 590 down-regulated genes, similar to the 724 and 535 genes described in the equivalent samples in the wild strain IMI58289. To compare over or under-expressed transcripts, we used the proposed ortholog equivalences between the genes in the two *F. fujikuroi* strains proposed in the work in which the sequencing of FKMC1995 was published (Niehaus et al., 2017), although it implied the loss of some information about the genes in this strain which did not have orthologs. 836 upregulated genes and 515 downregulated genes of FKMC1995 after 60 min of illumination had a best-bidirectional hit gene in the IMI58289 genome. Nevertheless, and quite surprisingly, the overlap between those genes and the DEG in IMI58289 was not as high as expected (Fig. C3.3H), with 349 coincident up regulated and 128 downregulated genes. Nevertheless, although more than half of the photoinduced genes were only found in one of the strains, the genes which are commonly upregulated by light in both wild strains presented a higher fold-change than the specific ones, especially in FKMC1995 (Fig. C3.I), suggesting that many of the discrepancies corresponded to genes with a fold change not far from the log2 = 1 threshold. In the case of repression, there seemed to be no differences in terms of fold-change level. It must be noted that there were differences in the experimental conditions between the two sets of data, since the experiments with IMI58289 did not include the 4-h adaption step in the Petri dish before illumination. Moreover, only two replicates were done in that case, against the three replicates used in this Thesis with FKMC1995.

As an additional approach to analyze the variability of the responses to light in the FKMC1995 strain, a hierarchical clustering heat map was done to visualize the expression values for the differentially expressed transcripts at the different illumination times (Fig. C3.4A). The result showed that the effect of light was frequently transient. The highest induction usually took place after 60 min of illumination (called intermediate induction in the graph). There were 161 genes in this category. Variations among them were found in the level of adaptation to longer illumination, with higher or lower decreases after 240 min compared to levels at 60 min. This indicates that there are genes whose response to light might be needed while the stimulus input is maintained, while in others expression gradually fall. Two other groups could be distinguished in the clustering: a set of 94 transcripts exhibiting rapid induction after 15 min (fast induction), and a set of 43 transcripts that reached their higher levels after 240 min (slow induction). The results of the clustering analysis of transcripts whose expression decreased with light revealed two major sets, consisting of 132 that exhibited significant repression after 60 min of light (intermediate repression) and 27 genes with a sharp decrease in mRNA levels only after 240 min of illumination (slow repression).

FUNCTIONAL CATEGORIES OF GENES INFLUENCED BY LIGHT

GO enrichment analyses were performed to study the putative functions of the genes controlled by light in *F. fujikuroi* FKMC1995. This strain has received less attention than IMI58289, and its genome was only available as a draft version in 2017 (Niehaus et al., 2017). Therefore, its annotation is not as curated as the one of IMI58289. Although several tools were tested, including a *de novo* annotation with Blast2GO and GO enrichment within the same platform (Gotz et al., 2008), we finally opted for the FunCat algorithm, currently working online in the FungiFun2 platform (Priebe et al., 2015) and the Gene Ontology Enrichment tool in the FungiDB database (Basenko et al., 2018), that provides reliable data using a fast and amenable procedure. A disadvantage of these bioinformatics tools is that the annotation of the FKMC1995 genome has not been included yet, so we used the same system as for the comparison with the IMI58289 data and we used the corresponding BBHs, with the risk of loss of a minor part of the information. However, we considered that the potential benefits outweighed the risks for this exploratory analysis.

GO enrichment analysis revealed some of the significant functional categories affected by light in the FKMC1995 transcriptome. In general, photoinduced DEG provided more biologically significant data than photorepressed ones. According to FungiDB annotation, among the photoinduced transcripts enriched GO categories shifted temporally along the photoinduction process, although there were some shared ones that were maintained (Fig. C3.4B). The lists included the DEG obtained from comparisons between WT0 and the different illumination times, resulting in lists that contained 67, 226, and 116 upregulated DEG after 15 min, 60 min, and 240 min light exposures. Processes conserved along different illuminations times were 'response to stimulus' and 'response to stress'. This second category basically corresponded to 'response to oxidative stress', as has already been published for other fungi and for IMI58289 of *F. fujikuroi* (Ruger-Herreros et al., 2019). Another observed functional subcategory, included in the more general processes of 'pigment biosynthesis' or 'glyceraldehyde−3−phosphate metabolism', was 'carotenoid biosynthesis'. A specific subgroup of GO categories which appeared after longer illumination times was 'cell wall remodeling', absent after 15 min of light exposure. The groups of genes resulting from the data clustering, nevertheless, did not give any significant results using FungiDB database.

FunCat data on significant functional categories, on the other hand, revealed reliable results for the set of genes induced by light for 60 min (Fig. C3.4C), but interestingly, they reached a different biological depth. The list included 154 genes, belonging to 15 major categories and subcategories involved in very diverse metabolic functions, including 'metabolism related with carotenoid biosynthesis´. Most of them belonged to two major groups, 'cell rescue defense and virulence' and 'interaction with the environment'.

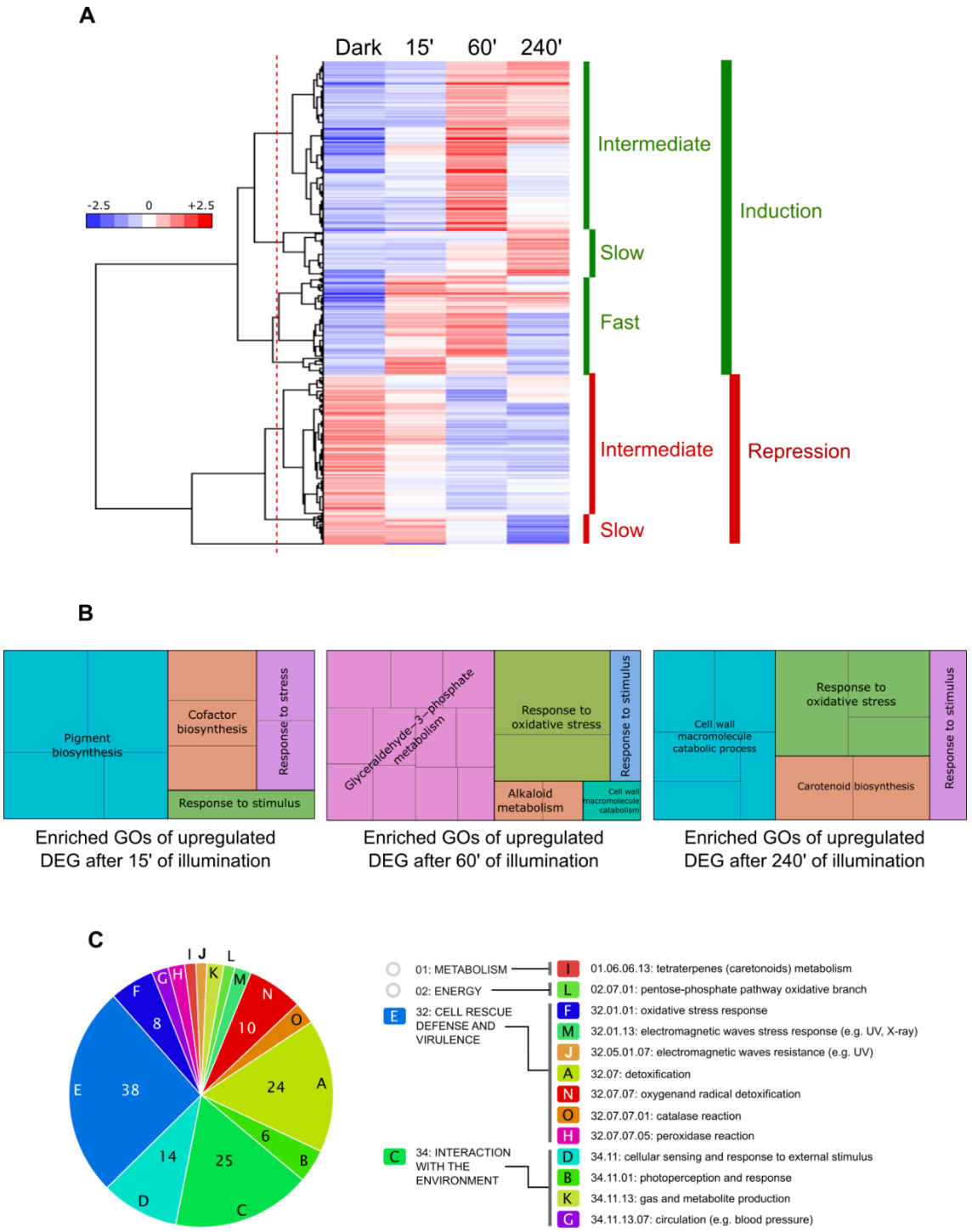

Figure C3.4. Effect of illumination time on the wild strain transcriptome. (A) Hierarchical heatmap of the genes induced or repressed under the illumination times indicated. (B) GO enriched categories of the upregulated DEG after 15 min, 60 min, and 240 min of photoinduction using FungiDB. (C) FunCat GO categories of the clustered genes with induction at 60 min.

The first one included several genes encoding proteins homologous to enzymes with presumable detoxification functions, such as a thioredoxin (*FFC1_12309,* log2 fold change 2.2), a thioredoxin peroxidase (*FFC1_05108*, log2 = 2.6), a glutathione S-transferase II (*FFC1_12341*, log2 = 2.7), an organic hydroperoxide resistance protein (*FFC1_02122*, log2 = 5.0), and two

catalases (*FFC1_14936*, log2 = 2.4, and *FFC1_13476*, log2 = 3.2). The second one included a putative HSP30 heat shock protein of the HSP30 family (*FFC1_12352*, log2 = 8.3), and some putative photoreceptors that remain to be investigated in this fungus, one similar to the phototropin 'nonphototropic hypocotyl protein 1' (*FFC1_12444*, log2 = 3.2), and a deoxyribodipyrimidine photo-lyase gene (*FFC1_07528*, log2 = 2.2), encoding a putative plant cryptochrome. Two other genes encoding proteins belonging to the deoxyribodipyrimidine photo-lyase group in *Fusarium*, the DASH cryptochrome CryD and the photolyase PHR, were detected as significant with this methodology only in the group of the early expressed genes, although they also exhibited a very strong photoinduction after 60 min of illumination (*cryD*: *FFC1_04237*, log2 = 8.9; *phr*: *FFC1_00478*, log2 = 5.2).

The FunCat results were less consistent for genes induced after 15 min or 240 min, or for genes repressed by light. A parallel analysis performed for the entire set of light-induced genes, grouping those induced after 15, 60, or 240 min of light, provided results like those obtained with 60 min**. I**n this case the total number of categories raised to 19, but not adding significant information.

EFFECT OF LIGHT IN THE *WCOA* MUTANT TRANSCRIPTOME

The absence of a functional WcoA had a drastic effect on the number of transcripts affected by light, showing a strong reduction in their numbers (Fig. C3.5A). Photoinduction of transcripts practically disappeared after short term light exposures and only after the longest time (240 min) a higher number of transcripts with a fold change above log2 = 2 were upregulated or downregulated. This was clearly visible in comparisons of scatter plots with those of the wild strain (data for 15, 60, and 240 min of illumination in Figure C3.5B, scatter plot of the effect of 60 min of illumination on wild-type transcriptome in Figure C3.5C for comparison purposes, the other two times can be found in Fig C3.3D). None of the transcripts induced or repressed after 15 or 60 min of illumination in the wild strain were significantly affected by light in the *wcoA* mutant, and the few genes induced by light in the mutant after these light exposures were not affected by light in the wild strain after the same illumination. Even more, the only transcripts deregulated in the *wcoA* mutant after 240 min of light exposure, 26 induced and 22 repressed (Fig. C3.5A), did not show major overlap with the equivalent gene sets in the wild strain, with only 3 activated and 4 repressed genes coincident (Fig. C3.5B). Taken together, the data point to WcoA as the major photoreceptor responsible for photoregulation of gene expression in *F. fujikuroi*.

Only four genes were induced by light in the *wcoA* mutant after 15 or 60 min, with a highest induction ratio of log2 = 3.4 (*FFC1_15159*, coding for an uncharacterized protein), and only two of them were also present in the set of 22 genes induced after 240 min (Fig. C3.5D). The pattern of transcript levels after illumination for the 26 genes induced by light was more homogeneous in the *wcoA* mutant (Fig. C3.5E), with a clear separation between 4 genes exhibiting a relatively fast response (Intermediate induction) and 24 exhibiting a slower response (Slow induction). However, the 22 genes that were repressed by light in the mutant

responded slowly, with significant reductions only after 240 min of illumination (Slow repression).

The 24 transcripts induced by 240 min of light in the *wcoA* mutant included those for *carRA* and *carB*, already found to show photoinduction in our RT-PCR assays of this strain (Figure 1C). This set also included genes for at least five proteins presumably associated to stress control: *FFC1_04281* (related to multidrug resistance protein), *FFC1_01433* (probable heat shock protein 30), *FFC1_09886* (related to AHA1-stress-regulated cochaperone), *FFC1_09644* (related to ADH4-alcohol dehydrogenase IV), and *FFC1_12341* (related to glutathione S-transferase II). Of these five genes, only *FFC1_12341* exhibited a significant induction by light in the wild strain, which was delayed in the mutant. On the other hand, the 22 transcripts repressed after 240 min light in the *wcoA* mutant included 8 genes associated to transport through the membrane: *FFC1_08950* (probable Na^+-transporting ATPase ENA-1), *FFC1_05826* (related to zinc transporter), *FFC1_09497* (probable SIT1-Transporter of the bacterial siderophore ferrioxamine B), *FFC1_04029* (related to peptide transport protein), *FFC1_14622* (NAAP-1 amino acid permease NAAP1), *FFC1_09245* (related to permeases-unknown function), *FFC1_09585* (probable general amino acid permease), *FFC1_15542* (probable uracil permease), as well as three other integral membrane proteins of unknown function.

EFFECT OF THE *WCOA* MUTATION IN THE *F. FUJIKUROI* TRANSCRIPTOME

Leaving aside the effect of illumination, the *wcoA* mutation had a high impact on the *F. fujikuroi* transcriptome compared to the wild strain (Table C3.3). As can be seen qualitatively in the corresponding scatter plots the effect of the mutation was huge regardless of the illumination time (Fig. C3.6). In the dark, a total of 674 and 2,130 transcripts were found to be activated or repressed in the *wcoA* mutant, respectively, relative to the wild strain. Similar numbers of activated or repressed transcripts were also found after 15-, 60-, and 240-min illumination (866, 810, and 661 for activation, and 1,787, 2,075, and 1,694 for repression, respectively). Globally, considering the matches between the different DET sets (Figure C3.7A), 2,843 transcripts were repressed and 1,297 were activated in the *wcoA* mutant. This means that 4,140 transcripts, *ca*. 1/4 of the total number of annotated genes, changed at least four-fold their levels due to the *wcoA* mutation in at least one of the conditions tested.

Even considering that these transcripts may include a high proportion of cascading effects, the results suggest that WcoA is an important transcription regulator in *F. fujikuroi*. Moreover, the abundance of downregulated genes in the *wcoA* mutant indicates a predominant role for WcoA as a positive regulator. Although there were variations in the transcript levels according to the illumination time, either up- or downregulation was usually maintained by most of the genes irrespective of light. Therefore, although WcoA is the key regulator involved in the control of gene expression by light, its major regulatory role seems to be light independent.

Figure C3.5. Effect of illumination time on the *wcoA* mutant transcriptome. (A) Numbers of genes upregulated (green) or downregulated (red) after 15-, 60-, or 240-min illumination. For comparison, the data for the wild strain are shown in pale color. (B) Venn diagrams of the genes induced (above) or repressed (below) after 240 min illumination in the wild strain and in the *wcoA* mutant. The intersection

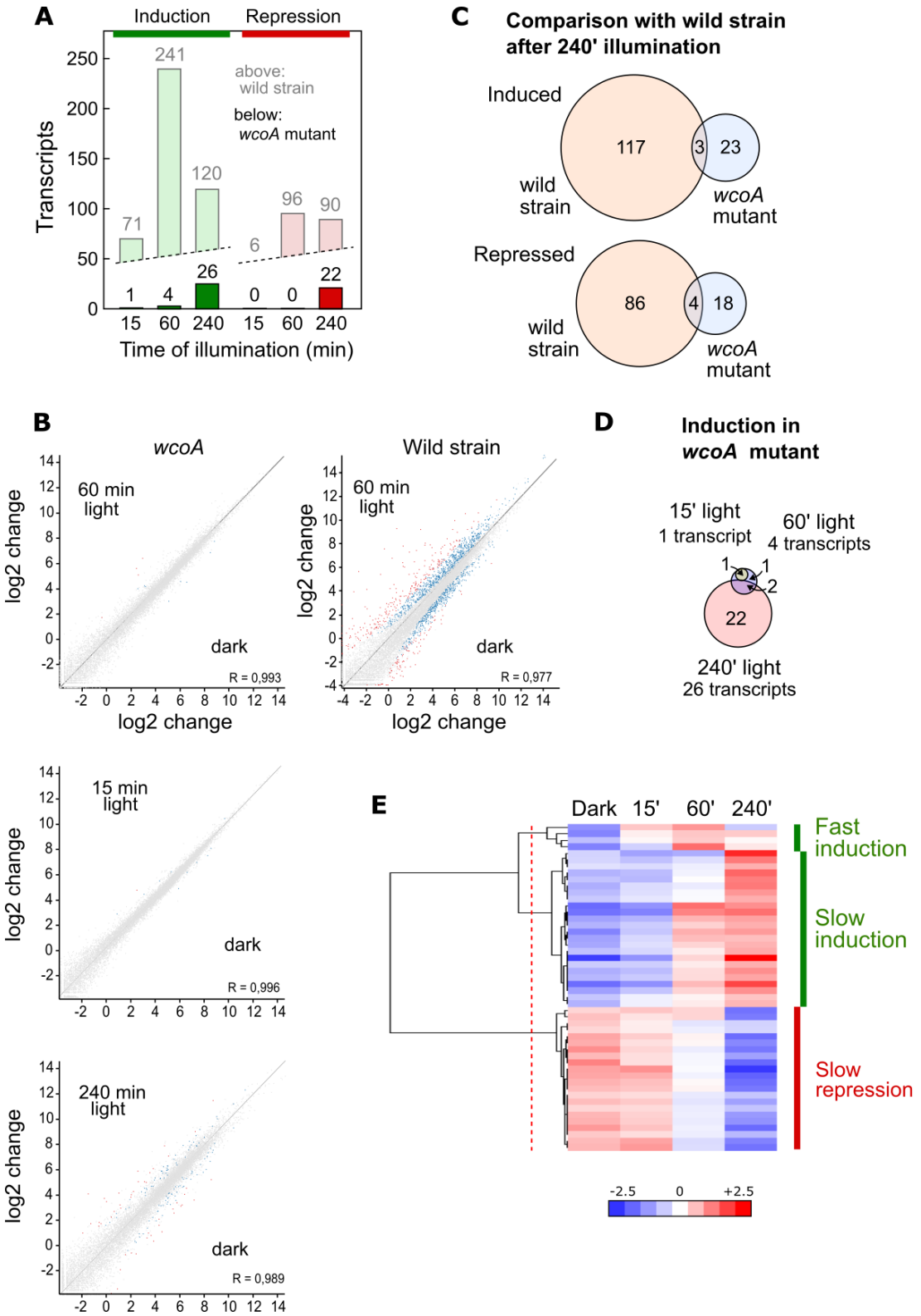

shows the number of genes induced in both strains. (C) Scatter plot representations of the effect of 15-, 60- and 240-min illumination in the *wcoA* mutant. Genes differentially expressed according to the Deseq analysis of the Seqmonk program are indicated in blue. Genes exceeding the log2 values of ± 2 are indicated in red. (D) Scatter plot representations of the effect of 60 min illumination in the wild strain for comparison purposes. (E) Hierarchical heatmap of the genes induced or repressed under the indicated illumination times in the *wcoA* mutant.

Due to the major consequences the *wcoA* mutation has on the *F. fujikuroi* transcriptome, the high number of affected genes makes difficult to discriminate between primary and secondary regulatory effects. Therefore, an alternative approach was used to extract the most affected processes in the investigated samples. The alteration of a biological system, in this case generated either by light or by the absence of a functional WcoA protein, is expected to affect large numbers of genes as the whole system becomes destabilized. Therefore, we applied the intensity difference filter tool, which checks the distribution of differences to find those whose change is not explained by the general level of disruption in the system. This method is expected to detect transcripts that changed in a stronger way as they directly respond to the stimulus, thus possibly reducing the list of hits. In our case, the intensity difference filter of SeqMonk detected 559 transcripts, which predictably explain the major transcriptomic differences in the *wcoA* mutant compared to the wild strain.

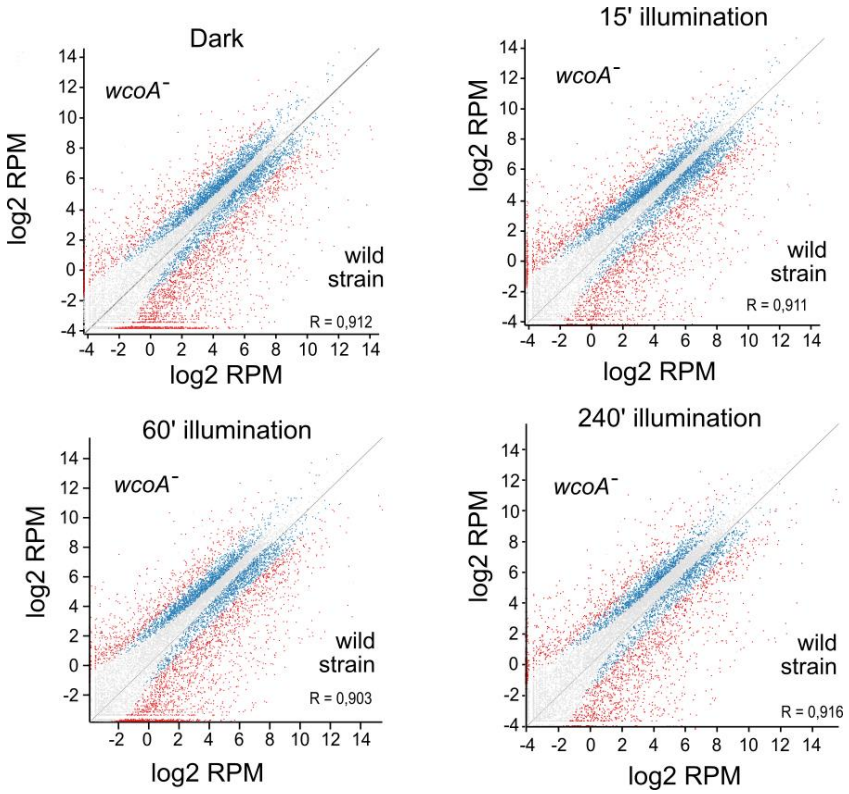

Figure C3.6. Scatter plot representations of the effect of *wcoA* mutation compared to the wild strain transcriptome in the dark and after each of the illumination times (15, 60 and 240 min). Genes differentially expressed according to the Deseq analysis of the Seqmonk program are indicated in blue. Genes exceeding the log2 values of ± 2 are indicated in red.

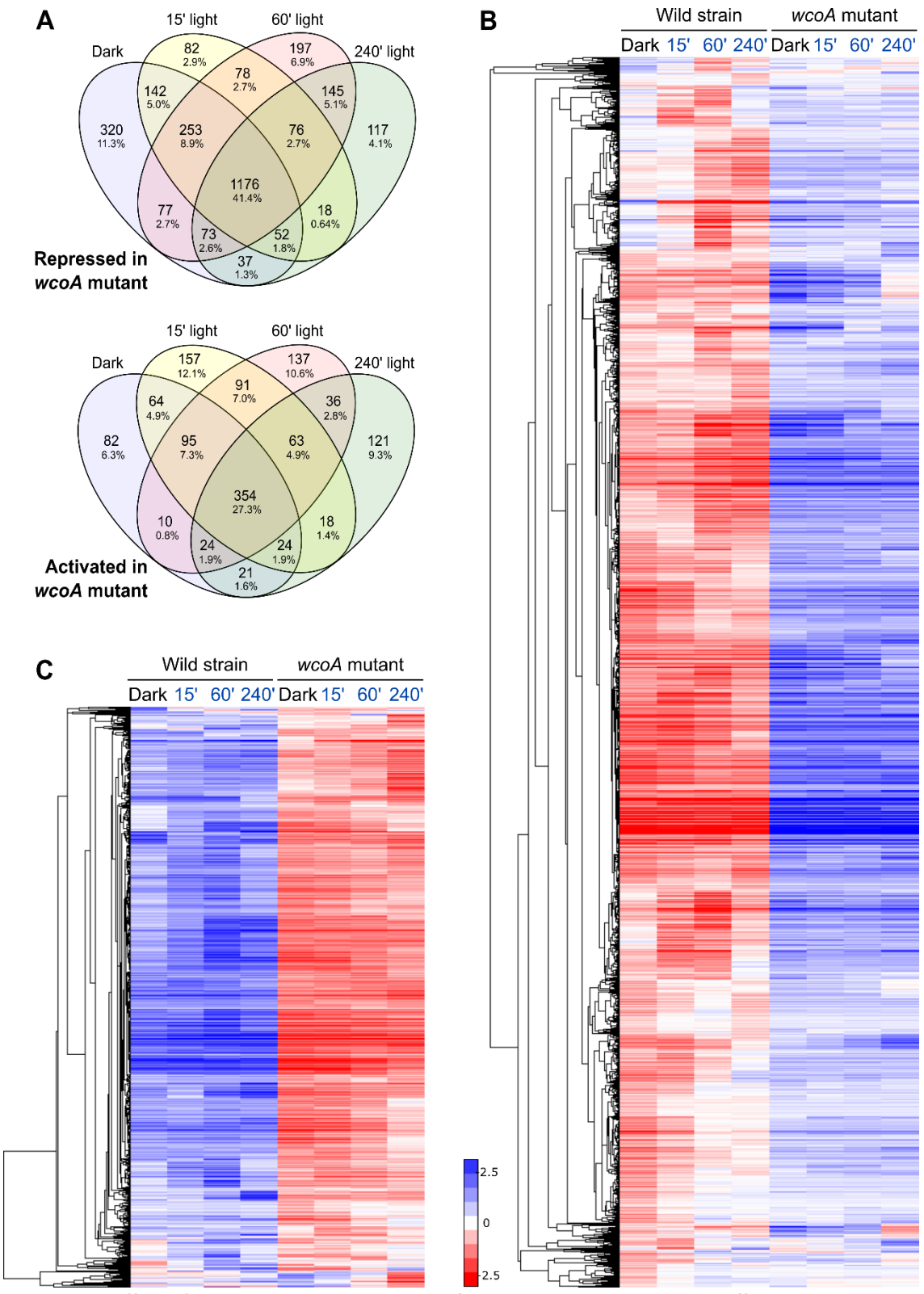

Figure C3.7. Effect of the *wcoA* mutation on the *F. fujikuroi* transcriptome under different light regimes. (A) Venn diagrams of the genes repressed (above) or induced (below) in the *wcoA* mutant in the dark or after the illumination times indicated. (B, C) Hierarchical heatmaps of the genes repressed (B) or induced (C) in the *wcoA* mutant under the illumination times indicated above.

The fact that most of the effects derived from the *wcoA* mutation are independent of light allows the use of the different light exposure datasets as experimental repeats for such effects, helping to discriminate among the processes affected. For more reliability, GO analyses of the WcoA-controlled genes were limited to those that changed in the mutant in all four conditions tested (dark, and 15-, 60- and 240-min illumination). These were found to be 354 induced and 1176 repressed in the *wcoA* mutant (Fig. C3.7A and 7B). FungiDB GO results, represented in word cloud graphs, already gave some hints about which processes were unregulated in the mutant. E.g., most of the affected upregulated genes seemed to be related to 'transmembrane transport' (Fig. C3.8A), particularly in 'metal transport', while the downregulated genes were mostly assigned to 'oxidative stress response' (Fig. C3.8B) and possibly, 'secondary metabolism'. Representations of the gene distributions in significant GO categories in FunCat (Fig. C3.8C and 8D) showed that the largest set of genes, corresponding to those with decreased mRNA levels in the *wcoA* mutant, showed less diversity of enriched functional categories, while more functional categories were observed in the set of upregulated genes (Fig. C3.8C and 8D). In both cases, the most relevant classes were related to metabolism, especially those involving secondary metabolism, which will be discussed below in more detail. Among the upregulated genes, stood out those related to transport systems (categories I, H, B, C, D, F in Figure C3.8C) and ion homeostasis (M, O, G). Other highly represented groups in both lists included genes of the 'cell rescue defense and virulence' categories, suggesting a possible participation of WcoA in pathogenesis.

When the genes deregulated in the *wcoA* mutant were contemplated from the perspective of photoinduction (Fig. C3.9), that is, if those that responded to light in the wild strain were separated from those that did not, secondary metabolism was also a predominant category in the genes not controlled by light, together with other functional categories already described in Figure C3.8C and 8D. The genes regulated by light in the wild strain, and affected by the *wcoA* mutation, included those of carotenoid metabolism and others involved in detoxification, especially the genes with catalase functions, already mentioned when the effect of light on the wild strain was described. FunCat categories were also applied to the list of 559 WcoA-influenced genes resulting after application of the SeqMonk intensity difference filter. The results reinforced the categories related to secondary metabolism and transport systems as those more relevant in the genes not regulated by light, while stress resistance and ion homeostasis were prevalent among the light-controlled genes (Fig. C3.10C).

Photoreceptors are a heterogenous group of proteins, and therefore, were not identified as a GO category by any of the databases. Former data showed that the genes for the DASH cryptochrome CryD (Castrillo et al., 2013), the small flavoprotein VvdA (Castrillo and Avalos, 2014), and the photolyase Phr (Ruger-Herreros et al., 2019), are among the most photoinduced genes in *F. fujikuroi*, and at least in the first two cases, their inductions are mediated by WcoA. The RNA-seq data confirmed these photoinductions (Fig. C3.9E). Moreover, the *carO* rhodopsin gene, which also belongs to the *car* cluster, also owed its photoinduction to WcoA, as the rest of the genes of the cluster. The second rhodopsin gene, *opsA*, was not photoinduced, but

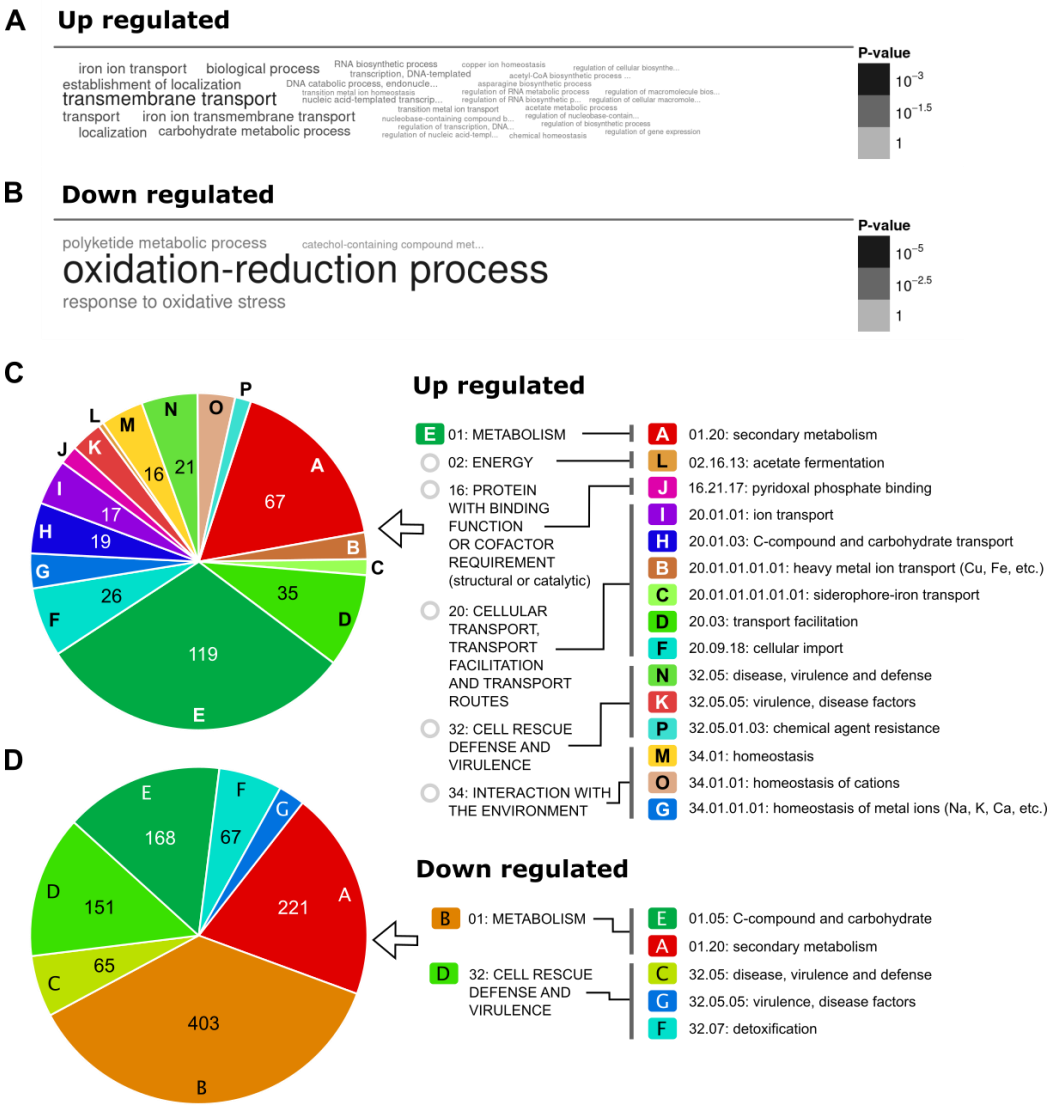

Figure C3.8. GO enrichment analysis of the differentially expressed genes due to the *wcoA* mutation in *F. fujikuroi*. (A) Word cloud graph of genes induced in the *wcoA* mutant (therefore, downregulated by WcoA) analyzed with FungiDB. (B) Word cloud graph of genes repressed in the *wcoA* mutant (therefore, upregulated by WcoA) according to FungiDB. (C) Categories of genes induced in the *wcoA* mutant (therefore, downregulated by WcoA) analyzed with FunCat. (D) Categories of genes repressed in the *wcoA* mutant (therefore, upregulated by WcoA) according to FunCat.

unexpectedly its expression was highly dependent on WcoA. The genes for two other predicted photoreceptors, the cryptochrome CryP (which has also been grouped as a 6,4 -PP photolyase (Cohrs and Schumacher, 2017; Cohrs et al., 2016) and the phytochrome Phy1, exhibited a slight photoinduction, with a clear dependence on WcoA only in the case of *cryP.* Finally, the photoinduction of a newly discovered putative phototropin gene, already mentioned in the effects of light on the wild strain transcriptome, which we call Phot1, was also lost in the *wcoA* mutant.

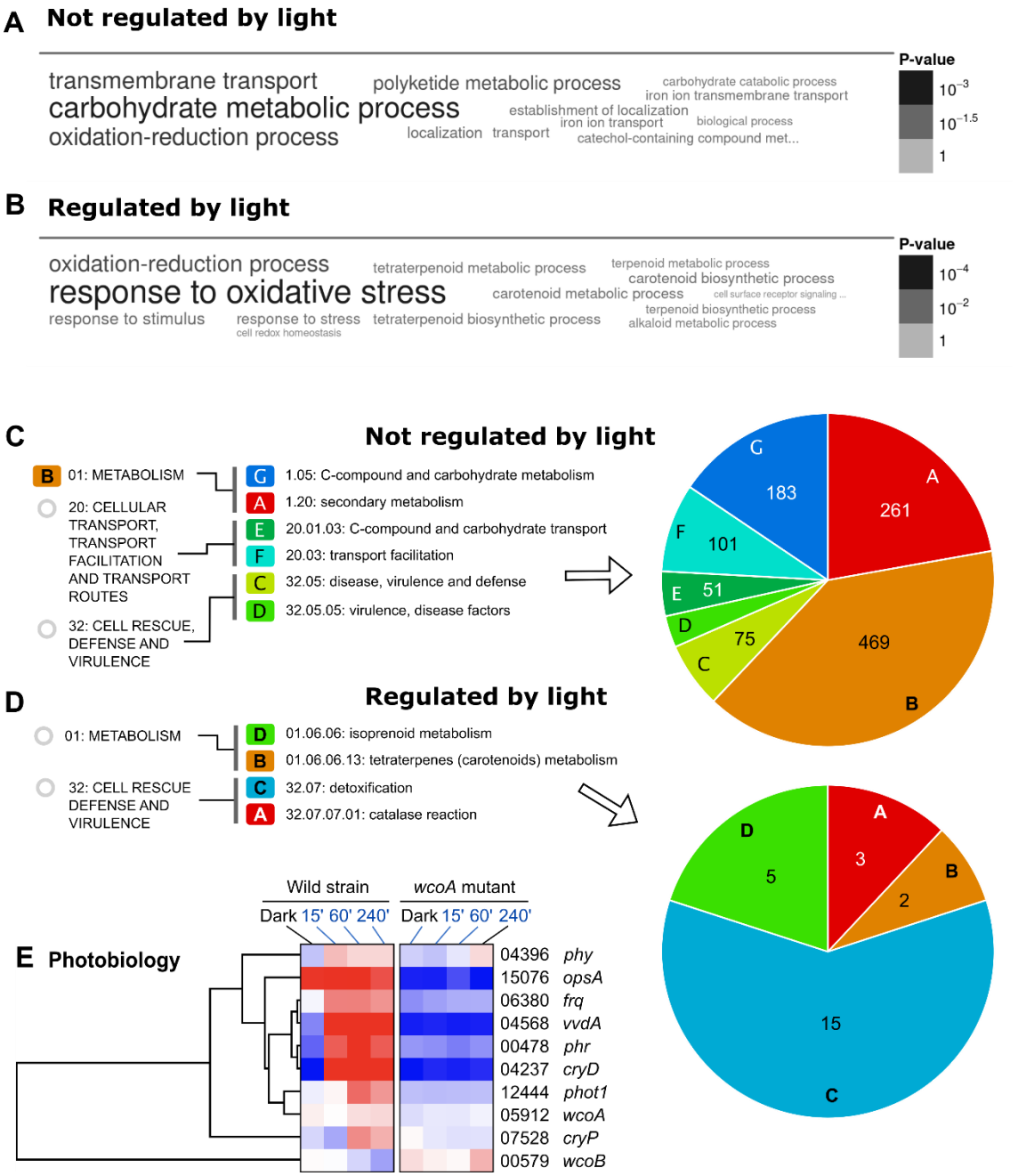

Figure C3.9. GO enrichment analysis of photoinduced and not photoinduced differentially expressed genes due to the *wcoA* mutation in *F. fujikuroi* and pattern of expression within the datasets of photoreceptor genes. (A) Word cloud graph of genes not regulated by light in the wild strain whose transcripts changed in the *wcoA* mutant analyzed with FungiDB. (B) Word cloud graph of genes regulated by light in the wild strain whose transcripts changed in the *wcoA* mutant analyzed with FungiDB. (C) Categories of genes not regulated by light in the wild strain whose transcripts changed in the *wcoA* mutant analyzed with FunCat. (D) Categories of genes regulated by light in the wild strain whose transcripts changed in the *wcoA* mutant analyzed with FunCat. (E) Hierarchical heatmaps for the effect of illumination and/or the *wcoA* mutation on the mRNA levels of genes related to *F. fujikuroi* photobiology. *FFC1_* numbers of the genes, and names given in the literature, are indicated on the right.

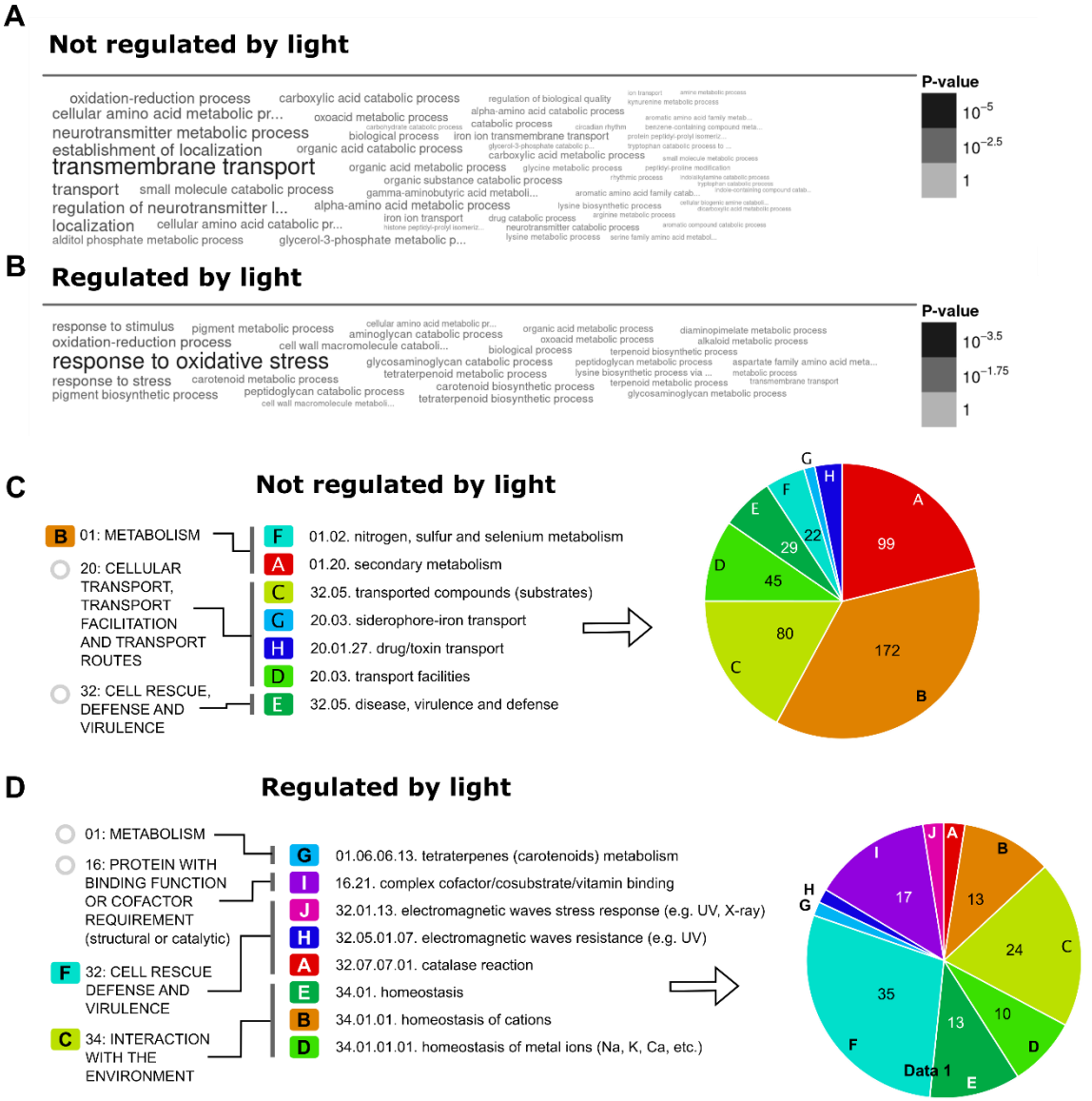

Figure C3.10. GO enrichment analysis of the genes affected by the *wcoA* mutation after application of the intensity difference filter. (A) Word cloud graph of genes not regulated by light in the wild strain whose transcripts changed in the *wcoA* mutant analyzed with FungiDB. (B) Word cloud graph of genes regulated by light in the wild strain whose transcripts changed in the *wcoA* mutant analyzed with FungiDB. (C) Categories of genes not regulated by light in the wild strain whose transcripts changed in the *wcoA* mutant analyzed with FunCat. (D) Categories of genes regulated by light in the wild strain whose transcripts changed in the *wcoA* mutant analyzed with FunCat.

The *wcoA* mutant phenotype includes a reduced mycelial hydrophobicity (Estrada and Avalos, 2008). A recent analysis in *F. graminearum* revealed five genes with hydrophobin domains, that were named *Fghyd1-5* (Quarantin et al., 2019). The *F. fujikuroi* genome contains orthologs for these genes, abbreviated here as *hyd1-5*. The analysis of the RNA-seq data for these genes showed that *hyd3* stood out among the others because of its very high mRNA amounts at the growth conditions tested (Fig. C3.11), while there where very low mRNA levels for *hyd2*, *hyd4*, and *hyd5* and no mRNA could be detected for *hyd1*. Interestingly, the amount of *hyd3* mRNA was strongly reduced in the *wcoA* mutant, while that of *hyd4* was increased, although it remained at low levels compared to those of *hyd2*.

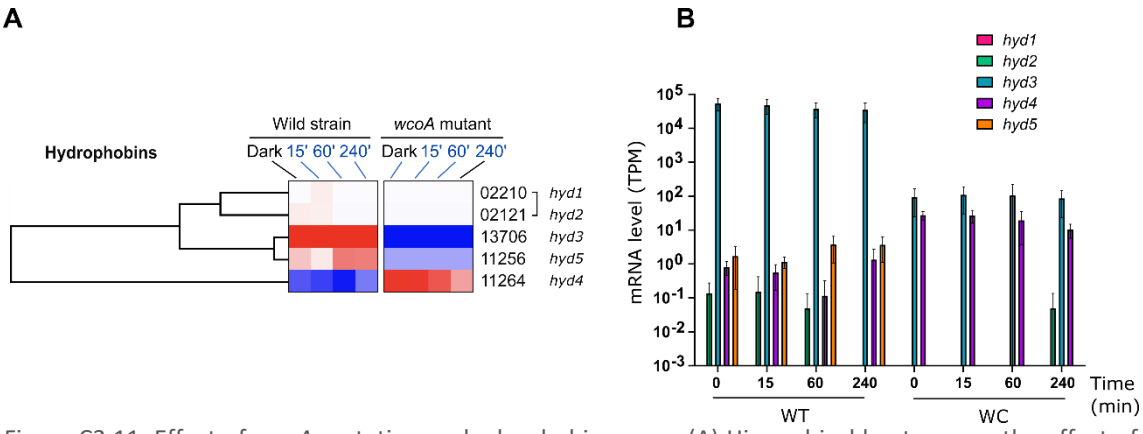

Figure C3.11. Effect of *wcoA* mutation on hydrophobin genes. (A) Hierarchical heatmap on the effect of illumination and/or the *wcoA* mutation on the mRNA levels of the five hydrophobin genes *hyd1*, *hyd2*, *hyd3*, *hyd4,* and *hyd5*. (B) Graphical representation of the transcript levels (TPM) of the five genes under all the conditions investigated.

ROLE OF WCOA IN SECONDARY METABOLISM

GO enrichment analyses showed that secondary metabolism (SM) was one of the processes whose deregulation in the *wcoA* mutant stood out. This is particulary outstanding, considering the relevance of *F. fujikuroi* in the study of the production of different metabolites (Janevska and Tudzynski, 2018). Genes involved in the production of SMs are usually clustered in the *F. fujikuroi* genome. A detailed view in heat map representations of the effect of WcoA on SM gene clusters is displayed in figure C3.12A, together with the genomic organizations of the clusters. The absence of a functional WcoA protein affected the analyzed clusters in different ways. Clusters for fusaric acid, fusarin, gibberellin, and echisetin/trichotecin production were mostly downregulated in the *wcoA* mutant. This was not observed for all genes, e.g., the PKS-NRPS-21 gene, encoding the key enzyme for echisetin/trichotecin production, was barely affected by the *wcoA* mutation, and the genes of the fusarin and gibberellin clusters PKS4 and P450-2 exhibited an opposite regulation, with larger transcript levels in the *wcoA* mutant. On the other hand, the bikaverin cluster showed the opposite regulation, with larger mRNA levels for all *bik* genes in the absence of a functional WcoA protein. Interestingly, the beauvericin and gybepirone clusters contained few genes, but with drastic regulatory differences. However, their genes for the key biosynthetic enzymes GPY1 and BEA1 showed strong WcoA regulations. In contrast, although there were minor effects in some of them, the *wcoA* mutation did not significantly affect most genes in the apicidin, fusarubin, and fumonisin clusters.

F. fujikuroi is predictably capable to produce a wide array of secondary metabolites, as indicates the large number of genes encoding enzymes of the NRPS, PKS, terpene cyclase families, as well as others. Only 7 of 18 functional PKS genes identified in the *F. fujikuroi* FKMC1995 genome (Niehaus et al., 2017) are mentioned in figure C3.11A. However, three other PKS genes of unknown function (*FFC1_04787*, *FFC1_12077*, and *FFC1_00016*) were significantly affected by the *wcoA* mutation. This was also the case for other presumptive SM genes not mentioned in figure C3.11, such as four genes for predicted NRPS enzymes (*FFC1_07944*, *FFC1_10414*, *FFC1_02152*, and *FFC1_12145*), three genes encoding putative

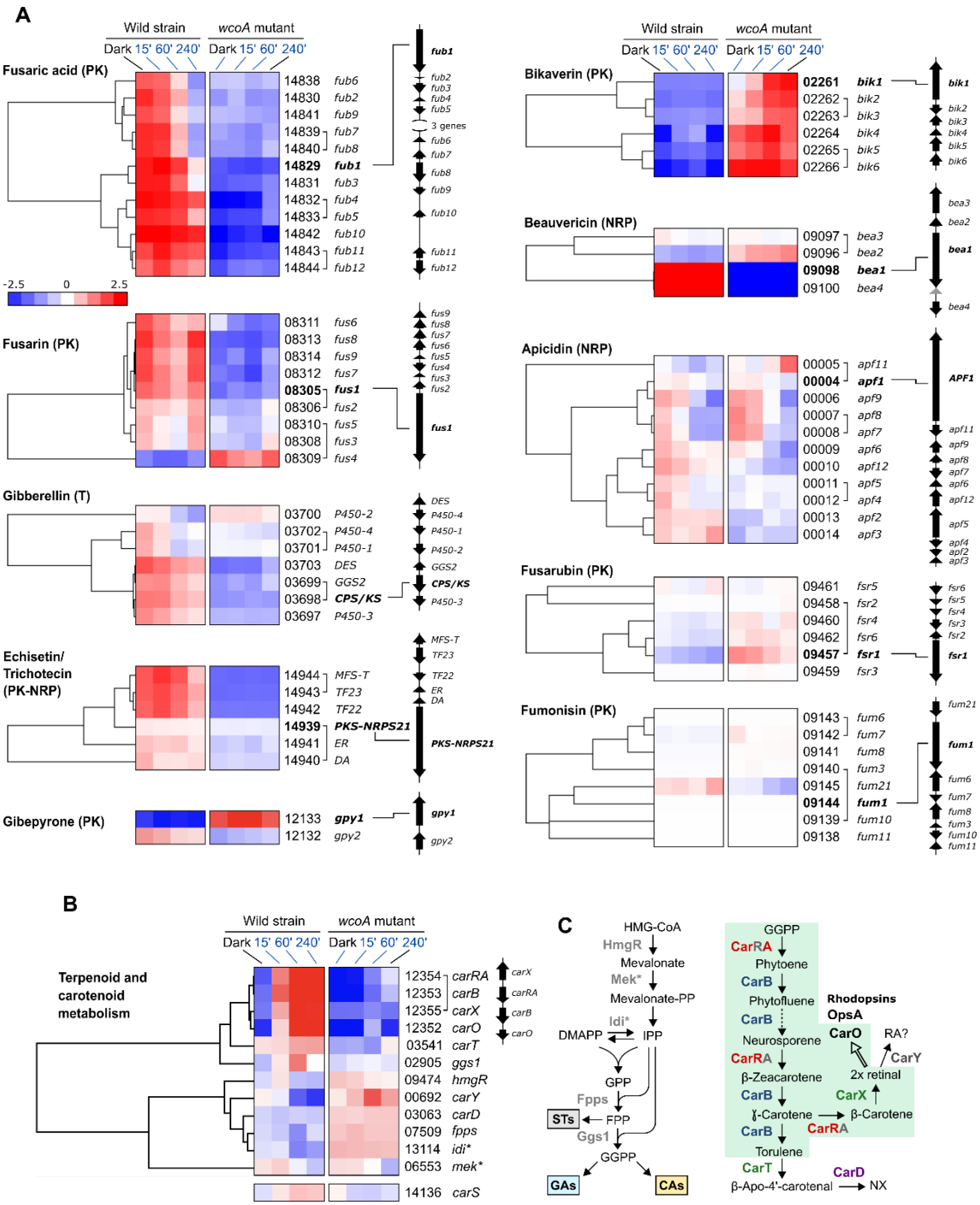

Figure C3.12. Effect of illumination and/or the *wcoA* mutation on secondary metabolism. (A) mRNA levels for the genes of the indicated SM clusters shown as hierarchical heatmaps. *FFC1_* numbers of the genes, and names given in the literature, are indicated on the right, together with their genomic organizations. Genes divergently transcribed are joined with a bracket. The most relevant gene in the biosynthetic pathway is indicated in bold letters. (B) Hierarchical heatmap of the genes involved in carotenoid biosynthesis and heatmap of the regulatory gene *carS*. (C) Identification of gene functions in the early steps of terpenoid biosynthesis (STs: sterols; GAs: gibberellins; CAs: carotenoids) and carotenoid metabolism in *F. fujikuroi*. The green area indicates the steps involving proteins of the *car* cluster.

dimethylallytryptophane synthases (*FFC1_09207*, *FFC1_05684*, and *FFC1_5464*), two genes for terpene cyclases, excluding *carRA* (*FFC1_00068* and *FFC1_12027*), a P450-1 gene predictably involved in cytokinin biosynthesis (*FFC1_079749*), and a gene involved in auxin production (*FFC1_08093*). These results reaffirm a central role for WcoA in the control of a large diversity of SM pathways in *F. fujikuroi*.

The function of WcoA as a positive regulator was particularly manifest in the case of the four genes of the carotenoid cluster, *carRA*, *carB*, *carX,* and *carO*, which agrees with the previous observations for *carRA* and *carB* in the RT-PCR analyses (Figure C3.1). The genes *ggs1*, responsible for the formation of the CarRA substrate GGPP, and *carT*, responsible for the cleaving step in NX biosynthesis, were also downregulated in the *wcoA* mutant, and formed a separate group with the genes of the *car* cluster upregulated by WcoA. In contrast, the gene for the final step of NX biosynthesis, *carD*, exhibited an opposite pattern. In this case, WcoA seemed to act more as a negative regulator, as was also observed for three genes for early steps of terpenoid biosynthesis (Figure C3.12C), *hmgR* (Woitek et al., 1997), *fpps* (Homann et al., 1996), and the gene for the probable isopentenyl-diphosphate delta-isomerase *idi*. The gene *carY* (*FFC1_00692*), a likely retinoic acid-forming enzyme (Díaz-Sánchez et al., 2016) (Figure C3.12C), exhibited a similar regulation, while the gene for the putative mevalonate kinase (which we call here Mek) was hardly affected by the *wcoA* mutation. Due to its central role in the control of the *car* cluster, the gene for the RING finger protein CarS was included in this study. As previously published, the *carS* gene was moderately induced by light, although not as strongly as the genes of the *car* cluster, and this photoinduction required a functional WcoA protein.

Effect of CryD in the *F. fujikuroi* transcriptome

The influence of the CryD photoreceptor on the transcriptome was analyzed in parallel to the *wcoA* mutant. However, due to the volume of the data and the different light exposure times used in the analysis of the *wcoA* strain, in this case only samples corresponding to darkness and 60 min of illumination were used for sequencing. The mapping was the same as the previously used for WcoA. Likewise, data similarity parameters were plotted. WcoA mutant samples were used as an outer control and for comparison purposes. Unlike in the case of the *wcoA* mutation, the PCA plot showed that the *cryD* mutation did not contribute importantly to the divergence of the transcriptomes after the quantification, with the effect of light having a greater weight. No differences were observed among samples in the bean plot graph or the cumulative distribution plot (Figure C3.13A and 13D). These data already suggested that, in the case of existing significative differences between the *cryD* mutant and the wild strain, the transcriptomic effects would be much lesser than the one of light. As a lower number of DET was expected after Deseq2 quantification, a less stringent log2 fold change of 1 and the usual *p*-value of 0.05 were used as criteria for differential expression. Based on such criteria, the number of genes activated and repressed by light in the wild strain, and in the *wcoA* and *cryD* mutants, as well as the effect of the mutations of these genes in relation to the wild strain, are shown in Table C3.4.

Table C3.4. Number of genes whose expression changed more than two-fold (log2 = 1) above (activated) or below (repressed) the controls, under the indicated conditions, using the Deseq2 protocol. The percentage refers to the total number of genes annotated in the reference genome (15,095). New transcripts not formerly annotated are indicated in parenthesis. [a] Comparisons between wild strain and *cryD* mutant. [b] Comparisons between wild strain and *wcoA* mutant

	Activated	%	Repressed	%
Effect of light in the wild strain	731 (15)	4.77	389 (3)	2.58
Effect of light in the *cryD* mutant	148	0.98	19	0.12
Effect of light in the *wcoA* mutant	7	0.04	4	0.03
Effect of *cryD* mutation in the dark [a]	19	0.13	8	0.05
Effect of *cryD* mutation in the light [a]	2	0.01	6	0.04
Effect of *wcoA* mutation in the dark [b]	1623 (45)	10.75	3035 (85)	20.11
Effect of *wcoA* mutation in the light [b]	1827 (60)	12.10	2919 (69)	19.33

The scatter plots of the corresponding comparisons confirmed a minor effect of the *cryD* mutation compared with that of the *wcoA* mutation (Figure C3.14). However, the results of the DESEQ analyses showed unexpected discrepancies. Even though *cryD* mutation seemed to have a big effect on the number of photoregulated transcripts (7,5% DET in the wild strain *vs*. 1.1% DET in the *cryD* mutant), fewer differences were detected in the mutant when compared to the wild strain either in the dark or after illumination. This low number of differentially expressed genes did not correlate with the drop of photoinduced and, particularly, photorepressed transcripts, and were not expected considering the phenotypic alterations exhibited by the *cryD* mutant.

This difference could be due to the greater demand of the Deseq2 algorithm. Therefore, the data were reanalyzed following the protocol used for the first transcriptomic analysis of the light effect on *F. fujikuroi* (Ruger-Herreros et al., 2019).

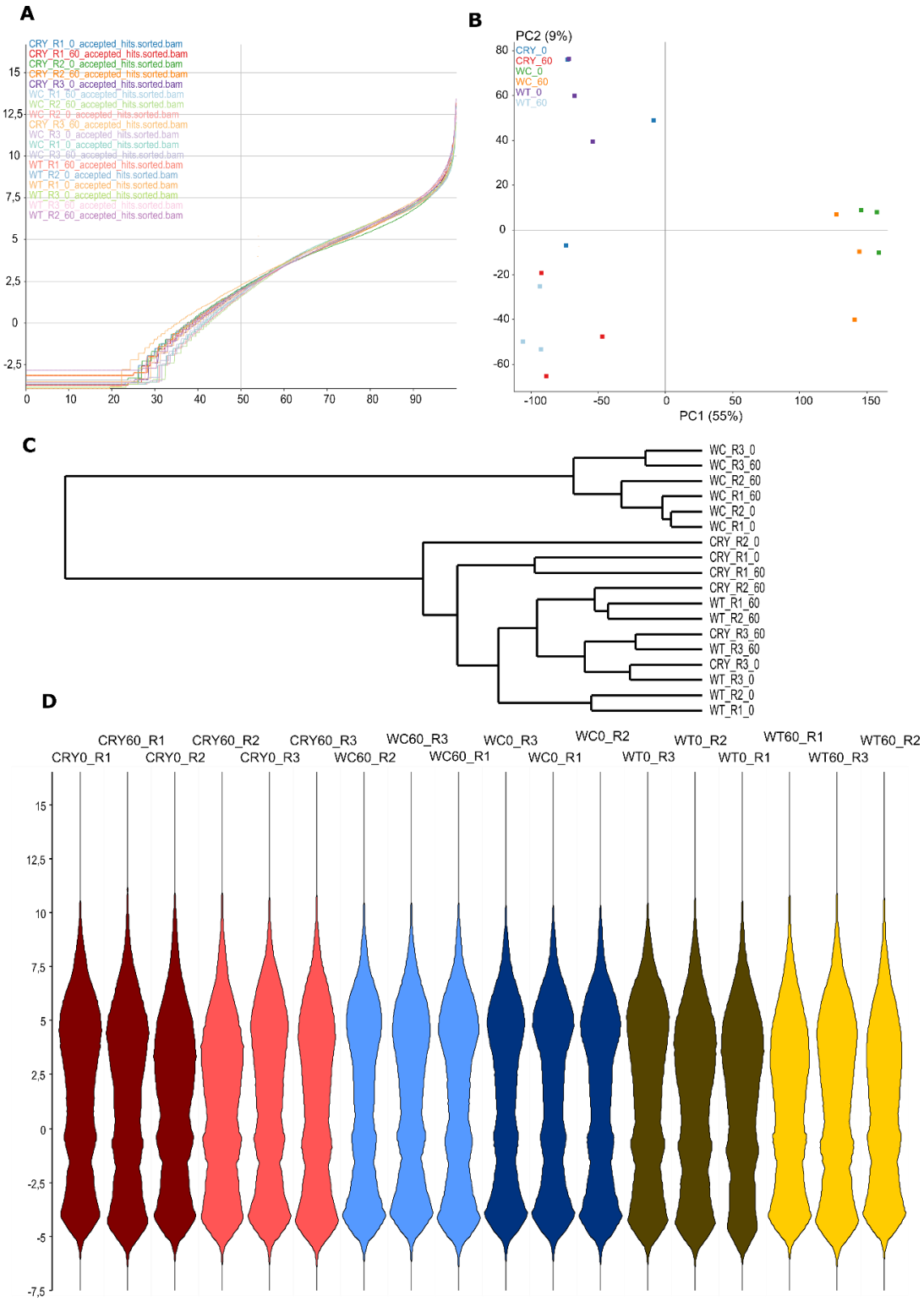

Figure C3.13. Dispersion and distribution graphs for RNA-seq samples of the wild strain, and the *cryD* and *wcoA* mutants. (A) Cumulative distribution plot after percentile normalization. (B) PCA plot. (C) Statastore Tree. (D) Bean distribution plot.

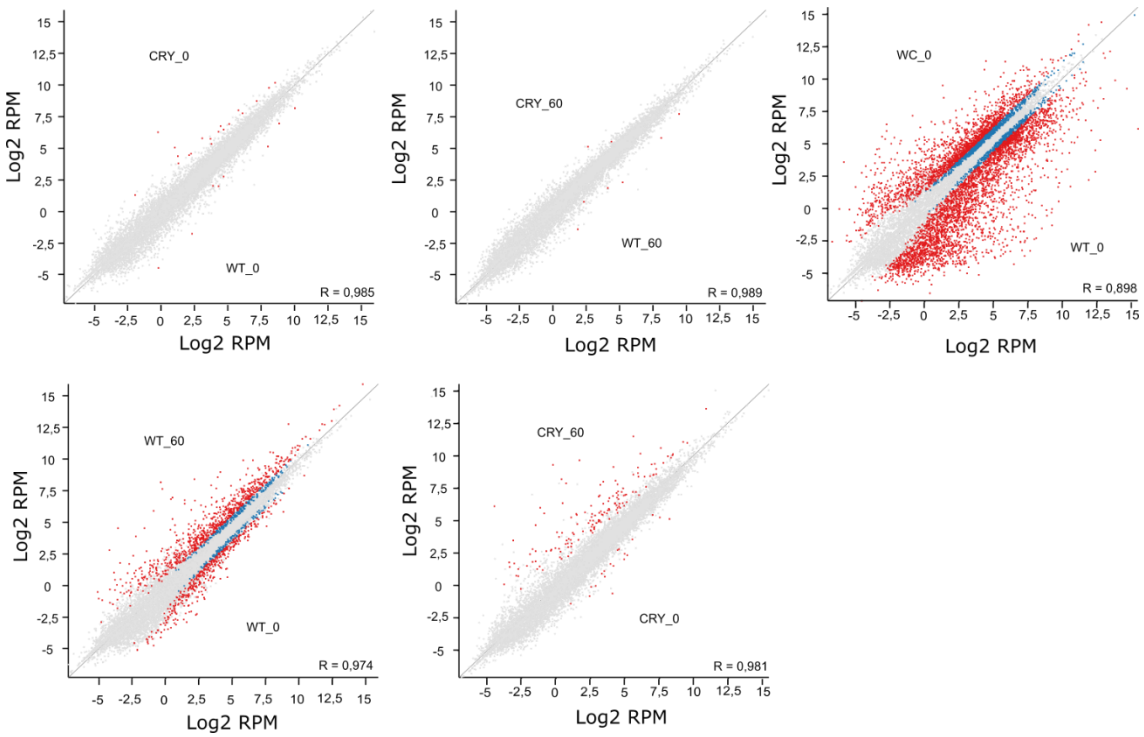

Figure C3.14. Scatter plot representations of the effect of *cryD* deletion compared to the wild strain transcriptome in the dark and after 60 min of illumination. The *wcoA* sample compared to the wild-type transcriptome (WT) in the dark was added for comparison purposes. Genes differentially expressed according to the Deseq analysis of the Seqmonk program are indicated in blue. Genes exceeding the log2 values of ±1 are indicated in red.

Table C3.5. Number of genes whose expression changed more than two-fold (log2 = 1) above (activated) or below (repressed) the controls, under the indicated conditions, using the TUXEDO protocol. The percentage refers to the total number of genes annotated in the reference genome (15,095). New transcripts not formerly annotated are indicated in parenthesis.

	Activated	%	Repressed	%
Effect of light in the wild strain	884 (36)	5.86	556 (33)	3.68
Effect of light in the cryD mutant	206 (14)	1.63	43 (5)	0.28
Effect of light in the wcoA mutant	105 (8)	0.70	26 (4)	0.17
Effect of cryD mutation in the dark a	147 (7)	0.97	67 (9)	0.44
Effect of cryD mutation in the light a	125 (10)	0.82	81	0.53
Effect of wcoA mutation in the dark b	1813 (83)	12.01	2711 (103)	17.96
Effect of wcoA mutation in the light b	2010 (93)	13.32	2582 (89)	17.11

[a] Comparisons between wild strain and *cryD* mutant. [b] Comparisons between wild strain and *wcoA* mutant.

The new quantification by the Tuxedo protocol (Trapnell et al., 2012) proved to be less stringent. In this case, the number of differentially expressed transcripts varied specially for the comparisons between the wild strain and the *cryD* mutant both in dark and under illumination, although the amount of photorepressed and photoinduced transcripts did not increase substantially in the *cryD* mutant compared to the previous quantification.

EFFECT OF LIGHT IN THE *CRYD* MUTANT TRANSCRIPTOME

The number of photoregulated transcripts decreased notably in the *cryD* mutant. Only 206 genes were photoinduced compared to 884 in the wild strain. This reduction was even more noticeable in the case of photorepression, with lower mRNA levels for 56 genes after light in the mutant while in the wild strain the number was 556, that is, about a tenfold reduction. As the overlap in the Venn diagram shows (Fig. C3.15A), most of the photoregulated genes in the *cryD* mutant were also photoregulated in the wild strain. Nevertheless, when analyzing the overall set of photoregulated 1,549 transcripts from both strains on a heatmap (Fig. C3.15B), the effect of the *cryD* mutation was more commensurate compared to the wild strain. Most genes which showed photoinduction or photorepression in the wild strain also showed photoinduction or photorepression in the *cryD* mutant, but many of them exhibited changes in the intensity of the response. This is logical, considering that the major photoreceptor responsible of light regulation is actually WcoA. Therefore, CryD is an accessory photoreceptor modulating the degree of the photoresponse of many genes. The hierarchical clustering of the mRNA values led to the identification of several groups of genes, with a subgroup whose average expression was higher in the *cryD* mutant under illumination, and two subgroups which were less photoinduced (343) and less photorepressed (63) than in the wild strain. Interestingly, two small subsets presented higher (45) or lower (11) amounts of transcripts in the dark in the *cryD* mutant compared to the wild strain. This was unexpected considering that CryD is expressed at very low level in the dark.

Some enriched FunCat categories were found in the subgroup of genes which presented a higher photoinduction in the *cryD* mutant (Fig. C3.15C): 'cellular sensing and response to external stimulus', which is directly linked with photoreception and photoresponse. This includes genes already mentioned, as the cryptochrome *FFC1_07528*, and the putative phototropin *FFC1_12444*. Another category was 'tetracyclic and pentacyclic triterpenes (cholesterin, steroids and hopanoids) metabolism', which includes the *ggs1* gene and *FFC1_11060*, ortholog to *bli-4*. The group of less photoinduced genes showed no enrichment when analyzed with FunCat database, but with FungiDB (Fig. C3.15D) there were some processes which seemed to be affected, of which is worth to mention circadian rhythm, with the *frq* gene.

EFFECT OF THE *CRYD* MUTATION IN THE *F. FUJIKUROI* TRANSCRIPTOME

The number of differentially expressed genes in the *cryD* mutant independently of illumination was quite low compared to the *wcoA* mutant. There were 230 differentially expressed transcripts with a two-fold change between the wild strain and the *cryD* mutant in the dark, 154 upregulated and 76 downregulated, while the numbers under illumination were 216 differentially expressed, of which 135 upregulated and 81 downregulated. Although both

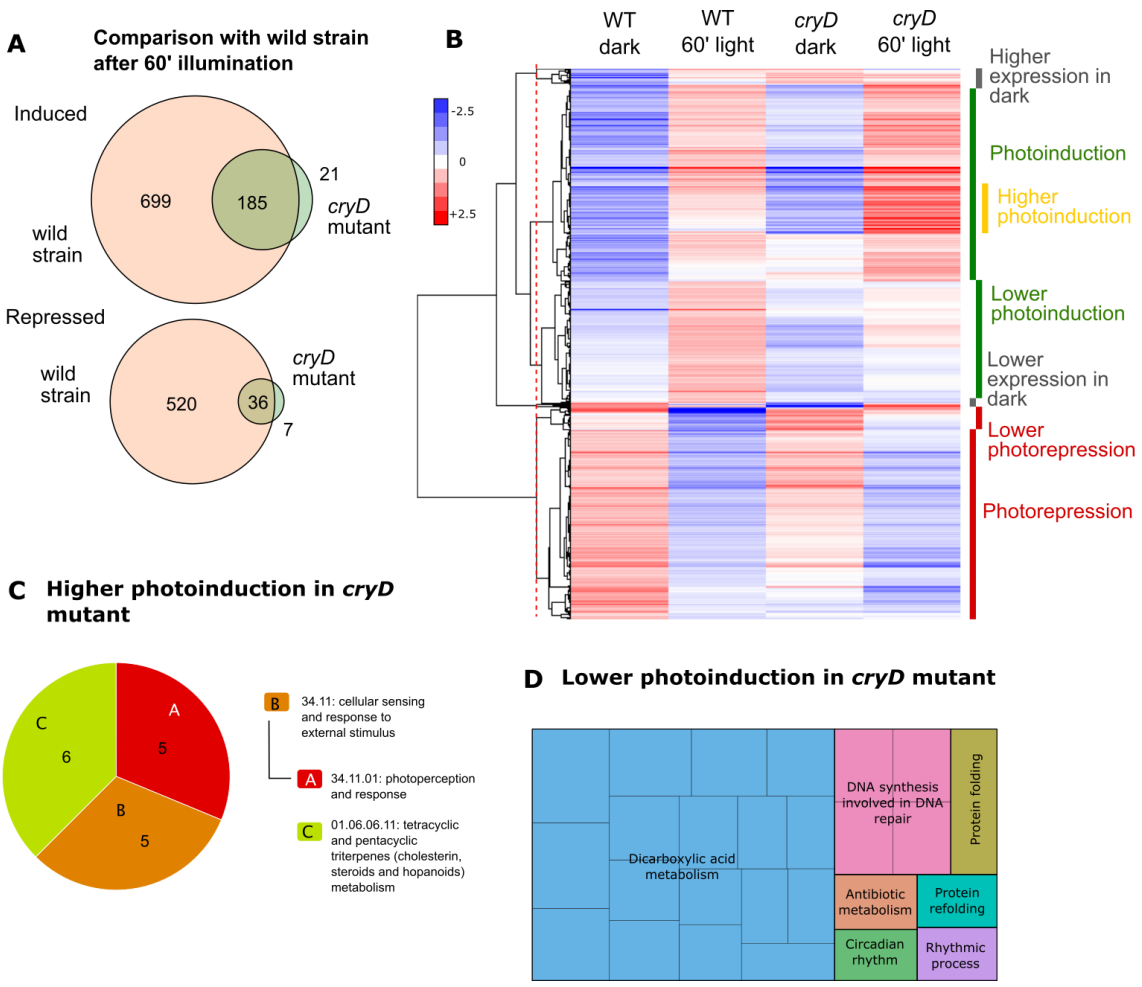

Figure C3.15. Effect of illumination time on the *cryD* mutant strain transcriptome. (A) Venn diagrams of the genes induced (above) or repressed (below) after 60 min illumination in the wild strain and in the *cryD* mutant. The intersection shows the number of genes induced in both strains. (B) Hierarchical heatmap of the genes induced or repressed after 60 min of illumination in the wild strain and/or in the *wcoA* mutant. (C) Categories of genes with a higher photoinduction in the *cryD* mutant analyzed with FunCat. (D) GO enriched categories of DEG with a lower photoinduction in the *cryD* mutant after 60 min of illumination using FungiDB.

sets of upregulated and downregulated DETs were very similar in number, the overlap between them was not very high, with only 36 coincidences in the activated genes and 26 in the repressed ones (Fig. C3.16A). As already done when we considered as genes differentially expressed in the *wcoA* mutant those showing differences under all the tested conditions, for comparison with the *cryD* mutant, we determined the lists of differentially expressed genes for each photoreceptor mutant in the two conditions tested, darkness and 60 min illumination, using in this case the log2 = 1 threshold. This led to a group of 3,333 *wcoA*-dependent DETs and 382 *cryD*-dependent DETs (230 in the dark and 216 in the light). Approximately half of them (138 in the dark and 114 in the light) were shared between the two photoreceptors (Fig. C3.15B). Nevertheless, 92 and 102 of the transcripts were specific of the *cryD* mutation, with a low overlap between those identified in the dark and after light. This differential effect between light and dark in the *cryD* mutant raises interesting questions. As already stated, the expression of the gene in darkness is very low (Fig C3.16C), and its induced expression in the light depends on

WcoA. It would be logical to expect that the CryD-dependent DETs found in illumination should be contained in the DETs of the *wcoA* mutant.

GO enrichment analyses with the FunCat database were not very revealing, providing no enriched categories for the group DETs in the *cryD* mutant under illumination, and very few categories for the DETs observed in the dark (Fig C3.15F). 'C-compounds and carbohydrates metabolism' was the enriched GO category which included more genes (31) among the ones detected by FunCat, while two other categories, 'biosynthesis of lysine' (4) and 'metabolism of aspartate' (3) were less represented. Wordclouds of the corresponding enriched GO categories from FungiDB provide some clues about the processes that might be deregulated in the mutant (Fig C3.15D and 15E). The presence of ammonium permease *FFC1_12351*, adjacent to the *car* cluster and differentially expressed with opposite patterns in dark and under illumination, together with the appearance of categories related to the synthesis of amino acids in the dark, suggest a possible link of this photoreceptor with nitrogen regulation.

As for the WcoA photoreceptor, the absence of CryD also plays a role in the regulation of secondary metabolism in *F. fujikuroi*, although its influence was much lower. The gene *gpy1*, responsible for the synthesis of gybepyrones, was overexpressed in the dark in the *cryD* mutant (*FFC1_12133*, FC=2.38), as it was the terpene cyclase *stc4*, which synthesizes koraiol (*FFC1_11028*, FC=1.91). The gene corresponding to the non-assigned NRPS23 (*FFC1_12145*) was repressed in the *cryD* mutant both in the dark (FC= -1.58) and after illumination (FC= -1.21). On the other hand, the NRPS11 was upregulated in light (*FFC1_10414*, FC=2.66). Interestingly, although *F. fujikuroi* does not have a functional trichotecene cluster, it does retain the pseudogene *TRI201* (Kimura et al., 2003; Proctor et al., 2009), which produces the 3-*O*-acetyltransferase. This gene (*FFC1_00151*) was overexpressed both in the dark (FC= 1.69) and under illumination (FC=1.61), along with its two adjacent neighbor genes (*FFC1_00150*, FC dark=3.17, FC light=2.60; *FFC1_00152*, FC dark=2.88, FC light=2.48). In the comparison with the wild strain under illumination, the *cryD* mutant also presented higher levels for some of the genes involved in carotenoid metabolism, including *carX*, *carO,* and *carD*.

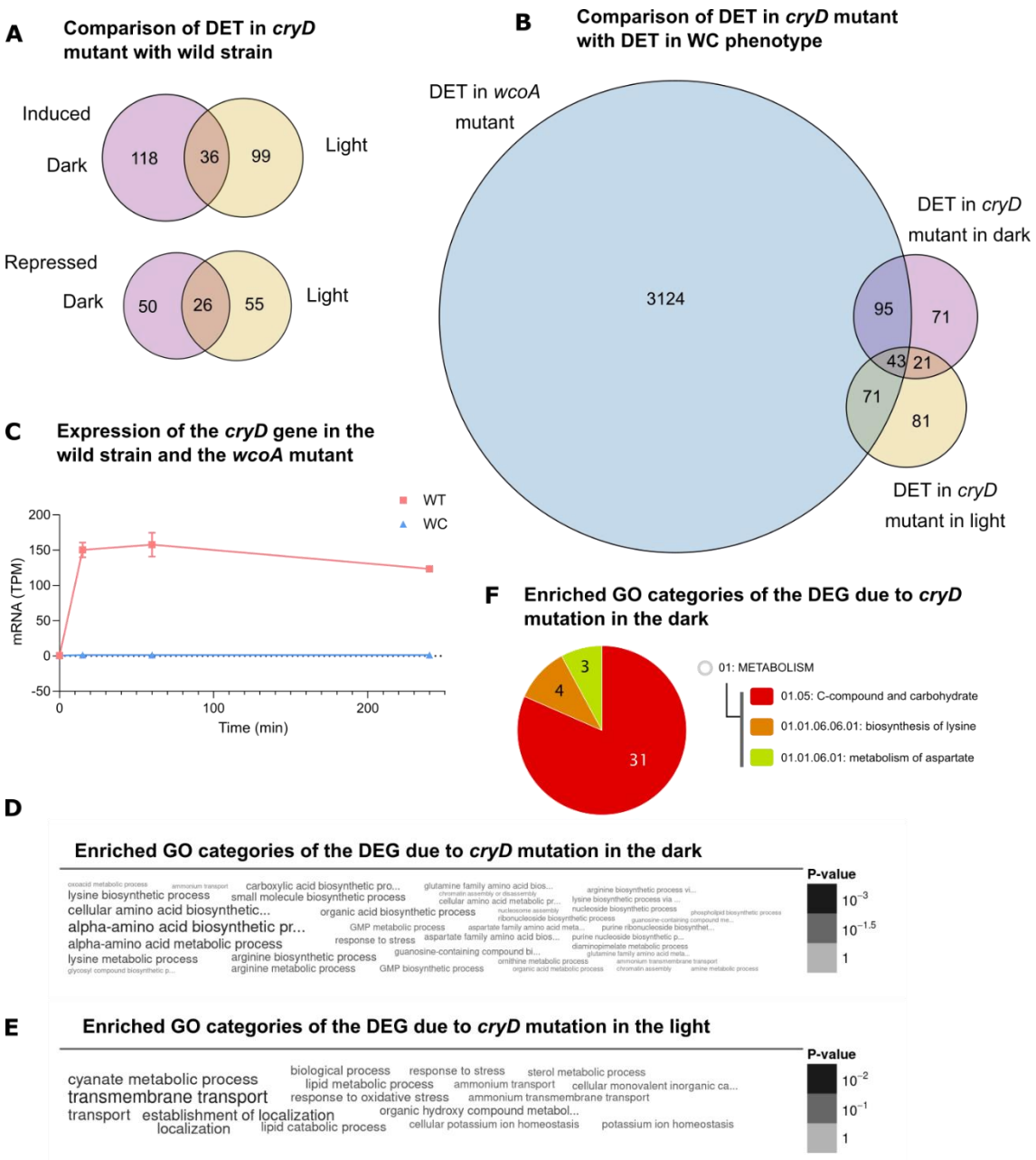

Figure C3.16. Effect of *cryD* mutation on *F. fujikuroi* transcriptome in the dark and after 60 min of illumination. (A) Venn diagrams of the genes induced (above) or repressed (below) in the *cryD* mutant in the dark (purple) and after 60 min of illumination (yellow) compared to the wild strain. The intersection shows the number of genes induced in both strains. (B) Venn diagrams of the DETs in *wcoA* mutant (in the dark and after 60 min of illumination) and the DETs in the *cryD* mutant in the dark (purple) and after 60 min illumination (yellow) compared to the wild strain. (C) Transcript levels of the *cryD* gene in the wild strain and the *wcoA* mutant strains. (D) Word cloud graph of the enriched GO categories of the DEG due to the *cryD* mutation in the dark. (E) Word cloud graph of the enriched GO categories of the DEG due to the *cryD* mutation after 60 min of illumination. (F) Enriched GO categories of the DEG due to the *cryD* mutation in the dark using FunCat.

DISCUSSION

The goal of this chapter was to investigate the role of WcoA and CryD as regulatory proteins in *F. fujikuroi*. The transcriptomic study of the effect produced by the loss of both photoreceptors has provided extensive data about their biological role, especially outstanding in the case of the WcoA protein.

WcoA has been extensively described in other fungi and its function as a key photoreceptor is already known (Corrochano, 2019; Fuller et al., 2015). In *Fusarium*, the effect of *wcoA* mutation has been investigated not only in *F. fujikuroi* (Estrada and Avalos 2008), in which this work is a further step in its study, but also in *F. oxysporum* (Ruiz-Roldán et al., 2008), *F. graminearum* (Kim et al., 2015), and *F. asiaticum* (Tang et al., 2020). In this chapter, a detailed analysis of the effect of illumination time on the transcriptome of a *wcoA* mutant was performed compared to its control wild strain. This is not the first work regarding the transcriptomic effect of light in *F. fujikuroi*. Previous results on a different wild strain, IMI58289, showed changes on an extensive number of genes, with a predominance of light-activating effects (Ruger-Herreros et al., 2019). Nevertheless, as already estated, the *wcoA* mutant was obtained in a different genetic background and experiments were carried out with its reference wild strain, FKMC1995. There are significant genomic differences between both strains, as indicates the finding of 2,496 transcripts in FKMC1995 with not directly assigned ortholog in IMI58289.

The effect of light on fungal transcriptomes has been investigated in several organisms with different techniques (Corrochano, 2019; Fuller et al., 2016), usually concluding that it affects the mRNA levels of hundreds of genes. In *A. fumigatus*, a microarray assay was used to investigate the effect of 15, 30, 60, and 120 min of light exposures, concluding that 2.6% of the genes were regulated by light (FC 1.5) in this species (Fuller et al., 2013). In *P. blakesleeanus* large-scale cDNA sequencing estimated that about 5.2% of the genes changed their mRNA levels at least five-fold after 30-min illumination (Tagua et al., 2020). Nevertheless, studies combining the effect of light on the transcriptome with the effect of mutations in *wc* genes are available in very few fungi. Microarray data from *T. reseei* showed that 2.8% of the genes were differentially expressed under continuous illumination compared to a dark control, trending towards upregulation too (Tisch and Schmoll, 2013). Surprisingly, the lack of the WC complex resulted in an altered adaptation to constant illumination, as the number of DEG in the light increased to about 9% in the wc mutant *blr1* and in the mutants of the wc-2 ortholog *brl2*. The experimental conditions of a later study performed in *T. atroviride* were more similar to those of this work, which found 246 and 215 genes up- and downregulated after a 30-min light pulse (Cetz-Chel et al., 2016), around 3.9% of its genome, even though the effect of *blr1* absence was not investigated. In *Sordaria fimicola*, the effect of 15 min and 45 min illumination on the transcriptome was checked in the wild strain and in a defective *sfwc-1* mutant, with the unexpected result that of the 874 light-regulated genes, 466 lost the photoinduction in the mutant, suggesting the participation of another blue-light photoreceptor (Krobanan et al., 2019). Light is less influential in other fungi, as *Ustilago maydis*, in which only 60 genes were induced by light, all dependent on the *wco1* gene (Brych et al., 2016). Other fungi, however, are

apparently insensitive to light; in the basidiomycete fungus *Cryptococcus neoformans*, only one gene was found to be significantly affected by illumination (Idnurm and Heitman, 2010).

N. crassa is probably been the fungus in which the effect of light has been more deeply studied. About 5-6% of its genes were found to be differentially expressed during the first 90 min after light onset, a response largely mediated by the WC complex (Chen et al. 2009). Comparison of microarray expression data after eight illumination times, from 5 to 240 min, revealed at least two classes of induction patterns, leading to the classification of genes as early- and late-responsive. A posterior and more precise RNA-seq study elevated to 31% the proportion of genes with at least a two-fold change in mRNA levels (Wu et al., 2014). The similarity of the illumination conditions used in this study with our conditions, with light exposures of 15, 60, 120, and 240 min, facilitate the comparison with the results in *F. fujikuroi*. In both species, induction predominated over repression. Different patterns of induction were also observed, separated in this case in four clusters, although the classification as early- and late-responsive genes was conserved. It called the attention in this report the occurrence of a large set of light-repressed genes, none of them showing early repression. WC-1 may also act a as repressing protein through a light responsive GATA element which was found to be involved in the binding of WC-1 to form a repressing complex in the dark (Brenna and Talora, 2019). Nevertheless, the lack of a fast photorepressive response suggests that downregulatory effects could be rather caused by other negative regulators, which would be activated earlier by WC-1. This was also the case in *F. fujikuroi*, in which intermediate and late responsive genes were identified in those regulated by light, but early responsive genes were only found among the light-induced ones.

The GO enrichment analyses of the genes regulated by light or by WcoA in *F. fujikuroi* showed a large diversity of functions. Their functional assignations are reminiscent to those for the more than two thousand genes affected by light at least two-fold in *N. crassa*, but only if comparison is made with those regulated by WcoA in *F. fujikuroi*. Coinciding categories include those for C-compound and carbohydrate metabolism, secondary metabolism, and detoxification in the upregulated genes, and cellular transport, and metabolism in downregulated genes. GO categories were less significant for the genes regulated by light in *F. fujikuroi* possibly because of their lower number compared to *N. crassa*. This is consistent with a more important role of light in regulation by Wc-1 in *N. crassa* than in *F. fujikuroi*, where the WcoA protein participates in the control of many genes for which light is a less influential signal.

It is assumed that illumination causes oxidative stress, and that carotenoids are accumulated to alleviate oxidative damage (Avalos and Limón, 2015). This may explain that, in both fungi, the genes *carB/al-1* and *carRA*/*al-2* appear among the 15-top genes with higher early photoinductions (15 min of illumination) in both species (Wu et al., 2014). An explanation for the possible role of the WC protein as a coordinator of other photoresponses is the fact that three photoreceptors appear in the same top list in both species: Vivid (VvdA, *FFC1_04568*; VVD, *NCU03967*), the DASH cryptochrome (CryD, *FFC1_04237*; CRY*, NCU00582*), and a photolyase (Phr, *FFC1_00478*, PHR, *NCU08626*). These data also uncovered a possible additional photoreceptor in *Fusarium*, formerly disregarded, also controlled by WcoA, the gene

FFC1_12444, which encodes a protein with sequence similarity with the phototropin Phot1 of *Arabidopsis thaliana* (Sullivan et al., 2016). No information is available on biological roles of phototropins in fungi, which opens a new area of research in fungal photobiology.

One of the main points of interest of this work is the broad changes in the transcriptome of the *wcoA* mutant, which are consistent with the visible phenotypic alterations of its colonies, either in the dark or under illumination (Castrillo and Avalos 2015). These alterations included defective growth, morphological changes, lower hydrophobicity, reduced conidiation, and changes in pigmentation and secondary metabolite production (Estrada and Avalos 2008). The high number of affected genes in the mutant suggests that many of the transcriptional alterations are indirect, probably caused by the WcoA-dependent expression of other regulatory genes, which would result in cascading effects. These effects have been reported in *N. crassa*, where WC-1 binds to the promoters of other genes controlling the expression of 24 transcription factors (Smith et al., 2010). E.g., the WC complex activates the gene *sub-1*, encoding a GATA transcription factor responsible for most of the late photoresponses in *N. crassa* (Chen et al. 2009). The closest *sub-1* homolog in *F. fujikuroi*, the NsdA-related protein *FFC1_02938* (48.1% identity with SUB-1), is not significantly affected by light or by the *wcoA* mutation, but other genes encoding intriguing regulatory proteins are strongly influenced by WcoA. An interesting example is provided by *FFC1_06993*, homolog of the C2H2 transcription factors LTF2 of *B. cinerea* and Sah-1 of *N. crassa*. In *B. cinerea* LTF2 is induced by light and stimulates conidiation (Cohrs et al., 2016), but in *N. crassa* the loss of *sah-1* (from "short aereal hyphae") results in enhanced earlier conidiation (Sun et al., 2012). Therefore, the reduced expression of *FFC1_06993* in the *wcoA* mutant could be related with the lower conidiation in DG medium in this strain (Estrada and Avalos 2008). Not surprisingly, *sah-1* is induced also by light in *N. crassa* in a WC-dependent manner (Chen et al. 2009). The effect of the WcoA mutation on conidiation could be the result of more complex interactions. WcoA downregulates the homeobox protein *FFC1_07148*, called Htf1 in other *Fusarium* species, where it participates in conidia development, most specially macroconidia formation (Zheng et al., 2012). *F. fujikuroi* differs in the regulation of conidiation from other *Fusarium* species, since it produces mostly microconidia and macroconidia are more rarely observed.

In the large functional diversity of the genes affected by the *wcoA* mutation, the most abundant category was secondary metabolism. The influence on SM production could be even greater, considering that downregulating roles of WcoA could be disregarded in our study for SM clusters not expressed in the investigated culture conditions. SMs production is subject to different regulations, usually sensing environmental cues, as pH, or stress conditions. As an example, the presence of nitrogen in the medium is a negative regulatory signal to produce gibberellins and bikaverin, but it is a positive signal to produce fusarins (Tudzynski, 2014). In the absence of WcoA, the bikaverin pathway is upregulated, counteracting the presence of nitrogen, but the opposite effect was observed with the genes for GA production. However, since GAs are downregulated in our culture conditions, a strong effect of WcoA would not be expected anyway. SM regulation frequently involves the participation of different regulatory proteins, in which WcoA may be one of the master regulators. The genes regulated by WcoA included other

transcription factors in addition to those indicated in the previous paragraph, whose altered expression may affect the regulation of SM gene clusters. One of them is Sge1 (*FFC1_03440*), a phosphoprotein homolog to MIT1 of *S. cerevisiae* with known orthologs in other fungi, whose expression is upregulated ca. 10-fold in the *wcoA* mutant. Sge1 was found to regulate positively the production of gibberellins, bikaverin, fumonisin, fusarin, fusaric acid, and apicidin in the IMI58289 wild strain of *F. fujikuroi* (Michielse et al., 2015). This could be additive with other regulatory effects. E. g., transcript levels of *FFC1_04144*, ortholog of the LaeA-like methyltransferase MrcA of *A. nidulans*, increased in the *wcoA* mutant about 2-fold in the dark, and about 3-fold and 5-fold after 60 min and 240 min of illumination. Deletion of *mrcA* in *A. nidulans* resulted in a higher production of different SMs, and the altered expression of more than 1,000 genes (Grau et al., 2019).

The altered hydrophobicity of the *wcoA* mutants of *F. fujikuroi*, a trait also described for the *wc1* mutants in *F. oxysporum* (Ruiz-Roldán et al., 2008), led us to investigate the effect of the *wcoA* mutation on the hydrophobin genes orthologous to the *Fghyd1-Fghyd5* of *F. graminearum* (Quarantin et al., 2019). The RNA-seq data showed that *hyd3* was predominantly expressed under our culture conditions, a result that agreed with the data in *F. graminearum*, where *Fghyd3* also exhibited the highest mRNA content. Light exerted minor changes in the *hyd* transcript levels in *F. fujikuroi*, compared to the drastic changes caused by the *wcoA* mutation in some of the *hyd* genes. The reduced hydrophobicity exhibited by the colonies of the *wcoA/wc1* mutants could be explained by the strong reduction in *hyd3* transcripts, although it remained the *hyd* gene with the highest expression level. In fact, mutant analysis revealed a role of Fghyd3 in hyphal attachment to hydrophobic surfaces in *F. graminearum* (Quarantin et al., 2019). Therefore, one of the roles of WcoA is to participate in the control of hydrophobins expression in *Fusarium*.

The effects caused by the WcoA mutation are so wide on the transcriptome of *F. fujikuroi* that in comparison, the deletion of the *cryD* mutant can only confirm its role as just an accessory photoreceptor. This work constitutes, to our knowledge, the first approach to a transcriptomic study on a cry-DASH mutant in fungi. Fungal cry-DASH still pose many unknowns regarding their balance between regulatory and repair functions. In some species, as *M. circinelloides* and *P. blakesleeanus*, cry-DASH proteins seem fulfill the repair role in absence of other proteins of the family (Navarro et al., 2020; Tagua et al., 2015) while in other fungi, as the proteins diversify, classic photolyases fulfill this activity, and the cry-DASH proteins evolve to perform regulatory functions. That is the case, of the *B. cinerea* cry-DASH protein that represses conidiation in white light and especially black/UV light, while a classic CPD photolyase covers repair functions (Cohrs and Schumacher, 2017). Fungal cry-DASH proteins have been shown to participate in other regulatory processes, as regulation of circadian ryhtm in *N. crassa* (Froehlich et al., 2010), fruiting body development, and secondary metabolism in *C. militaris* (Wang et al., 2017a), and alterations in the development in *S. sclerotiorum* (Veluchamy and Rollins, 2008). The roles of *cryD* in *F. fujikuroi* in the synthesis of carotenoids and other secondary metabolites or in conidiation suggest a higher number of transcriptomic changes than the ones actually osberved. Nevertheless, in a first analytical approach, almost no differences were

observed between the wild strain and the *cryD* mutant transcriptomes, while a higher number of genes lost the photoregulation in Δ*cryD*. This constituted a puzzling result, that could be due to either data dispersion or to variations in the threshold of activation. The latter seems a likely explanation, since the use of a slightly less stringent protocol led to more coherent numbers of differentially expressed genes between the two strains.

The considerable drop in the number of photoinduced genes in the *cryD* mutant raises questions about the extent of its role as a photoreceptor in the light response in this fungus. Nevertheless, this effect must be carefully taken, as it was not supported when the average values of expression were individually checked. It seems clear, however, that the *cryD* mutation affects the intensity of the photoresponses for many genes. To further confirm it, expression of individual genes should be analyzed by other techniques in order to be compared with the RNA-seq results. Interestingly, the analysis of clustering average values revealed a group of genes with a higher photoinduction than in the wild strain, which included several genes related with photoreception and the gene *frq*, indicating a possible influence of CryD in circadian rhythmicity in a similar manner to *N. crassa* (Froehlich et al., 2010). For a more complete identification of genes affected by CryD deletion, the effect of longer illumination times, such as 240 min, could be very informative, especially considering the visible phenotypic alterations shown by the *cryD* mutant under constant illumination (Castrillo et al., 2013). However, this was not adressed in this work because of limitations in the amount of samples that could be afforded in the ongoing project.

As observed with *wcoA*, *cryD* deletion also showed alterations in the mRNA profiles of several genes involved in secondary metabolism. Particulary interesting is the case for the remaining genes of the tricothenen biosynthesis cluster *F. fujikuroi*, that raises the question of wether CryD could participate in the regulation of trichotecens production. This can be particularly interesting in related fungi, as *F. graminearum*, in which this biosynthetic pathway has been studied in more detail (Chen et al., 2019). Nevertheless, no effect was observed in the bikaverin or gibberellin biosynthetic clusters, whose syntheses were altered in the mutant. It must be noted that mRNA levels for relevant structural genes for these pathways were checked during those analyses (Castrillo et al., 2013) and the authors did not find a correspondence with the phenotypic alterations observed in metabolite production. The finding of RNA-binding by this protein (Castrillo et al., 2015), unlike other described cryptochromes, has already been proposed as the basis for a possible mechanism responsible for a non-transcriptional regulation. So, it is not surprising that we did not find changes on mRNA levels on those clusters. RNA inmunoprecipitation experiments were carried out in this Thesis in an attempt to identify CryD-bound RNAs, but lack of success prompted us not to include this negative data. Unfortunately, it was not possible to extend the time dedicated to this aproach, that no doubt should provide very valuable data on the post-transcriptional molecular mechanism of action of CryD and the identification of its regulatory targets.

As a final consideration, the transcriptomic analyses performed in this chapter constitutes the most complete approach to date on the regulatory effects of light in *F. fujikuroi* at expression level, confirming the major role of WcoA in *Fusarium* photobiology, as well as the

participation of the DASH cryptochrome CryD, presumably at a post-transcriptional level. In addition, it has broadened the regulatory role initially expected for WcoA, extending its influence on thousands of genes in the dark and making it a major regulator in this fungus.

General discussion

In recent decades, some filamentous fungi have arisen as suitable models for the study of different biological processes. Among them, it is worth mentioning the control of sporulation in *A. nidulans* (Oiartzabal-Arano et al., 2016), the regulation by light and the circadian rhythm in *N. crassa* (Corrochano, 2019; Diernfellner and Brunner, 2020; Dunlap and Loros, 2017), or the pathogenesis and pathogen-plant interactions in *Fusarium oxysporum* (Gordon, 2017). Unlike the genera *Aspergillus* and *Neurospora*, the genus *Fusarium* has enormous taxonomic complexity, with hundreds of identified species, usually plant pathogens (Summerell, 2019). The interest of their study lies in its impact on agriculture, on which the ability of this group of fungi to produce a great diversity of secondary metabolites also plays a very important role (Li et al., 2020). In this regard, the fungus object of this Thesis, *F. fujikuroi*, formerly *Gibberella fujikuroi*, has stood out as one of the most studied models because of the richness of its secondary metabolism (Avalos et al., 2007; Niehaus et al., 2016). Early in the last century, *F. fujikuroi* called the attention of researchers due to its ability to produce gibberellins, a very unusual metabolite in the fungi world (Tudzynski, 2005; Tudzynski et al., 2016). In recent years, this species has also become one of the best studied models for carotenoid synthesis (Avalos et al., 2017b). The group in which this work has been carried out has identified all the genes for the enzymes of the pathway and has devoted its attention in recent years to the study of their regulatory mechanism, in which protein CarS and light play central roles (Ruger-Herreros et al., 2019).

This Thesis has been dedicated to deepening into into the mechanisms that control the synthesis of carotenoids, among other processes regulated by light in *F. fujikuroi*. Specific details on the results of the different chapters have been already discussed, and this section is only dedicated to some general considerations. One of the starting points of the described work was the suspected participation of a small regulatory gene upstream of the *carS* gene, initially discovered as a possible precursor of miRNA detected by sequence analysis with a computer program (Rodríguez-Ortiz, 2012). The data presented in this Thesis contradict the hypothesis of the participation of a small RNA in the regulation of the carotenoid pathway. Nevertheless, it has led to the discovery of a regulatory RNA of a different nature, a long non-coding one, supposedly transcribed and polyadenylated by RNA polymerase II (Parra-Rivero et al., 2020b). However, this line of research was continued at a genomic scale, which led to investigate for the first time the existence of small RNAs in this fungus, which was supported by the presence of all the genes that encode the pieces of machinery necessary for their formation and processing. The demonstrated existence of small RNAs in other *Fusarium* species (Chen et al., 2014, 2015) made it possible to anticipate their presence also in *F. fujikuroi*, which has been confirmed by massive sequencing analysis of small RNAs.

A particularly unexpected result of this study, as judged by those described in other fungi (Carreras-Villaseñor et al., 2013; Chen et al., 2015), was the impossibility of obtaining targeted mutants for the gene for the Dicer1 protein, *dcl1*. After the unsuccessful analysis of more than one hundred candidate transformants, which showed that the transformation process itself was not a limiting factor, it was concluded that the method followed for the generation of the mutant

does not allow it to be obtained. However, following the same protocol and analyzing a much lower number of transformants, it was possible to isolate two mutants of the gene *dcl2,* coding for Dicer2 protein. The question arises whether the mutants of the *dcl1* gene could be not viable, or at least that the Dicer1 protein could be necessary for the process of regeneration of protoplasts. Alternatively, it may happen that the region of the gene *dcl1* was not accessible to the recombination machinery that allows integration of the vector. In favor of the hypothesis of the essential role of the Dicer1 protein is the fact of the apparent lack of phenotype of the *dcl2* gene mutants. In none of the cultivation conditions tested it was possible to appreciate significant differences between the mutants of this gene and the wild strain, a result that is reinforced by the lack of effects of the *dcl2* mutation in the *F. fujikuroi* transcriptome. However, it is important to bear in mind that the *dcl2* gene shows higher levels of transcript, approximately 10 times higher, than the *dcl1* gene, which seems to contradict the hypothesis of the lower biological relevance of *dcl2*. In any case, it is possible that small RNAs do not play important roles in the growth and development of this species, at least under laboratory conditions. However, the ubiquity of this sRNA-producing machinery in *Fusarium* species strongly indicate that they perform biological functions that have been of interest on an evolutionary scale, as the presence of small antisense RNAs of presumed transposable elements seems to suggest.

As already mentioned, the study of the small regulatory RNAs in this fungus has unexpectedly led to the identification of a long regulatory RNA, called *carP*, which plays a role as a positive effector of carotenogenesis, evidenced by the albino phenotype of the mutants lacking this regulatory element (Parra-Rivero et al., 2020b). The simultaneous analysis of the same sequence in *F. oxysporum* allowed us to conclude without any doubt its nature as a long noncoding RNA. The characterization of *carP* in this Thesis has led to interesting conclusions about its possible regulatory mechanism. On the one hand, its efficiency is surprising for the very low transcript levels detected in RNA-seq analyses. The *carS* gene, located downstream in the same direction of transcription, does not show very high levels of expression either. On the other hand, its action on carotenogenesis requires its location upstream of *carS*, which leads to suspect a possible interference with the transcription of the *carS* gene. The transformants analyzed in the Δc*arP* complementation experiments in some cases showed the integration of *carP* in its native site, but the Southern blots revealed the presence of additional *carP* sequences in the genome, making more complex the interpretation of the complementing phenotypes. It must be assumed that a single clean *carP* restitution in its native site would result in the recovery of a wild phenotype. We do not know if the differences observed in the complementing transformants with respect to the wild-type background are due to the simultaneous action of *carP* in situ and in other places of the genome, or to differences in *carP* expression in the native site due to the neighbor sequence of the selection cassette.

The experiments described, however, leave many doubts that will have to be resolved in future research. It is surprising, for example, that the strong induction by light of the transcription of the *carB* gene in the complemented transformant *carP* #18 does not result in a proportional increase in the carotenoid content in its mycelium. It seems clear that if an increase in *carB* mRNA levels is not enough, there must be some type of post-transcriptional mechanism

that regulates the translation of the mRNA or the activity of the enzymes that synthesize these pigments. Another aspect that remains to be analyzed in greater depth is the existence of genes that are apparently regulated by *carP* independently of *carS*. Evolutionarily it is very likely that *carP* comes from the acquisition of an autonomous function of a segment of the primitive 5' UTR of the *carS* gene (Parra-Rivero et al., 2020b), as the *carP* and *carS* genes are transcribed in a single RNA molecule in *F. verticillioides* line 7600. However, the results of this Thesis support the idea that *carP* has found other regulatory functions as an autonomous lncRNA, which opens a new line of research. Another aspect that will require attention is the regulatory relationship between *carP* and light. It is possible that this relationship is due to its regulation on *carS*, which in turn was previously shown that it has an influence on the expression of many genes that are regulated by light (Ruger-Herreros et al., 2019), but an independent regulatory effect at post-transcription level on components of the light-regulation machinery is not ruled out.

The regulation of *Fusarium* carotenogenesis by light is emerging as one of the most complex ones described so far in fungi. In other well-known light regulation systems, such as that of *N. crasa*, this regulation resides practically exclusively in the control by the proteins of the White-collar complex (Dasgupta et al., 2016). A similar complex seems to also act in mucoral fungi, where a greater diversity of White Collar 1 and 2 proteins have been described, possibly able to form heterodimers in different combinations (Corrochano, 2019; Corrochano and Garre, 2010). However, only one White collar 1 protein is directly responsible for the photoinduction of carotenogenesis in *M. circinelloides* (Silva et al., 2006). One of the aims of this Thesis was to deepen into the role of the WcoA protein in *Fusarium* because previous results of the group showed that the elimination of its unique White collar 1 protein did not lead to the complete loss of photoinduction of carotenogenesis, as was observed in *N. crasa* (Estrada and Avalos, 2008). Therefore, at least a second photoreceptor must participate in this regulation. Previous data pointed to the cryptochrome CryD as responsible for an additional level of regulation to that exerted by the White-collar system (Castrillo and Avalos, 2015). It is interesting to note that the *cryD* gene is hardly expressed in the dark and that its mRNA levels are strongly increased under illumination by the action of the WcoA protein (Castrillo and Avalos, 2015). Since previous purification of heterologous expressed CryD in *E. coli* demonstrated that RNA molecules were bound to this protein (Castrillo et al., 2015), it was hypothesized that such RNA could play a role in the regulation of carotenogenesis, for which *carP* could be a possible candidate. Therefore, CryD labeling experiments were carried out in *F. fujikuroi* (results not shown in the Thesis) in order to purify the RNA molecules bound to this protein. Surprisingly, despite its strong induction at the mRNA level, the detection of the CryD protein was not possible in western experiments, which lead to suspect of the existence of possible post-transcriptional regulatory mechanisms of this protein, or perhaps a very short half-life. It is tempting to hypothesize that the binding of *carP* to CryD stabilizes it or produces a conformational change that facilitates a positive action on the biosynthetic activity of carotenoids by a mechanism yet to be elucidated.

The previously investigated insertional mutant of the *wcoA* gene showed a pleiotropic phenotype, that affected to morphology and the synthesis of other metabolites (Estrada and Avalos, 2008). For this reason, it was decided to learn more about the role of this protein by

investigating the effect of its mutation on the *F. fujikuroi* transcriptome. The result exceeded all expectations, since it showed that WcoA directly or indirectly influences the expression of approximately 20% of the genes of this fungus. On the other hand, the mutation alters the regulation of practically all the genes controlled by light, which shows that WcoA conserves its function as a critical photoreceptor in the regulation by light of *Fusarium*. However, its effects in the dark are even more extensive, and affect a wide variety of cellular functions, pointing to WcoA as a central regulatory protein, capable of integrating different responses, of which light is only one of them. What are these other signals, apart from light, to which WcoA could respond constitutes one of the future challenges in the investigation of the functions of this protein. Some of these signals must be involved in the regulation of secondary metabolism, since many of the pathways for these compounds change their regulatory pattern in the *wcoA* mutant. The genes responsible for these pathways are usually organized in clusters, often located in subtelomeric regions, suggesting a possible regulatory role for WcoA at the chromatin structure level. In *F. asiaticum*, different phenotypes have been linked to the LOV and the Zn finger domain of the protein (Tang et al., 2020). An interesting approach for future works could be to investigate the roles of the different domains of the WcoA protein in *F. fujikuroi*, confirming if light-independent phenotypes are indeed dependent only on the Zn finger domain, that is, if they are due to a role of WcoA as a standard transcription factor in which the flavin binding domain plays no function.

The study of the effect of the WcoA mutation on the transcriptome was also extended to the *cryD* gene mutant in experiments carried out in parallel for one of the illumination times, which facilitates the comparison of the results with those obtained with the *wcoA* mutant. As expected, the *cryD* mutation affected a much lower number of genes than the *wcoA* mutation, but nevertheless the number of genes influenced by light was reduced in the *cryD* mutant, confirming its possible role as a supplementary photoreceptor to WcoA in this fungus. The *cryD* deletion is not less interesting, although with a less striking effect than the *wcoA* mutation because CryD is not a transcription factor as WcoA. In any case, the regulatory function of CryD is dependent on WcoA, since as indicated above, its expression is regulated by WcoA.

The fact that neither *wcoA* nor *carP* mutations can completely abolish the photoinduction of mRNA levels of the structural *car* genes points to an alternative regulation pathway. As it has been mentioned, based on the kinetics response exhibited by its mutants (Castrillo and Avalos, 2015), CryD has been postulated as a complementary photoreceptor in photocarotenogenesis, but this remains to be experimentally confirmed. The participation of other photoreceptors, as the phytochrome, the plant-type cryptochrome, or the phototropin-like protein discovered in this Thesis, should be analyzed. In the case of the phytochrome, the phenotype of a null mutant was investigated in *F. graminearum*, but the involvement in carotenogenesis was not investigated (Kim et al., 2015). Nevertheless, the transcriptomic data allow us to identify the sets of genes affected by each of these mutations and can lead us to propose a tentative transduction pathway involved in the activation of the *car* genes. Even though the occurrence of a direct transcriptional regulator has not been demonstrated, the transcriptomic results may help in the search for other transcription factors that could also

participate directly or indirectly in the regulation of the cluster. A bioinformatic search for the presence of the consensus WC-1 DNA-binding elements in the promoters of the structural *car* genes did not identify clear hits (J. Pardo Medina, unpublished). Assuming similar DNA-binding elements for its *F. fujikuroi* counterpart, this result suggests that WcoA might exert its regulatory function modulating the activity of another transcription factor specific for carotenogenesis in the presence of light. There are at least four putative transcription factors whose expression changes more than 4-fold after 15 min of illumination, and many others with smaller fold changes, which could be potential candidates to regulate the *car* cluster upon their activation by WcoA. Chip-seq experiments would be very useful to discriminate direct regulatory targets of the WCC in *F. fujikuroi* from indirect transcriptomic effects, while confirming if it is able or not to bind the promoters of the *car* genes.

Considered globally, this Thesis provides different results that confirm the available information and the high degree of sophistication of the regulation of carotenogenesis in *F. fujikuroi*. A simplified model summarizing the available information on the light regulation process and its relationship with CarS is represented in Figure D1. The more we know about the regulation exerted by CarS, the greater the complexity found, making it a fascinating multilayered biological problem to study. The unexpected regulation by a lncRNA is joined to other levels of regulation not investigated in this Thesis. These include the existence of several alternative removal sites for a small intron in the carboxy-terminal region, which can give rise to different variants of the CarS protein with different regulatory properties (Parra-Rivero, 2018; Ruger-Herreros, 2016). Probably because of its low expression, previous attempts by the group to detect the CarS protein in western experiments have not yielded satisfactory results, making it a very elusive protein for study. Regulatory complexity is probably inherent to any biological problem investigated at molecular level, in the sense that when studying any process in sufficient depth, new elements will be found that will add complexity to its regulation. It seems likely that CarS has a particularly intricate regulation reflecting its functional diversification, as suggest former results (Ruger-Herreros et al. 2019) that indicated that its function goes beyond the regulation of carotenoid production. In fact, in addition to the genes related to the synthesis of carotenoids, genes related with oxidative stress are subject to CarS regulation (Ruger-Herreros, 2016; Ruger-Herreros et al., 2019). As described in the general introduction, there is a close relationship between light and oxidative stress, providing a logic to the regulation of carotenogenesis by light. *Fusarium* has other pigments that could contribute to a defense against light-induced damage, but the carotenoids are particularly efficient in this protection. In addition, carotenoids are lipophilic pigments, and they probably exert beneficial effects protecting membrane proteins against oxidative damage. Therefore, CarS could be postulated as a light-protection modulator factor, which exerts a repressive function on several groups of genes which seem to play a role in photoprotection.

It is expected that this work will stimulate the continuation of research on the *carS* gene, its protein, and its regulatory targets, which presumably may include the WcoA protein, as a transcription factor that could mediate the light-induced transcription of the carotenoid genes in this fungus. The interest in *carS* regulation is not merely solving a basic research problem.

Recently, neurosporaxanthin, the main carotenoid accumulated in *carS* mutants in *Fusarium*, has proved to be a compound with potential antioxidant properties which make it very interesting for biotechnology purposes (Parra-Rivero et al., 2020a).

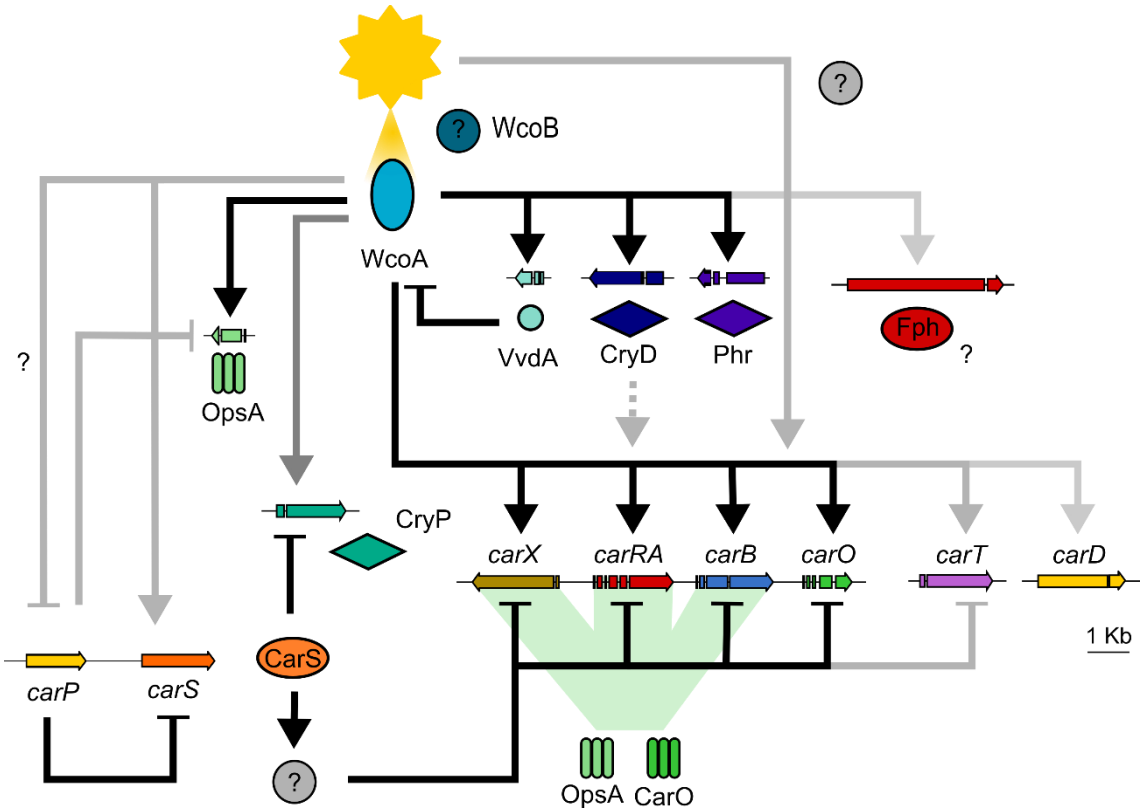

Figure D1. Model summarizing regulatory interconnections between genes involved in light detection and carotenogenesis in *F. fujikuroi*. Connections are based in transcriptomic data from this Thesis and experimental data from previous works. The intensity of the arrows represents the impact of each element on their targets. The discontinuous line which links CryD to the *car* genes represents the unknown molecular mechanism for this action. The green flux connects the genes involved in retinal production with the rhodopsin photoreceptors, indicating the putative use of retinal as chromophore. Grey elements correspond to hypothesized regulators which are still unknown.

Conclusions

1. *F. fujikuroi* has all the core components for siRNA production, RdRPs, Ago, and Dicer proteins, indicating a possible role of the interfering small RNA in its biology. Deletion of *dcl2* showed no phenotype under the studied conditions, while it was not possible to delete *dcl1*.

2. Data from small RNA sequencing points to the participation of specific siRNAs in gene silencing of some active transposons of *F. fujikuroi* and *F. oxysporum*.

3. Analysis of small RNAs did not find putative RNA-related elements in the upstream region of *carS* gene, refuting a former hypothesis on the implication of such elements in the regulation of this gene.

4. Different evidences support the existence of a gene that is transcribed to a lncRNA, located in the region upstream the *carS* gene. This lncRNA, which has been called *carP*, is a positive regulator of carotenogenesis in *F. fujikuroi*, as indicated the drastic reduction in gene expression of the structural genes resulting from *carP* deletion.

5. The *carP* gene upregulates carotenogenesis only in *cis,* as ectopic integration of the gene was not able to complement the *carP* mutant phenotype.

6. Deletion of *carP* widely changes transcriptome, including a three-fold decrease of the number of photoregulated genes compared to the wild strain. The most affected transcripts belong to a group of photoinducible genes that include many of the genes overexpressed in the *carS* mutant, whose mRNA levels decrease sharply in the *carP* mutant.

7. Many of the transcriptomic effects of *carP* deletion are presumably due to *carS* upregulation. Nevertheless, there is a group of genes differentially expressed in the absence of *carP* whose expression is not altered in the *carS* mutant, pointing to regulatory effects of *carP* unrelated to the action of CarS protein.

8. The transcriptomic effects of three times of illumination revealed a diversity of kinetics patterns in mRNA accumulation. Photoinduced genes exhibited fast, intermediate and late responses, but only intermediate or late responses were found among the photorepressed genes. Lack of rapid repressions may be explained by the persistence of mRNA previously synthesized in the dark.

9. WcoA is a master regulatory protein in *F. fujikuroi*, whose mutation, directly or indirectly, affects the expression of several thousand of genes involved in a great diversity of cellular processes, including the control of essentially all the light-regulated genes.

10. Although WcoA constitutes the main photoreceptor in *F. fujikuroi*, most functions performed by WcoA in *F. fujikuroi* are carried out without the involvement of light detection.

11. The RNA-seq data of a *wcoA* mutant have revealed its influence in the expression of a diversity of secondary metabolites biosynthetic clusters in a light-independent manner, indicating that WcoA plays a key role in the regulation of secondary metabolism in *F. fujikuroi*.

12. CryD deletion results in changes in the degrees of photoinduction or photorepression of many genes, suggesting an accessory function in *Fusarium* photobiology.

Materials and Methods

ORGANISMS

STRAINS OF *FUSARIUM*

The *F. fujikuroi* strains used in this Thesis, as well as their phenotypes and origins are described in Table M.1.

Table M.1. Strains of *F. fujikuroi* used in this Thesis.

Strains	Relevant genetic feature	Phenotype for carotenogenesis	Strain origin	Reference
IMI58289		Wild type	Imperial Mycological Institute (Kew, Surrey, UK)	
SG39	*carS* mutant obtained by NG mutagenesis	Carotenoid overproducer	IMI58289	Avalos and Cerdá-Olmedo, 1987
SG256	SG39 strain complemented with wild-type *carS* alelle	Wild type	SG39	Ruger-Herreros et al. 2019
Δ*dcl2*-3 and Δ*dcl2*-4	*dcl2* deletion	Wild type	IMI58289	This Thesis
SG268, SG267 and SG270	*carP* deletion	Albino	IMI58289	This Thesis
carP #2 and *carP* #21	Ectopic *carP* integration	Albino	SG268	This Thesis
carP #3 and *carP* #18	*carP* integration	Altered carotenogenesis (#3<WT, #18>WT)	SG268	This Thesis
FKMC1995		Wild type	Kansas state university (USA)	
SF226 and SF229	*wcoA* disruption	Reduced photoinduction	FKMC1995	Estrada and Avalos, 2008
SF236 and SF237	*cryD* deletion	Slower photoinduction	FKMC1995	Castrillo et al., 2013

(*NG = N-methyl-N'-nitro-N-nitrosoguanidine)

BACTERIA STRAIN

Escherichia coli strain DH5α (F– ϕ80l*ac*ZΔM15, Δ(*lacZYA-argF)U169, recA1, endA1, hsdR17(rK–, mK+), phoA, supE44, λ–, thi-1, gyrA96, relA1*) was employed for transformation and plasmid replication (Hanahan, 1983).

YEAST STRAIN

Saccharomyces cerevisiae strain FY834 (*MATα, hisΔ200, ura3-52, leu2Δ1, lysΔ202, trp1Δ63*) was used to construct plasmids by homologous recombination (Colot et al., 2006).

CULTURE MEDIA

E. COLI CULTURE MEDIA

- LB medium: LB (Luria Bertani) is a rich medium for enterobacteria, whose components are: 5 g l^{-1} of yeast extract, 10 g l^{-1} of peptone, and 10 g l^{-1} of NaCl. For solid media, 20 g l^{-1} of agar are added (Sambrook and Russell, 2001). Final pH is adjusted to 7-7.5 if required.

- Antibiotics and other medium supplements: to select transformant colonies, ampicillin was added to LB media at 100 mg l^{-1}. To detect insertions in the multiple cloning sites of plasmids and to induce the production of proteins in the expression vectors, X-gal and IPTG were added at 40 mg l^{-1} and 20 mg l^{-1} respectively.

- SOB medium: used to generate *E. coli* competent cells for transformation (Inoue et al., 1990) and for electroporation recuperation. The composition is: 5 g l^{-1} of yeast extract, 20 g l^{-1} of tryptone, 0.5 g l^{-1} of NaCl, and 10 ml l^{-1} of a 250 mM KCl solution. Once autoclaved, $MgCl_2$ was added to a final concentration of 10 mM.

S. CEREVISIAE CULTURE MEDIA

- YPD medium: Its composition per liter of distilled water is 10 g of yeast extract, 20 g of Bacto™ peptone, and 20 g of glucose. For solid medium, 20 g of agar were added.

- Minimal SC medium: Its composition per liter of distilled water is 1.7 g of Yeast Nitrogen Base (devoid of amino acids and NH_4SO_4, abbreviated YNB), 5 g of NH_4SO_4, and 20 g of glucose. In case of solid medium, 20 g of agar were added. This medium was supplemented with the required amino acids according to the experiment.

- Amino acids and bases in SC-Ura medium: 0.03% L-isoleucine, 0.15% L-valine, 0.02% L-arginine-HCl, 0.03% L-lysine-HCl, 0.02% L-methionine, 0.05% L-phenylalanine, 0.2% L-threonine, 0.02% L-tryptophan, 0.03% L-tyrosine, 0.02% L-histidine HCl monohydrate, 0.1% leucine, 0.1% L-glutamic acid, 0.1% L-aspartic acid, 0.4% L-serine, and 0.02% L-adenine hemisulfate.

FUSARIUM CULTURE MEDIA AND SOLUTIONS

F. fujikuroi was grown either in liquid or solid media. Solid media were prepared by adding 16 g of agar per liter to the composition listed below.

- DG minimal medium: standard medium used for *F. fujikuroi* growth for routine laboratory manipulations. The composition is 30 g l^{-1} of glucose, 3 g l^{-1} of $NaNO_3$, 1 g l^{-1} of KH_2PO_4, 0.5 g l^{-1} of KCl, 0.5 g l^{-1} of $MgSO_4 \cdot 7H_2O$ and 2 ml L^{-1} of a microelement solution (Avalos et al., 1985).

- DG microelements solution. 0.5 mg of H_3BO_3, 5 mg of $CuSO_4$, 10 mg of $FeCl_3$, 1 mg of $NaMoO_4$, 1 mg of $MnCl_2$ and 100 mg of $ZnSO_4$ in 100 ml of distilled water (Avalos et al., 1985).

- DG asparagine (DGasn): DG minimal medium in which the 3 g l^{-1} of $NaNO_3$ are replaced by 3 g l^{-1} of L-asparagine.

- EG medium: used as solid medium for sporulation purposes with IMI58289 and derived strains. The composition per liter is 1 g o glucose, 1 g of yeast extract, 1 g of NO_3NH_4, 1 g of KH_2PO_4, 0.5 g of $MgSO_4 \cdot 7H_2O$, and 16 g of agar.

- Low nitrogen DG or low nitrogen DGasn: the concentration of either $NaNO_3$ or asparagine was reduced to 0.625 g l^{-1}.

- DG pH 7: DG minimal medium in which 1 g l^{-1} of KH_2PO_4 was replaced by 1 g l^{-1} of K_2HPO_4.

- ICI medium: used as high nitrogen conditions in experiments for production of secondary metabolites. It contains 80 g l^{-1} of glucose, 4.8 g l^{-1} of NH_4NO_3, 5 g l^{-1} of KH_2PO_4, 1 g l^{-1} of $MgSO_4 \cdot 7H_2O$, and 2 ml l^{-1} of microelement solution (Geissman et al., 1966).

- 10% ICI medium: ICI medium with 10% of nitrogen source (0.48 g l^{-1} of NH_4NO_3).

- ICI microelements solution: 100 mg of $FeSO_4 \cdot 7H_2O$, 15 mg of $CuSO_4 \cdot 5H_2O$, 161 mg of $ZnSO_4 \cdot 7H_2O$, 10 mg of $MnSO_4 \cdot 7H_2O$, and 10 mg of $(NH_4)_6Mo_7O_{24} \cdot 4H_2O$) in 100 ml of distilled water (Geissman et al., 1966).

- Darken medium: used to prepare the inoculum for the transformation protocol. Composed of 15 g of corn steep liquor (Sigma), 30 g of sucrose, 2 g of $(NH_4)_2SO_4$, and 7 g of $CaCO_3$ in 1 L of distilled water.

- Regeneration medium 2X: a rich medium used for protoplast regeneration after the transformation protocol. The composition is 2 g l^{-1} of yeast extract, 2 g l^{-1} of casein (N-Z amino acids, Sigma), and 32 g l^{-1} of agar. This medium is mixed with 1.6 M sucrose in equal volumes to obtain regeneration medium 1X.

- Top-agar for regeneration medium 2X: 2 g l^{-1} of yeast extract, 2 g l^{-1} of N-Z amino acids, and 20 g l^{-1} of agarose. This medium is mixed with 1.6 M sucrose in equal volumes to obtain regeneration medium 1X. In the case of antibiotic selection, 50 mg l^{-1} of hygromycin or 250 mg l^{-1} geneticin were added to the medium and to top agar.

- Potato Dextrose Broth (PDB): 24 g of PDB (Formedium, LTD) per liter. In the case of solid medium (Potato Dextrose Agar, or PDA) 16 g of agar was added.

- Selective medium: DG or DGasn were supplemented with 100 mg l^{-1} of hygromycin B (Roche) or 100 mg l^{-1} geneticin (G-418 disulphate salt, Sigma).

PLASMIDS

PLASMIDS PREVIOUSLY AVAILABLE

- pGEMT-easy (Promega): commercial vector used for cloning of PCR products. This 3 kb plasmid contains the β-lactamase gene *bla,* which confers resistance to the antibiotic ampicillin. It also includes the β-galactosidase gene *lacZ* interrupted by a multiple cloning site (MCS) for detection of right clones by color screening through β-galactosidase activity on X-gal (5-bromo-4-cloro-3-indolil-β-galactopiranoside) upon IPTG (isopropil- β-D-1-tiogalactopira-noside) induction.

- pSpark I (Canvax): commercial vector used for cloning of PCR products. This 3 kb plasmid contains the β-lactamase gene *bla,* which confers resistance to the antibiotic ampicillin. It also includes the β-galactosidase gene *lacZ* interrupted by a multiple cloning site (MCS) for detection of right clones by color screening through β-galactosidase activity on X-gal (5-bromo-4-cloro-3-indolil-β-galactopiranoside) upon IPTG (isopropil-β-D-1-tiogalactopira-noside) induction.

- PRS426 (available from the Fungal Genetics Stocks Center, FGSC): cloning vector designed for genetic manipulation through of the host *S. cerevisiae*, and which is also functional in *E. coli*. Contains the gene that confers resistance to ampicillin and the *URA3* gene of *S. cerevisiae*, used as selection markers. The size is 5.7 kb.

- pCSN44 (available from FGSC): plasmid derived from pDH25 (Cullen et al., 1987). It contains the gene for resistance to hygromycin B under the control of the promoter and terminator of the *A. nidulans trpC* gene. The size is 3.4 kb.

- pNTP2 (kindly provided by Dr. Attila Adám): vector that contains a geneticin resistance cassette consisting of the neomycin phosphotransferase II gene (*nptII*) under control of a duplicated cauliflower mosaic virus 35S promoter (CaMV). Used as a plasmid with an alternative selection marker. The size is 4.8 kb.

- pGmir1F and pGmir1R: plasmids containing the putative *mir1* sequence in the two possible orientations, amplified from *F. fujikuroi* genomic DNA with PS1.1 primer set and cloned in vector pGEM-T. Both plasmids were used to sequence that DNA fragment and to produce radioactive riboprobes for northern-blot hybridization experiments of small RNA. Their sizes are 3.4 kb.

- pGmir2F and pGmir2R: plasmids containing the putative *mir2* sequence in the two possible orientations, amplified from *F. fujikuroi* genomic DNA with PS1.2 primer set and cloned in pGEM-T. Plasmids were used to sequence *mir2* and to produce radioactive riboprobes for northern-blot hybridization of small RNA. The size of each plasmid is 3.5 kb.

- pGpcarSF and pGpcarSR: plasmids containing the fragment between the putative *mir1* and the putative *mir2* of *F. fujikuroi* in the two possible orientations, amplified with PS1.3 and cloned in pGEM-T. Used to produce radioactive riboprobes for small RNA northern-blot hybridization experiments. The size of both plasmids is 5.1 kb.

- pdcl2hyg: plasmid used to delete the *dcl2* gene. It was constructed by homologous recombination in *S. cerevisiae* ligating the vector pRS426 with three fragments obtained by PCR with primers containing tails of homologous sequences with the other fragments and the vector: the 5' region of *dcl2* (amplified with PS1.4), its 3' region (amplified with PS1.5), and the hygromycin resistance cassette (amplified with PS1.6). The size is 8.8 kb.

- pSdcl1: plasmid containing the *dcl1* gene, including around 1.2 kb of upstream and downstream DNA (amplified by PCR with PS1.10), cloned in the pSpark plasmid. The size is 10.1 kb.

- pGneo2p: plasmid containing the *neoR* G418 resistance cassette, surrounded by an *Asc*I restriction site at each side (amplified by PCR from plasmid pTNP2 with PS1.12), cloned in pGEM-T. The size is 4.9 kb.

- pdcl1neo: plasmid used to try to delete the *dcl1* gene, formed by the ligation of an inverse PCR fragment, amplified from plasmid pSdcl1 with PS1.11, which avoids *dcl1* ORF. The inverse PCR fragment was obtained with *Asc*I restriction site containing primers. It includes the G418 resistance cassette obtained by digestion of PGneo2P with *Asc*I. The size is 7.4 kb.

- pcarPhyg: plasmid used to delete the *carP* lncRNA sequence. It was constructed by homologous recombination in *S. cerevisiae* ligating the vector pRS426 with three fragments obtained by PCR with primers containing tails of homologous sequences with the other fragments and the vector: the 5' region of *carP* (amplified with PS2.11), its 3'

region (amplified with PS2.12) and the hygromycin resistance cassette (amplified with PS1.6). The size is 9.4 kb.

- pcarPneo: plasmid used to complement the *carP* lncRNA sequence. It was constructed by homologous recombination in *S. cerevisiae* ligating the vector pRS426 with two fragments obtained by PCR with primers containing tails of homologous sequences with the other fragments and the vector: *neoR* G418 (amplified with PS2.19) resistance cassette, and the *carP* gene including its presumptive promoter and terminator sequences (amplified with PS2.20). The size is 10.3 kb.

CULTURE CONDITIONS OF MICROORGANISMS

Culture conditions for *Escherichia coli*

The *E. coli* bacteria were cultured in LB at 37 °C, shaking at 200 rpm in the case of liquid medium. When necessary, the required antibiotic was added (usually ampicillin) and / or other compounds, such as X-Gal and IPTG. Lomng-term conservation of bacterial strains was carried out in LB medium with 30 % glycerol (v/v) at -80 °C. For short-term periods colonies were kept on agar plates at 4 °C.

Culture conditions for *S. cerevisiae*

S. cerevisiae cells were grown on solid YPD to refresh collection strains or in liquid YPD to obtain biomass as pre-inoculums for transformation experiments or plasmid extractions. In transformation experiments, the yeast cells were grown in minimal medium SC-Ura supplemented with amino acids and bases. The medium lacks uracil, as plasmid pRS426 contains the *URA3* gene, as a selection marker, which allows the complementation of the uracil auxotrophic mutation of the FY834 strain.

Culture conditions for *F. fujikuroi*

For standard maintenance, *F. fujikuroi* strains were grown in solid DG or DGasn media at 30 °C. To collect conidia, *F. fujikuroi* was inoculated from fresh isolated colonies at seven equidistant points using sterile toothpicks on Petri dishes containing EG agar medium. The strains were grown for 7-10 days at 26 °C under white light. This inoculation system was also used in experiments for carotenoid measurements except that Petri dishes contained DG agar medium. In this case, strains were grown at 30 °C for 7 days under light or kept in the dark in a paperboard box. After being collected, mycelial samples were frozen and preserved from light until carotenoids extraction.

Conidia were collected from mycelia spreading 5-10 ml of sterile distilled H_2O with a metal rod. The conidia suspension was filtered through a borosilicate filter crucible of size pore 1 (30 ml and 30 mm Ø, Robu, Hatter, Germany) attached to a 100 ml flask. The scraping was repeated, and the successive samples were filtered and collected in the same flask. The content of each flask was poured into a 50 ml Falcon tube, centrifuged for 10 min at 2,000 rpm and the

supernatant was discarded. Two washing steps with 5 ml of sterile H_2O were done and the conidia pellets were resuspended in 1 ml of sterile H_2O and transferred to a sterile 1.5 ml Eppendorf tube. Concentrations of conidia were calculated in a hemocytometer using a DM1000 Leica microscope with 40X magnification or using a TC20™ Automated Cell Counter (BioRad). Depending on their concentrations, dilutions were required before counting.

To quantify production of conidia, mycelia from agar cultures inoculated at 7 points were washed twice with 7.5 ml of distilled water and collected in a 50 ml Falcon tube. Three parallel Petri dishes per strain were cultured in each experiment. Afterwards mycelia were washed twice with 10 ml of distilled water and collected to the same tube. Aliquots were taken to calculate conidia concentration in the TC20™ Automated Cell Counter (BioRad). Total amount of conidia was calculated per Petri dish.

For genomic DNA extraction, *F. fujikuroi* mycelium was grown in 50-, 250-, or 500-mL Erlenmeyer flasks containing one fifth of volume of DG or DGasn medium. Media were inoculated either with conidia or with a mycelium plug and incubated for 3 days under indirect illumination at 200 rpm at 30° C. The whole culture was filtered through filter paper with a Kitasato using a vacuum device. The mycelia were frozen at –20 °C.

For expression analyses in *F. fujikuroi*, 500-ml Erlenmeyer flasks containing 100 ml of DG medium were inoculated with 10^6 conidia of the corresponding strains and cultured in the dark for three days on an orbital shaker at 150 rpm. Subsequently, 25-ml samples of the cultures were transferred to standard Petri dishes under red safelight and incubated for four hours (or different times if indicated in the experiment) to adapt the mycelia to static conditions. Then, they were incubated for one hour in the dark or under white light. Upon incubation, the mycelium was removed from the medium by vacuum filtration, washed with distilled water, immediately frozen in liquid nitrogen, and stored at −80 °C. Light exposures were performed under a platform with 4 fluorescent tubes (Philips TL-D 18 W/840) at *ca*. 60 cm, providing a light intensity of 7 W m^{-2} (420 Lm W^{-1}), as in the case of carotenoids production experiments. Total darkness was achieved by incubating the plates in closed paperboard boxes or wrapping the flasks with aluminum foil surrounded by black plastic bags.

NUCLEIC ACID ISOLATION

PURIFICATION OF PLASMID DNA FROM *E. COLI*

Three different methods were used depending on the quality and purity of the plasmid DNA intended to isolate.

- Small-scale plasmid preparations (miniprep). Adapted from the alkaline lysis protocol (Sambrook and Russell, 2001; Stephen et al., 1990), this protocol was used to obtain DNA amounts lower than 10 µg. *E. coli* cultures, usually of 3 ml, were grown overnight at 37 °C. A 1.5-ml aliquot was centrifuged at maximum speed (13,200 rpm) for 1 min and the supernatant was removed. The cell pellet was resuspended in 200 µl

of cold solution I (50 mM Tris, 10 mM EDTA, pH 7.5 and 10 mg l^{-1} RNase). 200 µl of fresh solution II (0.2 M NaOH, 10 g l^{-1} SDS) were added to the sample, carefully inverted to clear up the cell suspension, and kept in ice. To neutralize the lysis process, 150 µl of cold solution III (3 M Potassium acetate, 11.5% glacial acetic acid, pH 4.8) were added and vortexed. The mixture was centrifuged for 10 min at 13,200 rpm and the supernatant was carefully transferred to a clean 1.5 ml tube. For DNA precipitation the sample was mixed with 500 µl of isopropanol and centrifuged again for 5 min at maximum speed. The supernatant was discarded, and the pellet was washed with 70 % ethanol. After 5 min of centrifugation, the precipitated DNA was dried and resuspended in 20-30 µl of TE.

- Plasmid DNA extraction kit (<10 µg). It was used when high-purity plasmid DNA was required, as for sequencing reactions. The commercial NucleoSpin Plasmid kit (Macherey-Nagel) was used, following the manufacturer's instructions.

- Large scale plasmid preparations (midiprep). The miniprep protocol yields DNA amounts over 500 µg, with average concentrations between 1 and 3 µg μ^{l-1}. A culture of *E. coli* was grown in 50 ml of LB overnight at 37 °C. The centrifugation steps were done at 4 °C and 4,500 rpm. All the steps were carried out in 50-ml Falcon tubes. The pellet obtained was resuspended in 1.6 ml of solution I and kept on ice for 5 min. 3.2 ml and 2.4 ml of solution II and III respectively were added proceeding as above and the lysed suspensions were centrifuged for 10 min. The supernatant was filtered through a sterile gauze and 6.4 ml of a mixture of phenol:chloroform:isoamilic alcohol (25:24:1) were added, mixed, and centrifuged for 10 min. Afterwards, the supernatant was transferred to a clean 50 ml tube and precipitated with 2 volumes of ethanol 96 % at -80 °C for 10 min. The sample was centrifuged for 10 min and the pellet was washed with 3.2 ml of ethanol 70%. A final centrifugation step was performed to remove the ethanol and the pellet was dried at 37 °C. The plasmid DNA was finally resuspended in 0.5-1 ml of TE.

ISOLATION OF PLASMID DNA FROM *S. CEREVISIAE*

Purification of plasmid DNA from *S. cerevisiae* followed a similar protocol to the extraction of plasmid DNA from bacteria, with small modifications. The starting material was yeast biomass obtained from a 10-12 h inoculum incubated for 24 hours in selective medium. Yeast cells were centrifuged for 1 min at 13,000 rpm and resuspended in water to wash them. Then, they were centrifuged again for 1 min at 13,000 rpm and the pellet was resuspended in 640 µl of a solution of 0.9 M Sorbitol 0.1 M EDTA pH 8. 6.4 µl of β-mercaptoethanol and 10 µl of 20T zimolyase (10 mg mL^{-1}) were added to this mixture, an enzymatic cocktail to break down yeast cell wall, and the mix was incubated for 1 hour at 37 °C. After incubation, the reaction was centrifuged for 1 min at 13,000 rpm and the extraction protocol continued as the bacterial plasmid miniprep extraction described above.

F. FUJIKUROI DNA EXTRACTION

For genomic DNA isolation two procedures were followed. Both required fine mycelia powder as the starting sample, obtained by grinding an appropriate mycelium amount with liquid nitrogen in a mortar with a pestle.

- Small DNA amounts for PCR tests were obtained with the GenElute Plant Genomic DNA Miniprep kit (Sigma-Aldrich, USA) or the Nucleo Spin Plant II (Macherey-Nagel), according with manufacturer's instructions. When the Nucleo Spin Plant II was used, section 5.2 ("Genomic DNA from fungi") of the protocol was applied.

- Large quantities of genomic DNA were extracted for Southern blot analyses as described in Weinkove et al. 1998: 7 ml of the extraction solution (Tris-HCl 50 mM, EDTA 20 mM, pH 7.5) were added to the fine powder and resuspended carefully on ice. Afterwards the sample was incubated at 65°C for 30 min with 0.5 ml of SDS 10%. The sample was cooled for 30-60 min in ice and 2 ml of neutralizing solution (Potassium acetate 5 M) were added prior to centrifugation at 4°C and 14,000 rpm for 10 min. The supernatant was transferred to a new 50-ml tube and precipitated with 2 volumes of ethanol 96% at -80°C for 1h. After this time, the sample was centrifuged for 20 min at 14,000 rpm (4°C) and the pellet was washed with 1 volume of ethanol 70% and centrifuged again. Finally, the pellet was dried and resuspended in 1 ml of TE (10 mM Tris, 1 mM EDTA pH 7.5). RNase treatment with 10 µg ml^{-1} Ribonuclease A (Sigma) was carried out for 30 min at 37°C, followed by enzyme inactivation at 65°C. Additional steps of Phenol:chloroform:isoamyl alcohol (25:24:1) extraction were implemented at the end of the process to ensure DNA purity (Sambrook and Russell, 2001).

F. FUJIKUROI RNA EXTRACTION

RNA extraction also had two variants depending on the quantity and/or purity necessary for its use.

-Small scale (<40 µg of RNA). Mycelia were ground with the FAST-PREP24 (Biomedicals, LLC Europe, France) disruption system and extraction was achieved with the commercial RNeasy® Plant Mini Kit (QIAGEN) or the NucleoSpin plant II (Machenerey-Nagel), following the manufacturer's instructions, with the specificities for fungal starting material. In general, the quality of the obtained RNA was high.

-Large scale (> 50 µg of RNA). At least 150 mg of mycelium were crushed in a mortar with liquid nitrogen as for DNA extraction. The protocol was always done on ice to avoid RNA degradation. The obtained powder was resuspended in 750 µl of TRIzol (TRIzol Reagent, Ambion), homogenized and kept at cold temperature for at least 5 min. 150 µl of chloroform were added, vigorously vortexed for 15 seconds, and kept for 2-3 min in ice. It was then centrifuged at 12,000 rpm for 15 min at 4 °C. The aqueous phase was collected, with extreme care of not touching the interphase, and transferred to a clean tube, where 375 µl of isopropanol were added. After mixing, the tube was incubated in ice for 10 min, centrifuged for 10 min at

12,000 rpm at 4 °C, and the supernatant was discarded. The RNA pellet was washed with 70% ethanol and centrifuged 5 min at 12,000 rpm at 4 °C. Finally, the supernatant was removed, and the precipitate was dried and resuspended in RNase-free bdH_2O. Finally, the samples were incubated in a bath at 60 °C for 10-15 min and stored at -80 °C until used.

This Trizol RNA extraction method was also used for the RNA-seq samples, since it provides large amounts of RNA in a small volume. In this case an additional RNA purification step was performed. RNA samples were passed 2 times through an RNA purification column of the commercial kit NucleoSpin RNA (Macherey-Nagel) following the manufacturer's instructions. This procedure allowed obtaining RNA of sufficient quality for the sequencing process.

A small RNA enrichment procedure was performed for northern-blot experiments of small RNA during the Trizol extraction. After chloroform phase separation, the aqueous phase was transferred to a new tube and 900 µl of isopropanol were added. Samples were incubated at -20 °C between 2 hours or overnight for precipitation of nucleic acids. They were centrifuged for 10 min at 12,000 rpm at 4 °C, and the supernatant was discarded. The pellets were washed with 1 ml of 75% ethanol and centrifuged again for 5 min. The resulting pellets were dried for 15 min and resuspended in 300 µl of water. Then, 40 µl of 50% PEG 8000 and 50 µL of 4 M NaCl were added, the mix was incubated for 30 min in ice, and centrifuged afterwards for 10 min at 12,000 rpm at 4 °C. The supernatant was precipitated with 3 volumes of absolute ethanol during 30 min in ice. Then it was centrifuged again, and the pellet was washed with ethanol 80%. The small RNA enriched samples were air dried and resuspended in 30 µl of RNAse-free bi-distilled water.

NUCLEIC ACID MANIPULATION

Nucleic acid quantification

The concentration of the DNA or RNA samples were determined by optical density at 260 nm using a Nanodrop® ND-1000 spectrophotometer, paying also attention to the relationships A260/A280 and A260/A230 in order to determine the quality and purity of the sample. In some cases, the quantification was carried out by densitometry in agarose gel electrophoresis, comparing the intensity of the bands with known amounts of a 1 kb DNA Ladder size marker (Nippon Genetics, Europe GmbH).

Nucleic acid electrophoresis on agarose gels

The separation and identification of DNA and RNA molecules was performed by electrophoresis in gels prepared with low electroendosmosis (D1 EEO) agarose (Intron Biotechnology) and TAE buffer (40 mM Tris-acetate; 1 mM EDTA pH 8). The agarose concentrations were 7 g l^{-1} for routine electrophoresis and 20 g l^{-1} when bands with sizes smaller than 200 bp needed to be differentiated. To visualize nucleic acids adjusted concentrations of ethidium bromide or 5 µl of Midori Green Advance (Nippon Genetics) were added per 100 ml of gel. Electrophoresis was run in horizontal cells (Ecogen, Barcelona) filled

with TAE and connected to a power supply (Pharmacia Biotech EPS 200 or Bio-Rad PowerPac™ Basic Power Supply). DNA samples mixed with 10X loading buffer (1% SDS, 50% glycerol and 0.05% bromophenol blue, Takara). RNA samples were mixed with special loading buffer, the 10X RNA Stock Buffer (50% v/v glycerol, 1 mM EDTA pH 8, 0.25% w/v bromophenol blue). Nucleic acids were run in parallel with commercial size markers, as the 1 kb DNA Ladder RTU (Nippon Genetics), containing fragments ranging from 250 bp to 10 kb. Known amounts of lambda phage DNA digested with *Hin*dIII was used to calculate DNA concentrations. Electrophoresis was performed in a horizontal cell with TAE buffer at a constant voltage of 1-4 V cm^{-1}. DNA was visualized in the gels by UV radiation in a Gel Doc™ EZ Imaging System (BioRad) and images were processed with Image Lab™ Software (BioRad).

Recovery of DNA fragments in agarose gels

The purification of DNA fragments from agarose gels was carried out cutting out the agarose plug which contained the band with a blade and using the commercial ISOLATE II PCR and Gel Kit (Bioline), following the manufacturer instructions. To avoid UV-induced mutations in DNA fragments used for sequencing or cloning, DNA was visualized with an UV hand lamp (312 nm).

DNA digestions

Restriction enzymes were purchased either to New England Biolabs (Ipswich, MA, USA) or to Takara (Shiga, Japan). The enzymes were supplied at concentrations ranging from 10 to 20 U μl^{-1} and with specific reaction buffers (10X). Plasmid DNA and PCR fragments were digested in a total volume of 10-20 µl using 0.2 µl of the enzyme. Incubation temperatures varied according to the manufacturer's instruction for each enzyme, and incubation times were usually of at least 90 min. When required, digestions were followed by enzyme inactivation at high temperature (65-80 °C).

For Southern blot analyses, due to the larger DNA amount needed, more enzymatic units and longer incubation times were used. Usually, two-step digestions were performed. About 10 µg of genomic DNA were first treated with 10 units of the corresponding enzyme for 1 h, and then another 10 units were added for an overnight incubation. The digested sample was finally precipitated at -80°C for 1 h with 0.1 volume of sodium acetate and 2 volumes of ethanol 96%. After centrifugation at 13,200 rpm for 10 min, the DNA pellet was washed with 2 volumes of ethanol 70%, centrifuged, and dried. The sample was resuspended in an appropriate volume of TE (20-40 µl) and loaded in an agarose gel.

Dephosphorylation

When a vector was linearized with a restriction enzyme to be ligated with a DNA fragment digested with the same enzyme, the monophosphate group of the 5' end of the vector was removed to avoid recircularization and increase the efficiency of the ligation. One unit of

alkaline phosphatase (Roche) was incubated with DNA at 37 °C for 15 min followed by heat inactivation at 65 °C.

DNA precipitation

In different protocols it was necessary to carry out DNA precipitation. Typically, it was used to remove buffers, polymerases, and leftover dNTPs from a PCR, or to increase the DNA concentration of a sample. Routine DNA precipitation was carried out by adding 0.1 volumes of 3 M sodium acetate and 2 volumes of cold 96° ethanol. The mix was incubated at -20 °C for 60 min and centrifuged for 15 min at 13,000 rpm. The supernatant was removed, and the pellet was washed with 70% ethanol (v/v). It was centrifuged again for 5 min, the supernatant discarded and the precipitated allowed to dry. Finally, it was resuspended in bidistilled water in the desired volume.

Ligation

DNA ligations were performed using 1 U of T4 DNA ligase (Roche), suitable DNA amounts of fragments and ligase buffer supplied that includes ATP. Final reaction volume was 10-15 µl. Ligations were incubated at 16 °C overnight, or at room temperature for 1 hour.

DNase treatment

RNA samples were treated with recombinant DNase I, RNase-free (purchased either from USB, Affymetrix or from Sigma) to ensure no traces of DNA in the samples. 2.5 µg of RNA were incubated with 10 U of DNase at 25 °C for 15 min. The 10X buffer was provided by the supplier. To inactivate the enzyme, 1 µl of STOP solution (50 mM EDTA, pH 8) was added and incubated at 65 °C for 10 min.

Polymerase chain reaction (PCR)

PCR amplifications from genomic or plasmid DNA were done with different enzymes: for standard reactions BIOTAQTM DNA polymerase (London, UK) was used; for high fidelity reactions, such as those used for cloning or sequencing purposes, the Expand High Fidelity PCR system (Roche) or the Velocity DNA polymerase (Bioline) were chosen because of their lower mutation rates. The reaction conditions were those indicated in the manufacturer's instructions and according to the primer sequences and the length of the synthesized DNA. In general, an initial denaturation step at 94 °C for 2 min was followed by 35 cycles of DNA amplification, consisting of strand denaturation (94 °C, 20s), primers hybridization (50-60°C, 30s), and polymerase elongation (68°C for fragments > 3 kb or 72°C for fragments < 3 kb, 1 min kb^{-1}). Last step was a final polymerization cycle at 72 °C for 5-10 min. The reactions were carried out with an amount of template DNA that ranged from 10 to 100 ng for genomic DNA and between 1 and 10 ng for plasmid DNA. Primer sets used in the different PCR reactions are described in Methods Annex 1.

cDNA synthesis

Complementary DNA was obtained from DNase-treated RNA samples using the Transcriptor First Strand cDNA Synthesis Kit (Roche) and following the manufacturer's protocol: 2.5 µg of RNA were incubated with 2.5 µM anchored oligo (dT)18 primers and 2.5 µM of random hexanucleotides at 65°C for 10 min. Reversed transcription was performed at 25 °C for 10 min followed by 30 min at 55°C with 1X Transcriptor RT reaction buffer, 20 U of RNase inhibitors, 1 mM dNTPs, and 10 U of reverse transcriptase. Finally, the enzyme was inactivated at 85 °C for 5 min. Assuming a reverse transcriptase efficiency of 70%, samples were diluted to 25 ng μl^{-1}.

A variant of this protocol was used to analyze the direction of the transcript of the *carP* gene. The poly-T primer, used in the synthesis of standard cDNA, was substituted by a mixture of specific primers for each of the strands, so that only cDNA molecules were obtained corresponding to the orientation of the transcript. Each primer mix was composed of three different primers, of about 20 bp, covering different parts of the transcript in a single orientation. Subsequently, a standard PCR was performed with both substrates so that the PCR product is only expected to be visible on the substrate generated by the mixture of primers complementary to the orientation of the transcribed *carP*.

Real time PCR

Quantitative PCR was performed with the two-step system of Roche. Complementary DNA synthesis was as described above, and mRNA quantification was made in a Light Cycler 480 device (Roche) in 384 wells plates by using the Light Cycler 480 SYBR Green Master I kit. Reaction samples contained 50 ng of cDNA (2 µl at 25 ng μl^{-1}), 0.4 µM of forward and reverse primers (0.4 µl of 10 µM stock), 5 µl of 1X SYBR Green I Master (hot start PCR mix), which includes FastStart Taq DNA polymerase, reaction buffer, dNTPs mix, SYBR Green I Dye and $MgCl_2$. The final volume in each well was 10 µl. The program used for cDNA amplification and quantification was as described in the supplier's manual and consists of a pre-incubation phase (95 °C, 5 min), 45 cycles of amplification and quantification (95 °C 10 s, 60 °C 10 s, 72 °C 10 s) with single acquisition mode, a melting curve to check the specificity of the product (5 s at 95 °C, 1 min at 65 °C and subsequent raise to 97 °C for continuous acquisition), and finally, a cooling phase (40 °C for 30 s). The mRNA levels of *F. fujikuroi* genes were detected by RT-qPCR, using the cDNA as template for the reaction with pairs of appropriate primers and amplifying products with a length between 70 and 200 bp. For each cDNA sample and gene measured, 3 simultaneous technical replicates were performed. The relative levels of RT-qPCR products were determined using the ΔΔCt method (Livak and Schmittgen, 2001; Pfaffl, 2001), being the Ct values normalized according to the Ct value obtained for the β-tubulin or the glyceraldehyde dehydrogenase genes used as the endogenous references (Relative expression = $2^{-(\text{Ct gene} - \text{Ct reference gene})}$). Primer sets used in the RT-PCR expression analyses are described in Methods Annex 2.

Statistical significance of differences between mRNA values was checked with the Welch's t test using the GraphPad Prism GraphPad Prism version 8.0.2 for Windows (GraphPad Software, San Diego, CA, U.S.A.), as for carotenoids quantifications. Since data were relativized

to the value of the wild strain grown in the dark, tests against these values were carried out with the one sample *t* test.

NUCLEIC ACID HYBRIDIZATION

DNA HYBRIDIZATION PROTOCOL: SOUTHERN BLOT

Radioactive labeling of the DNA probe

For hybridization, 100 ng (15 µl) of purified probe were labeled with [α-^{32}P] dCTP (Perkin-Elmer, Boston, MA). The sample was heated at 100 °C for 10 min and stored on ice. Labeling was performed adding 2 µl of a pool of dATP, dGTP and dTT (0.5 mM), 2-4 µl [α-^{32}P] dCTP (3000 Ci mmol^{-1}), depending on its activity, 2 µl of random hexanucleotides 10X (Roche) and 2 U of Klenow enzyme (Roche). The volume reaction was completed to 20 µl with bdH_2O, and the mixture was incubated at 37°C for 3-4 h. Finally, the radioactive probe and markers were purified with the GFX DNA purification kit (GE, Healthcare).

Electrophoresis and membrane DNA transfer

The digested genomic DNA was run in 0.8% agarose electrophoresis. 5-10 µg of the DNA were loaded in the gel and run for 5 h at 60 V. Afterwards, the DNA was denatured and subsequently hybridized. Treatments were carried out at room temperature with gentle shaking. The DNA was first subjected to acid depurinization (partial hydrolysis). For this, the gel was submerged 10 min in 0.25 M HCl and washed with distilled water. It was followed by two washing steps in denaturing solution (1.5 M NaCl, 0.5 M NaOH) for 15 min and two subsequent washing steps in neutralization solution (0.5 M Tris-HCl, 3 M NaCl, pH 7.5). Transfer was performed by capillarity in 20X SSC (3 M NaCl, 300 mM sodium citrate) as described (Sambrook and Russell, 2001). A piece of Hybond-N nylon membrane (Amersham Biosciences) was cut with a size to fit the gel dimensions and the same procedure was followed to cut two pieces of Whatman paper 3MM and several pieces of standard filter paper. The gel was placed at the bottom of a container filled with 20X SSC and the membrane, Whatman and filter papers were placed over in this order and left overnight with some balanced weight on top of it. As far as possible air bubbles that could remain between Whatman 3MM paper and gel, or between gel and nylon membrane, were avoided. After transfer, the membrane was washed in 2X SSC, dried and exposed to 700 J m^{-2} in a crosslinker RPN 2500 (Amersham) for DNA linking.

Radioactive probe hybridization and detection

The procedure was as described (Sambrook and Russell, 2001). The membrane was incubated in an oven (HB-100 Hybridizer, UVP) at 65°C for 30 min in a hybridization tube with 20 ml of pre-heated hybridization solution (0.5 M Na_2HPO_4 pH 7, SDS 7%). Then, the solution was replaced by another 20 ml and the probe was heated at 100 °C for 5 min prior to addition to the hybridization tube. The radioactive probe was incubated with the DNA overnight. The hybridization solution was discarded safely as radioactive waste, and the membrane was

washed with 40 ml of 65°C pre-heated washing solution (0.1% SSPE, 0.5% SDS, 5 mM EDTA) for 5 min to eliminate non-bound probe. Another washing step was repeated for 1 h at 65°C. The solution was discarded, and the radioactive membrane was covered with transparent film, placed between two acetate sheets and stored in an exposing cassette. The radioactive signals on the membrane were visualized in a FujiFilm FLA 5100 equipment (Life Science) which also allows image analysis of active, fluorescent and chemiluminescent signals.

Digoxigenin labeling of DNA probes

The digoxigenin (DIG) labelled probe was obtained by PCR amplification substituting the standard dNTPs with DIG labelled dNTPs (PCR DIG Labeling Mix, MERCK). The reaction was performed according to manufacturer's instructions. DIG-DNA probe was precipitated and quantified. To test the efficiency of the labelling, serial dilutions were prepared for the sample and a control (a well labelled probe or the DNA DIG marker). In a Hybond-N nylon membrane (Amersham Biosciences) 1 µl drops were placed (1 ng, 0.1 ng, 0.01 ng, 0.001 ng, 0.0001 ng, 0.00001 ng) of both DNAs and the membrane was UV crosslinked. Membrane was washed with 10 ml of maleic buffer for 2 min and treated with 10 ml of blocking solution, containing 1 µl anti-DIG (1: 10 000), for 30 min. The membrane was washed twice with 10 ml of maleic buffer with 0.3 % tween20 for 15 min and equilibrated with 10 ml of detection buffer for 2 min. The membrane was then placed in an acetate with 200 µl of CPD-star ready to use. It was covered with another acetate and after 2-10 min of incubation and the membrane's signal from the probe was detected in the Odyssey Fc Imaging System.

Digoxigenin-labelled probe hybridization and detection

The membrane was preincubated with "DIG Easy Hyb™ Granules (Roche) buffer solution for 1 h in a glass cylinder in a hybridization oven (HB-100 Hybridizer, UVP) and then 35 ng mL^{-1} DIG-labelled probe were added to new buffer solution for overnight incubation. Both the pre- and the hybridization were done in the same incubation tube. Two washes with 2X SSC + 0.1% SDS at room temperature for 5 min and two washes with 2X SSC +0.1% SDS at 68 °C during 15 min were done the following day. The membrane was equilibrated with maleic buffer and incubated in Blocking Reagent solution (Roche) for an hour. Then new stock of blocking solution with anti-DIG-alkaline phosphatase antibody (1:10000) (Merck) was added for 30 min. Membrane was washed twice for 15 min with maleic buffer + 0.3% Tween20, covered with detection buffer and placed in an acetate. Then, CDP-Star® ready to use (Roche) was added and the membrane was covered with another acetate. After a short incubation in the dark, the membrane's signal was detected in the Odyssey Fc Imaging System (LI-COR, Lincoln, NE, USA).

SMALL RNA HYBRIDIZATION PROTOCOL: NORTHERN BLOT

Electrophoresis and membrane RNA transfer

The small RNA-enriched samples were run in 1-mm wide 15% acrylamide gel in denaturing conditions (6 M Urea) with 0.5X TBE as buffer. Around 20-30 µg of RNA were loaded

concentrated in *ca*. 7 ul, to which the same volume of loading buffer (0.5 mM EDTA, 0.1% bromophenol blue, 0.1 % xylene cianol, 95% formamide), was added after being denatured. Electrophoresis was run in a Mini Protean 3 system at 100 V for about 2 hours. The gels were cut below the bromophenol blue line, and the upper part was dyed with ethidium bromide and used as a loading control. Semi Dry transference of the gel was performed using a nitrocellulose membrane NX for 1 h at 250 mA with TBE buffer. The crosslinking was done in a buffer containing 40.7 µl of 1-methylimidazol in 4 ml of RNAse free bidistilled water at pH 8 which were mixed with 0.11 g of 1-Ethyl-3-(3-dimethylaminopropyl) carbodiimide. In a transparent plastic film, a Whatman paper with the membrane size was soaked with the mix. The membrane was placed over it, covered with the film and kept at 60 °C for 120 min. Then the membrane was washed with distilled water for 10 min with gentle shaking.

Radioactive riboprobe preparation

The DNA fragments used as a template to synthesize the riboprobes were cloned in vector pGEM-T easy, with a promoter for T7 polymerase flanking the multicloning site. 20-30 µg of the plasmid were linearized with an appropriate restriction enzyme and the fragment was precipitated and resuspended in 10 µl. 500 ng of the linearized plasmid were used for the *in vitro* transcription reaction using the Ambion® MAXIscript® T7 In Vitro Transcription Kit, along with 1 µl of the corresponding buffer, 0,5 µl of ATP, CTP and GTP, 1 µl of the T7 polymerase, and 2,5 µl radioactively labelled UTP. The reaction was incubated for 10 min at 37 °C, 1 µl of DNAse was added and incubated during 15 min, and 1 µl of 0,5 M EDTA pH 8 was added to stop the reaction. The riboprobes were purified using Sephadex G50 columns and 300 µl of 80 mM sodium bicarbonate, 120 mM sodium carbonate was added to them. The mix was incubated during 3 h at 60 °C to digest partially the RNA, and 20 µl of 3M sodium acetate pH 5.2 were added to stop the reaction. To test the production of sRNAs in a determined region in both strands, the template sequence was cloned in both directions in the vector.

Hybridization and detection

The membranes were prehybridized for 2 h at 37 °C with approximately 5 ml of Ultrahyb®-Oligo Hybridization buffer (Ambion). The riboprobe was denatured and added to the prehybridization buffer. The hybridization was performed overnight at 37 °C in an oven HB-1000 Hybridizer (UVP). The next day, the membrane was washed twice with 2X SSC + 0.2% SDS at 37 °C in the same oven. The membranes were placed in transparent film and exposed at the FujiFilm FLA 5100 equipment.

GENETIC TRANSFORMATION

Transformation of *E. coli*

E. coli DH5α competent cells were prepared according to a published protocol (Inoue et al., 1990). A 1-liter Erlenmeyer flask containing 200 ml of SOC medium was inoculated with 1 ml of an *E. coli* preculture in stationary phase and incubated at 22°C. When the optical density

reached 0.5, the culture was cooled in ice for 10 min and centrifuged at 4°C for 10 min at 2,500 g. The pellet was resuspended in 80 ml of cold TB buffer (10 mM PIPES, 15 mM $CaCl_2 \cdot 2H_2O$, 250 mM KCl, 55 mM $MnCl_2 \cdot 6H_2O$, pH 6.7) and incubated for 10 min in ice. The sample was centrifuged as described above and resuspended in a volume of 20 ml of TB. To preserve cells from freezing, 1.5 ml of DMSO was added and left 10 min in ice. The cells were then distributed in 0.2 ml aliquots in sterile 1.5 ml tubes and frozen immediately in liquid nitrogen. Aliquots of 100 µl were stored at -80°C.

For a transformation, 0.1 ml of competent cells were thawed in ice and mixed with 1 µl of a plasmid sample or 5 µl of a ligation mixture. The samples were incubated in ice for 30 min, subjected to a heat shock at 42°C for 45 s, and cooled in ice for 2 min. Afterwards, 0.8 ml of LB medium was added to the transformation mixture and incubated at 37°C for 1h. Finally, the cells were plated on ampicillin-supplemented LB medium with appropriate dilutions to ensure the formation of isolated colonies. The typical procedure consisted of plating 10 µl, 100 µl and the rest of the sample after centrifugation. Plates were incubated at 37°C for 12-16h.

E. coli electroporation

Competent cells were prepared inoculating 1 liter of LB medium with 1 ml of *E. coli* preculture. Cells were grown until an optical density between 0.5 and 0.6. The culture was kept in ice for 30 min, after this incubation it was centrifuged at 4,500 rpm at 4°C for 15 min. The supernatant was discarded, and cells were resuspended in 200 ml of cold H_2O. The centrifugation was repeated, and cells were resuspended again in 100 ml of cold H_2O. A third centrifugation step was performed, and cells were resuspended in 5 ml of cold 10% glycerol. Cells were centrifuged again and resuspended in a final volume of 2-3 ml of cold 10% glycerol. Aliquots of 40 µl were stored at -80°C.

Purified DNA resuspended in water was used to transform the cells. Cuvettes were precooled in ice while around 1 µl DNA was mixed with the cells. Afterwards, cells were pipetted into the cuvette and electroporated (5 kV, 25 µF, 200 Ω, 125 µF). One ml of SOB was immediately added, cells were incubated for 60 min at 37 °C, and dilutions were plated on the appropriate selective media.

Transformation of *S. cerevisiae*

The protocol described by (Daniel Gietz and Woods, 2002) was used, with some modifications. A preinoculum of yeast cells was incubated for 12-14 hours in YPD medium. Then, they were used to inoculate 100 ml YPD cultures that grew until an optical density of 0.5-0.6 at 600 nm. The obtained cells were centrifuged, washed first with sterile H_2O and then with a solution of 100 mM lithium acetate in TE buffer (10 mM Tris, 1 mM EDTA pH 7.5). After being centrifuged again, they were resuspended in 2 ml of the same solution and kept at 30 °C for 1 hour stirring at 200 rpm. For each transformation, 150 µl of competent cells were mixed with 500 µl of 50% PEG 3350 in 0.1 M lithium acetate, 10 µl salmon sperm DNA (10 mg / ml) and 10 µl of the DNA used to transform. The mixture was kept stirring at 30 °C for 30 min and heat

shocked at 42 °C for 20 min. Finally, the cells were washed with H_2O, sowed in different dilutions on Petri dishes with selective culture medium, and incubated at 30 °C till colonies appeared.

F. fujikuroi transformation

The protocol was described (Marente et al., 2020).

As a starting material, 50 ml of Darken medium were inoculated with a small mycelium plug, and incubated for 3 days at standard conditions. The day before transformation, 1 ml of the culture was used to inoculate 100 ml of fresh ICI medium, and it was incubated overnight at 30 °C and 150 rpm. In the morning, a fresh enzyme solution was prepared with 100 mg of Lysing enzymes from *Trichoderma harzianum* (Sigma), 75 mg of Driselase from basidiomycetes (Fluca), 7.5 mg of Lyticase (Sigma), and 5 mg of BSA in 25 ml of osmostabilization buffer (1.2 M KCl, 0.66 M $CaCl_2$, pH 5.5). The enzymes were mixed with a magnetic stirrer bar during at least 30 min and later sterilized through a 0.42 µm filter. The young mycelium was vacuum filtered through a sterile filter paper and washed with sterile osmostabilization buffer. The mycelium was removed from the filter with a sterile spatula and resuspended in 25 ml of an enzyme solution. The mix was incubated for 3-4 h at 30°C at 100-150 rpm. Subsequently, the protoplasts were separated from mycelia through two borosilicate crucibles filters. After the pore size 0 filter (160–250 µm), the filtrate was collected and passed through pore size 1 filter (100–160 µm). The resulting protoplast-containing filtrate was centrifuged for 15 min at 2,000 g, the supernatant was discarded, and the protoplasts were resuspended and washed with osmostabilization buffer. Then, the centrifugation was repeated, the supernatant was discarded again, and the protoplasts were resuspended in 500 µl of osmostabilization buffer using cut pipette tips. The protoplasts were counted under the microscope using a Neubauer chamber.

Two sterile 1.5-ml Eppendorf tubes were prepared with around $3 \cdot 10^7$ protoplasts each one. To the transformation tube, 50 µl of 2X STC (2.4 M sorbitol, 20 mM Tris-HCl pH 8, 100 mM $CaCl_2$) and 10-15 µg of DNA (circular plasmid or a linearized fragment) were added and filled up to 200 µl with H_2O. In parallel, 100 µl of 1X STC were added to the second tube used as a control. The tubes were gently inverted, 50 µl of 30% PEG (30% PEG 8000, 10 mM Tris-HCl pH 8, $CaCl_2$ 50 mM) were added and followed by 20 min incubation in ice. Then, the samples were transferred to 10 ml sterile tubes and 2 ml of 30% PEG were added again and mixed by inversion. After 10 min of incubation in ice, 4 ml of 1X STC were added and carefully mixed. The content of the transformation tube was mixed with 120 ml of regeneration medium and poured into Petri dishes. Similarly, two Petri dishes were prepared with the corresponding number of protoplasts from the control reaction and appropriate serial dilutions to assess protoplast viability.

These plates were incubated at 30 °C for 15 h to allow protoplast regeneration and the expression of the antibiotic resistance cassette. Before the endo of this incubation, 5 ml of top agar were introduced in 10-ml tubes and were kept in a bath at 55°C. Then, 40 µl of 50 mg ml^{-1} hygromycin B or 30 µl of G418 (150 mg ml^{-1}) were added, carefully mixed, and laid over the transformation plates and one of the control plates (negative control). The remaining control plate served as a viability and regeneration control and only 5 ml of top agar were added. All the

plates were then incubated at 30 °C for 7-10 days. The colonies grown on the transformation plates were subcultured in 6 cm Ø Petri dishes with antibiotic-supplemented DG medium. The colonies growing in the selective medium were transferred again to EG sporulation medium. Conidia were collected from each transformant and plated at an appropriate dilution to obtain isolate colonies. To ensure homokaryosis, this step was repeated at least three times.

Targeted gene inactivation

The deletion of *F. fujikuroi* genes was carried out by targeted gene replacement using the gene inactivation technique widely used to generate the collection of deletion mutants in *N. crassa* (Colot et al., 2006). This technique is based on the replacement of the target gene with an antibiotic resistance cassette by homologous recombination between surrounding sequences of the target gene, and the same sequences also present in the vector surrounding the cassette. For vector construction, the homologous recombination mechanism of *S. cerevisiae* was used.

Fragments from the 5‘ and the 3’ end of the target genes were amplified by PCR with primers which included 20 nt tails with sequences homologous to either the vector pRS426 or the selection marker used to delete the gene. The tails were oriented in a way that the internal regions of the 5’ and 3’ fragments shared the homology with the marker gene, so that the order of the transformation cassette was 5’ gene fragment - selection marker - 3’ gene fragment. These fragments had a length of around 1.2 kb to ensure recombination with the homologous sequence in the fungus. Plasmid pRS426 was linearized by digestion with *Xho*I and *Eco*RI, restriction enzymes with cutting sites included in its multicloning sequence, to avoid autoligation. Once that all the fragments were obtained, they were introduced by transformation into FY834 strain of *S. cerevisiae*, where the different fragments will recombine by the homologous sequences included at their ends. In this way, a pRS426-derived plasmid was generated containing a resistance cassette surrounded by the promoter and terminator sequences of the target gene. This vector was used later to transform *F. fujikuroi* and to generate the desired mutants.

CAROTENOID EXTRACTION AND ANALYSIS

The carotenoid extraction was described in Marente et al. 2020. The carotenoids were extracted from mycelium samples grown in Petri dishes with solid DG medium using 2 Petri dishes per assay/sample. Due to the inoculating method, each Petri dish contained seven symmetrically distributed colonies. After one week of incubation under dark or light conditions, the colonies were carefully separated from the agar with a scalpel, the rests of agar were removed from the mycelium, and the samples were frozen, lyophilized and weighed. The amounts of lyophilized mycelium used for the carotenoid extractions ranged from 25 mg to 50 mg depending on the estimated carotenoid content. Carotenoid extractions were made in 2 ml screw-cap microcentrifuge tubes, using a FastPrep 24 Instrument cell homogenizer (MP Biomedicals). To each lyophilized mycelium sample (25-50 mg), 200 µl of beach sand and 1 ml of acetone were added and the tubes were subjected to 2 pulses of 30 seconds at 6.5 m s^{-1} in the homogenizer with a 5-min rest between both pulses. After these two steps, the samples

were centrifuged for 1 min at 13,000 rpm and the acetone supernatant was transferred to a clean microcentrifuge tube, in which the extracted carotenoids were accumulated. The procedure was repeated until the mycelium was completely colorless, usually four extraction cycles were used for the analyzed samples. When the extraction was complete, the collected acetone was centrifuged at 13,000 rpm to remove any remains of mycelium and sand, it was transferred to a clean tube, and left to dry in a Speedvac or vacuum centrifuge (Eppendorf) at a temperature below 40 °C. The extracts were dissolved in acetone and absorption spectra were determined from 350 to 650 nm in a Beckman DU 640 spectrophotometer (Beckman Coulter, Foullerton, California, USA). The carotenoid concentration was estimated from the maximum absorption values of the spectra in acetone, assuming an average extinction coefficient, ε, of 200 mg $^{-1}$ ml cm $^{-1}$.

BIOINFORMATICS

PRIMER DESIGN

To calculate physical properties of oligonucleotides, such as G+C content, melting temperature, self-complementarity or hairpin formation, the online tool OligoCalc was used (version 3.26, http://www.basic.northwestern.edu/biotools/oligocalc.html, North-western University©). In the case of RT-PCR primers, the oligonucleotides were designed with the PrimerExpressTM V2.0.0 (Applied Biosystems) program or the online tool Primer3plus (http://primer3plus.com/cgi-bin/dev/primer3plus.cgi). Synthesis of primers was ordered either to StabVida (Oeiras, Portugal) or to Integrated DNA Technologies (https://www.idtdna.com).

SEQUENCE ANALYSIS AND TREATMENT

DNA sequences and genome information were obtained through the Broad Institute server (www.broadinstitute.org), the National Center of Biotechnology and Informatics (NCBI) (https://www.ncbi.nlm.nih.gov/) and the Ensembl Fungi server (http://fungi.ensembl.org). The BLAST and BLASTP analyses were performed through the NCBI server. When needed, samples were purified and sent with the recommended concentration to StabVida (Portugal) where they were sequenced with the Sanger method in an ABI 3730XL DNA analyzer (Applied Biosystems). DNA sequencing data were analyzed with Chromas version 2.6.4 (Technelysium Pty Ltd) and with the Clustal Omega sequence alignment software (European Bioinformatics Institute of the European Molecular Biology Laboratory, EMBL-EBI, https://www.ebi.ac.uk/Tools/msa/clustalo/). Restriction maps, and complementary DNA sequences were analyzed with the Serial Cloner 2.6.1 (Serial Basic 2004-2013) program. Open Reading Frames were searched with ORFfinder software (https://www.ncbi.nlm.nih.gov/orffinder) at NCBI platform. The analysis of protein domains was performed with the Pfam database, from the EMBL-EBI (http://pfam.xfam.org/).

GENERATION AND PROCESSING OF RNA-SEQ DATA

The sequencing process for the transcriptomic analysis was carried out by the company

LifeSequencing (Valencia) through the Illumina platform. Initial quality parameters were assessed at the home laboratory. Purity and integrity of the RNA samples was evaluated by spectrophotometry in nanodrop (A260/A280>1.8 and A260/A230>1.5) and visualization after agarose gel electrophoresis. RNA integrity number (RIN), critical for successful sequencing, was done by the company upon reception of the samples. RIN values were checked in a 2100 Bioanalyzer (Agilent) using an RNA 6000 Nano Chip (Agilent). Results for all samples studied were higher than 8, being this the minimal RIN value for a sample to be considered of good quality. The characteristics of the RNA samples investigated in this Thesis are summarized in the Annex A1.

Sequencing was carried out using the Illumina platform (Metzker 2010). Samples were sequenced through the Illumina protocol, which can be summarized in the following steps. First, considering that most RNA molecules present in the cells are ribosomal, a poly-adenylated RNA enrichment was done to ensure that an adequate amount of RNA was obtained for the analysis of interest. After RNA purification, RNA was fragmented to sizes of 100 to 300 bp. Then double-stranded cDNA was synthesized through a poly-T primer binding and reverse transcription of the samples. Adapters were bound to the ends of the cDNA sequences and those were selected and amplified by PCR.

For RNA-seq analysis of small RNAs, an enrichment protocol was implemented. RNA below 150 nt of the two samples from each analyzed condition, covering the sRNAs and their precursors, was used to construct small RNA libraries, that were sequenced on Illumina's Hiseq platform in 50 bp single read mode. The rest of them were used to identify standard mRNAs, samples, and were sequenced on Illumina's NextSeq platform in 75 bp single read mode. “Bcl2fastq2” version 2.19.1 provided by Illumina was used for the conversion of “bcl” files into “fastq” sequence files, a program that also removes the sequencing adapters.

Raw reads for all samples were trimmed, filtered and quality controlled with AfterQC (Chen et al., 2017) or FastQC (https://www.bioinformatics.babraham.ac.uk/projects/fastqc/) packages. The information of the different transcriptomic experiments is provided at the beginning of each results section. The processing of the sequencing data by the Illumina platform was performed using the Tuxedo protocol, with the advice and collaboration of Prof. Dr. Gabriel Gutiérrez, from the Genetics Department of the University of Seville. The analysis of the sRNA sequences was performed in collaboration with Dr. Tim Dahlman and Dr. Minou Nowrussian from the University of Bochum (Germany).

IMI58289 sequences were mapped with STAR (Dobin et al., 2013), using the Ensemble Fungi annotation and genome corresponding to the strain. FKMC1995 sequences were mapped with TopHat 2.1.1 (Trapnell et al., 2009) with the corresponding genome of this strain (Niehaus et al., 2016). A meta-assembly of the transcriptome with the Cufflinks-Cuffmerge protocol (Roberts et al., 2011) was generated to improve the level of annotation of the FKMC1995 strain. The Integrative Genomics Viewer IGV application (IGV) version 2.8 was used for mapping visualization (Robinson et al., 2011). Mapped sequences were analyzed using SeqMonk (version 1.45.41, https://github.com/s-andrews/SeqMonk). Quantification was performed using the

RNA-seq quantitation pipeline with either the IMI58289 annotation or the improved mRNA annotation generated by Cuffmerge for FKMC1995, merging transcripts and counting reads over exons and percentile normalized. Deseq2 tool (Love et al., 2014), implemented in SeqMonk, which needs raw counts for quantitation, was used to compare among conditions. The differentially expressed genes were selected based on criteria combining a log2 fold change of either 1 or 2, depending on the experiment, and a *p*-value of 0.05. Log2 RPM (reads per feature per million reads of library) were used for data visualization and intensity tests, with a minimum *p*-value of 0.05 multiple testing correction applied with a sample size of 100 when constructing the control distributions. Venny 2.1 was used to draw Venn Diagrams. Transcript levels were measured as TPM (transcript per million) to represent the heatmaps. Heatmap figures were performed using the mean between the three samples in TPM for each strain and condition, then data were log transformed and centered using the mean between them, and hierarchically clustered with Gene Cluster 3.0 (de Hoon et al., 2004). The visualization was performed with Java TreeView3 (Saldanha, 2004).

To perform GO enrichment analysis, the *F. fujikuroi* FKMC1995 proteome was annotated using the corresponding IMI58289 orthologs annotation data from Fungi DB. To assign orthologs a formerly proposed equivalence was used (Niehaus et al., 2016). GO terms corresponding to each subset of genes for both strains were extracted and tested with a *p*-value of 0.05 as cut off. Computed and curated terms were used in the analysis. Results were visualized using Revigo (Supek et al., 2011) with 0.7 allowed similarity and using *p*-values. FunCat GO enrichment results were obtained from the FungiFun database using a significance level of 0.05 and testing for enrichment with FDR correction (Priebe et al., 2015).

For small RNA analysis, mapping was done with Bowtie v1.1.1 or Bowtie2 v2.2.9. Reads that occurred several times within the dataset were collapsed to a single entry and the read count was added to the fasta header (10 counts = _x10) of the corresponding read. The gff annotation files from both fungi were used to extract fasta files, containing coding, intronic, and intergenic sequences. The extraction was done after creating the corresponding features with the genome browser Artemis 16.0.0. To find sense and antisense transcribed features that may be differentially expressed during growth in light and dark, each sample was aligned separately to the reference genome. The read counts for each dataset were calculated with the R script summarizeOverlaps, part of the Bioconductor GenomicAlignments package (https://www.bioconductor.org/). After normalization, features that showed differential formation of small RNAs were calculated with DESeq2. For calculation of read counts R v2.3.2 and Rstudio was used on a Windows 7 machine. The Bioconductor 'RNA-seq workflow at gene level' was used (http://www.bioconductor.org/help/workflows/rnaseqGene/). After eliminating whitespaces from the genome fasta files and collapsed reads shorter than 17 nt, miRDeep2 was started without any additional information ('none none none' = no information of *Fusarium* milRNAs, other fungal milRNAs, or known *Fusarium* precursors). No score cut off was used and all precursors were analyzed (Friedländer et al., 2012).

Table A1. Quality parameters of the RNA samples to be sequenced during the Thesis. Samples corresponding to the first chapter are portrayed in yellow. Those corresponding to the second chapter in light blue (the ones labelled in green were used in chapters 1 and 2). The samples corresponding to the third chapter are marked in orange.

Sample	Conc. (ng/ul)	A260/A280	A260/230	RIN
Ffuj_dark_R1	118	2.1	2.45	10
Ffuj_dark_R2	201	2.1	2.41	10
Ffuj_light_R1	183	1.99	1.92	9.9
Ffuj_light_R2	150	2.1	2.4	10
Foxy_dark_R1	177	2.1		9.8
Foxy_dark_R2	187	2.09		10
Foxy_light_R1	200	2.1		9.8
Foxy_light_R2	223	2.04		9.7
WT.0.R2*	1632	2.23	2.39	8.7
WT.0.R3*	2166	2.19	2.4	8.9
WT.0.R4*	1431	2.23	2.43	8.6
WT.60.R2	792	2.22	2.48	8.7
WT.60.R3	2268	2.18	2.41	8.6
WT.60.R4	1264	2.22	2.45	8.8
SG268.0.R2	821	2.22	2.4	8.5
SG268.0.R3	2828	2.22	2.47	8.8
SG268.0.R4	1339	2.23	2.45	8.7
SG268.60.R2	552	2.19	2.44	8.7
SG268.60.R3	2785	2.23	2.48	8.9
SG268.60.R4	1428	2.22	2.45	8.5
dcl2.4.0.R2*	788	2.23	2.43	9
dcl2.4.0.R3*	2036	2.2	2.41	9.4
dcl2.4.0.R4*	2251	2.18	2.41	9.1
WT0_R1	1378	2.1	2.49	9.9
WT0_R2	1211	2.1	2.46	10
WT0_R3	900	2.08	2.5	10
WT15_R1	1078	2.1	2.44	10

WT15_R2	1132	2.09	2.44	10
WT15_R3	1303	2.1	2.44	9.8
WT60_R1	1368	2.1	2.44	9.9
WT60_R2	1537	2.09	2.47	10
WT60_R3	898	2.09	2.52	10
WT240_R1	1600	2.09	2.45	10
WT240_R2	1517	2.1	2.29	10
WT240_R3	1388	2.1	2.09	10
WC0_R1	1398	2.1	2.44	10
WC0_R2	1516	2.09	2.47	10
WC0_R3	1359	2.09	2.48	10
WC15_R1	1751	2.09	2.44	10
WC15_R2	1967	2.08	2.46	10
WC15_R3	1073	2.09	2.4	10
WC60_R1	1329	2.09	2.39	10
WC60_R2	2052	2.08	2.41	10
WC60_R3	1744	2.08	2.36	10
WC240_R1	1304	2.1	2.46	10
WC240_R2	1015	2.09	2.44	10
WC240_R3	1793	2.09	2.44	10
CRY0_R1	873	2.08	2.04	10
CRY0_R2	1445	2.08	2.39	9.5
CRY0_R3	1528	2.06	2.41	10
CRY60_R1	1051	2.08	2.46	10
CRY60_R2	1469	2.07	2.43	9.6
CRY60_R3	1654	2.06	2.36	9.9

Table A2. Primer sets used for PCR experiments of this Thesis.

Set	Primer name	Collection number	5'-3' Sequence	Experimental use
PS1.1	Ff-mir1-3F	OMP-779	CAACTCTCCCCTTTCTGGAG	Construction of pGmir1 F and R
	Ff-mir1-3R	OMP-780	GGGAGACTTGAGACTTGAG	
PS1.2	Ff-mir2-3F	OMP-781	TGTAGGTGCCCTTCCTTTAAT	Construction of pGmir2 F and R
	Ff-mir2-3R	OMP-782	TGAAGATAAGGGAAAAGGGC	
PS1.3	OMP-809	Ff-mir0-1F	AGAGAGCTTAGTTCAGCTATT	Construction of pGpcarS F and R
	Ff-mir2-3R	OMP-782	TGAAGATAAGGGAAAAGGGC	
PS1.4	Ff-dcl2-pRS246-F	OMP-862	GTAACGCCAGGGTTTTCCCAGTCACGACGTGGCT ATCTGTGATTTTAGTGTAC	5' *dcl2* segment of pDcl2hyg PCR
	Ff-dcl2-hph-R	OMP-865	ATCCACTTAACGTTACTGAAATCTCCAACCATTTTC CTATCATGGGGGAG	
PS1.5	Ff-dcl2-pRS246-R	OMP-863	GCGGATAACAATTTCACACAGGAAACAGCCCAAA GTCGATGCCGCTCT	3' *dcl2* segment pDcl2hyg PCR
	Ff-dcl2-hph-F	OMP-864	CTCCTTCAATATCATCTTCTGTCTCCGACGAAGGG GATCATGTACACGC	
PS1.6	HPH-6F	OMP-692	GTCGGAGACAGAAGATGATATTGAAGGAGC	Hyg^R cassette PCR
	HPH-6R	OMP-693	GTTGGAGATTTCAGTAACG TTAAGTGGAT	
PS1.7	Ff-predcl2-1F	OMP-932	CTCTTGTTGGCTTTCCATGCCG	PCR test 5'*dcl2* - Hyg^R
	HPH-6F	OMP-692	GTCGGAGACAGAAGATGATATTGAAGGAGC	
PS1.8	Ff-predcl2-1F	OMP-932	CTCTTGTTGGCTTTCCATGCCG	PCR test *dcl2* - Hyg^R
	Ff-postdcl2-1R	OMP-938	CTTCTTGCGCACGACATACGAG	
PS1.9	Ff-postdcl2-1F	OMP-947	GGAAGGCACCCTAACTGAGAACTC	Southern probe of *dcl2*
	Ff-postdcl2-1R	OMP-938	CTTCTTGCGCACGACATACGAG	
PS1.10	Ff-predcl1F	OMP-958	TAGAACACGGGCATTGATGCGA	Amplification of *dcl1*
	Ff-postdcl1R	OMP-959	CCAAGGACCTATTGTTCTCGC	

PS1.11	Ff-asc1-pdcl1R	OMP-960	TTGGCGCGCCGTTGAGGAGTAGATTATTTACTG	Inverse *dcl1* PCR with *Asc*I restriction sites
	Ff-asc1-pdcl1F	OMP-961	TTGGCGCGCCGCTGAAGTCGGCAGTAGAG	
PS1.12	Ff-neo-asc1F	OMP-962	ATGGCGCGCCCCAACATGGTGGAGCACGAC	neoR amplification with *Asc*I restriction sites
	Ff-neo-asc1R	OMP-963	TTGGCGCGCCGGATCTGGATTTTAGTACTGG	
PS1.13	Ff-predcl1-2F	OMP-936	GCTGAAAACTCTCTGGTTGAGTCAC	5'-*dcl1* PCR
	Ff-neo-asc1R	OMP-963	TTGGCGCGCCGGATCTGGATTTTAGTACTGG	
PS1.14	Ff-neo-asc1F	OMP-962	ATGGCGCGCCCCAACATGGTGGAGCACGAC	3'-*dcl1* PCR
	Ff-postdcl1-2R	OMP-937	CATGAAGCATTTGAATCGCCTGCG	
PS2.1	RT-Ff-pcarS2a-F	VAR-357	GCCGAGAGTCCCTTTTACGA	*carP* (F) strand specific RNA retrotranscription
	RT-Ff-pcarS2b-F	VAR-359	CCATTGAGCTGGGATGTGTTTT	
	RT-Ff-pcarS3-F	VAR-361	CTCGGCGTCATGAGTCCAT	
PS2.2	RT-Ff-pcarS2a-R	VAR-358	GCGCAGTCGAAAAAATGCA	*carP* (R) strand specific RNA retrotranscription
	RT-Ff-pcarS2b-R	VAR-360	TGCGCTGTGCTGTAAACCA	
	RT-Ff-pcarS3-R	VAR-362	CACAACAGCAGCATCAACTTCTG	
PS2.3	RT-Ff-pcarS2a-F	VAR-357	GCCGAGAGTCCCTTTTACGA	*carP* PCR
	RT-Ff-pcarS3-R	VAR-362	CACAACAGCAGCATCAACTTCTG	
PS2.4	Tub-1F	OMP-225	ACCATGGACGCCGTCCGTGC	*β-tub* (F) strand specific RNA retrotranscription
PS2.5	Tub-1R	OMP-226	GTTCTTGGGGTCGAACATCTG	*β-tub* (R) strand specific RNA

				retrotranscription
PS2.6	Tub-1F	OMP-225	ACCATGGACGCCGTCCGTGC	*β-tub* PCR
	Tub-1R	OMP-226	GTTCTTGGGGTCGAACATCTG	
PS2.7	Ff-pcarS-heF	OMP-956	CGTCGATGCGCCAGTTGATT	*carP* PCR
	Ff-pcarS-heR	OMP-957	AGCAAGCGCCTAGTGGCC	
PS2.8	CarS-2F	OMP-760	TTCTCTAGAGTACTATACGCACGCAA	*carS* PCR
	FfcarS-SalI-stop-R	OMP-613	CAGGTCGACGGGCAAGCATTGTCAATCAGA	
PS2.9	FF-mir2-2F	OMP-769	CTGTTGTGTGACTCGAGAGTTC	*carP-carS* PCR
	CarS-9R	OMP-990	GCAGGGGAGGCTGATGGGCT	
PS2.10	HPH-6F	OMP-692	GTCGGAGACAGAAGATGATATTGAAGGAGC	Hyg^R cassette PCR
	HPH-6R	OMP-693	GTTGGAGATTTCAGTAACG TTAAGTGGAT	
PS2.11	Ff-precarS1-pRS246-5F	OMP-964	GTAACGCCAGGGTTTTCCCAGTCACGACGGGAGATGGTCTAGAACAATTG	5' *carP* segment of pCarphyg PCR
	Ff-precarS-hph-5R	OMP-965	ATCCACTTAACGTTACTGAAATCTCCAACATCGACGCTACTTAATAGTCGAG	
PS2.12	Ff-precarS-hph-3F	OMP-966	CTCCTTCAATATCATCTTCTGTCTCCGACGGCGCTTGCTAGGAACTGCC	3' *carP* segment pCarphyg PCR
	Ff-precarS1-pRS246-3R	OMP-967	GCGGATAACAATTTCACACAGGAAACAGCGCCTTGACCGTTATATGATGTG	
PS2.13	Ff-carPhyg-1F	OMP-1035	GGAGATGGTCTAGAACAATTG	Replacement cassette *carP* PCR
	Ff-carPhyg-1R	OMP-1036	GCCTTGACCGTTATATGATGTG	
PS2.14	Ff-prepcarS-1F	OMP-933	GATGAGTGTGTGAGTGTGTGATGTTG	PCR test 5'*carP* - Hyg^R
	HPH-6F	OMP-692	GTCGGAGACAGAAGATGATATTGAAGGAGC	
PS2.15	Ff-postpcars-1F	OMP-939	CCTTCAAATATGTACCGCGTAGACTATG	PCR test 3'*carP* - Hyg^R

	HPH-6R	OMP-693	GTTGGAGATTTCAGTAACGTTAAGTGGAT	
PS2.16	Ff-prepcarS-1F	OMP-933	GATGAGTGTGTGAGTGTGTGATGTTG	PCR test 5′*carP*
	Ff-pcarS-heR	OMP-957	AGCAAGCGCCTAGTGGCC	
PS2.17	Ff-pcarS-heF	OMP-956	CGTCGATGCGCCAGTTGATT	PCR test 3′*carP*
	Ff-pcarS-heR	OMP-957	AGCAAGCGCCTAGTGGCC	
PS2.18	Ff-carP-2F	OMP-1099	CCATTTCTGTTCCCTTCCCTG	Southern probe for *carP*
	Ff-carP-2R	OMP-1100	CCGTCATACACCAGAGAGAC	
PS2.19	Ff-PRS426-neo-1F	OMP-1308	GTAACGCCAGGGTTTTCCCAGTCACACGGCTTGCCAACATGGTGGAGCACGACACTC	Neo^R segment pRS246neocarP
	Ff-carP-neo-1R	OMP-1309	TGGATGACGCTTACTATAGTCTTGTCCCAACAAAAGCTGGAGCTCCACCGCGGTGGC	
PS2.20	Ff-neo-carP-1F	OMP-1310	GCCACCGCGGTGGAGCTCCAGCTTTTGTTGGGACAAGACTATAGTAAGCGTCATCCA	*carP* segment pRS246neocarP
	Ff-pRS426-carP-1R	OMP-1311	GCGGATAACAATTTCACACAGGAAACAGCCAATCCGGGGACAATTCTAGAGGCACGCG	
PS2.21	Ff-pcarS-heF	OMP-956	CGTCGATGCGCCAGTTGATT	*carP-carS* PCR
	PCR-mir2-07-1R	OMP-826	GTGTAGAGATTGGTGGGGGTT	

Table A3. Primer sets used for RT-PCR analyses in the Thesis

Set	Primer name	Collection number	5'-3' Sequence	Experimental use
RTPS.1.1		VAR-282	CTTGGCAGTGGTTCTCACACA	Mir1.1
		VAR-283	AGATGACGAGGGACATTGATT	
RTPS.1.2	RTmiARN1Ff-2F	VAR-294	TGACGCCAACGACTTTCTTTT	Mir1.2
	RTmiARN1Ff-2R	VAR-295	TGGCAGGGCTGGCGTAT	
RTPS1.3	RTmiARNinterFf-1F	VAR-312	TGCCCTGTATCCAATGCTTCT	Intermediate sequence
	RtmiARNinterFf-2R	VAR-314	AGCGTAACCGAAGAGTTGCC	
RTPS1.4		VAR-284	CATCCGTTTTGCCTTGTAAGA	Mir2.1
		VAR-285	CAGGAATGAAGCCAGTGATAT	
RTPS1.5	RTmiARN2Ff-2F	VAR-296	CTA GGG CCT CTC CAC CAA GTT T	Mir2.2
	RTmiARN2Ff-2R	VAR-297	GGA ACT CAG GGA AGG GAA CAG	
RTPS.1	RT-Ff-pcarS1-F	VAR-355	CAGCAGCGAGAAGTGAACGA	upstream region of *carS* RT-qPCR
	RT-Ff-pcarS1-R	VAR-356	CAGCCTCCCTTGCAACGA	
RTPS.2	RT-Ff-pcarS2b-F	VAR-359	CCATTGAGCTGGGATGTGTTTT	*carP* (A) RT-qPCR
	RT-Ff-pcarS2b-R	VAR-360	TGCGCTGTGCTGTAAACCA	
RTPS.3	RT-Ff-pcarS3-F	VAR-361	CTCGGCGTCATGAGTCCAT	*carP* (B) RT-qPCR
	RT-Ff-pcarS3-R	VAR-362	CACAACAGCAGCATCAACTTCTG	
RTPS.4	RTcarB-1F	VAR-29	TCGGTGTCGAGTACCGTCTCT	*carB* RT-qPCR
	RTcarB-1R	VAR-30	TGCCTTGCCGGTTGCTT	
RTPS.5	Tub-2F	VAR-27	CCGGTGCTGGAAACAACTG	*β-tub* RT-qPCR
	Tub-2R	VAR-28	CGAGGACCTGGTCGACAAGT	
RTPS.6	RTcarRA-1F	VAR-9	CAGAAGCTGTTCCCGAAGACA	*carRA* RT-qPCR

	RTcarRA-1R	VAR-10	TGCGATGCCCATTTCTTGA	
RTPS.7	RtFfcarS-1F	VAR-246	GATACCCGGCGGAAAGGTTA	*carS* RT-qPCR
	RtFfcarS-1R	VAR-247	CTGACAGTCCATTTCAGCGC	
RTPS.8	RTwcoA-1F	VAR-37	TGAGATTGTCGGCCAGAATTG	*wcoA* RT-qPCR
	RTwcoA-1R	VAR-38	GAGCCCGCTTCGACTTTG	
RTPS.9	RT-CRY-1F	VAR-176	CGGGACTACATGCGATTGTG	*cryD* RT-qPCR
	RT-Cry-1R	VAR-177	CTTGAAAAGACGTGAGCCAAACT	
RTPS.10	vvd-2F	VAR-300	GCACCACCAGGGCATGA	*vvdA* RT-qPCR
	vvd-2R	VAR-301	GCGGTGTGAAGCGACCTT	
RTPS.11	RT-gdph-1F	VAR-148	GTGACCTCAAGGGCGTTCTG	*gpd* RT-qPCR
	Rt-Ff-gdph-1R	VAR-471	CGAAGATGGAGTTTGTGTT	

References

REFERENCES

Aasen, A.J., and Jensen, S.L. (1965). Fungal carotenoids. II. The structure of the carotenoid acid neurosporaxanthin. Acta Chem. Scand. 19, 1843–1853.

Adam, A., Deimel, S., Pardo-Medina, J., García-Martínez, J., Konte, T., Limón, M., Avalos, J., and Terpitz, U. (2018). Protein Activity of the *Fusarium fujikuroi* Rhodopsins CarO and OpsA and Their Relation to Fungus–Plant Interaction. Int. J. Mol. Sci. 19, 215.

Adám, A.L., García-Martínez, J., Szucs, E.P., Avalos, J., and Hornok, L. (2011). The *MAT1-2-1* mating-type gene upregulates photo-inducible carotenoid biosynthesis in *Fusarium verticillioides*. FEMS Microbiol. Lett. 318, 76–83.

Adrio, J.L., and Demain, A.L. (2003). Fungal biotechnology. Int. Microbiol. 6, 191–199.

Alejandre-Durán, E., Roldán-Arjona, T., Ariza, R.R., and Ruiz-Rubio, M. (2003). The photolyase gene from the plant pathogen *Fusarium oxysporum f. sp. lycopersici* is induced by visible light and alpha-tomatine from tomato plant. Fungal Genet. Biol. FG B 40, 159–165.

Arrach, N., Fernández-Martín, R., Cerdá-Olmedo, E., and Avalos, J. (2001). A single gene for lycopene cyclase, phytoene synthase, and regulation of carotene biosynthesis in *Phycomyces*. Proc. Natl. Acad. Sci. U. S. A. 98, 1687–1692.

Arrach, N., Schmidhauser, T.J., and Avalos, J. (2002). Mutants of the carotene cyclase domain of *al-2* from *Neurospora crassa*. Mol. Genet. Genomics MGG 266, 914–921.

Arthanari, Y., Heintzen, C., Griffiths-Jones, S., and Crosthwaite, S.K. (2014). Natural antisense transcripts and long non-coding RNA in *Neurospora crassa*. PloS One 9, e91353.

Austin, D.J., Bu'Lock, J.D., and Drake, D. (1970). The biosynthesis of trisporic acids from beta-carotene via retinal and trisporol. Experientia 26, 348–349.

Ávalos, J., and Cerdá-Olmedo, E. (1986). Chemical modification of carotenogenesis in *Gibberella fujikuroi*. Phytochemistry 25, 1837–1841.

Avalos, J., and Cerdà-Olmedo, E. (1987). Carotenoid mutants of *Gibberella fujikuroi*. Curr. Genet. 11, 505–511.

Avalos, J., and Cerdá-Olmedo, E. (2004). Fungal carotenoid production. In Handbook of Fungal Biotechnology, D.K. Arora, ed. (New York: Marcel Dekker, Inc.), pp. 367–378.

Avalos, J., and Corrochano, L.M. (2013). Carotenoid Biosynthesis in *Neurospora*. In *Neurospora*: Genomics and Molecular Biology, p. 15.

Avalos, J., and Estrada, A.F. (2010). Regulation by light in *Fusarium*. Fungal Genet. Biol. 47, 930–938.

Avalos, J., and Limón, M.C. (2015). Biological roles of fungal carotenoids. Curr. Genet. 61, 309–324.

Avalos, J., Casadesus, J., and Cerda-Olmedo, E. (1985). *Gibberella fujikuroi* mutants obtained with UV radiation and N-methyl-N'-nitro-N-nitrosoguanidine. Appl. Environ. Microbiol. 49, 187–191.

Avalos, J., Bejarano, E.R., and Cerdá-Olmedo, E. (1993). Photoinduction of carotenoid biosynthesis. In Methods in Enzymology, (Academic Press), pp. 283–294.

Avalos, J., Cerda-Olmedo, E., Reyes, F., and Barrero, A. (2007). Gibberellins and Other Metabolites of *Fusarium fujikuroi* and Related Fungi. Curr. Org. Chem. 11, 721–737.

Avalos, J., Díaz-Sánchez, V., García-Martínez, J., Castrillo, M., Ruger-Herreros, M., and Limón, M. (2014). Carotenoids. In Biosynthesis and Molecular Genetics of Fungal Secondary Metabolites, (Springer), pp. 149–185.

Avalos, J., Nordzieke, S., Parra, O., Pardo-Medina, J., and Carmen Limón, M. (2017a). Carotenoid Production by Filamentous Fungi and Yeasts. In Biotechnology of Yeasts and Filamentous Fungi, A.A. Sibirny, ed. (Cham: Springer International Publishing), pp. 225–279.

Avalos, J., Pardo-Medina, J., Parra-Rivero, O., Ruger-Herreros, M., Rodríguez-Ortiz, R., Hornero-Méndez, D., and Limón, M. (2017b). Carotenoid Biosynthesis in *Fusarium*. J. Fungi 3, 39.

Van Bakel, H., Nislow, C., Blencowe, B.J., and Hughes, T.R. (2010). Most "'Dark Matter'" Transcripts Are Associated With Known Genes. PLoS Biol 8, 1000371.

Ballario, P., Vittorioso, P., Magrelli, A., Talora, C., Cabibbo, A., and Macino, G. (1996). White collar-1, a central regulator of blue light responses in *Neurospora*, is a zinc finger protein. EMBO J. 15, 1650–1657.

Basenko, E., Pulman, J., Shanmugasundram, A., Harb, O., Crouch, K., Starns, D., Warrenfeltz, S., Aurrecoechea, C., Stoeckert, C., Kissinger, J., et al. (2018). FungiDB: An Integrated Bioinformatic Resource for Fungi and Oomycetes. J. Fungi 4, 39.

Bayram, O., Biesemann, C., Krappmann, S., Galland, P., and Braus, G.H. (2008a). More than a repair enzyme: *Aspergillus nidulans* photolyase-like CryA is a regulator of sexual development. Mol. Biol. Cell 19, 3254–3262.

Bayram, O., Krappmann, S., Ni, M., Bok, J.W., Helmstaedt, K., Valerius, O., Braus-Stromeyer, S., Kwon, N.-J., Keller, N.P., Yu, J.-H., et al. (2008b). VelB/VeA/LaeA complex coordinates light signal with fungal development and secondary metabolism. Science 320, 1504–1506.

Beattie, G.A., Hatfield, B.M., Dong, H., and McGrane, R.S. (2018). Seeing the Light: The Roles of Red- and Blue-Light Sensing in Plant Microbes. Annu. Rev. Phytopathol. 56, 41–66.

Bejarano, E.R., Avalos, J., Lipson, E.D., and Cerdá-Olmedo, E. (1991). Photoinduced accumulation of carotene in *Phycomyces*. Planta 183, 1–9.

Bergman, K., Eslava, A.P., and Cerdá-Olmedo, E. (1973). Mutants of *Phycomyces* with abnormal phototropism. Mol. Gen. Genet. MGG 123, 1–16.

Billmyre, R.B., Calo, S., Feretzaki, M., Wang, X., and Heitman, J. (2013). RNAi function, diversity, and loss in the fungal kingdom. Chromosome Res. 21, 561–572.

Bindl, E., Lang, W., and Rau, W. (1970). Untersuchungen über die lichtabhängige Carotinoidsynthese: VI. Zeitlicher Verlauf der Synthese der einzelnen Carotinoide bei *Fusarium aquaeductuum* unter verschiedenen Induktionsbedingungen. Planta 94, 156–174.

Blumenstein, A., Vienken, K., Tasler, R., Purschwitz, J., Veith, D., Frankenberg-Dinkel, N., and Fischer, R. (2005). The *Aspergillus nidulans* Phytochrome FphA Represses Sexual Development in Red Light. Curr. Biol. 15, 1833–1838.

Booth, C. (1971). The genus *Fusarium* (Farnham Royal: Commonwealth Agricultural Bureaux [for the] Commonwealth Mycological Institute).

Brandl, J., and Andersen, M.R. (2017). Aspergilli: Models for systems biology in filamentous fungi. Curr. Opin. Syst. Biol. 6, 67–73.

Brenna, A., and Talora, C. (2019). WC-1 and the Proximal GATA Sequence Mediate a Cis-/Trans-Acting Repressive Regulation of Light-Dependent Gene Transcription in the Dark. Int. J. Mol. Sci. 20, 2854.

Brenna, A., Grimaldi, B., Filetici, P., and Ballario, P. (2012). Physical association of the WC-1 photoreceptor and the histone acetyltransferase NGF-1 is required for blue light signal transduction in *Neurospora crassa*. Mol. Biol. Cell 23, 3863–3872.

Briggs, W.R. (2007). The LOV domain: a chromophore module servicing multiple photoreceptors. J. Biomed. Sci. 14, 499–504.

Britton, G., Liaaen-Jensen, S., and Pfander, H. (1998). Carotenoids (Basel: Birkhäuser Verlag).

Brockdorff, N., Bowness, J.S., and Wei, G. (2020). Progress toward understanding chromosome silencing by *Xist* RNA. Genes Dev. 34, 733–744.

Brych, A., Mascarenhas, J., Jaeger, E., Charkiewicz, E., Pokorny, R., Bölker, M., Doehlemann, G., and Batschauer, A. (2016). White collar 1 ‐ induced photolyase expression contributes to UV tolerance of *Ustilago maydis*. MicrobiologyOpen 5, 224–243.

Bumgarner, S.L., Dowell, R.D., Grisafi, P., Gifford, D.K., and Fink, G.R. (2009). Toggle involving cis-interfering noncoding RNAs controls variegated gene expression in yeast. Proc. Natl. Acad. Sci. U. S. A. 106, 18321–18326.

Cai, Q., He, B., Weiberg, A., Buck, A.H., and Jin, H. (2019). Small RNAs and extracellular vesicles: New mechanisms of cross-species communication and innovative tools for disease control. PLOS Pathog. 15, e1008090.

Calvo, A.M. (2008). The VeA regulatory system and its role in morphological and chemical development in fungi. Fungal Genet. Biol. FG B 45, 1053–1061.

Calvo, A.M., Wilson, R.A., Bok, J.W., and Keller, N.P. (2002). Relationship between Secondary Metabolism and Fungal Development. Microbiol. Mol. Biol. Rev. 66, 447–459.

Camblong, J., Beyrouthy, N., Guffanti, E., Schlaepfer, G., Steinmetz, L.M., and Stutz, F. (2009). Trans-acting antisense RNAs mediate transcriptional gene cosuppression in *S. cerevisiae*. Genes Dev. 23, 1534–1545.

Candau, R., Avalos, J., and Cerdá-Olmedo, E. (1991). Gibberellins and Carotenoids in the Wild Type and Mutants of *Gibberella fujikuroi*. Appl. Environ. Microbiol. 57, 3378–3382.

Canessa, P., Schumacher, J., Hevia, M.A., Tudzynski, P., and Larrondo, L.F. (2013). Assessing the effects of light on differentiation and virulence of the plant pathogen *Botrytis cinerea*: characterization of the White Collar Complex. PloS One 8, e84223.

Carninci, P., Kasukawa, T., Katayama, S., Gough, J., Frith, M.C., Maeda, N., Oyama, R., Ravasi, T., Lenhard, B., Wells, C., et al. (2005). The Transcriptional Landscape of the Mammalian Genome. Science 309, 1559–1563.

Carreras-Villaseñor, N., Esquivel-Naranjo, E.U., Villalobos-Escobedo, J.M., Abreu-Goodger, C., and Herrera-Estrella, A. (2013). The RNAi machinery regulates growth and development in the filamentous fungus *Trichoderma atroviride*. Mol. Microbiol. 89, 96–112.

Carthew, R.W., and Sontheimer, E.J. (2009). Origins and Mechanisms of miRNAs and siRNAs. Cell 136, 642–655.

Casas-Flores, S., and Herrera-Estrella, A. (2016). The Bright and Dark Sides of Fungal Life. In Environmental and Microbial Relationships, I.S. Druzhinina, and C.P. Kubicek, eds. (Cham: Springer International Publishing), pp. 41–77.

Castellanos, F., Schmoll, M., Martínez, P., Tisch, D., Kubicek, C.P., Herrera-Estrella, A., and Esquivel-Naranjo, E.U. (2010). Crucial factors of the light perception machinery and their impact on growth and cellulase gene transcription in *Trichoderma reesei*. Fungal Genet. Biol. FG B 47, 468–476.

Castrillo, M. (2014). Functional Analysis of Photoproteins in *Fusarium*. University of Seville.

Castrillo, M., and Avalos, J. (2014). Light-mediated participation of the VIVID-like protein of *Fusarium fujikuroi* VvdA in pigmentation and development. Fungal Genet. Biol. 71, 9–20.

Castrillo, M., and Avalos, J. (2015). The Flavoproteins CryD and VvdA Cooperate with the White Collar Protein WcoA in the Control of Photocarotenogenesis in *Fusarium fujikuroi*. PLOS ONE 10, e0119785.

Castrillo, M., García-Martínez, J., and Avalos, J. (2013). Light-dependent functions of the *Fusarium fujikuroi* CryD DASH cryptochrome in development and secondary metabolism. Appl. Environ. Microbiol. 79, 2777–2788.

Castrillo, M., Bernhardt, A., Ávalos, J., Batschauer, A., and Pokorny, R. (2015). Biochemical Characterization of the DASH-Type Cryptochrome CryD From *Fusarium fujikuroi*. Photochem. Photobiol. 91, 1356–1367.

Catalanotto, C., Azzalin, G., Macino, G., and Cogoni, C. (2002). Involvement of small RNAs and role of the *qde* genes in the gene silencing pathway in *Neurospora*. Genes Dev. 16, 790–795.

Cemel, I.A., Ha, N., Schermann, G., Yonekawa, S., and Brunner, M. (2017). The coding and noncoding transcriptome of *Neurospora crassa*. BMC Genomics 18, 978.

Cerdá-Olmedo, E. (1987). Carotene. In *Phycomyces*, E. Cerdá-Olmedo, and E.D. Lipson, eds. (New York: Cold Spring Harbor Laboratory Press), pp. 199–222.

Cetz-Chel, J.E., Balcázar-López, E., Esquivel-Naranjo, E.U., and Herrera-Estrella, A. (2016). The *Trichoderma atroviride* putative transcription factor Blu7 controls light responsiveness and tolerance. BMC Genomics 17, 327.

Chaves, I., Pokorny, R., Byrdin, M., Hoang, N., Ritz, T., Brettel, K., Essen, L.-O., van der Horst, G.T.J., Batschauer, A., and Ahmad, M. (2011). The Cryptochromes: Blue Light Photoreceptors in Plants and Animals. Annu. Rev. Plant Biol. 62, 335–364.

Chen, C.-H., Ringelberg, C.S., Gross, R.H., Dunlap, J.C., and Loros, J.J. (2009). Genome-wide analysis of light-inducible responses reveals hierarchical light signalling in *Neurospora*. EMBO J. 28, 1029–1042.

Chen, C.-H., DeMay, B.S., Gladfelter, A.S., Dunlap, J.C., and Loros, J.J. (2010). Physical interaction between VIVID and white collar complex regulates photoadaptation in *Neurospora*. Proc. Natl. Acad. Sci. U. S. A. 107, 16715–16720.

Chen, R., Jiang, N., Jiang, Q., Sun, X., Wang, Y., Zhang, H., and Hu, Z. (2014). Exploring MicroRNA-Like Small RNAs in the Filamentous Fungus *Fusarium oxysporum*. PloS One 9, e104956.

Chen, S., Huang, T., Zhou, Y., Han, Y., Xu, M., and Gu, J. (2017). AfterQC: automatic filtering, trimming, error removing and quality control for fastq data. BMC Bioinformatics 18, 80.

Chen, Y., Gao, Q., Huang, M., Liu, Y., Liu, Z., Liu, X., and Ma, Z. (2015). Characterization of RNA silencing components in the plant pathogenic fungus *Fusarium graminearum*. Sci. Rep. 5, 12500.

Chen, Y., Kistler, H.C., and Ma, Z. (2019). *Fusarium graminearum* Trichothecene Mycotoxins: Biosynthesis, Regulation, and Management. Annu. Rev. Phytopathol. 57, 15–39.

Cheng, P., Yang, Y., Gardner, K.H., and Liu, Y. (2002). PAS domain-mediated WC-1/WC-2 interaction is essential for maintaining the steady-state level of WC-1 and the function of both proteins in circadian clock and light responses of *Neurospora*. Mol. Cell. Biol. 22, 517–524.

Cogoni, C., and Macino, G. (1997). Isolation of quelling-defective (*qde*) mutants impaired in posttranscriptional transgene-induced gene silencing in *Neurospora crassa*. Proc. Natl. Acad. Sci. U. S. A. 94, 10233–10238.

Cohrs, K.C., and Schumacher, J. (2017). The Two Cryptochrome/Photolyase Family Proteins Fulfill Distinct Roles in DNA Photorepair and Regulation of Conidiation in the Gray Mold Fungus *Botrytis cinerea*. Appl. Environ. Microbiol. 83, e00812-17, e00812-17.

Cohrs, K.C., Simon, A., Viaud, M., and Schumacher, J. (2016). Light governs asexual differentiation in the grey mold fungus *Botrytis cinerea* via the putative transcription factor BcLTF2: BcLTF2 regulates conidiation in *Botrytis cinerea*. Environ. Microbiol. 18, 4068–4086.

Colot, H.V., Park, G., Turner, G.E., Ringelberg, C., Crew, C.M., Litvinkova, L., Weiss, R.L., Borkovich, K.A., and Dunlap, J.C. (2006). A high-throughput gene knockout procedure for *Neurospora* reveals functions for multiple transcription factors. Proc. Natl. Acad. Sci. 103, 10352–10357.

Conesa, A., Madrigal, P., Tarazona, S., Gomez-Cabrero, D., Cervera, A., McPherson, A., Szcześniak, M.W., Gaffney, D.J., Elo, L.L., Zhang, X., et al. (2016). A survey of best practices for RNA-seq data analysis. Genome Biol. 17, 13.

Connolly, L.R., Smith, K.M., and Freitag, M. (2013). The *Fusarium graminearum* Histone H3 K27 Methyltransferase KMT6 Regulates Development and Expression of Secondary Metabolite Gene Clusters. PLoS Genet. 9, e1003916.

Corrochano, L.M. (2019). Light in the Fungal World: From Photoreception to Gene Transcription and Beyond. Annu. Rev. Genet. 53, 149–170.

Corrochano, L.M., and Garre, V. (2010). Photobiology in the Zygomycota: multiple photoreceptor genes for complex responses to light. Fungal Genet. Biol. FG B 47, 893–899.

Costa, T.P.C., Rodrigues, E.M., Dias, L.P., Pupin, B., Ferreira, P.C., and Rangel, D.E.N. (2020). Different wavelengths of visible light influence the conidial production and tolerance to ultra-violet radiation of the plant pathogens *Colletotrichum acutatum* and *Fusarium fujikuroi*. Eur. J. Plant Pathol.

Crosson, S., and Moffat, K. (2002). Photoexcited structure of a plant photoreceptor domain reveals a light-driven molecular switch. Plant Cell 14, 1067–1075.

Cullen, D., Leong, S.A., Wilson, L.J., and Henner, D.J. (1987). Transformation of *Aspergillus nidulans* with the hygromycin-resistance gene, *hph*. Gene 57, 21–26.

Dahlmann, T.A., and Kück, U. (2015). Dicer-Dependent Biogenesis of Small RNAs and Evidence for MicroRNA-Like RNAs in the Penicillin Producing Fungus *Penicillium chrysogenum*. PloS One 10, e0125989.

D'Andrea, L., Amenós, M., and Rodríguez-Concepción, M. (2014). Confocal laser scanning microscopy detection of chlorophylls and carotenoids in chloroplasts and chromoplasts of tomato fruit. Methods Mol. Biol. Clifton NJ 1153, 227–232.

Daniel Gietz, R., and Woods, R.A. (2002). Transformation of yeast by lithium acetate/single-stranded carrier DNA/polyethylene glycol method. In Methods in Enzymology, C. Guthrie, and G.R. Fink, eds. (Academic Press), pp. 87–96.

Dasgupta, A., Chen, C.-H., Lee, C., Gladfelter, A.S., Dunlap, J.C., and Loros, J.J. (2015). Biological Significance of Photoreceptor Photocycle Length: VIVID Photocycle Governs the Dynamic VIVID-White Collar Complex Pool Mediating Photo-adaptation and Response to Changes in Light Intensity. PLoS Genet. 11, e1005215.

Dasgupta, A., Fuller, K.K., Dunlap, J.C., and Loros, J.J. (2016). Seeing the world differently: variability in the photosensory mechanisms of two model fungi: Photobiology of *N. crassa* and *Aspergillus*. Environ. Microbiol. 18, 5–20.

Davis, R.H. (2000). *Neurospora*: contributions of a model organism (New York: Oxford University Press).

Dawson, M.I. (2000). The importance of vitamin A in nutrition. Curr. Pharm. Des. 6, 311–325.

De Fabo, E.C., Harding, R.W., and Shropshire, W. (1976). Action Spectrum between 260 and 800 Nanometers for the Photoinduction of Carotenoid Biosynthesis in *Neurospora crassa*. Plant Physiol. 57, 440–445.

Degli-Innocenti, F., and Russo, V.E. (1984). Isolation of new white collar mutants of *Neurospora crassa* and studies on their behavior in the blue light-induced formation of protoperithecia. J. Bacteriol. 159, 757–761.

Díaz-Sánchez, V. (2013). Enzimas fúngicas implicadas en la síntesis y modificación de compuestos de interés aplicado. University of Seville.

Díaz-Sánchez, V., Estrada, A.F., Trautmann, D., Limón, M.C., Al-Babili, S., and Avalos, J. (2011a). Analysis of *al-2* mutations in *Neurospora*. PloS One 6, e21948.

Díaz-Sánchez, V., Estrada, A.F., Trautmann, D., Al-Babili, S., and Avalos, J. (2011b). The gene *carD* encodes the aldehyde dehydrogenase responsible for neurosporaxanthin biosynthesis in *Fusarium fujikuroi*. FEBS J. 278, 3164–3176.

Díaz-Sánchez, V., Limón, M.C., Schaub, P., Al-Babili, S., and Avalos, J. (2016). A RALDH-like enzyme involved in *Fusarium verticillioides* development. Fungal Genet. Biol. 86, 20–32.

Diernfellner, A.C.R., and Brunner, M. (2020). Phosphorylation Timers in the *Neurospora crassa* Circadian Clock. J. Mol. Biol. 432, 3449–3465.

Djebali, S., Davis, C.A., Merkel, A., Dobin, A., Lassmann, T., Mortazavi, A., Tanzer, A., Lagarde, J., Lin, W., Schlesinger, F., et al. (2012). Landscape of transcription in human cells. Nature 488.

Dobin, A., Davis, C.A., Schlesinger, F., Drenkow, J., Zaleski, C., Jha, S., Batut, P., Chaisson, M., and Gingeras, T.R. (2013). STAR: ultrafast universal RNA-seq aligner. Bioinformatics 29, 15–21.

Domenech, C.E., Giordano, W., Avalos, J., and Cerdá-Olmedo, E. (1996). Separate compartments for the production of sterols, carotenoids and gibberellins in *Gibberella fujikuroi*. Eur. J. Biochem. 239, 720–725.

Dunlap, J.C., and Loros, J.J. (2017). Making Time: Conservation of Biological Clocks from Fungi to Animals. In The Fungal Kingdom, Heitman, Howlett, Crous, Stukenbrock, James, and Gow, eds. (American Society of Microbiology), pp. 515–534.

Eggersdorfer, M., and Wyss, A. (2018). Carotenoids in human nutrition and health. Arch. Biochem. Biophys. 652, 18–26.

Estrada, A.F., and Avalos, J. (2008). The White Collar protein WcoA of *Fusarium fujikuroi* is not essential for photocarotenogenesis, but is involved in the regulation of secondary metabolism and conidiation. Fungal Genet. Biol. 45, 705–718.

Estrada, A.F., and Avalos, J. (2009). Regulation and Targeted Mutation of *opsA*, Coding for the NOP-1 Opsin Orthologue in *Fusarium fujikuroi*. J. Mol. Biol. 387, 59–73.

Estrada, A.F., Youssar, L., Scherzinger, D., Al-Babili, S., and Avalos, J. (2008a). The *ylo-1* gene encodes an aldehyde dehydrogenase responsible for the last reaction in the *Neurospora* carotenoid pathway. Mol. Microbiol. 69, 1207–1220.

Estrada, A.F., Maier, D., Scherzinger, D., Avalos, J., and Al-Babili, S. (2008b). Novel apocarotenoid intermediates in *Neurospora crassa* mutants imply a new biosynthetic reaction sequence leading to neurosporaxanthin formation. Fungal Genet. Biol. 45, 1497–1505.

Estrada, A.F., Brefort, T., Mengel, C., Díaz-Sánchez, V., Alder, A., Al-Babili, S., and Avalos, J. (2009). *Ustilago maydis* accumulates beta-carotene at levels determined by a retinal-forming carotenoid oxygenase. Fungal Genet. Biol. FG B 46, 803–813.

Fernández-Martín, R., Cerdá-Olmedo, E., and Avalos, J. (2000). Homologous recombination and allele replacement in transformants of *Fusarium fujikuroi*. Mol. Gen. Genet. MGG 263, 838–845.

Finn, R.D., Bateman, A., Clements, J., Coggill, P., Eberhardt, R.Y., Eddy, S.R., Heger, A., Hetherington, K., Holm, L., Mistry, J., et al. (2014). Pfam: the protein families database. Nucleic Acids Res. 42, D222–D230.

Fischer, R., Aguirre, J., Herrera-Estrella, A., and Corrochano, L.M. (2017). The Complexity of Fungal Vision. In The Fungal Kingdom, Heitman, Howlett, Crous, Stukenbrock, James, and Gow, eds. (American Society of Microbiology), pp. 441–461.

Fisher, M.C., Gurr, S.J., Cuomo, C.A., Blehert, D.S., Jin, H., Stukenbrock, E.H., Stajich, J.E., Kahmann, R., Boone, C., Denning, D.W., et al. (2020). Threats Posed by the Fungal Kingdom to Humans, Wildlife, and Agriculture. MBio 11, e00449-20, /mbio/11/3/mBio.00449-20.atom.

Franchi, L., Fulci, V., and Macino, G. (2005). Protein kinase C modulates light responses in *Neurospora* by regulating the blue light photoreceptor WC-1. Mol. Microbiol. 56, 334–345.

Fraser, P.D., Ruiz-Hidalgo, M.J., Lopez-Matas, M.A., Alvarez, M.I., Eslava, A.P., and Bramley, P.M. (1996). Carotenoid biosynthesis in wild type and mutant strains of *Mucor circinelloides*. Biochim. Biophys. Acta 1289, 203–208.

Friedländer, M.R., Mackowiak, S.D., Li, N., Chen, W., and Rajewsky, N. (2012). miRDeep2 accurately identifies known and hundreds of novel microRNA genes in seven animal clades. Nucleic Acids Res. 40, 37–52.

Froehlich, A.C., Noh, B., Vierstra, R.D., Loros, J., and Dunlap, J.C. (2005). Genetic and Molecular Analysis of Phytochromes from the Filamentous Fungus *Neurospora crassa*. Eukaryot. Cell 4, 2140–2152.

Froehlich, A.C., Chen, C.-H., Belden, W.J., Madeti, C., Roenneberg, T., Merrow, M., Loros, J.J., and Dunlap, J.C. (2010). Genetic and Molecular Characterization of a Cryptochrome from the Filamentous Fungus *Neurospora crassa*. Eukaryot. Cell 9, 738–750.

Fuller, K.K., Ringelberg, C.S., Loros, J.J., and Dunlap, J.C. (2013). The Fungal Pathogen *Aspergillus fumigatus* Regulates Growth, Metabolism, and Stress Resistance in Response to Light. MBio 4, e00142-13.

Fuller, K.K., Loros, J.J., and Dunlap, J.C. (2015). Fungal photobiology: visible light as a signal for stress, space and time. Curr. Genet. 61, 275–288.

Fuller, K.K., Dunlap, J.C., and Loros, J.J. (2016). Fungal Light Sensing at the Bench and Beyond. In Advances in Genetics, (Elsevier), pp. 1–51.

Gaffar, F.Y., Imani, J., Karlovsky, P., Koch, A., and Kogel, K.-H. (2019). Different Components of the RNA Interference Machinery Are Required for Conidiation, Ascosporogenesis, Virulence, Deoxynivalenol Production, and Fungal Inhibition by Exogenous Double-Stranded RNA in the Head Blight Pathogen *Fusarium graminearum*. Front. Microbiol. 10, 1662.

Garbayo, I., Vílchez, C., Nava-Saucedo, J.E., and Barbotin, J.N. (2003). Nitrogen, carbon and light-mediated regulation studies of carotenoid biosynthesis in immobilized mycelia of *Gibberella fujikuroi*. Enzyme Microb. Technol. 33, 629–634.

García-Martínez, J., Ádám, A.L., and Avalos, J. (2012). Adenylyl Cyclase Plays a Regulatory Role in Development, Stress Resistance and Secondary Metabolism in *Fusarium fujikuroi*. PLoS ONE 7, e28849.

García-Martínez, J., Brunk, M., Avalos, J., and Terpitz, U. (2015). The CarO rhodopsin of the fungus *Fusarium fujikuroi* is a light-driven proton pump that retards spore germination. Sci. Rep. 5, 7798.

Garg, A., Sanchez, A.M., Shuman, S., and Schwer, B. (2018). A long noncoding (lnc)RNA governs expression of the phosphate transporter Pho84 in fission yeast and has cascading effects on the flanking *prt* lncRNA and *pho1* genes. J. Biol. Chem. 293, 4456–4467.

Geiser, D.M., Aoki, T., Bacon, C.W., Baker, S.E., Bhattacharyya, M.K., Brandt, M.E., Brown, D.W., Burgess, L.W., Chulze, S., Coleman, J.J., et al. (2013). One fungus, one name: defining the genus *Fusarium* in a scientifically robust way that preserves longstanding use. Phytopathology 103, 400–408.

Geisler, S., Lojek, L., Khalil, A.M., Baker, K.E., and Coller, J. (2012). Decapping of Long Noncoding RNAs Regulates Inducible Genes. Mol. Cell 45, 279–291.

Geissman, T.A., Verbiscar, A.J., Phinney, B.O., and Cragg, G. (1966). Studies on the biosynthesis of gibberellins from (−)-kaurenoic acid in cultures of *Gibberella Fujikuroi*. Phytochemistry 5, 933–947.

Gerke, J., and Braus, G.H. (2014). Manipulation of fungal development as source of novel secondary metabolites for biotechnology. Appl. Microbiol. Biotechnol. 98, 8443–8455.

Gessler, N.N., Sokolov, A.V., Bykhovsky, V.Ya., and Belozerskaya, T.A. (2002). Superoxide Dismutase and Catalase Activities in Carotenoid-Synthesizing Fungi *Blakeslea trispora* and *Neurospora crassa* Fungi in Oxidative Stress. Appl. Biochem. Microbiol. 38, 205–209.

Gmoser, R., Ferreira, J.A., Lennartsson, P.R., and Taherzadeh, M.J. (2017). Filamentous ascomycetes fungi as a source of natural pigments. Fungal Biol. Biotechnol. 4, 4.

Goldie, A.H., and Subden, R.E. (1973). The neutral carotenoids of wild-type and mutant strains of *Neurospora crassa*. Biochem. Genet. 10, 275–284.

Goodwin, T. (1980). The Biochemistry of the Carotenoids: Volume I Plants (Springer Netherlands).

Gordon, T.R. (2017). *Fusarium oxysporum* and the *Fusarium* Wilt Syndrome. Annu. Rev. Phytopathol. 55, 23–39.

Gotz, S., Garcia-Gomez, J.M., Terol, J., Williams, T.D., Nagaraj, S.H., Nueda, M.J., Robles, M., Talon, M., Dopazo, J., and Conesa, A. (2008). High-throughput functional annotation and data mining with the Blast2GO suite. Nucleic Acids Res. 36, 3420–3435.

Grau, M.F., Entwistle, R., Oakley, C.E., Wang, C.C.C., and Oakley, B.R. (2019). Overexpression of an LaeA-like Methyltransferase Upregulates Secondary Metabolite Production in *Aspergillus nidulans*. ACS Chem. Biol. 14, 1643–1651.

Grimaldi, B., Coiro, P., Filetici, P., Berge, E., Dobosy, J.R., Freitag, M., Selker, E.U., and Ballario, P. (2006). The *Neurospora crassa* White Collar-1 dependent blue light response requires acetylation of histone H3 lysine 14 by NGF-1. Mol. Biol. Cell 17, 4576–4583.

Guo, M., Yang, P., Zhang, J., Liu, G., Yuan, Q., He, W., Nian, J., Yi, S., Huang, T., and Liao, Y. (2019). Expression of microRNA-like RNA-2 (*Fgmil-2*) and *bioH1* from a single transcript in *Fusarium graminearum* are inversely correlated to regulate biotin synthesis during vegetative growth and host infection. Mol. Plant Pathol. 20, 1574–1581.

Halic, M., and Moazed, D. (2010). Dicer-independent primal RNAs trigger RNAi and heterochromatin formation. Cell 140, 504–516.

Hammond, T.M., and Keller, N.P. (2005). RNA Silencing in *Aspergillus nidulans* Is Independent of RNA-Dependent RNA Polymerases. Genetics 169, 607–617.

Hanahan, D. (1983). Studies on transformation of *Escherichia coli* with plasmids. J. Mol. Biol. 166, 557–580.

Harding, R.W., and Turner, R.V. (1981). Photoregulation of the Carotenoid Biosynthetic Pathway in Albino and White Collar Mutants of *Neurospora crassa*. Plant Physiol. 68, 745–749.

Hashimoto, H., Uragami, C., and Cogdell, R.J. (2016). Carotenoids and Photosynthesis. In Carotenoids in Nature: Biosynthesis, Regulation and Function, C. Stange, ed. (Cham: Springer International Publishing), pp. 111–139.

He, Q., and Liu, Y. (2005). Molecular mechanism of light responses in *Neurospora*: from light-induced transcription to photoadaptation. Genes Dev. 19, 2888–2899.

He, Q., Cheng, P., Yang, Y., Wang, L., Gardner, K.H., and Liu, L. (2002). White Collar-1, a DNA Binding Transcription Factor and a Light Sensor. Science 297, 840–843.

Hedden, P., and Sponsel, V. (2015). A Century of Gibberellin Research. J. Plant Growth Regul. 34, 740–760.

Hernández-García, J., Briones-Moreno, A., and Blázquez, M.A. (2020). Origin and evolution of gibberellin signaling and metabolism in plants. Semin. Cell Dev. Biol.

Hevia, M.A., Canessa, P., Müller-Esparza, H., and Larrondo, L.F. (2015). A circadian oscillator in the fungus *Botrytis cinerea* regulates virulence when infecting *Arabidopsis thaliana*. Proc. Natl. Acad. Sci. 112, 8744–8749.

Homann, V., Mende, K., Arntz, C., Ilardi, V., Macino, G., Morelli, G., Bose, G., and Tudzynski, B. (1996). The isoprenoid pathway: cloning and characterization of fungal FPPS genes. Curr. Genet. 30, 232–239.

Hoogendoorn, K., Barra, L., Waalwijk, C., Dickschat, J.S., van der Lee, T.A.J., and Medema, M.H. (2018). Evolution and Diversity of Biosynthetic Gene Clusters in *Fusarium*. Front. Microbiol. 9, 1158.

de Hoon, M.J.L., Imoto, S., Nolan, J., and Miyano, S. (2004). Open source clustering software. Bioinformatics 20, 1453–1454.

van der Horst, M.A., and Hellingwerf, K.J. (2004). Photoreceptor proteins, “star actors of modern times”: a review of the functional dynamics in the structure of representative members of six different photoreceptor families. Acc. Chem. Res. 37, 13–20.

Houseley, J., Rubbi, L., Grunstein, M., Tollervey, D., and Vogelauer, M. (2008). A ncRNA Modulates Histone Modification and mRNA Induction in the Yeast GAL Gene Cluster. Mol. Cell 32, 685–695.

Hu, Z., Parekh, U., Maruta, N., Trusov, Y., and Botella, J.R. (2015). Down-regulation of *Fusarium oxysporum* endogenous genes by Host-Delivered RNA interference enhances disease resistance. Front. Chem. 3.

Huber, F., Bunina, D., Gupta, I., Theer, P., Steinmetz, L.M., and Correspondence, M.K. (2016). Protein Abundance Control by Non-coding Antisense Transcription.

Hunt, S.M., Thompson, S., Elvin, M., and Heintzen, C. (2010). VIVID interacts with the WHITE COLLAR complex and FREQUENCY-interacting RNA helicase to alter light and clock responses in *Neurospora*. Proc. Natl. Acad. Sci. U. S. A. 107, 16709–16714.

Idnurm, A., and Heitman, J. (2005). Light controls growth and development via a conserved pathway in the fungal kingdom. PLoS Biol. 3, e95.

Idnurm, A., and Heitman, J. (2010). Ferrochelatase is a conserved downstream target of the blue light-sensing White-collar complex in fungi. Microbiology 156, 2393–2407.

Idnurm, A., Verma, S., and Corrochano, L.M. (2010). A glimpse into the basis of vision in the kingdom Mycota. Fungal Genet. Biol. FG B 47, 881–892.

Iigusa, H., Yoshida, Y., and Hasunuma, K. (2005). Oxygen and hydrogen peroxide enhance light-induced carotenoid synthesis in *Neurospora crassa*. FEBS Lett. 579, 4012–4016.

Inoue, H., Nojima, H., and Okayama, H. (1990). High efficiency transformation of *Escherichia coli* with plasmids. Gene 96, 23–28.

Jain, S., and Keller, N. (2013). Insights to fungal biology through LaeA sleuthing. Fungal Biol. Rev. 27, 51–59.

Janevska, S., and Tudzynski, B. (2018). Secondary metabolism in *Fusarium fujikuroi*: strategies to unravel the function of biosynthetic pathways. Appl. Microbiol. Biotechnol. 102, 615–630.

Janik, E., Niemcewicz, M., Ceremuga, M., Stela, M., Saluk-Bijak, J., Siadkowski, A., and Bijak, M. (2020). Molecular Aspects of Mycotoxins—A Serious Problem for Human Health. Int. J. Mol. Sci. 21, 8187.

Jian, J., and Liang, X. (2019). One Small RNA of *Fusarium graminearum* Targets and Silences CEBiP Gene in Common Wheat. Microorganisms 7, 425.

Jiang, J., Liu, X., Yin, Y., and Ma, Z. (2011). Involvement of a velvet protein FgVeA in the regulation of asexual development, lipid and secondary metabolisms and virulence in *Fusarium graminearum*. PloS One 6, e28291.

Jin, J.-M., Lee, J., and Lee, Y.-W. (2010). Characterization of carotenoid biosynthetic genes in the ascomycete *Gibberella zeae*. FEMS Microbiol. Lett. 302, 197–202.

Jo, S.-M., Ayukawa, Y., Yun, S.-H., Komatsu, K., and Arie, T. (2018). A putative RNA silencing component protein FoQde-2 is involved in virulence of the tomato wilt fungus *Fusarium oxysporum f. sp. lycopersici*. J. Gen. Plant Pathol. 84, 395–398.

Johnson, E.A., and Schroeder, W.A. (1996). Biotechnology of Astaxanthin Production in *Phaffia rhodozyma*. In Biotechnology for Improved Foods and Flavors, G.R. Takeoka, R. Teranishi, P.J. Williams, and A. Kobayashi, eds. (Washington, DC: American Chemical Society), pp. 39–50.

Káldi, K., González, B.H., and Brunner, M. (2006). Transcriptional regulation of the *Neurospora* circadian clock gene *wc-1* affects the phase of circadian output. EMBO Rep. 7, 199–204.

Kang, K., Zhong, J., Jiang, L., Liu, G., Gou, C.Y., Wu, Q., Wang, Y., Luo, J., and Gou, D. (2013). Identification of microRNA-Like RNAs in the Filamentous Fungus *Trichoderma reesei* by Solexa Sequencing. PLoS ONE 8, 1–7.

Keller, N.P. (2019). Fungal secondary metabolism: regulation, function and drug discovery. Nat. Rev. Microbiol. 17, 167–180.

Kim, H., Son, H., and Lee, Y.-W. (2014). Effects of light on secondary metabolism and fungal development of *Fusarium graminearum*. J. Appl. Microbiol. 116, 380–389.

Kim, H., Kim, H.-K., Lee, S., and Yun, S.-H. (2015). The White-Collar Complex Is Involved in Sexual Development of *Fusarium graminearum*. PLOS ONE 10, e0120293.

Kim, W., Miguel-Rojas, C., Wang, J., Townsend, J.P., and Trail, F. (2018). Developmental Dynamics of Long Noncoding RNA Expression during Sexual Fruiting Body Formation in *Fusarium graminearum*. MBio 9.

Kimura, M., Tokai, T., Matsumoto, G., Fujimura, M., Hamamoto, H., Yoneyama, K., Shibata, T., and Yamaguchi, I. (2003). Trichothecene Nonproducer *Gibberella* Species Have Both Functional and Nonfunctional 3-O-Acetyltransferase Genes. 8.

Kiontke, S., Göbel, T., Brych, A., and Batschauer, A. (2020). DASH-type cryptochromes – solved and open questions. Biol. Chem. 401, 1487–1493.

Kodedová, M., and Sychrová, H. (2015). Changes in the Sterol Composition of the Plasma Membrane Affect Membrane Potential, Salt Tolerance and the Activity of Multidrug Resistance Pumps in *Saccharomyces cerevisiae*. PLOS ONE 10, e0139306.

Krobanan, K., Liang, S.-W., Chiu, H.-C., and Shen, W.-C. (2019). The Blue-Light Photoreceptor Sfwc-1 Gene Regulates the Phototropic Response and Fruiting-Body Development in the Homothallic Ascomycete *Sordaria fimicola*. Appl. Environ. Microbiol. 85, e02206-18, /aem/85/12/AEM.02206-18.atom.

Kuhlman, E.G. (1982). Varieties of *Gibberella fujikuroi* with Anamorphs in *Fusarium* Section Liseola. Mycologia 74, 759–768.

Kvas, M., Marasas, W.F.O., Wingfield, B.D., Wingfield, M.J., and Steenkamp, E.T. (2009). Diversity and evolution of *Fusarium* species in the *Gibberella fujikuroi* complex. Fungal Divers. 34, 1–21.

Lax, C., Tahiri, G., Patiño-Medina, J.A., Cánovas-Márquez, J.T., Pérez-Ruiz, J.A., Osorio-Concepción, M., Navarro, E., and Calo, S. (2020). The Evolutionary Significance of RNAi in the Fungal Kingdom. Int. J. Mol. Sci. 21, 9348.

Lee, H.-C., Chang, S.-S., Choudhary, S., Aalto, A.P., Maiti, M., Bamford, D.H., and Liu, Y. (2009). qiRNA is a new type of small interfering RNA induced by DNA damage. Nature 459, 274–277.

Lee, H.C., Li, L., Gu, W., Xue, Z., Crosthwaite, S.K., Pertsemlidis, A., Lewis, Z. a., Freitag, M., Selker, E.U., Mello, C.C., et al. (2010). Diverse Pathways Generate MicroRNA-like RNAs and Dicer-Independent Small Interfering RNAs in Fungi. Mol. Cell 38, 803–814.

Leong, H.S., Dawson, K., Wirth, C., Li, Y., Connolly, Y., Smith, D.L., Wilkinson, C.R.M., and Miller, C.J. (2014). A global non-coding RNA system modulates fission yeast protein levels in response to stress. Nat. Commun. 5, 3947.

Leppek, K., Das, R., and Barna, M. (2018). Functional 5′ UTR mRNA structures in eukaryotic translation regulation and how to find them. Nat. Rev. Mol. Cell Biol. 19, 158–174.

Leslie, J.F., and Summerell, B.A. (2006). The *Fusarium* laboratory manual (Ames, Iowa: Blackwell Pub).

Leslie, J.F., Summerell, B.A., Bullock, S., and Doe, F.J. (2005). Description of *Gibberella sacchari* and neotypification of its anamorph *Fusarium sacchari*. Mycologia 97, 718–724.

Li, L., Chang, S.S., and Liu, Y. (2010). RNA interference pathways in filamentous fungi. Cell. Mol. Life Sci. 67, 3849–3863.

Li, M., Yu, R., Bai, X., Wang, H., and Zhang, H. (2020). *Fusarium* : a treasure trove of bioactive secondary metabolites. Nat. Prod. Rep. 10.1039.D0NP00038H.

Li, W., Li, C., Li, S., and Peng, M. (2017). Long noncoding RNAs that respond to *Fusarium oxysporum* infection in 'Cavendish' banana (Musa acuminata). Sci. Rep. 7, 16939.

Limón, M.C., Rodríguez-Ortiz, R., and Avalos, J. (2010). Bikaverin production and applications. Appl. Microbiol. Biotechnol. 87, 21–29.

Lin, L., and Xu, J. (2020). Fungal Pigments and Their Roles Associated with Human Health. J. Fungi 6, 280.

Linden, H., and Macino, G. (1997). White collar 2, a partner in blue-light signal transduction, controlling expression of light-regulated genes in *Neurospora crassa*. EMBO J. 16, 98–109.

Linnemannstöns, P., Prado, M.M., Fernández-Martín, R., Tudzynski, B., and Avalos, J. (2002). A carotenoid biosynthesis gene cluster in *Fusarium fujikuroi*: the genes *carB* and *carRA*. Mol. Genet. Genomics MGG 267, 593–602.

von Lintig, J. (2010). Colors with functions: elucidating the biochemical and molecular basis of carotenoid metabolism. Annu. Rev. Nutr. 30, 35–56.

Livak, K.J., and Schmittgen, T.D. (2001). Analysis of relative gene expression data using real-time quantitative PCR and the 2(-Delta Delta C(T)) Method. Methods San Diego Calif 25, 402–408.

Lorca-Pascual, J.M., Murcia-Flores, L., Garre, V., Torres-Martínez, S., and Ruiz-Vázquez, R.M. (2004). The RING-finger domain of the fungal repressor *crgA* is essential for accurate light regulation of carotenogenesis. Mol. Microbiol. 52, 1463–1474.

Love, M.I., Huber, W., and Anders, S. (2014). Moderated estimation of fold change and dispersion for RNA-seq data with DESeq2. Genome Biol. 15, 550.

Luke, B., and Lingner, J. (2009). TERRA: telomeric repeat-containing RNA. EMBO J. 28, 2503–2510.

Ma, L., Bajic, V.B., and Zhang, Z. (2013). On the classification of long non-coding RNAs. RNA Biol. 10, 924–933.

Malzahn, E., Ciprianidis, S., Káldi, K., Schafmeier, T., and Brunner, M. (2010). Photoadaptation in *Neurospora* by competitive interaction of activating and inhibitory LOV domains. Cell 142, 762–772.

Marente, J., Ortega, P., Pardo-Medina, J., Avalos, J., and Limón, M.C. (2020). Modulation of Activity of a Carotenoid Pathway Through the Use of the TeT-on Regulatory System: Application in the Fungus *Fusarium fujikuroi*. In Plant and Food Carotenoids, M. Rodríguez-Concepción, and R. Welsch, eds. (New York, NY: Springer US), pp. 343–360.

Marente, J., Avalos, J., and Limón, M.C. (2021). Controlled Transcription of Regulator Gene *carS* by Tet-on or by a Strong Promoter Confirms Its Role as a Repressor of Carotenoid Biosynthesis in *Fusarium fujikuroi*. Microorganisms 9, 71.

Mattick, J.S., and Makunin, I. V. (2006). Non-coding RNA. Hum. Mol. Genet. 15 Spec No, R17–R29.

Mehta, B.J., Obraztsova, I.N., and Cerdá-Olmedo, E. (2003). Mutants and Intersexual Heterokaryons of *Blakeslea trispora* for Production of β-Carotene and Lycopene. Appl. Environ. Microbiol. 69, 4043–4048.

Meléndez-Martínez, A.J., Britton, G., Vicario, I.M., and Heredia, F.J. (2007). Relationship between the colour and the chemical structure of carotenoid pigments. Food Chem. 101, 1145–1150.

Mende, K., Homann, V., and Tudzynski, B. (1997). The geranylgeranyl diphosphate synthase gene of *Gibberella fujikuroi*: isolation and expression. Mol. Gen. Genet. MGG 255, 96–105.

Meng, H., Wang, Z., Wang, Y., Zhu, H., and Huang, B. (2017). Dicer and Argonaute Genes Involved in RNA Interference in the Entomopathogenic Fungus *Metarhizium robertsii*. Appl. Environ. Microbiol. 83, e03230-16, e03230-16.

Mercer, T.R., and Mattick, J.S. (2013). Structure and function of long noncoding RNAs in epigenetic regulation. Nat. Struct. Mol. Biol. 20, 300–307.

Merhej, J., Urban, M., Dufresne, M., Hammond-Kosack, K.E., Richard-Forget, F., and Barreau, C. (2012). The velvet gene, *FgVe1*, affects fungal development and positively regulates trichothecene biosynthesis and pathogenicity in *Fusarium graminearum*. Mol. Plant Pathol. 13, 363–374.

Metzker, M.L. (2010). Sequencing technologies — the next generation. Nat. Rev. Genet. 11, 31–46.

Michán, S., Lledías, F., and Hansberg, W. (2003). Asexual development is increased in *Neurospora crassa* cat-3-null mutant strains. Eukaryot. Cell 2, 798–808.

Michielse, C.B., Studt, L., Janevska, S., Sieber, C.M.K., Arndt, B., Espino, J.J., Humpf, H.-U., Güldener, U., and Tudzynski, B. (2015). The global regulator FfSge1 is required for expression of secondary metabolite gene clusters but not for pathogenicity in *Fusarium fujikuroi*: FfSge1, a regulator of secondary metabolism. Environ. Microbiol. 17, 2690–2708.

Milo-Cochavi, S., Adar, S., and Covo, S. (2019). Developmentally Regulated Oscillations in the Expression of UV Repair Genes in a Soilborne Plant Pathogen Dictate UV Repair Efficiency and Survival. MBio 10.

Moliné, M., Flores, M.R., Libkind, D., Diéguez, M. del C., Farías, M.E., and van Broock, M. (2010). Photoprotection by carotenoid pigments in the yeast *Rhodotorula mucilaginosa*: the role of torularhodin. Photochem. Photobiol. Sci. Off. J. Eur. Photochem. Assoc. Eur. Soc. Photobiol. 9, 1145–1151.

Moran, N.A., and Jarvik, T. (2010). Lateral transfer of genes from fungi underlies carotenoid production in aphids. Science 328, 624–627.

Morelli, G., Nelson, M.A., Ballario, P., and Macino, G. (1993). Photoregulated carotenoid biosynthetic genes of *Neurospora crassa*. In Methods in Enzymology, (Academic Press), pp. 412–424.

Morris, S.A.C., and Subden, R.E. (1974). Effects of ultraviolet radiation on carotenoid containing and albino strains of *Neurospora crassa*. Mutat. Res. Mol. Mech. Mutagen. 22, 105–109.

Moss, M.O., and Smith, J.E. (1982). The Applied mycology of *Fusarium* (Cambridge: Cambridge University Press).

Murcia-Flores, L., Lorca-Pascual, J.M., Garre, V., Torres-Martínez, S., and Ruiz-Vázquez, R.M. (2007). Non-AUG translation initiation of a fungal RING finger repressor involved in photocarotenogenesis. J. Biol. Chem. 282, 15394–15403.

Nadal-Ribelles, M., Solé, C., Xu, Z., Steinmetz, L.M., de Nadal, E., and Posas, F. (2014). Control of Cdc28 CDK1 by a Stress-Induced lncRNA. Mol. Cell 53, 549–561.

Nagalakshmi, U., Wang, Z., Waern, K., Shou, C., Raha, D., Gerstein, M., and Snyder, M. (2008). The transcriptional landscape of the yeast genome defined by RNA sequencing. Science 320, 1344–1349.

Navarro, E., Sandmann, G., and Torres-Martínez, S. (1995). Mutants of the Carotenoid Biosynthetic Pathway of *Mucor circinelloides*. Exp. Mycol. 19, 186–190.

Navarro, E., Ruiz-Pérez, V.L., and Torres-Martínez, S. (2000). Overexpression of the *crgA* gene abolishes light requirement for carotenoid biosynthesis in *Mucor circinelloides*. Eur. J. Biochem. 267, 800–807.

Navarro, E., Lorca-Pascual, J., Quiles-Rosillo, M., Nicolás, F., Garre, V., Torres-Martínez, S., and Ruiz-Vázquez, R. (2001). A negative regulator of light-inducible carotenogenesis in *Mucor circinelloides*. Mol. Genet. Genomics 266, 463–470.

Navarro, E., Niemann, N., Kock, D., Dadaeva, T., Gutiérrez, G., Engelsdorf, T., Kiontke, S., Corrochano, L.M., Batschauer, A., and Garre, V. (2020). The DASH-type Cryptochrome from the Fungus *Mucor circinelloides* Is a Canonical CPD-Photolyase. Curr. Biol. S0960982220312410.

Nelson, P.E., Toussoun, T.A., and Marasas, W.F.O. (1983). *Fusarium* species: an illustrated manual for identification (University Park: Pennsylvania State University Press).

Nicolas, F.E., Moxon, S., de Haro, J.P., Calo, S., Grigoriev, I.V., Torres-Martínez, S., Moulton, V., Ruiz-Vázquez, R.M., and Dalmay, T. (2010). Endogenous short RNAs generated by Dicer 2 and RNA-dependent RNA polymerase 1 regulate mRNAs in the basal fungus *Mucor circinelloides*. Nucleic Acids Res. 38, 5535–5541.

Nicolás, F.E., Murcia, L., Navarro, E., Cánovas-Márquez, J.T., and Garre, V. (2020). Small RNAs in Fungi. In Genetics and Biotechnology, J.P. Benz, and K. Schipper, eds. (Cham: Springer International Publishing), pp. 105–122.

Niederer, R.O., Hass, E.P., and Zappulla, D.C. (2017). Long Noncoding RNAs in the Yeast *S. cerevisiae*. In Advances in Experimental Medicine and Biology, pp. 119–132.

Niehaus, E.-M., Münsterkötter, M., Proctor, R.H., Brown, D.W., Sharon, A., Idan, Y., Oren-Young, L., Sieber, C.M., Novák, O., Pěnčík, A., et al. (2016). Comparative "Omics" of the *Fusarium fujikuroi* Species Complex Highlights Differences in Genetic Potential and Metabolite Synthesis. Genome Biol. Evol. 8, 3574–3599.

Niehaus, E.-M., Kim, H.-K., Münsterkötter, M., Janevska, S., Arndt, B., Kalinina, S.A., Houterman, P.M., Ahn, I.-P., Alberti, I., Tonti, S., et al. (2017). Comparative genomics of geographically distant *Fusarium fujikuroi* isolates revealed two distinct pathotypes correlating with secondary metabolite profiles. PLOS Pathog. 13, e1006670.

Niehaus, E.-M., Rindermann, L., Janevska, S., Münsterkötter, M., Güldener, U., and Tudzynski, B. (2018). Analysis of the global regulator Lae1 uncovers a connection between Lae1 and the histone acetyltransferase HAT1 in *Fusarium fujikuroi*. Appl. Microbiol. Biotechnol. 102, 279–295.

Oakley, B.R. (2017). *Aspergillus nidulans*. In Reference Module in Life Sciences, (Elsevier), p.

O'Donnell, K., Cigelnik, E., and Nirenberg, H.I. (1998). Molecular Systematics and Phylogeography of the *Gibberella fujikuroi* Species Complex. Mycologia 90, 465.

Oiartzabal-Arano, E., Perez-de-Nanclares-Arregi, E., Espeso, E.A., and Etxebeste, O. (2016). Apical control of conidiation in *Aspergillus nidulans*. Curr. Genet. 62, 371–377.

Ojima, K., Breitenbach, J., Visser, H., Setoguchi, Y., Tabata, K., Hoshino, T., van den Berg, J., and Sandmann, G. (2006). Cloning of the astaxanthin synthase gene from *Xanthophyllomyces dendrorhous* (*Phaffia rhodozyma*) and its assignment as a beta-carotene 3-hydroxylase/4-ketolase. Mol. Genet. Genomics MGG 275, 148–158.

Olmedo, M., Ruger-Herreros, C., Luque, E.M., and Corrochano, L.M. (2010). A complex photoreceptor system mediates the regulation by light of the conidiation genes *con-10* and *con-6* in *Neurospora crassa*. Fungal Genet. Biol. 47, 352–363.

Ootaki, T., Lighty, A.C., Delbrück, M., and Hsu, W.J. (1973). Complementation between mutants of *Phycomyces* deficient with respect to carotenogenesis. Mol. Gen. Genet. MGG 121, 57–70.

Ou, S.H. (1985). Rice diseases (Kew, Surrey, UK: Commonwealth Mycological Institute).

Ozturk, N. (2017). Phylogenetic and Functional Classification of the Photolyase/Cryptochrome Family. Photochem. Photobiol. 93, 104–111.

Pang, K.C., Frith, M.C., and Mattick, J.S. (2006). Rapid evolution of noncoding RNAs: Lack of conservation does not mean lack of function. Trends Genet. 22, 1–5.

Pardo-Medina, J. (2014). Producción de ARN no codificante en la región intergénica anterior al gen *carS* en *Fusarium fujikuroi*. Trabajo de fin de máster en Genética molecular y Biotecnología. Universidad de Sevilla.

Pardo-Medina, J., Gutiérrez, G., Limón, M.C., and Avalos, J. (2021). Impact of the White Collar Photoreceptor WcoA on the *Fusarium fujikuroi* Transcriptome. Front. Microbiol. 11, 619474.

Parra-Rivero, O. (2018). Nuevos mecanismos moleculares de regulación de la carotenogénesis en *Fusarium oxysporum*. University of Seville.

Parra-Rivero, O., Paes de Barros, M., Prado, M. del M., Gil, J.-V., Hornero-Méndez, D., Zacarías, L., Rodrigo, M.J., Limón, M.C., and Avalos, J. (2020a). Neurosporaxanthin Overproduction by *Fusarium fujikuroi* and Evaluation of Its Antioxidant Properties. Antioxidants 9, 528.

Parra-Rivero, O., Pardo-Medina, J., Gutiérrez, G., Limón, M.C., and Avalos, J. (2020b). A novel lncRNA as a positive regulator of carotenoid biosynthesis in *Fusarium*. Sci. Rep. 10, 678.

Perkins, D.D., and Davis, R.H. (2000). *Neurospora* at the Millennium. Fungal Genet. Biol. 31, 153–167.

Pfaffl, M.W. (2001). A new mathematical model for relative quantification in real-time RT-PCR. Nucleic Acids Res. 29, e45.

Pfeifer, A., Majerus, T., Zikihara, K., Matsuoka, D., Tokutomi, S., Heberle, J., and Kottke, T. (2009). Time-resolved Fourier transform infrared study on photoadduct formation and secondary structural changes within the phototropin LOV domain. Biophys. J. 96, 1462–1470.

Pickford, A.S., and Cogoni, C. (2003). RNA-mediated gene silencing. Cell. Mol. Life Sci. CMLS 60, 871–882.

Polaino, S., Herrador, M.M., Cerdá-Olmedo, E., and Barrero, A.F. (2010). Splitting of beta-carotene in the sexual interaction of *Phycomyces*. Org. Biomol. Chem. 8, 4229–4231.

Ponting, C.P., Oliver, P.L., and Reik, W. (2009). Evolution and Functions of Long Noncoding RNAs. Cell 136, 629–641.

Porter, J.W., and Lincoln, R.E. (1950). Lycopersicon selections containing a high content of carotenes and colorless polyenes; the mechanism of carotene biosynthesis. Arch. Biochem. 27, 390–403.

Prado, M.M., Prado-Cabrero, A., Fernández-Martín, R., and Avalos, J. (2004). A gene of the opsin family in the carotenoid gene cluster of *Fusarium fujikuroi*. Curr. Genet. 46, 47–58.

Prado-Cabrero, A., Scherzinger, D., Avalos, J., and Al-Babili, S. (2007a). Retinal biosynthesis in fungi: Characterization of the carotenoid oxygenase CarX from *Fusarium fujikuroi*. Eukaryot. Cell 6, 650–657.

Prado-Cabrero, A., Estrada, A.F., Al-Babili, S., and Avalos, J. (2007b). Identification and biochemical characterization of a novel carotenoid oxygenase: Elucidation of the cleavage step in the *Fusarium* carotenoid pathway. Mol. Microbiol. 64, 448–460.

Prado-Cabrero, A., Schaub, P., Díaz-Sánchez, V., Estrada, A.F., Al-Babili, S., and Avalos, J. (2009). Deviation of the neurosporaxanthin pathway towards β-carotene biosynthesis in *Fusarium fujikuroi* by a point mutation in the phytoene desaturase gene. FEBS J. 276, 4582–4597.

Priebe, S., Kreisel, C., Horn, F., Guthke, R., and Linde, J. (2015). FungiFun2: a comprehensive online resource for systematic analysis of gene lists from fungal species. Bioinformatics 31, 445–446.

Proctor, R.H., McCormick, S.P., Alexander, N.J., and Desjardins, A.E. (2009). Evidence that a secondary metabolic biosynthetic gene cluster has grown by gene relocation during evolution of the filamentous fungus *Fusarium*. Mol. Microbiol. 74, 1128–1142.

Purschwitz, J., Müller, S., Kastner, C., Schöser, M., Haas, H., Espeso, E.A., Atoui, A., Calvo, A.M., and Fischer, R. (2008). Functional and physical interaction of blue- and red-light sensors in *Aspergillus nidulans*. Curr. Biol. CB 18, 255–259.

Qi, Y., Sun, X., Ma, L., Wen, Q., Qiu, L., and Shen, J. (2020). Identification of two *Pleurotus ostreatus* blue light receptor genes (PoWC-1 and PoWC-2) and in vivo confirmation of complex PoWC-12 formation through yeast two hybrid system. Fungal Biol. 124, 8–14.

Quan, M., Chen, J., and Zhang, D. (2015). Exploring the Secrets of Long Noncoding RNAs. Int. J. Mol. Sci. 16, 5467–5496.

Quarantin, A., Hadeler, B., Kröger, C., Schäfer, W., Favaron, F., Sella, L., and Martínez-Rocha, A.L. (2019). Different Hydrophobins of *Fusarium graminearum* Are Involved in Hyphal Growth, Attachment, Water-Air Interface Penetration and Plant Infection. Front. Microbiol. 10, 751.

Quiles-Rosillo, M.D., Torres-Martínez, S., and Garre, V. (2003). *cigA*, a light-inducible gene involved in vegetative growth in *Mucor circinelloides* is regulated by the carotenogenic repressor *crgA*. Fungal Genet. Biol. FG B 38, 122–132.

Quiles-Rosillo, M.D., Ruiz-Vázquez, R.M., Torres-Martínez, S., and Garre, V. (2005). Light induction of the carotenoid biosynthesis pathway in *Blakeslea trispora*. Fungal Genet. Biol. FG B 42, 141–153.

Rao, a. V., and Rao, L.G. (2007). Carotenoids and human health. Pharmacol. Res. 55, 207–216.

Rau, W. (1967). Untersuchungen über die lichtabhängige Carotinoidsynthese: II. Ersatz der Lichtinduktion durch Mercuribenzoat. Planta 74, 263–277.

Rau, W. (1971). Untersuchungen über die lichtabhängige Carotinoidsynthese. Planta 101, 251–264.

Rau, W., Feuser, B., and Rau-Hund, A. (1967). Substitution of p-chloro- or p-hydroxymercuribenzoate for light in carotenoid synthesis by *Fusarium aquaeductuum*. Biochim. Biophys. Acta 136, 589–590.

Rensing, S.A., Sheerin, D.J., and Hiltbrunner, A. (2016). Phytochromes: More Than Meets the Eye. Trends Plant Sci. 21, 543–546.

Rinn, J.L., Kertesz, M., Wang, J.K., Squazzo, S.L., Xu, X., Brugmann, S.A., Goodnough, L.H., Helms, J.A., Farnham, P.J., Segal, E., et al. (2007). Functional Demarcation of Active and Silent Chromatin Domains in Human *HOX* Loci by Noncoding RNAs. Cell 129, 1311–1323.

Roberts, A., Pimentel, H., Trapnell, C., and Pachter, L. (2011). Identification of novel transcripts in annotated genomes using RNA-Seq. Bioinformatics 27, 2325–2329.

Robinson, J.T., Thorvaldsdóttir, H., Winckler, W., Guttman, M., Lander, E.S., Getz, G., and Mesirov, J.P. (2011). Integrative genomics viewer. Nat. Biotechnol. 29, 24–26.

Rodríguez-Ortiz, R. (2012). Análisis genético y molecular del fenotipo *carS* en *Fusarium*. University of Seville.

Rodríguez-Ortiz, R., Limón, M.C., and Avalos, J. (2009). Regulation of carotenogenesis and secondary metabolism by nitrogen in wild-type *Fusarium fujikuroi* and carotenoid-overproducing mutants. Appl. Environ. Microbiol. 75, 405–413.

Rodríguez-Ortiz, R., Michielse, C., Rep, M., Limón, M.C., and Avalos, J. (2012). Genetic basis of carotenoid overproduction in *Fusarium oxysporum*. Fungal Genet. Biol. FG B 49, 684–696.

Rodríguez-Ortiz, R., Limón, M.C., and Avalos, J. (2013). Functional analysis of the *carS* gene of *Fusarium fujikuroi*. Mol. Genet. Genomics 288, 157–173.

Rodriguez-Romero, J., Hedtke, M., Kastner, C., Müller, S., and Fischer, R. (2010). Fungi, hidden in soil or up in the air: light makes a difference. Annu. Rev. Microbiol. 64, 585–610.

Röhrig, J., Kastner, C., and Fischer, R. (2013). Light inhibits spore germination through phytochrome in *Aspergillus nidulans*. Curr. Genet. 59, 55–62.

Roncero, M.I., and Cerdá-Olmedo, E. (1982). Genetics of carotene biosynthesis in *Phycomyces*. Curr. Genet. 5, 5–8.

Ruesch, C.E., Ramakrishnan, M., Park, J., Li, N., Chong, H.S., Zaman, R., Joska, T.M., and Belden, W.J. (2014). The histone H3 lysine 9 methyltransferase DIM-5 modifies chromatin at frequency and represses light-activated gene expression. G3 5, 93–101.

Ruger-Herreros, M. (2016). Participación de la proteína CarS en la regulación de la carotenogénesis y el estrés en *Fusarium fujikuroi*. University of Seville.

Ruger-Herreros, C., Rodríguez-Romero, J., Fernández-Barranco, R., Olmedo, M., Fischer, R., Corrochano, L.M., and Canovas, D. (2011). Regulation of Conidiation by Light in *Aspergillus nidulans*. Genetics 188, 809–822.

Ruger-Herreros, C., Gil-Sánchez, M. del M., Sancar, G., Brunner, M., and Corrochano, L.M. (2014). Alteration of light-dependent gene regulation by the absence of the RCO-1/RCM-1 repressor complex in the fungus *Neurospora crassa*. PloS One 9, e95069.

Ruger-Herreros, M., Parra-Rivero, O., Pardo-Medina, J., Romero-Campero, F.J., Limón, M.C., and Avalos, J. (2019). Comparative transcriptomic analysis unveils interactions between the regulatory CarS protein and light response in *Fusarium*. BMC Genomics 20, 67.

Ruiz-Roldán, M.C., Garre, V., Guarro, J., Mariné, M., and Roncero, M.I.G. (2008). Role of the White Collar 1 Photoreceptor in Carotenogenesis, UV Resistance, Hydrophobicity, and Virulence of *Fusarium oxysporum*. Eukaryot. Cell 7, 1227–1230.

Saelices, L., Youssar, L., Holdermann, I., Al-Babili, S., and Avalos, J. (2007). Identification of the gene responsible for torulene cleavage in the *Neurospora* carotenoid pathway. Mol. Genet. Genomics MGG 278, 527–537.

Sakaki, H., Kaneno, H., Sumiya, Y., Tsushima, M., Miki, W., Kishimoto, N., Fujita, T., Matsumoto, S., Komemushi, S., and Sawabe, A. (2002). A new carotenoid glycosyl ester isolated from a marine microorganism, *Fusarium* strain T-1. J. Nat. Prod. 65, 1683–1684.

Saldanha, A.J. (2004). Java Treeview--extensible visualization of microarray data. Bioinforma. Oxf. Engl. 20, 3246–3248.

Sambrook, J., and Russell, D.W. (2001). Molecular cloning: a laboratory manual (Cold Spring Harbor Laboratory Press).

Sancar, A. (2004). Photolyase and cryptochrome blue-light photoreceptors. Adv. Protein Chem. 69, 73–100.

Sancar, C., Ha, N., Yilmaz, R., Tesorero, R., Fisher, T., Brunner, M., and Sancar, G. (2015). Combinatorial Control of Light Induced Chromatin Remodeling and Gene Activation in *Neurospora*. PLOS Genet. 11, e1005105.

Sandmann, G. (1993). Photoregulation of Carotenoid Biosynthesis in Mutants of *Neurospora crassa*: Activities of Enzymes Involved in the Synthesis and Conversion of Phytoene. Z. Für Naturforschung C 48, 570–574.

Sandmann, G. (2019). Antioxidant Protection from UV- and Light-Stress Related to Carotenoid Structures. Antioxid. Basel Switz. 8.

Sandmann, G., and Misawa, N. (2002). Fungal Carotenoids. In The Mycota X. Industrial Applications, (Springer Verlag), pp. 247–262.

Sanz, C., Rodríguez-Romero, J., Idnurm, A., Christie, J.M., Heitman, J., Corrochano, L.M., and Eslava, A.P. (2009). *Phycomyces* MADB interacts with MADA to form the primary photoreceptor complex for fungal phototropism. Proc. Natl. Acad. Sci. U. S. A. 106, 7095–7100.

Schafmeier, T., and Diernfellner, A.C.R. (2011). Light input and processing in the circadian clock of *Neurospora*. FEBS Lett. 585, 1467–1473.

Schafmeier, T., Haase, A., Káldi, K., Scholz, J., Fuchs, M., and Brunner, M. (2005). Transcriptional feedback of *Neurospora* circadian clock gene by phosphorylation-dependent inactivation of its transcription factor. Cell 122, 235–246.

Schmidhauser, T.J., Lauter, F.R., Russo, V.E., and Yanofsky, C. (1990). Cloning, sequence, and photoregulation of *al-1*, a carotenoid biosynthetic gene of *Neurospora crassa*. Mol. Cell. Biol. 10, 5064–5070.

Schmidhauser, T.J., Lauter, F.R., Schumacher, M., Zhou, W., Russo, V.E., and Yanofsky, C. (1994). Characterization of *al-2*, the phytoene synthase gene of *Neurospora crassa*. Cloning, sequence analysis, and photoregulation. J. Biol. Chem. 269, 12060–12066.

Schmoll, M. (2011). Assessing the Relevance of Light for Fungi. In Advances in Applied Microbiology, (Elsevier), pp. 27–78.

Schmoll, M. (2018). Light, stress, sex and carbon – The photoreceptor ENVOY as a central checkpoint in the physiology of *Trichoderma reesei*. Fungal Biol. 122, 479–486.

Schmoll, M., Zeilinger, S., Mach, R.L., and Kubicek, C.P. (2004). Cloning of genes expressed early during cellulase induction in *Hypocrea jecorina* by a rapid subtraction hybridization approach. Fungal Genet. Biol. FG B 41, 877–887.

Schmoll, M., Franchi, L., and Kubicek, C.P. (2005). Envoy, a PAS/LOV domain protein of *Hypocrea jecorina* (Anamorph *Trichoderma reesei*), modulates cellulase gene transcription in response to light. Eukaryot. Cell 4, 1998–2007.

Schroeder, A., Mueller, O., Stocker, S., Salowsky, R., Leiber, M., Gassmann, M., Lightfoot, S., Menzel, W., Granzow, M., and Ragg, T. (2006). The RIN: an RNA integrity number for assigning integrity values to RNA measurements. BMC Mol. Biol. 7, 3.

Schumacher, J. (2017). How light affects the life of *Botrytis*. Fungal Genet. Biol. 106, 26–41.

Schumacher, J., and Gorbushina, A.A. (2020). Light sensing in plant- and rock-associated black fungi. Fungal Biol. 124, 407–417.

Schwerdtfeger, C., and Linden, H. (2000). Localization and light-dependent phosphorylation of white collar 1 and 2, the two central components of blue light signaling in *Neurospora crassa*. Eur. J. Biochem. 267, 414–422.

Schwerdtfeger, C., and Linden, H. (2001). Blue light adaptation and desensitization of light signal transduction in *Neurospora crassa*. Mol. Microbiol. 39, 1080–1087.

Schwerdtfeger, C., and Linden, H. (2003). VIVID is a flavoprotein and serves as a fungal blue light photoreceptor for photoadaptation. EMBO J. 22, 4846–4855.

Shearwin, K.E., Callen, B.P., and Egan, J.B. (2005). Transcriptional interference-a crash course. Trends Genet 21, 339–345.

Shiu, P.K.T., and Metzenberg, R.L. (2002). Meiotic silencing by unpaired DNA: Properties, regulation and suppression. Genetics 161, 1483–1495.

Silva, F., Torres-Martínez, S., and Garre, V. (2006). Distinct white collar-1 genes control specific light responses in *Mucor circinelloides*. Mol. Microbiol. 61, 1023–1037.

Silva, F., Navarro, E., Peñaranda, A., Murcia-Flores, L., Torres-Martínez, S., and Garre, V. (2008). A RING-finger protein regulates carotenogenesis via proteolysis-independent ubiquitylation of a White Collar-1-like activator. Mol. Microbiol. 70, 1026–1036.

Smith, K.M., Sancar, G., Dekhang, R., Sullivan, C.M., Li, S., Tag, A.G., Sancar, C., Bredeweg, E.L., Priest, H.D., McCormick, R.F., et al. (2010). Transcription Factors in Light and Circadian Clock Signaling Networks Revealed by Genomewide Mapping of Direct Targets for *Neurospora* White Collar Complex. Eukaryot. Cell 9, 1549–1556.

Smith, K.N., Miller, S.C., Varani, G., Calabrese, J.M., and Magnuson, T. (2019). Multimodal long noncoding RNA interaction networks: Control panels for cell fate specification. Genetics 213, 1093–1110.

Sokolovsky, V.Y., Lauter, F.-R., Müller-röber, B., Ricci, M., Schmidhauser, T.J., and Russo, V.E.A. (1992). Nitrogen regulation of blue light-inducible genes in *Neurospora crassa*. Microbiology, 138, 2045–2049.

Son, H., Min, K., Lee, J., Raju, N.B., and Lee, Y.W. (2011). Meiotic silencing in the homothallic fungus *Gibberella zeae*. Fungal Biol. 115, 1290–1302.

Son, H., Park, A.R., Lim, J.Y., Shin, C., and Lee, Y.-W. (2017). Genome-wide exonic small interference RNA-mediated gene silencing regulates sexual reproduction in the homothallic fungus *Fusarium graminearum*. PLOS Genet. 13, e1006595.

Spadaro, D. (2017). The puzzle of bakanae disease through interactions between *Fusarium fujikuroi* and rice. Front. Biosci. 9, 333–344.

Stahl, W., and Sies, H. (2002). Carotenoids and protection against solar UV radiation. Skin Pharmacol. Appl. Skin Physiol. 15, 291–296.

Steenkamp, E.T., Wingfield, B.D., Coutinho, T.A., Zeller, K.A., Wingfield, M.J., Marasas, W.F.O., and Leslie, J.F. (2000). PCR-Based Identification of MAT-1 and MAT-2 in the *Gibberella fujikuroi* Species Complex. Appl. Environ. Microbiol. 66, 4378–4382.

Stephen, D., Jones, C., and Schofield, J.P. (1990). A rapid method for isolating high quality plasmid DNA suitable for DNA sequencing. Nucleic Acids Res. 18, 7463–7464.

Sui, X., Kiser, P.D., Lintig, J. von, and Palczewski, K. (2013). Structural basis of carotenoid cleavage: from bacteria to mammals. Arch. Biochem. Biophys. 539, 203–213.

Sullivan, S., Takemiya, A., Kharshiing, E., Cloix, C., Shimazaki, K., and Christie, J.M. (2016). Functional characterization of *Arabidopsis* phototropin 1 in the hypocotyl apex. Plant J. 88, 907–920.

Summerell, B.A. (2019). Resolving *Fusarium*: Current Status of the Genus. Annu. Rev. Phytopathol. 57, 323–339.

Sun, T., Yuan, H., Cao, H., Yazdani, M., Tadmor, Y., and Li, L. (2018). Carotenoid Metabolism in Plants: The Role of Plastids. Mol. Plant 11, 58–74.

Sun, X., Yu, L., Lan, N., Wei, S., Yu, Y., Zhang, H., Zhang, X., and Li, S. (2012). Analysis of the role of transcription factor VAD-5 in conidiation of *Neurospora crassa*. Fungal Genet. Biol. 49, 379–387.

Supek, F., Bošnjak, M., Škunca, N., and Šmuc, T. (2011). REVIGO Summarizes and Visualizes Long Lists of Gene Ontology Terms. PLOS ONE 6, e21800.

Sutter, R.P. (1975). Mutations affecting sexual development in *Phycomyces blakesleeanus*. Proc. Natl. Acad. Sci. U. S. A. 72, 127–130.

Tagua, V.G., Pausch, M., Eckel, M., Gutiérrez, G., Miralles-Durán, A., Sanz, C., Eslava, A.P., Pokorny, R., Corrochano, L.M., and Batschauer, A. (2015). Fungal cryptochrome with DNA repair activity reveals an early stage in cryptochrome evolution. Proc. Natl. Acad. Sci. U. S. A. 112, 15130–15135.

Tagua, V.G., Navarro, E., Gutiérrez, G., Garre, V., and Corrochano, L.M. (2020). Light regulates a *Phycomyces blakesleeanus* gene family similar to the carotenogenic repressor gene of *Mucor circinelloides*. Fungal Biol. 124, 338–351.

Tang, Y., Zhu, P., Lu, Z., Qu, Y., Huang, L., Zheng, N., Wang, Y., Nie, H., Jiang, Y., and Xu, L. (2020). The Photoreceptor Components FaWC1 and FaWC2 of *Fusarium asiaticum* Cooperatively Regulate Light Responses but Play Independent Roles in Virulence Expression. Microorganisms 8, 365.

Taylor, B.L., and Zhulin, I.B. (1999). PAS Domains: Internal Sensors of Oxygen, Redox Potential, and Light. Microbiol. Mol. Biol. Rev. 63, 479–506.

Theimer, R.R., and Rau, W. (1972). Untersuchungen über die lichtabhängige Carotinoidsynthese. Planta 106, 331–343.

Thewes, S., Prado-Cabrero, A., Prado, M.M., Tudzynski, B., and Avalos, J. (2005). Characterization of a gene in the car cluster of *Fusarium fujikuroi* that codes for a protein of the carotenoid oxygenase family. Mol. Genet. Genomics 274, 217–228.

Till, P., Mach, R.L., and Mach-Aigner, A.R. (2018a). A current view on long noncoding RNAs in yeast and filamentous fungi. Appl. Microbiol. Biotechnol. 102, 7319–7331.

Till, P., Pucher, M.E., Mach, R.L., and Mach-Aigner, A.R. (2018b). A long noncoding RNA promotes cellulase expression in *Trichoderma reesei*. Biotechnol. Biofuels 11, 78.

Till, P., Derntl, C., Kiesenhofer, D.P., Mach, R.L., Yaver, D., and Mach-Aigner, A.R. (2020). Regulation of gene expression by the action of a fungal lncRNA on a transactivator. RNA Biol. 17, 47–61.

Tisch, D., and Schmoll, M. (2010). Light regulation of metabolic pathways in fungi. Appl. Microbiol. Biotechnol. 85, 1259–1277.

Tisch, D., and Schmoll, M. (2013). Targets of light signalling in *Trichoderma reesei*. BMC Genomics 14, 657.

Tokai, T., Fujimura, M., Inoue, H., Aoki, T., Ohta, K., Shibata, T., Yamaguchi, I., and Kimura, M. (2005). Concordant evolution of trichothecene 3-O-acetyltransferase and an rDNA species phylogeny of trichothecene-producing and non-producing fusaria and other ascomycetous fungi. Microbiology 151, 509–519.

Torres-Martínez, S., and Ruiz-Vázquez, R.M. (2016). RNAi pathways in *Mucor*: A tale of proteins, small RNAs and functional diversity. Fungal Genet. Biol. 9.

Torres-Martínez, S., and Ruiz-Vázquez, R.M. (2017). The RNAi Universe in Fungi: A Varied Landscape of Small RNAs and Biological Functions. Annu. Rev. Microbiol. 71, 371–391.

Torres-Martínez, S., Murillo, F.J., and Cerdá-Olmedo, E. (1980). Genetics of lycopene cyclization and substrate transfer in beta-carotene biosynthesis in *Phycomyces*. Genet. Res. 36, 299–309.

Trail, F., Xu, H., Loranger, R., and Gadoury, D. (2002). Physiological and environmental aspects of ascospore discharge in *Gibberella zeae* (anamorph *Fusarium graminearum*). Mycologia 94, 181–189.

Trapnell, C., Pachter, L., and Salzberg, S.L. (2009). TopHat: discovering splice junctions with RNA-Seq. Bioinformatics 25, 1105–1111.

Trapnell, C., Roberts, A., Goff, L., Pertea, G., Kim, D., Kelley, D.R., Pimentel, H., Salzberg, S.L., Rinn, J.L., and Pachter, L. (2012). Differential gene and transcript expression analysis of RNA-seq experiments with TopHat and Cufflinks. Nat. Protoc. 7, 562–578.

Treiber, T., Treiber, N., and Meister, G. (2019). Regulation of microRNA biogenesis and its crosstalk with other cellular pathways. Nat. Rev. Mol. Cell Biol. 20, 5–20.

Trieu, T.A., Navarro-Mendoza, M.I., Pérez-Arques, C., Sanchis, M., Capilla, J., Navarro-Rodriguez, P., Lopez-Fernandez, L., Torres-Martínez, S., Garre, V., Ruiz-Vázquez, R.M., et al. (2017). RNAi-Based Functional Genomics Identifies New Virulence Determinants in Mucormycosis. PLOS Pathog. 13, e1006150.

Tschanz, A.T., Horst, R.K., and Nelson, P.E. (1976). The Effect of Environment on Sexual Reproduction of *Gibberella zeae*. Mycologia 68, 327.

Tudzynski, B. (2005). Gibberellin biosynthesis in fungi: Genes, enzymes, evolution, and impact on biotechnology. Appl. Microbiol. Biotechnol. 66, 597–611.

Tudzynski, B. (2014). Nitrogen regulation of fungal secondary metabolism in fungi. Front. Microbiol. 5.

Tudzynski, B., Studt, L., and Rojas, M.C. (2016). Gibberellins in fungi, bacteria and lower plants: biosynthesis, function and evolution. In Annual Plant Reviews, Volume 49, P. Hedden, and S.G. Thomas, eds. (Chichester, UK: John Wiley & Sons, Ltd), pp. 121–152.

Veluchamy, S., and Rollins, J.A. (2008). A CRY-DASH-type photolyase/cryptochrome from *Sclerotinia sclerotiorum* mediates minor UV-A-specific effects on development. Fungal Genet. Biol. 45, 1265–1276.

Verdoes, J.C., Krubasik, K.P., Sandmann, G., and van Ooyen, A.J. (1999a). Isolation and functional characterisation of a novel type of carotenoid biosynthetic gene from *Xanthophyllomyces dendrorhous*. Mol. Gen. Genet. MGG 262, 453–461.

Verdoes, J.C., Misawa, N., and van Ooyen, A.J. (1999b). Cloning and characterization of the astaxanthin biosynthetic gene encoding phytoene desaturase of *Xanthophyllomyces dendrorhous*. Biotechnol. Bioeng. 63, 750–755.

Villalobos-Escobedo, J.M., Herrera-Estrella, A., and Carreras-Villaseñor, N. (2016). The interaction of fungi with the environment orchestrated by RNAi. Mycologia 108, 556–571.

Wang, F., Song, X., Dong, X., Zhang, J., and Dong, C. (2017a). DASH-type cryptochromes regulate fruiting body development and secondary metabolism differently than CmWC-1 in the fungus *Cordyceps militaris*. Appl. Microbiol. Biotechnol. 101, 4645–4657.

Wang, M., Weiberg, A., Dellota, E., Yamane, D., and Jin, H. (2017b). *Botrytis* small RNA *Bc-siR37* suppresses plant defense genes by cross-kingdom RNAi. RNA Biol. 14, 421–428.

Wang, X., Hsueh, Y.P., Li, W., Floyd, A., Skalsky, R., and Heitman, J. (2010). Sex-induced silencing defends the genome of *Cryptococcus* neoformans via RNAi. Genes Dev. 24, 2566–2582.

Wang, Y., Shao, Y., Zhu, Y., Wang, K., Ma, B., Zhou, Q., Chen, A., and Chen, H. (2019a). XRN1 associated long non-coding RNAs may contribute to fungal virulence and sexual development in entomopathogenic fungus *Cordyceps militaris*. Pest Manag. Sci. 75, 3302–3311.

Wang, Z., Wang, J., Li, N., Li, J., Trail, F., Dunlap, J.C., and Townsend, J.P. (2018). Light sensing by opsins and fungal ecology: NOP-1 modulates entry into sexual reproduction in response to environmental cues. Mol. Ecol. 27, 216–232.

Wang, Z., Jiang, Y., Wu, H., Xie, X., and Huang, B. (2019b). Genome-Wide Identification and Functional Prediction of Long Non-coding RNAs Involved in the Heat Stress Response in *Metarhizium robertsii*. Front. Microbiol. 10, 2336.

Weinkove, D., Poyatos, J.A., Greiner, H., Oltra, E., Avalos, J., Fukshansky, L., Barrero, A.F., and Cerdá-Olmedo, E. (1998). Mutants of *Phycomyces* with decreased gallic acid content. Fungal Genet. Biol. FG B 25, 196–203.

Whitehead, R.D., Ozakinci, G., and Perrett, D.I. (2012). Attractive skin coloration: harnessing sexual selection to improve diet and health. Evol. Psychol. Int. J. Evol. Approaches Psychol. Behav. 10, 842–854.

Wiemann, P., Brown, D.W., Kleigrewe, K., Bok, J.W., Keller, N.P., Humpf, H.-U., and Tudzynski, B. (2010). FfVel1 and FfLae1, components of a velvet-like complex in *Fusarium fujikuroi*, affect differentiation, secondary metabolism and virulence: Identification of a velvet-like complex in *F. fujikuroi*. Mol. Microbiol. no-no.

Wiemann, P., Sieber, C.M.K., von Bargen, K.W., Studt, L., Niehaus, E.-M., Espino, J.J., Huß, K., Michielse, C.B., Albermann, S., Wagner, D., et al. (2013). Deciphering the Cryptic Genome: Genome-wide Analyses of the Rice Pathogen *Fusarium fujikuroi* Reveal Complex Regulation of Secondary Metabolism and Novel Metabolites. PLoS Pathog. 9, e1003475.

Woitek, S., Unkles, S.E., Kinghorn, J.R., and Tudzynski, B. (1997). 3-Hydroxy-3-methylglutaryl-CoA reductase gene of *Gibberella fujikuroi*: isolation and characterization. Curr. Genet. 31, 38–47.

Wu, C., Yang, F., Smith, K.M., Peterson, M., Dekhang, R., Zhang, Y., Zucker, J., Bredeweg, E.L., Mallappa, C., Zhou, X., et al. (2014). Genome-Wide Characterization of Light-Regulated Genes in *Neurospora crassa*. G3 4, 1731–1745.

Xue, Z., Ye, Q., Anson, S.R., Yang, J., Xiao, G., Kowbel, D., Glass, N.L., Crosthwaite, S.K., and Liu, Y. (2014). Transcriptional interference by antisense RNA is required for circadian clock function. Nature 514, 650–653.

Yamaguchi, S. (2008). Gibberellin metabolism and its regulation. Annu. Rev. Plant Biol. 59, 225–251.

Yamashita, A., Shichino, Y., and Yamamoto, M. (2016). The long non-coding RNA world in yeasts. Biochim. Biophys. Acta BBA - Gene Regul. Mech. 1859, 147–154.

Yang, Q., Li, L., Xue, Z., Ye, Q., Zhang, L., Li, S., and Liu, Y. (2013). Transcription of the major *Neurospora crassa* microRNA-like small RNAs relies on RNA polymerase III. PLoS Genet. 9, e1003227.

Yoshida, Y., and Hasunuma, K. (2004). Reactive oxygen species affect photomorphogenesis in *Neurospora crassa*. J. Biol. Chem. 279, 6986–6993.

Yu, Z., and Fischer, R. (2019). Light sensing and responses in fungi. Nat. Rev. Microbiol. 17, 25–36.

Yu, J., Lee, K.-M., Cho, W.K., Park, J.Y., and Kim, K.-H. (2018). Differential Contribution of RNA Interference Components in Response to Distinct *Fusarium graminearum* Virus Infections. J. Virol. 92, e01756-17.

Zheng, W., Zhao, X., Xie, Q., Huang, Q., Zhang, C., Zhai, H., Xu, L., Lu, G., Shim, W.-B., and Wang, Z. (2012). A Conserved Homeobox Transcription Factor Htf1 Is Required for Phialide Development and Conidiogenesis in *Fusarium* Species. PLoS ONE 7, e45432.

Zhou, J., Fu, Y., Xie, J., Li, B., Jiang, D., Li, G., and Cheng, J. (2012). Identification of microRNA-like RNAs in a plant pathogenic fungus *Sclerotinia sclerotiorum* by high-throughput sequencing. Mol. Genet. Genomics 287, 275–282.

Zhou, Q., Su, X., Wang, A., Xu, J., and Ning, K. (2013). QC-Chain: Fast and Holistic Quality Control Method for Next-Generation Sequencing Data. PLoS ONE 8, e60234.

Zhu, Q.H., Stephen, S., Taylor, J., Helliwell, C.A., and Wang, M.B. (2014). Long noncoding RNAs responsive to *Fusarium oxysporum* infection in Arabidopsis thaliana. New Phytol. 201, 574–584.

Zoltowski, B.D., and Crane, B.R. (2008). Light activation of the LOV protein vivid generates a rapidly exchanging dimer. Biochemistry 47, 7012–7019.

Annex

Table S1.1 De novo predicted miRNA-like RNAs in the merged sRNA dataset of *F. oxysporum*.

F. oxysporum		read count						
id	score	total	mature	loop	star	p-value	mature sequence	precursor sequence
11_43465	7.4e+3	14537	14536	0	1	no	ggugagauggccgaguugguuaug	ugugcuggucaagaacucuaauaaaaugcuuugucaucaagcaaaucggugagauggccgaguugguuaug
10_56582	1.5e+3	3114	3072	0	42	no	ugcgagaggucccggguuca	ugcgagaggucccggguucaaucccccggccagacccu
8_116257	1.4e+3	2862	2853	0	9	no	uccugaagguuaucgguuca	uccugaagguuaucgguucaaaauccggugugccucaaacuuuucuu
2_267694	2.7	2	1	0	1	yes	ugugccgccgggugcucgg	ugugccgccgggugcucggcggcaccccuagcacccggaccauaguaggcg
1_335695	2.6	3	1	0	2	yes	cugcugcuguccca gcucuggca	cugcugcugucccagcucuggcaguaacugcguaccagaguaucaagcguggacugcagcuucaa
10_56973	2.6	3	2	0	1	yes	gaguuacgcgcug uggggacu	uuugcacggcgcgggggauguuggagggcagauguguuguuuugucagcgagagaguuacgcgcuguggggacu
7_126340	2.6	3	1	0	2	yes	uacgucgugucuc caagcc	uacgucgugucuccaagccuugguuacucacuucauccugaagugccuugaucuugugccaagucuugaggcgccggccgacag
7_125213	2.6	3	2	0	1	yes	uuauguccaccgu ugucagaucg	guaggcggcgguggugggugauuuguaggauccaaaucaggucgcaguuggugaaccauccacgaauuauguccaccguugucagaucg
DS231743_8517	2.3	1783	1783	0	0	yes	uccuugggccuggc ugg	uccuugggccuggcugggacuuggccaggguucgagggac
9_82056	2.3	2	1	0	1	yes	uguuggccgccagg gcagggc	uuguaaaccuugaggcuggcgcauuuuccgucugagcagaggugggggaauauacuguuggccgccagggcagggc
2_237016	2.1	2	1	0	1	yes	ugccgagcuccucu guuuca	ugccgagcuccucuguuucauuccuugcgggagacucggcaca
15_52019	2.1	408	407	1	0	yes	uuuggcaucguua cuggggc	uuuggcaucguuacuggggcucucuguuugucggggguccuuucgucuucgauaauuaguguccuggcaguagcgggaagaacu
15_52731	2.1	408	407	1	0	yes	uuuggcaucguua cuggggc	uuuggcaucguuacuggggcucucuguuugucggggguccuucgucuucgauaauuaguguccuggcaguagcgggaagaacu
2_240888	2.0	641	641	0	0	yes	ugggcugggcugg gcugggcu	ugggcugggcugggcugggcuaccgcagccucagccaucagc
6_150126	2.0	65	62	3	0	yes	uuuggcaucguua cugggg	uuuggcaucguuacuggggucucuguugucggggguccuucaucuucgauguuuucug
8_102980	1.9	400	400	0	0	yes	ugggcugggcugg gcugggcu	ugggcugggcugggcugggcugcuucggcugcuuccaagucuuugguucaauggaguaaauuggauccggguccuuguccuug
1_317974	1.9	2	1	0	1	yes	ucaauguccca gccgacaca	cguuggugggcuuguugaacuugagguugagguucauucuggcaaugcgcuucaugucccuccucaucaaugucccagccgacaca
2_244571	1.8	4424	4424	0	0	yes	uuugacucguucg gcacc	agacggucgacucaggcaugcuguuugacucguucggcacc
3_272619	1.7	14	14	0	0	yes	aaaagcaacugug gggc	cccgcuauuagcgucuugcuagggucaagaauuuuugcaagccaaaauggcaggaaaagcaacugugggc
1_295196	1.7	580	580	0	0	yes	ugggcugggcugg gcugggcu	ugggcugggcugggcugggcuugauccauccauuggaucuacagggucccuuucuucccaggaggaugucucucgcccaccuccauc
DS231729_13742	1.7	14	14	0	0	yes	aaaagcaacugug gggc	cccgcuauuagcgucuugcuagggucaagaauuuuugcaagccaaaauggcaggaaaagcaacugugggc
6_161128	1.7	14	14	0	0	yes	aaaagcaacugug gggc	cccgcuauuagcgucuugcuagggucaagaauuuuugcaagccaaaauggcaggaaaagcaacugugggc
10_65887	1.7	368	368	0	0	yes	ucccuccgccucca cca	cuggaggggagcuaaaauaucgauucguucccucccgccuccacca
3_286906	1.7	14	14	0	0	yes	aaaagcaacugug gggc	cccgcuauuagcgucuugcuagggucaagaauuuuugcaagccaaaauggcaggaaaagcaacugugggc
8_94087	1.7	2	1	0	1	yes	uaacccagcuggag agccuu	uaacccagcuggagagccuuacuugcucuucagcuggccccaa

3_273233	1.5	13	13	0	0	yes	ucugagaccacugaagcccuu	gccgcaaguggcuuagagucuuaccuacacagaaaccccacucuuuuacagacucugagaccacugaagcccuu
6_160514	1.3	13	13	0	0	yes	ucugagaccacugaagcccuu	aggccgcaaguggcuuagagucuuaccuacacagaaaccccacucuuuuacagacucugagaccacugaagcccuu
3_286278	1.3	13	13	0	0	yes	ucugagaccacugaagcccuu	aggccgcaaguggcuuagagucuuaccuacacagaaaccccacucuuuuacagacucugagaccacugaagcccuu
15_55864	1.2	3	2	0	1	yes	ucgugggacucgauucgaa	uugaaucgguccucacucgauugggauuuccacauuucacaauucagucagacaucucaacucgugggacucgauucgaa
DS231725_16640	1.2	3	2	0	1	yes	ucgugggacucgauucgaa	uugaaucgguccucacucgauugggauuuccacauuucacaauucagucagacaucucaacucgugggacucgauucgaa
5_186818	0.8	9	5	0	4	yes	aagggcccuggacugucauc	aagggcccuggacugucaucucuugauaguccagggccuu
6_150301	0.8	3	2	0	1	yes	ucgugggacucgauucgaa	uugaaucgguccucacucgauugggauuuccacauuucacaauucagucagacaucucaacucgugggacucgauucgaa
9_72867	0.7	163877	163829	34	14	yes	ucauuuuugagaucuacauuc	uuggauccgucguuaaucucgacaccuaguuuuaccgucuaggugucguuucauuuuugagaucuacauuc

Table S1.2 Total differentially expressed genes included in the second chapter RNA-seq analysis, corresponding to the study of the effect of *dcl2* deletion (EdgeR stats p<0.05 after correction), including the differential fold change for each of the comparisons analyzed.

ID	Description	P-value	FDR	Log2 Fold Change
FFUJ_09878	uncharacterized protein	1.40E-45	2.44E-41	-5.2226424
FFUJ_09877	related to Dcl-2 dicer RNA helicase/RNAseIII CAF	3.71E-18	1.86E-14	4.562785
FFUJ_09875	related to exostosin-like 3	3.31E-20	2.50E-16	-3.048495
FFUJ_14373	uncharacterized protein	3.63E-07	0.00137163	-5.6086974
FFUJ_14259	probable GTP cyclohydrolase I	3.17E-06	0.00955772	-3.6413677

Table S2. Total differentially expressed genes included in the second chapter RNA-seq analysis, corresponding to the study of the effect of *carP* deletion (DESeq with p<0.05 after correction), including the differential fold change for each of the comparisons analyzed.

Gene	Description	Log2 FC (WT0 WT60)	Log2 FC (SG268_0 SG268_60)	Log2 FC (SG268_0 WT_0)	Log2 FC (SG268_60 WT_60)
FFUJ_06628	related to NAD(P)H-dependent oxidoreductase	12.283			11.754
FFUJ_11801	related to lignostilbene alphabeta-dioxygenase I	12.272			13.561
FFUJ_02302	related to pentafunctional arom polypeptide	12.183			12.464
FFUJ_12435	uncharacterized protein	11.812			11.686
FFUJ_11472	probable catalase isozyme P	11.457			7.990
FFUJ_11804	related to HSP30 heat shock protein Yro1p	10.906			9.682
FFUJ_10321	probable alcohol dehydrogenase homolog Bli-4	10.428			13.302
FFUJ_05402	uncharacterized protein	10.305	3.267		5.296
FFUJ_09337	uncharacterized protein	9.557	3.713		7.782
FFUJ_09310	related to NmrA-like family protein	9.315			4.811
FFUJ_09119	related to flavin-containing amine oxidasedehydrogenase	9.296	3.070		6.043
FFUJ_09320	related to Rds1 protein	9.172			7.322
FFUJ_10895	related to galactinol synthase	8.973			6.816
FFUJ_03574	uncharacterized protein	8.905			4.613
FFUJ_14129	uncharacterized protein	8.794			7.308
FFUJ_05524	uncharacterized protein	8.698			4.360
FFUJ_05128	probable CTT1-catalase T%2C cytosolic	8.646			3.073
FFUJ_08272	uncharacterized protein	8.338	5.056		3.317
FFUJ_10692	related to NADH oxidase	8.330			
FFUJ_01292	uncharacterized protein	8.266	5.568		2.265
FFUJ_00131	uncharacterized protein	8.078	7.301		
FFUJ_03970	uncharacterized protein	7.949			4.638
FFUJ_03418	uncharacterized protein	7.893			7.726
FFUJ_06562	related to molybdopterin biosynthesis protein moeA	7.605			
FFUJ_10322	uncharacterized protein	7.557			7.030
FFUJ_02691	probable glucose repressible protein Grg1	7.485			3.535
FFUJ_10367	related to sensory transduction histidine kinase	7.443	6.023		
FFUJ_12794	uncharacterized protein	7.356			6.824
FFUJ_06561	probable periplasmic nitrate reductase	7.327			
FFUJ_13751	uncharacterized protein	7.246	5.329		1.771
FFUJ_13896	related to TGF beta induced protein ig-h3 precursor	7.218		1.704	8.417
FFUJ_10705	uncharacterized protein	7.199			6.159
FFUJ_06055	probable vivid PAS protein VVD	7.136	7.174		
FFUJ_06304	probable glucose repressible protein Grg1	7.057	3.882		1.144
FFUJ_01088	related to short-chain alcohol dehydrogenase	7.017	3.101		4.519
FFUJ_11877	uncharacterized protein	6.985	6.000		
FFUJ_03586	uncharacterized protein	6.934			7.119
FFUJ_00295	CON-10 conidation-specific protein CON-10	6.921	3.838		4.378
FFUJ_10896	related to 2%2C5-diketo-D-gluconic acid reductase	6.917		3.862	9.137
FFUJ_11471	uncharacterized protein	6.886			7.315
FFUJ_10505	uncharacterized protein	6.880			6.656
FFUJ_14257	uncharacterized protein	6.871			2.749
FFUJ_08014	related to formaldehyde dehydrogenase	6.750			5.283
FFUJ_08327	uncharacterized protein	6.704	2.971		4.681
FFUJ_00691	uncharacterized protein	6.681	3.379		
FFUJ_05585	related to NAD(P)H-dependent oxidoreductase	6.599	1.500		4.842
FFUJ_05082	uncharacterized protein	6.552	1.537		5.366
FFUJ_11003	uncharacterized protein	6.534	2.244		5.529
FFUJ_03784	related to tryptophan 2%2C3 dioxygenase	6.454			
EFFFUG00000000013	0	6.390			
FFUJ_07351	related to mfs-multidrug-resistance transporter	6.379	2.121		4.390
FFUJ_08281	uncharacterized protein	6.377			6.495
FFUJ_10453	uncharacterized protein	6.366			4.237
FFUJ_03407	related to CTA1-catalase A%2C peroxisomal	6.351			5.702
FFUJ_03452	related to xylulose-5-phosphate/fructose-6-phosphate phosphoketolase	6.348	4.010		2.516
FFUJ_06800	uncharacterized protein	6.321			3.928
FFUJ_05934	uncharacterized protein	6.293	2.551		4.574
FFUJ_11854	uncharacterized protein	6.170			
FFUJ_11615	uncharacterized protein	6.156			5.210
FFUJ_01396	related to mitochondrial integral membrane protein	6.077			2.866
FFUJ_01909	uncharacterized protein	6.045	2.801		
FFUJ_11802	probable geranylgeranyl-diphosphate geranylgeranyltransferase (AL-2)	5.985		5.892	8.770
FFUJ_05732	related to deoxyribodipyrimidine photo-lyase	5.970	5.177		0.868
FFUJ_09358	probable general amidase	5.921			8.455
FFUJ_06923	probable MNN4-regulates the mannosylphosphorylation	5.887	3.208		2.002
FFUJ_07032	uncharacterized protein	5.883	3.169		2.075
FFUJ_02301	uncharacterized protein	5.875		3.252	7.828

FFUJ_14324	related to acid phosphatase precursor (pH 6-optimum acid phosphatase)	5.869			
FFUJ_04654	related to 2-polyprenyl-6-methoxyphenol hydroxylase and related FAD-dependent oxidoreductases	5.843			6.961
FFUJ_11043	uncharacterized protein	5.791	4.040		
FFUJ_10257	putative NADH cytb-reductase	5.778			5.248
FFUJ_11562	related to PHO11-secreted acid phosphatase	5.747	3.625		2.516
FFUJ_10918	uncharacterized protein	5.733			
FFUJ_07302	related to pall protein	5.716	3.463		
FFUJ_03451	probable catalase-1	5.661	3.756		
FFUJ_01996	related to C4-dicarboxylate transport protein mae1	5.639	4.259		1.120
FFUJ_11803	probable phytoene dehydrogenase AL-1 (carotenoid biosynthesis protein al-1)	5.630	4.487	6.668	7.792
FFUJ_00230	uncharacterized protein	5.557			
FFUJ_01785	uncharacterized protein	5.549			5.293
FFUJ_06907	related to dehydroshikimate dehydratase	5.503	2.907		2.784
FFUJ_14760	related to acid phosphatase	5.483			1.888
FFUJ_01993	probable organic hydroperoxide resistance protein	5.432			4.468
FFUJ_08230	related to integral membrane protein PTH11	5.427			
FFUJ_06163	uncharacterized protein	5.412			5.005
FFUJ_04061	related to 2-polyprenyl-6-methoxyphenol hydroxylase and related FAD-dependent oxidoreductases	5.392	2.313		5.119
FFUJ_04335	uncharacterized protein	5.344	2.847		2.814
FFUJ_06988	related to aryl-alcohol dehydrogenases	5.323			4.520
FFUJ_03408	probable gibberellin biosynthesis-related	5.321			5.610
FFUJ_06701	uncharacterized protein	5.316			4.629
FFUJ_07962	related to beta-carotene 15%2C15`-dioxygenase	5.292			5.122
FFUJ_09120	related to 4-hydroxybenzoate transporter	5.274	2.479		5.147
FFUJ_02297	probable low-affinity hexose transporter HXT3	5.233	3.485		
FFUJ_09413	uncharacterized protein	5.227			1.824
FFUJ_04508	probable blue-light-inducible Bli-3 protein	5.221	2.427		3.425
FFUJ_09007	probable alcohol dehydrogenase (NADP+)	5.216			3.707
FFUJ_01887	uncharacterized protein	5.199			
FFUJ_00130	probable Phenylalanine ammonia-lyase	5.189			
FFUJ_01907	uncharacterized protein	5.181			
FFUJ_10665	related to salicylate 1-monooxygenase	5.175			
FFUJ_06906	uncharacterized protein	5.164			
FFUJ_05515	probable ATP-binding multidrug cassette transport protein	5.103	3.212		3.101
FFUJ_10747	probable iron-dependent peroxidase	5.083			
FFUJ_00436	probable deoxyribodipyrimidine photo-lyase PHR	5.060	4.381		0.966
FFUJ_11713	related to nonphototropic hypocotyl protein 1	5.054	5.049		
FFUJ_13888	related to ECM14-involved in cell wall biogenesis and architecture	5.046			7.171
FFUJ_11042	related to oxidoreductase	5.029			3.576
FFUJ_11824	uncharacterized protein	5.010	2.986		3.327
FFUJ_09338	uncharacterized protein	4.990			6.332
FFUJ_10489	uncharacterized protein	4.982			
FFUJ_09284	uncharacterized protein	4.965			6.539
FFUJ_13276	uncharacterized protein	4.936	2.849		1.948
FFUJ_07515	related to arabinose 5-phosphate isomerase	4.883	2.257		3.080
FFUJ_08102	related to lambda-crystallin	4.841			
FFUJ_11961	uncharacterized protein	4.772	3.287		
FFUJ_05360	uncharacterized protein	4.771			5.021
FFUJ_07396	related to mismatched base pair and cruciform dna recognition protein	4.765	2.414		1.384
FFUJ_04672	uncharacterized protein	4.734			
FFUJ_10691	related to maackiain detoxification protein 1	4.710			
FFUJ_06705	uncharacterized protein	4.699			4.571
FFUJ_09378	uncharacterized protein	4.696			4.035
FFUJ_14546	uncharacterized protein	4.689			4.277
FFUJ_06981	related to myo-inositol transport protein ITR1	4.667			1.264
FFUJ_05834	probable oxidoreductase CipA-like	4.661			3.464
FFUJ_10598	uncharacterized protein	4.650			2.478
FFUJ_06160	related to short chain dehydrogenase	4.617	1.456		4.010
FFUJ_06373	uncharacterized protein	4.593	1.890		1.376
FFUJ_02524	related to glutamic acid decarboxylase	4.590	3.347		
FFUJ_11610	uncharacterized protein	4.586			3.131
FFUJ_05482	related to calcium-binding protein caleosin	4.562	2.599		
FFUJ_08013	related to putidaredoxin reductase	4.549			
FFUJ_11978	related to 6-phosphogluconate dehydrogenase	4.547	2.528	-1.689	
FFUJ_10092	related to quinate transport protein	4.523			
FFUJ_05481	related to aldo-keto reductase family protein	4.506			
FFUJ_07815	related to anthranilate synthase component II	4.472			2.911
FFUJ_11846	related to thioredoxin	4.446	1.855		2.383
FFUJ_11224	related to allantoate permease	4.422	3.404		
FFUJ_00034	related to vegetatible incompatibility protein HET-E-1	4.395	2.225	2.027	4.169
FFUJ_07384	uncharacterized protein	4.391			

FFUJ_10836	related to xylosidase/arabinosidase	4.389	1.759		2.541
FFUJ_00275	related to DUF636 domain protein	4.381			3.727
FFUJ_13754	related to diacylglycerol pyrophosphate phosphatase DPP1	4.331	1.376		2.378
FFUJ_11698	uncharacterized protein	4.326	1.793		2.786
FFUJ_13124	uncharacterized protein	4.319			
FFUJ_10466	related to Auxin Efflux Carrier superfamily	4.318	2.258		4.026
FFUJ_07759	related to isoflavone reductase family protein	4.309			2.979
FFUJ_11900	uncharacterized protein	4.254	2.304		1.534
FFUJ_11686	related to diacylglycerol pyrophosphate phosphatase DPP1	4.253			
FFUJ_05570	uncharacterized protein	4.236	2.401		1.625
FFUJ_09818	uncharacterized protein	4.234	2.386		1.811
FFUJ_10020	related to RTM1 protein	4.208			
FFUJ_10897	uncharacterized protein	4.206			3.721
FFUJ_05185	uncharacterized protein	4.182			
FFUJ_06572	uncharacterized protein	4.180			4.656
FFUJ_08931	related to short-chain alcohol dehydrogenase	4.167			2.383
FFUJ_06194	uncharacterized protein	4.164	2.666		1.595
FFUJ_05190	uncharacterized protein	4.161	1.921		
FFUJ_03848	uncharacterized protein	4.133			
FFUJ_02067	uncharacterized protein	4.108			
FFUJ_14325	related to dTDP-glucose 4%2C6-dehydratase	4.106		-2.810	
FFUJ_00148	related to nucleoside-diphosphate-sugar epimerase	4.105			1.824
FFUJ_10518	probable beta-glucosidase 1 precursor	4.090			
FFUJ_01296	related to glycosyl hydrolase%2C family 15	4.078	1.694		2.591
FFUJ_03979	uncharacterized protein	4.065			
FFUJ_00337	probable catechol O-methyltransferase	4.043			4.461
FFUJ_03926	probable phosphate transport protein MIR1	3.991			
FFUJ_03267	related to DUF1295 domain protein	3.982			3.709
FFUJ_08747	related to PET8 protein%2C member of the mitochondrial carrier (MCF) family	3.977			1.902
FFUJ_01016	related to meiotic expression up-regulated protein 14	3.957			1.854
FFUJ_11509	related to DNA repair exonuclease SIA1	3.952	3.421		1.611
FFUJ_12719	uncharacterized protein	3.947			3.941
FFUJ_13152	uncharacterized protein	3.935	2.170		2.137
FFUJ_11223	uncharacterized protein	3.920	3.010		
FFUJ_11876	uncharacterized protein	3.919	3.192		
FFUJ_09319	related to HHE domain protein	3.919	2.903		1.822
FFUJ_14761	uncharacterized protein	3.859			1.971
FFUJ_06977	related to DUF1264 domain protein	3.849	1.999		1.272
FFUJ_13569	related to subtilisin-like serine protease	3.834	4.119		
FFUJ_03105	related to deoxyribodipyrimidine photo-lyase PHR	3.820		1.216	4.590
FFUJ_12782	related to chitin synthase class IV	3.810			
FFUJ_11045	related to phospholipase A2%2C cytosolic	3.797			3.727
FFUJ_14904	related to serum paraoxonase/arylesterase family protein	3.748		1.844	4.479
566073	0	3.729			
FFUJ_11537	uncharacterized protein	3.728			4.424
FFUJ_07454	uncharacterized protein	3.711	1.833		1.861
FFUJ_03482	uncharacterized protein	3.706			
FFUJ_09845	related to putative transmembrane protein	3.699			2.422
126174	0	3.697			
FFUJ_03481	related to flavin oxidoreductase	3.691			
FFUJ_06570	probable thioredoxin peroxidase%2C mitochondrial isoform	3.690	1.938		1.954
FFUJ_05523	related to oxidoreductase	3.688			
FFUJ_11440	related to ADH2-alcohol dehydrogenase II	3.675			
FFUJ_01212	related to benzodiazepine receptor%2C peripheral-type	3.673	3.182		1.369
FFUJ_13729	related to phosphatidylserine decarboxylase 2	3.654	2.025		
FFUJ_13183	related to CYTOCHROME B561	3.648			
FFUJ_11546	uncharacterized protein	3.642	1.962		
FFUJ_06546	related to quinone oxidoreductase	3.642			2.704
FFUJ_05984	uncharacterized protein	3.641			
FFUJ_04757	uncharacterized protein	3.641	2.949		
FFUJ_12699	uncharacterized protein	3.633			2.203
FFUJ_02346	related to multidrug resistant protein	3.629	3.704		
FFUJ_10344	uncharacterized protein	3.609	3.011		
FFUJ_t15	0	3.608			
FFUJ_10800	uncharacterized protein	3.595			
FFUJ_12693	related to reductases	3.582			3.927
FFUJ_08104	probable bifunctional P-450:NADPH-P450 reductase	3.571			
FFUJ_07699	uncharacterized protein	3.559	1.407		2.404
FFUJ_11815	related to Glutathione S-transferase II	3.558			
FFUJ_10519	related to aflatoxin efflux pump AFLT	3.542			
FFUJ_06474	related to Cu-binding metallothionein	3.535			
FFUJ_06982	uncharacterized protein	3.522			5.133
FFUJ_03975	uncharacterized protein	3.516	4.900		
FFUJ_06003	uncharacterized protein	3.516			1.350
FFUJ_11953	uncharacterized protein	3.513	1.663	-1.485	
FFUJ_00756	related to UDP-glucuronosyltransferase 2C1 microsomal	3.511			3.638

FFUJ_06265	uncharacterized protein	3.506			
FFUJ_07352	probable farnesyltranstransferase (al-3)	3.476			2.897
FFUJ_03471	related to ACB 4-hydroxyacetophenone monooxygenase	3.471	2.345		
FFUJ_05866	related to stilbene synthase 2	3.469			3.449
FFUJ_13161	related to YER185w%2C Rta1p	3.461			4.436
FFUJ_14667	probable catalase isozyme P	3.460		-3.505	
FFUJ_10429	uncharacterized protein	3.447			
FFUJ_12387	uncharacterized protein	3.441	3.369		
FFUJ_08100	related to flavin-containing monooxygenase	3.439			
FFUJ_04336	uncharacterized protein	3.436	2.782		
FFUJ_06138	uncharacterized protein	3.410			2.276
FFUJ_11664	related to multidrug resistance protein	3.407			2.309
FFUJ_11845	uncharacterized protein	3.404			
FFUJ_04810	uncharacterized protein	3.404			1.657
FFUJ_08275	related to monosaccharide transporter	3.401			2.659
FFUJ_00026	uncharacterized protein	3.372	1.685		
FFUJ_02582	probable succinate dehydrogenase (ubiquinone) flavoprotein precursor%2C mitochondrial	3.364			
FFUJ_11665	uncharacterized protein	3.359		-1.698	1.987
FFUJ_14823	uncharacterized protein	3.336	1.116		2.109
FFUJ_11505	uncharacterized protein	3.331			
FFUJ_11952	uncharacterized protein	3.329			
FFUJ_02772	uncharacterized protein	3.313	1.211		2.279
FFUJ_00033	probable 3-hydroxyisobutyrate dehydrogenase%2C mitochondrial precursor	3.313			2.342
FFUJ_12690	uncharacterized protein	3.312			2.054
FFUJ_14029	uncharacterized protein	3.304			
FFUJ_07199	uncharacterized protein	3.290	2.152		1.310
FFUJ_05779	uncharacterized protein	3.289			1.587
FFUJ_10890	related to chitinase	3.284			2.213
FFUJ_06002	MUC1-Extracellular alpha-1%2C4-glucan glucosidase	3.267			
FFUJ_08084	related to 3-(3-Hydroxyphenyl)propionate 2-hydroxylase	3.260			4.842
FFUJ_06427	uncharacterized protein	3.255	1.854		
FFUJ_02581	uncharacterized protein	3.248			2.763
FFUJ_10167	uncharacterized protein	3.240			3.677
FFUJ_01910	uncharacterized protein	3.237	2.821		
FFUJ_05502	uncharacterized protein	3.235			1.351
FFUJ_04367	related to M.capricolum transcription repressor	3.234			2.706
FFUJ_13708	related to pathway-specific regulatory protein nit-4	3.232	1.905		
FFUJ_10970	related to NmrA-like family protein	3.224			4.513
FFUJ_09510	uncharacterized protein	3.212			2.037
FFUJ_14043	related to isoamyl alcohol oxidase	3.205			3.915
FFUJ_11486	probable Cyanamide hydratase	3.201			2.635
FFUJ_10900	related to nonribosomal peptide synthetase MxcG	3.154			3.224
FFUJ_06448	related to DUF1237 domain protein	3.151			
FFUJ_02494	related to FK506 suppressor Sfk1	3.138			
FFUJ_14082	uncharacterized protein	3.115	3.455		
FFUJ_11487	related to ankyrin	3.114			2.872
FFUJ_01361	uncharacterized protein	3.109			1.644
FFUJ_06958	uncharacterized protein	3.093	2.021		
FFUJ_05854	uncharacterized protein	3.077	1.402		1.440
FFUJ_11459	related to hydroxylase	3.068			2.598
FFUJ_11222	uncharacterized protein	3.021	2.607		
FFUJ_03576	related to short-chain alcohol dehydrogenase	3.012			
FFUJ_14529	uncharacterized protein	3.004	2.183		
FFUJ_01724	uncharacterized protein	3.002			2.657
FFUJ_01451	related to DNA repair family protein	2.999			2.746
FFUJ_04556	probable ferrochelatase	2.998	3.197		
FFUJ_03404	related to alcohol dehydrogenase I-ADH1	2.990			
FFUJ_06571	related to 5-methylcytosine G/T mismatch-specific DNA glycosylase	2.987			3.223
FFUJ_06207	related to D-arabinono-1%2C4-lactone oxidase	2.970			
FFUJ_07211	probable conidiation protein 6 (con-6)	2.967			2.724
FFUJ_11806	related to 3-(3-Hydroxyphenyl)propionate 2-hydroxylase	2.957			2.089
FFUJ_09104	related to KES1-involved in ergosterol biosynthesis	2.957	3.664		
FFUJ_11751	uncharacterized protein	2.950			2.820
FFUJ_03861	probable lysosomal cobalamin transporter	2.946			
FFUJ_06722	related to IQ calmodulin-binding motif protein	2.937			
FFUJ_07608	probable brefeldin A resistance protein	2.918	1.602		1.118
FFUJ_02232	uncharacterized protein	2.917			3.213
FFUJ_04133	uncharacterized protein	2.914	0.723		2.438
FFUJ_12444	uncharacterized protein	2.911			
FFUJ_02317	related to light induced alcohol dehydrogenase Bli-4	2.907			
FFUJ_12437	related to cytosine deaminase and related metal-dependent hydrolases	2.906			2.023
FFUJ_09006	related to NonF protein%2C involved in nonactin biosynthesis	2.900			

FFUJ_11685	uncharacterized protein	2.894			
FFUJ_10818	probable NADPH2 dehydrogenase chain OYE2	2.880			
FFUJ_09299	related to monoamine oxidase N	2.864			
FFUJ_05514	uncharacterized protein	2.862	2.459		1.219
FFUJ_08269	uncharacterized protein	2.860			2.559
FFUJ_03785	related to kynureninase	2.858			
FFUJ_03974	related to zinc finger protein odd-paired-like (opl)	2.854	4.323		
FFUJ_10316	uncharacterized protein	2.851			3.179
FFUJ_12300	related to phospholipase A2%2C cytosolic	2.846	1.429		1.176
FFUJ_00469	related to beta-glucosidase	2.817	3.563		
FFUJ_13851	uncharacterized protein	2.815			
FFUJ_11895	uncharacterized protein	2.813	3.017		
FFUJ_11535	uncharacterized protein	2.806			1.910
FFUJ_14327	related to aldehyde dehydrogenase	2.805			
FFUJ_06723	related to transcriptional activator Mut3p	2.790			
FFUJ_01908	uncharacterized protein	2.777	1.652		0.737
FFUJ_10993	related to reductases	2.774			2.790
FFUJ_11470	related to channel proteins	2.771	1.845		
FFUJ_07144	related to UPF0591 membrane protein C15E1.02c	2.766			1.646
FFUJ_06781	related to alcohol dehydrogenase%2C class C	2.764			
FFUJ_10756	uncharacterized protein	2.763		1.341	3.448
FFUJ_05300	related to Oxidoreductase%2C short-chain dehydrogenase	2.761			2.274
FFUJ_07825	uncharacterized protein	2.736	1.684		
FFUJ_00345	uncharacterized protein	2.727			1.926
FFUJ_07367	related to carrier protein YMC1%2C mitochondrial	2.708			2.589
FFUJ_00164	uncharacterized protein	2.700	1.404		
FFUJ_12178	related to purine transporter azgA	2.695			
FFUJ_07916	related to glutathione S-transferase	2.681			2.460
FFUJ_08523	uncharacterized protein	2.674	1.228		1.598
FFUJ_11542	related to DNA repair exonuclease SIA1	2.674	2.979		
FFUJ_00322	related to ketoreductases	2.668			3.008
FFUJ_06191	uncharacterized protein	2.653			
FFUJ_04725	probable 3^-phosphoadenosine 5^-phosphosulfate sulfotransferase (PAPS reductase)/FAD synthetase and related enzymes	2.643			2.605
FFUJ_11614	uncharacterized protein	2.636	1.311		0.702
FFUJ_04572	related to mannose-6-phosphate isomerase	2.635			1.139
FFUJ_07015	related to COQ2-para-hydroxybenzoate--polyprenyltransferase	2.635	1.725		1.029
FFUJ_13992	uncharacterized protein	2.629	1.495		1.211
FFUJ_08745	probable succinate dehydrogenase (ubiquinone) iron-sulfur protein precursor	2.628			
FFUJ_10256	related to 3-hydroxybutyryl-CoA dehydrogenase	2.609	2.050		
FFUJ_04190	uncharacterized protein	2.579			2.222
FFUJ_08451	uncharacterized protein	2.569	1.587		
FFUJ_09359	uncharacterized protein	2.566			2.627
FFUJ_07198	uncharacterized protein	2.551	1.702		1.333
FFUJ_10520	related to dienelactone hydrolase and related enzymes	2.548	1.805		
FFUJ_00718	related to endoplasmic reticulum 25 kDa transmembrane protein	2.546	1.296		1.453
FFUJ_08714	uncharacterized protein	2.545		-3.579	-1.813
FFUJ_00427	probable malate dehydrogenase (oxaloacetate decarboxylating) (NADP+)	2.537	1.635		
FFUJ_09919	uncharacterized protein	2.536			
FFUJ_01463	related to RNA binding protein	2.529	1.655		1.020
FFUJ_00122	uncharacterized protein	2.524	4.902		
FFUJ_03973	uncharacterized protein	2.520			
FFUJ_11843	uncharacterized protein	2.518			
FFUJ_14510	uncharacterized protein	2.511	2.480		
FFUJ_07162	related to acyl-coa dehydrogenase%2C long-chain specific precursor	2.508			
FFUJ_10815	related to PET8 protein%2C member of the mitochondrial carrier (MCF) family	2.504			1.877
FFUJ_01273	probable SIS1 Heat shock protein	2.502	1.453		
FFUJ_04228	uncharacterized protein	2.500			3.182
FFUJ_06980	uncharacterized protein	2.498			
FFUJ_11397	related to membrane protein	2.494			
FFUJ_14045	probable alpha-galactosidase C precursor	2.486			
FFUJ_10095	related to DUF1295 domain protein	2.476			
FFUJ_13182	related to two-component histidine kinase chk-1	2.476	1.657		
FFUJ_06610	uncharacterized protein	2.475			
FFUJ_02352	related to YRO2 protein	2.475			1.888
FFUJ_06889	uncharacterized protein	2.471			
FFUJ_09438	uncharacterized protein	2.469			
FFUJ_05077	uncharacterized protein	2.465			
FFUJ_07181	probable RIC1 protein	2.459	1.553		
FFUJ_01091	related to hxB protein	2.455	2.148		

FFUJ_08282	uncharacterized protein	2.455			2.439
FFUJ_10526	uncharacterized protein	2.452			2.454
FFUJ_07673	uncharacterized protein	2.450	2.210		
FFUJ_09958	uncharacterized protein	2.444	2.108		1.426
FFUJ_07140	related to REX3-RNA exonuclease%2C member of the family of 3`-5` exonucleases	2.438	1.531		
FFUJ_10495	related to pathway-specific regulatory protein nit-4	2.427			
FFUJ_00720	probable meiotic expression up-regulated protein 14	2.418	1.363		0.784
FFUJ_02493	uncharacterized protein	2.415			
FFUJ_08536	uncharacterized protein	2.408			
FFUJ_07745	uncharacterized protein	2.398			1.826
FFUJ_02678	related to ATP-binding cassette (ABC) transporter	2.390			2.809
FFUJ_05604	uncharacterized protein	2.390			
FFUJ_03136	probable oxidoreductase	2.384			1.515
FFUJ_06205	related to FMP45 Cell cortex protein involved in sporulation	2.379			
FFUJ_03547	uncharacterized protein	2.375			
FFUJ_09580	uncharacterized protein	2.373	0.582		1.925
FFUJ_00845	uncharacterized protein	2.360	3.076		
FFUJ_11380	uncharacterized protein	2.359			2.192
FFUJ_09936	related to histidine kinase	2.348			
FFUJ_13168	related to Mechanosensitive ion channel family	2.345	1.884		
FFUJ_11277	uncharacterized protein	2.341			
FFUJ_14685	related to integral membrane protein PTH11	2.338	3.620		
FFUJ_02439	uncharacterized protein	2.324			1.313
FFUJ_05665	related to calcium-binding protein caleosin	2.324			
FFUJ_07878	uncharacterized protein	2.311	1.020		1.440
FFUJ_10474	catalase	2.303			2.583
FFUJ_06721	uncharacterized protein	2.297			1.506
FFUJ_10366	uncharacterized protein	2.294			
FFUJ_06987	related to pyridoxine 4-dehydrogenase	2.291			
FFUJ_11420	related to lipase 1	2.289			1.916
FFUJ_03778	related to RSB1-integral membrane transporter or flippase that may transport LCBs from the cytoplasmic side toward the extracytoplasmic side of the membrane	2.286	2.025		
FFUJ_13069	uncharacterized protein	2.279			
FFUJ_08319	probable cytochrome c	2.275			
FFUJ_10898	related to multidrug resistance protein	2.272			
FFUJ_12394	related to alcohol dehydrogenase homolog Bli-4	2.268			
FFUJ_07165	related to galactinol synthase	2.260			2.421
FFUJ_01546	related to diacylglycerol acyltransferase type 2a	2.249	1.404		0.933
FFUJ_03391	uncharacterized protein	2.248			
FFUJ_04580	uncharacterized protein	2.247	3.343		
FFUJ_09806	uncharacterized protein	2.240			
FFUJ_06780	probable chaperone protein hchA	2.239			
FFUJ_00965	related to Acylphosphatase	2.232	1.212		
FFUJ_14571	probable carnitine transport protein	2.224	1.279		1.466
FFUJ_05723	uncharacterized protein	2.216	1.449		
FFUJ_11977	uncharacterized protein	2.206			
FFUJ_09382	related to lactate 2-monooxygenase	2.204			
FFUJ_05874	probable holocytochrome-c synthase	2.204	1.190		
FFUJ_13608	probable CHO1-CDP-diacylglycerol serine O-phosphatidyltransferase	2.201	1.201		0.876
FFUJ_04548	uncharacterized protein	2.200			1.959
FFUJ_13406	uncharacterized protein	2.187	1.815		0.749
FFUJ_05953	uncharacterized protein	2.187			
FFUJ_14913	uncharacterized protein	2.181	2.751		
FFUJ_03470	uncharacterized protein	2.172	1.650		
FFUJ_07430	related to TGL2-triacylglycerol lipase	2.169	1.202		
FFUJ_08144	uncharacterized protein	2.166			
FFUJ_11735	uncharacterized protein	2.163			
FFUJ_10899	related to fungal transcriptional regulatory protein	2.151			1.877
FFUJ_10549	related to adenine phosphoribosyltransferase	2.151	3.249		
FFUJ_11469	related to thermoresistant gluconokinase	2.149			
FFUJ_10606	uncharacterized protein	2.146			
FFUJ_09758	uncharacterized protein	2.146	1.965		
FFUJ_04604	uncharacterized protein	2.145	1.047		1.136
FFUJ_11712	uncharacterized protein	2.143			
FFUJ_00208	related to tetracycline resistance protein (probable transport protein)	2.137	1.404		0.997
FFUJ_07453	related to integral membrane protein	2.133	1.867		
FFUJ_11536	related to nitrate assimilation regulatory protein nirA	2.132			1.008
FFUJ_11951	uncharacterized protein	2.131			1.175
FFUJ_06056	related to DNA repair protein MMS21	2.131	1.929		
FFUJ_02214	uncharacterized protein	2.129			
FFUJ_13188	uncharacterized protein	2.120			
FFUJ_00334	uncharacterized protein	2.119			
FFUJ_05875	uncharacterized protein	2.111			

FFUJ_05739	related to DNA damage-responsive protein 48	2.109	2.475		
FFUJ_11687	uncharacterized protein	2.097			
FFUJ_06257	uncharacterized protein	2.095			1.797
FFUJ_08932	probable sulfonate biosynthesis enzyme	2.078			
FFUJ_11945	probable hexokinase	2.074		-4.155	-2.162
FFUJ_05614	uncharacterized protein	2.073			
FFUJ_05987	related to 2%2C4-dienoyl-CoA reductase precursor	2.067	1.025		1.303
FFUJ_13229	probable beta (1-3) glucanosyltransferase	2.067			1.703
FFUJ_07659	related to the plant PR-1 class of pathogen related proteins	2.065			1.187
FFUJ_05873	related to aminoglycoside acetyltransferase regulator from P. stuartii	2.064	0.781		0.925
FFUJ_12948	related to dienelactone hydrolase family protein	2.060			4.250
FFUJ_06242	probable oxidoreductase%2C short chain dehydrogenase/reductase family superfamily	2.059			1.281
FFUJ_00149	uncharacterized protein	2.057			
FFUJ_00994	uncharacterized protein	2.049			
FFUJ_00163	uncharacterized protein	2.049			
FFUJ_00449	related to serine/threonine-protein kinase	2.045	1.149		
FFUJ_10767	uncharacterized protein	2.044		-2.744	
FFUJ_08987	probable UV-endonuclease UVE-1	2.040	1.660		
FFUJ_05591	related to multidrug resistance protein	2.038			2.091
FFUJ_12878	related to ALO1-D-arabinono-1%2C4-lactone oxidase	2.035	1.967		
FFUJ_13895	uncharacterized protein	2.031			1.038
FFUJ_04202	related to RTG2-retrograde regulation protein	2.029	2.272		
FFUJ_13453	uncharacterized protein	2.028			2.311
FFUJ_00450	uncharacterized protein	2.026			
FFUJ_03411	uncharacterized protein	2.022			2.056
FFUJ_04185	uncharacterized protein	2.019			
FFUJ_09157	uncharacterized protein	2.015			
FFUJ_05474	uncharacterized protein	2.013			1.176
FFUJ_04800	probable 4-alpha-glucanotransferase / amylo-1%2C6-glucosidase (glycogen-debranching enzyme)	2.008	2.043		
FFUJ_13511	probable glucan 1%2C4-alpha-glucosidase	2.007			
FFUJ_06049	related to sarcosine oxidase	2.006	2.629		
FFUJ_11851	related to short chain dehydrogenase	2.006	1.046		0.942
FFUJ_04459	probable 3-isopropylmalate dehydratase	2.003			
FFUJ_02679	uncharacterized protein	1.994			2.152
FFUJ_04745	related to IST2 protein	1.993			1.072
FFUJ_06922	related to vacuolar protein sorting-associated protein VPS13	1.990			0.803
FFUJ_09141	uncharacterized protein	1.988			
FFUJ_02606	related to finger protein AZF1	1.988	2.176		
FFUJ_03089	uncharacterized protein	1.988			4.016
FFUJ_13147	uncharacterized protein	1.986			
FFUJ_08838	related to proliferation associated SNF2-like protein	1.982			2.143
FFUJ_06155	uncharacterized protein	1.982	1.203		
FFUJ_03421	uncharacterized protein	1.981	0.849		
FFUJ_01223	uncharacterized protein	1.980			1.107
FFUJ_13436	related to quinate transport protein	1.979			1.618
FFUJ_08866	related to D-arabinitol 2-dehydrogenase	1.977	2.393		
FFUJ_04331	related to Rtm1p	1.975			
FFUJ_05316	uncharacterized protein	1.973			
FFUJ_11705	related to lipid binding protein Tfs1p	1.972			1.568
FFUJ_00207	related to arsenic resistance protein ArsH	1.972			
FFUJ_07717	related to spherulin 1B precursor	1.969	2.293		
FFUJ_10748	uncharacterized protein	1.966			
FFUJ_07872	probable membrane-bound O-acyltransferase domain-containing protein 5	1.963			
FFUJ_02814	uncharacterized protein	1.958	2.816		
FFUJ_03780	uncharacterized protein	1.958	2.060		
FFUJ_03761	uncharacterized protein	1.953			3.055
FFUJ_12370	uncharacterized protein	1.951			1.395
FFUJ_01439	probable cytochrome-c peroxidase precursor	1.948			
FFUJ_04484	probable osmotic sensitive-2 protein (putative mitogen-activated protein (MAP) kinase homolog)	1.941	1.926		
FFUJ_02868	uncharacterized protein	1.938	0.834		1.169
FFUJ_06223	related to bacterial aminoglycoside acetyltransferase regulators	1.938	0.799		1.190
FFUJ_10209	related to cutinase transcription factor 1 beta	1.929			
FFUJ_00492	related to nitrogen permease regulator	1.926			1.090
FFUJ_09606	uncharacterized protein	1.921			
FFUJ_06554	uncharacterized protein	1.913			
FFUJ_00722	related to RAD13	1.912	0.831		1.214
FFUJ_06991	uncharacterized protein	1.909			
FFUJ_11508	uncharacterized protein	1.899			
FFUJ_05447	probable beta-succinyl CoA synthetase precursor	1.898			
FFUJ_00751	probable cytochrome-b5 reductase%2C mitochondrial outer membrane form	1.898			0.805

FFUJ_05994	uncharacterized protein	1.896	1.305		
FFUJ_10554	related to glyoxalase family protein	1.886			
FFUJ_02205	related to galactinol synthase	1.885	3.157		
FFUJ_06185	related to ubiquinol--cytochrome-c reductase assembly factor	1.885			1.185
FFUJ_11235	uncharacterized protein	1.884			
FFUJ_11220	uncharacterized protein	1.883			
FFUJ_08783	related to TAD2-tRNA-specific adenosine deaminase 2	1.882			2.041
FFUJ_06758	uncharacterized protein	1.878	1.448		
FFUJ_10667	related to nucleoside-diphosphate-sugar epimerase	1.876			
FFUJ_02914	uncharacterized protein	1.872			
FFUJ_00882	probable MNR2-Manganese resistance protein	1.870	0.979		1.086
FFUJ_14694	related to SUC2-invertase (sucrose hydrolyzing enzyme)	1.870	1.325		1.358
FFUJ_13902	related to dihydroxyacetone kinase	1.867			3.803
FFUJ_14317	probable aldehyde dehydrogenase	1.867			5.150
FFUJ_03253	uncharacterized protein	1.866	1.400		0.689
FFUJ_05588	uncharacterized protein	1.863		-2.728	
FFUJ_11909	uncharacterized protein	1.861			
FFUJ_11052	related to quinone reductase	1.861			
FFUJ_04078	related to haloacetate dehalogenase H-1	1.858			1.608
FFUJ_09741	related to polyphosphoinositide phosphatase family member	1.858	1.611		
FFUJ_06202	related to pyridoxamine phosphate oxidase	1.854			1.118
FFUJ_13125	related to acetylhydrolase	1.847			
FFUJ_13474	related to aldo-keto reductase YPR1	1.843			
FFUJ_01726	uncharacterized protein	1.842			1.827
FFUJ_04705	related to cell wall protein cwl1	1.840	1.077		
FFUJ_14205	uncharacterized protein	1.837			
FFUJ_04877	uncharacterized protein	1.836			
FFUJ_05497	uncharacterized protein	1.830			
FFUJ_06310	related to aflatoxin efflux pump AFLT	1.829	1.294		
FFUJ_13753	uncharacterized protein	1.828			1.304
FFUJ_08412	probable acyl-CoA dehydrogenase	1.824			
FFUJ_01888	uncharacterized protein	1.821			
FFUJ_10073	probable DFG5 protein	1.817	1.536		
FFUJ_06959	related to metallo-beta-lactamase family protein	1.815			
FFUJ_05205	related to polyadenylate-binding protein	1.804	1.586		
FFUJ_09929	related to O-methylsterigmatocystin oxidoreductase	1.804			3.491
FFUJ_04875	related to excision repair protein RAD4	1.803			1.542
FFUJ_13678	probable aconitase	1.796			
FFUJ_10826	uncharacterized protein	1.795			
FFUJ_10874	uncharacterized protein	1.778	1.954		
FFUJ_02373	uncharacterized protein	1.777			
FFUJ_r2	0	1.774			
FFUJ_01986	related to immune-responsive protein 1	1.772	1.792		
FFUJ_02652	probable cutinase transcription factor 1 beta	1.771	2.920		
FFUJ_03511	probable extragenic suppressor of the bimD6 mutation	1.761			1.890
FFUJ_00951	related to CAF120 CCR4 Associated Factor 120 kDa	1.757	1.217		
FFUJ_06164	related to cytosine C5-DNA methyltransferase	1.754			1.573
FFUJ_07805	probable NADH dehydrogenase (ubiquinone)%2C 64 kD subunit%2C mitochondrial	1.753			
FFUJ_01741	probable CYB2-lactate dehydrogenase cytochrome b2	1.741			
FFUJ_14569	related to hydrolase related to dienelactone hydrolase	1.735	1.377		
FFUJ_10693	related to tol protein	1.734			2.050
FFUJ_08716	uncharacterized protein	1.731			
FFUJ_09461	related to histidine triad protein	1.731			
FFUJ_01664	uncharacterized protein	1.729			
FFUJ_14180	uncharacterized protein	1.728			
FFUJ_00239	probable glutamine synthetase	1.728			
FFUJ_09624	related to YVC1-vacuolar cation channel	1.726	1.763		
FFUJ_04584	uncharacterized protein	1.723			
FFUJ_09652	related to carboxylic acid transporter protein	1.719			
FFUJ_01258	uncharacterized protein	1.713			
FFUJ_01090	related to cytosolic Cu/Zn superoxide dismutase	1.712	1.558		
FFUJ_05061	uncharacterized protein	1.708			1.189
FFUJ_01266	related to YjeF domain protein	1.708	0.894		0.845
FFUJ_05114	related to PHM7-similarity to A.thaliana hyp1 protein	1.707			
FFUJ_11506	uncharacterized protein	1.707			
FFUJ_07383	related to NsdD protein	1.704	1.400		
FFUJ_04164	uncharacterized protein	1.697			
FFUJ_10506	related to ketoreductases	1.696			2.795
FFUJ_09999	uncharacterized protein	1.694			
FFUJ_13149	uncharacterized protein	1.693			2.057
FFUJ_08868	uncharacterized protein	1.693			
FFUJ_09572	related to sexual differentiation and meiosis protein ste20	1.691	1.694		
FFUJ_09309	related to transcriptional activator Mut3p	1.687			
FFUJ_14547	related to chitinase	1.686			1.910
FFUJ_09674	related to members of the aldo/keto reductase family	1.673	1.574		

FFUJ_08020	uncharacterized protein	1.672			
FFUJ_13578	uncharacterized protein	1.671			
FFUJ_07874	related to ketoreductases	1.671	1.486		
FFUJ_01879	probable ATP dependent RNA helicase	1.668	1.684		
FFUJ_03112	probable RMD1-protein required for Meiotic Division	1.664	0.742		0.922
FFUJ_10457	related to nitrate assimilation regulatory protein nirA	1.664			1.891
FFUJ_04289	related to human TGR-CL10C	1.658	1.380		
FFUJ_13647	probable SAP1-member of the AAA-protein family	1.656	1.354		
FFUJ_14921	related to transcription factor Ask10p	1.653	1.198		
FFUJ_09808	uncharacterized protein	1.651	0.980		
FFUJ_01891	uncharacterized protein	1.651	0.787		0.910
FFUJ_01346	probable heat shock protein 30	1.650			
FFUJ_08865	uncharacterized protein	1.638			1.503
FFUJ_13702	uncharacterized protein	1.630			1.133
FFUJ_12327	uncharacterized protein	1.623			2.487
FFUJ_01621	related to rna-binding protein fus/tls	1.621			
FFUJ_00204	related to endo-polygalacturonase 6	1.619			
FFUJ_07303	uncharacterized protein	1.617	1.654		
FFUJ_01397	uncharacterized protein	1.613	0.929		
FFUJ_05483	related to vegetatible incompatibility protein HET-E-1	1.613			
FFUJ_09538	related to Na+/H+ antiporter CNH1	1.612	1.355		
FFUJ_12309	related to aspartate-tRNA ligase%2C cytosolic	1.611			
FFUJ_05700	related to Calcium_related spray protein	1.610			
FFUJ_14350	probable pectate lyase	1.607			
FFUJ_01853	uncharacterized protein	1.607			
FFUJ_09742	uncharacterized protein	1.606			
FFUJ_00776	probable heat shock protein 70 (hsp70)	1.601			
FFUJ_03384	related to SCS3 Inositol phospholipid synthesis protein	1.598	0.714		0.852
FFUJ_00499	uncharacterized protein	1.597	1.359		
FFUJ_13534	related to FMP25 Found in Mitochondrial Proteome	1.596			
FFUJ_06096	uncharacterized protein	1.593	2.744		
FFUJ_10397	uncharacterized protein	1.592			
FFUJ_07503	related to aldehyde dehydrogenase	1.590			1.983
FFUJ_01563	uncharacterized protein	1.590	1.283		
FFUJ_04805	related to A.thaliana hyp1 protein	1.585	0.880		
FFUJ_05051	uncharacterized protein	1.582			
FFUJ_01363	related to Zn-dependent oxidoreductases	1.581			
FFUJ_08273	related to AVO2 Component of a complex containing the Tor2p kinase and other proteins%2C which may have a role in regulation of cell growth	1.580			
FFUJ_07852	uncharacterized protein	1.575	1.420	-1.618	-1.478
FFUJ_13700	uncharacterized protein	1.574			
FFUJ_11510	related to polyamine oxidase precursor	1.572			1.294
FFUJ_04158	related to human PTC protein involved in nevoid basal cell carcinoma syndrome	1.572			1.080
FFUJ_13701	related to light induced alcohol dehydrogenase Bli-4	1.559			
FFUJ_14814	related to heterokaryon incompatibility protein (het-6OR allele)	1.559			1.319
FFUJ_03311	LEU2-Beta-isopropyl-malate dehydrogenase	1.557			
FFUJ_11239	related to aldehyde-alcohol dehydrogenase	1.552			
FFUJ_04162	probable NADH2 dehydrogenase (ubiquinone) flavoprotein 1 precursor	1.551			
FFUJ_13776	uncharacterized protein	1.551			
FFUJ_03782	mannitol dehydrogenase	1.539			0.981
FFUJ_00231	uncharacterized protein	1.538			
FFUJ_01589	uncharacterized protein	1.537			
FFUJ_14686	related to monooxigenase	1.536	1.808		
FFUJ_03526	uncharacterized protein	1.532			1.171
FFUJ_12986	uncharacterized protein	1.532			1.145
FFUJ_14179	uncharacterized protein	1.522			
FFUJ_00721	uncharacterized protein	1.520			1.467
FFUJ_02280	related to histidine kinase	1.518	1.583		
FFUJ_02977	related to sucrose transporter SUT1D	1.516	1.082		
FFUJ_14635	related to POX1-acyl-CoA oxidase	1.514			1.103
FFUJ_04669	related to helicase-like transcription factor	1.512	1.212		
FFUJ_05729	uncharacterized protein	1.509	1.634		
FFUJ_08733	related to F1F0-ATPase complex assembly protein ATP11	1.505	0.978		
FFUJ_03508	related to transporter-like protein CTL2	1.504	0.855		1.150
FFUJ_00473	related to pisatin demethylase (cytochrome P450)	1.504			
FFUJ_00243	uncharacterized protein	1.503			
FFUJ_02467	probable cyanate lyase	1.503			1.376
FFUJ_11979	related to fluconazole resistance protein	1.501			
FFUJ_08864	related to phosphatidylinositol/phosphatidylcholine transfer protein	1.499	1.330		
FFUJ_06818	related to multidrug efflux pump	1.498			
FFUJ_14895	related to dna polymerase delta small subunit	1.496			1.497
FFUJ_05836	related to heterokaryon incompatibility protein het-6	1.496			1.345

FFUJ_10702	related to isoamyl alcohol oxidase	1.491			2.521
FFUJ_05893	probable PCK1-phosphoenolpyruvate carboxykinase	1.489			
FFUJ_14238	uncharacterized protein	1.488	0.974		
FFUJ_09428	related to oxidoreductase	1.485			1.306
FFUJ_01647	related to putative plasma membrane protein YRO2	1.485			
FFUJ_05657	related to DNA polymerase eta	1.482			
FFUJ_08801	related to HD family hydrolase	1.482			
FFUJ_13257	uncharacterized protein	1.475	0.544	0.510	1.425
FFUJ_02489	uncharacterized protein	1.474			1.210
FFUJ_12027	related to hydrolases or acyltransferases (alpha/beta hydrolase superfamily)	1.474			
FFUJ_09102	related to putative nucleotide binding protein (NUPB)	1.473			
FFUJ_13151	related to DUF967 domain protein	1.472			
FFUJ_13522	uncharacterized protein	1.469			
FFUJ_02539	probable abc1 protein precursor	1.468			1.333
FFUJ_09471	uncharacterized protein	1.468	1.611		
FFUJ_13427	related to nik-1 protein (Os-1p protein)	1.467	1.249		
FFUJ_07875	related to P.aeruginosa regulatory protein mmsR	1.463	1.364		
FFUJ_13262	related to benzoate 4-monooxygenase cytochrome P450	1.460			
FFUJ_02368	uncharacterized protein	1.459			1.216
FFUJ_11697	uncharacterized protein	1.456			2.014
FFUJ_08978	uncharacterized protein	1.455			
FFUJ_07236	probable NADH-ubiquinone oxidoreductase 19.3 kDa subunit%2C mitochondrial precursor	1.454			
FFUJ_04323	uncharacterized protein	1.454	1.149		
FFUJ_09944	probable SOD2-superoxide dismutase (Mn) precursor%2C mitochondrial	1.452	1.456		
FFUJ_05577	related to nitrate assimilation regulatory protein nirA	1.450	1.171		
FFUJ_05522	related to oxidoreductase	1.447			1.263
FFUJ_07310	related to transcription factor atf1+	1.447			
FFUJ_09942	uncharacterized protein	1.444			
FFUJ_00792	probable methyltransferase	1.443			1.537
FFUJ_05129	uncharacterized protein	1.443			
FFUJ_10491	related to LSB3-possible role in the regulation of actin cytoskeletal organization	1.439			
FFUJ_07309	related to hexamer-binding protein HEXBP	1.439			
FFUJ_08588	uncharacterized protein	1.429	1.177		
FFUJ_11847	related to M.genitalium alanine--tRNA ligase	1.426			1.106
FFUJ_13378	uncharacterized protein	1.421			
FFUJ_07065	uncharacterized protein	1.420			
FFUJ_05926	related to triacylglycerol lipase	1.418			
FFUJ_07599	related to acyl-CoA cholesterol acyltransferase	1.418			
FFUJ_07253	probable cytochrome b5	1.417			
FFUJ_03512	probable aspartic proteinase precursor	1.417			
FFUJ_10755	related to ARCA protein	1.417			2.052
FFUJ_05760	uncharacterized protein	1.413			1.543
FFUJ_02440	related to non-ribosomal peptide synthetase	1.413			
FFUJ_05499	uncharacterized protein	1.412			
FFUJ_02892	uncharacterized protein	1.411			
FFUJ_13070	related to 24-dehydrocholesterol reductase precursor	1.410	0.971	-0.814	
FFUJ_07798	related to transcription factor medusa	1.403			
FFUJ_03236	related to CBP3-required for assembly of cytochrome bc1 complex	1.400			1.131
FFUJ_09927	uncharacterized protein	1.399	1.122		
FFUJ_01588	uncharacterized protein	1.397			1.331
FFUJ_09771	uncharacterized protein	1.397			1.438
FFUJ_08800	uncharacterized protein	1.396	1.481		
FFUJ_13670	related to YTP1	1.394	1.066		
FFUJ_04053	uncharacterized protein	1.391			1.570
FFUJ_08621	uncharacterized protein	1.391			
FFUJ_09701	related to microsomal dipeptidase precursor	1.389			
FFUJ_09324	related to putative lipid binding protein TFS1	1.383			
FFUJ_01780	related to hormone-sensitive lipase	1.379			
FFUJ_10458	probable endothiapepsin precursor	1.377			2.125
FFUJ_03847	probable Na+-transporting ATPase ENA-1 (sodium P-type ATPase ENA-1)	1.373			
FFUJ_04964	probable Lon proteinase%2C mitochondrial precursor	1.372			
FFUJ_02566	uncharacterized protein	1.364			
FFUJ_06544	uncharacterized protein	1.363			
FFUJ_04347	probable GLO1-glyoxalase I	1.362	0.625		0.935
FFUJ_05855	related to actin cytoskeleton protein (VIP1)	1.362			0.761
FFUJ_04186	uncharacterized protein	1.361			
FFUJ_14730	uncharacterized protein	1.359			0.868
FFUJ_05606	uncharacterized protein	1.359			
FFUJ_08404	uncharacterized protein	1.359	2.271		
FFUJ_12419	related to NIT3 Nitrilase	1.359			1.338
FFUJ_06057	related to carboxypeptidase	1.358	1.340		

FFUJ_06275	related to hydrolase related to dienelactone hydrolase	1.355			0.810
FFUJ_07009	related to 2`-hydroxyisoflavone reductase	1.355			
FFUJ_08458	related to actin cytoskeleton organization and biogenesis	1.351			
FFUJ_02682	uncharacterized protein	1.348			
FFUJ_01687	related to aldehyde reductase II	1.348			
FFUJ_14044	related to cytosine deaminase	1.347			2.062
FFUJ_10029	uncharacterized protein	1.345			1.423
FFUJ_07604	related to DUF159 domain protein	1.345			1.133
FFUJ_13344	uncharacterized protein	1.338	1.503		
FFUJ_03735	uncharacterized protein	1.338	1.174		
FFUJ_03043	related to MUTS protein homolog 1	1.337	1.176		
FFUJ_05780	related to nitrate assimilation regulatory protein nirA	1.337			2.472
FFUJ_07421	related to putative multidrug transporter	1.333	0.606		1.011
FFUJ_11754	uncharacterized protein	1.331			
FFUJ_03075	probable RIC1 protein	1.331			
FFUJ_07884	probable mitochondrial import inner membrane translocase subunit TIM8	1.328			0.679
FFUJ_04643	uncharacterized protein	1.325			
FFUJ_05865	related to cytochrome P450 94A1	1.322			1.883
FFUJ_02940	uncharacterized protein	1.320			
FFUJ_08574	related to lysophosphatidic acid phosphatase	1.320			0.765
FFUJ_06378	uncharacterized protein	1.319			1.319
FFUJ_08782	uncharacterized protein	1.318			1.205
FFUJ_08790	related to A.thaliana hyp1 protein	1.317			
FFUJ_07954	related to 6-hydroxy-D-nicotine oxidase	1.312			1.114
FFUJ_07139	related to lipase/serine esterase	1.303			
FFUJ_02854	related to PET127	1.296			
FFUJ_09835	probable fluconazole resistance protein	1.296			
FFUJ_10038	probable glutaredoxin	1.295			
FFUJ_01405	uncharacterized protein	1.293	1.714		
FFUJ_08788	related to alcohol oxidase	1.290			
FFUJ_00325	related to heterokaryon incompatibility protein het-6	1.288			
FFUJ_12306	related to phospholipase D	1.288			0.983
FFUJ_10825	related to 2%2C5-diketo-D-gluconic acid reductase	1.287			
FFUJ_00494	related to succinate dehydrogenase precursor	1.286			
FFUJ_06058	probable COQ3-enzyme of ubiquinone (coenzyme Q) biosynthesis	1.286	0.905		
FFUJ_07873	probable Golgi GDP-mannose transporter	1.282	1.163		
FFUJ_13553	related to DNA ligase (ATP)	1.282			1.224
FFUJ_06087	probable flavoprotein-ubiquinone oxidoreductase	1.280			
FFUJ_07059	uncharacterized protein	1.275			
FFUJ_00801	probable glucosidase I	1.272			
FFUJ_08715	uncharacterized protein	1.271			
FFUJ_13073	uncharacterized protein	1.271			
FFUJ_08650	uncharacterized protein	1.269			
FFUJ_07014	related to aerobactin siderophore biosynthesis protein iucB	1.269			
FFUJ_10618	related to dihydroflavonol-4-reductases	1.268			
FFUJ_01915	related to alcohol dehydrogenase%2C class C	1.266			
FFUJ_02666	uncharacterized protein	1.265	1.206		
FFUJ_03855	uncharacterized protein	1.259			
FFUJ_03256	uncharacterized protein	1.259	0.814		0.689
FFUJ_03185	related to members of the aldo/keto reductase family	1.256			
FFUJ_09527	uncharacterized protein	1.254	1.242		
FFUJ_07163	related to anon-37cs protein	1.253			
FFUJ_07860	related to PMU1-high copy suppressor of ts tps2 mutant phenotype	1.252			
FFUJ_14434	related to MDM35 Mitochondrial Distribution and Morphology protein	1.251			0.990
FFUJ_11058	related to aspartic proteinase OPSB	1.251	0.760		
FFUJ_02424	related to nik-1 protein (Os-1p protein)	1.250			
FFUJ_13739	related to type-III integral membrane protein%2C involved in copper and iron homeostasis	1.250			
FFUJ_05950	related to pathogenesis-related protein PR5K (thaumatin family)	1.249			
FFUJ_04403	related to bood POZ containing protein	1.248			1.114
FFUJ_13897	related to cyclin CCL1	1.248			1.549
FFUJ_09588	related to chitinase	1.246			
FFUJ_04280	related to NIPSNAP protein	1.245			
FFUJ_09800	related to multidrug resistance protein	1.243			
FFUJ_05469	related to acetyltransferase%2C GNAT family	1.242			
FFUJ_08354	uncharacterized protein	1.242			
FFUJ_09849	uncharacterized protein	1.238	1.339		
FFUJ_04257	uncharacterized protein	1.238			
FFUJ_03994	related to YPC1-Alkaline Ceramidase	1.231	1.382		
FFUJ_03432	related to Altered inheritance of mitochondria protein 1	1.231			
FFUJ_06307	related to acetyl-hydrolase	1.230			1.001
FFUJ_00998	uncharacterized protein	1.228			

FFUJ_06960	uncharacterized protein	1.227			-0.886
FFUJ_04152	related to switching protein SWI10	1.227			
FFUJ_10369	uncharacterized protein	1.227	1.555		-1.415
FFUJ_13275	related to Y.lipolytica GPR1 protein and Fun34p	1.225			
FFUJ_05065	related to phospholipase C	1.223			
FFUJ_04896	uncharacterized protein	1.220	1.638		
FFUJ_04121	related to sexual differentiation process protein	1.219			
FFUJ_04785	uncharacterized protein	1.219			0.815
FFUJ_04339	uncharacterized protein	1.218			1.324
FFUJ_06543	related to Pseudomonas L-fucose dehydrogenase	1.218			2.131
FFUJ_01869	related to MDR1-Mac1p interacting protein	1.212			0.647
FFUJ_13832	related to inositol polyphosphate 5-phosphatase ocrl-1	1.211			0.948
FFUJ_09101	probable S-adenosylmethionine decarboxylase (spe-2)	1.206	1.045		
FFUJ_05908	related to protein yhhW	1.206			
FFUJ_05050	uncharacterized protein	1.206			
FFUJ_08504	related to formaldehyde dehydrogenase	1.203			1.532
FFUJ_06866	related to fumarate reductase flavoprotein subunit precursor	1.202			
FFUJ_02959	probable UPF0047 domain protein	1.200			
FFUJ_01663	related to short-chain dehydrogenase/reductase	1.198			
FFUJ_09086	uncharacterized protein	1.198			1.494
FFUJ_01852	related to NADPH quinone oxidoreductase homolog PIG3	1.193			1.160
FFUJ_10819	uncharacterized protein	1.192			
FFUJ_11507	related to nitrate assimilation regulatory protein nirA	1.189			
FFUJ_07580	related to cat eye syndrome critical region protein 5 precursor	1.189			
FFUJ_08534	related to RNA binding protein Nrd1	1.187			
FFUJ_06990	probable benzoate 4-monooxygenase cytochrome P450	1.185			
FFUJ_04778	uncharacterized protein	1.184			
FFUJ_06556	related to NmrA-like family protein	1.183			
FFUJ_01331	uncharacterized protein	1.183			
FFUJ_08867	uncharacterized protein	1.182			
FFUJ_10765	related to beta-galactosidase	1.182			2.317
FFUJ_01434	related to triacylglycerol lipase	1.177			
FFUJ_06206	related to LIP2-lipoic acid ligase	1.176			
FFUJ_10140	uncharacterized protein	1.176			
FFUJ_01190	related to cold sensitive U2 snRNA supressor	1.175	0.464		0.872
FFUJ_08313	related to Fe/S cluster assembly protein ISA1	1.173			
FFUJ_12988	uncharacterized protein	1.173	1.331		
FFUJ_09005	uncharacterized protein	1.170			
FFUJ_13611	related to transcription factor Ask10p	1.169	0.614		
FFUJ_13607	related to jacalin-like lectin domain-containing protein	1.168			
FFUJ_04251	related to putative C2H2 zinc finger protein flbC	1.167			
FFUJ_02855	related to proteins containing regions of low-complexity	1.160			
FFUJ_05712	uncharacterized protein	1.160			
FFUJ_10026	related to carbonic anhydrase	1.158	1.672		
FFUJ_09661	uncharacterized protein	1.157	1.513		
FFUJ_02516	uncharacterized protein	1.157			
FFUJ_04270	probable Altered inheritance of mitochondria protein 31%2C mitochondrial	1.156			
FFUJ_01906	related to WSS1 Protein involved in sister chromatid separation and segregation	1.155			
FFUJ_07929	related to DNA repair helicase ERCC6	1.155			0.796
FFUJ_08941	related to vesicle-associated membrane protein 722	1.152			0.596
FFUJ_03018	uncharacterized protein	1.147	0.989		
FFUJ_11091	uncharacterized protein	1.145			
FFUJ_02466	uncharacterized protein	1.144			
FFUJ_05092	related to dihydrodipicolinate synthase	1.143			
FFUJ_11832	uncharacterized protein	1.143			
FFUJ_01725	uncharacterized protein	1.138			1.889
FFUJ_00693	uncharacterized protein	1.137	1.143		
FFUJ_00412	related to growth hormone inducible transmembrane protein	1.132			
FFUJ_09844	uncharacterized protein	1.132			
FFUJ_04374	uncharacterized protein	1.131			0.800
FFUJ_08863	related to magnesium dependent phosphatase	1.129			
FFUJ_01291	probable phenylalanine-tRNA ligase beta chain	1.128			
FFUJ_13559	related to SKI3-antiviral protein	1.128			1.013
FFUJ_01415	related to zinc-binding protein	1.128	1.191		
FFUJ_00585	related to mitochondrial hypoxia responsive domain protein	1.128			
FFUJ_11706	probable catalase 2	1.127			
FFUJ_01180	uncharacterized protein	1.127			0.807
FFUJ_01520	uncharacterized protein	1.127			0.830
FFUJ_07050	uncharacterized protein	1.124			
FFUJ_04682	related to Fe-S oxidoreductase	1.123			
FFUJ_08439	uncharacterized protein	1.123			
FFUJ_14512	reductase	1.122			

FFUJ_13797	related to HRT2-high level expression reduced Ty3 transposition	1.120			
FFUJ_14862	related to UPC2-regulatory protein involved in control of sterol uptake	1.119			
FFUJ_07189	probable NADH-ubiquinone oxidoreductase 24 kDa subunit%2C mitochondrial precursor	1.117			
FFUJ_08869	related to protein-tyrosine phosphatase	1.117			
FFUJ_08520	related to peroxisomal ATP carrier	1.116			
FFUJ_02429	uncharacterized protein	1.113			
FFUJ_04822	uncharacterized protein	1.113			1.299
FFUJ_09915	uncharacterized protein	1.112			
FFUJ_13212	uncharacterized protein	1.111			
FFUJ_11460	related to aminotriazole resistance protein	1.108			
FFUJ_01665	uncharacterized protein	1.108			
FFUJ_09595	uncharacterized protein	1.108			0.738
FFUJ_05922	related to multidrug resistance protein fnx1	1.106			
FFUJ_07561	related to Lactobacillus putative histidine protein kinase SppK	1.105			0.681
FFUJ_07275	DUF636 domain protein	1.104			
FFUJ_13889	probable conserved mitochondrial protein	1.104			
FFUJ_12158	uncharacterized protein	1.099	0.711		
FFUJ_06004	uncharacterized protein	1.099			
FFUJ_12385	uncharacterized protein	1.097			
FFUJ_07312	related to EMI5-protein required for transcriptional induction of the early meiotic-specific transcription factor IME1	1.097			
FFUJ_01493	related to acetate kinase	1.096			1.922
FFUJ_01928	probable pH-response regulator palA protein	1.096	0.793		0.475
FFUJ_04079	related to mitochondrial carrier family protein	1.095			
FFUJ_01280	probable UTR1 protein%2C associated with ferric reductase activity	1.094			
FFUJ_08605	uncharacterized protein	1.094	1.022		
FFUJ_10295	related to glucan 1%2C3-beta-glucosidase	1.091			
FFUJ_07282	related to BSC1 Transcript encoded by this ORF shows a high level of stop codon bypass	1.090			
FFUJ_13755	uncharacterized protein	1.090			
FFUJ_09381	related to pathway-specific regulatory protein nit-4	1.087			
FFUJ_14522	uncharacterized protein	1.086			
FFUJ_05605	related to sterol glucosyltransferase	1.086	0.828		
FFUJ_12290	related to proteinase inhibitor PBI2	1.085			
FFUJ_04994	probable SSC1-mitochondrial heat shock protein 70-related protein	1.085			
FFUJ_11681	related to heterokaryon incompatibility protein	1.084			
FFUJ_13613	probable LRO1-a lecithin cholesterol acyltransferase-like gene%2C mediates diacylglycerol esterification	1.083	0.930		
FFUJ_08781	uncharacterized protein	1.082	0.763		
FFUJ_07514	uncharacterized protein	1.081			
FFUJ_13443	related to Rossmann fold nucleotide-binding protein	1.081			
FFUJ_08609	probable heat shock protein HSP104 (endopeptidase Clp ATP-binding chain HSP104)	1.081			
FFUJ_04330	uncharacterized protein	1.080			
FFUJ_02416	related to nitrate reductase	1.077			
FFUJ_13345	related to lethal(2) denticleless protein	1.074			0.762
FFUJ_02510	related to cyclin dependent kinase C	1.074	1.304		
FFUJ_13757	uncharacterized protein	1.074			
FFUJ_03158	related to Putative transferase CAF17%2C mitochondrial	1.073			
FFUJ_01637	related to D-ribulokinase	1.073			
FFUJ_13273	uncharacterized protein	1.073			
FFUJ_02492	uncharacterized protein	1.072	1.009		
FFUJ_13263	related to CWH43-putative sensor/transporter protein	1.070			
FFUJ_13226	related to DNA polymerase delta subunit 4	1.070			0.945
FFUJ_01098	uncharacterized protein	1.069			
FFUJ_13779	probable NADH-ubiquinone oxidoreductase complex 1/LYR family protein	1.065			
FFUJ_13887	probable succinyl-CoA 3-ketoacid-coenzyme A transferase%2C mitochondrial precursor	1.061			
FFUJ_02780	uncharacterized protein	1.061			
FFUJ_13885	uncharacterized protein	1.060	0.890		
FFUJ_04846	probable acyl-CoA dehydrogenase short-branched chain precursor	1.060			
FFUJ_04175	probable NADH-ubiquinone oxidoreductase 30.4 kDa subunit%2C mitochondrial precursor	1.059			
FFUJ_03514	uncharacterized protein	1.058			
FFUJ_07779	related to mitochondrial intermembrane space protein Mia40	1.058			
FFUJ_07637	related to sialidase	1.056			
FFUJ_04978	uncharacterized protein	1.052			1.264
FFUJ_01895	related to DNA repair protein RAD14	1.052			

FFUJ_07047	related to FMP21 Found in Mitochondrial Proteome	1.049	0.845		
FFUJ_07286	uncharacterized protein	1.047	1.195		
FFUJ_06497	related to transmembrane transporter Liz1p	1.046			
FFUJ_12299	related to RNA-binding protein La1	1.046	0.707		
FFUJ_07780	uncharacterized protein	1.046			
FFUJ_00887	probable NADH dehydrogenase (ubiquinone) 49K chain	1.045			
FFUJ_13245	probable period clock protein FRQ	1.044			
FFUJ_01475	probable ZWF1-glucose-6-phosphate dehydrogenase	1.044			
FFUJ_13655	uncharacterized protein	1.042			0.890
FFUJ_06051	uncharacterized protein	1.042	1.605		
FFUJ_02620	probable ATP-binding cassette transporter protein YOR1	1.041			1.184
FFUJ_00379	uncharacterized protein	1.039			
FFUJ_04583	uncharacterized protein	1.036			
FFUJ_01195	probable chaperonin ClpB	1.033			
FFUJ_05181	related to interferon-regulated resistance GTP-binding protein	1.033			
FFUJ_10817	related to NonF protein%2C involved in nonactin biosynthesis	1.033			
FFUJ_13791	related to vacuolar protein sorting protein Vps66	1.032			
FFUJ_06274	related to sensory transduction histidine kinase	1.032	1.203		
FFUJ_00922	related to acetate regulatory DNA binding protein FacB	1.027	1.045		
FFUJ_06386	uncharacterized protein	1.026			
FFUJ_03264	uncharacterized protein	1.026			1.158
FFUJ_04986	related to SNARE binding protein	1.025			
FFUJ_07630	probable KES1-involved in ergosterol biosynthesis	1.024			
FFUJ_06203	related to ZSP1 Zinc Sensitive Phenotype 1	1.023			
FFUJ_12711	related to cytochrome P450 monooxigenase	1.023			1.693
FFUJ_08771	related to histidinol-phosphatase	1.023			
FFUJ_03410	related to cercosporin resistance protein	1.022			
FFUJ_01839	related to mannosylphosphorylation protein MNN4	1.021			0.622
FFUJ_10649	related to toxD gene	1.021			1.444
FFUJ_08649	probable sterol glucosyltransferase	1.020			
FFUJ_10835	related to photosystem II protein D2	1.019			
FFUJ_04941	probable heat shock protein 10 (chaperonin CPN10)	1.018			
FFUJ_06204	related to tyrosine protein kinase of the MAP kinase kinase family	1.017	1.035		
FFUJ_00447	related to DUF1275 domain protein	1.015			
FFUJ_03186	uncharacterized protein	1.013			
FFUJ_07824	uncharacterized protein	1.013	0.772		
FFUJ_09693	uncharacterized protein	1.011			
FFUJ_09662	related to XAP-5 protein	1.011	1.293		
FFUJ_12244	related to O-methylsterigmatocystin oxidoreductase	1.009			
FFUJ_10330	related to glycerol dehydrogenase	1.009			
FFUJ_03084	related to methionine adenosyltransferase regulatory beta subunit	1.009			1.103
FFUJ_00778	related to mitochondrial rRNA processing protein PRP12	1.008			
FFUJ_12179	related to 26S proteasome-associated ubiquitin carboxyl-terminal hydrolase	1.007			0.686
FFUJ_04959	uncharacterized protein	1.007	1.924		-1.607
FFUJ_11478	probable potassium transporter TRK-1	1.004			
FFUJ_13595	related to transcription factor BOM	1.004	1.304		
FFUJ_01047	related to phytase	1.004			
FFUJ_07218	uncharacterized protein	1.004			
FFUJ_05315	related to glyoxal oxidase precursor	1.002			
FFUJ_08734	uncharacterized protein	1.002			
FFUJ_03412	uncharacterized protein	1.000			
FFUJ_00446	related to MUC1 Extracellular alpha-1%2C4-glucan glucosidase	-1.001			
FFUJ_03934	uncharacterized protein	-1.001			
FFUJ_09114	related to glu/asp-tRNA amidotransferase subunit A	-1.002			
FFUJ_08057	uncharacterized protein	-1.002			
FFUJ_09524	uncharacterized protein	-1.003			
FFUJ_09658	uncharacterized protein	-1.004			
FFUJ_06946	related to pyridoxine 4-dehydrogenase	-1.006			
FFUJ_04501	uncharacterized protein	-1.008			
FFUJ_10954	uncharacterized protein	-1.009			
FFUJ_08732	related to triacylglycerol lipase	-1.010			
FFUJ_01126	related to asparagine synthases	-1.010			
FFUJ_01041	uncharacterized protein	-1.012	-0.840		
FFUJ_10936	probable GUT1-glycerol kinase	-1.012			
FFUJ_11917	uncharacterized protein	-1.012			
FFUJ_02142	related to beta transducin-like protein	-1.012			
FFUJ_11210	uncharacterized protein	-1.013			
FFUJ_12901	related to ankyrin	-1.013			
FFUJ_00060	uncharacterized protein	-1.016			
FFUJ_06283	uncharacterized protein	-1.017	-0.768		
FFUJ_12559	related to methyltransferase	-1.017			

FFUJ_09496	related to extracellular cellulase CelA/allergen Asp F7-like%2C putative	-1.019			
FFUJ_01802	uncharacterized protein	-1.019			
FFUJ_11591	uncharacterized protein	-1.019			
FFUJ_00261	related to alcohol oxidase	-1.020			
FFUJ_10947	uncharacterized protein	-1.020			
FFUJ_02360	related to multidrug resistance protein	-1.020			
FFUJ_11410	probable lactonohydrolase	-1.021		1.137	
FFUJ_14225	uncharacterized protein	-1.021			
FFUJ_02253	related to ankyrin	-1.022			
FFUJ_11295	related to integral membrane protein PTH11	-1.022	-0.785	0.956	0.703
FFUJ_05613	uncharacterized protein	-1.022	-1.264		
FFUJ_09071	putative protein	-1.022			
FFUJ_05788	related to short-chain alcohol dehydrogenase	-1.023	-1.139		
FFUJ_10864	uncharacterized protein	-1.024			
FFUJ_05841	probable GCV3-glycine decarboxylase%2C subunit H	-1.025	-1.233		
FFUJ_10413	uncharacterized protein	-1.026			
FFUJ_02824	related to AGA1 A-agglutinin anchor subunit	-1.027			
FFUJ_07466	probable potassium channel beta subunit protein	-1.029	-1.088		
FFUJ_09881	related to alpha-1%2C2-galactosyltransferase	-1.030	-0.847		
FFUJ_02050	related beta-lactamase	-1.030			
FFUJ_04241	probable CDC11-septin	-1.031			
FFUJ_11964	uncharacterized protein	-1.032			
FFUJ_06088	related to Meiotically up-regulated gene 157 protein	-1.033			
FFUJ_04566	related to transcription activator	-1.034			
FFUJ_06517	related to novobiocin biosynthesis protein novR	-1.035			
FFUJ_00675	uncharacterized protein	-1.036			
FFUJ_08619	related to DUF453 domain protein	-1.037			
FFUJ_04216	probable Metacaspase-1	-1.037	-0.809		
FFUJ_03388	beta-tubulin	-1.037			
FFUJ_05694	uncharacterized protein	-1.037	-0.718		
FFUJ_03109	related to von Willebrand and RING finger domain protein	-1.038	-0.706		
FFUJ_13105	related to PDR16 protein	-1.039			
FFUJ_13565	probable xylulose-5-phosphate phosphoketolase	-1.041	-1.595		
FFUJ_05149	uncharacterized protein	-1.041			
FFUJ_04862	probable rho GDP dissociation inhibitor	-1.042			
FFUJ_11063	related to fructosyl amino acid oxidase	-1.042			-1.254
FFUJ_03187	probable beta-glucosidase	-1.043			
FFUJ_13116	uncharacterized protein	-1.044			
FFUJ_12555	uncharacterized protein	-1.044			
FFUJ_03524	related to coactosin	-1.045			
FFUJ_03693	related to aldehyde dehydrogenase	-1.046			
FFUJ_08727	related to cyclopropane-fatty-acyl-phospholipid synthase	-1.047			
FFUJ_09357	related to integral membrane protein PTH11	-1.049	-0.776	0.827	
FFUJ_00193	related to capsule-associated protein	-1.051			
FFUJ_04734	related to zinc/cadmium resistance protein	-1.054	-1.776		
FFUJ_01913	related to kinesin-like protein	-1.056			
FFUJ_07158	related to tol protein	-1.056			
FFUJ_06935	related to zinc finger protein	-1.056	-0.880		
FFUJ_11524	uncharacterized protein	-1.056			
FFUJ_12564	related to transmembrane transporter Liz1p	-1.056			
FFUJ_06734	related to nitrate assimilation regulatory protein nirA	-1.057			
FFUJ_14738	probable zinc-binding oxidoreductase	-1.058			
FFUJ_13285	related to acetoacetyl-CoA synthetase	-1.059			
FFUJ_02644	uncharacterized protein	-1.060			
FFUJ_00444	related to novobiocin biosynthesis protein novR	-1.060			
FFUJ_05817	uncharacterized protein	-1.060			
FFUJ_06868	uncharacterized protein	-1.062			
FFUJ_06666	related to myo-inositol transport protein ITR1	-1.062			-1.224
FFUJ_08009	related to transcriptional regulator	-1.062			
FFUJ_14736	uncharacterized protein	-1.062			
FFUJ_11549	related to aromatic-L-amino-acid decarboxylase	-1.063			
FFUJ_00169	uncharacterized protein	-1.065			
FFUJ_00018	related to ketoreductase	-1.065			
FFUJ_13315	related to endo-1%2C3(4)-beta-glucanase	-1.065			
FFUJ_10658	related to microcin C7 self-immunity protein mccF	-1.066			
FFUJ_06488	uncharacterized protein	-1.066			
FFUJ_12837	related to thermostable alkaline protease precursor	-1.067			-1.277
FFUJ_14901	uncharacterized protein	-1.068			
FFUJ_12927	uncharacterized protein	-1.068			
FFUJ_05057	uncharacterized protein	-1.068	-0.885		
FFUJ_08571	uncharacterized protein	-1.069			
FFUJ_07152	related to DOT5-involved in derepression of telomeric silencing	-1.069			
FFUJ_02708	uncharacterized protein	-1.070			
FFUJ_11414	related to beta transducin-like protein	-1.070			
FFUJ_13952	uncharacterized protein	-1.071			

FFUJ_05567	uncharacterized protein	-1.074			
FFUJ_03876	related to heterokaryon incompatibility protein (het-6OR allele)	-1.077	-1.167		
FFUJ_06905	uncharacterized protein	-1.078			
FFUJ_13640	probable delta 8-sphingolipid desaturase	-1.079			
FFUJ_10865	uncharacterized protein	-1.079			
FFUJ_05842	probable glycine decarboxylase P subunit	-1.079	-1.263		-0.649
FFUJ_03841	uncharacterized protein	-1.080			
FFUJ_11944	uncharacterized protein	-1.081			
FFUJ_06827	related to potential drug facilitator PEP5	-1.081			
FFUJ_03498	uncharacterized protein	-1.081			
FFUJ_11786	related to methyltransferase	-1.082			
FFUJ_05510	related beta-lactamase	-1.083			-1.868
FFUJ_11748	probable DFG5 protein	-1.085			
FFUJ_10638	uncharacterized protein	-1.086			
FFUJ_07318	uncharacterized protein	-1.086			
FFUJ_00206	HET-6OR heterokaryon incompatibility protein (het-6OR allele)	-1.089			
FFUJ_14503	uncharacterized protein	-1.091			
FFUJ_04441	probable MET13-putative methylene tetrahydrofolate reductase	-1.097			
FFUJ_02788	uncharacterized protein	-1.097			
FFUJ_09446	related to glu/asp-tRNA amidotransferase subunit A	-1.098			
FFUJ_10863	uncharacterized protein	-1.099			
FFUJ_00024	uncharacterized protein	-1.101			
FFUJ_12664	uncharacterized protein	-1.101			
FFUJ_12701	related to methyltransferase	-1.102			
FFUJ_12033	related to transcription activator protein acu-15	-1.106			
FFUJ_02623	related to CSI2 protein	-1.107	-0.888		
FFUJ_06434	related to GABA transport protein	-1.108			
FFUJ_04497	uncharacterized protein	-1.108			
FFUJ_00192	uncharacterized protein	-1.110			
FFUJ_02976	uncharacterized protein	-1.110			
FFUJ_12015	related to monooxygenase	-1.111			
FFUJ_02269	related to HOL1-Putative substrate-H+ antiporter-unknown biological function	-1.112			
FFUJ_05289	related to delta-12 fatty acid desaturase	-1.112			
FFUJ_11937	related to tol protein	-1.113			
FFUJ_10634	uncharacterized protein	-1.114			
FFUJ_14850	uncharacterized protein	-1.114			
FFUJ_09974	uncharacterized protein	-1.115			
FFUJ_03873	related to allantoate permease	-1.115			
FFUJ_02250	related to phthalate 4%2C5-dioxygenase oxygenase reductase subunit	-1.115			
FFUJ_08392	related to C6 zink-finger protein PRO1A	-1.115	-1.412		
FFUJ_04783	probable isopentenyl-diphosphate delta-isomerase	-1.116	-0.956		
FFUJ_01429	probable alpha-glucosidase (maltase)	-1.117			
FFUJ_14752	uncharacterized protein	-1.119			-1.128
FFUJ_07775	uncharacterized protein	-1.120			-1.113
FFUJ_08892	related to heterokaryon incompatibility protein (het-6OR allele)	-1.120			
FFUJ_02568	probable cell division control protein CDC12	-1.120			
FFUJ_13083	uncharacterized protein	-1.121			
FFUJ_12092	uncharacterized protein	-1.122			
FFUJ_09395	uncharacterized protein	-1.123			
FFUJ_08024	related to dibenzothiophene desulfurization enzyme C%2C thermophilic	-1.123			
FFUJ_02053	probable acetyl-CoA synthetase	-1.124			
FFUJ_02502	related to secretory pathway protein YSY6	-1.124			
FFUJ_10637	uncharacterized protein	-1.125			
FFUJ_09144	uncharacterized protein	-1.126			
FFUJ_07918	related to glucosyltransferase	-1.126	-1.254		
FFUJ_13230	probable ATP citrate lyase subunit 2	-1.129			
FFUJ_02642	related to exo-alpha-sialidase / neuraminidase	-1.130			
FFUJ_10945	related to prenyl cysteine carboxyl methyltransferase	-1.130			
FFUJ_08828	related to monooxygenase	-1.132			
FFUJ_07959	related to beta-glucosidase	-1.133			
FFUJ_10586	uncharacterized protein	-1.135			
FFUJ_14338	related to het-6-heterokaryon incompatibility protein	-1.135			
FFUJ_08091	uncharacterized protein	-1.135			
FFUJ_07985	uncharacterized protein	-1.136			
FFUJ_05165	uncharacterized protein	-1.136			
FFUJ_02105	polyketide synthase	-1.140			
FFUJ_14853	uncharacterized protein	-1.141			
FFUJ_11582	related to cholinesterase	-1.146			
FFUJ_10478	uncharacterized protein	-1.149			
FFUJ_09883	uncharacterized protein	-1.150	-1.141		

FFUJ_01008	related to phenol 2-monooxygenase	-1.151	-1.090		
FFUJ_06392	uncharacterized protein	-1.152			
FFUJ_10479	uncharacterized protein	-1.152			
FFUJ_00667	uncharacterized protein	-1.152			
FFUJ_10937	related to channel proteins	-1.153			
FFUJ_13235	uncharacterized protein	-1.157	-1.162		
FFUJ_00961	related to programmed cell death protein (calcium-binding protein)	-1.157	-0.771		
FFUJ_05278	uncharacterized protein	-1.158			
FFUJ_05374	related to ROT2-glucosidase II%2C catalytic subunit	-1.158			
FFUJ_01333	uncharacterized protein	-1.159			
FFUJ_10464	related to D-arabinitol 2-dehydrogenase	-1.162			-3.023
FFUJ_06414	uncharacterized protein	-1.162			
FFUJ_01427	related to ECM39 protein%2C involved in cell wall biogenesis and architecture	-1.162	-1.082		
FFUJ_08095	related to methyltransferase	-1.162			
FFUJ_06422	related to cocaine esterase	-1.163			
FFUJ_01179	probable cytochrome P450 51 (eburicol 14 alpha-demethylase)	-1.164			
FFUJ_10889	galactose oxidase precursor	-1.169		-2.954	-3.094
FFUJ_08417	uncharacterized protein	-1.169			
FFUJ_14791	probable sulfate permease II	-1.169			
FFUJ_09088	related to LCB2-serine C-palmitoyltransferase subunit	-1.172			
FFUJ_13231	probable ATP citrate lyase subunit 1	-1.178			
FFUJ_09916	uncharacterized protein	-1.179			
FFUJ_11203	related to O-methylsterigmatocystin oxidoreductase	-1.179	-1.040		
FFUJ_04388	related to tyrosinase precursor	-1.180			
FFUJ_14576	uncharacterized protein	-1.184			
FFUJ_02023	uncharacterized protein	-1.186			
FFUJ_12461	related to ankyrin 3	-1.187			
FFUJ_09568	related to NADPH oxidase cytosolic protein p67phox	-1.188			
FFUJ_10923	related to integral membrane protein	-1.188			
FFUJ_11642	related to glutamyl-tRNA	-1.189			
FFUJ_08877	related to methyltransferase	-1.190			
FFUJ_02544	related to calcium-independent phospholipase A2	-1.192			
FFUJ_09917	related to L-2.3-butanediol dehydrogenase	-1.194			
FFUJ_12097	uncharacterized protein	-1.196			
FFUJ_11396	uncharacterized protein	-1.199			
FFUJ_12584	uncharacterized protein	-1.205	-0.725	-1.551	-2.045
FFUJ_14593	uncharacterized protein	-1.206			
FFUJ_06660	related to ankyrin 1	-1.207		-1.119	-1.703
FFUJ_03013	related to ELMO2 protein	-1.207	-1.271		
FFUJ_13836	probable ammonium transporter MEPa	-1.208			
FFUJ_01083	related to calcium-related spray protein	-1.211			
FFUJ_08586	related to ATX2-Putative Golgi transporter involved in homeostasis of manganese ions	-1.211	-0.990		
FFUJ_05429	uncharacterized protein	-1.211			
FFUJ_02982	uncharacterized protein	-1.212			
FFUJ_08055	related to aminopeptidase	-1.213	-1.375		
FFUJ_06224	probable septin aspE	-1.213	-0.973		
FFUJ_14739	related to ZRT1 Zinc transporter I	-1.214			
FFUJ_11770	uncharacterized protein	-1.214			
FFUJ_08463	probable alpha-glucoside transport protein	-1.218	-1.080		
FFUJ_01338	related to PPN1-vacuolar endopolyphosphatase	-1.218			
FFUJ_02276	uncharacterized protein	-1.219			
FFUJ_09145	related to galactose oxidase precursor	-1.220			
FFUJ_14359	related to heterokaryon incompatibility protein het-6	-1.221	-0.971		
FFUJ_03593	uncharacterized protein	-1.222			
FFUJ_00614	probable alpha-tubulin B	-1.223			
FFUJ_12098	uncharacterized protein	-1.223			
FFUJ_12189	related to malate dehydrogenase	-1.223			
FFUJ_06887	probable ASP3-1-L-asparaginase II	-1.224			
FFUJ_07342	uncharacterized protein	-1.224			
FFUJ_00274	related to heterokaryon incompatibility protein (het-6OR allele)	-1.224	-0.971		
FFUJ_02801	related to krueppel protein	-1.226	-1.603		
FFUJ_05494	related to GNAT family acetyltransferase	-1.226	-1.077		-1.194
FFUJ_10044	uncharacterized protein	-1.228			
FFUJ_13981	uncharacterized protein	-1.229			
FFUJ_01055	related to major facilitator MirA	-1.229			
FFUJ_14607	probable pantothenate kinase	-1.229			
FFUJ_12341	uncharacterized protein	-1.230			
FFUJ_00634	probable aldehyde dehydrogenase	-1.237			
FFUJ_05840	probable glycine hydroxymethyltransferase	-1.239	-1.442		
FFUJ_14039	uncharacterized protein	-1.240			
FFUJ_11413	uncharacterized protein	-1.240			
FFUJ_06863	uncharacterized protein	-1.240			

FFUJ_13348	related to acriflavine sensitivity control protein ACR-2	-1.242	-1.154		
FFUJ_08040	uncharacterized protein	-1.243			
FFUJ_14691	related to aminotransferase GliI	-1.243			
FFUJ_11073	uncharacterized protein	-1.243			
FFUJ_08386	uncharacterized protein	-1.244			
FFUJ_14591	uncharacterized protein	-1.244			
FFUJ_02062	uncharacterized protein	-1.245			
FFUJ_09327	related to O-methylsterigmatocystin oxidoreductase	-1.246			
FFUJ_11173	uncharacterized protein	-1.247			
FFUJ_02347	uncharacterized protein	-1.247			
FFUJ_06431	uncharacterized protein	-1.249			
FFUJ_04739	related to C2H2 zinc finger protein	-1.252			
FFUJ_10942	uncharacterized protein	-1.255			
FFUJ_03541	Weak similarity to Y.pseudotuberculosis CDP-3%2C6-dideoxy-D-glycero-L-glycero-4-hexulose-5-epimerase	-1.258			-1.074
FFUJ_07109	probable beta transducin-like protein	-1.259			
FFUJ_06103	probable glucosamine-6-phosphate isomerase	-1.259	-1.069		
FFUJ_11409	uncharacterized protein	-1.259	-0.797		
FFUJ_05120	related to putative tartrate transporter	-1.261			
FFUJ_02007	related to tol protein	-1.261			
FFUJ_12551	related to pisatin demethylase cytochrome P450	-1.262			
FFUJ_11725	uncharacterized protein	-1.263			
FFUJ_11138	uncharacterized protein	-1.263			
FFUJ_07688	uncharacterized protein	-1.263			
FFUJ_14737	uncharacterized protein	-1.266	-0.813		
FFUJ_10699	related to DFG5 protein	-1.267			
FFUJ_04397	beta-tubulin	-1.268			
FFUJ_02631	probable C-8 sterol isomerase erg-1	-1.268			
FFUJ_00653	uncharacterized protein	-1.269			
FFUJ_09973	related to glucose transporter-3	-1.274			
FFUJ_07117	uncharacterized protein	-1.274			
FFUJ_02643	related to amino-terminal amidase	-1.274			
FFUJ_10467	uncharacterized protein	-1.278	-0.917		
FFUJ_05500	related to TAM domain methyltransferase	-1.280			
FFUJ_02685	related to acid phosphatase	-1.282			-1.133
FFUJ_04406	uncharacterized protein	-1.283			
FFUJ_11142	probable general amino acid permease	-1.287			
FFUJ_10055	fusarin C cluster-peptidase	-1.288			
FFUJ_10981	uncharacterized protein	-1.288			
FFUJ_00530	probable zinc finger protein white collar 2 (wc-2)	-1.288			
FFUJ_14108	uncharacterized protein	-1.289			
FFUJ_03884	related to cell division control protein/predicted DNA repair exonuclease	-1.289	-1.075		
FFUJ_14611	uncharacterized protein	-1.292			
FFUJ_00589	probable class I alpha-mannosidase	-1.292	-0.739		
FFUJ_12846	uncharacterized protein	-1.292			
FFUJ_00187	related to nicotinamide mononucleotide permease	-1.293			
FFUJ_10493	related to putative tartrate transporter	-1.296			
FFUJ_14713	uncharacterized protein	-1.296			
FFUJ_14631	uncharacterized protein	-1.296			
FFUJ_03905	related to 3-oxoacyl-[acyl-carrier-protein] reductase	-1.298			-0.719
FFUJ_10399	uncharacterized protein	-1.301	-1.135		
FFUJ_10156	uncharacterized protein	-1.303	-0.880		
FFUJ_08919	related to beta-1%2C4-mannosyl-glycoprotein 4-beta-N-acetylglucosaminyltransferase	-1.303			
FFUJ_13024	probable protein urg3	-1.304	-0.883		
FFUJ_14371	related to D-mandelate dehydrogenase	-1.305			
FFUJ_02052	uncharacterized protein	-1.307	-0.798		
FFUJ_02521	related to GNT1 alphaN-acetylglucosamine transferase K. lactis	-1.307			
FFUJ_11756	related to integral membrane protein PTH11	-1.310			
FFUJ_10308	related to integral membrane protein	-1.310			
FFUJ_00527	related to flavin-containing monooxygenase	-1.313			
FFUJ_06864	related to HXT3-Low-affinity hexose facilitator	-1.313	-1.230		
FFUJ_11548	uncharacterized protein	-1.315			
FFUJ_10995	related to triacylglycerol lipase II precursor	-1.315			
FFUJ_04119	related to CRH1-family of putative glycosidases might exert a common role in cell wall organization	-1.316	-1.119		
FFUJ_03542	related to C6 finger domain protein	-1.321			-1.110
FFUJ_00265	related to HNM1-Choline permease	-1.323			
FFUJ_07400	uncharacterized protein	-1.324	-0.985		
FFUJ_02036	uncharacterized protein	-1.324			
FFUJ_14774	uncharacterized protein	-1.325			
FFUJ_03880	uncharacterized protein	-1.332			
FFUJ_00689	related to TOS1 Target of SBF	-1.334		-2.671	-2.646
FFUJ_09604	related to integral membrane protein	-1.334	-1.184		
FFUJ_09686	related to glycosyl transferase	-1.335			

FFUJ_09683	probable chitosanase precursor	-1.337			
FFUJ_10853	related to Putative sterigmatocystin biosynthesis lipase/esterase STCI	-1.339			-1.604
FFUJ_04033	uncharacterized protein	-1.341			-1.224
FFUJ_00082	uncharacterized protein	-1.341			
FFUJ_08031	related to pisatin demethylase	-1.343			
FFUJ_10712	related to DHA14-like major facilitator efflux transporter (MFS transporter)	-1.343			
FFUJ_11840	uncharacterized protein	-1.344			
FFUJ_11332	PRC1-Carboxypeptidase y%2C serine-type protease	-1.345			
FFUJ_14797	related to dehydrogenase/reductase SDR family member 7 precursor	-1.346			
FFUJ_10450	related to integral membrane protein PTH11	-1.352			
FFUJ_14592	probable fusarubin cluster-esterase	-1.352	-1.125		
FFUJ_05917	related to Fre1p and Fre2p	-1.354			
FFUJ_00414	related to TIM barrel metal-dependent hydrolase	-1.354	-1.200		
FFUJ_01973	related to uracil permease	-1.355	-1.288		
FFUJ_12410	related to integral membrane protein PTH11	-1.356			
FFUJ_11913	uncharacterized protein	-1.358	-1.043		
FFUJ_02284	related to tol protein	-1.360			
FFUJ_09912	related to ankyrin 1	-1.362			
FFUJ_09794	uncharacterized protein	-1.363			
FFUJ_10557	related to PMU1-high copy suppressor of ts tps2 mutant phenotype	-1.363	-1.269		
FFUJ_12446	related to tol protein	-1.365			
FFUJ_05036	related to Uth1p%2C Nca3p%2C YIL123w and Sun4p	-1.366			
FFUJ_14601	uncharacterized protein	-1.368			-1.552
FFUJ_13228	probable CDC10 cell division control protein 10	-1.370			
FFUJ_02305	uncharacterized protein	-1.371			
FFUJ_10866	uncharacterized protein	-1.374			
FFUJ_02769	uncharacterized protein	-1.377	-1.091		
FFUJ_07769	uncharacterized protein	-1.378			
FFUJ_02289	related to Dextranase	-1.379			
FFUJ_09536	uncharacterized protein	-1.382			
FFUJ_11334	uncharacterized protein	-1.384			
FFUJ_09687	uncharacterized protein	-1.385			
FFUJ_03662	related to tol protein	-1.386			
FFUJ_11995	uncharacterized protein	-1.386			
FFUJ_04466	uncharacterized protein	-1.387			
FFUJ_04747	related to endo-1%2C6-alpha-D-mannanase	-1.388			
FFUJ_00374	related to oxidoreductase	-1.391			
FFUJ_02116	probable L-lactate dehydrogenase (cytochrome)	-1.396			
FFUJ_11727	related to small s protein	-1.396			-1.737
FFUJ_06408	uncharacterized protein	-1.398			
FFUJ_06754	uncharacterized protein	-1.401			
FFUJ_13987	uncharacterized protein	-1.406			
FFUJ_03540	uncharacterized protein	-1.406	-0.881		
FFUJ_10338	related to calcium-independent phospholipase A2	-1.406			
FFUJ_10743	related to integral membrane protein PTH11	-1.406			
FFUJ_10881	uncharacterized protein	-1.410	-0.996		
FFUJ_06617	uncharacterized protein	-1.412			
FFUJ_03599	related to N-carbamoyl-L-amino acid hydrolase	-1.418			
FFUJ_08799	related to chitin binding protein	-1.419		1.641	
FFUJ_02838	probable DFG5 protein	-1.422			
FFUJ_01605	uncharacterized protein	-1.425			
FFUJ_05467	related to Amid-like NADH oxidoreductase	-1.426			-0.929
FFUJ_02098	related to helix-loop-helix protein	-1.427			
FFUJ_11465	uncharacterized protein	-1.427			
FFUJ_10378	related to lipase 1	-1.428			
FFUJ_02256	related to methyltransferase	-1.428			
FFUJ_02349	related to transcription co-repressor GAL80	-1.429			
FFUJ_12448	related to GAL4-like transcriptional activator	-1.433			
FFUJ_03839	uncharacterized protein	-1.433	-1.259		
FFUJ_12654	related to GrpB domain protein	-1.433			
FFUJ_06119	related to glucosidase II%2C alpha subunit	-1.434			
FFUJ_05673	related to alpha-1%2C6-mannosyltransferase HOC1	-1.435	-1.043		
FFUJ_12847	related to pisatin demethylase (cytochrome P450)	-1.437			
FFUJ_14709	related to Transaldolase B	-1.438			
FFUJ_09277	uncharacterized protein	-1.438	-0.955		
FFUJ_07733	uncharacterized protein	-1.441		-2.079	-2.433
FFUJ_06413	uncharacterized protein	-1.443			
FFUJ_01056	related to GNAT family acetyltransferase	-1.445	-1.099		
FFUJ_12798	uncharacterized protein	-1.451			
FFUJ_00723	related to morphogenesis-related protein MSB1	-1.452			
FFUJ_09994	uncharacterized protein	-1.454			
FFUJ_12882	uncharacterized protein	-1.457			-1.732

FFUJ_06663	SRY1-Not a Serine Racemase of Yeast%2C threo-3-hydroxyaspartate ammonia-lyase activity	-1.460			
FFUJ_07919	related to EMP47 Golgi membrane protein	-1.460	-1.497		
FFUJ_14349	uncharacterized protein	-1.462			
FFUJ_11388	uncharacterized protein	-1.462			
FFUJ_10294	uncharacterized protein	-1.466			
FFUJ_07684	uncharacterized protein	-1.470	-1.556		
FFUJ_14030	uncharacterized protein	-1.473	-1.322	1.336	1.179
FFUJ_10632	related to ankyrin	-1.478			
FFUJ_03846	uncharacterized protein	-1.479			-2.145
FFUJ_12583	uncharacterized protein	-1.481		-1.624	-2.000
FFUJ_02481	probable cyclophilin	-1.482	-1.510		
FFUJ_05843	uncharacterized protein	-1.482			
FFUJ_05290	uncharacterized protein	-1.484			
FFUJ_14918	uncharacterized protein	-1.484			
FFUJ_10911	uncharacterized protein	-1.486			
FFUJ_14341	related to phosphoglycerate mutase family protein	-1.487			
FFUJ_03086	probable farnesyl-pyrophosphate synthetase	-1.487			
FFUJ_04639	uncharacterized protein	-1.488			
FFUJ_01967	uncharacterized protein	-1.489			
FFUJ_05958	uncharacterized protein	-1.490			
FFUJ_03900	related to proteoglycan	-1.491		1.215	
FFUJ_12462	uncharacterized protein	-1.492	-1.113	1.251	
FFUJ_07428	related to phospholipid-translocating ATPase	-1.493	-1.254		
FFUJ_14505	uncharacterized protein	-1.496			
FFUJ_02387	uncharacterized protein	-1.496			
FFUJ_08089	uncharacterized protein	-1.497		1.107	
FFUJ_05362	probable mutanase (glucan endo-1%2C3-alpha-glucosidase)	-1.499			
FFUJ_08181	related to TAM domain methyltransferase	-1.500	-1.272		
FFUJ_05415	uncharacterized protein	-1.500			
FFUJ_14773	uncharacterized protein	-1.500			
FFUJ_14675	related to laccase precursor	-1.502			
FFUJ_14034	related to dihydrodipicolinate synthetase	-1.502			
FFUJ_13281	uncharacterized protein	-1.505			
FFUJ_12663	related to integral membrane protein	-1.511			
FFUJ_09518	related to O-methyltransferase B	-1.511	-1.314		
FFUJ_09369	uncharacterized protein	-1.514	-1.445		
FFUJ_09680	uncharacterized protein	-1.514			
FFUJ_07519	uncharacterized protein	-1.516			
FFUJ_05560	related to dis1-suppressing protein kinase dsk1	-1.516			
FFUJ_10234	related to beta-mannosidase	-1.517			
FFUJ_02590	uncharacterized protein	-1.517			
FFUJ_09067	uncharacterized protein	-1.524			
FFUJ_14540	related to Proline racemase	-1.524	-0.839		
FFUJ_11325	related to SUR1-required for mannosylation of sphingolipids	-1.526	-1.379		
FFUJ_03633	probable dityrosine transporter	-1.529			
FFUJ_10887	related to beta-galactosidase	-1.532			
FFUJ_12735	uncharacterized protein	-1.532			
FFUJ_07174	related to DUF6 domain protein	-1.535	-1.159		
FFUJ_06071	uncharacterized protein	-1.539			
FFUJ_00094	uncharacterized protein	-1.540			
FFUJ_07053	uncharacterized protein	-1.540			
FFUJ_14856	related to carboxypeptidase A	-1.540			
FFUJ_13719	uncharacterized protein	-1.544			
FFUJ_03292	probable DDR48-heat shock protein	-1.544	-1.141		
FFUJ_14584	uncharacterized protein	-1.547			
FFUJ_10772	uncharacterized protein	-1.548			
FFUJ_05746	related to major facilitator MirA	-1.548		-2.914	-3.852
FFUJ_02707	related to integral membrane protein pth11	-1.550	-1.181	0.765	
FFUJ_08179	related to integral membrane protein PTH11	-1.551			
FFUJ_07905	uncharacterized protein	-1.551	-1.227		
FFUJ_08452	uncharacterized protein	-1.551	-2.185		0.926
FFUJ_03823	related to aspartate--tRNA ligase%2C mitochondrial	-1.553			
FFUJ_05491	uncharacterized protein	-1.556			
FFUJ_04215	related to NPL3-nucleolar protein	-1.557	-1.198		
FFUJ_08129	related to DUF124 domain protein	-1.559			
FFUJ_03047	uncharacterized protein	-1.559			
FFUJ_10053	fusarin C cluster-transporter	-1.559			
FFUJ_11383	related to tol protein	-1.563			
FFUJ_14693	related to multidrug resistance protein fnx1	-1.564			
FFUJ_11839	related to GABA permease	-1.569			
FFUJ_02314	uncharacterized protein	-1.570			
FFUJ_11523	related to PHO12-secreted acid phosphatase	-1.570			
FFUJ_10271	related to formaldehyde dehydrogenase	-1.573			
FFUJ_06420	related to Oxidoreductase	-1.577			
FFUJ_13029	uncharacterized protein	-1.577			
FFUJ_03881	uncharacterized protein	-1.579	-1.200		

FFUJ_06882	probable protein disulfide-isomerase precursor	-1.586			
FFUJ_10754	related to benzoate 4-monooxygenase cytochrome P450	-1.587			
FFUJ_09074	related to zinc finger protein odd-paired-like (opl)	-1.589			
FFUJ_04046	related to 3-isopropylmalate dehydrogenase	-1.590			
FFUJ_06665	related to tol protein	-1.592			
FFUJ_10449	related to alcohol oxidase	-1.594			
FFUJ_01732	probable D-xylose reductase	-1.595	-2.127	0.831	1.349
FFUJ_05909	related to endochitinase 2 precursor	-1.597		1.761	1.430
FFUJ_02785	related to C6 zink-finger protein PRO1A	-1.598	-1.699		
FFUJ_06120	related to beta-glucosidase	-1.601			
FFUJ_04145	probable hydroxymethylglutaryl-CoA synthase	-1.601			
FFUJ_05561	related to myc-type bHLH transcription factor	-1.604	-2.109		
FFUJ_09684	uncharacterized protein	-1.607			
FFUJ_09501	uncharacterized protein	-1.607			
FFUJ_14539	uncharacterized protein	-1.607	-1.350		
FFUJ_04815	probable peptidylprolyl isomerase (FK506-binding protein homolog)	-1.609			
FFUJ_08768	related to Erv1p and rat ALR protein	-1.610	-1.329		
FFUJ_08575	related to RNA binding protein Nrd1	-1.613	-1.227		
FFUJ_04037	related to heterokaryon incompatibility protein	-1.615	-1.437		
FFUJ_00197	related to nucleoside-diphosphate-sugar epimerase	-1.617	-1.582		
FFUJ_04021	probable SIT1-Transporter of the bacterial siderophore ferrioxamine B	-1.619	-1.056		
FFUJ_08150	uncharacterized protein	-1.619	-0.916		
FFUJ_03598	related to allantoate transport protein	-1.620			
FFUJ_05398	related to monomeric sarcosine oxidase	-1.623			
FFUJ_03882	uncharacterized protein	-1.625	-1.242		
FFUJ_05777	uncharacterized protein	-1.626			
FFUJ_11579	uncharacterized protein	-1.628			
FFUJ_04207	related to monocarboxylate transporter 2	-1.629			
FFUJ_09276	uncharacterized protein	-1.631			
FFUJ_07325	related to acetyl coenzyme A synthetase	-1.633			-1.545
FFUJ_11454	related to methyltransferase	-1.635	-1.538		
FFUJ_04295	uncharacterized protein	-1.637			
FFUJ_12589	uncharacterized protein	-1.639			
FFUJ_10563	related to interferon-regulated resistance GTP-binding protein	-1.642			
FFUJ_06445	uncharacterized protein	-1.643	-1.332		
FFUJ_11994	probable branched-chain amino acids aminotransferase	-1.645			
FFUJ_11365	related to fructosyl amino acid oxidase	-1.647			
FFUJ_07765	related to sporulation-specific protein Sps2p	-1.651			
FFUJ_02180	related to methyltransferase	-1.652			
FFUJ_02043	related to D-alanine aminotransferase	-1.654			
FFUJ_11387	probable amino acid transport protein GAP1	-1.655	-1.257		
FFUJ_06045	related to excitatory amino acid transporter	-1.657			
FFUJ_01441	probable protein disulfide-isomerase precursor	-1.657	-1.331		
FFUJ_05184	uncharacterized protein	-1.658			
FFUJ_03501	related to calpain-like protein	-1.668	-2.354		
FFUJ_09163	related to tol protein	-1.669			
FFUJ_08471	probable coproporphyrinogen oxidase precursor	-1.670	-1.431		
FFUJ_01039	related to extracellular matrix protein precursor	-1.671			
FFUJ_06921	related to sodium/nucleoside cotransporter 1	-1.672			
FFUJ_11776	uncharacterized protein	-1.672			
FFUJ_05541	uncharacterized protein	-1.674			
FFUJ_05595	probable DELTA(24)-STEROL C-METHYLTRANSFERASE (ERG6)	-1.674			
FFUJ_10428	probable cutinase 1 precursor	-1.682		-2.951	-3.067
FFUJ_02322	uncharacterized protein	-1.683			
FFUJ_06789	uncharacterized protein	-1.683			-1.924
FFUJ_14053	uncharacterized protein	-1.684			
FFUJ_10799	related to oxalate decarboxylase	-1.686			-1.944
FFUJ_09493	uncharacterized protein	-1.692	-1.713		
FFUJ_11771	uncharacterized protein	-1.696	-1.264		
FFUJ_10761	related to TOB3 (member of AAA-ATPase family)	-1.701	-1.877		-1.052
FFUJ_10877	uncharacterized protein	-1.704			
FFUJ_14616	uncharacterized protein	-1.707			
FFUJ_10326	uncharacterized protein	-1.708			
FFUJ_03465	related to aminopeptidase Y precursor%2C vacuolar	-1.712			
FFUJ_10402	related to tol protein	-1.715			
FFUJ_14832	uncharacterized protein	-1.716			
FFUJ_04022	uncharacterized protein	-1.720			
FFUJ_00099	uncharacterized protein	-1.728			
FFUJ_01609	related to hydroxyproline-rich glycoprotein precursor	-1.728	-1.479		
FFUJ_08591	uncharacterized protein	-1.730			
FFUJ_10046	uncharacterized protein	-1.731			
FFUJ_12423	uncharacterized protein	-1.731			
FFUJ_09681	uncharacterized protein	-1.733			
FFUJ_08169	related to polyamine oxidase precursor	-1.739	-1.467		

FFUJ_09072	uncharacterized protein	-1.739			
FFUJ_11122	uncharacterized protein	-1.740			
FFUJ_11859	related to methyltransferase	-1.742	-1.102		
FFUJ_14708	uncharacterized protein	-1.746			
FFUJ_06409	uncharacterized protein	-1.755			
FFUJ_07522	uncharacterized protein	-1.758	-1.324		
FFUJ_06796	probable 3-isopropylmalate dehydrogenase beta	-1.761			
FFUJ_11352	related to methyltransferase	-1.762	-1.585		
FFUJ_10180	related to antibiotic resistance protein	-1.769			
FFUJ_03678	related to ATP adenylyltransferase II	-1.773			
FFUJ_02210	related to ankyrin	-1.775			
FFUJ_10181	uncharacterized protein	-1.777			
FFUJ_00500	related to histidine kinase	-1.782	-1.214		
FFUJ_06860	related to TRI13-cytochrome P450	-1.786			
FFUJ_10179	uncharacterized protein	-1.791			
FFUJ_07037	uncharacterized protein	-1.792			-1.004
FFUJ_06662	related to microbial serine proteinase	-1.792	-1.441		-1.303
FFUJ_08448	related to lustrin A	-1.794			
FFUJ_07892	probable sterol delta 5%2C6-desaturase	-1.794	-1.990		
FFUJ_06600	uncharacterized protein	-1.794			
FFUJ_12892	related to chitinase	-1.797			
FFUJ_09343	related to class I alpha-mannosidase 1B	-1.797			
FFUJ_00198	related to ARG81-transcription factor involved in arginine metabolism	-1.798			
FFUJ_08825	uncharacterized protein	-1.803			
FFUJ_05109	uncharacterized protein	-1.806			
FFUJ_08903	uncharacterized protein	-1.807			
FFUJ_09275	related to sulfatase	-1.812			
FFUJ_14750	uncharacterized protein	-1.812	-1.806		
FFUJ_04206	related to phospholipid-translocating ATPase	-1.816	-2.046		
FFUJ_11733	uncharacterized protein	-1.816			
FFUJ_05539	related to peptide transport protein	-1.817			
FFUJ_12021	related to multidrug resistance protein	-1.823			-1.882
FFUJ_14518	related to N%2CN-dimethylglycine oxidase	-1.825			
FFUJ_04670	uncharacterized protein	-1.829			
FFUJ_03901	uncharacterized protein	-1.831			
FFUJ_14297	uncharacterized protein	-1.832	-1.621		
FFUJ_08823	uncharacterized protein	-1.833			-2.263
FFUJ_11650	uncharacterized protein	-1.833	-1.405	1.321	
FFUJ_02181	related to ceramidase	-1.834		-1.990	-2.373
FFUJ_12688	probable subtilisin-like serine protease	-1.837			
FFUJ_09281	uncharacterized protein	-1.838			-1.040
FFUJ_08044	uncharacterized protein	-1.839			
FFUJ_14117	uncharacterized protein	-1.840	-0.867		
FFUJ_06762	uncharacterized protein	-1.841			
FFUJ_02030	uncharacterized protein	-1.841			-1.554
FFUJ_04262	related to arylamine N-acetyltransferase	-1.844	-1.239		
FFUJ_05265	related to monooxigenase	-1.846			
FFUJ_01162	uncharacterized protein	-1.846	-1.375		
FFUJ_03597	uncharacterized protein	-1.851		-2.710	-3.804
FFUJ_14050	uncharacterized protein	-1.852			
FFUJ_08878	uncharacterized protein	-1.861			
FFUJ_08367	uncharacterized protein	-1.861	-1.784		
FFUJ_03265	uncharacterized protein	-1.865			
FFUJ_02037	uncharacterized protein	-1.869			
FFUJ_12020	polyketide synthase	-1.871		-1.389	-2.618
FFUJ_05308	related to MFS transporter	-1.873	-1.574		
FFUJ_10587	related to heterokaryon incompatibility protein (het-6OR allele)	-1.877			
FFUJ_02255	related to agglutinin isolectin 1 precursor	-1.878	-1.155		-1.116
FFUJ_11294	related to O-methyltransferase B	-1.883	-1.469	1.254	
FFUJ_04182	related to myosin heavy chain	-1.885	-1.435		
FFUJ_03879	uncharacterized protein	-1.885			
FFUJ_00260	related to integral membrane protein PTH11	-1.885			-1.604
FFUJ_10162	related to protein-arginine deiminase type II	-1.886			-1.512
FFUJ_05566	uncharacterized protein	-1.888	-1.542		
FFUJ_04259	uncharacterized protein	-1.892			
FFUJ_10564	uncharacterized protein	-1.892			
FFUJ_12409	probable isoamyl alcohol oxidase	-1.897	-1.434		
FFUJ_14573	related to monocarboxylate transporter	-1.902	-1.736		
FFUJ_10332	uncharacterized protein	-1.903			
FFUJ_10187	uncharacterized protein	-1.905			
FFUJ_09647	uncharacterized protein	-1.912			
FFUJ_09179	related to tryptophan dimethylallyltransferase	-1.913			
FFUJ_08426	probable Putative glutathione-dependent formaldehyde-activating enzyme	-1.914			
FFUJ_05076	probable ACC deaminase	-1.916			

FFUJ_10043	related to PMU1-high copy suppressor of ts tps2 mutant phenotype	-1.917	-1.777		
FFUJ_09300	uncharacterized protein	-1.919			
FFUJ_14922	uncharacterized protein	-1.920			
FFUJ_10623	probable ATP-binding protein PRP16	-1.926			
FFUJ_02543	uncharacterized protein	-1.928	-2.085		
FFUJ_03656	related to aspartic-type signal peptidase	-1.929			
FFUJ_08160	related to 3-oxoacyl-[acyl-carrier-protein] reductase	-1.931			
FFUJ_08913	probable amino acid permease NAAP1	-1.935			
FFUJ_09162	uncharacterized protein	-1.946			
FFUJ_05376	related to methyltransferase	-1.947			
FFUJ_09397	related to 6-hydroxy-d-nicotine oxidase	-1.949			
FFUJ_03827	uncharacterized protein	-1.954			
FFUJ_05797	related to trichodiene oxygenase cytochrome P450	-1.956	-1.652		
FFUJ_02784	uncharacterized protein	-1.957	-1.841		
FFUJ_11272	related to beta-glucosidase	-1.961			
FFUJ_08904	uncharacterized protein	-1.970			
FFUJ_10313	related to toxD gene	-1.974			
FFUJ_01604	uncharacterized protein	-1.974	-1.727		
FFUJ_10868	uncharacterized protein	-1.978			
FFUJ_03817	uncharacterized protein	-1.979			
FFUJ_14726	uncharacterized protein	-1.981			
FFUJ_10163	uncharacterized protein	-1.985		-3.445	-4.545
FFUJ_14343	uncharacterized protein	-1.988			
FFUJ_13950	related to Ras guanine-nucleotide exchange protein Cdc25p	-1.988			
FFUJ_04023	probable neutral amino acid permease	-1.992			
FFUJ_14261	related to qde-1 RNA-dependent RNA polymerase (RdRP)	-1.997			
FFUJ_06108	uncharacterized protein	-1.999	-1.728		
FFUJ_02054	related to methyltransferase	-2.001	-1.028		-1.421
FFUJ_11775	uncharacterized protein	-2.003			
FFUJ_11880	uncharacterized protein	-2.017			
FFUJ_00264	uncharacterized protein	-2.018			
FFUJ_10862	related to multidrug transporter	-2.024			
FFUJ_13349	related to kinesin-related protein KLPA	-2.026	-1.366		
FFUJ_06236	probable 100 kDa protein P100	-2.027	-1.738		
FFUJ_13948	uncharacterized protein	-2.029	-2.213		
FFUJ_12137	uncharacterized protein	-2.029			
FFUJ_03545	related to xylosidase/arabinosidase	-2.032			
FFUJ_08088	uncharacterized protein	-2.037			
FFUJ_10182	uncharacterized protein	-2.041			
FFUJ_12992	uncharacterized protein	-2.046	-2.431		
FFUJ_10807	uncharacterized protein	-2.048			
FFUJ_14038	related to aryl-alcohol dehydrogenases	-2.048			
FFUJ_14300	uncharacterized protein	-2.056		-3.453	-3.596
FFUJ_02123	related to IBR finger domain protein	-2.063			
FFUJ_10351	related to tol protein	-2.073			
FFUJ_07074	related to putative fatty acid desaturase (mld)	-2.075	-1.669		
FFUJ_02271	related to acid phosphatase precursor	-2.087			
FFUJ_05409	uncharacterized protein	-2.095	-2.111		
FFUJ_10503	uncharacterized protein	-2.097			
FFUJ_02313	related to ankyrin	-2.099			
FFUJ_03824	related to integral membrane protein	-2.107	-1.392		
FFUJ_11560	uncharacterized protein	-2.108			
FFUJ_14727	uncharacterized protein	-2.108			
FFUJ_08234	related to GNT1 alphaN-acetylglucosamine transferase K. lactis	-2.108			
FFUJ_10742	related to oxidoreductase	-2.111			
FFUJ_13912	related to multidrug resistance-associated protein	-2.118			
FFUJ_14175	uncharacterized protein	-2.127			
FFUJ_12991	probable sugar transport protein STL1	-2.132	-2.167		
FFUJ_00358	uncharacterized protein	-2.136			
FFUJ_12307	probable het-c2 protein	-2.144			
FFUJ_08097	related to 2-hydroxyacid dehydrogenase	-2.145			
FFUJ_00263	uncharacterized protein	-2.146			
FFUJ_10509	uncharacterized protein	-2.147	-1.348		
FFUJ_14173	uncharacterized protein	-2.151			
FFUJ_04787	uncharacterized protein	-2.155	-1.536	-1.467	-2.092
FFUJ_01066	related to ankyrin repeat protein	-2.162			
FFUJ_14908	uncharacterized protein	-2.168			
FFUJ_05419	uncharacterized protein	-2.170			
FFUJ_06611	related to major facilitator MirA	-2.171			
FFUJ_14572	uncharacterized protein	-2.179			
FFUJ_07016	probable MVD1-mevalonate pyrophosphate decarboxylase	-2.185			
FFUJ_13988	uncharacterized protein	-2.186			
FFUJ_06528	related to BCS1 protein precursor	-2.186			
FFUJ_02182	uncharacterized protein	-2.186			
FFUJ_07508	uncharacterized protein	-2.188			

FFUJ_14634	uncharacterized protein	-2.189			
FFUJ_08773	uncharacterized protein	-2.190	-1.642		
FFUJ_12558	uncharacterized protein	-2.198	-1.849		
FFUJ_10451	related to TPN1 Pyridoxine transporter	-2.203			
FFUJ_12655	related to ankyrin	-2.204	-1.571		
FFUJ_14586	uncharacterized protein	-2.210			
FFUJ_01798	uncharacterized protein	-2.211	-1.743		
FFUJ_09062	related to RBTMx2 protein	-2.211	-1.608		
FFUJ_08170	uncharacterized protein	-2.214			
FFUJ_09938	related to 6-hydroxy-d-nicotine oxidase	-2.217			
FFUJ_02115	related to nonribosomal peptide synthetase MxcG (component of the myxochelin iron transport regulon)	-2.220			
FFUJ_10541	uncharacterized protein	-2.224			
FFUJ_06419	uncharacterized protein	-2.226			
FFUJ_10192	probable polysaccharide deacetylase family protein	-2.246			
FFUJ_03822	related to signal peptide protein	-2.257			
FFUJ_02770	related to triacylglycerol lipase II precursor	-2.262			
FFUJ_10764	related to sexual differentiation process protein isp4	-2.273	-1.901		
FFUJ_10194	related to general amidase	-2.283			-1.976
FFUJ_11912	uncharacterized protein	-2.306			
FFUJ_10239	related to integral membrane protein PTH11	-2.307			
FFUJ_11233	related to 15-hydroxyprostaglandin dehydrogenase	-2.308	-1.256		
FFUJ_10709	related to methyltransferase	-2.309			
FFUJ_12698	uncharacterized protein	-2.313	-1.842		
FFUJ_12505	uncharacterized protein	-2.319			
FFUJ_02889	related to F-box protein Fbl2	-2.320	-2.008		
FFUJ_00955	uncharacterized protein	-2.337	-1.706		
FFUJ_00196	probable aldehyde dehydrogenase	-2.347	-1.663		
FFUJ_13722	probable DUF895 domain membrane protein	-2.347			
FFUJ_02038	related to tol protein	-2.371			
FFUJ_06531	uncharacterized protein	-2.382			
FFUJ_12656	uncharacterized protein	-2.384			
FFUJ_05451	related to integral membrane protein	-2.396			
FFUJ_08236	related to beta-N-hexosaminidase	-2.401	-2.210		
FFUJ_10971	related to Ca2+/H+-exchanging protein%2C vacuolar	-2.410			
FFUJ_00118	polyketide synthase	-2.411			
FFUJ_09301	uncharacterized protein	-2.419			
FFUJ_12470	uncharacterized protein	-2.432	-2.449		
FFUJ_06661	uncharacterized protein	-2.441	-1.805	-1.671	-2.322
FFUJ_02254	related to chitinase	-2.450			
FFUJ_11626	related to beta-glucosidase	-2.459			
FFUJ_05117	uncharacterized protein	-2.460			
FFUJ_08190	related to dipeptidyl aminopeptidase B	-2.470			
FFUJ_14174	related to fructosyl amino acid oxidase	-2.476			
FFUJ_11861	related to nitric-oxide synthase%2C salivary gland	-2.504	-1.787		
FFUJ_02856	related to epoxide hydrolase	-2.509			
FFUJ_14581	related to agmatinase	-2.513			
FFUJ_02045	related to 3-oxoacyl-[acyl-carrier-protein] reductase	-2.514			
FFUJ_10753	related to endopeptidase K	-2.527			-1.351
FFUJ_06635	uncharacterized protein	-2.557	-2.475		
FFUJ_10200	related to ARO8-aromatic amino acid aminotransferase I	-2.581	-1.624		
FFUJ_01978	related to TOB3 (member of AAA-ATPase family)	-2.587			
FFUJ_13996	uncharacterized protein	-2.588			
FFUJ_03578	uncharacterized protein	-2.589			
FFUJ_11774	uncharacterized protein	-2.595			
FFUJ_12603	related to aliphatic nitrilase	-2.601			
FFUJ_10468	related to peptide transporter	-2.606			
FFUJ_13190	related to UDP-galactopyranose mutase	-2.613			
FFUJ_09180	uncharacterized protein	-2.629	-3.077		
FFUJ_02114	probable O-acetylhomoserine (thiol)-lyase	-2.631	-4.570		3.138
FFUJ_02862	uncharacterized protein	-2.644			
FFUJ_02385	uncharacterized protein	-2.672			
FFUJ_11134	uncharacterized protein	-2.672			
FFUJ_02532	uncharacterized protein	-2.702			
FFUJ_03620	uncharacterized protein	-2.714			
FFUJ_08167	related to TAM domain methyltransferase	-2.723	-2.133		
FFUJ_10146	uncharacterized protein	-2.733	-1.879		
FFUJ_07239	uncharacterized protein	-2.743	-1.739		
FFUJ_00056	uncharacterized protein	-2.745			
FFUJ_08826	related to ethanolamine utilization protein (EutQ)	-2.759			
FFUJ_12909	uncharacterized protein	-2.759			
FFUJ_12849	uncharacterized protein	-2.761	-1.516		
FFUJ_11021	uncharacterized protein	-2.776			
FFUJ_09125	uncharacterized protein	-2.778			
FFUJ_01118	probable ASP3-1-L-asparaginase II	-2.778			
FFUJ_06636	uncharacterized protein	-2.799			
FFUJ_12730	probable GTP-binding protein	-2.836			

FFUJ_06524	uncharacterized protein	-2.855			
FFUJ_09996	related to UDP-galactopyranose mutase	-2.857	-1.781	-3.736	-4.803
FFUJ_03811	uncharacterized protein	-2.864			
FFUJ_10246	related to proteoglycan	-2.903	-1.598		
FFUJ_03679	PTR2-Di-and tripeptide permease	-2.906			
FFUJ_12620	related to endo-1%2C4-beta-xylanase	-2.907			
FFUJ_09204	uncharacterized protein	-2.909			
FFUJ_10739	related to isoamyl alcohol oxidase	-2.934			
FFUJ_08158	related to KP4 killer toxin	-2.947			
FFUJ_02106	uncharacterized protein	-2.965			
FFUJ_14098	related to heterokaryon incompatibility protein (het-6OR allele)	-2.993			
FFUJ_00081	related to tenascin X precursor	-3.004			
FFUJ_12032	related to antifungal protein	-3.009			
FFUJ_08881	related to cyanovirin-N family protein	-3.025			
FFUJ_11234	related to integral membrane protein PTH11	-3.039			
FFUJ_00059	probable amino acid aldolase or racemase	-3.044	-2.460		
FFUJ_02542	uncharacterized protein	-3.053	-2.241		
FFUJ_11426	related to nik-1 protein (Os-1p protein)	-3.091			
FFUJ_00288	related to DAL5-Allantoate and ureidosuccinate permease	-3.097			
FFUJ_03792	related to heterokaryon incompatibility protein het-6	-3.102			
FFUJ_08026	uncharacterized protein	-3.119			
FFUJ_10237	related to alkaline protease (oryzin)	-3.141			
FFUJ_03815	uncharacterized protein	-3.153			
FFUJ_10556	related to heterokaryon incompatibility protein	-3.159			-2.799
FFUJ_06876	uncharacterized protein	-3.172	-1.866		
FFUJ_09184	related to class I alpha-mannosidase 1B	-3.177		-2.929	-4.738
FFUJ_03758	related to 6-hydroxy-D-nicotine oxidase	-3.179			
FFUJ_12031	uncharacterized protein	-3.203			
FFUJ_09685	probable UDP-glucose 6-dehydrogenase	-3.206	-2.231		
FFUJ_06633	uncharacterized protein	-3.242	-1.783		-1.419
FFUJ_03816	related to permeases-unknown function	-3.254	-3.521		
FFUJ_00133	uncharacterized protein	-3.262			
FFUJ_10602	related to methyltransferase LaeA-like	-3.270	-5.122		
FFUJ_10128	uncharacterized protein	-3.289			
FFUJ_00057	related to lipase 2	-3.299	-2.428		
FFUJ_05807	uncharacterized protein	-3.325			
FFUJ_14661	related to DUF614 domain protein	-3.327		-1.533	-3.435
FFUJ_09914	related to microbial serine proteinase	-3.354	-2.876		
FFUJ_13314	uncharacterized protein	-3.361	-3.218		
FFUJ_10875	uncharacterized protein	-3.382	-2.502		
FFUJ_06112	related to alcohol oxidase	-3.429			-1.772
FFUJ_09303	uncharacterized protein	-3.436			
FFUJ_03721	uncharacterized protein	-3.503	-2.292	-1.458	-2.708
FFUJ_14009	uncharacterized protein	-3.512	-2.648		
FFUJ_03613	uncharacterized protein	-3.538	-2.548		
FFUJ_14370	related to laminaripentaose-producing beta-1%2C3-glucanase	-3.542			
FFUJ_11613	uncharacterized protein	-3.736		-3.111	-5.794
FFUJ_14620	probable glucosamine-phosphate N-acetyltransferase	-3.822			
FFUJ_11793	probable aspartate aminotransferase%2C cytoplasmic	-3.851			
FFUJ_02291	uncharacterized protein	-3.854			
FFUJ_11430	related to tripeptidyl-peptidase I	-3.859			
FFUJ_11520	uncharacterized protein	-3.865			
FFUJ_08168	uncharacterized protein	-3.881			
FFUJ_11333	related to PRC1-carboxypeptidase y%2C serine-type protease	-3.887			
FFUJ_12107	related to chitinase	-3.894			
FFUJ_02039	uncharacterized protein	-3.969	-2.743		
FFUJ_11427	uncharacterized protein	-4.003			
FFUJ_09977	uncharacterized protein	-4.038	-3.511	3.974	3.438
FFUJ_14706	uncharacterized protein	-4.129			
FFUJ_06688	related to monocarboxylate transporter 2	-4.133			
FFUJ_08047	related to tol protein	-4.222			
FFUJ_02109	probable homoserine O-acetyltransferase	-4.235			
FFUJ_14026	related to Putative sterigmatocystin biosynthesis lipase/esterase STCI	-4.239			
FFUJ_11107	related to putative tartrate transporter	-4.264			
FFUJ_13763	related to 6-HYDROXY-D-NICOTINE OXIDASE	-4.269	-3.570		
FFUJ_07160	uncharacterized protein	-4.270			
FFUJ_03590	related to 2%2C4-dihydroxyhept-2-ene-1%2C7-dioic acid aldolase	-4.276			
FFUJ_13945	uncharacterized protein	-4.285			
FFUJ_10740	related to integral membrane protein PTH11	-4.370			
FFUJ_03634	uncharacterized protein	-4.371			
FFUJ_12850	probable PGU1-Endo-polygalacturonase	-4.409			
FFUJ_12891	probable glucan 1%2C3-beta-glucosidase	-4.447			
FFUJ_03986	fusarubin cluster-monooxygenase	-4.449			

FFUJ_06482	uncharacterized protein	-4.465			
FFUJ_12441	uncharacterized protein	-4.480			
FFUJ_00058	related to putative tartrate transporter	-4.499	-3.214		
FFUJ_09280	uncharacterized protein	-4.509			
FFUJ_03387	uncharacterized protein	-4.654			
FFUJ_14134	related to tol protein	-4.680			
FFUJ_14299	uncharacterized protein	-4.683			
FFUJ_13721	uncharacterized protein	-4.726			
FFUJ_12495	related to triacylglycerol lipase II precursor	-4.815	-3.302		
FFUJ_12859	uncharacterized protein	-4.830			
FFUJ_03793	uncharacterized protein	-4.859			
FFUJ_14025	related to toxD protein	-4.872			
FFUJ_14329	uncharacterized protein	-4.875			
FFUJ_10325	uncharacterized protein	-4.942	-3.180		
FFUJ_03751	related to cis-1%2C2-dihydro-1%2C2-dihydroxynaphthalene dehydrogenase	-4.942			
FFUJ_10280	uncharacterized protein	-4.944			
FFUJ_06855	probable acetylxylan esterase precursor	-4.963			
FFUJ_11035	related to integral membrane protein PTH11	-5.026			
FFUJ_10353	uncharacterized protein	-5.035	-2.483		
FFUJ_14271	uncharacterized protein	-5.073			
FFUJ_11412	uncharacterized protein	-5.130			
FFUJ_05118	related to chitinase	-5.269	-4.655		
FFUJ_10176	related to trichothecene 3-O-acetyltransferase	-5.363			
FFUJ_12552	uncharacterized protein	-5.507			
FFUJ_00079	related to carbonic anhydrase precursor	-5.517	-2.819		
FFUJ_00138	uncharacterized protein	-5.522			
FFUJ_10216	related to G protein coupled receptor like protein	-5.547	-3.187		
FFUJ_11910	related to Carboxypeptidase 2	-5.568			
FFUJ_06113	related to integral membrane protein PTH11	-5.682			
FFUJ_06525	uncharacterized protein	-5.975			
FFUJ_08927	related to aminopeptidase Y precursor%2C vacuolar	-6.878			
FFUJ_00438	uncharacterized protein	0.865	1.022		
FFUJ_00817	uncharacterized protein		2.658		
FFUJ_01330	probable delta-1-pyrroline-5-carboxylate dehydrogenase	0.604	1.235		
FFUJ_01398	uncharacterized protein	0.770	1.013		
FFUJ_01494	related to transcriptional repressor		1.087		
FFUJ_03390	related to TOB3 (member of AAA-ATPase family)	0.987	1.079		
FFUJ_03646	uncharacterized protein		1.341		
FFUJ_03976	uncharacterized protein		2.571		
FFUJ_03978	related to conidial hydrophobin RodB		2.258	3.689	2.967
FFUJ_04856	related to NUF2-outer kinetochore protein-part of Ndc80p complex	0.957	1.154		
FFUJ_05728	related to potato small nuclear ribonucleoprotein U2B and human splicing factor homolog	0.893	1.058		
FFUJ_05733	probable 2-methylcitrate dehydratase	0.680	1.206		
FFUJ_05734	related to SH3 domain protein	0.990	1.182		
FFUJ_06144	probable protein kinase DBF20	0.880	1.194		
FFUJ_06745	bikaverin cluster-transcription factor enhancer		2.129		
FFUJ_07772	related to nik-1 protein (Os-1p protein)		1.060		
FFUJ_08405	related to asn-tRNA synthetase%2C mitochondrial		1.013		
FFUJ_09467	related to RSN1 Overexpression rescues sro7/sop1 in NaCl	0.934	1.082		
FFUJ_09591	probable chitin binding protein		3.240		
FFUJ_12295	uncharacterized protein	0.937	1.052		
FFUJ_12668	related to 5-carboxyvanillate decarboxylase		1.305		
FFUJ_13141	related to SGT1 protein	0.773	1.027		
FFUJ_13389	uncharacterized protein	0.915	1.221		
FFUJ_14382	related to integral membrane protein PTH11		1.014		
FFUJ_14666	related to nitrate reductase		4.121		
FFUJ_02531	uncharacterized protein	-0.855	-1.017		
FFUJ_04132	uncharacterized protein	-0.934	-1.028		
FFUJ_04701	related to TAP42%2C component of the Tor signaling pathway	-0.721	-1.043		
FFUJ_00514	uncharacterized protein	-0.881	-1.044		
FFUJ_14535	probable bifunctional D12/D15 fatty acid desaturase	-0.835	-1.081		
FFUJ_12469	related to lysophospholipase		-1.104		
FFUJ_13960	uncharacterized protein		-1.141		
FFUJ_00577	related to multidrug transporter (yeast bile transporter)	-0.941	-1.149		
FFUJ_13898	related to lysophosphatidic acid acyltransferase endophilin/SH3GL%2C involved in synaptic vesicle formation	-0.747	-1.177		1.001
FFUJ_00014	related to ferric reductase Fre2p		-1.187		
FFUJ_08842	related to exopolyphosphatase	-0.690	-1.187		
FFUJ_10662	uncharacterized protein		-1.217		
FFUJ_10063	uncharacterized protein		-1.227		
FFUJ_14013	uncharacterized protein		-1.232		
FFUJ_10728	related to glycine-rich RNA-binding protein	-0.852	-1.243		
FFUJ_03774	uncharacterized protein		-1.261		

FFUJ_14681	uncharacterized protein		-1.319		
FFUJ_09430	probable vegetatible incompatibility protein HET-E-1		-1.477		
FFUJ_11428	uncharacterized protein		-1.512		
FFUJ_06105	related to N-acetylglucosamine-6-phosphate deacetylase		-1.586		
FFUJ_01007	related to a retinal short-chain dehydrogenase/reductase	-0.750	-1.631		1.392
FFUJ_14707	uncharacterized protein		-1.670		
FFUJ_12496	related to integral membrane protein PTH11		-1.698		
FFUJ_00161	uncharacterized protein		-1.736		
FFUJ_12585	related to pentalenene synthase		-1.802	-2.055	
FFUJ_03775	uncharacterized protein		-1.815		
FFUJ_03773	uncharacterized protein		-1.914		
FFUJ_08290	related to stomatin	-0.685	-2.164		1.335
FFUJ_09152	uncharacterized protein		-2.183		
FFUJ_09185	uncharacterized protein		-2.246		
FFUJ_00069	related to glucan 1%2C3-beta-glucosidase		-2.444	-4.323	
FFUJ_14683	uncharacterized protein			5.708	
FFUJ_11707	related to 6-hydroxy-d-nicotine oxidase			5.497	
126222	0			4.915	
FFUJ_06424	uncharacterized protein			3.845	5.074
FFUJ_11920	related to integral membrane protein			3.632	2.658
FFUJ_09376	related to monooxygenase			3.530	
FFUJ_14684	related to aliphatic nitrilase			2.731	
FFUJ_00934	probable nitrate transport protein crnA			2.496	2.094
FFUJ_14553	related to zinc transporter			2.421	
FFUJ_14552	uncharacterized protein			2.296	
FFUJ_09694	related to sodium-and chloride-dependent GABA transporter 1	-0.993		2.242	1.970
FFUJ_12120	related to integral membrane protein			2.197	1.535
FFUJ_12121	uncharacterized protein	-0.847		1.948	1.822
FFUJ_12853	uncharacterized protein			1.912	2.102
FFUJ_05054	related to multidrug resistance protein	-0.790		1.518	1.382
FFUJ_06435	related to integral membrane protein			1.400	
FFUJ_09699	related to Ca2+-transporting ATPase			1.366	1.282
FFUJ_13568	related to zinc transporter			1.203	0.921
FFUJ_01416	related to acetylxylan esterase	-0.834		1.181	
FFUJ_14641	uncharacterized protein			1.153	1.015
FFUJ_07854	uncharacterized protein			-1.041	
FFUJ_10364	uncharacterized protein			-1.064	
FFUJ_05745	uncharacterized protein	-0.828		-1.466	-1.740
FFUJ_10406	uncharacterized protein			-1.607	
FFUJ_14654	related to short-chain alcohol dehydrogenase			-1.670	-2.899
FFUJ_05183	related to PNG1-protein with de-N-glycosylation function (N-glycanase)			-1.726	-1.643
FFUJ_11842	uncharacterized protein			-1.730	
FFUJ_10517	probable galactose oxidase			-1.794	-1.380
FFUJ_14803	probable 3-polyprenyl-4-hydroxybenzoate decarboxylase and related decarboxylases			-1.801	-1.761
FFUJ_03618	related to beta-glucosidase			-1.922	
FFUJ_12586	probable glucan 1%2C4-alpha-glucosidase			-1.940	-1.578
FFUJ_03329	uncharacterized protein			-1.981	
FFUJ_12117	related to tetracycline efflux protein (otrb)			-1.996	
FFUJ_14321	related to integral membrane protein			-2.006	
FFUJ_00563	uncharacterized protein			-2.131	-2.863
FFUJ_09334	related to myo-inositol transport protein ITR1			-2.144	
FFUJ_04585	uncharacterized protein			-2.264	
FFUJ_02308	uncharacterized protein			-2.312	
FFUJ_05645	uncharacterized protein			-2.314	-2.110
FFUJ_11186	related to endo-1%2C3-beta-glucanase			-2.346	-2.801
FFUJ_03814	uncharacterized protein			-2.483	-2.520
FFUJ_09384	uncharacterized protein			-2.621	-1.713
FFUJ_12118	probable cysteine synthase B			-2.691	-2.462
FFUJ_03607	related to arachidonate 5-lipoxygenase			-2.752	-2.924
FFUJ_03543	uncharacterized protein			-2.782	-2.711
FFUJ_11554	related to L-fucose permease			-2.898	-3.723
FFUJ_11724	related to Y.lipolytica GPR1 protein and Fun34p			-3.116	-3.290
FFUJ_02202	uncharacterized protein			-3.164	-5.323
FFUJ_14071	related to chitin synthase/hyaluronan synthase (glycosyltransferases)			-3.200	-3.983
FFUJ_10609	related to C4-dicarboxylate transport protein mae1			-3.257	-3.491
FFUJ_09084	uncharacterized protein			-3.709	-4.041
FFUJ_08713	uncharacterized protein			-3.938	-4.059
FFUJ_12578	uncharacterized protein			-4.065	
FFUJ_10555	related to GPI anchored protein			-4.390	-4.292
FFUJ_14072	uncharacterized protein			-4.637	-6.408
FFUJ_06773	probable rhamnogalacturonase A precursor			-4.767	-6.115
FFUJ_14063	uncharacterized protein			-4.818	-5.817
FFUJ_10514	uncharacterized protein			-7.724	-7.323

FFUJ_02203	related to integral membrane protein			-8.083	-5.667
FFUJ_10773	uncharacterized protein				6.130
FFUJ_14318	uncharacterized protein				6.085
FFUJ_14513	related to nitrate reductase				4.053
FFUJ_01810	related to PHO89-Na+/phosphate co-transporter				3.563
FFUJ_14669	uncharacterized protein				3.394
FFUJ_12277	probable nitrate reductase				3.115
FFUJ_09682	related to short-chain dehydrogenase/reductase family protein%2C putative				2.971
FFUJ_03972	uncharacterized protein				2.892
FFUJ_11004	probable endopolygalacturonase				2.807
FFUJ_06099	probable nitrite reductase				2.780
FFUJ_05126	uncharacterized protein				2.484
FFUJ_05163	uncharacterized protein				2.432
FFUJ_11826	related to putative transporter SEO1				2.376
FFUJ_04803	related to major facilitator MirA				2.101
FFUJ_05351	related to cytochrome P450 monooxygenase (lovA)				2.028
FFUJ_00741	uncharacterized protein				1.988
FFUJ_00531	uncharacterized protein		-0.832	0.639	1.869
FFUJ_11384	uncharacterized protein	0.962			1.857
FFUJ_11800	related to positive activator of transcription	0.863			1.734
FFUJ_09930	uncharacterized protein				1.733
FFUJ_05916	uncharacterized protein				1.706
FFUJ_11521	related to long-chain-fatty-acid--CoA ligase				1.605
FFUJ_05411	related to methyltransferase				1.583
FFUJ_05659	uncharacterized protein	0.563			1.543
FFUJ_05186	related to FAD binding domain protein	0.750			1.498
FFUJ_05859	related to ABC transporter	0.983			1.493
FFUJ_00466	uncharacterized protein	0.791			1.469
FFUJ_00247	related to nucleoside diphosphate-sugar hydrolase of the MutT (NUDIX) family	0.983			1.459
FFUJ_07190	uncharacterized protein	0.500	-0.708		1.425
FFUJ_03504	related to methyltransferase	0.940			1.393
FFUJ_12486	uncharacterized protein				1.344
FFUJ_07843	related to integral membrane protein PTH11				1.326
FFUJ_04972	related to phospholipase D				1.323
FFUJ_14565	uncharacterized protein				1.310
FFUJ_12154	uncharacterized protein	0.933			1.294
FFUJ_11844	uncharacterized protein	0.911			1.290
FFUJ_02580	related to dityrosine transporter	0.602			1.281
FFUJ_04726	related to glia maturation factor beta	0.844			1.279
FFUJ_05473	uncharacterized protein				1.246
FFUJ_12212	related to DNA polymerase Tdt-N	0.850			1.239
FFUJ_02972	probable PRC1-carboxypeptidase y%2C serine-type protease	0.835			1.234
FFUJ_02358	uncharacterized protein				1.229
FFUJ_13762	related to neutral amino acid permease	0.627			1.207
FFUJ_08469	related to tocopherol O-methyltransferase				1.204
FFUJ_09989	related to phospholipid-translocating ATPase				1.187
FFUJ_13380	uncharacterized protein	0.761			1.155
FFUJ_14670	uncharacterized protein				1.130
FFUJ_10901	uncharacterized protein				1.109
FFUJ_03104	uncharacterized protein	0.872			1.099
FFUJ_03862	uncharacterized protein	0.987			1.094
FFUJ_10419	related to monocarboxylate transporter 2				1.093
FFUJ_03783	related to nicotinamide mononucleotide permease				1.073
FFUJ_02409	uncharacterized protein	0.741			1.069
FFUJ_02734	related to DNA mismatch repair protein	0.709			1.060
FFUJ_11690	uncharacterized protein				1.057
FFUJ_00434	uncharacterized protein	0.828			1.028
FFUJ_03398	probable c-14 sterol reductase ERG-3	0.893			1.012
FFUJ_00824	related to D-xylose reductase II%2CIII protein	0.662			1.010
FFUJ_02333	related to lactose permease	-0.723			1.009
FFUJ_09667	related to delta-24-sterol methyltransferase				-1.072
FFUJ_10003	related to TRI7-trichothecene biosynthesis gene cluster	-0.853			-1.072
FFUJ_09778	related to multidrug resistant protein				-1.078
FFUJ_00088	uncharacterized protein				-1.098
FFUJ_11415	related to multidrug resistant protein				-1.103
FFUJ_01169	uncharacterized protein	-0.730			-1.104
FFUJ_04360	related to D-arabinitol 2-dehydrogenase				-1.106
FFUJ_11292	probable ABC1 transport protein				-1.119
FFUJ_05952	probable GUT1-glycerol kinase				-1.141
FFUJ_14278	uncharacterized protein				-1.168
FFUJ_14435	uncharacterized protein	-0.532			-1.174
FFUJ_06511	related to RTM1 protein				-1.253
FFUJ_10319	uncharacterized protein				-1.263
FFUJ_02653	related to malate dehydrogenase (oxaloacetate-decarboxylating) (NADP+)				-1.265

FFUJ_10771	uncharacterized protein				-1.272
FFUJ_06646	uncharacterized protein				-1.300
FFUJ_05999	uncharacterized protein	-0.966			-1.325
FFUJ_03313	uncharacterized protein				-1.329
FFUJ_10944	uncharacterized protein				-1.403
FFUJ_05653	uncharacterized protein				-1.439
FFUJ_08033	probable putative methyltransferase				-1.445
FFUJ_00342	uncharacterized protein				-1.479
FFUJ_06962	probable maltase				-1.486
FFUJ_05996	related to D-arabinitol 2-dehydrogenase				-1.489
FFUJ_12809	related to 2%2C3-dihydroxybiphenyl-1%2C2-dioxygenase				-1.602
FFUJ_09706	related to dehydrogenases with different specificities (related to short-chain alcohol dehydrogenases)	-0.920			-1.612
FFUJ_03617	uncharacterized protein				-1.617
FFUJ_00089	uncharacterized protein				-1.665
FFUJ_10839	related to ADH3-alcohol dehydrogenase III				-1.679
FFUJ_05744	related to dis1-suppressing protein kinase dsk1				-1.682
FFUJ_01985	putative trichothecene biosynthesis gene				-1.739
FFUJ_06213	probable DAL7-malate synthase 2				-1.746
FFUJ_11016	related to myo-inositol transport protein ITR1				-1.746
FFUJ_14119	related to delta3-cis-delta2-trans-enoyl-CoA isomerase				-1.762
FFUJ_06547	probable monosaccharide transporter				-1.789
FFUJ_13173	uncharacterized protein				-1.866
FFUJ_09657	related to glutamine rich protein%2C nitrogen starvation-induced				-1.937
FFUJ_04015	related to phosphatidylcholine-sterol acyltransferase precursor				-1.948
FFUJ_09690	related to glutamyl-tRNA				-1.958
FFUJ_07819	uncharacterized protein				-1.976
FFUJ_05222	uncharacterized protein				-1.992
FFUJ_02060	uncharacterized protein				-2.031
FFUJ_07946	probable alpha/beta fold family hydrolase				-2.086
FFUJ_05529	related to 3-hydroxybutyryl-CoA dehydratase				-2.127
FFUJ_11569	related to 4-coumarate--CoA ligase				-2.135
FFUJ_00021	related to NonF protein%2C involved in nonactin biosynthesis				-2.153
FFUJ_14002	uncharacterized protein				-2.204
FFUJ_11570	uncharacterized protein				-2.209
FFUJ_10318	uncharacterized protein				-2.319
FFUJ_10386	uncharacterized protein				-2.336
FFUJ_14804	probable 3-octaprenyl-4-hydroxybenzoate carboxy-lyase				-2.385
FFUJ_12808	related to bifunctional 4-hydroxyphenylacetate degradation enzyme				-2.425
FFUJ_14652	related to 15-hydroxyprostaglandin dehydrogenase				-2.450
FFUJ_10610	uncharacterized protein				-2.553
FFUJ_00744	uncharacterized protein				-2.611
FFUJ_03619	related to hexose transporter protein				-2.780
FFUJ_12621	related to cellulose binding protein CEL1				-2.834
FFUJ_14151	uncharacterized protein				-3.016
FFUJ_09392	uncharacterized protein				-4.736
FFUJ_10794	uncharacterized protein				-6.620

Table S3. Total differentially expressed genes included in the third chapter RNA-seq analysis, corresponding to the study of the effect of *wcoA* mutation (DESeq with p<0.05 after correction), including the differential fold change for each of the comparisons analyzed.

Probe	C95	IMI	Protein name	Log2 FC (WT0 WT15)	Log2 FC (WT0 WT60)	Log2 FC (WT0 WT240)	Log2 FC (WC0 WC15)	Log2 FC (WC0 WC60)	Log2 FC (WC0 WC240)	Log2 FC (WC0 WT0)	Log2 FC (WC15 WT15)	Log2 FC (WC60 WT60)	Log2 FC (WC240 WT240)
XLOC_001215	FFC1_00009	FFUJ_00008	related to O-methyltransferase										2.82
XLOC_001216	FFC1_00010	FFUJ_00009	uncharacterized protein FFUJ_00009							2.10	2.26	3.10	3.21
XLOC_000006	FFC1_00013	FFUJ_00012	uncharacterized protein FFUJ_00012							2.03	1.72		1.60
XLOC_001218	FFC1_00014	FFUJ_00013	related to PRO3-delta 1-pyrroline-5-carboxylate reductase							2.20	1.17	1.91	2.42
XLOC_001219	FFC1_00016									4.35			3.96
XLOC_001222	FFC1_00021									2.15	1.19	1.37	1.65
XLOC_000009	FFC1_00022									3.08			
XLOC_000017	FFC1_00035				-2.99					-1.50	-3.16	-5.12	-1.95
XLOC_001229	FFC1_00035									-2.20	-5.14	-5.79	-5.21
XLOC_001231	FFC1_00037									3.50			1.39
XLOC_000018	FFC1_00038								2.01	3.22	2.61	1.87	1.27
XLOC_000019	FFC1_00040									6.64	5.83	6.25	4.46
XLOC_001234	FFC1_00041									8.92	9.63	8.06	5.56
XLOC_000022	FFC1_00044									5.70	4.81		
XLOC_001235	FFC1_00045									-3.56	-4.28	-4.85	-5.95
XLOC_001236	FFC1_00046	FFUJ_00014	related to ferric reductase Fre2p							-5.13	-5.01	-5.63	-5.05
XLOC_001237	FFC1_00047	FFUJ_00015	uncharacterized protein FFUJ_00015						0.97	-2.16	-2.53	-3.22	-2.54
XLOC_000023	FFC1_00050	FFUJ_00018	related to ketoreductase							-1.29	-2.12	-2.54	-2.94
XLOC_001243	FFC1_00055	FFUJ_00023	uncharacterized protein FFUJ_00023							-1.98	-3.04	-3.58	-3.92
XLOC_001244	null										-2.08	-1.98	
XLOC_000026	FFC1_00057	FFUJ_00025	related to aldehyde reductase II							4.14	2.81	1.77	2.17
XLOC_000027	FFC1_00058	FFUJ_00026	uncharacterized protein FFUJ_00026	1.67						5.94	7.08	5.90	5.67
XLOC_001245	FFC1_00059	FFUJ_00027	probable benzoate 4-monooxygenase cytochrome P450							4.41	4.73	5.36	4.49
XLOC_001248	FFC1_00065	FFUJ_00033	probable 3-hydroxyisobutyrate dehydrogenase, mitochondrial precursor									3.85	
XLOC_000031	FFC1_00066	FFUJ_00034	related to vegetatible incompatibility protein HET-E-1	2.16	3.85	3.18					1.34	3.13	2.13
XLOC_001249	FFC1_00067	FFUJ_00035	uncharacterized protein FFUJ_00035							-4.19	-4.96	-2.45	-2.46
XLOC_001250	FFC1_00068	FFUJ_00036	uncharacterized protein FFUJ_00036							-7.18	-6.36	-5.88	-8.49
XLOC_000032	FFC1_00069	FFUJ_00037	uncharacterized protein FFUJ_00037							-3.77	-4.59	-4.19	-5.90
XLOC_000034	FFC1_00073	FFUJ_00041	uncharacterized protein FFUJ_00041								-1.97	-2.26	
XLOC_001257	FFC1_00081	FFUJ_00049	related to pisatin demethylase cytochrome P450							8.12	3.90	3.72	5.72
XLOC_001260	FFC1_00087	FFUJ_00055	related to ankyrin							6.11	4.94		
XLOC_001261	FFC1_00088				-2.79					7.54	6.56		7.19
XLOC_000041	FFC1_00089				-1.97					5.35	5.23	4.04	5.69
XLOC_001262	FFC1_00090	FFUJ_00057	related to lipase 2		-1.91					2.81	1.91		
XLOC_000042	FFC1_00091	FFUJ_00058	related to putative tartrate transporter							5.94			
XLOC_000043	FFC1_00092	FFUJ_00059	probable amino acid aldolase or racemase		-2.05								
XLOC_001267	FFC1_00102	FFUJ_00070	probable aspartic proteinase precursor									7.70	
XLOC_001273	FFC1_00113	FFUJ_00080	uncharacterized protein FFUJ_00080			-2.23				8.34	8.62	8.81	6.28
XLOC_001274	FFC1_00114	FFUJ_00081	related to tenascin X precursor			-2.02				10.01	9.67	8.77	8.13
XLOC_000054	FFC1_00115	FFUJ_00082	uncharacterized protein FFUJ_00082			-2.29				9.72	6.89	6.71	7.60
XLOC_000060	FFC1_00123	FFUJ_00090	uncharacterized protein FFUJ_00090							5.29	5.13	5.28	
XLOC_000061	FFC1_00124									2.28	1.84		
XLOC_000062	FFC1_00125	FFUJ_00091	uncharacterized protein FFUJ_00091							2.11	1.80		
XLOC_001277	FFC1_00126	FFUJ_00092	uncharacterized protein FFUJ_00092										2.12
XLOC_000063	FFC1_00127	FFUJ_00093	related to aliphatic nitrilase								-4.18		
XLOC_001278	FFC1_00128	FFUJ_00094	uncharacterized protein FFUJ_00094							-1.98	-3.32	-2.70	
XLOC_000065	FFC1_00132	FFUJ_00098	uncharacterized protein FFUJ_00098								-4.89		
XLOC_000074	FFC1_00150	FFUJ_00115	uncharacterized protein FFUJ_00115							3.32	2.95	2.25	2.58
XLOC_001290	FFC1_00151	FFUJ_00116	related to Tri201-trichothecene 3-O-acetyltransferase							2.09	1.85		1.73
XLOC_000075	FFC1_00152	FFUJ_00117	related to integral membrane protein PTH11							2.77	2.47	2.09	
XLOC_001292	FFC1_00156									3.90	3.86	3.62	3.53
XLOC_000078	FFC1_00159	FFUJ_00122	uncharacterized protein FFUJ_00122							6.29	8.49	7.16	4.93
XLOC_000083	FFC1_00171									5.64	5.34		
XLOC_000084	FFC1_00172				-4.33					5.98	5.44		4.94
XLOC_000085	FFC1_00173	FFUJ_00134	uncharacterized protein FFUJ_00134							3.07	3.03	2.15	2.80
XLOC_000086	FFC1_00174	FFUJ_00138	uncharacterized protein FFUJ_00138							8.12	8.97	6.74	7.49
XLOC_001302	FFC1_00179	FFUJ_00143	uncharacterized protein FFUJ_00143							1.82	1.81	2.25	
XLOC_001304	FFC1_00184	FFUJ_00148	related to nucleoside-diphosphate-sugar epimerase		2.31	1.64				3.77	3.04	4.38	4.24
XLOC_000093	FFC1_00185	FFUJ_00150	probable NADPH2 dehydrogenase chain OYE2							5.43		6.41	6.26
XLOC_001307	FFC1_00188	FFUJ_00153	related to small s protein							3.10	1.84		
XLOC_000098	FFC1_00195	FFUJ_00159	uncharacterized protein FFUJ_00159							2.36	1.46		
XLOC_001311	FFC1_00198	FFUJ_00163	uncharacterized protein FFUJ_00163							9.29	9.29	9.17	6.85
XLOC_001312	FFC1_00199	FFUJ_00164	uncharacterized protein FFUJ_00164		1.12					5.54	4.91	5.03	
XLOC_001313	FFC1_00200	FFUJ_00165	related to hexose transporter protein							4.22			
XLOC_000104	FFC1_00206	FFUJ_00170	uncharacterized protein FFUJ_00170		-1.95						-1.31	-2.17	
XLOC_001314	FFC1_00208	FFUJ_00172	uncharacterized protein FFUJ_00172							5.09	5.63	6.67	6.83
XLOC_001315	FFC1_00209	FFUJ_00173	related to nicotinamide mononucleotide permease							6.11	6.19	7.34	7.53
XLOC_000106	FFC1_00210	FFUJ_00174	related to ankyrin 3							3.22	2.73	2.69	
XLOC_000107	FFC1_00211	FFUJ_00175	uncharacterized protein FFUJ_00175							3.46	3.01	3.20	2.18

XLOC_000108	FFC1_00212	FFUJ_00176	related to flavin-containing monooxygenase							2.60	2.32	2.23	1.80
XLOC_000109	FFC1_00214	FFUJ_00178	uncharacterized protein FFUJ_00178									3.50	
XLOC_000111	FFC1_00218									6.72	5.36	7.69	4.90
XLOC_001319	FFC1_00219	FFUJ_00182	uncharacterized protein FFUJ_00182		-5.67	-5.88				6.35			
XLOC_000112	FFC1_00220	FFUJ_00183	related to hsp70 protein		-5.83	-4.15				6.51	5.61		
XLOC_001324	FFC1_00230	FFUJ_00190	related to neutral amino acid permease							2.69	2.64	2.91	
XLOC_000118	FFC1_00231	FFUJ_00191	uncharacterized protein FFUJ_00191							4.75	4.73	3.56	3.48
XLOC_001325	FFC1_00232	FFUJ_00192	uncharacterized protein FFUJ_00192							1.38	1.51	2.06	1.79
XLOC_001326	FFC1_00236	FFUJ_00196	probable aldehyde dehydrogenase							2.44	1.89		2.40
XLOC_000122	FFC1_00238	FFUJ_00198	related to ARG81-transcription factor involved in arginine metabolism							-2.90			
XLOC_001329	FFC1_00240	FFUJ_00200	uncharacterized protein FFUJ_00200								-4.40		
XLOC_000125	FFC1_00244	FFUJ_14413	related to neutral amino acid permease			-1.54				4.18	4.26	4.23	3.59
XLOC_001331	FFC1_00245	FFUJ_00204	related to endo-polygalacturonase 6		2.07				1.30	3.34	2.84	5.01	2.02
XLOC_000127	FFC1_00248	FFUJ_00207	related to arsenic resistance protein ArsH		1.32					7.06	7.77	7.33	8.23
XLOC_001333	FFC1_00249	FFUJ_00208	related to tetracycline resistance protein (probable transport protein)		1.37					1.80	2.18	2.84	2.43
XLOC_000130	FFC1_00251	FFUJ_00210	uncharacterized protein FFUJ_00210										-6.55
XLOC_000133	FFC1_00255	FFUJ_00214	related to succinate-semialdehyde dehydrogenase							4.38	3.56	3.47	2.96
XLOC_000134	FFC1_00256	FFUJ_00215	uncharacterized protein FFUJ_00215							5.68	4.27	5.90	
XLOC_000141	FFC1_00267	FFUJ_00225	probable unsaturated glucuronyl hydrolase involved in regulation of bacterial surface properties, and related proteins		-2.40	-3.81				2.84			
XLOC_000145	FFC1_00272	FFUJ_00230	uncharacterized protein FFUJ_00230	1.34	1.96					7.32	5.06	6.96	5.16
XLOC_000146	FFC1_00275	FFUJ_00233	related to glutathione transferase omega 1							1.96	1.78	2.52	1.63
XLOC_000148	FFC1_00277	FFUJ_00235	uncharacterized protein FFUJ_00235							-2.91	-2.39	-2.07	-1.97
XLOC_001342	FFC1_00278	FFUJ_00236	probable methylcitrate synthase							2.18			
XLOC_001344	FFC1_00282	FFUJ_00240	uncharacterized protein FFUJ_00240		-1.06	-1.12				1.96	2.13	1.55	1.44
XLOC_001345	FFC1_00283	FFUJ_00241	uncharacterized protein FFUJ_00241							2.40	2.50	2.13	2.58
XLOC_001347	FFC1_00285	FFUJ_00243	uncharacterized protein FFUJ_00243							2.89	2.19	2.12	2.17
XLOC_000152	FFC1_00287	FFUJ_00245	uncharacterized protein FFUJ_00245							5.59	5.09	3.38	4.18
XLOC_001348	FFC1_00288	FFUJ_00246	related to YSA1 sugar-nucleotide hydrolase			1.27				-2.47	-2.56	-2.23	
XLOC_001350	FFC1_00290	FFUJ_00248	uncharacterized protein FFUJ_00248							3.41	2.72	2.87	
XLOC_000156	FFC1_00298	FFUJ_00256	uncharacterized protein FFUJ_00256							3.48	4.05	4.59	4.23
XLOC_001356	null												-3.07
XLOC_001357	FFC1_00300	FFUJ_00258	related to monocarboxylate transporter 2							-2.40			
XLOC_001358	FFC1_00302	FFUJ_00260	related to integral membrane protein PTH11							2.63	3.39	2.83	2.04
XLOC_001363	FFC1_00310	FFUJ_00268	uncharacterized protein FFUJ_00268		-2.00					4.10	2.16	1.61	1.69
XLOC_001367	FFC1_00317	FFUJ_00275	related to DUF636 domain protein		1.97	1.35				3.48	3.19	6.31	5.26
XLOC_001368	FFC1_00319	FFUJ_00277	uncharacterized protein FFUJ_00277							5.59			5.87
XLOC_001369	FFC1_00321	FFUJ_00278	uncharacterized protein FFUJ_00278							8.24	6.60	5.76	7.24
XLOC_000166	FFC1_00322	FFUJ_00279	uncharacterized protein FFUJ_00279							5.02	3.70	3.86	3.41
XLOC_001371	FFC1_00326	FFUJ_00283	uncharacterized protein FFUJ_00283							1.60	2.47	2.65	3.36
XLOC_000170	FFC1_00328	FFUJ_00285	related to sodium-dependent serotonin transporter							7.05		5.83	
XLOC_001372	FFC1_00329	FFUJ_00286	related to microsomal dipeptidase precursor							5.73	4.88		4.88
XLOC_000172	FFC1_00331	FFUJ_00288	related to DAL5-Allantoate and ureidosuccinate permease							9.63	9.59	8.40	8.23
XLOC_000173	FFC1_00336	FFUJ_00293	related to multidrug resistant protein		1.31					-2.59	-1.09		-1.41
XLOC_000174	FFC1_00338	FFUJ_00295	CON-10 conidation-specific protein CON-10		3.41	3.33				7.01	6.14	6.97	8.07
XLOC_000176	FFC1_00341	FFUJ_00298	related to acetyltransferase							-3.62	-3.25	-3.52	-2.80
XLOC_001380	FFC1_00344	FFUJ_00301	related to alcohol dehydrogenase homolog Bli-4							5.24			
XLOC_000179	FFC1_00346	FFUJ_00303	related to GTPase-activating protein of the rho/rac family (LRG1 protein)							2.20			2.85
XLOC_001384	FFC1_00351	FFUJ_00308	uncharacterized protein FFUJ_00308							-2.31	-2.42	-3.25	
XLOC_001385	FFC1_00352	FFUJ_00309	probable Alcohol dehydrogenase								-4.09		-4.28
XLOC_000181	FFC1_00353	FFUJ_00310	uncharacterized protein FFUJ_00310							-3.09	-5.21	-4.70	
XLOC_001391	FFC1_00364	FFUJ_00322	related to ketoreductases		1.23	1.84				3.50	3.20	3.75	4.32
XLOC_001392	FFC1_00365	FFUJ_00323	uncharacterized protein FFUJ_00323		-1.49	-1.22				2.02	0.95		
XLOC_000189	FFC1_00366	FFUJ_00324	uncharacterized protein FFUJ_00324		-1.23	-1.72				5.32	4.74	4.65	3.43
XLOC_000196	FFC1_00376	FFUJ_00334	uncharacterized protein FFUJ_00334									5.45	5.83
XLOC_000200	FFC1_00380	FFUJ_00337	probable catechol O-methyltransferase		3.12							2.39	
XLOC_000204	FFC1_00385	FFUJ_00342	uncharacterized protein FFUJ_00342							-1.62	-2.37		
XLOC_000209	FFC1_00391	FFUJ_00348	uncharacterized protein FFUJ_00348							-0.91	-1.70	-1.48	-2.29
XLOC_000212	FFC1_00394	FFUJ_00351	probable galactose oxidase precursor							-3.39	-3.85	-4.26	-5.30
XLOC_000214	FFC1_00396	FFUJ_00353	uncharacterized protein FFUJ_00353								-2.73		
XLOC_001400	FFC1_00401	FFUJ_00358	uncharacterized protein FFUJ_00358			-1.26						-2.90	-4.81
XLOC_001406	FFC1_00411	FFUJ_00367	uncharacterized protein FFUJ_00367							-1.87	-2.37	-2.25	-1.64
XLOC_000221	FFC1_00412	FFUJ_00368	related to protein BTN1		-1.21	-0.86				-1.65	-2.12	-2.70	-1.99
XLOC_000224	null									5.53			
XLOC_000225	FFC1_00416	FFUJ_00372	related to PNG1-protein with de-N-glycosylation function (N-glycanase)							2.72	2.90	2.66	2.68
XLOC_000226	FFC1_00417	FFUJ_00373	uncharacterized protein FFUJ_00373							2.16	2.34	2.69	2.16
XLOC_001408	FFC1_00419	FFUJ_00375	uncharacterized protein FFUJ_00375							6.04	6.77	7.61	6.81
XLOC_000228	FFC1_00422	FFUJ_00377	uncharacterized protein FFUJ_00377							1.72	1.43	2.30	2.51
XLOC_001411	FFC1_00423	FFUJ_00378	related to mannose-P-dolichol utilization defect 1 protein							2.72	2.37	2.42	
XLOC_000229	FFC1_00424	FFUJ_00379	uncharacterized protein FFUJ_00379							4.76	4.14	4.24	3.37
XLOC_001412	tRNA-Pro(CGG)										4.68	5.98	6.72
XLOC_000233	FFC1_00429	FFUJ_00384	related to DNA repair exonuclease rad1		0.95	0.80				2.53	2.25	3.13	3.27

XLOC_000234	FFC1_00430	FFUJ_00385	uncharacterized protein FFUJ_00385		0.97	0.94				4.79	4.11	4.55	5.42
XLOC_000235	FFC1_00431	FFUJ_00386	uncharacterized protein FFUJ_00386			-1.15				2.26	2.69	1.83	1.47
XLOC_000244	FFC1_00447	FFUJ_00402	uncharacterized protein FFUJ_00402								-5.97	-3.14	
XLOC_001423	FFC1_00450	FFUJ_00405	uncharacterized protein FFUJ_00405							1.96	1.50	2.05	2.65
XLOC_001424	FFC1_00451	FFUJ_00407	uncharacterized protein FFUJ_00407							-1.22	-2.23	-1.77	
XLOC_001425	FFC1_00452	FFUJ_00410	uncharacterized protein FFUJ_00410							-1.30	-1.98	-2.06	
XLOC_000248	FFC1_00454	FFUJ_00412	related to growth hormone inducible transmembrane protein		1.43					3.71	3.64	4.05	3.57
XLOC_000249	FFC1_00456	FFUJ_00414	related to TIM barrel metal-dependent hydrolase		-1.84	-2.69					-1.31	-1.30	-1.87
XLOC_001428	FFC1_00459	FFUJ_00417	related to aquaporin							-2.07	-1.96	-2.03	
XLOC_000251	FFC1_00463	FFUJ_00421	related to GTP-binding protein rab4b							1.73	1.88	2.37	2.32
XLOC_000252	FFC1_00464	FFUJ_00422	related to beta-mannosidase			1.39				1.73	1.19	2.65	3.27
XLOC_000253	FFC1_00465	FFUJ_00423	uncharacterized protein FFUJ_00423							7.44	6.00	5.99	6.20
XLOC_000255	FFC1_00467	FFUJ_00425	uncharacterized protein FFUJ_00425										5.45
XLOC_000256	FFC1_00468	FFUJ_00426	related to quinate transport protein								-1.29	-1.47	-2.67
XLOC_000257	FFC1_00469	FFUJ_00427	probable malate dehydrogenase (oxaloacetate decarboxylating) (NADP+)	1.33	1.87					0.80	1.68	2.29	1.28
XLOC_000261	FFC1_00474	FFUJ_00432	uncharacterized protein FFUJ_00432		1.35	1.50				4.03	2.81	4.28	4.42
XLOC_001436	FFC1_00478	FFUJ_00436	probable deoxyribodipyrimidine photo-lyase PHR	4.09	5.18	4.13					3.78	5.15	3.81
XLOC_001439	null									2.37	1.74	2.41	1.72
XLOC_001440	FFC1_00483	FFUJ_00441	related to protein kinase							2.49	2.44	3.09	2.87
XLOC_000270	FFC1_00491	FFUJ_00449	related to serine/threonine-protein kinase							2.69	2.45	2.78	2.64
XLOC_001444	FFC1_00492	FFUJ_00450	uncharacterized protein FFUJ_00450		1.40	1.67						2.04	2.58
XLOC_001445	FFC1_00493	FFUJ_00451	uncharacterized protein FFUJ_00451								2.61	3.83	3.42
XLOC_000271	FFC1_00494	FFUJ_00452	related to acetylxylan esterase precursor							5.78	6.22	6.28	7.41
XLOC_000272	FFC1_00495	FFUJ_00453	related to acetylxylan esterase precursor									-2.52	
XLOC_001448	FFC1_00499	FFUJ_00457	uncharacterized protein FFUJ_00457										-2.81
XLOC_000276	FFC1_00503	FFUJ_00461	uncharacterized protein FFUJ_00461							2.23	1.70	1.29	
XLOC_000277	FFC1_00504	FFUJ_00462	uncharacterized protein FFUJ_00462							2.39	1.76	1.68	
XLOC_001461	FFC1_00521	FFUJ_00477	uncharacterized protein FFUJ_00477							2.53			
XLOC_000283	FFC1_00522	FFUJ_00478	uncharacterized protein FFUJ_00478							3.27		1.61	
XLOC_001463	FFC1_00524	FFUJ_00479	related to stress-induced protein STI1		1.38	1.28				2.35	1.76	2.00	2.80
XLOC_001464	FFC1_00525	FFUJ_00480	related to arginyl-tRNA synthetase, cytosolic							1.87	1.29	2.64	2.26
XLOC_001465	FFC1_00526	FFUJ_00481	uncharacterized protein FFUJ_00481			2.50				2.92	2.50	4.36	7.08
XLOC_001466	null											5.42	
XLOC_001468	FFC1_00527				1.52				-1.97	1.84	1.94	4.20	4.20
XLOC_001470	FFC1_00528	FFUJ_00482	uncharacterized protein FFUJ_00482							1.84	1.77	2.96	2.98
XLOC_000288	FFC1_00538	FFUJ_00492	related to nitrogen permease regulator		1.90	2.06						1.30	1.66
XLOC_000291	FFC1_00543	FFUJ_00497	probable urease							-1.61	-1.97	-2.12	-1.59
XLOC_001478	FFC1_00544	FFUJ_00498	probable NADPH oxidase heavy chain subunit							2.24	1.93	1.35	1.41
XLOC_000292	null									3.54	6.17		
XLOC_000293	FFC1_00545	FFUJ_00499	uncharacterized protein FFUJ_00499							2.41	2.47	2.69	2.59
XLOC_001479	FFC1_00546	FFUJ_00500	related to histidine kinase	1.09						-1.63		-1.58	-2.25
XLOC_001480	null											-5.01	
XLOC_001482	FFC1_00549	FFUJ_00502	uncharacterized protein FFUJ_00502	2.15	3.08				-2.04	-2.31			
XLOC_001491	FFC1_00565	FFUJ_00517	uncharacterized protein FFUJ_00517							-2.62	-2.96	-3.47	-3.84
XLOC_000304	FFC1_00569	FFUJ_00520	uncharacterized protein FFUJ_00520								-3.02		
XLOC_000305	FFC1_00570	FFUJ_00521	related to aldehyde dehydrogenase		-1.10					-1.73	-1.96	-2.58	-1.75
XLOC_001496	FFC1_00575	FFUJ_00526	related to STB5-SIN3 binding protein		-1.07					-1.44	-1.68	-2.36	-1.98
XLOC_000308	FFC1_00576	FFUJ_00527	related to flavin-containing monooxygenase		-1.23	-1.82				-1.92	-2.40	-3.19	-3.53
XLOC_000309	null												-4.00
XLOC_000313	FFC1_00583	FFUJ_00534	uncharacterized protein FFUJ_00534							4.10	4.18	3.65	2.31
XLOC_000314	FFC1_00586	FFUJ_00537	related to enoyl-CoA hydratase							1.93	1.64	2.02	
XLOC_001503	FFC1_00588										2.15		
XLOC_000315	FFC1_00588									1.65	2.73	3.16	2.80
XLOC_000317	FFC1_00590	FFUJ_00539	related to polysaccharide synthase Cps1								2.29		
XLOC_000321	FFC1_00595	FFUJ_00543	related to manganese resistance protein							1.77	2.51	2.68	1.43
XLOC_000327	FFC1_00603	FFUJ_00551	uncharacterized protein FFUJ_00551								-1.55	-2.15	-1.38
XLOC_000328	FFC1_00604										-1.66		-2.53
XLOC_000336	FFC1_00615	FFUJ_00559	related to folylpolyglutamate synthetase							-1.87	-2.19	-1.39	-1.61
XLOC_001511	FFC1_00616	FFUJ_00560	probable tetrahydrofolylpolyglutamate synthase (met6+)		-0.94					-1.94	-2.24	-2.24	-0.97
XLOC_001513	null												-5.11
XLOC_000338	FFC1_00619	FFUJ_00563	uncharacterized protein FFUJ_00563							-4.33	-4.62	-4.14	-5.24
XLOC_001514	FFC1_00620	FFUJ_00564	uncharacterized protein FFUJ_00564							-3.12	-6.21	-3.72	-4.54
XLOC_001518	FFC1_00632	FFUJ_00576	uncharacterized protein FFUJ_00576							-1.71	-2.73	-1.49	-1.41
XLOC_000348	FFC1_00633	FFUJ_02620	probable ATP-binding cassette transporter protein YOR1							-3.20	-2.96	-3.01	-2.67
XLOC_001519	FFC1_00634	FFUJ_00578	probable Arylsulfatase							-1.72	-2.24		
XLOC_001520	FFC1_00637	FFUJ_00581	uncharacterized protein FFUJ_00581							-1.88	-2.62		-1.66
XLOC_001528	FFC1_00653	FFUJ_00596	related to NFU-1 protein (iron homeostasis)							2.17	1.72	2.26	1.88
XLOC_000362	FFC1_00656	FFUJ_00599	uncharacterized protein FFUJ_00599		0.94					1.95	1.67	2.56	2.21
XLOC_000364	FFC1_00658	FFUJ_00601	uncharacterized protein FFUJ_00601										4.04
XLOC_000379	FFC1_00685	FFUJ_00627	related to recQ gene for DNA helicase							-1.65	-2.26	-1.90	-1.82
XLOC_000380	FFC1_00688	FFUJ_00630	uncharacterized protein FFUJ_00630										-4.19
XLOC_001548	FFC1_00692	FFUJ_00634	probable aldehyde dehydrogenase		-1.41	-2.01						-2.79	
XLOC_000383	FFC1_00694	FFUJ_00635	uncharacterized protein FFUJ_00635									-4.01	
XLOC_001556	FFC1_00707	FFUJ_00647	related to methyltransferase							2.00	0.76	1.30	1.00
XLOC_001559	FFC1_00714	FFUJ_00653	uncharacterized protein FFUJ_00653		-1.61	-1.93				2.53	1.89		
XLOC_001561	null									3.36		3.99	3.03
XLOC_001562	FFC1_00721	FFUJ_00659	related to heat shock transcription factor							1.79	2.39	2.44	1.89
XLOC_000405	FFC1_00729	FFUJ_00667	uncharacterized protein FFUJ_00667			-1.12				3.63	3.83	2.64	2.35
XLOC_000414	FFC1_00743	FFUJ_00680	probable histidine biosynthesis trifunctional protein (his-3)							-2.33	-1.54		

XLOC_000419	FFC1_00749	FFUJ_00686	related to G/T mismatch-specific thymine DNA glycosylase		1.79					1.51	1.31	3.52	2.49
XLOC_000421	FFC1_00754	FFUJ_00691	uncharacterized protein FFUJ_00691	2.39	3.19	1.73				6.77	7.58	7.97	6.63
XLOC_001578	FFC1_00755	FFUJ_00692	uncharacterized protein FFUJ_00692							3.61		5.51	
XLOC_001580	FFC1_00757	FFUJ_00694	uncharacterized protein FFUJ_00694		1.29					1.33	1.37	2.32	2.32
XLOC_001592	FFC1_00781	FFUJ_00718	related to endoplasmic reticulum 25 kDa transmembrane protein	0.76	1.23					1.26	1.77	2.27	1.13
XLOC_000436	FFC1_00783	FFUJ_00720	probable meiotic expression up-regulated protein 14	0.90	1.73					2.42	2.58	3.27	2.60
XLOC_001597	FFC1_00790	FFUJ_00727	uncharacterized protein FFUJ_00727		2.39						0.91	2.42	0.87
XLOC_000445	FFC1_00800	FFUJ_00737	uncharacterized protein FFUJ_00737							4.13	4.33	4.92	2.73
XLOC_000454	FFC1_00820	FFUJ_00756	related to UDP-glucuronosyltransferase 2C1 microsomal		2.50	1.76				-1.75		1.87	
XLOC_000460	null									7.73	8.64	8.22	4.79
XLOC_000461	null									4.01	2.99	2.88	1.61
XLOC_000462	FFC1_00829	FFUJ_00765	related to suppressor protein PSP1							3.47	3.22	2.87	2.47
XLOC_000471	FFC1_00840	FFUJ_00776	probable heat shock protein 70 (hsp70)		1.46					5.14	4.15	3.74	5.15
XLOC_001621	FFC1_00841	FFUJ_00777	uncharacterized protein FFUJ_00777		1.82	2.20				2.20	2.65	4.12	4.19
XLOC_000476	FFC1_00851	FFUJ_00787	related to 7alpha-cephem-methoxylase P8 chain							5.59	5.98	7.24	6.05
XLOC_000480	null												-6.65
XLOC_001631	FFC1_00859	FFUJ_00794	probable nitrilase							-1.39	-2.14	-1.57	-0.90
XLOC_001642	null										-5.27		-2.67
XLOC_001649	FFC1_00882	FFUJ_00817	uncharacterized protein FFUJ_00817							2.63	3.09	4.57	5.11
XLOC_001652	FFC1_00887	FFUJ_00820	uncharacterized protein FFUJ_00820								-2.62		
XLOC_000491	FFC1_00889	FFUJ_00821	related to DRPLA protein		0.95					2.57	2.73	3.63	2.36
XLOC_000498	FFC1_00901	FFUJ_00833	probable acetyl-CoA synthetase							-1.09	-0.95	-2.09	-2.25
XLOC_000506	null				2.67	2.44					1.24	1.46	1.17
XLOC_000507	FFC1_00913	FFUJ_00845	uncharacterized protein FFUJ_00845		2.17	1.74					0.75	1.56	
XLOC_001665	FFC1_00917	FFUJ_00848	uncharacterized protein FFUJ_00848							4.02	3.34	3.47	2.84
XLOC_001668	FFC1_00921	FFUJ_00852	uncharacterized protein FFUJ_00852							4.75	4.39	4.27	4.75
XLOC_000514	FFC1_00931	FFUJ_00862	uncharacterized protein FFUJ_00862			-2.32				2.58	2.48		
XLOC_001688	FFC1_00954	FFUJ_00885	related to SRC1-regulation of cohesion (Splice variant I)							2.54	2.45	2.70	1.90
XLOC_001690	FFC1_00957	FFUJ_00888	uncharacterized protein FFUJ_00888		-1.21	-0.93				-3.11	-3.52	-3.61	-2.74
XLOC_001698	FFC1_00971	FFUJ_00902	uncharacterized protein FFUJ_00902		2.09	2.48				-1.65	-1.03		1.10
XLOC_000536	FFC1_00973	FFUJ_00904	uncharacterized protein FFUJ_00904		2.10	2.12				4.70	5.00	6.56	6.39
XLOC_001700	FFC1_00974	FFUJ_00905	uncharacterized protein FFUJ_00905		1.32	1.30				4.39	4.45	5.74	5.87
XLOC_001701	null									5.68	3.67	5.26	6.42
XLOC_001702	FFC1_00975	FFUJ_00906	uncharacterized protein FFUJ_00906		0.98					6.96	6.09	6.38	4.77
XLOC_000544	FFC1_00984	FFUJ_00914	related to UGA4-GABA permease-also involved in delta-aminolevulinate transport							-4.09	-2.47	-3.83	-5.88
XLOC_000549	FFC1_00992	FFUJ_00921	uncharacterized protein FFUJ_00921							1.24	1.07	2.09	2.40
XLOC_000550	FFC1_00994									1.72	2.24		1.87
XLOC_001711	FFC1_00996	FFUJ_00924	uncharacterized protein FFUJ_00924							-2.19	-2.30	-2.11	-2.08
XLOC_000554	FFC1_01000	FFUJ_00928	uncharacterized protein FFUJ_00928							3.47	3.42	3.43	2.93
XLOC_000555	FFC1_01001	FFUJ_00929	uncharacterized protein FFUJ_00929							5.97	5.36	5.12	4.59
XLOC_001714	FFC1_01002	FFUJ_00930	uncharacterized protein FFUJ_00930							8.14	6.87	7.94	9.48
XLOC_000556	FFC1_01003	FFUJ_00931	related to hsp70 protein							2.56	3.03	2.66	3.62
XLOC_000563	FFC1_01014	FFUJ_00941	related to phosphatidylinositol phospholipase		-1.29					-1.50	-2.07	-2.58	-1.47
XLOC_001724	FFC1_01024	FFUJ_00951	related to CAF120 CCR4 Associated Factor 120 kDa	1.07	1.35	0.94				1.00	1.77	2.07	2.13
XLOC_001725	null			1.30	1.55						1.76	2.21	2.16
XLOC_000574	FFC1_01028	FFUJ_00955	uncharacterized protein FFUJ_00955		-1.01	-1.00			-1.04	-1.76	-1.83	-2.45	-1.71
XLOC_001728	FFC1_01031	FFUJ_00958	uncharacterized protein FFUJ_00958							-1.20	-2.55		-3.40
XLOC_001732	null									-4.71	-5.11		-5.44
XLOC_000584	FFC1_01044	FFUJ_00971	uncharacterized protein FFUJ_00971										-4.07
XLOC_001734	FFC1_01045	FFUJ_00972	related to cystathionine gamma-synthases							-3.01	-3.38	-3.50	-2.61
XLOC_000585	FFC1_01047	FFUJ_00974	uncharacterized protein FFUJ_00974							-3.63	-3.03	-2.97	-5.37
XLOC_001753	FFC1_01070	FFUJ_00996	probable 2-dehydro-3-deoxyphosphoheptonate aldolase							-2.40	-1.85	-1.54	
XLOC_000600	FFC1_01077	FFUJ_01003	uncharacterized protein FFUJ_01003							-3.01	-2.95	-2.63	
XLOC_001758	FFC1_01079	FFUJ_01005	related to carbohydrate kinase, contains PfkB domain							-2.75	-3.10	-3.11	-1.76
XLOC_000601	FFC1_01080	FFUJ_01006	uncharacterized protein FFUJ_01006							-2.91	-3.17	-3.37	-2.38
XLOC_000602	FFC1_01081	FFUJ_01007	related to a retinal short-chain dehydrogenase/reductase								-2.56	-2.04	-2.33
XLOC_001764	FFC1_01090	FFUJ_01016	related to meiotic expression up-regulated protein 14		1.94					1.47	1.77	3.19	2.24
XLOC_000606	FFC1_01092									-1.59	-2.10	-2.25	-1.22
XLOC_000608	FFC1_01096	FFUJ_01022	related to O-succinylhomoserine (thiol)-lyase							-3.39	-5.82		
XLOC_000618	null										-4.49		
XLOC_001778	FFC1_01122	FFUJ_01048	related to TfdA family oxidoreductase							-2.75	-2.32		-1.32
XLOC_001780	FFC1_01125	FFUJ_01051	uncharacterized protein FFUJ_01051		2.07	2.21						2.00	1.39
XLOC_001784	FFC1_01130	FFUJ_01056	related to GNAT family acetyltransferase							4.94	7.90	4.58	
XLOC_000627	FFC1_01131	FFUJ_09800	related to multidrug resistance protein			-1.09				1.55	2.14		1.82
XLOC_001792	FFC1_01144	FFUJ_01070	uncharacterized protein FFUJ_01070							3.94	4.00	4.25	3.43
XLOC_001804	FFC1_01162	FFUJ_01088	related to short-chain alcohol dehydrogenase	2.14	4.95	2.31				2.18	3.76	6.07	4.59
XLOC_000643	FFC1_01167	FFUJ_01091	related to hxB protein		2.64					1.46	1.68	3.07	2.22
XLOC_000646	FFC1_01171	FFUJ_01095	related to HXT3-Low-affinity hexose facilitator							-1.90	-2.49	-2.92	-3.18
XLOC_001813	FFC1_01180	FFUJ_01103	related to papaya ringspot virus polyprotein	2.23	1.69	1.38				-1.42			
XLOC_001817	FFC1_01187	FFUJ_01109	uncharacterized protein FFUJ_01109	1.19	1.44					1.54	2.89	3.30	2.32
XLOC_000659	FFC1_01194	FFUJ_01116	uncharacterized protein FFUJ_01116							2.26	1.98	1.64	
XLOC_001820	FFC1_01196	FFUJ_01118	probable ASP3-1-L-asparaginase II	-1.33	-2.08	-2.25				2.02	1.26		

XLOC_000660	FFC1_01198	FFUJ_01120	related to anthranilate phosphoribosyltransferase							-1.86	-2.12	-1.95	
XLOC_001824	FFC1_01203	FFUJ_01125	uncharacterized protein FFUJ_01125							-2.05	-1.91	-1.93	-1.30
XLOC_001825	FFC1_01204	FFUJ_01126	related to asparagine synthases							-2.27	-2.51	-2.52	-2.19
XLOC_001827	FFC1_01206	FFUJ_01128	uncharacterized protein FFUJ_01128							3.26	2.89	2.64	1.86
XLOC_000664	FFC1_01210	FFUJ_01132	probable BRT1 protein, down-regulated by mating factor B							-2.02	-2.31	-2.02	-0.84
XLOC_000668	FFC1_01215	FFUJ_01137	probable amino acid transport protein GAP1		-0.91					-1.27	-1.61	-2.32	-1.90
XLOC_000669	FFC1_01217	FFUJ_01139	related to carboxypeptidase Y-sorting protein PEP1 precursor							1.47	2.12	1.98	1.53
XLOC_000672	FFC1_01221	FFUJ_01143	uncharacterized protein FFUJ_01143							-1.90	-3.14	-2.55	-2.37
XLOC_001834	null									-4.82	-4.59		
XLOC_000673	FFC1_01222	FFUJ_01144	probable ammonium transporter MEPa							-1.41	-1.83	-2.05	
XLOC_000674	FFC1_01223	FFUJ_01145	related to DNA-directed DNA polymerase lambda							-1.45	-2.33	-1.64	
XLOC_000685	FFC1_01243	FFUJ_01165	uncharacterized protein FFUJ_01165							2.03	1.68	2.40	2.27
XLOC_000687	FFC1_01245	FFUJ_01167	probable rhamnogalacturonase B precursor									5.38	
XLOC_000693	FFC1_01256	FFUJ_01178	uncharacterized protein FFUJ_01178							2.18	1.71	1.39	
XLOC_001851	FFC1_01262	FFUJ_01184	related to kinesin motor protein		0.89					1.27	1.34	2.10	1.56
XLOC_001859	FFC1_01273	FFUJ_01195	probable chaperonin ClpB							4.89	4.41	3.62	3.72
XLOC_000710	FFC1_01292	FFUJ_01212	related to benzodiazepine receptor, peripheral-type	1.54	2.67	2.17					1.39	2.57	2.05
XLOC_001872	FFC1_01296	FFUJ_01216	related to alpha-L-rhamnosidase A									2.64	2.52
XLOC_001873	FFC1_01298	FFUJ_01217	probable DNA repair protein MUS-42		1.19	1.07				0.70	0.78	2.05	1.74
XLOC_001874	FFC1_01301	FFUJ_01220	related to TPC1-mitochondrial transport protein								0.93	2.23	1.23
XLOC_000716	FFC1_01304	FFUJ_01223	uncharacterized protein FFUJ_01223			-1.03				1.90	1.88	2.17	
XLOC_001881	FFC1_01320	FFUJ_01239	uncharacterized protein FFUJ_01239							-3.59	-4.36	-3.09	-3.62
XLOC_000740	FFC1_01339	FFUJ_01258	uncharacterized protein FFUJ_01258		1.05					2.10	1.96	2.17	1.49
XLOC_001890	FFC1_01340	FFUJ_01259	uncharacterized protein FFUJ_01259		2.37	1.71				2.95	3.56	5.32	3.81
XLOC_001891	FFC1_01341				2.11					4.08	4.78	8.78	4.92
XLOC_001895	FFC1_01346	FFUJ_01264	uncharacterized protein FFUJ_01264									-4.15	-4.23
XLOC_000742	FFC1_01347	FFUJ_01265	uncharacterized protein FFUJ_01265							3.73			
XLOC_000743	FFC1_01348	FFUJ_01266	related to YjeF domain protein							1.30	1.63	2.28	
XLOC_000745	FFC1_01351	FFUJ_01269	uncharacterized protein FFUJ_01269								4.01		
XLOC_001899	FFC1_01357	FFUJ_01273	probable SIS1 Heat shock protein		0.75				1.21	2.26	2.44	2.46	1.35
XLOC_000761	FFC1_01379	FFUJ_01292	uncharacterized protein FFUJ_01292	3.27	4.59	4.78				2.35	4.85	5.84	6.21
XLOC_001913	FFC1_01383	FFUJ_01296	related to glycosyl hydrolase, family 15		2.51	1.15					1.27	3.02	1.80
XLOC_001918	FFC1_01391	FFUJ_01304	uncharacterized protein FFUJ_01304							-1.75	-2.61	-2.25	
XLOC_001922	FFC1_01396	FFUJ_01309	related to verprolin			-2.02				3.52	3.29	2.33	2.07
XLOC_001936	FFC1_01420	FFUJ_01333	uncharacterized protein FFUJ_01333			1.64						2.42	3.81
XLOC_001937	FFC1_01421	FFUJ_01334	uncharacterized protein FFUJ_01334										5.10
XLOC_000779	null									-1.82	-3.94		
XLOC_001946	FFC1_01433	FFUJ_01346	probable heat shock protein 30		1.54	1.66			3.18	5.74	5.36	3.77	4.24
XLOC_000785	FFC1_01440	FFUJ_01353	related to DNA mismatch repair protein PMS2			1.05				1.08	0.91	1.30	2.19
XLOC_000789	FFC1_01447	FFUJ_01361	uncharacterized protein FFUJ_01361		1.18					2.29	2.58	3.14	2.49
XLOC_000790	FFC1_01448	FFUJ_01362	uncharacterized protein FFUJ_01362							3.07	3.12	3.39	3.76
XLOC_001954	null											4.07	
XLOC_000791	FFC1_01449	FFUJ_01363	related to Zn-dependent oxidoreductases		1.05				3.56	7.98	7.60	5.81	5.48
XLOC_001955	FFC1_01450	FFUJ_01364	uncharacterized protein FFUJ_01364		1.62					4.85	5.22	6.67	5.09
XLOC_000794	FFC1_01456	FFUJ_01369	probable cystathionine gamma-lyase							2.56	2.56	3.06	2.83
XLOC_000797	null										1.91	2.05	4.00
XLOC_000798	FFC1_01461	FFUJ_01373	uncharacterized protein FFUJ_01373							1.47	1.90	1.93	2.07
XLOC_001961	FFC1_01463	FFUJ_01374	uncharacterized protein FFUJ_01374							-1.51	-1.86	-2.66	-2.29
XLOC_000805	FFC1_01473	FFUJ_01384	uncharacterized protein FFUJ_01384								3.89		
XLOC_001975	FFC1_01486	FFUJ_01396	related to mitochondrial integral membrane protein		2.50	2.06				4.42	3.59	4.51	
XLOC_001976	FFC1_01487	FFUJ_01397	uncharacterized protein FFUJ_01397							2.44	1.81	2.72	
XLOC_001980	FFC1_01498	FFUJ_04517	probable URA2-multifunctional pyrimidine biosynthesis protein	1.36	1.05	1.18				-2.04			
XLOC_001982	null									-1.45	-2.17		
XLOC_000824	FFC1_01506	FFUJ_01415	related to zinc-binding protein		2.16								
XLOC_000825	FFC1_01507	FFUJ_01416	related to acetylxylan esterase						-1.94	-3.79	-3.94	-3.71	-2.41
XLOC_000835	FFC1_01518	FFUJ_01427	related to ECM39 protein, involved in cell wall biogenesis and architecture		-1.04					-1.86	-2.58	-2.55	-1.71
XLOC_000838	FFC1_01524	FFUJ_01433	uncharacterized protein FFUJ_01433							-1.31	-1.67	-1.86	-2.30
XLOC_001989	null										-3.80		
XLOC_000842	FFC1_01530	FFUJ_01439	probable cytochrome-c peroxidase precursor							4.19	3.64	3.35	3.79
XLOC_000851	FFC1_01542										-3.94		-4.53
XLOC_000852	FFC1_01544	FFUJ_01451	related to DNA repair family protein							2.41	2.12	3.01	2.12
XLOC_000858	FFC1_01556	FFUJ_01462	uncharacterized protein FFUJ_01462							1.36		1.97	2.39
XLOC_002011	FFC1_01572	FFUJ_01478	related to nuclear poly(A)-binding protein							2.25	1.97	2.75	2.54
XLOC_002012	FFC1_01575	FFUJ_01481	related to ARO8-aromatic amino acid aminotransferase I							-3.13	-2.47	-4.07	-3.91
XLOC_002013	FFC1_01576										-3.69		
XLOC_000877	FFC1_01585	FFUJ_01490	related to glutathione transferase omega 1	2.18							1.38		
XLOC_002016	FFC1_01586	FFUJ_01491	related to high-affinity phosphate permease, phosphate-repressible							-1.28	-1.01	-1.48	-2.01
XLOC_002017	FFC1_01589	FFUJ_01494	related to transcriptional repressor	2.17	2.15	1.38				2.19	4.19	3.84	2.65
XLOC_002018	FFC1_01590	FFUJ_01495	related to U4/U6 snRNP-associated 61 kDa protein		0.98	0.96				1.00	1.81	2.02	1.70
XLOC_002019	FFC1_01592	FFUJ_01497	uncharacterized protein FFUJ_01497	0.65	0.71					1.79	2.42	2.30	1.76
XLOC_000888	FFC1_01606	FFUJ_01509	uncharacterized protein FFUJ_01509		0.93					-2.12	-1.32	-1.18	-2.16
XLOC_002033	null									-1.79		-3.08	-2.15
XLOC_000899	FFC1_01624	FFUJ_01527	uncharacterized protein FFUJ_01527							2.13	2.14	1.90	

XLOC_002046	FFC1_01637	FFUJ_01539	probable alternative oxidase precursor, mitochondrial	1.03						-1.70	-1.31	-1.91	-2.85
XLOC_002049	FFC1_01645	FFUJ_01546	related to diacylglycerol acyltransferase type 2a		0.88					2.15	2.43	2.52	1.40
XLOC_002050	FFC1_01646	FFUJ_01547	related to zinc finger protein crol gamma							1.35	2.01	1.63	0.88
XLOC_000913	FFC1_01649	FFUJ_01549	related to MFS amino acid transporter							2.26	1.52	1.68	
XLOC_002069	FFC1_01689	FFUJ_01583	uncharacterized protein FFUJ_01583							8.69	9.17	8.03	7.24
XLOC_002082	FFC1_01711	FFUJ_01604	uncharacterized protein FFUJ_01604		-1.12					-1.67	-2.60	-2.81	-3.03
XLOC_002083	FFC1_01712	FFUJ_01605	uncharacterized protein FFUJ_01605		-1.64					-1.41	-2.27	-2.72	-2.17
XLOC_002084	FFC1_01714	FFUJ_01607	probable 1,4-Benzoquinone reductase		2.10	1.80				-2.99	-2.53		
XLOC_000950	null									-5.08			
XLOC_000958	FFC1_01730	FFUJ_01623	uncharacterized protein FFUJ_01623							-1.85	-2.47	-1.55	-2.23
XLOC_002093	FFC1_01731	FFUJ_01624	probable O-acetylhomoserine (thiol)-lyase							-3.29	-4.73	-4.12	-2.32
XLOC_002098	null										5.68		
XLOC_002099	FFC1_01743	FFUJ_01633	uncharacterized protein FFUJ_01633							-2.24	-1.73	-1.82	
XLOC_000966	FFC1_01744	FFUJ_01634	uncharacterized protein FFUJ_01634							-1.96	-2.24	-1.16	
XLOC_000969	FFC1_01757	FFUJ_01647	related to putative plasma membrane protein YRO2		1.44					1.88	1.92	2.02	
XLOC_002111	FFC1_01762	FFUJ_01652	related to serine protease		-1.50	-1.74			-1.12	-1.25	-1.52	-2.24	-1.85
XLOC_000984	FFC1_01779	FFUJ_01668	uncharacterized protein FFUJ_01668							6.90	5.54	8.16	6.31
XLOC_002123	FFC1_01789	FFUJ_01678	uncharacterized protein FFUJ_01678			2.20				7.50	6.48	7.97	7.45
XLOC_002124	FFC1_01790	FFUJ_01679	probable zinc finger protein ZPR1							2.25	2.31	2.95	2.87
XLOC_000991	FFC1_01794	FFUJ_01683	related to glycerophosphocholine (GroPCho) phosphodiesterase							-1.58	-0.97	-1.40	-2.18
XLOC_000997	FFC1_01800	FFUJ_01687	related to aldehyde reductase II							2.86	2.44	2.82	3.18
XLOC_001000	FFC1_01809	FFUJ_01696	anaphase promoting complex subunit 11							-1.58	-1.97	-2.06	-1.84
XLOC_001002	FFC1_01811	FFUJ_01698	uncharacterized protein FFUJ_01698								-2.39		
XLOC_001010	FFC1_01823	FFUJ_01709	probable choline-sulfatase							-4.36	-6.08	-5.16	-5.53
XLOC_001013	FFC1_01826	FFUJ_01712	uncharacterized protein FFUJ_01712							-2.98	-3.26	-3.23	-2.57
XLOC_001014	FFC1_01827	FFUJ_01713	uncharacterized protein FFUJ_01713							-1.94	-2.27	-2.15	-2.82
XLOC_001018	FFC1_01832	FFUJ_01718	related to DAHP synthase class II							-2.46	-1.97	-2.45	-2.06
XLOC_002146	FFC1_01840	FFUJ_01725	uncharacterized protein FFUJ_01725							-4.17	-3.89	-2.51	-2.23
XLOC_002151	FFC1_01849	FFUJ_01734	uncharacterized protein FFUJ_01734									-3.07	-2.94
XLOC_001029	FFC1_01857	FFUJ_01742	uncharacterized protein FFUJ_01742							1.84	3.12	2.87	1.81
XLOC_002156	FFC1_01858	FFUJ_01743	related to arginase									3.62	4.46
XLOC_001043	FFC1_01884	FFUJ_01767	related to heterokaryon incompatibility protein het-6							-1.89	-2.22	-2.23	-2.10
XLOC_001048	null										-4.86		
XLOC_001053	FFC1_01895	FFUJ_01775	probable AAH1-adenosine deaminase		1.07	1.26				1.04	0.78	1.84	2.09
XLOC_002173	FFC1_01896	FFUJ_01776	probable ubiquitin fusion degradation protein 2		0.87					1.07	1.16	2.01	1.82
XLOC_002174	FFC1_01897	FFUJ_01777	related to traf5 protein							2.71	2.83	2.79	2.80
XLOC_002175	null									5.00			
XLOC_001054	FFC1_01898	FFUJ_01778	related to calpain							1.61	2.13	1.72	1.46
XLOC_001055	FFC1_01899	FFUJ_01779	uncharacterized protein FFUJ_01779							-1.86	-2.31	-1.60	-1.63
XLOC_001057	FFC1_01900	FFUJ_01780	related to hormone-sensitive lipase							2.96	1.95	1.69	
XLOC_002176	FFC1_01902	FFUJ_01782	probable acetylornithine aminotransferase precursor							-2.08			
XLOC_002177	FFC1_01904	FFUJ_01784	related to Y.lipolytica GPR1 protein and Fun34p							2.06	2.03		
XLOC_001060	FFC1_01905	FFUJ_01785	uncharacterized protein FFUJ_01785		2.72							3.11	1.52
XLOC_002183	FFC1_01916	FFUJ_01794	related to putative multidrug transporter Mfs1.1 (major facilitator family protein)							2.07			
XLOC_002185	null									5.77	5.88	5.97	
XLOC_002186	FFC1_01917	FFUJ_01795	uncharacterized protein FFUJ_01795							7.82	7.99	8.30	7.69
XLOC_002187	null									5.51			
XLOC_002188	null										5.44	6.21	
XLOC_002189	FFC1_01918									7.52	8.38	8.35	7.46
XLOC_002190	FFC1_01919	FFUJ_01796	uncharacterized protein FFUJ_01796							5.45	6.30	6.56	5.72
XLOC_002191	FFC1_01920	FFUJ_01797	uncharacterized protein FFUJ_01797							10.56	9.93	12.28	10.77
XLOC_002192	null										6.08		6.18
XLOC_002193	null									5.85	6.20		
XLOC_002194	null					-1.35				9.60	10.34	10.02	8.38
XLOC_002198	FFC1_01927									-2.96	-3.07	-2.77	-1.96
XLOC_001070	FFC1_01929	FFUJ_02110	uncharacterized protein FFUJ_02110							-0.89	-1.12	-2.13	-1.34
XLOC_002200	FFC1_01933	FFUJ_01808	uncharacterized protein FFUJ_01808							4.58	3.94	3.96	4.10
XLOC_001074	FFC1_01935	FFUJ_01810	related to PHO89-Na+/phosphate co-transporter									5.16	5.88
XLOC_002202	FFC1_01936	FFUJ_01811	uncharacterized protein FFUJ_01811							4.58	5.06	5.19	5.66
XLOC_002204	FFC1_01940	FFUJ_01815	uncharacterized protein FFUJ_01815							5.19		5.39	
XLOC_002205	FFC1_01941									4.58			
XLOC_002209	FFC1_01946	FFUJ_01821	uncharacterized protein FFUJ_01821		1.12	1.32				4.87	4.80	5.66	5.92
XLOC_002210	FFC1_01947	FFUJ_01822	probable protein-tyrosine-phosphatase		0.83					1.92	1.92	2.63	2.37
XLOC_002213	FFC1_01950									2.05		2.82	
XLOC_002228	FFC1_01972	FFUJ_01844	probable cellulase precursor							-3.76	-3.87	-3.36	-3.68
XLOC_001089	FFC1_01978	FFUJ_01850	uncharacterized protein FFUJ_01850								-4.85		
XLOC_002236	FFC1_01986	FFUJ_01858	related to triacylglycerol lipase										-3.47
XLOC_001097	null											-4.73	-5.55
XLOC_001098	null											-5.38	-6.09
XLOC_002242	FFC1_01997	FFUJ_01869	related to MDR1-Mac1p interacting protein							1.38	1.65	2.51	2.11
XLOC_002248	FFC1_02010	FFUJ_01882	related to E.coli dioxygenase							6.97	6.20	5.36	3.49
XLOC_001108	FFC1_02011	FFUJ_01883	related to permease							2.74			
XLOC_002251	FFC1_02014	FFUJ_01887	uncharacterized protein FFUJ_01887								-2.94		
XLOC_001109	FFC1_02015	FFUJ_01888	uncharacterized protein FFUJ_01888							-1.36	-2.31	-1.48	-1.62
XLOC_002252	FFC1_02016	FFUJ_01889	probable thiamine repressed nmt1 protein							-1.93	-2.37	-2.35	
XLOC_001115	FFC1_02026	FFUJ_01899	uncharacterized protein FFUJ_01899								-1.19		-2.17
XLOC_001116	FFC1_02028	FFUJ_01901	related to beta-glucosidase							-3.03	-3.50		

XLOC_002261	FFC1_02033	FFUJ_01906	related to WSS1 Protein involved in sister chromatid separation and segregation						1.50	4.95	4.54	4.73	4.40
XLOC_002262	FFC1_02034	FFUJ_01907	uncharacterized protein FFUJ_01907		1.40			2.27		9.90	9.19	9.03	9.22
XLOC_001120	FFC1_02035	FFUJ_01908	uncharacterized protein FFUJ_01908		0.84					6.70	5.01	6.09	5.41
XLOC_001121	FFC1_02036	FFUJ_01909	uncharacterized protein FFUJ_01909		1.65					9.43	8.98	9.03	9.10
XLOC_001122	FFC1_02037	FFUJ_01910	uncharacterized protein FFUJ_01910		0.96					6.03	6.24	6.10	5.83
XLOC_001123	FFC1_02038	FFUJ_01911	uncharacterized protein FFUJ_01911							3.67	3.64	4.50	3.91
XLOC_002265	FFC1_02042	FFUJ_01915	related to alcohol dehydrogenase, class C		2.02					2.40	2.79	4.42	3.35
XLOC_002266	FFC1_02044	FFUJ_01917	uncharacterized protein FFUJ_01917							2.31		3.26	1.95
XLOC_001126	FFC1_02046	FFUJ_01919	uncharacterized protein FFUJ_01919							4.16	6.07	7.53	5.00
XLOC_002269	FFC1_02049	FFUJ_01922	uncharacterized protein FFUJ_01922							5.12			
XLOC_001128	FFC1_02050	FFUJ_01923	uncharacterized protein FFUJ_01923							1.52	1.21	2.02	
XLOC_001129	FFC1_02051	FFUJ_01925	uncharacterized protein FFUJ_01925							5.21	3.46	4.70	3.50
XLOC_001130	FFC1_02053	FFUJ_01927	uncharacterized protein FFUJ_01927		1.86					2.91	2.86	4.41	3.66
XLOC_002271	FFC1_02055	FFUJ_01929	related to UDPglucose 4-epimerase		2.15					-2.51	-2.31		
XLOC_001132	FFC1_02057	FFUJ_01931	related to nodulin							2.52	2.59	2.71	
XLOC_001137	FFC1_02069	FFUJ_01941	uncharacterized protein FFUJ_01941			2.74							3.64
XLOC_001139	FFC1_02071	FFUJ_01943	related to cholinesterase							3.62	3.67	4.66	6.60
XLOC_001140	FFC1_02074	FFUJ_01946	uncharacterized protein FFUJ_01946							-5.66	-5.39	-3.69	-4.33
XLOC_001141	FFC1_02075	FFUJ_01947	uncharacterized protein FFUJ_01947							-4.45	-5.14	-4.48	-3.88
XLOC_002282	FFC1_02076	FFUJ_01948	uncharacterized protein FFUJ_01948							-4.40	-5.11	-4.85	-5.05
XLOC_001142	FFC1_02077	FFUJ_01949	uncharacterized protein FFUJ_01949							-2.82	-2.27	-3.06	-2.37
XLOC_002283	FFC1_02077	FFUJ_01950	related to epoxide hydrolase							-2.79	-2.40	-3.02	-2.52
XLOC_002284	FFC1_02079	FFUJ_01951	related to flavonol synthase-like protein							-1.34	-1.69	-2.26	-1.61
XLOC_001147	FFC1_02089									4.62			
XLOC_001151	FFC1_02095	FFUJ_01967	uncharacterized protein FFUJ_01967							9.45	8.78	6.45	6.30
XLOC_002293	FFC1_02096	FFUJ_01968	related to heterokaryon incompatibility protein							4.94			
XLOC_002299	FFC1_02106	FFUJ_01978	related to TOB3 (member of AAA-ATPase family)		-1.86	-2.02				7.64	7.19	6.64	5.77
XLOC_001157	FFC1_02107	FFUJ_01979	uncharacterized protein FFUJ_01979							6.96	4.90	5.37	
XLOC_001158	FFC1_02109	FFUJ_01981	uncharacterized protein FFUJ_01981			1.82							3.03
XLOC_002303	FFC1_02114	FFUJ_01985	putative trichothecene biosynthesis gene							3.54	3.07	3.60	3.86
XLOC_002304	FFC1_02115	FFUJ_01986	related to immune-responsive protein 1							1.89	2.33	3.10	
XLOC_002308	FFC1_02122	FFUJ_01993	probable organic hydroperoxide resistance protein		4.96	2.61				3.41	3.43	6.00	5.16
XLOC_001164	FFC1_02123	FFUJ_01994	related to salicylate 1-monooxygenase (flavoprotein monooxygenase)									2.19	
XLOC_001165	FFC1_02124	FFUJ_01995	related to cytochrome P450 monooxygenase							4.60			
XLOC_002309	FFC1_02125	FFUJ_01996	related to C4-dicarboxylate transport protein mae1	1.77	1.63					3.19	4.26	4.04	
XLOC_002310	FFC1_02126	FFUJ_01998	related to hsp70 protein							3.36	2.49	1.90	
XLOC_001166	FFC1_02127	FFUJ_01997	uncharacterized protein FFUJ_01997							2.87	2.09	2.24	
XLOC_002311	FFC1_02128	FFUJ_01999	uncharacterized protein FFUJ_01999							2.83	2.69	2.73	
XLOC_001175	FFC1_02143	FFUJ_02013	uncharacterized protein FFUJ_02013			-2.76				5.00	6.99	6.48	
XLOC_002318	FFC1_02144	FFUJ_02014	uncharacterized protein FFUJ_02014							-1.41	-1.82	-2.01	-1.62
XLOC_002319	FFC1_02145	FFUJ_02015	uncharacterized protein FFUJ_02015							4.49	3.69		
XLOC_002322	FFC1_02149	FFUJ_02019	aurofusarin/rubrofusarin efflux pump AFLT			1.24				10.39	9.82	8.38	6.29
XLOC_001178	FFC1_02150	FFUJ_02020	related to 2,4-dienoyl-CoA reductase precursor							9.48	9.12	8.85	7.83
XLOC_002323	FFC1_02151	FFUJ_02021	uncharacterized protein FFUJ_02021							10.43	10.41	10.96	9.35
XLOC_001179	FFC1_02152					1.21				9.66	8.50	6.92	6.78
XLOC_002324	FFC1_02153	FFUJ_02023	uncharacterized protein FFUJ_02023		-0.95					-1.44	-2.17	-2.60	-2.23
XLOC_002329	FFC1_02161	FFUJ_02030	uncharacterized protein FFUJ_02030							3.61	2.55	2.63	
XLOC_002330	FFC1_02163	FFUJ_02032	related to tol protein							2.32			
XLOC_002331	FFC1_02165	FFUJ_02034	uncharacterized protein FFUJ_02034							-1.26	-1.08		-2.31
XLOC_001185	FFC1_02166	FFUJ_02035	related to WSC2 Glucoamylase III (alpha-1,4-glucan-glucosidase)			-1.75				-1.10	-1.27	-1.64	-3.22
XLOC_001186	FFC1_02167	FFUJ_02036	uncharacterized protein FFUJ_02036							3.65	3.20	2.85	2.79
XLOC_001188	FFC1_02169	FFUJ_02038	related to tol protein		-1.41	-1.72				5.91	6.84	5.85	8.20
XLOC_001189	FFC1_02170	FFUJ_02039	uncharacterized protein FFUJ_02039							-9.34	-8.94	-8.07	-7.65
XLOC_002332	FFC1_02171	FFUJ_02040	uncharacterized protein FFUJ_02040		-1.49					3.76	3.01	2.09	2.93
XLOC_001190	FFC1_02172	FFUJ_02041	uncharacterized protein FFUJ_02041							2.58	2.56	1.75	3.75
XLOC_002336	FFC1_02176	FFUJ_02044	uncharacterized protein FFUJ_02044							-2.49			
XLOC_002337	FFC1_02177	FFUJ_02045	related to 3-oxoacyl								-5.08		
XLOC_001195	FFC1_02184	FFUJ_02052	uncharacterized protein FFUJ_02052							-3.68	-6.70	-5.48	-2.72
XLOC_002340	FFC1_02185	FFUJ_02053	probable acetyl-CoA synthetase							-2.73	-3.13	-3.29	-2.52
XLOC_001197	FFC1_02190	FFUJ_02058	related to pisatin demethylase cytochrome P450							4.78	6.53	6.23	6.61
XLOC_002344	FFC1_02191	FFUJ_02059	probable amidases related to nicotinamidase							3.61	2.95	3.44	2.71
XLOC_002345	FFC1_02192	FFUJ_02060	uncharacterized protein FFUJ_02060							3.74	3.62	3.47	3.20
XLOC_001198	FFC1_02193	FFUJ_02061	related to cutinase transcription factor 1 beta							3.81	3.72	3.64	3.72
XLOC_002346	FFC1_02194	FFUJ_02062	uncharacterized protein FFUJ_02062		1.60	1.75				2.51	2.11	4.43	3.61
XLOC_002347	FFC1_02195	FFUJ_02063	related to ketoreductase									6.62	6.49
XLOC_002349	FFC1_02197	FFUJ_02065	related to Protein indc11							-2.55	-2.48	-1.74	-2.06
XLOC_001202	FFC1_02203	FFUJ_02072	related to C6 zink-finger protein PRO1A							-1.83	-2.75	-1.63	
XLOC_002354	FFC1_02207	FFUJ_02076	related to MFS transporter		-1.34						-1.78	-2.17	-1.09
XLOC_001206	FFC1_02212	FFUJ_02081	uncharacterized protein FFUJ_02081							-2.53	-3.24	-3.46	-2.95
XLOC_002358	null									5.51	6.79	5.13	
XLOC_002364	FFC1_02230	FFUJ_06714	uncharacterized protein FFUJ_06714									-5.00	
XLOC_002365	FFC1_02232	FFUJ_06716	uncharacterized protein FFUJ_06716							-2.15	-2.56	-3.25	-2.28
XLOC_003200	FFC1_02240	FFUJ_06722	related to IQ calmodulin-binding motif protein							-1.99	-2.04		
XLOC_003201	FFC1_02241	FFUJ_06723	related to transcriptional activator Mut3p	2.12	2.80						2.39	2.80	
XLOC_003202	FFC1_02242	FFUJ_06724	related to DUF1446 domain protein	5.85	7.53						5.83	7.42	

XLOC_002369	FFC1_02243	FFUJ_06725	related to acyl-CoA transferases/carnitine dehydratase		4.38							3.51	
XLOC_002372	FFC1_02247	FFUJ_06729	related to 4-cresol dehydrogenase flavoprotein subunit							5.71			3.96
XLOC_003205	FFC1_02249	FFUJ_06731	uncharacterized protein FFUJ_06731		4.61						5.57	5.81	4.45
XLOC_003209	FFC1_02257	FFUJ_06739	uncharacterized protein FFUJ_06739							5.89	4.52	5.01	
XLOC_003212	FFC1_02261	FFUJ_03984	fusarubin cluster-polyketide synthase					3.26	3.46	-7.74	-8.49	-7.96	-11.63
XLOC_003213	FFC1_02262	FFUJ_06743	bikaverin cluster-monooxygenase							-7.75	-5.39	-5.89	-9.40
XLOC_002377	FFC1_02263	FFUJ_06744	bikaverin cluster-O-methyltransferase							-7.50	-6.34	-5.32	-8.49
XLOC_002378	FFC1_02264	FFUJ_06745	bikaverin cluster-transcription factor enhancer							-5.12			
XLOC_003214	FFC1_02265	FFUJ_06746	bikaverin cluster-transcription factor							-3.16	-2.93	-3.16	-3.08
XLOC_002379	FFC1_02266	FFUJ_06747	bikaverin cluster-efflux pump							-6.16	-4.39		-4.87
XLOC_002380	FFC1_02267	FFUJ_06748	uncharacterized protein FFUJ_06748							-3.47	-5.22	-3.86	-8.04
XLOC_003217	FFC1_02270	FFUJ_06751	related to C2H2 zinc finger protein							-3.04	-5.65	-4.52	
XLOC_003219	FFC1_02273	FFUJ_06754	uncharacterized protein FFUJ_06754								-3.92		
XLOC_002382	FFC1_02275	FFUJ_06756	related to D-amino acid hydantoin hydrolase (hydantoinase)							5.63	2.99		3.27
XLOC_002384	FFC1_02278	FFUJ_06759	HET-6OR heterokaryon incompatibility protein (het-6OR allele)								-3.51		
XLOC_002385	FFC1_02279	FFUJ_06760	uncharacterized protein FFUJ_06760							-3.70	-4.32	-4.08	-2.30
XLOC_002389	FFC1_02285									5.04		5.64	
XLOC_002390	FFC1_02289	FFUJ_06769	uncharacterized protein FFUJ_06769			2.05				-2.93	-4.41	-2.53	
XLOC_003228	FFC1_02293	FFUJ_06773	probable rhamnogalacturonase A precursor								5.00		5.71
XLOC_003231	FFC1_02299	FFUJ_06779	uncharacterized protein FFUJ_06779							2.55			
XLOC_003232	FFC1_02300	FFUJ_06780	probable chaperone protein hchA									4.48	
XLOC_002396	FFC1_02301	FFUJ_06781	related to alcohol dehydrogenase, class C							3.70	2.15	3.96	2.96
XLOC_003236	FFC1_02310	FFUJ_06788	uncharacterized protein FFUJ_06788							-4.58			
XLOC_002404	FFC1_02314	FFUJ_06791	related to tol protein								-4.13	-4.78	
XLOC_003238	FFC1_02315	FFUJ_06792	uncharacterized protein FFUJ_06792							-4.02	-5.52	-4.95	-4.51
XLOC_003243	FFC1_02323	FFUJ_06800	uncharacterized protein FFUJ_06800							-2.83	-2.73	-2.56	-3.17
XLOC_003247	FFC1_02329	FFUJ_06806	related to lipoxygenase 1							6.76	5.76	6.18	6.42
XLOC_002415	FFC1_02342	FFUJ_06818	related to multidrug efflux pump							4.08	3.34	4.30	2.71
XLOC_003255	FFC1_02344	FFUJ_06820	probable molecular chaperone distantly related to HSP70-fold metalloproteases										5.05
XLOC_003256	FFC1_02346	FFUJ_06822	related to C6 transcription factor							-1.77	-2.07	-2.18	-1.56
XLOC_002420	FFC1_02351	FFUJ_06827	related to potential drug facilitator PEP5							4.16			
XLOC_002421	FFC1_02352	FFUJ_06828	related to multidrug resistance protein		-2.36	-1.81				2.63	1.99		
XLOC_003259	FFC1_02354	FFUJ_06830	related to Fe-containing alcohol dehydrogenase							2.82			
XLOC_003261	FFC1_02358	FFUJ_06834	related to 3-carboxy-cis,cis-muconate cycloisomerase							4.30			5.98
XLOC_003262	FFC1_02360	FFUJ_06836	uncharacterized protein FFUJ_06836							4.61			
XLOC_003265	FFC1_02364	FFUJ_06840	related to D-arabinitol 2-dehydrogenase							4.90			
XLOC_002428	FFC1_02366	FFUJ_06842	uncharacterized protein FFUJ_06842								4.82		
XLOC_002436	FFC1_02381	FFUJ_06859	related to integral membrane protein									4.84	
XLOC_003276	FFC1_02389	FFUJ_06866	related to fumarate reductase flavoprotein subunit precursor							-2.05	-2.41	-2.88	-4.67
XLOC_002441	FFC1_02392	FFUJ_06868	uncharacterized protein FFUJ_06868		-2.21						-2.19	-3.60	
XLOC_002450	FFC1_02403	FFUJ_06878	related to phenazine biosynthesis protein phzC							-3.24	-3.06	-2.64	-2.57
XLOC_003281	FFC1_02406	FFUJ_06881	uncharacterized protein FFUJ_06881							-8.89	-9.37	-9.01	-7.97
XLOC_002453	FFC1_02407	FFUJ_06882	probable protein disulfide-isomerase precursor							-4.66	-4.90	-5.84	-5.90
XLOC_002454	FFC1_02408	FFUJ_06883	related to heterokaryon incompatibility protein (het-6OR allele)							-1.07	-2.18	-2.23	-1.57
XLOC_003287	FFC1_02418	FFUJ_06893	uncharacterized protein FFUJ_06893							4.75	8.55	5.25	
XLOC_003291	FFC1_02424	FFUJ_06898	probable PTR2-Di-and tripeptide permease								-2.22	-2.75	
XLOC_003292	FFC1_02427	FFUJ_06901	related to DAL81-transcriptional activator for allantoin and GABA catabolic genes							-2.27	-2.36	-3.20	-2.11
XLOC_002463	FFC1_02429	FFUJ_06903	related to beta transducin-like protein							2.44			
XLOC_002466	FFC1_02433	FFUJ_06907	related to dehydroshikimate dehydratase		1.94					7.81	3.92	6.31	5.17
XLOC_003296	FFC1_02436	FFUJ_06910	uncharacterized protein FFUJ_06910							4.53	3.10	4.10	4.78
XLOC_002468	FFC1_02440	FFUJ_06914	uncharacterized protein FFUJ_06914							-5.80	-6.53	-5.75	-4.61
XLOC_002471	FFC1_02444	FFUJ_06918	related to ornithine aminotransferase	-1.93	-4.06	-2.75				1.40		-2.68	
XLOC_002472	FFC1_02445	FFUJ_06919	uncharacterized protein FFUJ_06919			-1.48				2.02	2.71	2.08	
XLOC_002474	FFC1_02446	FFUJ_06920	related to ahmp1 protein							2.28	2.35	2.38	1.85
XLOC_003302	FFC1_02447	FFUJ_06921	related to sodium/nucleoside cotransporter 1							-2.51	-1.82	-3.05	-2.84
XLOC_002475	FFC1_02450	FFUJ_06923	probable MNN4-regulates the mannosylphosphorylation	1.87	3.62	1.65				3.25	5.14	5.85	5.23
XLOC_002482	FFC1_02462									-1.61	-2.03	-1.45	-1.90
XLOC_003312	FFC1_02470	FFUJ_06941	uncharacterized protein FFUJ_06941								-5.13		
XLOC_003314	FFC1_02473	FFUJ_06944	uncharacterized protein FFUJ_06944							-2.24	-3.83	-4.58	
XLOC_003315	FFC1_02474	FFUJ_06945	probable homoaconitase precursor									4.79	
XLOC_003316	FFC1_02476	FFUJ_06947	uncharacterized protein FFUJ_06947							-2.46	-2.41	-2.71	-2.62
XLOC_003317	FFC1_02477	FFUJ_06948	related to monocarboxylate transporter 2							-2.40	-2.51		-1.64
XLOC_002490	FFC1_02480	FFUJ_06950	uncharacterized protein FFUJ_06950							-2.52	-2.57	-2.01	-2.15
XLOC_003320	FFC1_02484	FFUJ_06954	uncharacterized protein FFUJ_06954							-5.55	-5.95	-6.20	-4.29
XLOC_003321	FFC1_02485	FFUJ_06955	uncharacterized protein FFUJ_06955							-4.99	-7.54	-5.60	-5.41
XLOC_002495	FFC1_02489	FFUJ_06958	uncharacterized protein FFUJ_06958		1.37					1.74	2.23	3.37	1.69
XLOC_002496	FFC1_02490	FFUJ_06959	related to metallo-beta-lactamase family protein		1.75					1.88	2.14	3.01	
XLOC_002497	FFC1_02492									-3.19	-3.95	-2.12	-2.75
XLOC_003325	FFC1_02494	FFUJ_06962	probable maltase	4.08	4.37						4.21	4.86	
XLOC_002498	FFC1_02495	FFUJ_06963	probable Maltose permease									4.83	
XLOC_003326	FFC1_02496	FFUJ_06964	related to DAL81-transcriptional activator for allantoin and GABA catabolic genes							-3.68	-4.18		-2.44

XLOC_003328	FFC1_02499	FFUJ_06967	related to tpa inducible protein							-3.41	-3.65	-3.69	-3.82
XLOC_003330	FFC1_02504	FFUJ_06972	uncharacterized protein FFUJ_06972		-2.37	-2.33				8.34	6.47	5.84	3.32
XLOC_002504	FFC1_02505	FFUJ_06973	uncharacterized protein FFUJ_06973		-1.65	-1.69				5.35	7.26	6.01	5.30
XLOC_003333	FFC1_02509	FFUJ_06977	related to DUF1264 domain protein		2.25	1.91				3.19	3.93	4.70	4.43
XLOC_003334	FFC1_02510	FFUJ_06978	uncharacterized protein FFUJ_06978										5.92
XLOC_002506	FFC1_02513	FFUJ_06981	related to myo-inositol transport protein ITR1	1.66	1.54					6.59	9.21	6.10	4.47
XLOC_002508	FFC1_02515				2.31						5.81	4.66	2.98
XLOC_002511	FFC1_02518	FFUJ_06985	related to DHA14-like major facilitator efflux transporter (MFS transporter)										2.25
XLOC_003338	FFC1_02520	FFUJ_06987	related to pyridoxine 4-dehydrogenase		2.28	1.25						1.69	
XLOC_002512	FFC1_02521	FFUJ_06988	related to aryl-alcohol dehydrogenases							5.01		6.17	5.91
XLOC_002514	FFC1_02525	FFUJ_06991	uncharacterized protein FFUJ_06991		1.21					3.40	2.76	3.94	2.25
XLOC_002516	FFC1_02528	FFUJ_06994	related to carbonic anhydrase							2.72	4.39	3.86	5.48
XLOC_002518	FFC1_02531	FFUJ_06998	uncharacterized protein FFUJ_06998							2.14	2.18	3.79	3.56
XLOC_002520	FFC1_02535	FFUJ_07002	uncharacterized protein FFUJ_07002										4.94
XLOC_003348	FFC1_02540	FFUJ_07007	related to glutathione S-transferase GST-6.0										4.95
XLOC_002524	FFC1_02543	FFUJ_07010	related to oxidoreductase										5.66
XLOC_002525	FFC1_02544	FFUJ_07011	uncharacterized protein FFUJ_07011			4.75						5.92	6.73
XLOC_003350	FFC1_02545	FFUJ_07012	related to hydrolases or acyltransferases (alpha/beta hydrolase superfamily)		2.15	2.83				1.93	2.38	4.67	4.21
XLOC_003351	FFC1_02546	FFUJ_07013	related to 6-hydroxy-D-nicotine oxidase		2.11	2.71				2.14	2.29	4.78	4.05
XLOC_003352	FFC1_02547	FFUJ_07014	related to aerobactin siderophore biosynthesis protein iucB		1.06	0.83				2.16	2.54	2.97	2.49
XLOC_003360	FFC1_02560	FFUJ_07027	probable O-acetylhomoserine (thiol)-lyase								5.28	5.49	
XLOC_002531	FFC1_02561	FFUJ_07028	uncharacterized protein FFUJ_07028							3.56	4.14	3.26	2.95
XLOC_002532	FFC1_02562	FFUJ_07029	uncharacterized protein FFUJ_07029							1.60	2.14	2.26	1.71
XLOC_003361	FFC1_02563	FFUJ_07030	probable homoserine O-acetyltransferase							2.43	2.52	3.01	2.57
XLOC_002533	FFC1_02564	FFUJ_07031	related to ATP-binding cassette transporter protein YOR1							2.83	3.04	3.24	2.55
XLOC_002534	FFC1_02565	FFUJ_07032	uncharacterized protein FFUJ_07032	2.42	3.59	1.69				6.57	7.63	7.98	7.07
XLOC_002537	FFC1_02568	FFUJ_07035	related to mfs-multidrug-resistance transporter									5.27	5.56
XLOC_003364	FFC1_02573	FFUJ_07040	probable endo-1,4-beta-xylanase							4.36	6.67	6.28	3.11
XLOC_003368	FFC1_02579	FFUJ_07044	uncharacterized protein FFUJ_07044								-4.18	-4.69	-2.94
XLOC_002545	FFC1_02584	FFUJ_07049	uncharacterized protein FFUJ_07049							2.78	1.51	2.23	1.75
XLOC_002547	FFC1_02588	FFUJ_07052	uncharacterized protein FFUJ_07052							-1.56	-2.33	-2.31	-1.73
XLOC_002548	FFC1_02590	FFUJ_07054	related to laccase precursor			2.01				6.75	7.01	7.23	8.90
XLOC_003374	FFC1_02591	FFUJ_07055	related to lysine permease							2.50	1.97	1.68	1.85
XLOC_002549	FFC1_02592	FFUJ_07056	uncharacterized protein FFUJ_07056		1.27							2.09	1.26
XLOC_002551	FFC1_02595									5.76	4.27	5.10	3.64
XLOC_003376	FFC1_02596	FFUJ_07059	uncharacterized protein FFUJ_07059							3.11	2.73	2.67	2.03
XLOC_003377	FFC1_02597	FFUJ_07060	related to ERV41-component of copii vesicles involved in transport between the ER and golgi complex							2.44	1.96	2.53	2.34
XLOC_002553	FFC1_02599	FFUJ_07062	uncharacterized protein FFUJ_07062							7.14	5.12		
XLOC_002554	FFC1_02601	FFUJ_07064	probable MBP1-transcription factor, subunit of the MBF factor							3.23	3.42	4.25	3.99
XLOC_002559	FFC1_02607	FFUJ_07070	related to DUF218 domain protein							-2.00	-3.88	-5.01	
XLOC_003382	FFC1_02608	FFUJ_07071	uncharacterized protein FFUJ_07071							-2.46	-2.38	-2.39	-1.89
XLOC_002561	FFC1_02611	FFUJ_07074	related to putative fatty acid desaturase (mld)		-1.37					-1.25	-1.76	-2.74	-1.91
XLOC_002562	FFC1_02613	FFUJ_07076	uncharacterized protein FFUJ_07076							-1.71	-1.92	-2.34	-1.60
XLOC_003386	FFC1_02617	FFUJ_07080	uncharacterized protein FFUJ_07080							-2.64	-3.67	-3.28	-2.14
XLOC_002567	FFC1_02619	FFUJ_07082	uncharacterized protein FFUJ_07082							2.63	1.80	2.07	
XLOC_003388	FFC1_02622	FFUJ_07085	uncharacterized protein FFUJ_07085							3.27	3.15	3.71	3.39
XLOC_002570	FFC1_02624	FFUJ_07087	related to putative tartrate transporter							-3.25	-2.91	-3.46	-3.18
XLOC_002572	FFC1_02628	FFUJ_07091	uncharacterized protein FFUJ_07091							2.12	1.94	2.09	1.62
XLOC_002573	null									4.29	2.74		2.96
XLOC_003392	FFC1_02631	FFUJ_07094	probable DTD1-D-Tyr-tRNA(Tyr) deacylase activity							-2.27	-2.22	-2.08	-1.18
XLOC_002577	FFC1_02634	FFUJ_07096	uncharacterized protein FFUJ_07096			-2.09				2.34	2.00	1.89	
XLOC_003399	FFC1_02646										2.26	1.93	
XLOC_002584	FFC1_02649	FFUJ_07109	probable beta transducin-like protein										2.15
XLOC_003402	FFC1_02650	FFUJ_07110	uncharacterized protein FFUJ_07110							3.34		2.22	
XLOC_003404	FFC1_02652	FFUJ_07112	related to 3-oxoacyl							-5.13	-5.41	-5.26	-5.77
XLOC_002585	FFC1_02653	FFUJ_07113	related to sugar transporter							-2.74	-4.19	-5.46	-5.65
XLOC_003405	FFC1_02656	FFUJ_07115	uncharacterized protein FFUJ_07115		2.51							3.02	
XLOC_003412	FFC1_02668	FFUJ_07127	uncharacterized protein FFUJ_07127							2.88	2.79	2.85	2.30
XLOC_002596	FFC1_02670	FFUJ_07129	probable protein involved in intramitochondrial protein sorting		1.00	1.07				2.61	2.96	3.19	2.78
XLOC_002597	FFC1_02673	FFUJ_07132	uncharacterized protein FFUJ_07132		-3.40	-4.13				6.17	2.64		
XLOC_002598	FFC1_02675	FFUJ_07134	related to general amidase							-2.05	-3.66	-3.46	-3.95
XLOC_002599	FFC1_02678	FFUJ_07137	uncharacterized protein FFUJ_07137		2.28	2.38						1.74	
XLOC_003418	FFC1_02679	FFUJ_07138	related to UPS1 Mitochondrial intermembrane space protein that regulates alternative processing and sorting of Mgm1p and other proteins							3.89	3.26	3.44	3.78
XLOC_003421	FFC1_02685	FFUJ_07144	related to UPF0591 membrane protein C15E1.02c		1.85					2.57	2.70	3.27	1.53
XLOC_002604	FFC1_02689	FFUJ_07148	uncharacterized protein FFUJ_07148							3.36	3.28	3.14	3.47
XLOC_003433	FFC1_02705	FFUJ_07162	related to acyl-coa dehydrogenase, long-chain specific precursor		1.84						1.76	2.77	
XLOC_003438	FFC1_02712	FFUJ_07169	related to dihydrodipicolinate synthase							-1.52	-2.38	-1.79	
XLOC_003440	FFC1_02715	FFUJ_07172	uncharacterized protein FFUJ_07172			1.89				1.84		2.34	3.05
XLOC_003444	FFC1_02723	FFUJ_07180	related to DNA repair protein RAD26							1.66	1.29	2.90	2.38
XLOC_002619	FFC1_02726	FFUJ_07183	uncharacterized protein FFUJ_07183							2.17	2.00	2.15	2.18
XLOC_002628	FFC1_02742	FFUJ_07199	uncharacterized protein FFUJ_07199	1.52	2.85						0.86	1.65	
XLOC_002637	FFC1_02763	FFUJ_07219	uncharacterized protein FFUJ_07219							-1.64	-1.96	-2.13	-1.79

XLOC_002638	null											-4.27	
XLOC_003471	FFC1_02766	FFUJ_07222	uncharacterized protein FFUJ_07222							-6.16	-3.59	-2.91	
XLOC_003475	FFC1_02771									-1.57	-2.15	-1.95	-1.15
XLOC_002647	FFC1_02787	FFUJ_07239	uncharacterized protein FFUJ_07239							5.20	3.87	4.01	4.44
XLOC_003485	FFC1_02788	FFUJ_07240	uncharacterized protein FFUJ_07240							-2.19	-1.79	-2.66	-3.16
XLOC_002648	FFC1_02792	FFUJ_07243	uncharacterized protein FFUJ_07243							2.60	2.02	1.90	
XLOC_003491	FFC1_02793	FFUJ_07244	related to DNA repair protein NTG1							2.04	1.71	2.30	2.07
XLOC_003492	FFC1_02794	FFUJ_07245	probable alcohol dehydrogenase (FDH1)							-1.87	-2.26	-2.46	-2.50
XLOC_002650	FFC1_02796	FFUJ_07247	related to aconitate hydratase precursor		1.58	0.96						1.30	2.31
XLOC_002654	null										-3.32		
XLOC_003498	FFC1_02805	FFUJ_07256	related to methyltransferase							-3.76	-3.11	-3.26	-2.55
XLOC_003510	FFC1_02835	FFUJ_07286	uncharacterized protein FFUJ_07286							-2.31	-2.07	-1.77	-1.49
XLOC_002676	FFC1_02837	FFUJ_07288	uncharacterized protein FFUJ_07288								2.69		3.47
XLOC_002679	FFC1_02845	FFUJ_07296	uncharacterized protein FFUJ_07296							-1.25	-2.28	-2.29	-1.78
XLOC_003516	FFC1_02846	FFUJ_07297	uncharacterized protein FFUJ_07297							-2.43	-2.25	-1.23	-1.90
XLOC_003519	FFC1_02851	FFUJ_07302	related to pall protein		1.35				1.66	3.15	3.60	3.64	2.00
XLOC_003530	FFC1_02869	FFUJ_07319	related to HD superfamily hydrolase							-1.76	-1.84	-2.17	-1.24
XLOC_002692	FFC1_02871	FFUJ_07320	related to SRP40 Suppressor of mutant AC40 of RNA polymerase I and III							5.34	5.21	4.95	4.17
XLOC_002693	null										5.36		
XLOC_003534	null									-3.70			
XLOC_003535	FFC1_02877	FFUJ_07325	related to acetyl coenzyme A synthetase							-2.93	-3.47	-3.65	-2.57
XLOC_002698	FFC1_02883	FFUJ_07331	related to dityrosine transporter							-2.03	-1.26	-1.89	-2.22
XLOC_002701	null									-3.14	-4.53	-5.47	-4.38
XLOC_002702	FFC1_02892	FFUJ_07339	related to nuclear migration protein ami1							-1.90	-2.10	-2.83	-1.93
XLOC_003553	FFC1_02904	FFUJ_07351	related to mfs-multidrug-resistance transporter	1.67	3.57							3.71	
XLOC_002708	FFC1_02905	FFUJ_07352	probable farnesyltranstransferase (al-3)	1.08	2.46	0.93					0.97	2.26	0.88
XLOC_003563	FFC1_02924	FFUJ_07369	uncharacterized protein FFUJ_07369							-1.62	-1.13		-2.05
XLOC_003567	FFC1_02931	FFUJ_07376	probable bifunctional histidine biosynthesis protein hishf			0.84				-2.38	-2.33	-2.02	-0.99
XLOC_002722	FFC1_02932	FFUJ_07377	uncharacterized protein FFUJ_07377							-1.31	-1.88	-2.04	-1.71
XLOC_003571	FFC1_02940	FFUJ_07384	uncharacterized protein FFUJ_07384	2.09	3.18	1.38				3.80	4.89	5.53	4.18
XLOC_003579	FFC1_02951	FFUJ_07395	probable sterol C-24 reductase		0.83					-2.20	-1.48	-1.45	-1.69
XLOC_003580	FFC1_02952	FFUJ_07396	related to mismatched base pair and cruciform dna recognition protein	1.91	2.58					5.76	6.93	7.26	5.05
XLOC_003583	null											-5.43	
XLOC_002743	FFC1_02969	FFUJ_07412	uncharacterized protein FFUJ_07412			1.90				7.35	4.85	5.41	5.86
XLOC_003589	FFC1_02970	FFUJ_07413	uncharacterized protein FFUJ_07413			1.92				3.24	3.15	3.85	4.45
XLOC_002748	FFC1_02977											-2.40	-2.74
XLOC_003593	FFC1_02980	FFUJ_07423	related to ferric-chelate reductase										3.67
XLOC_002750	FFC1_02982	FFUJ_07425	related to sorbitol utilization protein sou1								-2.51	-4.12	
XLOC_003596	FFC1_02984	FFUJ_07427	uncharacterized protein FFUJ_07427							3.94	2.36	4.64	3.26
XLOC_003597	FFC1_02985	FFUJ_07428	related to phospholipid-translocating ATPase			-1.68				4.80	4.41	3.73	3.27
XLOC_002752	FFC1_02987	FFUJ_07430	related to TGL2-triacylglycerol lipase							2.46	2.13	2.50	1.91
XLOC_002758	FFC1_02995	FFUJ_07438	uncharacterized protein FFUJ_07438			-2.90				-1.41	-2.60	-2.57	-3.94
XLOC_003601	FFC1_02996	FFUJ_07439	related to epoxide hydrolase							-1.43	-2.68	-1.56	-1.80
XLOC_002761	FFC1_02999	FFUJ_07442	uncharacterized protein FFUJ_07442							-3.90	-4.27	-4.16	-4.54
XLOC_002762	FFC1_03000	FFUJ_14918	uncharacterized protein FFUJ_14918							-1.30	-1.67	-2.20	-1.41
XLOC_002765	FFC1_03006	FFUJ_07448	uncharacterized protein FFUJ_07448							-2.64	-3.10		
XLOC_002769	FFC1_03013	FFUJ_07453	related to integral membrane protein							6.40	5.98	5.68	
XLOC_002770	FFC1_03014	FFUJ_07454	uncharacterized protein FFUJ_07454	2.03	2.91					3.28	5.21	5.95	3.19
XLOC_003615	FFC1_03025	FFUJ_07465	probable FMN-dependent 2-nitropropane dioxygenase							3.19	2.53	3.35	2.69
XLOC_002778	FFC1_03030									5.31			
XLOC_003623	FFC1_03043	FFUJ_07482	uncharacterized protein FFUJ_07482							-2.96	-2.70		-2.06
XLOC_002788	FFC1_03047	FFUJ_07486	related to protein-tyrosine phosphatase							5.02		4.42	6.19
XLOC_002789	FFC1_03048	FFUJ_07487	uncharacterized protein FFUJ_07487							3.86	3.19	3.52	3.18
XLOC_002790	FFC1_03050	FFUJ_07489	related to protein N-acetyltransferase NAT2		0.96					2.44	2.20	2.86	2.36
XLOC_002791	FFC1_03051	FFUJ_07490	uncharacterized protein FFUJ_07490			2.04				5.97	7.38	7.29	8.14
XLOC_002793	null									-5.20			-4.21
XLOC_002795	null											-3.09	-5.86
XLOC_002798	FFC1_03057	FFUJ_07497	related to ATPase family protein							1.41	1.10	2.35	2.56
XLOC_002806	FFC1_03075	FFUJ_07515	related to arabinose 5-phosphate isomerase	4.57	3.60	1.93					4.59	3.56	1.77
XLOC_002817	FFC1_03090	FFUJ_07530	probable asparagine synthase							-2.24	-1.47	-1.58	
XLOC_003649	FFC1_03092				1.03	0.91				1.15	1.48	2.09	2.02
XLOC_003659	FFC1_03112									2.19	1.81		
XLOC_002838	FFC1_03131	FFUJ_07569	related to MPE1 Role in mRNA 3` end formation							2.18	1.64	2.04	2.04
XLOC_003672	FFC1_03134	FFUJ_07572	uncharacterized protein FFUJ_07572							2.09	2.02	1.51	
XLOC_003673	null									3.12		2.06	
XLOC_003674	null									4.76	2.45		
XLOC_002840	FFC1_03138	FFUJ_07576	related to endo alpha-1,4 polygalactosaminidase precusor						-0.70	-2.34	-2.20	-1.98	-2.03
XLOC_002841	FFC1_03140	FFUJ_07578	probable starvation sensing protein rspA							-0.99	-1.68	-2.35	-1.89
XLOC_002842	FFC1_03141	FFUJ_07579	related to short-chain alcohol dehydrogenase							-1.38	-1.75	-2.34	-1.59
XLOC_003679	FFC1_03143	FFUJ_07581	uncharacterized protein FFUJ_07581		-0.74					-1.81	-2.72	-2.37	-1.88
XLOC_002855	FFC1_03162	FFUJ_07599	related to acyl-CoA cholesterol acyltransferase	1.82	2.27	-0.85				2.74	3.16	4.74	1.66
XLOC_002860	null											6.59	
XLOC_002861	null											5.31	6.20
XLOC_002863	FFC1_03169									4.20	3.86	3.42	3.29
XLOC_003692	FFC1_03174	FFUJ_07608	probable brefeldin A resistance protein	0.67	1.38					2.44	2.91	3.53	2.74
XLOC_002868	FFC1_03181	FFUJ_07615	probable TRM11 Catalytic subunit of an adoMet-dependent tRNA							2.26	2.06	2.04	2.03

			methyltransferase complex (Trm11p-Trm112p)										
XLOC_002871	FFC1_03187	FFUJ_07621	uncharacterized protein FFUJ_07621							2.55	2.55	2.17	2.15
XLOC_003701	FFC1_03190	FFUJ_07624	uncharacterized protein FFUJ_07624							3.10	2.73	3.08	3.68
XLOC_002876	FFC1_03199	FFUJ_07633	uncharacterized protein FFUJ_07633							-1.53	-2.44	-2.30	-2.33
XLOC_002877	FFC1_03200	FFUJ_07634	probable amino acid transporter							-2.47	-2.98	-2.86	-2.16
XLOC_002879	FFC1_03203	FFUJ_07637	related to sialidase							-1.20			-2.21
XLOC_003710	FFC1_03208	FFUJ_07642	uncharacterized protein FFUJ_07642							2.35	2.55	2.36	2.31
XLOC_003713	FFC1_03212	FFUJ_07646	uncharacterized protein FFUJ_07646							-1.15	-1.40	-2.33	-2.62
XLOC_003714	FFC1_03214	FFUJ_07648	related to pyridoxine 4-dehydrogenase		1.14					0.81	1.66	2.27	
XLOC_003717	null												-3.92
XLOC_003718	null												-3.63
XLOC_003720	null									-5.55			
XLOC_003721	null									-4.97			
XLOC_002888	FFC1_03219	FFUJ_07655	related to monocarboxylate transporter 2							-2.32	-1.92		
XLOC_003722	FFC1_03220	FFUJ_07656	uncharacterized protein FFUJ_07656							1.57		2.35	2.63
XLOC_003723	FFC1_03221	FFUJ_07657	related to DNA-binding protein							2.18	1.88	1.83	1.63
XLOC_002890	FFC1_03224	FFUJ_07659	related to the plant PR-1 class of pathogen related proteins	1.39	2.09	1.19					0.67	1.17	
XLOC_002896	FFC1_03231	FFUJ_07666	related to ECM22 Sterol regulatory element binding protein, member of the fungus-specific Z							-1.33	-2.28	-1.87	-1.26
XLOC_003727	FFC1_03235	FFUJ_07670	uncharacterized protein FFUJ_07670							1.91	3.45	3.91	1.60
XLOC_002901	FFC1_03243	FFUJ_07674	uncharacterized protein FFUJ_07674							-1.68	-1.03	-1.66	-2.52
XLOC_002907	FFC1_03251	FFUJ_07682	uncharacterized protein FFUJ_07682							4.46	2.87	2.81	
XLOC_002908	FFC1_03252	FFUJ_07683	uncharacterized protein FFUJ_07683							8.80	8.19	9.44	7.82
XLOC_003737	null									7.05	7.69	3.19	3.60
XLOC_002909	FFC1_03253									5.08	4.32	4.35	4.03
XLOC_002910	FFC1_03254	FFUJ_07684	uncharacterized protein FFUJ_07684		-2.06	-1.79				1.84			
XLOC_003738	FFC1_03255	FFUJ_07685	uncharacterized protein FFUJ_07685							2.42	2.25	2.88	3.19
XLOC_003747	FFC1_03266	FFUJ_07696	related to FMN-dependent 2-nitropropane dioxygenase							-1.76	-2.37		
XLOC_002914	FFC1_03269	FFUJ_07699	uncharacterized protein FFUJ_07699		1.88					1.48	2.23	3.38	
XLOC_002924	FFC1_03285	FFUJ_07715	uncharacterized protein FFUJ_07715										-2.88
XLOC_003758	FFC1_03286	FFUJ_07716	uncharacterized protein FFUJ_07716							-2.19			-2.75
XLOC_002925	FFC1_03287	FFUJ_07717	related to spherulin 1B precursor							6.61	3.46	3.16	
XLOC_002926	FFC1_03288									4.02	2.15	2.85	
XLOC_002927	FFC1_03289	FFUJ_07718	uncharacterized protein FFUJ_07718										-2.48
XLOC_002930	FFC1_03295	FFUJ_07721	uncharacterized protein FFUJ_07721								-4.38		
XLOC_002935	FFC1_03302	FFUJ_07728	related to monooxigenase							3.60			
XLOC_002937	FFC1_03304	FFUJ_07730	related to thermophilic desulfurizing enzyme								-5.06		
XLOC_003770	FFC1_03314	FFUJ_07740	uncharacterized protein FFUJ_07740							2.01		1.77	
XLOC_002943	FFC1_03316	FFUJ_07742	probable HOL1-Putative substrate-H+ antiporter-unknown biological function							2.17	1.73	1.59	1.56
XLOC_002944	FFC1_03317	FFUJ_07743	uncharacterized protein FFUJ_07743							6.37	6.33	6.96	7.88
XLOC_003771	FFC1_03319	FFUJ_07745	uncharacterized protein FFUJ_07745		1.27					1.29	1.11	2.18	1.72
XLOC_002946	FFC1_03320	FFUJ_07746	related to ribonucleases							6.14	5.99	5.12	6.55
XLOC_003772	FFC1_03323	FFUJ_07749	probable cytochrome P450 monooxygenase (lovA)							8.94	10.91	10.87	8.36
XLOC_003773	FFC1_03324	FFUJ_07750	uncharacterized protein FFUJ_07750							4.25	3.57	3.39	3.02
XLOC_002949	FFC1_03325	FFUJ_07751	uncharacterized protein FFUJ_07751							3.60	5.12	4.51	3.91
XLOC_002950	null									5.50	4.85		
XLOC_003774	FFC1_03326	FFUJ_07752	uncharacterized protein FFUJ_07752							8.42	7.73	8.02	6.65
XLOC_003780	FFC1_03335	FFUJ_07763	uncharacterized protein FFUJ_07763							2.77	2.45	1.96	2.04
XLOC_002955	FFC1_03339	FFUJ_07767	related to GNAT family acetyltransferase							-3.20	-1.96	-3.35	-4.25
XLOC_003784	FFC1_03341	FFUJ_07769	uncharacterized protein FFUJ_07769							-2.75	-5.27	-5.61	-6.41
XLOC_002957	FFC1_03342	FFUJ_07770	uncharacterized protein FFUJ_07770							-6.13	-7.79	-6.32	-5.45
XLOC_002960	FFC1_03348	FFUJ_07776	related to Acyl-coenzyme A:6-aminopenicillanic-acid-acyltransferase 40 kDa form			2.01				2.76	2.80	4.60	5.36
XLOC_002961	FFC1_03349	FFUJ_07777	related to acyl-coenzyme A:6-aminopenicillanic-acid-acyltransferase precursor			1.01				1.67	1.27	1.94	2.41
XLOC_002962	FFC1_03351	FFUJ_07779	related to mitochondrial intermembrane space protein Mia40							2.97	2.60	2.96	2.74
XLOC_003789	FFC1_03352				0.56					2.55	2.18	2.61	2.16
XLOC_003790	FFC1_03353	FFUJ_07780	uncharacterized protein FFUJ_07780									1.88	2.01
XLOC_002965	FFC1_03356	FFUJ_07783	related to pisatin demethylase		1.43							2.21	
XLOC_003791	FFC1_03357	FFUJ_07784	related to lipase/esterase		1.68					1.90	2.16	3.11	2.48
XLOC_002966	FFC1_03358	FFUJ_07785	probable SPF1-P-type ATPase-unknown function		0.95					1.26	1.40	1.81	2.03
XLOC_003793	FFC1_03362	FFUJ_07789	uncharacterized protein FFUJ_07789							-1.94	-1.85	-1.48	-2.10
XLOC_003794	FFC1_03363	FFUJ_07790	related to cysteine synthase B							2.83	1.95	2.15	2.13
XLOC_002970	FFC1_03365	FFUJ_07792	related to silencing protein							2.98	2.73	2.60	2.22
XLOC_002974	null										4.96		
XLOC_002975	null										1.46	2.49	
XLOC_002988	FFC1_03389	FFUJ_07815	related to anthranilate synthase component II	2.01	4.51	2.34					3.18	5.86	3.28
XLOC_003804	FFC1_03390	FFUJ_07816	related to dis1-suppressing protein kinase dsk1	-1.96	-2.14	-1.56					-2.12	-1.99	-1.68
XLOC_002994	FFC1_03397	FFUJ_07823	uncharacterized protein FFUJ_07823							3.59	3.02	3.70	3.63
XLOC_003808	FFC1_03399	FFUJ_07825	uncharacterized protein FFUJ_07825	1.86	2.31						2.22	2.42	1.30
XLOC_003810	FFC1_03402	FFUJ_07827	uncharacterized protein FFUJ_07827							-4.71	-5.18	-6.14	-6.89
XLOC_003813	null			3.44	3.72	3.95					6.62	6.80	4.89
XLOC_003004	FFC1_03419	FFUJ_07843	related to integral membrane protein PTH11		2.08					2.87	3.72	5.02	3.73
XLOC_003008	FFC1_03424	FFUJ_07848	related to dma1, component of spindle assembly checkpoint							2.37	2.19	2.07	1.32
XLOC_003823	FFC1_03426	FFUJ_07850	related to Rotein of unknown function							4.11	3.81	3.95	3.55

XLOC_003010	FFC1_03427	FFUJ_07851	related to ribosomal RNA processing protein RRP5							1.78	2.21	2.31	1.76
XLOC_003011	FFC1_03428	FFUJ_07852	uncharacterized protein FFUJ_07852		2.46					4.72	5.71	7.49	7.58
XLOC_003827	FFC1_03435	FFUJ_07859	uncharacterized protein FFUJ_07859							1.94	2.11	3.13	3.75
XLOC_003830	FFC1_03438	FFUJ_07862	uncharacterized protein FFUJ_07862							-1.16	-2.14	-1.53	-1.77
XLOC_003831	FFC1_03440	FFUJ_07864	related to S.pombe pac2 protein		-0.72					-2.55	-3.25	-3.04	-2.49
XLOC_003832	FFC1_03441	FFUJ_07865	uncharacterized protein FFUJ_07865							-1.74	-2.21	-2.21	-1.75
XLOC_003835	FFC1_03446	FFUJ_07870	related to CAAX prenyl protease 2							-1.21	-2.65	-1.11	
XLOC_003842	FFC1_03456	FFUJ_07880	uncharacterized protein FFUJ_07880			0.80				2.09	1.94	2.62	2.33
XLOC_003024	FFC1_03462	FFUJ_07886	uncharacterized protein FFUJ_07886							2.13	2.34	2.40	2.24
XLOC_003025	FFC1_03464	FFUJ_07888	related to serine/threonine-specific kinase KSP1							2.21	1.97	2.18	1.84
XLOC_003027	FFC1_03468	FFUJ_07892	probable sterol delta 5,6-desaturase			-1.27				-1.35	-1.85	-2.73	-2.67
XLOC_003850	FFC1_03474	FFUJ_07898	probable relatd to E3-like factor in the SUMO pathway							3.35	2.80	2.29	1.96
XLOC_003852	FFC1_03479	FFUJ_07903	uncharacterized protein FFUJ_07903		1.48					3.29	2.72	3.64	3.61
XLOC_003035	null									-2.66	-2.89	-5.69	-4.78
XLOC_003036	FFC1_03481	FFUJ_07905	uncharacterized protein FFUJ_07905		0.98	1.07				-2.05	-1.89	-0.89	
XLOC_003854	FFC1_03482	FFUJ_07906	related to helix-loop-helix protein							2.14	2.24	2.43	1.54
XLOC_003856	null												-3.32
XLOC_003037	null									2.45	2.01		
XLOC_003057	FFC1_03519	FFUJ_07942	related to mei2 protein								-3.95		
XLOC_003058	FFC1_03521	FFUJ_07944	uncharacterized protein FFUJ_07944			-1.71				3.40	3.60	3.11	6.26
XLOC_003059	FFC1_03522	FFUJ_07945	uncharacterized protein FFUJ_07945							6.48	5.86	4.94	5.77
XLOC_003068	FFC1_03538	FFUJ_07959	related to beta-glucosidase							-2.21	-2.34	-2.37	-3.12
XLOC_003882	FFC1_03539	FFUJ_07960	uncharacterized protein FFUJ_07960										4.21
XLOC_003069	FFC1_03541	FFUJ_07962	related to beta-carotene 15,15`-dioxygenase							2.38	2.32	3.70	1.71
XLOC_003885	FFC1_03543	FFUJ_07964	uncharacterized protein FFUJ_07964							3.19	3.91	4.89	3.32
XLOC_003073	FFC1_03551	FFUJ_07972	uncharacterized protein FFUJ_07972							-2.86	-2.57	-2.57	-5.24
XLOC_003074	FFC1_03552	FFUJ_07973	probable RCO3-glucose transporter		-0.72					-2.66	-3.76		-2.75
XLOC_003894	FFC1_03556	FFUJ_07976	related to Modin								-1.65	-2.52	-3.45
XLOC_003075	FFC1_03557	FFUJ_07977	related to micromolar calcium activated neutral protease 1 (capn1)		-1.11					-0.82	-1.46	-2.39	-2.20
XLOC_003079	FFC1_03561	FFUJ_07981	uncharacterized protein FFUJ_07981							2.66	3.16	4.82	5.72
XLOC_003081	FFC1_03565	FFUJ_07985	uncharacterized protein FFUJ_07985		-0.99					-2.70	-3.19	-3.72	-2.87
XLOC_003083	FFC1_03566	FFUJ_07986	uncharacterized protein FFUJ_07986							-1.35	-1.99	-2.11	-2.08
XLOC_003087	FFC1_03574	FFUJ_07994	related to endo-1,3-beta-glucanase									4.57	
XLOC_003903	FFC1_03582	FFUJ_08002	uncharacterized protein FFUJ_08002							-2.21	-2.63	-1.50	
XLOC_003905	FFC1_03584	FFUJ_08004	related to linoleate diol synthase		4.89							7.92	
XLOC_003093	FFC1_03588	FFUJ_08008	uncharacterized protein FFUJ_08008							6.01	3.73	4.20	3.88
XLOC_003908	FFC1_03589	FFUJ_08009	related to transcriptional regulator							2.23	1.36	1.45	
XLOC_003095	null												-3.35
XLOC_003096	FFC1_03593	FFUJ_08011	uncharacterized protein FFUJ_08011							3.15	2.72	3.80	2.56
XLOC_003911	FFC1_03594	FFUJ_08012	uncharacterized protein FFUJ_08012							2.60	2.60	2.98	2.40
XLOC_003097	FFC1_03595	FFUJ_08013	related to putidaredoxin reductase		1.16					6.17	6.00	6.74	6.34
XLOC_003098	FFC1_03596	FFUJ_08014	related to formaldehyde dehydrogenase		2.66	1.59				6.43	5.58	6.60	6.82
XLOC_003100	FFC1_03599	FFUJ_08017	related to monocarboxylate transporter 4		1.80	1.64					1.61	2.57	2.68
XLOC_003915	FFC1_03603	FFUJ_14426	uncharacterized protein FFUJ_14426							2.88	3.05	3.37	
XLOC_003918	FFC1_03608	FFUJ_08025	related to feebly like protein								3.76		
XLOC_003919	FFC1_03609	FFUJ_08026	uncharacterized protein FFUJ_08026							-6.70	-5.08	-5.06	-3.89
XLOC_003109	FFC1_03620	FFUJ_08035	related to DUF1275 domain protein							-2.41	-1.81	-1.81	
XLOC_003931	FFC1_03625	FFUJ_08040	uncharacterized protein FFUJ_08040		-2.03								
XLOC_003114	FFC1_03630	FFUJ_08045	uncharacterized protein FFUJ_08045							4.99			5.22
XLOC_003933	FFC1_03631	FFUJ_08046	uncharacterized protein FFUJ_08046								3.92		
XLOC_003935	FFC1_03633	FFUJ_08048	related to zinc finger protein							5.23	3.31	6.16	6.26
XLOC_003941	FFC1_03640	FFUJ_08055	related to aminopeptidase		-2.40	-2.78							
XLOC_003118	FFC1_03643	FFUJ_08058	related to galactoside O-acetyltransferase										2.25
XLOC_003944	FFC1_03644	FFUJ_08059	uncharacterized protein FFUJ_08059							4.59	8.19	7.88	
XLOC_003945	FFC1_03645	FFUJ_08060	uncharacterized protein FFUJ_08060							3.51		3.38	
XLOC_003120	FFC1_03648	FFUJ_14384	related to allantoate permease									5.08	
XLOC_003122	FFC1_03651	FFUJ_14381	probable thioredoxin							6.37	5.69	5.89	6.47
XLOC_003123	FFC1_03652	FFUJ_14380	uncharacterized protein FFUJ_14380		2.68	3.18						6.96	7.69
XLOC_003124	FFC1_03653	FFUJ_14379	uncharacterized protein FFUJ_14379									2.86	3.54
XLOC_003125	FFC1_03654	FFUJ_14378	uncharacterized protein FFUJ_14378			5.63							4.78
XLOC_003131	FFC1_03662	FFUJ_14371	related to D-mandelate dehydrogenase	-1.17	-1.91	-1.71				2.60	1.61		
XLOC_003133	FFC1_03665	FFUJ_14368	uncharacterized protein FFUJ_14368							3.63	2.61	4.09	3.50
XLOC_003134	FFC1_03666	FFUJ_14367	uncharacterized protein FFUJ_14367							2.20		3.87	3.00
XLOC_003951	FFC1_03667	FFUJ_04381	probable calcium P-type ATPase							1.45	1.94	1.51	2.04
XLOC_003958	FFC1_03678	FFUJ_14356	related to C.carbonum toxD gene							10.78	10.09	10.00	8.30
XLOC_003141	FFC1_03679	FFUJ_14355	related to multifunctional beta-oxidation protein							6.90	5.48	6.32	
XLOC_003144	FFC1_03683	FFUJ_14351	probable flavoprotein involved in K+ transport							3.59			
XLOC_003145	FFC1_03684	FFUJ_14350	probable pectate lyase							8.40	6.70	7.89	6.89
XLOC_003960	FFC1_03685	FFUJ_14349	uncharacterized protein FFUJ_14349							8.86	8.43	8.72	7.60
XLOC_003961	FFC1_03686	FFUJ_14348	uncharacterized protein FFUJ_14348							3.42	2.59	2.75	2.80
XLOC_003146	FFC1_03687	FFUJ_14347	uncharacterized protein FFUJ_14347							5.07	3.76	4.34	
XLOC_003963	FFC1_03689	FFUJ_14345	related to AAH1-adenosine deaminase								2.43		2.39
XLOC_003148	FFC1_03691	FFUJ_14343	uncharacterized protein FFUJ_14343							-4.32	-5.02	-6.76	-4.00
XLOC_003965	FFC1_03693	FFUJ_14341	related to phosphoglycerate mutase family protein							2.39	2.36		
XLOC_003149	FFC1_03694	FFUJ_14340	related to multidrug transporter							4.81		5.18	
XLOC_003150	FFC1_03696	FFUJ_14338	related to het-6-heterokaryon incompatibility protein							2.19			
XLOC_003967	FFC1_03697	FFUJ_14337	gibberellin cluster-C13-oxidase							2.40	2.12	1.97	
XLOC_003968	FFC1_03698	FFUJ_14336	gibberellin cluster-kaurensynthase							2.90	2.83	2.43	2.05
XLOC_003151	FFC1_03699	FFUJ_14335	gibberellin cluster-GGPP-synthase							2.64	2.48	2.40	
XLOC_003153	FFC1_03703	FFUJ_14331	gibberellin cluster-GA4-Desaturase							3.67	3.23	3.11	

XLOC_003971	FFC1_03704	FFUJ_14330	related to myo-inositol transport protein ITR1							8.34	6.26	6.53	6.20
XLOC_003154	FFC1_03705	FFUJ_14329	uncharacterized protein FFUJ_14329							8.39	7.60	8.13	5.53
XLOC_003155	FFC1_03706	FFUJ_14328	related to zinc-binding oxidoreductase							7.93	8.11	8.19	5.36
XLOC_003972	FFC1_03707	FFUJ_14327	related to aldehyde dehydrogenase							3.86	4.89	5.58	4.26
XLOC_003973	FFC1_03708	FFUJ_14326	related to class V chitinase							2.76	2.88	3.02	3.11
XLOC_003976	FFC1_03712	FFUJ_14322	uncharacterized protein FFUJ_14322							-6.62	-7.05	-7.28	-6.75
XLOC_003977	FFC1_03713	FFUJ_14321	related to integral membrane protein							-4.08	-4.86	-4.21	-6.52
XLOC_003158	FFC1_03716	FFUJ_14318	uncharacterized protein FFUJ_14318								-5.09	-6.28	
XLOC_003159	FFC1_03717	FFUJ_14317	probable aldehyde dehydrogenase							5.23	5.50	4.24	5.98
XLOC_003979	FFC1_03718	FFUJ_14316	uncharacterized protein FFUJ_14316									-3.85	
XLOC_003981	FFC1_03720	FFUJ_14314	uncharacterized protein FFUJ_14314								-4.49		
XLOC_003166	FFC1_03735	FFUJ_14300	uncharacterized protein FFUJ_14300		-1.68	-2.01			-1.48	-1.78	-2.11	-2.70	-2.29
XLOC_003991	FFC1_03739	FFUJ_14297	uncharacterized protein FFUJ_14297		-1.36	-1.72				7.44	7.01	7.23	5.23
XLOC_003992	FFC1_03740	FFUJ_14296	uncharacterized protein FFUJ_14296							7.05			5.28
XLOC_003169	FFC1_03741	FFUJ_14295	related to ankyrin 3							5.12	4.46	6.07	5.14
XLOC_003170	FFC1_03744	FFUJ_14292	uncharacterized protein FFUJ_14292		-4.99					5.67	5.37		
XLOC_003998	FFC1_03749	FFUJ_14287	uncharacterized protein FFUJ_14287							-2.45	-2.49	-2.75	-2.35
XLOC_003999	FFC1_03750	FFUJ_14286	probable aspartate aminotransferase, cytoplasmic							-6.58	-5.34	-5.53	-5.04
XLOC_004002	FFC1_03757	FFUJ_14280	related to neutral amino acid permease	2.79	2.93					-4.55			
XLOC_003176	FFC1_03758	FFUJ_14279	probable alpha-glucoside transport protein							8.60	8.37	8.08	
XLOC_004004	FFC1_03760	FFUJ_14277	related to 2`-hydroxyisoflavone reductase			2.13				5.46	6.45	7.32	7.74
XLOC_003177	FFC1_03761	FFUJ_14276	related to Zn-dependent hydrolases, including glyoxylases		2.90	2.96						6.39	6.70
XLOC_004005	FFC1_03762	FFUJ_14275	uncharacterized protein FFUJ_14275		4.68	5.16						4.55	3.36
XLOC_003180	FFC1_03773	FFUJ_14264	related to RSB1-integral membrane transporter or flippase that may transport LCBs from the cytoplasmic side toward the extracytoplasmic side of the membrane							1.90		3.07	2.27
XLOC_004015	FFC1_03774	FFUJ_14263	related to multidrug resistance protein							-3.31			
XLOC_003182	FFC1_03779									5.16	5.05		
XLOC_003184	FFC1_03784									-4.33	-6.19		
XLOC_004025	FFC1_03793				2.72					2.73		2.51	
XLOC_004826	FFC1_03797			-0.97	-1.64	-1.56				-1.60	-2.25	-2.91	-3.48
XLOC_004029	FFC1_03807	FFUJ_05330	uncharacterized protein FFUJ_05330									5.04	5.15
XLOC_004840	FFC1_03820	FFUJ_05343	uncharacterized protein FFUJ_05343							4.45	4.53	4.13	
XLOC_004845	FFC1_03827	FFUJ_05349	uncharacterized protein FFUJ_05349							-5.33	-5.73	-3.97	-5.61
XLOC_004848	FFC1_03832	FFUJ_05354	uncharacterized protein FFUJ_05354							-2.00	-2.12	-3.40	-3.80
XLOC_004042	FFC1_03842	FFUJ_05362	probable mutanase (glucan endo-1,3-alpha-glucosidase)		-2.01					0.75		-1.00	
XLOC_004857	FFC1_03846	FFUJ_05366	related to beta-glucosidase							2.10			
XLOC_004047	FFC1_03852	FFUJ_05372	uncharacterized protein FFUJ_05372								-3.82		
XLOC_004049	FFC1_03856	FFUJ_05376	related to methyltransferase		-0.79					6.24	5.71	4.71	3.80
XLOC_004056	FFC1_03877	FFUJ_05396	related to heterokaryon incompatibility protein het-6							5.73			
XLOC_004057	FFC1_03879	FFUJ_05398	related to monomeric sarcosine oxidase		-2.28					5.07	3.01		5.00
XLOC_004878	FFC1_03883	FFUJ_05402	uncharacterized protein FFUJ_05402		2.34					4.61	4.35	4.80	3.43
XLOC_004060	FFC1_03885	FFUJ_05404	uncharacterized protein FFUJ_05404	-5.25									
XLOC_004062	FFC1_03888	FFUJ_05409	uncharacterized protein FFUJ_05409		-1.74					3.70	1.93		
XLOC_004881	FFC1_03890	FFUJ_05411	related to methyltransferase		-1.25					2.46	1.47		1.97
XLOC_004882	FFC1_03891	FFUJ_05412	uncharacterized protein FFUJ_05412							7.17	6.93	7.48	6.06
XLOC_004064	FFC1_03892	FFUJ_05413	uncharacterized protein FFUJ_05413							7.29	6.14	7.96	4.55
XLOC_004065	FFC1_03893	FFUJ_05414	uncharacterized protein FFUJ_05414								4.91	4.99	
XLOC_004883	FFC1_03894	FFUJ_05417	uncharacterized protein FFUJ_05417								2.29		
XLOC_004066	FFC1_03895									3.21			
XLOC_004069	FFC1_03898	FFUJ_05419	uncharacterized protein FFUJ_05419		-1.69				-1.97	-1.47	-2.32		
XLOC_004070	FFC1_03900	FFUJ_05421	Protein of unknown function localised to cytoplasm			-5.76				7.94	4.81		
XLOC_004075	FFC1_03910	FFUJ_05425	uncharacterized protein FFUJ_05425							-2.82	-3.87	-2.71	-2.63
XLOC_004893	FFC1_03917	FFUJ_05432	related to aldehyde reductase II							-2.49	-2.80	-2.04	-2.19
XLOC_004080	FFC1_03919									-11.62	-9.88	-10.24	-10.14
XLOC_004088	FFC1_03932	FFUJ_05447	probable beta-succinyl CoA synthetase precursor							2.71			
XLOC_004899	FFC1_03933	FFUJ_05448	related to succinate-CoA ligase alpha and beta chain							2.50			
XLOC_004901	FFC1_03936	FFUJ_05451	related to integral membrane protein								-5.35		
XLOC_004902	FFC1_03937	FFUJ_05452	uncharacterized protein FFUJ_05452								-3.54	-5.11	
XLOC_004903	FFC1_03939	FFUJ_05454	uncharacterized protein FFUJ_05454							-1.54	-2.21	-1.55	-2.09
XLOC_004092	FFC1_03940	FFUJ_05455	uncharacterized protein FFUJ_05455							-6.01	-5.36		
XLOC_004093	FFC1_03941	FFUJ_05456	uncharacterized protein FFUJ_05456							-7.90	-7.04	-6.73	-7.35
XLOC_004904	FFC1_03942	FFUJ_11292	probable ABC1 transport protein							-4.47	-4.67	-5.67	-4.69
XLOC_004094	FFC1_03943	FFUJ_05458	uncharacterized protein FFUJ_05458			1.15			1.53	-2.21	-1.94	-1.52	-2.57
XLOC_004905	FFC1_03944	FFUJ_05459	uncharacterized protein FFUJ_05459		1.44	1.74				1.67	2.28	2.21	2.37
XLOC_004912	FFC1_03956	FFUJ_05468	uncharacterized protein FFUJ_05468							3.46	4.41	7.05	9.15
XLOC_004101	FFC1_03959	FFUJ_05471	related to integral membrane protein						-2.55	-7.51	-8.50	-7.53	-6.28
XLOC_004915	FFC1_03961	FFUJ_05473	uncharacterized protein FFUJ_05473							-1.89	-2.32	-1.79	-2.00
XLOC_004103	FFC1_03963	FFUJ_05475	related to gibberellin biosynthesis-related								-3.92	-3.93	
XLOC_004916	FFC1_03965	FFUJ_05477	related to alanine racemase								-2.33	-2.17	
XLOC_004917	FFC1_03968	FFUJ_05480	uncharacterized protein FFUJ_05480							5.25			
XLOC_004918	FFC1_03969	FFUJ_05481	related to aldo-keto reductase family protein		2.16					6.65	5.74	5.72	4.43
XLOC_004107	FFC1_03970	FFUJ_05482	related to calcium-binding protein caleosin		2.30					4.24	4.91	5.92	3.69
XLOC_004108	FFC1_03971	FFUJ_05483	related to vegetatible incompatibility protein HET-E-1							4.09	4.08	4.12	3.02
XLOC_004111	FFC1_03974	FFUJ_05486	related to transporter protein								3.71	6.40	5.39
XLOC_004920	FFC1_03976	FFUJ_05488	uncharacterized protein FFUJ_05488										-2.89

XLOC_004922	FFC1_03978	FFUJ_05490	uncharacterized protein FFUJ_05490							6.97	7.40	7.95	8.53
XLOC_004923	FFC1_03979	FFUJ_05491	uncharacterized protein FFUJ_05491							4.53	3.03	2.20	
XLOC_004925	FFC1_03981	FFUJ_05493	uncharacterized protein FFUJ_05493								-4.84	-4.62	-5.32
XLOC_004926	FFC1_03982	FFUJ_05494	related to GNAT family acetyltransferase							-5.81	-3.92	-3.11	-6.88
XLOC_004113	FFC1_03987	FFUJ_05499	uncharacterized protein FFUJ_05499							1.37	1.57	2.22	1.11
XLOC_004114	FFC1_03988	FFUJ_05500	related to TAM domain methyltransferase		-1.16					6.56	6.70	6.32	5.69
XLOC_004115	FFC1_03989	FFUJ_05501	related to cell wall glycosyl hydrolase YteR							4.99	5.00	7.56	4.94
XLOC_004116	FFC1_03990	FFUJ_05502	uncharacterized protein FFUJ_05502							3.60	3.64	3.67	2.83
XLOC_004118	FFC1_03992	FFUJ_05504	uncharacterized protein FFUJ_05504							-4.74	-4.27	-6.19	-4.36
XLOC_004930	FFC1_03993	FFUJ_05505	uncharacterized protein FFUJ_05505							-6.09	-5.24	-4.36	-5.57
XLOC_004931	FFC1_03994	FFUJ_05506	uncharacterized protein FFUJ_05506							-5.77	-5.99	-5.15	-6.28
XLOC_004119	FFC1_03995	FFUJ_05507	uncharacterized protein FFUJ_05507							-2.07	-2.51	-2.77	-2.30
XLOC_004932	FFC1_03996	FFUJ_05508	related to HPP family protein							3.19	3.01	3.58	
XLOC_004120	FFC1_03998	FFUJ_05510	related beta-lactamase								-2.36	-2.58	-3.91
XLOC_004123	FFC1_04000	FFUJ_05512	probable phenylacetyl-CoA ligase							3.62			
XLOC_004934	FFC1_04002	FFUJ_05514	uncharacterized protein FFUJ_05514	1.77	2.01	2.17				5.89	7.44	6.78	6.15
XLOC_004125	FFC1_04003	FFUJ_02574	probable ATP-binding multidrug cassette transport protein	2.40	4.29	2.92				3.48	5.37	6.62	4.64
XLOC_004126	FFC1_04004	FFUJ_05516	related to multidrug resistant protein							-2.36	-2.93	-3.75	-3.33
XLOC_004127	FFC1_04005	FFUJ_05517	related to major facilitator MirA							-2.46	-3.03	-3.58	-3.11
XLOC_004936	FFC1_04007	FFUJ_05519	related to MFS transporter							-2.78	-3.11	-3.19	-2.74
XLOC_004129	FFC1_04009	FFUJ_05521	uncharacterized protein FFUJ_05521							4.88	5.37	3.90	4.42
XLOC_004938	FFC1_04011	FFUJ_05523	related to oxidoreductase							4.75	4.61	4.32	3.92
XLOC_004939	FFC1_04012	FFUJ_05524	uncharacterized protein FFUJ_05524							5.72	6.26	8.17	7.77
XLOC_004941	FFC1_04015	FFUJ_05527	probable dis1-suppressing protein kinase dsk1							-2.69	-2.71	-2.21	
XLOC_004131	FFC1_04017	FFUJ_05529	related to 3-hydroxybutyryl-CoA dehydratase										-2.59
XLOC_004945	FFC1_04019					4.12							
XLOC_004136	FFC1_04025	FFUJ_05535	related to potassium:hydrogen antiporter							3.08	2.94	2.44	
XLOC_004946	FFC1_04026	FFUJ_05536	uncharacterized protein FFUJ_05536									5.65	5.33
XLOC_004138	FFC1_04028	FFUJ_05538	uncharacterized protein FFUJ_05538										5.16
XLOC_004947	FFC1_04029	FFUJ_05539	related to peptide transport protein						-3.39				
XLOC_004949	FFC1_04032	FFUJ_05542	uncharacterized protein FFUJ_05542							2.96			
XLOC_004141	FFC1_04033	FFUJ_05543	related to O-methylsterigmatocystin oxidoreductase							4.52	6.09	5.50	6.47
XLOC_004950	FFC1_04034	FFUJ_05544	related to DUF1680 domain protein							5.18			
XLOC_004953	FFC1_04039	FFUJ_05549	related to Vault poly							-2.17	-2.90	-2.08	-1.92
XLOC_004954	FFC1_04040	FFUJ_05550	uncharacterized protein FFUJ_05550							-2.01			
XLOC_004957	FFC1_04046	FFUJ_05554	uncharacterized protein FFUJ_05554							3.29			
XLOC_004148	null											-1.54	-2.13
XLOC_004150	FFC1_04051	FFUJ_05559	uncharacterized protein FFUJ_05559		-2.26	-2.37				2.65	1.48		
XLOC_004960	FFC1_04052	FFUJ_05560	related to dis1-suppressing protein kinase dsk1							-2.24	-4.13	-3.15	-3.22
XLOC_004151	FFC1_04053									-3.47	-3.93	-4.71	-4.95
XLOC_004962	FFC1_04055	FFUJ_05562	uncharacterized protein FFUJ_05562										6.09
XLOC_004153	FFC1_04056	FFUJ_05563	uncharacterized protein FFUJ_05563								5.05	5.41	6.23
XLOC_004154	FFC1_04058	FFUJ_05565	related to phospholipase a-2-activating protein							2.06	1.92	2.10	2.50
XLOC_004964	FFC1_04059	FFUJ_05566	uncharacterized protein FFUJ_05566							5.64	5.40	4.87	4.52
XLOC_004155	FFC1_04060	FFUJ_05567	uncharacterized protein FFUJ_05567							2.96	2.66	2.86	2.32
XLOC_004156	FFC1_04061	FFUJ_05568	uncharacterized protein FFUJ_05568							2.42	2.48	2.56	3.12
XLOC_004157	FFC1_04063	FFUJ_05570	uncharacterized protein FFUJ_05570	2.66	3.40					2.93	4.66	5.46	4.01
XLOC_004967	FFC1_04070	FFUJ_05576	related to NAM7-nonsense-mediated mRNA decay protein		1.43	1.73				1.95	1.83	2.89	3.77
XLOC_004168	FFC1_04079	FFUJ_05585	related to NAD(P)H-dependent oxidoreductase		1.86					2.43	2.30	3.73	2.21
XLOC_004973	FFC1_04080	FFUJ_05586	related to protein involved in sporulation and meiosis							2.37	1.92	2.76	2.53
XLOC_004976	FFC1_04082	FFUJ_05588	uncharacterized protein FFUJ_05588		1.14	1.02				3.26	3.01	3.36	2.64
XLOC_004169	FFC1_04083	FFUJ_05589	uncharacterized protein FFUJ_05589							1.20	1.25	2.27	1.68
XLOC_004170	FFC1_04085	FFUJ_05776	related to multidrug resistance protein			1.10							2.53
XLOC_004982	FFC1_04097	FFUJ_05603	probable permeases							-2.25	-1.99	-1.35	-1.24
XLOC_004983	null									-4.31	-3.09		
XLOC_004178	FFC1_04098	FFUJ_05604	uncharacterized protein FFUJ_05604							5.34	4.65	6.09	6.10
XLOC_004984	FFC1_04099	FFUJ_14424	uncharacterized protein FFUJ_14424									2.34	
XLOC_004986	FFC1_04101	FFUJ_05605	related to sterol glucosyltransferase		1.23					1.34	1.84	2.30	1.34
XLOC_004987	null				1.53					4.49	3.55	3.00	2.11
XLOC_004988	FFC1_04102	FFUJ_05606	uncharacterized protein FFUJ_05606							2.45	2.94	3.22	1.44
XLOC_004993	null											-2.04	
XLOC_004997	FFC1_04110	FFUJ_05614	uncharacterized protein FFUJ_05614							2.87	2.92	3.52	2.45
XLOC_004187	FFC1_04119	FFUJ_05623	uncharacterized protein FFUJ_05623							5.04			
XLOC_005004	FFC1_04126	FFUJ_05629	related to hypothetical protein yjjx								-2.67		
XLOC_004218	FFC1_04167	FFUJ_05664	uncharacterized protein FFUJ_05664							3.80	3.62	4.00	3.66
XLOC_005022	FFC1_04167	FFUJ_05664	uncharacterized protein FFUJ_05664							4.16	3.23	4.25	3.49
XLOC_004219	FFC1_04168	FFUJ_05665	related to calcium-binding protein caleosin							5.19	4.50	5.00	5.05
XLOC_004222	FFC1_04177	FFUJ_05674	related to N.crassa uvs2 protein						0.77	2.90	2.44	3.10	3.03
XLOC_005030	FFC1_04180	FFUJ_05679	probable catalytic subunit of DNA polymerase zeta UPR-1							1.54	1.74	2.16	2.46
XLOC_005032	FFC1_04185	FFUJ_05684	uncharacterized protein FFUJ_05684		1.63					6.85	7.48	8.38	7.39
XLOC_004231	FFC1_04194	FFUJ_05693	uncharacterized protein FFUJ_05693		-1.16	-1.51				-1.30	-1.85	-2.37	-2.77
XLOC_004232	FFC1_04195	FFUJ_05694	uncharacterized protein FFUJ_05694		-0.91					-1.04	-1.41	-2.04	-1.76
XLOC_004234	FFC1_04198	FFUJ_05697	uncharacterized protein FFUJ_05697			-1.35				3.84	3.13	2.31	1.89
XLOC_005038	FFC1_04199	FFUJ_05698	uncharacterized protein FFUJ_05698			-1.23				2.66	2.75	2.19	1.10
XLOC_005040	FFC1_04201	FFUJ_05700	related to Calcium_related spray protein							1.70	1.77	1.87	2.21
XLOC_004245	FFC1_04217	FFUJ_05712	uncharacterized protein FFUJ_05712							4.21	3.94	4.42	3.89
XLOC_004246	FFC1_04218	FFUJ_05713	uncharacterized protein FFUJ_05713							7.54	6.82	7.36	6.30
XLOC_004251	FFC1_04226	FFUJ_05721	uncharacterized protein FFUJ_05721							-2.99	-2.64	-2.31	-1.99
XLOC_004256	FFC1_04236	FFUJ_09492	related to alpha-1,3-mannosyltransferase	1.65	3.11	4.34				5.36	6.60	8.39	8.83

XLOC_005055	FFC1_04237	FFUJ_05732	related to deoxyribodipyrimidine photo-lyase	8.64	8.88	8.39					7.45	7.86	7.16
XLOC_004261	FFC1_04241	FFUJ_05736	uncharacterized protein FFUJ_05736							2.07	3.73	3.91	2.97
XLOC_005056	FFC1_04242	FFUJ_05737	uncharacterized protein FFUJ_05737							-3.94	-4.24	-3.34	-3.13
XLOC_004263	FFC1_04244	FFUJ_05738	related to TOB3 (member of AAA-ATPase family)							3.92			
XLOC_005057	FFC1_04245	FFUJ_05739	related to DNA damage-responsive protein 48							3.55	2.01	3.51	
XLOC_004265	FFC1_04249	FFUJ_05744	related to dis1-suppressing protein kinase dsk1								2.06		2.34
XLOC_004266	FFC1_04250									2.34	2.39	2.19	2.32
XLOC_005060	FFC1_04252	FFUJ_05747	probable phenylacetyl-CoA ligase							2.43			
XLOC_005063	FFC1_04259	FFUJ_05754	uncharacterized protein FFUJ_05754							-5.53	-5.09		
XLOC_004278	FFC1_04269	FFUJ_05764	related to C6 transcription factor							4.00	3.33		
XLOC_005068	FFC1_04271	FFUJ_12086	probable ATP-binding multidrug cassette transport protein		2.21	1.70				1.77	2.54	3.36	2.79
XLOC_004280	FFC1_04273	FFUJ_05768	uncharacterized protein FFUJ_05768							-2.44	-2.56	-1.70	-1.57
XLOC_004281	FFC1_04275	FFUJ_05770	uncharacterized protein FFUJ_05770							-1.83	-2.55	-3.84	-2.28
XLOC_005071	FFC1_04277	FFUJ_05772	uncharacterized protein FFUJ_05772							-1.92	-2.77	-2.44	-1.79
XLOC_005073	FFC1_04279	FFUJ_05774	related to dienelactone hydrolase family protein							4.74	4.08	3.45	4.27
XLOC_005074	FFC1_04280	FFUJ_05775	related to berberine bridge enzyme							2.91	2.38	1.77	2.54
XLOC_005075	FFC1_04281	FFUJ_05591	related to multidrug resistance protein						3.43		1.32		-2.79
XLOC_004284	FFC1_04283	FFUJ_05778	related to cofilin			6.32				-5.43			
XLOC_004285	FFC1_04284	FFUJ_05779	uncharacterized protein FFUJ_05779							3.09		2.93	1.70
XLOC_004286	FFC1_04285	FFUJ_05780	related to nitrate assimilation regulatory protein nirA							4.04	3.74	4.37	3.93
XLOC_005076	FFC1_04286	FFUJ_05781	related to phthalate 4,5-dioxygenase oxygenase reductase subunit							-2.20	-3.05	-2.74	-2.21
XLOC_005078	FFC1_04288										4.82	5.63	
XLOC_005085	FFC1_04303	FFUJ_05797	related to trichodiene oxygenase cytochrome P450	-1.09						-2.62	-3.75	-3.10	
XLOC_004298	null									-2.44	-2.98	-2.24	-2.38
XLOC_005086	null									-3.16	-3.91	-4.89	-2.89
XLOC_004299	null									-1.83		-5.29	
XLOC_005089	FFC1_04310	FFUJ_05804	related to long-chain-fatty-acid-CoA ligase							3.79	3.67	4.14	3.35
XLOC_004304	FFC1_04311	FFUJ_05805	related to n-alkane-inducible cytochrome P450							5.72		5.53	4.72
XLOC_005091	FFC1_04313	FFUJ_05807	uncharacterized protein FFUJ_05807	-1.54	-3.52	-2.60				6.83	4.28		3.42
XLOC_004305	FFC1_04314	FFUJ_05808	uncharacterized protein FFUJ_05808							2.87		3.48	3.30
XLOC_004307	null										-4.66		
XLOC_005100	null										-4.57		
XLOC_005103	FFC1_04335	FFUJ_05827	probable taurine dioxygenase								-2.10	-1.98	
XLOC_004321	FFC1_04338	FFUJ_05830	probable PMA1-H+-transporting P-type ATPase							6.77	4.55	4.24	6.40
XLOC_004323	FFC1_04340	FFUJ_05832	uncharacterized protein FFUJ_05832									-4.10	
XLOC_004324	FFC1_04341	FFUJ_05833	probable potassium channel beta subunit protein		-1.94						-2.77	-3.67	
XLOC_004326	FFC1_04343	FFUJ_05835	choline permease							-1.58		-2.49	
XLOC_005106	FFC1_04345	FFUJ_05837	uncharacterized protein FFUJ_05837							3.27	3.22	2.48	
XLOC_004331	FFC1_04352	FFUJ_05843	uncharacterized protein FFUJ_05843							3.65	3.04	2.52	
XLOC_004333	FFC1_04354	FFUJ_05845	uncharacterized protein FFUJ_05845		1.77	1.77				3.31	3.71	4.43	4.25
XLOC_004334	FFC1_04355	FFUJ_05846	related to ankyrin 3		2.24	2.20				5.60	5.48	6.80	6.07
XLOC_004335	FFC1_04356	FFUJ_05847	uncharacterized protein FFUJ_05847							3.79	3.10	3.76	4.43
XLOC_005110	FFC1_04357	FFUJ_12961	probable homogentisate 1,2-dioxygenase							4.55	4.05	4.39	3.43
XLOC_004339	FFC1_04361	FFUJ_05852	uncharacterized protein FFUJ_05852									2.02	2.60
XLOC_004340	FFC1_04363	FFUJ_05854	uncharacterized protein FFUJ_05854		1.42					3.64	3.75	4.22	3.91
XLOC_005114	FFC1_04364	FFUJ_05855	related to actin cytoskeleton protein (VIP1)		0.89					3.03	2.84	3.35	2.91
XLOC_004341	null									4.74	5.20		
XLOC_004343	FFC1_04370	FFUJ_05861	related to V.vinifera dihydroflavonol 4-reductase							-2.36	-2.12		
XLOC_004344	FFC1_04371	FFUJ_05862	uncharacterized protein FFUJ_05862								-2.02		
XLOC_005121	FFC1_04372				-1.29	-1.09				-0.65	-0.99	-2.89	-1.54
XLOC_005127	FFC1_04388	FFUJ_05877	uncharacterized protein FFUJ_05877							2.30	2.09	3.07	3.78
XLOC_004355	null									-3.50			
XLOC_004358	FFC1_04393	FFUJ_05885	uncharacterized protein FFUJ_05885							1.94	2.15	1.36	
XLOC_004359	null										-5.06		
XLOC_004361	FFC1_04395	FFUJ_05886	uncharacterized protein FFUJ_05886							-1.90	-1.93	-2.18	-1.97
XLOC_004365	FFC1_04402	FFUJ_05893	probable PCK1-phosphoenolpyruvate carboxykinase		1.28					2.17	1.41		
XLOC_005135	FFC1_04403	FFUJ_05894	related to ATP-dependent RNA helicase		1.71	1.98						3.44	3.15
XLOC_005139	null									6.95	4.64	7.94	5.11
XLOC_004373	FFC1_04417	FFUJ_05908	related to protein yhhW		2.69						1.85	3.11	1.74
XLOC_004374	FFC1_04418	FFUJ_05909	related to endochitinase 2 precursor							-2.13	-2.51	-2.20	-1.37
XLOC_005144	FFC1_04425	FFUJ_05916	uncharacterized protein FFUJ_05916							-1.78	-2.13	-2.58	-3.47
XLOC_005149	null										-4.22		
XLOC_004387	FFC1_04436	FFUJ_05927	related to YER185w, Rta1p									5.32	
XLOC_004390	FFC1_04443	FFUJ_05934	uncharacterized protein FFUJ_05934	2.72	5.34	3.70				1.61	3.98	6.34	4.84
XLOC_004396	FFC1_04452	FFUJ_05943	uncharacterized protein FFUJ_05943								-5.28		
XLOC_004401	FFC1_04462	FFUJ_05953	uncharacterized protein FFUJ_05953						2.07	3.01	2.98	3.36	1.93
XLOC_005165	FFC1_04463	FFUJ_05954	uncharacterized protein FFUJ_05954		0.59					-3.14	-3.00	-2.33	-2.13
XLOC_004404	FFC1_04468	FFUJ_05958	uncharacterized protein FFUJ_05958							-2.25	-2.82	-2.63	-1.62
XLOC_004408	FFC1_04477	FFUJ_05967	probable acetylglutamate kinase/N-acetyl-gamma-glutamyl-phosphate reductase precursor (ARG-6)		0.82	0.94				-2.56	-2.09	-1.85	-1.75
XLOC_005174	FFC1_04480	FFUJ_05970	uncharacterized protein FFUJ_05970							-2.19	-2.18	-1.93	-3.33
XLOC_005175	null											-4.15	
XLOC_004411	FFC1_04481	FFUJ_05971	related to beta-1,3-glucan binding protein						0.94	-1.19	-1.40	-2.10	-2.78
XLOC_004413	FFC1_04485				1.03					1.07	1.10	2.15	1.54

XLOC_004419	FFC1_04493	FFUJ_05983	uncharacterized protein FFUJ_05983		1.98					2.23		3.16	2.48
XLOC_004420	FFC1_04494	FFUJ_05984	uncharacterized protein FFUJ_05984		2.37	1.81				2.40	2.32	3.83	3.30
XLOC_004425	FFC1_04505	FFUJ_05994	uncharacterized protein FFUJ_05994		1.00					1.40	1.78	2.00	1.59
XLOC_005187	FFC1_04506	FFUJ_05995	uncharacterized protein FFUJ_05995							-1.48	-1.43	-1.19	-2.70
XLOC_005189	null										-4.85	-5.27	-5.79
XLOC_005190	FFC1_04507	FFUJ_05996	related to D-arabinitol 2-dehydrogenase							-1.74	-2.10	-1.52	
XLOC_005194	FFC1_04513	FFUJ_06002	MUC1-Extracellular alpha-1,4-glucan glucosidase							3.89	4.03	4.08	3.26
XLOC_005195	FFC1_04514	FFUJ_06003	uncharacterized protein FFUJ_06003		1.91					2.09	2.77	3.33	1.61
XLOC_004430	FFC1_04515	FFUJ_06004	uncharacterized protein FFUJ_06004							2.32	2.79	2.58	1.75
XLOC_004433	FFC1_04519	FFUJ_06008	uncharacterized protein FFUJ_06008							2.13	1.80	1.88	
XLOC_005206	FFC1_04538	FFUJ_06027	related to negative acting factor							-3.37	-6.54	-5.27	-3.17
XLOC_004454	FFC1_04555	FFUJ_06043	related to cyclin pclA							1.95	2.51	2.44	2.33
XLOC_005216	FFC1_04556	FFUJ_06044	related to CCC2-P-type ATPase involved in export of Cu++ from the cytosol into intracellular, secret							1.90	2.14	1.47	1.05
XLOC_004457	FFC1_04558	FFUJ_06045	related to excitatory amino acid transporter			-2.77				3.06	2.47	2.36	
XLOC_005218	FFC1_04560	FFUJ_06047	related to alkaline protease (oryzin)							-1.88	-2.39		-1.74
XLOC_005220	FFC1_04562	FFUJ_06049	related to sarcosine oxidase		1.53				1.53	2.99	3.20	3.89	2.38
XLOC_005221	FFC1_04563	FFUJ_06050	uncharacterized protein FFUJ_06050							3.88	4.03	3.45	2.45
XLOC_004460	null									1.43	1.75	1.56	2.09
XLOC_005222	FFC1_04565	FFUJ_06052	uncharacterized protein FFUJ_06052							3.77	3.27	2.82	2.15
XLOC_004461	null											3.68	
XLOC_005223	null				-5.79							-5.70	
XLOC_004463	null												5.89
XLOC_005225	FFC1_04568	FFUJ_06055	probable vivid PAS protein VVD	4.90	5.17	4.84				1.75	6.41	6.85	6.43
XLOC_004464	FFC1_04569	FFUJ_06056	related to DNA repair protein MMS21	2.58	2.00	1.60					2.30	2.15	1.54
XLOC_004469	FFC1_04580	FFUJ_06065	probable vacuolar aspartic proteasse							2.12	1.93	2.00	2.19
XLOC_005236	FFC1_04583	FFUJ_06068	probable alanine transaminases							1.78	1.89	1.99	2.08
XLOC_005237	null									-4.52	-3.87		-5.02
XLOC_005238	null									-5.46	-4.27		
XLOC_005241	FFC1_04589	FFUJ_06074	uncharacterized protein FFUJ_06074							8.53	9.48	9.81	9.25
XLOC_004474	FFC1_04590	FFUJ_06075	uncharacterized protein FFUJ_06075							9.40	8.32	9.38	8.89
XLOC_005253	FFC1_04604	FFUJ_06089	probable HUL5-ubiquitin-protein ligase (E3)		1.12	1.63				2.74	2.71	3.47	4.35
XLOC_005258	FFC1_04610	FFUJ_06096	uncharacterized protein FFUJ_06096		3.12						1.24	2.55	
XLOC_005259	FFC1_04613	FFUJ_06099	probable nitrite reductase							-1.88	-1.46	-1.48	-2.03
XLOC_004483	FFC1_04617	FFUJ_06103	probable glucosamine-6-phosphate isomerase							-1.46	-1.62	-1.51	-3.30
XLOC_005263	FFC1_04619	FFUJ_06105	related to N-acetylglucosamine-6-phosphate deacetylase								-1.32		-2.65
XLOC_005265	FFC1_04622	FFUJ_06108	uncharacterized protein FFUJ_06108		-1.41	-1.65				2.50	1.93		
XLOC_005266	FFC1_04624	FFUJ_06110	related to 6-HYDROXY-D-NICOTINE OXIDASE							3.20	3.51	5.61	
XLOC_004486	FFC1_04625	FFUJ_06111	related to integral membrane protein							3.44	2.25	2.94	2.04
XLOC_005267	FFC1_04626	FFUJ_06112	related to alcohol oxidase		-2.79	-3.56				2.83	3.08		
XLOC_004487	FFC1_04627	FFUJ_06113	related to integral membrane protein PTH11		-1.11	-1.81				8.98	9.25	7.80	7.29
XLOC_005270	FFC1_04633	FFUJ_06119	related to glucosidase II, alpha subunit							2.33			
XLOC_004491	FFC1_04634	FFUJ_06120	related to beta-glucosidase							2.23			
XLOC_005276	FFC1_04646	FFUJ_06132	uncharacterized protein FFUJ_06132		-1.57	-1.93				6.73	4.84	3.96	3.83
XLOC_004498	FFC1_04647	FFUJ_06133	related to multidrug resistant protein							2.78		2.96	
XLOC_005280	FFC1_04653	FFUJ_06138	uncharacterized protein FFUJ_06138		1.69					1.46	1.55	3.36	1.88
XLOC_005286	null										-2.81		
XLOC_005289	FFC1_04667									2.49	2.92	3.64	
XLOC_004512	FFC1_04671	FFUJ_06155	uncharacterized protein FFUJ_06155		1.26				1.06	3.17	3.03	3.36	2.55
XLOC_005292	FFC1_04676	FFUJ_06160	related to short chain dehydrogenase		2.23	1.47						2.13	
XLOC_005295	FFC1_04679	FFUJ_06163	uncharacterized protein FFUJ_06163	2.63	3.20	1.93				0.88	3.63	4.27	3.34
XLOC_005299	FFC1_04687	FFUJ_06170	uncharacterized protein FFUJ_06170		1.61	1.00				2.79	2.82	3.85	3.15
XLOC_005300	FFC1_04688				1.78		1.79		2.34	6.94	5.85	6.38	4.90
XLOC_005309	null									3.82	5.63	7.01	
XLOC_005317	FFC1_04714	FFUJ_06194	uncharacterized protein FFUJ_06194		2.05					3.70	3.82	4.42	2.80
XLOC_005322	FFC1_04721	FFUJ_06201	probable methylcrotonoyl-CoA carboxylase biotin carboxylase chain			-1.26				2.54	1.78	1.42	
XLOC_005325	FFC1_04728	FFUJ_06208	probable Pls1 tetraspanin							-1.74	-1.79	-1.95	-2.02
XLOC_005327	FFC1_04732											-4.84	-5.08
XLOC_004544	FFC1_04733	FFUJ_06212	related to finger protein							-1.93	-1.05	-2.14	-3.19
XLOC_005332	FFC1_04742	FFUJ_06221	uncharacterized protein FFUJ_06221							2.48	2.01	2.64	2.09
XLOC_005339	FFC1_04758									5.61	3.58	3.59	4.28
XLOC_004561	FFC1_04764									5.58	5.21		
XLOC_005344	FFC1_04765	FFUJ_06242	probable oxidoreductase, short chain dehydrogenase/reductase family superfamily		1.06					0.94	1.25	2.07	1.38
XLOC_005350	null									-3.51			
XLOC_004565	FFC1_04778									-1.84	-1.57	-2.30	
XLOC_005358	FFC1_04787									-3.16	-3.31	-3.14	-5.24
XLOC_004572	FFC1_04788	FFUJ_06261	related to multidrug transporter							-3.81	-4.80		
XLOC_005361	FFC1_04791				1.66				2.26	-2.32	-1.65	-0.89	-3.75
XLOC_004573	FFC1_04794	FFUJ_06265	uncharacterized protein FFUJ_06265							1.55	1.46	2.05	1.52
XLOC_005371	FFC1_04810	FFUJ_06281	probable glucokinase			-1.48				-2.12	-2.85	-3.46	-3.29
XLOC_004583	null										-4.49	-5.94	-4.12
XLOC_004585	FFC1_04815	FFUJ_06285	uncharacterized protein FFUJ_06285		-1.06					-1.33	-1.81	-2.14	-1.97
XLOC_004587	FFC1_04817	FFUJ_06287	UBI4-Ubiquitin		1.17		0.51			1.96	1.68	2.36	2.17
XLOC_004588	FFC1_04818	FFUJ_06288	related to cytoplasmic Zn-finger protein BRAP2 (BRCA1 associated protein)		1.16	0.97				1.89	1.83	2.38	2.06
XLOC_005377	null											-4.46	
XLOC_005384	FFC1_04836	FFUJ_06304	probable glucose repressible protein Grg1	2.31	3.89	1.51				6.07	7.38	8.55	7.26
XLOC_005391	FFC1_04850	FFUJ_06318	probable maltose permease (MalP)							-1.96	-2.17	-2.00	-1.67
XLOC_004609	FFC1_04856	FFUJ_06324	related to AP1-like transcription factor							2.06	1.91	2.33	1.61

XLOC_005398	FFC1_04862	FFUJ_06330	probable ubiquitin-conjugating enzyme							2.17	1.94	1.84	1.11
XLOC_004615	FFC1_04866			1.43	1.75	1.30				-3.00	-1.32	-1.52	-2.32
XLOC_004617	FFC1_04869	FFUJ_06336	related to methyltransferase							-5.15	-4.81	-6.84	-5.75
XLOC_004618	FFC1_04872	FFUJ_06338	related to ABC1 transport protein	2.02	2.01	1.91				-4.00	-1.74	-2.22	-2.70
XLOC_005406	FFC1_04880	FFUJ_06345	uncharacterized protein FFUJ_06345							2.94	3.47	4.56	3.85
XLOC_004622	FFC1_04882	FFUJ_06347	related to mouse T10 protein							2.97	2.78	2.53	1.76
XLOC_004623	FFC1_04883	FFUJ_06348	uncharacterized protein FFUJ_06348							9.48	11.02	9.05	11.63
XLOC_005409	FFC1_04885	FFUJ_06350	uncharacterized protein FFUJ_06350							-1.83	-1.55		-2.39
XLOC_005410	FFC1_04886	FFUJ_06351	related to esterase		-1.38	-1.29					-1.29	-1.92	-2.75
XLOC_004624	FFC1_04887	FFUJ_06352	probable proline racemase		-2.08	-1.75				1.34			
XLOC_004628	FFC1_04895	FFUJ_06360	uncharacterized protein FFUJ_06360							-1.08	-2.02	-1.47	-1.39
XLOC_004630	FFC1_04899	FFUJ_06364	uncharacterized protein FFUJ_06364							-2.78	-2.62	-3.69	-3.59
XLOC_004632	FFC1_04901	FFUJ_06366	probable acetyl-CoA C-acyltransferase precursor							-2.04	-1.51	-1.43	-1.98
XLOC_004634	FFC1_04903	FFUJ_06368	related to neutral proteinase							3.31		2.89	
XLOC_004635	FFC1_04906	FFUJ_06371	uncharacterized protein FFUJ_06371							4.29	3.92	4.16	3.95
XLOC_004636	FFC1_04907	FFUJ_06372	related to component of actin cortical patches LAS17							2.88	2.67	2.73	2.51
XLOC_005420	FFC1_04908	FFUJ_06373	uncharacterized protein FFUJ_06373	1.14	1.89					6.42	6.36	6.48	4.87
XLOC_004637	FFC1_04909	FFUJ_06374	uncharacterized protein FFUJ_06374		1.01					2.95	3.02	3.61	3.17
XLOC_005422	FFC1_04912	FFUJ_06377	uncharacterized protein FFUJ_06377										3.02
XLOC_004644	FFC1_04921	FFUJ_06387	uncharacterized protein FFUJ_06387							4.79	4.98		
XLOC_004645	FFC1_04923	FFUJ_06389	uncharacterized protein FFUJ_06389							-3.07	-3.13	-4.08	-2.77
XLOC_005429	FFC1_04925	FFUJ_06391	uncharacterized protein FFUJ_06391							-2.11	-2.16	-2.45	-1.66
XLOC_005430	FFC1_04926	FFUJ_06392	uncharacterized protein FFUJ_06392							-1.23	-1.40	-2.04	-1.56
XLOC_005431	FFC1_04930	FFUJ_06396	uncharacterized protein FFUJ_06396							3.04	2.18	1.84	2.22
XLOC_004653	null									5.96			
XLOC_004654	FFC1_04935	FFUJ_06401	probable chitosanase precursor							-3.46	-4.82	-5.42	-6.44
XLOC_005433	FFC1_04936										-4.31		
XLOC_004656	FFC1_04939	FFUJ_06406	uncharacterized protein FFUJ_06406							-2.72	-2.15	-1.48	-2.13
XLOC_005435	FFC1_04941	FFUJ_06408	uncharacterized protein FFUJ_06408							-3.78	-4.61	-3.38	
XLOC_005436	FFC1_04942	FFUJ_06409	uncharacterized protein FFUJ_06409							1.31	1.55	2.03	1.46
XLOC_005437	FFC1_04944					-1.23				-0.86	-2.10	-2.10	-1.85
XLOC_004663	FFC1_04951	FFUJ_06418	uncharacterized protein FFUJ_06418		1.86	1.68				4.62	4.82	6.47	7.47
XLOC_005441	FFC1_04953	FFUJ_06420	related to Oxidoreductase							3.66	2.80	3.46	3.56
XLOC_004664	null											-4.47	
XLOC_004665	FFC1_04956	FFUJ_06422	related to cocaine esterase							2.15	1.11		1.50
XLOC_004666	FFC1_04957	FFUJ_06423	uncharacterized protein FFUJ_06423								3.83	3.77	
XLOC_004667	FFC1_04958	FFUJ_06424	uncharacterized protein FFUJ_06424		1.83					6.64	5.69	5.43	3.81
XLOC_004669	FFC1_04961	FFUJ_06427	uncharacterized protein FFUJ_06427							4.27	3.74	4.51	3.31
XLOC_004671	FFC1_04963	FFUJ_06428	uncharacterized protein FFUJ_06428							4.95			
XLOC_004672	FFC1_04966	FFUJ_06432	related to aliphatic nitrilase							2.90	1.90	2.53	3.03
XLOC_005447	FFC1_04968	FFUJ_06434	related to GABA transport protein	0.85	0.99	1.07				7.92	7.15	8.06	7.20
XLOC_005448	FFC1_04969	FFUJ_06435	related to integral membrane protein	0.85		1.48				9.29	7.93	9.94	8.74
XLOC_004674	FFC1_04970	FFUJ_06436	related to GNAT family acetyltransferase			0.98				5.08	4.55	5.18	5.36
XLOC_005449	FFC1_04973	FFUJ_06439	related to calcium-independent phospholipase A2								-4.41		
XLOC_005455	FFC1_04983	FFUJ_06448	related to DUF1237 domain protein							6.41	6.67	6.16	5.17
XLOC_004681	FFC1_04984	FFUJ_06449	related to lipase/esterase							3.20	3.17	3.41	
XLOC_005458	FFC1_04988	FFUJ_06453	uncharacterized protein FFUJ_06453							-4.62	-4.47	-3.69	-3.89
XLOC_004683	FFC1_04990	FFUJ_06455	uncharacterized protein FFUJ_06455									2.81	
XLOC_005460	FFC1_04991	FFUJ_06456	uncharacterized protein FFUJ_06456							3.39	1.69		
XLOC_004684	FFC1_04993	FFUJ_06458	uncharacterized protein FFUJ_06458						-1.99	-1.90	-3.62		
XLOC_005464	FFC1_04997	FFUJ_06462	related to aldo-keto reductase YPR1							5.30			
XLOC_004686	FFC1_04999	FFUJ_06464	uncharacterized protein FFUJ_06464							7.11		5.22	
XLOC_005466	FFC1_05000	FFUJ_06465	related to C4-dicarboxylate transport protein mae1							4.10	4.44	3.72	3.47
XLOC_005469	FFC1_05005	FFUJ_06470	uncharacterized protein FFUJ_06470								-4.91		
XLOC_005470	FFC1_05006	FFUJ_06471	uncharacterized protein FFUJ_06471								-3.85	-3.94	-4.95
XLOC_004690	FFC1_05009	FFUJ_06474	related to Cu-binding metallothionein	2.31	3.84	1.94					2.12	2.78	3.61
XLOC_004694	FFC1_05017	FFUJ_06481	uncharacterized protein FFUJ_06481							3.34	2.92	3.00	
XLOC_004695	FFC1_05018	FFUJ_06482	uncharacterized protein FFUJ_06482							3.72			
XLOC_004699	FFC1_05024	FFUJ_06488	uncharacterized protein FFUJ_06488							-2.00	-4.36	-4.14	-3.58
XLOC_004700	FFC1_05025	FFUJ_06489	uncharacterized protein FFUJ_06489		-4.92								
XLOC_004702	FFC1_05028	FFUJ_06493	uncharacterized protein FFUJ_06493							7.61	6.82	6.83	7.27
XLOC_005483	FFC1_05029	FFUJ_06494	related to cell surface ferroxidase							-3.40	-3.83	-4.33	-4.64
XLOC_004703	FFC1_05030	FFUJ_06495	related to high-affinity iron permease		-1.07	-1.31				-4.38	-5.05	-5.62	-6.02
XLOC_005489	FFC1_05037	FFUJ_06500	flavin depend monooxygenase that catalyses the oxidation of rubrofusarin to 9-hydroxyrubrofusarin			-1.67				-2.36	-2.11	-1.84	-3.40
XLOC_005492	FFC1_05041	FFUJ_06504	probable potassium transporter hak-1								-3.25	-2.78	
XLOC_004707	null												-6.48
XLOC_004709	FFC1_05044	FFUJ_06507	related to HETEROKARYON incompatibility protein							3.38	3.03		
XLOC_004711	FFC1_05048	FFUJ_06511	related to RTM1 protein							-2.58	-2.12		-2.79
XLOC_005498	FFC1_05053	FFUJ_06516	probable UGA2-succinate semialdehyde dehydrogenase							-3.70			
XLOC_004714	FFC1_05054	FFUJ_06517	related to novobiocin biosynthesis protein novR								-4.30		-3.34
XLOC_004715	FFC1_05056	FFUJ_06519	probable L-lactate dehydrogenase (cytochrome)							-2.79	-3.86	-2.34	
XLOC_004717	FFC1_05061									-5.72	-6.31		
XLOC_005503	FFC1_05064	FFUJ_06526	uncharacterized protein FFUJ_06526							-1.59	-3.25	-2.12	-1.95
XLOC_005505	FFC1_05069	FFUJ_06531	uncharacterized protein FFUJ_06531			-3.61				3.48	4.51	2.99	
XLOC_005507	FFC1_05071	FFUJ_06533	related to glutamate carboxypeptidase II							4.27	5.11		
XLOC_005512	FFC1_05079	FFUJ_06541	related to PRLI-interacting factor K			1.28				3.16	3.04	4.15	4.07
XLOC_004728	FFC1_05082	FFUJ_06544	uncharacterized protein FFUJ_06544			1.35				2.76	2.71	3.14	2.40
XLOC_004729	FFC1_05083	FFUJ_06545	related to actin-like protein							2.08	1.49	1.29	
XLOC_005513	FFC1_05084	FFUJ_06546	related to quinone oxidoreductase			1.62				3.17	3.04	2.85	3.16
XLOC_005514	null								3.83				-4.64

XLOC_004730	FFC1_05085	FFUJ_06547	probable monosaccharide transporter			-1.95				-3.00	-3.71		
XLOC_005515	FFC1_05086	FFUJ_06548	related to putative cystathionine beta-lyase									-2.87	-2.95
XLOC_005516	FFC1_05087	FFUJ_06549	uncharacterized protein FFUJ_06549								-4.27		-4.98
XLOC_005519	FFC1_05096									5.31		5.08	3.94
XLOC_005521	FFC1_05098	FFUJ_06560	related to heterokaryon incompatibility protein (het-6OR allele)		-4.14	-4.85				7.12	4.97		
XLOC_004737	FFC1_05101	FFUJ_06562	related to molybdopterin biosynthesis protein moeA									6.23	
XLOC_005527	FFC1_05105	FFUJ_06566	related to beta transducin-like protein							5.68			
XLOC_004739	null											-4.50	
XLOC_005528	FFC1_05107	FFUJ_06569	uncharacterized protein FFUJ_06569							5.70	7.52	5.33	7.98
XLOC_004740	FFC1_05108	FFUJ_06570	probable thioredoxin peroxidase, mitochondrial isoform		2.57	1.61				3.74	4.56	5.62	4.21
XLOC_004742	FFC1_05110	FFUJ_06572	uncharacterized protein FFUJ_06572		3.64	4.56						3.94	4.29
XLOC_004744	FFC1_05114	FFUJ_06575	related to neutral amino acid permease							-2.06			
XLOC_005534	FFC1_05118										6.37		
XLOC_004747	FFC1_05122	FFUJ_06578	related to ARCA protein								-2.49		
XLOC_005536	FFC1_05123	FFUJ_06579	related to tol protein							5.87			5.07
XLOC_004748	FFC1_05124	FFUJ_06580	probable argonaute like post-transcriptional gene silencing protein QDE-2		-1.26					3.88	2.98	2.47	3.12
XLOC_004752	FFC1_05128	FFUJ_06584	related to pyridoxamine 5`-phosphate oxidase							-2.02	-2.03	-1.69	
XLOC_004753	FFC1_05129	FFUJ_06585	PMR1-Ca++-transporting P-type ATPase located in Golgi			-1.17				-2.49	-2.25	-2.47	-2.97
XLOC_004755	FFC1_05132	FFUJ_06588	probable benzoate 4-monooxygenase cytochrome P450							4.91			
XLOC_005538	FFC1_05133	FFUJ_06589	uncharacterized protein FFUJ_06589										-4.89
XLOC_004757	FFC1_05136	FFUJ_06592	uncharacterized protein FFUJ_06592							-4.75	-6.16	-4.75	-5.83
XLOC_004760	FFC1_05140	FFUJ_06596	uncharacterized protein FFUJ_06596			-1.68				6.59	4.18	3.22	
XLOC_005543	FFC1_05145	FFUJ_06600	uncharacterized protein FFUJ_06600							-4.24	-5.01	-7.12	
XLOC_005544	FFC1_05146									-5.85	-6.15	-5.36	
XLOC_004763	FFC1_05147	FFUJ_06601	uncharacterized protein FFUJ_06601	0.98	0.98					-1.93	-0.94	-1.13	-2.05
XLOC_005547	FFC1_05152	FFUJ_06606	related to aryl-alcohol dehydrogenases							6.43	3.71	4.45	5.52
XLOC_004766	FFC1_05153	FFUJ_06607	related to cutinase transcription factor 1 beta							4.32	4.36	4.36	2.71
XLOC_005548	FFC1_05154	FFUJ_06608	related to dehydrogenases and related proteins			-2.23				7.72	6.87	6.27	
XLOC_004767	FFC1_05156	FFUJ_06610	uncharacterized protein FFUJ_06610						3.73	5.46	4.63	4.80	2.25
XLOC_004768	FFC1_05157	FFUJ_06611	related to major facilitator MirA							3.52	2.94	3.04	2.94
XLOC_005551	FFC1_05160										-2.80	-3.02	
XLOC_004771	FFC1_05163	FFUJ_06616	uncharacterized protein FFUJ_06616		-4.11							-3.81	
XLOC_004772	FFC1_05164	FFUJ_06617	uncharacterized protein FFUJ_06617							4.18			
XLOC_005558	FFC1_05171	FFUJ_06621	probable UGA2-succinate semialdehyde dehydrogenase	3.45							3.21		
XLOC_004777	FFC1_05177	FFUJ_06627	probable quinate transport protein								5.70		
XLOC_005561	FFC1_05178	FFUJ_06628	related to NAD(P)H-dependent oxidoreductase		4.35							5.64	
XLOC_005563	FFC1_05180	FFUJ_06630	related to ankyrin		-1.95					5.27	3.02	4.74	5.25
XLOC_005565	FFC1_05182	FFUJ_06632	uncharacterized protein FFUJ_06632							5.21			
XLOC_005566	FFC1_05183	FFUJ_06633	uncharacterized protein FFUJ_06633		-2.81					7.79	4.60		
XLOC_004779	FFC1_05185	FFUJ_06635	uncharacterized protein FFUJ_06635							2.25			
XLOC_004783	FFC1_05190	FFUJ_06640	uncharacterized protein FFUJ_06640							1.88	1.10	1.54	2.04
XLOC_004785	FFC1_05192	FFUJ_06642	uncharacterized protein FFUJ_06642							5.85			
XLOC_004786	FFC1_05195	FFUJ_06645	uncharacterized protein FFUJ_06645							4.38	5.09	5.47	2.24
XLOC_004790	FFC1_05205	FFUJ_06653	uncharacterized protein FFUJ_06653		-2.56								
XLOC_005578	FFC1_05213	FFUJ_06661	uncharacterized protein FFUJ_06661							-2.16	-2.84	-2.56	
XLOC_004796	FFC1_05214	FFUJ_06662	related to microbial serine proteinase							-1.29	-1.59	-2.16	
XLOC_004801	FFC1_05219	FFUJ_06667	uncharacterized protein FFUJ_06667						1.44	-2.20	-1.94	-2.52	-2.66
XLOC_004810	FFC1_05236	FFUJ_06684	related to Zn(II)2Cys6 transcriptional activator		2.69	2.07				7.03	8.29	7.81	9.23
XLOC_004811	FFC1_05237	FFUJ_06685	uncharacterized protein FFUJ_06685		1.54	1.27				7.33	6.79	6.91	7.76
XLOC_004812	FFC1_05238	FFUJ_06686	related to hexose transporter protein							13.62	9.46	9.78	10.00
XLOC_004813	FFC1_05239	FFUJ_06687	related to isotrichodermin C-15 hydroxylase (cytochrome P-450 monooxygenase CYP65A1)	1.19	1.17					9.96	10.04	10.27	9.90
XLOC_005587	FFC1_05240	FFUJ_06688	related to monocarboxylate transporter 2							6.41	7.05	6.99	6.23
XLOC_005588	FFC1_05241	FFUJ_06689	related to choline dehydrogenase							8.30	7.51	7.30	7.15
XLOC_004814	FFC1_05242	FFUJ_06690	related to phosphoenolpyruvate phosphomutase							8.78	8.20		7.45
XLOC_004815	FFC1_05243	FFUJ_06691	uncharacterized protein FFUJ_06691							8.25	7.19	7.30	5.87
XLOC_004816	FFC1_05244	FFUJ_06692	related to monocarboxylate transporter 2							6.73	5.79	5.36	4.57
XLOC_005589	FFC1_05245	FFUJ_06693	probable Alpha-glucosidase precursor (Maltase)							7.74	6.60	6.43	6.29
XLOC_004817	FFC1_05246	FFUJ_06694	uncharacterized protein FFUJ_06694							11.01	9.24	7.58	7.80
XLOC_004818	FFC1_05247	FFUJ_06695	related to potassium channel beta subunit protein							2.02	0.94	0.88	
XLOC_005590	FFC1_05249	FFUJ_06697	related to cutinase transcription factor 1 beta							4.69			
XLOC_006428	FFC1_05250										5.28		
XLOC_005591	FFC1_05251									2.99	4.40	4.11	3.64
XLOC_005593	FFC1_05257												6.72
XLOC_006433	FFC1_05258									-8.62	-11.11	-8.87	-6.25
XLOC_006434	FFC1_05259									-6.99	-7.81	-8.62	-5.47
XLOC_006438	FFC1_05268											-1.25	-4.83
XLOC_005600	FFC1_05272									-2.64	-2.94	-2.87	-2.39
XLOC_005601	FFC1_05273									-5.04			
XLOC_006443	FFC1_05277	FFUJ_12834	related to sulfatase							-4.99	-4.36	-4.79	-3.32
XLOC_006444	FFC1_05278				-1.47					-2.06	-2.59	-3.44	-2.57

XLOC_005604	FFC1_05279									-3.20	-3.63	-4.25	-3.98
XLOC_005606	FFC1_05281												5.14
XLOC_006446	null									6.87	6.72	6.12	6.25
XLOC_006447	FFC1_05282									4.75	4.45	4.36	4.97
XLOC_005607	FFC1_05283									4.27	4.18	4.27	5.39
XLOC_005614	FFC1_05292					1.12				-4.16	-3.53	-3.20	-2.17
XLOC_006453	FFC1_05298									4.80	4.70		
XLOC_006455	FFC1_05301										2.43		
XLOC_006457	FFC1_05303									2.60	1.47		
XLOC_005618	FFC1_05304				1.96					5.18	5.56	3.34	
XLOC_006459	FFC1_05305									-3.04			
XLOC_005626	null									4.85			
XLOC_006473	FFC1_05327									-0.94			-2.50
XLOC_006474	FFC1_05328									-3.09	-2.55	-2.85	-4.16
XLOC_005630	FFC1_05330									5.80			
XLOC_006479	FFC1_05335									7.26	5.32		6.55
XLOC_005634	FFC1_05339				-1.04					2.67	2.13		3.10
XLOC_005638	FFC1_05347									2.25		2.61	2.25
XLOC_006488	FFC1_05353									-2.81	-3.73	-3.60	-3.42
XLOC_006489	FFC1_05354										-5.02		
XLOC_006490	FFC1_05355									-2.40	-2.85	-2.57	-1.80
XLOC_006492	FFC1_05358									4.11	4.48	4.89	4.62
XLOC_005644	FFC1_05360									6.96	6.37	5.57	6.27
XLOC_005645	FFC1_05362									5.25	5.59	5.56	
XLOC_005646	FFC1_05363									-5.24	-5.02	-4.08	-3.85
XLOC_006497	FFC1_05371									2.47		2.86	
XLOC_006501	FFC1_05378									-4.84			
XLOC_006503	FFC1_05380									4.28			3.55
XLOC_006504	FFC1_05381									-2.38			-1.50
XLOC_005657	FFC1_05383				1.79	0.99				1.38	1.76	2.55	1.40
XLOC_006505	FFC1_05384									-1.51	-2.47	-1.96	-1.94
XLOC_006506	FFC1_05385									-2.61	-2.84	-2.54	-3.95
XLOC_006508	FFC1_05389									-7.16	-8.60	-9.03	-6.02
XLOC_006509	FFC1_05392									5.42			
XLOC_006510	FFC1_05394			3.95	3.61					5.24	9.20	6.29	
XLOC_005663	FFC1_05395									2.38			
XLOC_006515	FFC1_05405									3.02			
XLOC_005672	FFC1_05411										-4.53	-5.58	-4.84
XLOC_006520	FFC1_05414									2.62		3.39	
XLOC_005676	FFC1_05415											4.50	
XLOC_006523	FFC1_05420									-2.44	-3.46		-2.37
XLOC_006524	FFC1_05421												-2.90
XLOC_005679	FFC1_05422												-7.21
XLOC_006525	FFC1_05423									-2.45			-4.82
XLOC_005684	FFC1_05430									-4.36	-3.98	-4.16	-4.73
XLOC_006533	FFC1_05439									5.42	5.08		4.40
XLOC_005689	FFC1_05441									8.40	8.63	8.62	8.77
XLOC_006538	FFC1_05446									4.26	6.64	6.29	7.75
XLOC_006539	FFC1_05447									3.44	3.46	3.71	2.68
XLOC_006542	FFC1_05455									5.49	3.49	4.88	
XLOC_006543	FFC1_05456									5.77	5.25	5.32	5.39
XLOC_006544	FFC1_05457									7.56	6.98	7.90	5.39
XLOC_005700	FFC1_05458									4.74	3.87	4.79	3.66
XLOC_006545	FFC1_05459									6.75	7.29	7.60	6.89
XLOC_005701	FFC1_05460									3.76	2.61	4.85	4.03
XLOC_006546	FFC1_05461					-2.33				8.08	7.44	6.70	3.99
XLOC_005703	FFC1_05463									8.90	7.61	6.72	6.73
XLOC_006547	FFC1_05464									5.38		5.98	
XLOC_005704	FFC1_05465									4.80			
XLOC_006549	FFC1_05468									4.44	2.72	3.22	
XLOC_005710	FFC1_05476	FFUJ_14874	related to ATP/GTP-binding protein							-4.78	-6.38	-6.32	-4.97
XLOC_005712	FFC1_05478	FFUJ_14872	related to putative tartrate transporter										2.95
XLOC_006554	FFC1_05483	FFUJ_14867	uncharacterized protein FFUJ_14867							-2.29	-2.22	-2.10	
XLOC_006562	FFC1_05495	FFUJ_14856	related to carboxypeptidase A								5.03	5.08	
XLOC_006565	FFC1_05500	FFUJ_14851	related to putative alpha-L-fucosidase precursor							5.77			
XLOC_006571	FFC1_05510	FFUJ_14842	related to catechol O-methyltransferase							3.04	2.36		2.49
XLOC_005730	FFC1_05512	FFUJ_14840	related to methyltransferase							2.91	1.95	1.92	3.23
XLOC_005733	FFC1_05520	FFUJ_14832	uncharacterized protein FFUJ_14832			-1.81				-2.97	-4.18	-3.21	-5.37
XLOC_005736	FFC1_05523	FFUJ_14829	uncharacterized protein FFUJ_14829										2.29
XLOC_006582	FFC1_05531	FFUJ_14822	related to Aspartate ammonia-lyase							1.62		2.55	1.28
XLOC_005744	FFC1_05538	FFUJ_14814	related to heterokaryon incompatibility protein (het-6OR allele)							2.74	2.38	2.66	
XLOC_005749	FFC1_05545	FFUJ_14807	uncharacterized protein FFUJ_14807						-1.41	-3.16	-2.20	-1.91	-2.57
XLOC_006591	FFC1_05548	FFUJ_14804	probable 3-octaprenyl-4-hydroxybenzoate carboxy-lyase										-2.30
XLOC_005751	FFC1_05549	FFUJ_14803	probable 3-polyprenyl-4-hydroxybenzoate decarboxylase and related decarboxylases			-1.42							-2.37
XLOC_006592	FFC1_05550	FFUJ_14802	uncharacterized protein FFUJ_14802							-1.03	-1.46	-1.75	-2.41
XLOC_005752	FFC1_05551	FFUJ_14801	uncharacterized protein FFUJ_14801										-2.11
XLOC_005756	FFC1_05560	FFUJ_14793	probable metallo-beta-lactamase domain protein									-3.55	
XLOC_006599	FFC1_05562	FFUJ_14791	probable sulfate permease II							-2.91	-2.55	-3.07	-5.49
XLOC_005758	FFC1_05566	FFUJ_14787	related to beta transducin-like protein							-1.92	-2.91	-2.14	
XLOC_005761	FFC1_05571	FFUJ_14782	related to acetyl-hydrolase							4.21		6.48	
XLOC_005762	FFC1_05572	FFUJ_14781	related to monooxygenase							6.01	5.59	7.73	6.39
XLOC_005768	FFC1_05579	FFUJ_14773	uncharacterized protein FFUJ_14773							-0.82	-1.33	-2.41	
XLOC_006606	FFC1_05581	FFUJ_14771	uncharacterized protein FFUJ_14771							6.97	3.11	6.75	4.16
XLOC_006607	FFC1_05583	FFUJ_14769	related to acetyltransferase							-5.50			

XLOC_005770	FFC1_05584	FFUJ_14397	related to tetracycline resistance protein (probable transport protein)						-2.83	-4.01	-3.08		
XLOC_006608	FFC1_05585	FFUJ_14396	related to formaldehyde dehydrogenase									-4.85	
XLOC_005772	FFC1_05590	FFUJ_14391	uncharacterized protein FFUJ_14391							-1.93	-3.90	-2.10	
XLOC_006614	FFC1_05594	FFUJ_14387	related to pathway-specific regulatory protein nit-4								-2.61		-2.31
XLOC_006616	FFC1_05598	FFUJ_14765	uncharacterized protein FFUJ_14765							3.55	2.90	4.28	2.13
XLOC_006617	FFC1_05600	FFUJ_14763	uncharacterized protein FFUJ_14763							5.44			
XLOC_006618	FFC1_05601	FFUJ_14762	related to tol protein							3.20	2.69	1.97	1.81
XLOC_005777	FFC1_05602	FFUJ_14761	uncharacterized protein FFUJ_14761							7.22	5.59	6.86	5.12
XLOC_005778	FFC1_05603	FFUJ_14760	related to acid phosphatase		1.92					5.47	5.44	6.51	5.00
XLOC_006620	FFC1_05606	FFUJ_14757	uncharacterized protein FFUJ_14757							2.56	2.92	3.13	
XLOC_006623	FFC1_05612									-3.49	-3.20	-2.24	-3.33
XLOC_005783	FFC1_05616	FFUJ_14750	uncharacterized protein FFUJ_14750								-4.52		
XLOC_006629	FFC1_05623	FFUJ_14743	related to peroxisomal short-chain alcohol dehydrogenase							6.76	6.80	5.90	7.04
XLOC_005788	FFC1_05627	FFUJ_14739	related to ZRT1 Zinc transporter I			-1.11				-1.97	-2.58	-3.02	-3.26
XLOC_006632	FFC1_05628	FFUJ_14738	probable zinc-binding oxidoreductase							2.15	1.24		
XLOC_005791	FFC1_05635	FFUJ_14731	uncharacterized protein FFUJ_14731							7.56	6.65	5.84	5.43
XLOC_006639	FFC1_05639	FFUJ_14727	uncharacterized protein FFUJ_14727							-5.00	-6.83	-5.47	-4.55
XLOC_006641	FFC1_05641	FFUJ_14725	related to dTDP-glucose 4,6-dehydratase										-3.07
XLOC_006642	FFC1_05642	FFUJ_14724	probable isoamyl alcohol oxidase							-5.62	-6.65	-6.63	-5.77
XLOC_005793	FFC1_05643	FFUJ_14723	related to integral membrane protein PTH11							-3.21	-2.86	-2.91	-3.09
XLOC_006643	FFC1_05644	FFUJ_14722	uncharacterized protein FFUJ_14722			2.13				5.57	7.94	6.41	5.91
XLOC_005795	FFC1_05646	FFUJ_14720	uncharacterized protein FFUJ_14720							-2.32	-1.82	-2.17	
XLOC_005801	FFC1_05658	FFUJ_14709	related to Transaldolase B		-2.48					2.18			
XLOC_006650	FFC1_05659	FFUJ_14708	uncharacterized protein FFUJ_14708		-1.46	-1.34				2.11			
XLOC_006651	FFC1_05660	FFUJ_14707	uncharacterized protein FFUJ_14707								-2.37	-3.10	-5.60
XLOC_005806	FFC1_05666	FFUJ_14701	uncharacterized protein FFUJ_14701										3.37
XLOC_006654	FFC1_05670	FFUJ_14697	related to MFS multidrug transporter							3.90	4.29	4.31	3.75
XLOC_006655	FFC1_05671	FFUJ_14696	related to C.carbonum toxD protein							3.14	3.14	3.45	2.34
XLOC_006656	FFC1_05674	FFUJ_14693	related to multidrug resistance protein fnx1							5.46			
XLOC_005811	FFC1_05675	FFUJ_14692	related to thioredoxin reductase							6.31	5.85	4.95	5.45
XLOC_006657	FFC1_05676	FFUJ_14691	related to aminotransferase GliI							6.69	6.31	5.56	6.56
XLOC_005812	FFC1_05677	FFUJ_14690	uncharacterized protein FFUJ_14690							6.19	5.91	7.34	5.97
XLOC_006658	FFC1_05678	FFUJ_14689	uncharacterized protein FFUJ_14689							3.61	3.10	3.56	5.01
XLOC_006660	FFC1_05681	FFUJ_14686	related to monooxigenase		1.38	1.44				5.71	6.12	6.54	7.16
XLOC_006661	FFC1_05682	FFUJ_14685	related to integral membrane protein PTH11	1.35	1.72	2.63				9.34	8.85	8.62	8.86
XLOC_005814	FFC1_05683	FFUJ_14684	related to aliphatic nitrilase							8.30	7.79	6.44	7.49
XLOC_005815	FFC1_05684	FFUJ_14683	uncharacterized protein FFUJ_14683	1.27	2.40	2.51				8.53	9.80	9.94	11.17
XLOC_006662	FFC1_05685	FFUJ_14682	uncharacterized protein FFUJ_14682							5.65	3.82	4.66	4.19
XLOC_006663	FFC1_05686	FFUJ_14681	uncharacterized protein FFUJ_14681								-2.10		
XLOC_005819	FFC1_05693	FFUJ_14675	related to laccase precursor	-1.45	-3.28								
XLOC_005822	FFC1_05697	FFUJ_14671	related to maltose permease (MalP)							5.07			
XLOC_006668	FFC1_05698	FFUJ_14670	uncharacterized protein FFUJ_14670							-1.94	-2.96	-1.93	-1.99
XLOC_006671	FFC1_05703	FFUJ_14665	related to trans-aconitate 3-methyltransferase		1.10					-2.61	-2.17	-1.62	-2.07
XLOC_006675	null									-5.53	-4.93	-4.67	-6.31
XLOC_005827	FFC1_05710	FFUJ_14659	uncharacterized protein FFUJ_14659							2.73	3.18	2.75	4.03
XLOC_006679	FFC1_05715	FFUJ_14654	related to short-chain alcohol dehydrogenase							5.34	3.45	5.87	6.23
XLOC_005831	FFC1_05717	FFUJ_14652	related to 15-hydroxyprostaglandin dehydrogenase							5.92			
XLOC_006684	FFC1_05725	FFUJ_14644	uncharacterized protein FFUJ_14644							4.68	5.16		
XLOC_006685	FFC1_05728	FFUJ_14641	uncharacterized protein FFUJ_14641							3.04	2.26	2.45	3.63
XLOC_006689	FFC1_05734	FFUJ_14636	related to gibberellin biosynthesis-related							5.37		5.20	5.77
XLOC_005843	FFC1_05741	FFUJ_14628	uncharacterized protein FFUJ_14628							-4.79	-4.27		-5.42
XLOC_006695	FFC1_05745	FFUJ_14624	uncharacterized protein FFUJ_14624							7.81	4.94	8.06	8.21
XLOC_006696	FFC1_05746	FFUJ_14622	uncharacterized protein FFUJ_14622							-3.05	-3.46	-2.80	-3.02
XLOC_005846	FFC1_05749	FFUJ_14619	related to dehydrogenases and related proteins							6.12	5.36	6.65	
XLOC_006698	FFC1_05750	FFUJ_14618	uncharacterized protein FFUJ_14618							4.46	3.36	4.82	
XLOC_006703	FFC1_05763	FFUJ_14606	uncharacterized protein FFUJ_14606							7.19	7.09	7.40	4.11
XLOC_006704	FFC1_05764	FFUJ_14605	uncharacterized protein FFUJ_14605							8.70	7.02	8.23	
XLOC_006705	FFC1_05765									5.88		5.44	4.48
XLOC_006706	FFC1_05766	FFUJ_14604	probable maltose permease (MalP)							3.99	4.60		
XLOC_006707	FFC1_05770	FFUJ_14601	uncharacterized protein FFUJ_14601							2.21	1.41	1.94	
XLOC_005858	FFC1_05771	FFUJ_14600	related to protein kinase							2.46		2.20	
XLOC_006708	FFC1_05772	FFUJ_14599	related to protein kinase							2.39			
XLOC_005864	FFC1_05779	FFUJ_14593	uncharacterized protein FFUJ_14593							-2.05	-2.84	-2.57	
XLOC_006710	null									-7.53	-6.82	-6.27	-6.17
XLOC_006711	FFC1_05780	FFUJ_14592	probable fusarubin cluster-esterase							-4.92	-5.67	-5.54	-4.30
XLOC_005865	FFC1_05781	FFUJ_14591	uncharacterized protein FFUJ_14591							-4.81	-5.51	-5.11	-4.34
XLOC_005866	FFC1_05783	FFUJ_14590	uncharacterized protein FFUJ_14590							3.65	2.81	3.93	2.58
XLOC_006713	FFC1_05785	FFUJ_14588	related to nonribosomal peptide synthetase MxcG							5.43	4.97	4.99	5.18
XLOC_006714	FFC1_05787	FFUJ_14586	uncharacterized protein FFUJ_14586							-3.24	-3.40		
XLOC_006715	FFC1_05788	FFUJ_14585	uncharacterized protein FFUJ_14585										4.99
XLOC_006719	null										-4.39		
XLOC_005874	FFC1_05797	FFUJ_14576	uncharacterized protein FFUJ_14576							2.68	2.78	2.68	
XLOC_006720	FFC1_05801	FFUJ_14573	related to monocarboxylate transporter		-1.49	-1.42				-2.75	-3.19	-3.62	-3.58
XLOC_006721	FFC1_05805	FFUJ_14571	probable carnitine transport protein	1.28						1.84	2.72	2.39	
XLOC_005880	null										5.77		
XLOC_006722	FFC1_05809	FFUJ_14567	related to protein carrier KAP123							2.66	3.15	3.35	3.60
XLOC_006723	FFC1_05810	FFUJ_14566	uncharacterized protein FFUJ_14566							3.75	3.44	4.08	4.17
XLOC_005884	FFC1_05811	FFUJ_14565	uncharacterized protein FFUJ_14565							6.30	5.66	6.43	6.84
XLOC_006724	FFC1_05812									9.74	5.57	6.41	9.80

XLOC_006725	FFC1_05815	FFUJ_14562	uncharacterized protein FFUJ_14562								1.48	2.24	3.11
XLOC_005887	FFC1_05816	FFUJ_14561	uncharacterized protein FFUJ_14561							1.21	1.18	2.36	2.90
XLOC_006729	FFC1_05826	FFUJ_14553	related to zinc transporter			-2.02			-2.75	3.24	4.31	3.39	3.98
XLOC_006730	FFC1_05827	FFUJ_14552	uncharacterized protein FFUJ_14552			-1.02				3.22	4.06	4.16	4.35
XLOC_005894	FFC1_05828	FFUJ_14551	related to putative trehalase			-1.28					2.17		1.36
XLOC_005895	FFC1_05829	FFUJ_14550	uncharacterized protein FFUJ_14550							-1.20	-1.27	-2.09	
XLOC_006731	FFC1_05830	FFUJ_14549	related to ARG8-acetylornithine aminotransferase									-3.17	-2.63
XLOC_006732	FFC1_05831	FFUJ_14548	related to Carboxypeptidase 2							4.20	4.33	3.08	
XLOC_005897	FFC1_05833	FFUJ_14546	uncharacterized protein FFUJ_14546		2.50	1.72					1.16	3.87	3.05
XLOC_006734	FFC1_05836	FFUJ_14542	related to fructosyl amino acid oxidase							-1.34	-2.01	-1.75	
XLOC_005900	FFC1_05839	FFUJ_14539	uncharacterized protein FFUJ_14539							3.21	3.03	2.76	2.53
XLOC_006736	FFC1_05840	FFUJ_14538	related to dehydrogenase/reductase							7.63	7.79	7.73	8.14
XLOC_006738	FFC1_05843	FFUJ_14535	probable bifunctional D12/D15 fatty acid desaturase							-2.78	-2.21	-2.51	-2.21
XLOC_005903	FFC1_05846	FFUJ_14531	phosphate transport protein							-2.15	-2.40	-1.83	-1.92
XLOC_005905	FFC1_05848	FFUJ_14529	uncharacterized protein FFUJ_14529	1.90	2.71					3.13	4.32	5.40	3.60
XLOC_006742	FFC1_05849	FFUJ_14528	related to succinate-CoA ligase alpha and beta chain								-1.99	-2.18	
XLOC_006743	FFC1_05853	FFUJ_14524	related to capsule polysaccharide biosynthesis protein							-1.99	-2.10		
XLOC_005909	FFC1_05855	FFUJ_14522	uncharacterized protein FFUJ_14522							3.08	2.99	2.97	2.72
XLOC_005913	FFC1_05862	FFUJ_14515	related to 2-haloalkanoic acid dehalogenase								-4.40	-3.93	
XLOC_005915	FFC1_05864	FFUJ_14513	related to nitrate reductase									3.18	1.68
XLOC_006750	FFC1_05865	FFUJ_14512	reductase		1.86	1.21				1.04		2.05	
XLOC_005917	FFC1_05867	FFUJ_14510	uncharacterized protein FFUJ_14510		3.81								
XLOC_005923	FFC1_05874	FFUJ_14504	uncharacterized protein FFUJ_14504							4.56		5.18	
XLOC_006753	null									2.80		3.22	2.42
XLOC_006760	FFC1_05886	FFUJ_13716	related to D-arabinitol 2-dehydrogenase							2.07	1.19	1.11	
XLOC_006762	FFC1_05888	FFUJ_13714	uncharacterized protein FFUJ_13714									4.87	6.03
XLOC_005932	FFC1_05890	FFUJ_13712	uncharacterized protein FFUJ_13712							2.06	1.54	2.29	3.77
XLOC_005933	FFC1_05892	FFUJ_13710	uncharacterized protein FFUJ_13710							1.57	1.58	1.90	2.19
XLOC_006765	FFC1_05894	FFUJ_13708	related to pathway-specific regulatory protein nit-4		1.49					5.13	5.00	5.72	4.54
XLOC_006767	FFC1_05896	FFUJ_13706	uncharacterized protein FFUJ_13706			2.15					5.42	4.88	
XLOC_006768	FFC1_05897	FFUJ_13705	uncharacterized protein FFUJ_13705	0.62	0.63	-0.62				1.45	1.77	2.10	1.08
XLOC_005938	FFC1_05900	FFUJ_13702	uncharacterized protein FFUJ_13702							2.42	2.59	3.02	2.68
XLOC_006769	FFC1_05901	FFUJ_13701	related to light induced alcohol dehydrogenase Bli-4	1.59	1.45					1.91	3.97	3.52	
XLOC_005940	FFC1_05903	FFUJ_13700	uncharacterized protein FFUJ_13700							2.85	3.34	3.14	2.24
XLOC_005941	FFC1_05906	FFUJ_13697	probable Alcohol dehydrogenase							1.80	0.79	2.91	2.56
XLOC_006774	null										-3.73		
XLOC_005949	FFC1_05925	FFUJ_13678	probable aconitase	1.10	1.41					1.60	2.14	1.95	1.46
XLOC_006786	null									2.50	3.11		
XLOC_005961	FFC1_05944	FFUJ_13659	uncharacterized protein FFUJ_13659							-3.47	-3.48	-3.28	-3.60
XLOC_005977	FFC1_05983	FFUJ_13626	probable aflatoxin efflux pump AFLT							2.82	2.50	3.20	3.35
XLOC_006818	FFC1_05985	FFUJ_13624	Oxidation resistance protein 1							3.07	2.59	2.83	2.67
XLOC_005980	FFC1_05990	FFUJ_13619	probable hydrolase (HAD superfamily)			-1.65				1.79	2.53	2.46	
XLOC_006823	FFC1_05991	FFUJ_13618	related to thiamine repressible genes regulatory protein thi1							1.81	2.97	2.10	1.39
XLOC_005984	null				2.30								
XLOC_006828	FFC1_06001	FFUJ_13608	probable CHO1-CDP-diacylglycerol serine O-phosphatidyltransferase	0.64	0.94					1.71	2.13	2.33	1.60
XLOC_005989	FFC1_06006	FFUJ_13603	probable caspase			1.14				0.85	0.95	1.71	2.03
XLOC_006834	FFC1_06013	FFUJ_13596	uncharacterized protein FFUJ_13596	1.41	1.39					3.01	4.21	3.91	2.16
XLOC_005993	FFC1_06014	FFUJ_13595	related to transcription factor BOM	1.50	1.19					1.44	2.85	2.14	1.37
XLOC_005995	FFC1_06017	FFUJ_13592	related to mfs-multidrug-resistance transporter	1.33						-3.61	-2.07	-3.41	-3.45
XLOC_006843	FFC1_06028	FFUJ_13581	uncharacterized protein FFUJ_13581							2.83	2.39	2.07	1.80
XLOC_006845	FFC1_06030	FFUJ_13579	probable succinyl-CoA:3-ketoacid-coenzyme A transferase, mitochondrial precursor	1.57						-1.13			-2.46
XLOC_006006	FFC1_06040	FFUJ_13569	related to subtilisin-like serine protease	1.19	2.14	2.93				1.43	2.66	3.36	3.30
XLOC_006008	FFC1_06043	FFUJ_13566	uncharacterized protein FFUJ_13566							-1.57	-1.99	-2.34	-2.09
XLOC_006852	FFC1_06044	FFUJ_13565	probable xylulose-5-phosphate phosphoketolase							-1.58	-2.12	-2.71	-2.29
XLOC_006009	null										-5.13		
XLOC_006854	FFC1_06047										5.34	4.77	4.91
XLOC_006858	FFC1_06054	FFUJ_13558	uncharacterized protein FFUJ_13558							-2.14	-1.89	-1.25	-1.89
XLOC_006019	null												-2.44
XLOC_006024	FFC1_06068	FFUJ_13544	probable SPT10-transcription regulatory protein							-2.38	-2.12	-2.35	-2.34
XLOC_006032	FFC1_06079	FFUJ_13533	related to protein tyrosine phosphatase phi							2.01	1.51	1.33	1.33
XLOC_006033	FFC1_06083	FFUJ_13529	uncharacterized protein FFUJ_13529										-5.16
XLOC_006040	FFC1_06092	FFUJ_13520	related to DNA Polymerase iota (POLI)							-1.55	-2.12		
XLOC_006042	FFC1_06097	FFUJ_13515	probable acetolactate synthase small subunit precursor							-2.72	-2.25	-2.03	
XLOC_006044	FFC1_06101	FFUJ_13511	probable glucan 1,4-alpha-glucosidase		1.71	1.64				-2.13	-2.08		
XLOC_006045	FFC1_06103	FFUJ_13509	related to a-agglutinin core protein AGA1							2.71	2.15	2.92	3.13
XLOC_006882	FFC1_06104	FFUJ_13508	related to Type 1 phosphatases regulator ypi-1							2.50	2.11	2.47	1.84
XLOC_006893	FFC1_06125	FFUJ_13489	uncharacterized protein FFUJ_13489							2.21	1.92	1.92	2.16
XLOC_006894	FFC1_06127	FFUJ_13487	uncharacterized protein FFUJ_13487									6.11	6.33
XLOC_006066	FFC1_06140	FFUJ_13475	related to mitotic apparatus protein p62							2.07	1.62	2.24	2.62
XLOC_006067	FFC1_06141	FFUJ_13474	related to aldo-keto reductase YPR1							2.00	1.54	2.00	1.96
XLOC_006079	FFC1_06162	FFUJ_13453	uncharacterized protein FFUJ_13453							1.94	1.73	2.72	1.65
XLOC_006087	FFC1_06179	FFUJ_13436	related to quinate transport protein	2.04	2.45	2.38					2.10	2.34	2.84
XLOC_006918	FFC1_06186	FFUJ_13429	probable GTPase activating protein							2.12	2.06	1.75	1.68

XLOC_006919	FFC1_06187	FFUJ_13428	related to integral membrane protein	1.05	0.98					1.40	2.18	2.08	
XLOC_006920	FFC1_06188				1.12					2.67	3.31	3.74	2.03
XLOC_006095	FFC1_06192	FFUJ_13424	uncharacterized protein FFUJ_13424									2.88	
XLOC_006924	FFC1_06193	FFUJ_13423	related to 1-aminocyclopropane-2-carboxylate synthase 2							-1.35	-1.67	-2.08	-1.58
XLOC_006929	FFC1_06199	FFUJ_13417	uncharacterized protein FFUJ_13417							2.90	2.96	3.08	2.99
XLOC_006100	FFC1_06206	FFUJ_13411	uncharacterized protein FFUJ_13411		1.85					3.67	3.09	3.78	3.77
XLOC_006104	FFC1_06211	FFUJ_13406	uncharacterized protein FFUJ_13406	1.68	2.28					-2.01	-0.52		-1.45
XLOC_006936	FFC1_06214	FFUJ_13403	uncharacterized protein FFUJ_13403							3.41	3.83	4.34	4.69
XLOC_006937	FFC1_06216	FFUJ_13401	probable FET3-cell surface ferroxidase, high affinity							-3.34	-2.94	-3.73	-3.83
XLOC_006107	FFC1_06217	FFUJ_13400	related to high-affinity iron permease							-3.53	-3.06	-4.42	-4.23
XLOC_006943	FFC1_06231	FFUJ_13386	uncharacterized protein FFUJ_13386							1.75	1.77	2.43	2.08
XLOC_006117	FFC1_06233	FFUJ_13384	probable P-Type ATPase related to neomycin resistance protein							4.22	3.92	3.74	3.65
XLOC_006949	FFC1_06242	FFUJ_13376	related to thioredoxin		1.45					1.82	1.48	3.39	2.95
XLOC_006952	FFC1_06250	FFUJ_13368	uncharacterized protein FFUJ_13368							-1.23	-1.81	-2.31	
XLOC_006128	FFC1_06252	FFUJ_13366	probable cpc-3 protein							-1.72	-1.70	-2.14	-1.55
XLOC_006130	FFC1_06255	FFUJ_13363	related to DNAJ-like protein homolog		1.36					2.88	2.45	3.09	3.40
XLOC_006132	FFC1_06259	FFUJ_13359	related to dihydrodipicolinate synthase							2.94	2.32	2.79	2.43
XLOC_006136	null											-5.32	
XLOC_006959	FFC1_06266	FFUJ_13349	related to kinesin-related protein KLPA							-2.83	-3.24		
XLOC_006965	FFC1_06274	FFUJ_13344	uncharacterized protein FFUJ_13344	1.46		1.01					2.31	1.48	1.38
XLOC_006143	FFC1_06279									-2.75	-2.25	-2.35	-2.28
XLOC_006978	FFC1_06294	FFUJ_13326	uncharacterized protein FFUJ_13326							-1.70	-2.06	-2.01	-1.99
XLOC_006149	FFC1_06296	FFUJ_13324	probable formate dehydrogenase			-2.66							
XLOC_006982	FFC1_06305	FFUJ_13315	related to endo-1,3(4)-beta-glucanase							-1.63	-2.11	-2.78	-3.24
XLOC_006983	FFC1_06306	FFUJ_13314	uncharacterized protein FFUJ_13314		-2.43	-2.48		-1.85					
XLOC_006161	FFC1_06318	FFUJ_13302	related to triose phosphate/3-phosphoglycerate/phosphate translocator							-2.53	-2.35	-2.90	-3.15
XLOC_006993	FFC1_06323	FFUJ_13297	uncharacterized protein FFUJ_13297							-1.47	-2.13	-1.97	-1.40
XLOC_006996	FFC1_06329	FFUJ_13293	probable arginosuccinate synthetase							-3.85	-3.13	-2.86	
XLOC_006169	FFC1_06336	FFUJ_13286	uncharacterized protein FFUJ_13286							2.21	1.65	2.19	
XLOC_006170	FFC1_06339	FFUJ_13283	related to disease resistance protein aig2							-1.96	-2.45	-2.75	-1.50
XLOC_007001	FFC1_06341	FFUJ_13281	uncharacterized protein FFUJ_13281							3.93	3.86	4.17	3.58
XLOC_006172	FFC1_06342	FFUJ_13280	related to ubiquitin carboxyl-terminal hydrolase 2							2.03	2.05	2.23	2.28
XLOC_006173	FFC1_06343	FFUJ_13279	uncharacterized protein FFUJ_13279		0.78					2.05	1.99	2.09	2.25
XLOC_006175	FFC1_06346	FFUJ_13276	uncharacterized protein FFUJ_13276		2.42					4.94	4.54	5.47	4.07
XLOC_006176	FFC1_06348	FFUJ_13274	uncharacterized protein FFUJ_13274							5.02		4.94	
XLOC_006180	FFC1_06353	FFUJ_13270	uncharacterized protein FFUJ_13270									-4.46	
XLOC_007009	null										-1.38	-2.09	
XLOC_007010	null												-4.70
XLOC_006185	FFC1_06361	FFUJ_13262	related to benzoate 4-monooxygenase cytochrome P450							3.86	3.38	3.53	
XLOC_007012	FFC1_06365	FFUJ_13259	probable DNA polymerase epsilon, calytic chain POL2							-2.11	-2.10	-1.85	-1.88
XLOC_006190	FFC1_06372	FFUJ_13252	related to GAL10-UDP-glucose 4-epimerase							-2.61	-3.33	-3.30	-2.86
XLOC_006195	null			1.80	1.92	1.46				0.97	2.69	2.62	2.37
XLOC_006196	FFC1_06380	FFUJ_13245	probable period clock protein FRQ	1.53	1.79	1.44				1.54	2.76	2.90	2.44
XLOC_006198	FFC1_06382	FFUJ_13243	related to C.cardunculus cypro4 protein							2.60	2.62	2.86	2.58
XLOC_006200	null									7.72	6.60	5.64	6.46
XLOC_006214	FFC1_06419	FFUJ_13207	related to hsp70 protein							8.40	7.17	5.93	6.46
XLOC_006215	FFC1_06420	FFUJ_13206	related to RING finger protein Dorfin							2.69	2.60	1.51	
XLOC_007045	FFC1_06423	FFUJ_13203	uncharacterized protein FFUJ_13203							4.38	4.23	4.05	4.35
XLOC_007051	FFC1_06432	FFUJ_13194	probable 4-hydroxyphenylpyruvate dioxygenase			-1.50							-2.17
XLOC_006221	FFC1_06433	FFUJ_13193	uncharacterized protein FFUJ_13193										-2.48
XLOC_007052	FFC1_06434	FFUJ_14909	uncharacterized protein FFUJ_14909							-1.79	-2.08	-2.17	-1.83
XLOC_006226	FFC1_06444	FFUJ_13183	related to CYTOCHROME B561		2.98	1.18					1.89	2.86	2.25
XLOC_006227	FFC1_06445	FFUJ_13182	related to two-component histidine kinase chk-1		1.55					1.95	2.39	2.71	1.96
XLOC_007059	FFC1_06446	FFUJ_13181	uncharacterized protein FFUJ_13181							5.31	5.21	4.41	4.02
XLOC_006228	FFC1_06447	FFUJ_13180	related to DUF1168 domain protein							2.05	1.88	1.42	1.32
XLOC_006229	FFC1_06449	FFUJ_13178	uncharacterized protein FFUJ_13178							4.22	4.86	4.46	5.07
XLOC_007061	FFC1_06450	FFUJ_13177	uncharacterized protein FFUJ_13177							4.17	3.80	4.29	4.72
XLOC_007073	FFC1_06466	FFUJ_13161	related to YER185w, Rta1p		2.75	2.03						2.32	
XLOC_007074	FFC1_06467	FFUJ_13160	uncharacterized protein FFUJ_13160							2.11	1.57	1.37	1.68
XLOC_007080	FFC1_06476	FFUJ_13152	uncharacterized protein FFUJ_13152	1.66	2.83					1.83	2.92	4.06	1.94
XLOC_006241	FFC1_06481	FFUJ_13147	uncharacterized protein FFUJ_13147		1.16					2.91	3.12	4.04	2.51
XLOC_007084	FFC1_06484	FFUJ_13144	uncharacterized protein FFUJ_13144		1.69					2.22	2.17	4.40	3.67
XLOC_007085	FFC1_06487	FFUJ_13141	related to SGT1 protein		2.01							1.44	0.96
XLOC_006244	FFC1_06489	FFUJ_13139	related to meiotic recombination protein rec12							-2.06	-2.10	-3.21	-2.02
XLOC_007088	FFC1_06492	FFUJ_13136	related to regulatory protein amdA							-2.47	-2.21	-2.18	-2.18
XLOC_007089	FFC1_06493	FFUJ_13135	DUR1,2-Urea amidolyase								-2.66		
XLOC_007091	FFC1_06495	FFUJ_13133	related to Lactam utilization protein lamB							-1.83	-2.29	-2.55	
XLOC_006246	FFC1_06496	FFUJ_13132	uncharacterized protein FFUJ_13132							-2.14	-1.92	-2.86	-3.26
XLOC_006247	FFC1_06497	FFUJ_13131	uncharacterized protein FFUJ_13131							-2.07	-1.89	-2.11	-2.49
XLOC_007094	FFC1_06501	FFUJ_13127	related to carboxyphosphonoenolpyruvate phosphonomutase-like protein							2.20		3.59	2.41
XLOC_006249	FFC1_06502	FFUJ_13126	uncharacterized protein FFUJ_13126							1.15	1.33	2.26	1.44
XLOC_006250	FFC1_06503	FFUJ_13125	related to acetylhydrolase		1.48				1.35	3.37	3.89	4.26	2.58
XLOC_007095	FFC1_06504	FFUJ_13124	uncharacterized protein FFUJ_13124							4.42	5.91	7.12	5.01
XLOC_007096	FFC1_06505	FFUJ_13123	related to triacylglycerol lipase V precursor							5.09	3.92	6.68	7.04
XLOC_007098	FFC1_06507	FFUJ_13121	probable CYB2-lactate dehydrogenase cytochrome b2							-6.83	-5.80	-3.79	

XLOC_006251	FFC1_06509	FFUJ_13119	related to carboxylic acid transport protein JEN1							3.19	3.10	3.10	2.98
XLOC_006268	FFC1_06544	FFUJ_13087	related to nucleotide exsicion repair protein RAD7			0.83				1.68	1.79	2.16	1.24
XLOC_006269	FFC1_06547	FFUJ_13084	related to RBTMx2 protein			-2.04				4.40	2.84	1.99	
XLOC_007121	FFC1_06548	FFUJ_13083	uncharacterized protein FFUJ_13083							1.68	2.25		2.04
XLOC_006276	FFC1_06559	FFUJ_13072	related to FMN-dependent 2-nitropropane dioxygenase							2.83	3.04	2.56	
XLOC_006283	FFC1_06568	FFUJ_13064	uncharacterized protein FFUJ_13064							7.22	7.29	8.09	9.11
XLOC_006284	FFC1_06569	FFUJ_13063	related to nitrate assimilation regulatory protein nirA	-0.95	-1.34	-0.78				2.47	1.60	1.34	2.19
XLOC_006305	FFC1_06604	FFUJ_13029	uncharacterized protein FFUJ_13029							3.17	2.82	3.02	3.80
XLOC_007149	null										3.83		
XLOC_007150	FFC1_06623	FFUJ_13010	uncharacterized protein FFUJ_13010							7.74	6.22	6.56	7.19
XLOC_006321	FFC1_06626	FFUJ_13007	uncharacterized protein FFUJ_13007							4.20	5.95	7.30	7.51
XLOC_006329	FFC1_06639	FFUJ_13001	uncharacterized protein FFUJ_13001							-3.15	-3.08	-3.05	-2.70
XLOC_006330	FFC1_06640	FFUJ_13000	uncharacterized protein FFUJ_13000							-2.78	-2.53	-2.73	-4.36
XLOC_006334	FFC1_06645	FFUJ_12995	uncharacterized protein FFUJ_12995			1.50				-2.32	-2.89	-2.61	-1.25
XLOC_007159	FFC1_06646	FFUJ_14907	uncharacterized protein FFUJ_14907							-2.74	-4.36	-2.83	-2.63
XLOC_007161	FFC1_06648	FFUJ_12993	uncharacterized protein FFUJ_12993								-3.25	-3.84	
XLOC_007162	FFC1_06649	FFUJ_12992	uncharacterized protein FFUJ_12992							-1.53	-4.10	-4.69	-4.29
XLOC_006336	FFC1_06653	FFUJ_12988	uncharacterized protein FFUJ_12988	2.29	1.16	1.21				-0.81	1.17		
XLOC_006340	FFC1_06659	FFUJ_12982	related to SAM-dependent methyltransferases			2.66				-3.71	-2.79	-2.69	-1.43
XLOC_007167	FFC1_06660	FFUJ_12981	uncharacterized protein FFUJ_12981								-2.41	-1.64	
XLOC_006342	FFC1_06665	FFUJ_12976	related to Vault poly							2.00	1.97		
XLOC_006343	FFC1_06666	FFUJ_12975	related to nicotinamide mononucleotide permease			-1.31				2.59	2.88	3.06	3.10
XLOC_007176	FFC1_06679	FFUJ_12962	probable fumarylacetoacetate hydrolase							2.01			
XLOC_006352	FFC1_06681	FFUJ_12960	probable SERINE-TYPE CARBOXYPEPTIDASE F PRECURSOR							2.97	3.09	3.77	
XLOC_007178	FFC1_06685	FFUJ_12956	uncharacterized protein FFUJ_12956								-2.94		
XLOC_006363	FFC1_06702									2.08			
XLOC_007187	FFC1_06703					-4.57				5.90	6.96	5.27	
XLOC_006364	FFC1_06704									7.65	6.30	7.70	5.71
XLOC_007189	FFC1_06707										2.55	3.24	
XLOC_006367	FFC1_06709			1.07	0.90					2.90	2.91	2.90	
XLOC_007192	FFC1_06715									5.50	5.05	4.37	5.03
XLOC_007194	FFC1_06717										4.61	6.27	
XLOC_006371	FFC1_06719									2.20	2.11	1.85	
XLOC_006372	FFC1_06720									9.17	7.90	8.12	7.03
XLOC_007196	FFC1_06721	FFUJ_05323	uncharacterized protein FFUJ_05323							6.38	5.82	7.90	7.73
XLOC_007201	FFC1_06730									4.15		5.21	6.24
XLOC_006379	FFC1_06734									4.36			3.56
XLOC_007204	FFC1_06736									3.04	2.76	2.47	2.62
XLOC_006385	FFC1_06743									4.52			
XLOC_007206	FFC1_06744					-2.90							
XLOC_007208	FFC1_06747						2.32	2.95					-4.91
XLOC_006389	FFC1_06749									5.78	6.43	5.97	6.28
XLOC_006390	FFC1_06750				-1.12	-1.25				3.38	3.72	2.57	2.77
XLOC_007209	FFC1_06751					-1.93				7.38	7.27	5.27	6.47
XLOC_007210	FFC1_06752									1.87			2.62
XLOC_006391	FFC1_06753									5.34	4.65	4.11	5.25
XLOC_007212	FFC1_06756									6.56	5.63	5.69	7.22
XLOC_007213	FFC1_06757									3.51	3.45	3.57	
XLOC_007214	FFC1_06758									5.20			
XLOC_006393	FFC1_06759												5.98
XLOC_007215	FFC1_06760									6.44	6.79	6.65	5.77
XLOC_007216	FFC1_06761									3.50	3.28	3.41	
XLOC_007218	FFC1_06764									-1.76	-1.40	-1.62	-2.42
XLOC_007221	FFC1_06772					-1.68				8.33	7.50	6.96	4.73
XLOC_007222	FFC1_06773					-1.13				3.70	4.07	3.89	2.62
XLOC_006400	FFC1_06774					-2.53				4.94	3.80	4.45	1.94
XLOC_007223	FFC1_06778					-5.33				5.81			
XLOC_006406	FFC1_06781									-5.36	-7.60	-7.35	
XLOC_007226	FFC1_06785									-6.93	-7.88	-6.97	
XLOC_006417	FFC1_06800									-3.73	-2.45	-2.40	-4.08
XLOC_006418	FFC1_06802									-3.55	-7.21		-2.96
XLOC_006421	FFC1_06807										-2.84	-3.54	
XLOC_006422	FFC1_06808									-2.57	-4.67	-2.91	
XLOC_007236	FFC1_06810										4.91	5.32	
XLOC_006423	FFC1_06811										4.33	3.28	
XLOC_007952	FFC1_06820	FFUJ_02437	uncharacterized protein FFUJ_02437							2.68	2.42		2.29
XLOC_007241	FFC1_06821	FFUJ_02438	uncharacterized protein FFUJ_02438							6.84	3.97	3.32	5.09
XLOC_007955	FFC1_06826	FFUJ_02443	uncharacterized protein FFUJ_02443		-1.09						-1.48	-2.00	-1.00
XLOC_007255	FFC1_06850	FFUJ_02467	probable cyanate lyase							-1.54	-2.63	-2.16	-1.87
XLOC_007969	FFC1_06855	FFUJ_02472	uncharacterized protein FFUJ_02472							4.00	3.61	4.82	5.74
XLOC_007970	null									-2.65	-6.80	-4.18	
XLOC_007977	FFC1_06868	FFUJ_02485	uncharacterized protein FFUJ_02485							-1.56	-2.22	-2.24	-2.52
XLOC_007270	FFC1_06878	FFUJ_02493	uncharacterized protein FFUJ_02493	0.65	0.80						1.41	2.02	1.33
XLOC_007983	FFC1_06879	FFUJ_02494	related to FK506 suppressor Sfk1	1.02	1.77	1.00				2.51	3.26	3.90	3.49
XLOC_007986	FFC1_06883	FFUJ_02498	probable aspartate kinase							-2.55	-2.50	-2.15	
XLOC_007991	FFC1_06890	FFUJ_02504	related to SRP40-suppressor of mutant AC40 of RNA polymerase I and III							2.88	3.23	2.92	1.56
XLOC_008004	FFC1_06907	FFUJ_02521	related to GNT1 alphaN-acetylglucosamine transferase K. lactis		-2.35	-1.61				-0.95	-1.93	-3.09	-1.92
XLOC_007283	FFC1_06909	FFUJ_02523	related to glutamic acid decarboxylase							-2.24	-3.48	-2.40	-1.85
XLOC_007284	FFC1_06910	FFUJ_02524	related to glutamic acid decarboxylase		3.05					-2.66	-2.24		
XLOC_008005	FFC1_06911	FFUJ_02525	uncharacterized protein FFUJ_02525							-2.07			
XLOC_008006	FFC1_06912	FFUJ_02526	uncharacterized protein FFUJ_02526								-1.65	-2.48	

XLOC_007287	FFC1_06918	FFUJ_02532	uncharacterized protein FFUJ_02532							2.07	1.40	1.29	
XLOC_007295	FFC1_06930	FFUJ_02544	related to calcium-independent phospholipase A2										-2.98
XLOC_007302	FFC1_06941	FFUJ_02554	related to nitrate assimilation regulatory protein nirA							-1.65	-1.37	-2.31	-1.90
XLOC_008025	FFC1_06945	FFUJ_02558	uncharacterized protein FFUJ_02558							-1.50	-2.65	-1.70	-1.58
XLOC_007307	FFC1_06950	FFUJ_02563	probable alkaline phosphatase							-3.88	-3.36	-3.09	-3.32
XLOC_008028	FFC1_06951	FFUJ_02564	uncharacterized protein FFUJ_02564							-2.01	-2.54	-2.52	-2.69
XLOC_007308	FFC1_06952	FFUJ_02565	related to phosphatase 2a inhibitor							-2.26		-1.88	
XLOC_007309	FFC1_06953	FFUJ_02566	uncharacterized protein FFUJ_02566							3.01	2.87	3.00	3.34
XLOC_008031	FFC1_06958	FFUJ_02571	related to hsp70 protein							-1.34	-2.38	-1.88	
XLOC_008036	FFC1_06967	FFUJ_02582	probable succinate dehydrogenase (ubiquinone) flavoprotein precursor, mitochondrial		2.28	1.14					0.90	2.14	1.55
XLOC_008039	null										2.77		
XLOC_008042	FFC1_06972	FFUJ_02587	uncharacterized protein FFUJ_02587		1.55	1.10					1.00	2.32	1.86
XLOC_008043	FFC1_06973	FFUJ_02588	uncharacterized protein FFUJ_02588		1.67					3.11	2.88	3.79	3.06
XLOC_008044	null				1.85					2.58	2.44	3.31	2.63
XLOC_008045	FFC1_06974	FFUJ_02589	uncharacterized protein FFUJ_02589		1.64					3.20	3.05	3.83	3.26
XLOC_008046	null				1.85					2.59	2.43	3.45	2.70
XLOC_008047	null				1.68					3.23	3.06	3.90	3.52
XLOC_007320	FFC1_06975									-2.69	-2.74	-2.91	-1.73
XLOC_007331	FFC1_06993	FFUJ_02606	related to finger protein AZF1	2.10	2.58	1.89				-2.09	0.65		
XLOC_008056	null										-2.43		
XLOC_007334	FFC1_06999	FFUJ_02612	probable FES1-Hsp70 nucleotide exchange factor							3.03	2.59	3.49	3.27
XLOC_007337	null											-3.06	
XLOC_007343	FFC1_07011	FFUJ_02622	related to TFIID and SAGA subunit TAF61							3.40	3.36	3.36	2.57
XLOC_008074	FFC1_07031	FFUJ_02642	related to exo-alpha-sialidase / neuraminidase	-1.90	-2.03	-1.83				2.22			
XLOC_007359	FFC1_07036	FFUJ_02647	related to exo-alpha-sialidase / neuraminidase							2.43	2.65	2.18	1.81
XLOC_007361	null											-1.64	-2.98
XLOC_007362	FFC1_07044	FFUJ_02655	related to flavin-containing monooxygenase							-2.55	-2.81	-2.79	-2.04
XLOC_007370	null									2.32			
XLOC_007372	FFC1_07059	FFUJ_02669	probable glutamate dehydrogenase (NADP+)		-2.43					-1.24	-3.03	-3.91	-2.19
XLOC_007381	FFC1_07074	FFUJ_02682	uncharacterized protein FFUJ_02682							2.35	2.57	2.01	1.73
XLOC_008095	FFC1_07077	FFUJ_02685	related to acid phosphatase			-1.18				4.37	3.98	3.09	2.98
XLOC_007384	FFC1_07083	FFUJ_02691	probable glucose repressible protein Grg1		2.64					6.05	7.15	8.57	5.59
XLOC_008108	FFC1_07104	FFUJ_02709	related to monocarboxylate transporter 4	1.49						-4.63	-2.72	-3.86	-4.25
XLOC_007410	FFC1_07126	FFUJ_02729	related to nonhistone chromosomal protein							1.99	2.24	2.12	1.46
XLOC_008130	FFC1_07142	FFUJ_02744	uncharacterized protein FFUJ_02744								3.12	4.10	3.32
XLOC_008134	FFC1_07148	FFUJ_02750	uncharacterized protein FFUJ_02750			-1.48				-2.52	-2.30	-3.46	-4.53
XLOC_008141	null									-3.15	-2.54	-2.26	
XLOC_007429	FFC1_07172	FFUJ_02770	related to triacylglycerol lipase II precursor		-2.01	-2.42					1.26		
XLOC_007435	FFC1_07184	FFUJ_02780	uncharacterized protein FFUJ_02780							2.15	1.99	1.97	
XLOC_008160	FFC1_07188	FFUJ_02784	uncharacterized protein FFUJ_02784		-1.20	-1.11				2.91	2.76	1.34	
XLOC_007438	FFC1_07190	FFUJ_02785	related to C6 zink-finger protein PRO1A		-1.68	-1.46				2.83	2.31		1.11
XLOC_007440	FFC1_07193	FFUJ_02788	uncharacterized protein FFUJ_02788							2.64	2.52	2.34	1.71
XLOC_008163	FFC1_07194	FFUJ_02789	uncharacterized protein FFUJ_02789							2.65	2.40	2.13	1.70
XLOC_008165	FFC1_07200	FFUJ_02795	related to C.elegans ZK688.3 protein and E.coli hpcEp							-1.65	-1.73	-2.01	
XLOC_008167	null									4.26			
XLOC_008177	FFC1_07221	FFUJ_02814	uncharacterized protein FFUJ_02814	3.28	1.99					1.09	4.54	2.82	1.76
XLOC_007457	null									-5.65	-5.65		
XLOC_007458	FFC1_07223	FFUJ_02816	uncharacterized protein FFUJ_02816							-2.53	-2.52	-2.55	
XLOC_007461	FFC1_07226	FFUJ_02819	uncharacterized protein FFUJ_02819							0.90	0.96	1.84	2.12
XLOC_008181	FFC1_07229	FFUJ_02822	related to MYND domain protein		1.62					1.59	1.20	2.36	1.73
XLOC_007470	FFC1_07246	FFUJ_02838	probable DFG5 protein		-0.85	-1.00				2.80	2.66	2.50	3.05
XLOC_008193	FFC1_07247	FFUJ_02839	uncharacterized protein FFUJ_02839							2.27	2.31	1.77	3.17
XLOC_007475	FFC1_07257	FFUJ_02849	uncharacterized protein FFUJ_02849							3.01	3.06	2.30	
XLOC_008203	FFC1_07263	FFUJ_02854	related to PET127		1.02					1.99	1.95	2.73	2.65
XLOC_007486	FFC1_07273	FFUJ_02864	related to regulatory protein for the arginine catabolic pathway							-1.30	-2.61	-1.81	
XLOC_008208	FFC1_07280	FFUJ_02871	uncharacterized protein FFUJ_02871							-1.46	-2.28	-2.56	
XLOC_008214	null									3.07			
XLOC_007495	FFC1_07289	FFUJ_02880	related to HUT1-weak similarity to human UDP-galactose transporter related isozyme 1							3.95	3.84	3.38	3.41
XLOC_008221	FFC1_07302	FFUJ_02890	uncharacterized protein FFUJ_02890							-1.26	-2.36	-1.79	-1.72
XLOC_007502	FFC1_07303	FFUJ_02891	related to transcription initiation factor	-1.11						-0.86	-1.90	-1.48	-2.03
XLOC_007511	FFC1_07315	FFUJ_02903	probable glycine--tRNA ligase GRS1							-2.01	-1.66	-1.68	-1.24
XLOC_008232	FFC1_07325	FFUJ_02913	probable alpha-aminoadipate reductase large subunit							-2.12	-1.79	-1.50	
XLOC_007518	FFC1_07329	FFUJ_02917	uncharacterized protein FFUJ_02917							2.88	2.31	2.23	2.05
XLOC_008239	FFC1_07339	FFUJ_02926	uncharacterized protein FFUJ_02926							-1.02	-1.09	-1.46	-2.12
XLOC_008240	null									-1.49	-1.31	-1.89	-2.50
XLOC_008241	null										-2.45	-3.29	-3.27
XLOC_007531	FFC1_07350	FFUJ_02936	uncharacterized protein FFUJ_02936							1.84		2.06	
XLOC_008251	null									-7.35	-3.75	-6.14	-3.12
XLOC_008262	FFC1_07377	FFUJ_02965	uncharacterized protein FFUJ_02965							-1.76	-1.82	-2.21	-1.89
XLOC_008263	FFC1_07378	FFUJ_02966	uncharacterized protein FFUJ_02966							-1.66	-1.53	-1.86	-2.09
XLOC_008265	FFC1_07383	FFUJ_02971	related to fatty acid elongation protein	1.65	1.07					-4.13	-2.43	-3.26	-3.94
XLOC_008270	FFC1_07390	FFUJ_02978	uncharacterized protein FFUJ_02978										2.53
XLOC_007554	FFC1_07395	FFUJ_02983	related to QRI7-similarity to H.influenzae sialoglycoprotease (gcp)							-1.80	-1.95	-2.22	-1.53

XLOC_007555	FFC1_07398	FFUJ_02986	uncharacterized protein FFUJ_02986		-1.51						-1.63	-2.14	
XLOC_008278	FFC1_07400	FFUJ_02988	uncharacterized protein FFUJ_02988							3.05	3.35	2.47	4.08
XLOC_007562	null										-4.61		
XLOC_008288	FFC1_07420	FFUJ_03003	probable pyridoxine 4-dehydrogenase							-1.91			-2.00
XLOC_008293	FFC1_07434	FFUJ_03018	uncharacterized protein FFUJ_03018		1.11					2.43	2.08	2.68	2.19
XLOC_007580	FFC1_07436	FFUJ_03019	uncharacterized protein FFUJ_03019		1.37					1.74	1.95	2.96	2.84
XLOC_007581	FFC1_07438	FFUJ_03021	probable valine--tRNA ligase							-2.06	-1.83	-1.60	-1.21
XLOC_007586	FFC1_07447	FFUJ_03030	uncharacterized protein FFUJ_03030							4.34	4.40	4.02	3.87
XLOC_007598	null									6.12	6.19		3.53
XLOC_008306	FFC1_07464	FFUJ_03046	probable YDJ1-mitochondrial and ER import protein						1.80	3.72	3.04	2.56	2.73
XLOC_007599	FFC1_07465	FFUJ_03047	uncharacterized protein FFUJ_03047							3.24	2.81	3.10	2.68
XLOC_008309	null										-3.66		
XLOC_007616	FFC1_07496	FFUJ_03073	uncharacterized protein FFUJ_03073							2.93			2.11
XLOC_007618	FFC1_07498	FFUJ_03075	probable RIC1 protein							2.42	2.36	2.60	2.66
XLOC_008332	FFC1_07513	FFUJ_03089	uncharacterized protein FFUJ_03089							3.58	2.86	3.66	3.77
XLOC_008334	null									4.34		6.56	
XLOC_008337	FFC1_07519	FFUJ_03094	uncharacterized protein FFUJ_03094							1.85	2.01	1.65	1.52
XLOC_007631	FFC1_07528	FFUJ_03105	related to deoxyribodipyrimidine photo-lyase PHR		2.21	1.64						2.44	1.90
XLOC_007633	null											-2.26	-2.08
XLOC_008349	FFC1_07535	FFUJ_03113	uncharacterized protein FFUJ_03113							-2.96	-3.19	-2.61	-2.44
XLOC_008351	FFC1_07544	FFUJ_03122	probable UGA2-succinate semialdehyde dehydrogenase								3.11	1.46	
XLOC_007644	FFC1_07545	FFUJ_03123	probable UGA1-4-aminobutyrate aminotransferase (GABA transaminase)								2.28		
XLOC_008372	FFC1_07580	FFUJ_03157	uncharacterized protein FFUJ_03157									3.07	
XLOC_008374	FFC1_07582	FFUJ_03159	uncharacterized protein FFUJ_03159	0.99	1.60						2.15	2.55	
XLOC_008377	FFC1_07584									4.81			
XLOC_007664	FFC1_07588	FFUJ_03164	probable peptidyl-prolyl cis-trans isomerase nima-interacting 4		-1.01					-2.01	-2.19	-2.76	-1.71
XLOC_007677	FFC1_07608	FFUJ_03184	related to AMP-binding protein							2.30		1.69	
XLOC_007678	FFC1_07610	FFUJ_03186	uncharacterized protein FFUJ_03186		1.60					1.73	1.63	2.19	1.74
XLOC_007681	FFC1_07615	FFUJ_03191	uncharacterized protein FFUJ_03191							1.82	1.55	2.24	
XLOC_008394	FFC1_07623	FFUJ_03199	related to mitochondrial cytosolically directed NADH dehydrogenase								-1.32		-2.28
XLOC_008395	FFC1_07624	FFUJ_03200	related to UTP10-U3 snoRNP protein	2.20	1.26					-1.28			
XLOC_008428	FFC1_07674	FFUJ_03249	uncharacterized protein FFUJ_03249							4.66			
XLOC_008434	FFC1_07680	FFUJ_03255	uncharacterized protein FFUJ_03255							5.55	5.48	5.96	6.03
XLOC_008442	FFC1_07691	FFUJ_03265	uncharacterized protein FFUJ_03265							5.23	4.48	4.60	
XLOC_008443	FFC1_07693	FFUJ_03267	related to DUF1295 domain protein		2.54	0.93				-0.66		1.90	
XLOC_007717	FFC1_07694	FFUJ_03268	related to DNA topoisomerase III							2.16	2.11	1.93	1.15
XLOC_008444	null									-2.91		-4.32	
XLOC_007733	FFC1_07717	FFUJ_03290	uncharacterized protein FFUJ_03290							2.11	1.43	1.04	1.91
XLOC_008455	FFC1_07719	FFUJ_03292	probable DDR48-heat shock protein									-2.34	
XLOC_007742	FFC1_07730	FFUJ_03303	probable esterase D							-1.86	-2.72	-2.87	-1.96
XLOC_008467	FFC1_07742	FFUJ_03315	uncharacterized protein FFUJ_03315		1.75					1.58	1.87	3.28	2.44
XLOC_008470	FFC1_07747	FFUJ_03320	uncharacterized protein FFUJ_03320							4.00	3.52	3.66	3.79
XLOC_008471	null									6.51	6.36	5.30	
XLOC_007754	FFC1_07759	FFUJ_03331	related to YER185w, Rta1p									-2.89	
XLOC_008485	FFC1_07770	FFUJ_03339	uncharacterized protein FFUJ_03339									3.81	3.55
XLOC_008487	FFC1_07772	FFUJ_03341	uncharacterized protein FFUJ_03341		1.08					0.92		2.11	1.71
XLOC_007760	FFC1_07775	FFUJ_03344	probable lipase 5							2.01	1.63	2.06	1.93
XLOC_008500	FFC1_07789	FFUJ_03357	uncharacterized protein FFUJ_03357									4.34	3.02
XLOC_008501	null				-4.34								
XLOC_008503	FFC1_07791	FFUJ_03359	probable actin cytoskeleton organization and biogenesis							1.92	1.87	2.00	1.47
XLOC_008504	null									1.50		2.34	
XLOC_007766	FFC1_07793	FFUJ_03361	uncharacterized protein FFUJ_03361		2.94					4.35	4.32	8.18	3.53
XLOC_008509	FFC1_07803	FFUJ_03371	related to cycloeucalenol cycloisomerase							3.06	3.15	4.04	3.03
XLOC_007773	FFC1_07804	FFUJ_03372	uncharacterized protein FFUJ_03372							2.01	1.33	1.88	
XLOC_008510	FFC1_07805	FFUJ_03373	related to multidrug resistant protein										5.23
XLOC_008511	FFC1_07807	FFUJ_03375	uncharacterized protein FFUJ_03375							6.69	6.92	6.31	6.32
XLOC_008513	FFC1_07809	FFUJ_03377	uncharacterized protein FFUJ_03377							-3.57	-4.08		
XLOC_008514	FFC1_07810	FFUJ_03378	related to alcohol dehydrogenase		-0.98					-1.48	-2.31	-2.96	-2.27
XLOC_007778	FFC1_07815	FFUJ_03383	uncharacterized protein FFUJ_03383			-3.30				6.31			
XLOC_007779	FFC1_07816	FFUJ_03384	related to SCS3 Inositol phospholipid synthesis protein							2.25	2.12	3.00	3.18
XLOC_008516	FFC1_07817	FFUJ_03385	related to amidohydrolase AmhX							7.52	6.77	6.78	
XLOC_008520	FFC1_07822	FFUJ_03390	related to TOB3 (member of AAA-ATPase family)			-1.30				2.18	1.87	2.12	1.58
XLOC_008523	FFC1_07826										1.47	2.08	1.83
XLOC_007786	FFC1_07832	FFUJ_03399	probable beta-glucosidase			-2.37							-3.52
XLOC_007788	FFC1_07834	FFUJ_03401	uncharacterized protein FFUJ_03401							-1.82	-2.14	-2.62	
XLOC_007789	FFC1_07836	FFUJ_03402	uncharacterized protein FFUJ_03402							2.37	2.05	1.37	
XLOC_007790	FFC1_07838	FFUJ_03404	related to alcohol dehydrogenase I-ADH1		2.04					1.97	2.23	2.54	
XLOC_008528	FFC1_07839	FFUJ_03405	uncharacterized protein FFUJ_03405									4.79	
XLOC_008529	FFC1_07840	FFUJ_03406	uncharacterized protein FFUJ_03406		3.04					4.68	3.24	5.19	3.33
XLOC_007791	FFC1_07841				3.94							7.03	
XLOC_007792	FFC1_07842	FFUJ_03407	related to CTA1-catalase A, peroxisomal									4.85	
XLOC_007793	FFC1_07843	FFUJ_03408	probable gibberellin biosynthesis-related	2.56	5.27	4.18					3.28	5.93	3.25
XLOC_008530	FFC1_07844	FFUJ_03409	uncharacterized protein FFUJ_03409		1.27	1.41				-1.89	-2.08		
XLOC_007796	null										5.90		-2.65
XLOC_008535	FFC1_07854	FFUJ_03418	uncharacterized protein FFUJ_03418		3.96							3.73	
XLOC_008538	null									2.36	2.40	2.02	2.31
XLOC_007807	FFC1_07860	FFUJ_03424	probable acetyl-CoA carboxylase	1.31						-1.88	-1.24	-1.60	-2.26
XLOC_008540	FFC1_07864	FFUJ_03428	uncharacterized protein FFUJ_03428							-1.82	-1.73	-2.00	-2.26
XLOC_008543	FFC1_07869	FFUJ_03433	probable arginyl-tRNA synthetase, cytosolic							-2.33	-1.43	-1.52	

XLOC_007814	FFC1_07873	FFUJ_03437	related to TWF1-twinfilin, an actin monomer sequestering protein									-2.01	
XLOC_008552	FFC1_07887	FFUJ_03451	probable catalase-1	2.22	3.55					3.05	5.37	6.40	4.54
XLOC_007821	FFC1_07888	FFUJ_03452	related to xylulose-5-phosphate/fructose-6-phosphate phosphoketolase	2.49	4.14	1.84				4.64	5.82	7.36	6.19
XLOC_008554	FFC1_07890	FFUJ_03454	related to NDP-N-acetyl-D-galactosaminuronic acid dehydrogenase										5.03
XLOC_007822	FFC1_07891	FFUJ_03455	related to chitin binding protein			2.24							3.32
XLOC_007825	FFC1_07894	FFUJ_03458	related to GABA permease		-5.64								
XLOC_008555	FFC1_07895	FFUJ_03459	related to TOB3 (member of AAA-ATPase family)							3.75	3.65	3.60	
XLOC_007826	FFC1_07896	FFUJ_03460	uncharacterized protein FFUJ_03460							6.95	5.38	3.58	
XLOC_007829	FFC1_07899	FFUJ_03462	uncharacterized protein FFUJ_03462							-4.97			
XLOC_008556	FFC1_07902	FFUJ_03465	related to aminopeptidase Y precursor, vacuolar							3.42	4.71	4.55	
XLOC_008558	null										-3.83		
XLOC_007834	FFC1_07906	FFUJ_03469	related to integral membrane protein PTH11		2.01	1.77						2.85	
XLOC_008559	FFC1_07907	FFUJ_03470	uncharacterized protein FFUJ_03470		0.92					2.38	2.68	2.92	1.71
XLOC_007835	FFC1_07908			1.10	1.22					4.06	4.52	4.60	3.51
XLOC_007836	FFC1_07909	FFUJ_03471	related to ACB 4-hydroxyacetophenone monooxygenase	1.17	1.33					4.00	4.55	4.59	3.55
XLOC_008560	FFC1_07911	FFUJ_03473	related to fructosyl amino acid oxidase		-1.15					7.70	7.27	7.54	7.00
XLOC_007838	FFC1_07912	FFUJ_03474	uncharacterized protein FFUJ_03474							2.28	2.05	2.04	1.76
XLOC_007839	FFC1_07914	FFUJ_03476	uncharacterized protein FFUJ_03476									2.30	3.34
XLOC_007842	FFC1_07919	FFUJ_03481	related to flavin oxidoreductase	1.76	2.67	2.03				1.37	2.69	3.34	2.31
XLOC_008567	FFC1_07924	FFUJ_03486	related to anthranilate synthase component							-2.25	-1.90	-1.87	
XLOC_007844	FFC1_07925	FFUJ_03487	uncharacterized protein FFUJ_03487							2.05	1.79	1.38	1.19
XLOC_008568	FFC1_07926	FFUJ_03488	uncharacterized protein FFUJ_03488							5.19	5.07	4.79	3.87
XLOC_008569	FFC1_07927	FFUJ_03489	uncharacterized protein FFUJ_03489								5.48		5.77
XLOC_007845	FFC1_07928	FFUJ_03490	uncharacterized protein FFUJ_03490							-5.51			-2.67
XLOC_008570	FFC1_07929	FFUJ_03491	uncharacterized protein FFUJ_03491							-1.71	-2.93	-2.59	-1.92
XLOC_007846	FFC1_07930	FFUJ_03492	uncharacterized protein FFUJ_03492									-4.00	
XLOC_007847	FFC1_07931	FFUJ_03493	related to thioesterase superfamily member 2								-1.94	-2.25	
XLOC_008571	FFC1_07932	FFUJ_03494	related to malate dehydrogenase							-1.34	-2.10	-2.03	-0.97
XLOC_007849	FFC1_07935	FFUJ_03497	related to short-chain alcohol dehydrogenase							-3.81	-3.73	-5.01	-2.33
XLOC_007853	FFC1_07939	FFUJ_03501	related to calpain-like protein			-1.05			1.11			-1.13	-2.43
XLOC_008573	FFC1_07941	FFUJ_03503	uncharacterized protein FFUJ_03503								5.63	4.91	5.47
XLOC_008574	FFC1_07942	FFUJ_03504	related to methyltransferase							1.72	2.00	2.72	2.37
XLOC_008575	FFC1_07943	FFUJ_03505	uncharacterized protein FFUJ_03505			-1.55				2.07	1.88	1.26	
XLOC_008576	FFC1_07944	FFUJ_03506	related to alpha-aminoadipate reductase large subunit		-0.67					-1.37	-1.29	-2.22	-1.56
XLOC_007858	FFC1_07952	FFUJ_03514	uncharacterized protein FFUJ_03514							4.19	4.56	4.48	2.69
XLOC_007860	FFC1_07954	FFUJ_03516	uncharacterized protein FFUJ_03516							2.79	2.66	2.90	3.49
XLOC_008583	FFC1_07959	FFUJ_03521	related to GIP2 Glc7p-interacting protein							2.73	2.33	2.25	2.02
XLOC_008584	null									2.48	2.20	2.02	1.86
XLOC_008585	null									2.47	1.81		
XLOC_008586	FFC1_07960	FFUJ_03522	uncharacterized protein FFUJ_03522							4.61	5.66	7.13	
XLOC_008593	FFC1_07969	FFUJ_03530	related to AAH1-adenosine deaminase							-2.75	-2.60	-2.04	-2.32
XLOC_008598	FFC1_07974	FFUJ_03535	related to pisatin demethylase cytochrome P450							4.17			
XLOC_008602	FFC1_07980	FFUJ_03541	Weak similarity to Y.pseudotuberculosis CDP-3,6-dideoxy-D-glycero-L-glycero-4-hexulose-5-epimerase							-1.74	-2.39	-1.91	-1.20
XLOC_007868	FFC1_07982	FFUJ_03543	uncharacterized protein FFUJ_03543							-1.93	-2.16	-2.14	-2.35
XLOC_007869	FFC1_07986	FFUJ_03547	uncharacterized protein FFUJ_03547							5.27	2.83	4.09	
XLOC_007870	FFC1_07987	FFUJ_03548	uncharacterized protein FFUJ_03548							-2.66	-2.84	-2.63	-2.96
XLOC_008606	FFC1_07989	FFUJ_03550	uncharacterized protein FFUJ_03550								-2.03		
XLOC_007874	FFC1_07994	FFUJ_03555	uncharacterized protein FFUJ_03555								2.71	1.72	
XLOC_007875	FFC1_07995	FFUJ_03556	related to haloacetate dehalogenase H-1		3.00							7.00	5.81
XLOC_008616	FFC1_08005	FFUJ_03566	probable pectin lyase precursor								-3.96		
XLOC_007880	FFC1_08008	FFUJ_03570	uncharacterized protein FFUJ_03570								-2.10		
XLOC_007884	FFC1_08012	FFUJ_03574	uncharacterized protein FFUJ_03574		3.56	2.47						3.70	
XLOC_008618	FFC1_08015	FFUJ_03576	related to short-chain alcohol dehydrogenase							6.41	4.71	4.86	
XLOC_007890	FFC1_08023	FFUJ_03586	uncharacterized protein FFUJ_03586		2.41							3.50	2.02
XLOC_008628	FFC1_08031	FFUJ_03593	uncharacterized protein FFUJ_03593							2.55			
XLOC_007894	FFC1_08036	FFUJ_03596	probable L-lactate dehydrogenase (cytochrome)							5.15			
XLOC_007895	FFC1_08037										-4.49		
XLOC_008632	FFC1_08038	FFUJ_03598	related to allantoate transport protein								3.82	5.03	
XLOC_007896	FFC1_08039	FFUJ_03599	related to N-carbamoyl-L-amino acid hydrolase								4.01	4.60	
XLOC_007899	FFC1_08042	FFUJ_03602	related to coenzyme a synthetase							4.03	4.33	3.85	4.84
XLOC_007900	FFC1_08043	FFUJ_03603	uncharacterized protein FFUJ_03603							-2.64		-1.99	-2.22
XLOC_008633	FFC1_08046	FFUJ_03606	related to YPC1-alkaline ceramidase							-3.28	-5.35		
XLOC_008636	FFC1_08050	FFUJ_03610	uncharacterized protein FFUJ_03610							4.39	5.44	5.73	4.88
XLOC_007904	FFC1_08051	FFUJ_03611	uncharacterized protein FFUJ_03611							3.03	4.18	4.01	4.67
XLOC_008637	FFC1_08052	FFUJ_03612	uncharacterized protein FFUJ_03612							-7.45	-7.48	-6.96	-6.09
XLOC_007905	FFC1_08053	FFUJ_03613	uncharacterized protein FFUJ_03613							-9.65	-8.73	-8.31	-8.18
XLOC_008639	FFC1_08057									-3.75	-4.32	-5.17	-4.96
XLOC_007908	FFC1_08058	FFUJ_03617	uncharacterized protein FFUJ_03617							-2.70	-3.18	-2.46	-2.92
XLOC_008640	FFC1_08059	FFUJ_03618	related to beta-glucosidase								-2.40		
XLOC_007909	FFC1_08060	FFUJ_03619	related to hexose transporter protein							-3.85	-4.30	-3.87	-3.68
XLOC_008641	FFC1_08061	FFUJ_03620	uncharacterized protein FFUJ_03620		-1.60				-1.45	-2.68	-3.30	-3.66	-1.75
XLOC_007910	FFC1_08062	FFUJ_03621	uncharacterized protein FFUJ_03621							-3.27	-3.22	-4.09	-1.73
XLOC_008647	FFC1_08075	FFUJ_03634	uncharacterized protein FFUJ_03634							6.62	3.59		4.13

XLOC_008650	FFC1_08079	FFUJ_03638	related to NAM7-nonsense-mediated mRNA decay protein (RdRP)		0.76					4.84	4.29	4.82	4.58
XLOC_008652	FFC1_08084	FFUJ_03644	uncharacterized protein FFUJ_03644		-1.78					-3.22	-3.21	-4.39	-2.84
XLOC_007922	FFC1_08085	FFUJ_03645	related to tripeptidyl-peptidase I							-4.17	-5.22	-7.55	-4.26
XLOC_007923	FFC1_08086	FFUJ_03646	uncharacterized protein FFUJ_03646		1.19	2.04				6.44	6.31	7.54	10.81
XLOC_007924	FFC1_08087	FFUJ_03647	uncharacterized protein FFUJ_03647							7.69	5.57	5.68	7.56
XLOC_008655	FFC1_08093	FFUJ_03653	uncharacterized protein FFUJ_03653							5.41		5.04	
XLOC_008656	FFC1_08095	FFUJ_03655	probable phosphate transport protein MIR1							-2.18	-2.50	-2.09	-1.88
XLOC_007929	FFC1_08096	FFUJ_03656	related to aspartic-type signal peptidase		-1.94					-2.53	-3.28	-3.94	-1.80
XLOC_008657	FFC1_08097	FFUJ_03657	uncharacterized protein FFUJ_03657	-1.48	-2.26	-1.79				-0.90	-2.19	-2.54	-2.23
XLOC_008659	FFC1_08101	FFUJ_03660	related to pathway-specific regulatory protein nit-4							-3.67	-5.95	-5.09	-4.21
XLOC_007933	FFC1_08103	FFUJ_14419	related to beta-mannosidase							5.12	5.34	2.86	2.26
XLOC_007934	FFC1_08104	FFUJ_03662	related to tol protein							4.43			
XLOC_007935	FFC1_08106	FFUJ_03663	uncharacterized protein FFUJ_03663							-5.12	-2.60	-5.49	
XLOC_008666	FFC1_08114	FFUJ_03671	probable glucokinase							-5.22		-5.15	-3.25
XLOC_007938	FFC1_08115	FFUJ_03672	uncharacterized protein FFUJ_03672							-3.05	-3.20	-3.51	-3.25
XLOC_008668	FFC1_08117	FFUJ_03674	related to OrfH, unknown gene in trichothecene gene cluster	1.89	2.47						3.24	3.50	2.67
XLOC_007939	FFC1_08118	FFUJ_03675	related to hexose transporter protein		2.66						1.68	2.39	
XLOC_007940	FFC1_08119	FFUJ_03676	related to beta-galactosidase	1.38	1.38					2.75	3.61	3.46	2.56
XLOC_008669	FFC1_08120	FFUJ_03677	GPM1-Phosphoglycerate mutase							4.10	4.12	4.39	3.97
XLOC_008670	FFC1_08121	FFUJ_03678	related to ATP adenylyltransferase II							4.81	4.71	4.47	4.31
XLOC_008671	FFC1_08122	FFUJ_03679	PTR2-Di-and tripeptide permease							6.33	5.05	7.19	5.21
XLOC_007941	FFC1_08123	FFUJ_03680	uncharacterized protein FFUJ_03680							5.27	4.76	5.57	5.63
XLOC_007946	FFC1_08129	FFUJ_03685	related to non-ribosomal peptide synthetase								5.22		
XLOC_008678	FFC1_08137	FFUJ_03693	related to aldehyde dehydrogenase		-1.88					2.91	1.88		2.38
XLOC_007950	FFC1_08151				-4.59					6.24			
XLOC_008693	FFC1_08156	FFUJ_10202	related to 2,4-dihydroxyhept-2-ene-1,7-dioic acid aldolase									-4.40	
XLOC_008694	FFC1_08157	FFUJ_10201	uncharacterized protein FFUJ_10201							-2.08	-3.35	-2.34	-1.51
XLOC_008695	FFC1_08158	FFUJ_10200	related to ARO8-aromatic amino acid aminotransferase I							-5.00	-4.77	-7.84	-6.70
XLOC_008696	FFC1_08160	FFUJ_10198	related to salicylate hydroxylase									4.41	
XLOC_009217	FFC1_08162	FFUJ_10196	related to synaptic vesicle transporter SV2 (major facilitator superfamily)							5.21			
XLOC_009218	FFC1_08163	FFUJ_10195	related to phenol 2-monooxygenase									-2.68	
XLOC_009222	FFC1_08169	FFUJ_10189	related to gibberellin 20-oxidase								-2.85	-2.57	
XLOC_009224	FFC1_08173	FFUJ_10185	uncharacterized protein FFUJ_10185							7.72	8.58	7.64	6.61
XLOC_008701	FFC1_08174	FFUJ_10184	uncharacterized protein FFUJ_10184							7.88	8.19	8.59	8.05
XLOC_008702	FFC1_08175									3.53	3.33	3.23	3.04
XLOC_008703	FFC1_08176	FFUJ_10183	related to pisatin demethylase cytochrome P450							5.94	5.33		
XLOC_008704	FFC1_08178	FFUJ_10181	uncharacterized protein FFUJ_10181		-2.32					2.51			
XLOC_009226	FFC1_08179	FFUJ_10180	related to antibiotic resistance protein							8.52	7.15	7.82	7.76
XLOC_008705	FFC1_08180	FFUJ_10179	uncharacterized protein FFUJ_10179							7.98	8.26	8.40	6.92
XLOC_009228	FFC1_08184	FFUJ_10175	related to dehydrogenase							5.16			5.57
XLOC_009232	FFC1_08192	FFUJ_10168	uncharacterized protein FFUJ_10168	0.89						6.17	7.08	7.46	5.27
XLOC_009233	FFC1_08193	FFUJ_10167	uncharacterized protein FFUJ_10167		1.48					3.34	3.62	5.85	3.58
XLOC_009234	FFC1_08194	FFUJ_10166	uncharacterized protein FFUJ_10166	1.62	2.21								
XLOC_008712	FFC1_08196	FFUJ_10164	related to integral membrane protein							2.84	4.92	5.21	5.66
XLOC_008713	FFC1_08197	FFUJ_10163	uncharacterized protein FFUJ_10163			-0.90				7.51	7.42	7.49	7.14
XLOC_009239	FFC1_08204	FFUJ_10156	uncharacterized protein FFUJ_10156							2.72			
XLOC_008720	FFC1_08216	FFUJ_10144	related to transaminase type I							-2.64	-3.65		
XLOC_009252	FFC1_08229	FFUJ_10131	related to low-affinity hexose transporter HXT3		-1.33	-1.66				6.74	5.14	4.55	3.49
XLOC_009255	FFC1_08235	FFUJ_10126	uncharacterized protein FFUJ_10126							-2.05	-2.22	-2.28	-2.56
XLOC_009257	FFC1_08237	FFUJ_10124	uncharacterized protein FFUJ_10124									5.10	
XLOC_009261	FFC1_08248	FFUJ_10115	uncharacterized protein FFUJ_10115		-2.03						-1.78	-2.47	
XLOC_008743	FFC1_08258	FFUJ_10104	uncharacterized protein FFUJ_10104							2.89	2.75	2.34	2.45
XLOC_008744	FFC1_08261	FFUJ_10102	uncharacterized protein FFUJ_10102								-4.12		
XLOC_008748	FFC1_08266	FFUJ_10095	related to DUF1295 domain protein							4.31	4.36	4.21	2.79
XLOC_008749	FFC1_08269	FFUJ_10094	uncharacterized protein FFUJ_10094								6.36	5.57	
XLOC_008750	FFC1_08271	FFUJ_10092	related to quinate transport protein		3.22							4.37	
XLOC_008751	FFC1_08272	FFUJ_10091	probable amino acid permease NAAP1									6.61	
XLOC_008761	FFC1_08287	FFUJ_10076	related to carbonic anhydrase							5.94	5.28	6.66	5.66
XLOC_009282	FFC1_08290	FFUJ_10073	probable DFG5 protein							3.67	4.15	4.71	2.97
XLOC_009283	FFC1_08291	FFUJ_10072	uncharacterized protein FFUJ_10072							1.88	2.09	0.86	1.30
XLOC_008763	FFC1_08296	FFUJ_10067	uncharacterized protein FFUJ_10067							-1.72	-3.95		-3.03
XLOC_008764	FFC1_08298	FFUJ_10065	related to HOL1, putative substrate-H+ antiporter							2.45	2.24	2.02	
XLOC_009288	FFC1_08299	FFUJ_10064	uncharacterized protein FFUJ_10064							-1.65	-3.36	-4.41	-2.31
XLOC_009292	FFC1_08305									3.79			
XLOC_009293	FFC1_08309	FFUJ_10055	fusarin C cluster-peptidase								-3.04	-2.58	
XLOC_008771	FFC1_08311	FFUJ_10053	fusarin C cluster-transporter							2.47	2.91	2.72	
XLOC_008772	FFC1_08312	FFUJ_10052	fusarin C cluster-oxidoreductase		-0.78						3.30		3.04
XLOC_008773	FFC1_08313	FFUJ_10051	fusarin C cluster-cytochrome P450							4.12	3.55		
XLOC_008774	FFC1_08314	FFUJ_10050	fusarin C cluster-methyltransferase							3.96		3.16	
XLOC_009296	FFC1_08317	FFUJ_11292	probable ABC1 transport protein							4.58	4.55	4.52	4.20
XLOC_008775	FFC1_08318	FFUJ_10046	uncharacterized protein FFUJ_10046							2.82	3.50	3.01	2.22
XLOC_009297	FFC1_08319	FFUJ_10045	uncharacterized protein FFUJ_10045	2.05	1.54					2.71	4.44	4.47	4.97
XLOC_008776	FFC1_08320				2.17					-2.18			
XLOC_009299	FFC1_08321	FFUJ_10043	related to PMU1-high copy suppressor of ts tps2 mutant phenotype							-2.40	-2.78	-2.94	-2.38
XLOC_008777	FFC1_08322	FFUJ_10042	related to phosphoethanolamine cytidylyltransferase							-2.11	-1.88	-2.06	-2.10
XLOC_008778	FFC1_08323	FFUJ_10041	probable branched-chain amino acids aminotransferase							-2.47	-1.83	-2.87	-4.70

XLOC_009300	FFC1_08324	FFUJ_10040	uncharacterized protein FFUJ_10040							3.68	3.05	3.44	2.13
XLOC_009302	FFC1_08327	FFUJ_10037	uncharacterized protein FFUJ_10037							3.03	2.08		
XLOC_009304	FFC1_08330	FFUJ_10033	related to lincomycin-condensing protein lmbA							3.47			
XLOC_008781	FFC1_08331	FFUJ_10032	uncharacterized protein FFUJ_10032							6.44	6.77	6.19	
XLOC_009308	FFC1_08340	FFUJ_10023	uncharacterized protein FFUJ_10023							-2.00	-1.44	-2.01	-1.68
XLOC_008788	FFC1_08341	FFUJ_10022	uncharacterized protein FFUJ_10022								-1.39	-1.19	-2.31
XLOC_009309	FFC1_08343	FFUJ_10020	related to RTM1 protein							1.80	2.21	3.12	3.59
XLOC_009314	FFC1_08349	FFUJ_10014	uncharacterized protein FFUJ_10014							5.00			
XLOC_009316	FFC1_08351	FFUJ_10012	uncharacterized protein FFUJ_10012							4.27	6.93	4.97	8.97
XLOC_008791	FFC1_08352	FFUJ_10011	uncharacterized protein FFUJ_10011							4.76	4.20	3.80	4.46
XLOC_009317	FFC1_08353	FFUJ_10010	uncharacterized protein FFUJ_10010							3.94	2.89	2.83	
XLOC_009320	FFC1_08357	FFUJ_10006	uncharacterized protein FFUJ_10006		-1.25					2.73	1.60		
XLOC_009323	FFC1_08360	FFUJ_10003	related to TRI7-trichothecene biosynthesis gene cluster							-1.73	-2.75	-3.20	
XLOC_009324	FFC1_08361	FFUJ_10002	related to YSC84-protein involved in the organization of the actin cytoskeleton									-4.23	
XLOC_008794	FFC1_08363	FFUJ_10000	related to dis1-suppressing protein kinase dsk1							8.72	7.19	8.98	7.84
XLOC_008795	FFC1_08364	FFUJ_09999	uncharacterized protein FFUJ_09999							2.87	1.82	2.37	3.56
XLOC_009325	FFC1_08365	FFUJ_09998	uncharacterized protein FFUJ_09998			2.06				5.41	5.73	4.18	8.58
XLOC_008797	FFC1_08367	FFUJ_09996	related to UDP-galactopyranose mutase							2.05	5.32		3.69
XLOC_009327	FFC1_08370	FFUJ_09993	related to PMR1-Ca++-transporting P-type ATPase located in Golgi		2.32					-2.16	-3.02		
XLOC_009328	FFC1_08371	FFUJ_09992	related to alcohol oxidase							-2.91	-3.00	-2.98	-2.78
XLOC_009329	FFC1_08372	FFUJ_09991	uncharacterized protein FFUJ_09991							-2.54	-2.81	-2.13	-2.44
XLOC_008799	FFC1_08374	FFUJ_09989	related to phospholipid-translocating ATPase							3.88	3.91	5.38	4.97
XLOC_009331	FFC1_08375	FFUJ_09988	uncharacterized protein FFUJ_09988									5.42	
XLOC_009334	FFC1_08382	FFUJ_09981	uncharacterized protein FFUJ_09981	-1.24	-1.61	-2.46				9.93	8.69	8.85	8.18
XLOC_009337	FFC1_08387	FFUJ_09977	uncharacterized protein FFUJ_09977							7.07	7.03	7.00	6.67
XLOC_009343	null									-1.04	-1.39	-2.32	
XLOC_009350	FFC1_08401	FFUJ_09964	uncharacterized protein FFUJ_09964							2.03	1.66		
XLOC_009354	FFC1_08406	FFUJ_09959	probable GTP cyclohydrolase II		1.30	1.39				1.00	1.03	2.13	2.46
XLOC_009355	FFC1_08407	FFUJ_09958	uncharacterized protein FFUJ_09958	1.03	1.13	0.81				1.43	2.15	2.57	2.51
XLOC_008812	FFC1_08411	FFUJ_09954	probable arylsulfatase							3.12	2.22	1.87	
XLOC_009358	FFC1_08415	FFUJ_09950	uncharacterized protein FFUJ_09950							-2.28	-1.88	-2.71	-3.50
XLOC_008816	FFC1_08419									3.59	2.74	1.99	
XLOC_008817	FFC1_08420	FFUJ_09945	uncharacterized protein FFUJ_09945							2.00	1.97	2.78	2.27
XLOC_009364	FFC1_08423	FFUJ_09942	uncharacterized protein FFUJ_09942	1.03	0.95	1.11				1.20	2.15	2.08	2.28
XLOC_008821	FFC1_08427	FFUJ_09938	related to 6-hydroxy-d-nicotine oxidase								6.01		
XLOC_009366	FFC1_08428	FFUJ_09937	uncharacterized protein FFUJ_09937							4.36			
XLOC_009367	FFC1_08429	FFUJ_09936	related to histidine kinase		0.68					2.81	2.84	3.17	2.33
XLOC_008822	FFC1_08430	FFUJ_09935	uncharacterized protein FFUJ_09935							4.21	4.32	4.78	3.67
XLOC_008823	FFC1_08436	FFUJ_09929	related to O-methylsterigmatocystin oxidoreductase							2.24		2.36	3.04
XLOC_008824	FFC1_08437	FFUJ_09928	related to integral membrane protein							-1.89	-2.51	-2.40	-2.04
XLOC_009373	FFC1_08438	FFUJ_09927	uncharacterized protein FFUJ_09927							3.23	2.82	2.80	2.73
XLOC_008829	FFC1_08445	FFUJ_09921	related to TEA1-TY1 enhancer activator			1.71				2.33	1.99	3.42	3.91
XLOC_009376	FFC1_08446	FFUJ_09920	related to glutathione S-transferase							5.33	4.79	5.51	4.04
XLOC_008832	FFC1_08450	FFUJ_09916	uncharacterized protein FFUJ_09916		-2.45					3.94	2.84		4.64
XLOC_008834	FFC1_08453	FFUJ_09913	uncharacterized protein FFUJ_09913							4.63			
XLOC_008836	FFC1_08455	FFUJ_09911	related to peroxidase										3.17
XLOC_008838	FFC1_08458	FFUJ_09908	related to allantoate permease							-6.82	-7.79	-6.87	-5.38
XLOC_008839	FFC1_08459	FFUJ_09907	related to Dal5p		-1.83					-3.96	-5.57	-6.58	-4.42
XLOC_008840	FFC1_08460	FFUJ_09906	related to pectinesterase							2.18			
XLOC_009380	FFC1_08461	FFUJ_09905	related to allantoate permease							6.96	5.63		
XLOC_008847	FFC1_08471	FFUJ_09895	related to multidrug resistance protein							2.06	1.62	2.17	1.98
XLOC_008851	FFC1_08480	FFUJ_09886	uncharacterized protein FFUJ_09886			1.23				3.32	3.26	5.52	4.70
XLOC_008858	FFC1_08496	FFUJ_09870	uncharacterized protein FFUJ_09870		5.10	5.70						4.99	5.80
XLOC_009402	FFC1_08501	FFUJ_09867	uncharacterized protein FFUJ_09867							-0.76	-1.32	-1.06	-2.11
XLOC_008865	FFC1_08514									-2.90			
XLOC_009413	FFC1_08518	FFUJ_09851	uncharacterized protein FFUJ_09851			1.50				2.45	2.30	3.28	2.57
XLOC_008869	FFC1_08520	FFUJ_09849	uncharacterized protein FFUJ_09849	1.81	2.44	2.14				-2.39	-0.80		-0.55
XLOC_008871	FFC1_08522	FFUJ_09847	uncharacterized protein FFUJ_09847							4.59		3.41	
XLOC_009416	FFC1_08524	FFUJ_09845	related to putative transmembrane protein	1.08	2.21	0.99				2.50	2.84	3.80	3.22
XLOC_008872	FFC1_08529	FFUJ_09840	uncharacterized protein FFUJ_09840							6.60	2.45	6.04	
XLOC_009421	FFC1_08530	FFUJ_09839	uncharacterized protein FFUJ_09839							-2.33	-3.41	-3.05	
XLOC_009428	FFC1_08542	FFUJ_09828	related to multistep phosphorelay regulator 1							-1.90	-1.57	-1.70	-2.30
XLOC_009431	FFC1_08546	FFUJ_09824	uncharacterized protein FFUJ_09824							3.42	3.34	2.75	2.59
XLOC_009435	FFC1_08550	FFUJ_09820	related to MOSC domain protein							-2.05	-2.15	-2.15	-1.87
XLOC_008881	FFC1_08552	FFUJ_09818	uncharacterized protein FFUJ_09818	1.07	1.73					3.66	3.80	4.15	3.02
XLOC_008884	FFC1_08557	FFUJ_09813	uncharacterized protein FFUJ_09813								4.99	6.90	5.29
XLOC_009438	null									2.28	3.38	1.80	
XLOC_008885	FFC1_08558	FFUJ_14906	uncharacterized protein FFUJ_14906							2.93	2.58	2.12	
XLOC_009440	FFC1_08560	FFUJ_09811	related to N-glycosyltransferase							2.66	2.71	2.59	2.65
XLOC_008889	FFC1_08564	FFUJ_09807	uncharacterized protein FFUJ_09807			2.88						4.27	7.75
XLOC_008895	FFC1_08574	FFUJ_09797	related to aerobactin siderophore biosynthesis protein iucB	1.02						-2.02	-1.11	-1.86	-2.29
XLOC_009447	FFC1_08575	FFUJ_09796	related to long-chain-fatty-acid-CoA ligase	1.25					1.08	-2.43	-1.46	-2.44	-3.34
XLOC_008904	FFC1_08585									3.05	2.79		
XLOC_009460	FFC1_08598	FFUJ_09775	uncharacterized protein FFUJ_09775		3.30							3.62	
XLOC_009468	FFC1_08610	FFUJ_09764	uncharacterized protein FFUJ_09764							2.31	1.98	1.97	2.10
XLOC_009469	FFC1_08611	FFUJ_09763	uncharacterized protein FFUJ_09763							6.78	4.98	3.96	4.43
XLOC_008914	FFC1_08612	FFUJ_09762	related to phenol 2-monooxygenase								2.04	1.46	
XLOC_008915	FFC1_08613	FFUJ_09761	related to Ubl-specific protease							2.31	2.06	1.94	1.97
XLOC_008916	null									-3.40	-5.32	-4.58	

XLOC_009470	FFC1_08616	FFUJ_09759	related to glycerol-3-phosphate dehydrogenase precursor			1.05				0.99	1.19	1.91	2.78
XLOC_009480	null				1.55					7.20	4.76	4.82	
XLOC_008925	FFC1_08628	FFUJ_09747	related to 26S proteasome subunit RPN4		1.41				1.86	4.65	4.86	5.38	3.93
XLOC_009481	FFC1_08629	FFUJ_09746	probable PENTAFUNCTIONAL AROM POLYPEPTIDE	0.76	1.13	1.06				-2.18	-1.48		
XLOC_009486	FFC1_08640	FFUJ_09742	uncharacterized protein FFUJ_09742							4.46	3.68	3.26	
XLOC_008932	FFC1_08641	FFUJ_09741	related to polyphosphoinositide phosphatase family member							2.42	2.82	2.43	
XLOC_009487	FFC1_08642	FFUJ_09740	uncharacterized protein FFUJ_09740							2.14	2.25	2.52	2.23
XLOC_008936	FFC1_08652	FFUJ_09729	uncharacterized protein FFUJ_09729							3.24	2.99	3.00	1.96
XLOC_009495	FFC1_08653	FFUJ_09728	related to apyrase (NDPase/NTPase)							2.55	2.28	2.35	2.53
XLOC_009496	FFC1_08654	FFUJ_09727	uncharacterized protein FFUJ_09727							3.26	3.22	3.31	3.67
XLOC_009497	FFC1_08655	FFUJ_09726	probable lactose regulatory protein							6.07	4.71	5.28	6.45
XLOC_009498	FFC1_08656	FFUJ_09725	probable lactose regulatory protein							2.70	1.51		
XLOC_009508	FFC1_08674	FFUJ_09707	uncharacterized protein FFUJ_09707								4.86	5.39	
XLOC_009511	FFC1_08681	FFUJ_09700	related to aminopeptidase Y precursor, vacuolar							5.09		6.07	5.61
XLOC_008950	FFC1_08684	FFUJ_08851	probable Na+-transporting ATPase ENA-1			-2.18			-2.28	2.05	2.48	1.60	2.20
XLOC_008954	FFC1_08689	FFUJ_09694	related to sodium-and chloride-dependent GABA transporter 1							7.63	3.93	6.64	5.86
XLOC_008955	FFC1_08690	FFUJ_09693	uncharacterized protein FFUJ_09693							2.79	2.70	3.31	3.92
XLOC_009521	FFC1_08700	FFUJ_09683	probable chitosanase precursor							2.23	2.71	2.06	3.19
XLOC_008960	FFC1_08701	FFUJ_09682	related to short-chain dehydrogenase/reductase family protein, putative							5.14	5.95	3.92	5.31
XLOC_009523	FFC1_08703	FFUJ_09680	uncharacterized protein FFUJ_09680		-2.31	-2.99				2.77	2.40		
XLOC_009532	FFC1_08717	FFUJ_09666	related to monocarboxylate transporter 2							-3.70	-4.61	-4.66	-1.91
XLOC_009533	FFC1_08718	FFUJ_09665	related to formaldehyde dehydrogenase							3.05	1.52	2.59	
XLOC_008966	FFC1_08721	FFUJ_09662	related to XAP-5 protein		1.39						1.72	2.30	
XLOC_009536	FFC1_08722	FFUJ_09661	uncharacterized protein FFUJ_09661		1.99					1.22	2.49	3.08	1.78
XLOC_009537	FFC1_08723	FFUJ_09660	probable transcriptional regulator			-2.05				5.18	4.00	3.83	
XLOC_008968	FFC1_08726	FFUJ_09657	related to glutamine rich protein, nitrogen starvation-induced		-2.54								
XLOC_009543	FFC1_08732	FFUJ_09652	related to carboxylic acid transporter protein						2.58	5.15	4.44	4.74	3.39
XLOC_008971	FFC1_08736	FFUJ_09648	uncharacterized protein FFUJ_09648							4.00	2.95	4.14	3.30
XLOC_008972	FFC1_08738	FFUJ_09646	uncharacterized protein FFUJ_09646							2.87	2.03	3.06	2.28
XLOC_008973	FFC1_08739	FFUJ_09645	uncharacterized protein FFUJ_09645							2.00	1.86	2.44	2.16
XLOC_008974	FFC1_08740	FFUJ_09644	uncharacterized protein FFUJ_09644							4.65	4.90	6.02	6.48
XLOC_009547	FFC1_08741	FFUJ_09643	related to protein involved in biosynthesis of mitomycin antibiotics/polyketide fumonisin		2.21	2.08					1.95	5.05	4.38
XLOC_008978	FFC1_08751	FFUJ_09634	related to major facilitator (MFS1) transporter							-3.54	-2.29	-1.74	-2.22
XLOC_008985	FFC1_08760	FFUJ_09626	uncharacterized protein FFUJ_09626							4.72	3.86	5.50	3.87
XLOC_008986	FFC1_08761	FFUJ_09625	related to LRP16 protein							2.36	2.58	3.16	2.51
XLOC_008987	FFC1_08763	FFUJ_09623	related to TOB3 (member of AAA-ATPase family)							4.59	4.28	4.64	4.02
XLOC_008990	FFC1_08768	FFUJ_09618	uncharacterized protein FFUJ_09618							2.08	1.67	1.88	
XLOC_009565	FFC1_08778	FFUJ_09608	uncharacterized protein FFUJ_09608							6.47	4.67	8.35	6.29
XLOC_008996	FFC1_08781	FFUJ_09605	related to FRE1-ferric (and cupric) reductase							4.42	4.69	3.27	5.02
XLOC_008999	FFC1_08786	FFUJ_09600	related to uracil phosphoribosyltransferase										-2.18
XLOC_009576	FFC1_08795	FFUJ_09591	probable chitin binding protein								-4.30		-5.09
XLOC_009005	FFC1_08798	FFUJ_09588	related to chitinase							-1.79	-3.07	-2.44	-1.29
XLOC_009006	null									3.54	1.87	2.60	2.50
XLOC_009582	FFC1_08806	FFUJ_09580	uncharacterized protein FFUJ_09580		1.62	0.90				0.79	1.72	2.50	1.90
XLOC_009583	null									3.58		5.55	6.42
XLOC_009584	FFC1_08807	FFUJ_09579	related to putative transcriptional regulator							-2.73	-2.36	-2.36	-2.55
XLOC_009588	FFC1_08810	FFUJ_09576	related to kynureninase		-0.71					-1.99	-2.13	-2.34	
XLOC_009011	FFC1_08815	FFUJ_09571	probable urate oxidase (uricase)								1.89	2.39	
XLOC_009595	FFC1_08823	FFUJ_09563	related to ATP dependent RNA helicase							1.90	2.05	1.90	1.78
XLOC_009597	null										2.83		
XLOC_009613	FFC1_08850	FFUJ_09536	uncharacterized protein FFUJ_09536								-3.86		
XLOC_009031	FFC1_08852	FFUJ_09534	probable cytochrome P450 51 (eburicol 14 alpha-demethylase)	2.10							4.15		
XLOC_009032	FFC1_08855	FFUJ_09531	uncharacterized protein FFUJ_09531								-1.95	-2.08	
XLOC_009622	FFC1_08864	FFUJ_09523	uncharacterized protein FFUJ_09523							5.95	4.08	6.52	4.76
XLOC_009038	FFC1_08865	FFUJ_09522	probable acetolactate synthase							-2.09			
XLOC_009041	FFC1_08873	FFUJ_09515	uncharacterized protein FFUJ_09515							-2.37	-3.76	-2.74	-2.94
XLOC_009628	FFC1_08875	FFUJ_09513	related to cell wall protein PhiA							4.10	5.21	4.52	3.71
XLOC_009044	FFC1_08876	FFUJ_09512	uncharacterized protein FFUJ_09512		2.84	2.47						3.37	3.53
XLOC_009630	FFC1_08878	FFUJ_09510	uncharacterized protein FFUJ_09510							6.02	5.37	5.88	5.77
XLOC_009632	null											-3.56	
XLOC_009635	FFC1_08884	FFUJ_09505	uncharacterized protein FFUJ_09505							4.11	3.26	4.31	3.46
XLOC_009636	FFC1_08886	FFUJ_09503	related to TRANSKETOLASE							2.11	2.07	1.88	
XLOC_009051	FFC1_08891	FFUJ_09498	related to regulatory protein for the arginine catabolic pathway							-1.02	-2.24		-1.50
XLOC_009053	FFC1_08893	FFUJ_09496	related to extracellular cellulase CelA/allergen Asp F7-like, putative			-1.94				-1.50	-2.03	-2.43	-2.93
XLOC_009055	FFC1_08895	FFUJ_09494	uncharacterized protein FFUJ_09494							-4.80	-4.90		
XLOC_009638	FFC1_08896	FFUJ_09493	uncharacterized protein FFUJ_09493							2.48	2.69	2.52	
XLOC_009057	FFC1_08899	FFUJ_09490	related to TOB3 (member of AAA-ATPase family)			-2.07				3.09	2.74		
XLOC_009642	FFC1_08905	FFUJ_09484	related to VHS1-protein kinase involved in G1/S transition							2.18	2.39	2.42	2.04
XLOC_009065	FFC1_08911	FFUJ_09477	uncharacterized protein FFUJ_09477							3.33	6.27		

XLOC_009071	FFC1_08920	FFUJ_09469	uncharacterized protein FFUJ_09469							2.05	1.76	2.64	2.18
XLOC_009074	FFC1_08924	FFUJ_09467	related to RSN1 Overexpression rescues sro7/sop1 in NaCl	1.35							2.01	0.91	
XLOC_009652	FFC1_08931	FFUJ_09460	uncharacterized protein FFUJ_09460							5.32	4.77	5.56	2.93
XLOC_009656	FFC1_08937	FFUJ_09454	uncharacterized protein FFUJ_09454								5.11	5.60	
XLOC_009659	FFC1_08941	FFUJ_09450	uncharacterized protein FFUJ_09450								4.40		
XLOC_009084	FFC1_08944	FFUJ_09447	related to integral membrane protein pth11			1.48				-2.68	-2.94	-3.04	-1.23
XLOC_009085	FFC1_08945	FFUJ_09446	related to glu/asp-tRNA amidotransferase subunit A							-2.07	-2.59	-2.64	-0.95
XLOC_009666	FFC1_08949	FFUJ_09442	uncharacterized protein FFUJ_09442								-1.81	-2.19	-1.61
XLOC_009086	FFC1_08953	FFUJ_09438	uncharacterized protein FFUJ_09438	1.49	1.80	1.73				3.90	4.68	4.97	5.06
XLOC_009670	FFC1_08954	FFUJ_09437	related to endo-1,3-beta-glucanase							-6.69	-5.57	-6.71	-5.95
XLOC_009675	FFC1_08960	FFUJ_09431	related to TOB3 (member of AAA-ATPase family)							2.41			
XLOC_009088	FFC1_08961	FFUJ_09430	probable vegetatible incompatibility protein HET-E-1							3.68		2.99	
XLOC_009678	FFC1_08964	FFUJ_09427	related to trichothecene 3-O-acetyltransferase							4.26	4.07		
XLOC_009094	FFC1_08978	FFUJ_09413	uncharacterized protein FFUJ_09413		2.26					3.65	3.82	4.94	3.57
XLOC_009100	FFC1_08987	FFUJ_09404	related to glomerulosclerosis protein Mpv17							2.36	1.77	1.64	
XLOC_009693	FFC1_08990	FFUJ_09401	uncharacterized protein FFUJ_09401							-1.66	-2.30		
XLOC_009695	FFC1_08992	FFUJ_09399	uncharacterized protein FFUJ_09399							-6.19	-6.04	-5.31	-3.90
XLOC_009103	FFC1_08994	FFUJ_09397	related to 6-hydroxy-d-nicotine oxidase			-1.89				8.23	4.71	5.58	4.13
XLOC_009696	FFC1_08995	FFUJ_09396	related to low affininty zinc transporter								5.56		
XLOC_009104	FFC1_08996	FFUJ_09395	uncharacterized protein FFUJ_09395							-2.10	-1.42	-1.95	
XLOC_009698	FFC1_08998	FFUJ_09393	uncharacterized protein FFUJ_09393								-3.57		-1.96
XLOC_009105	FFC1_08999	FFUJ_09392	uncharacterized protein FFUJ_09392								4.81	5.46	
XLOC_009106	FFC1_09001	FFUJ_09390	related to aldehyde reductase II							-1.55	-2.35	-3.60	
XLOC_009108	FFC1_09004	FFUJ_09387	related to C-4 methyl sterol oxidase							3.75	3.76	3.52	2.76
XLOC_009702	FFC1_09007	FFUJ_09384	uncharacterized protein FFUJ_09384							5.87	4.16	6.35	
XLOC_009704	FFC1_09009	FFUJ_09382	related to lactate 2-monooxygenase		3.38	2.28				2.36	3.65	4.68	3.32
XLOC_009706	FFC1_09011	FFUJ_09380	uncharacterized protein FFUJ_09380							2.29	2.27	3.19	4.65
XLOC_009707	FFC1_09012	FFUJ_09380	uncharacterized protein FFUJ_09380								5.85	6.81	6.65
XLOC_009708	FFC1_09014	FFUJ_09378	uncharacterized protein FFUJ_09378							3.51	4.79	4.26	4.47
XLOC_009709	FFC1_09015	FFUJ_14904	related to serum paraoxonase/arylesterase family protein		2.90	2.20						3.46	2.56
XLOC_009111	FFC1_09016	FFUJ_09376	related to monooxygenase							-4.34			
XLOC_009112	FFC1_09017	FFUJ_09375	related to S.fumigata Asp FII							-5.34	-4.55	-4.52	-3.73
XLOC_009710	FFC1_09018	FFUJ_09374	uncharacterized protein FFUJ_09374			2.72				5.99	4.57	5.44	7.28
XLOC_009711	FFC1_09019	FFUJ_09373	related to cellulose binding protein CEL1							2.83	2.41	3.30	3.83
XLOC_009114	FFC1_09024	FFUJ_09368	related to isoamyl alcohol oxidase		1.75	1.79				4.23	4.26	5.28	4.79
XLOC_009715	FFC1_09025	FFUJ_09367	related to serum paraoxonase/arylesterase		1.50					1.84	1.99	3.12	3.05
XLOC_009117	FFC1_09034	FFUJ_09358	probable general amidase		2.07							3.08	2.59
XLOC_009118	FFC1_09035	FFUJ_09357	related to integral membrane protein PTH11							-3.30	-2.77	-2.84	-2.52
XLOC_009723	FFC1_09039	FFUJ_09353	uncharacterized protein FFUJ_09353										2.38
XLOC_009121	FFC1_09040	FFUJ_09352	related to pisatin demethylase							1.88	1.68	2.44	2.54
XLOC_009122	FFC1_09041	FFUJ_09351	related to protein yneE									5.82	5.27
XLOC_009724	FFC1_09042	FFUJ_09350	related to zinc alcohol dehydrogenase							2.81	2.65	2.89	
XLOC_009727	FFC1_09045	FFUJ_09347	related to tol protein							5.32			
XLOC_009729	FFC1_09049	FFUJ_09344	uncharacterized protein FFUJ_09344							-4.37	-4.64	-3.85	-4.34
XLOC_009125	FFC1_09050	FFUJ_09343	related to class I alpha-mannosidase 1B							-1.36	-4.71		
XLOC_009127	FFC1_09052	FFUJ_09341	probable beta-galactosidase		0.93					3.89	3.85	5.13	4.00
XLOC_009730	FFC1_09054	FFUJ_09339	related to Cut9 interacting protein scn1									2.05	
XLOC_009129	FFC1_09055	FFUJ_09338	uncharacterized protein FFUJ_09338		2.11	2.00				2.86	3.94	5.61	5.33
XLOC_009130	FFC1_09056	FFUJ_09337	uncharacterized protein FFUJ_09337		3.27	3.95				2.77	4.53	5.12	6.76
XLOC_009731	FFC1_09057	FFUJ_09336	uncharacterized protein FFUJ_09336									5.46	6.59
XLOC_009131	FFC1_09059	FFUJ_09334	related to myo-inositol transport protein ITR1							3.34			
XLOC_009733	FFC1_09060	FFUJ_09333	related to allantoate permease							5.04	6.62	5.39	
XLOC_009132	FFC1_09061	FFUJ_09332	related to 2-deoxy-D-gluconate 3-dehydrogenase							4.95		5.31	
XLOC_009133	FFC1_09062	FFUJ_09331	probable starvation sensing protein rspA							6.50	6.07		5.02
XLOC_009135	FFC1_09064	FFUJ_09329	uncharacterized protein FFUJ_09329							3.04			
XLOC_009136	FFC1_09066	FFUJ_09327	related to O-methylsterigmatocystin oxidoreductase							4.12	2.12	2.07	2.63
XLOC_009735	FFC1_09068	FFUJ_09325	uncharacterized protein FFUJ_09325							4.29	4.76	5.46	
XLOC_009736	FFC1_09069	FFUJ_09324	related to putative lipid binding protein TFS1							2.53	1.87	2.15	2.40
XLOC_009138	FFC1_09070	FFUJ_09323	uncharacterized protein FFUJ_09323							1.75		2.20	3.33
XLOC_009737	FFC1_09071	FFUJ_09322	uncharacterized protein FFUJ_09322							4.65	4.10	3.48	3.91
XLOC_009738	FFC1_09072									5.70	4.09	4.92	3.54
XLOC_009139	FFC1_09073	FFUJ_09321	probable flavin-containing monooxygenase							2.60	2.33	1.92	2.19
XLOC_009739	FFC1_09074	FFUJ_09320	related to Rds1 protein		5.78	2.24				5.47	6.59	7.33	7.87
XLOC_009140	FFC1_09075	FFUJ_09319	related to HHE domain protein		4.99							4.45	
XLOC_009740	FFC1_09077	FFUJ_09317	probable RCO3 glucose transporter							5.57			
XLOC_009142	FFC1_09080	FFUJ_09314	probable SUC2-invertase (sucrose hydrolyzing enzyme)							3.53			
XLOC_009143	FFC1_09081	FFUJ_09313	related to tol protein							5.84	5.42	4.96	5.50
XLOC_009744	FFC1_09084	FFUJ_09310	related to NmrA-like family protein		3.59							7.44	5.17
XLOC_009145	FFC1_09085	FFUJ_09309	related to transcriptional activator Mut3p							2.38		3.53	3.32
XLOC_009146	FFC1_09086	FFUJ_09308	uncharacterized protein FFUJ_09308							6.70	2.28	7.53	5.60
XLOC_009746	FFC1_09089	FFUJ_09305	probable phenol 2-monooxygenase							2.84	2.95	2.39	5.03
XLOC_009748	FFC1_09091	FFUJ_09303	uncharacterized protein FFUJ_09303							-4.72	-5.18	-3.67	-2.56
XLOC_009749	FFC1_09092	FFUJ_09302	uncharacterized protein FFUJ_09302			-2.07					-1.20		-2.93
XLOC_009148	FFC1_09093	FFUJ_09301	uncharacterized protein FFUJ_09301							-3.39	-3.41	-3.97	-3.86

XLOC_009149	FFC1_09094	FFUJ_09300	uncharacterized protein FFUJ_09300							-3.33	-3.53	-3.29	-3.29
XLOC_009750	FFC1_09095	FFUJ_09299	related to monoamine oxidase N		2.16						1.88	3.32	
XLOC_009752	FFC1_09098									10.35	10.45	10.13	10.49
XLOC_009151	FFC1_09099	FFUJ_09295	related to 2-dehydropantoate 2-reductase							10.15	10.58	9.93	10.28
XLOC_009152	FFC1_09100	FFUJ_02991	related to multidrug resistance protein							6.79	6.69	6.86	7.01
XLOC_009754	FFC1_09101	FFUJ_09293	uncharacterized protein FFUJ_09293							5.15		4.78	
XLOC_009153	FFC1_09102	FFUJ_09292	uncharacterized protein FFUJ_09292							4.85	4.10	7.55	5.40
XLOC_009755	FFC1_09103	FFUJ_09291	uncharacterized protein FFUJ_09291										5.19
XLOC_009759	FFC1_09109	FFUJ_09285	uncharacterized protein FFUJ_09285							7.31	6.32	5.07	4.29
XLOC_009156	FFC1_09110	FFUJ_09284	uncharacterized protein FFUJ_09284									5.69	5.10
XLOC_009761	FFC1_09113	FFUJ_09281	uncharacterized protein FFUJ_09281							3.99	2.31	4.14	
XLOC_009160	FFC1_09116	FFUJ_09278	related to early nodulin 75 precursor							-1.96	-2.05	-1.79	-1.35
XLOC_009762	FFC1_09117	FFUJ_09277	uncharacterized protein FFUJ_09277							-4.20	-4.98	-4.98	-5.71
XLOC_009161	FFC1_09118	FFUJ_09276	uncharacterized protein FFUJ_09276							-3.89	-5.27	-5.02	-4.74
XLOC_009162	FFC1_09119	FFUJ_09275	related to sulfatase			-0.68				-3.88	-3.75	-3.64	-4.78
XLOC_009166	FFC1_09124	FFUJ_09270	uncharacterized protein FFUJ_09270							4.30	3.03	3.25	3.54
XLOC_009764	FFC1_09125	FFUJ_09269	uncharacterized protein FFUJ_09269							3.96			
XLOC_009772	FFC1_09142	FFUJ_09243	fumonisin cluster-dehydrogenase							5.00			
XLOC_009775	FFC1_09146	FFUJ_09239	related to transcription activator amyR							2.06	1.10	1.32	
XLOC_009178	FFC1_09149	FFUJ_09236	related to epoxide hydrolase									6.53	6.02
XLOC_009185	FFC1_09163	FFUJ_09222	related to maltose permease							5.63	6.03	5.82	6.50
XLOC_009194	FFC1_09177	FFUJ_09208	uncharacterized protein FFUJ_09208							2.72	3.05		3.28
XLOC_009790	FFC1_09182	FFUJ_09204	uncharacterized protein FFUJ_09204							5.59	5.61		5.59
XLOC_009198	FFC1_09183	FFUJ_09203	uncharacterized protein FFUJ_09203							3.30	3.52	3.45	3.00
XLOC_009791	FFC1_09184	FFUJ_09202	related to tol protein							7.60	7.68	6.33	5.55
XLOC_009792	FFC1_09185	FFUJ_09201	probable UGA2-succinate semialdehyde dehydrogenase							8.75	8.33	7.70	8.06
XLOC_009199	FFC1_09186	FFUJ_09200	related to short-chain alcohol dehydrogenase							8.32	7.10	7.35	7.30
XLOC_009793	FFC1_09187	FFUJ_09199	related to sugar transporter							8.51	8.62	7.87	8.60
XLOC_009200	FFC1_09188	FFUJ_09198	uncharacterized protein FFUJ_09198							8.56	9.58	8.37	9.05
XLOC_009201	FFC1_09189	FFUJ_09197	related to integral membrane protein							10.03	9.21	9.58	10.30
XLOC_009794	FFC1_09190	FFUJ_09196	related to putative tartrate transporter							9.16	10.11	9.62	9.43
XLOC_009798	FFC1_09197	FFUJ_09189	related to Chitin deacetylase 1							2.09			
XLOC_009800	FFC1_09200	FFUJ_09185	uncharacterized protein FFUJ_09185							2.66	3.22	3.35	1.85
XLOC_009801	FFC1_09201	FFUJ_09184	related to class I alpha-mannosidase 1B						-4.28	6.57	6.48	7.39	9.92
XLOC_009802	FFC1_09202	FFUJ_09183	uncharacterized protein FFUJ_09183			2.34				4.28	4.41	3.47	5.54
XLOC_009803	FFC1_09203	FFUJ_09182	uncharacterized protein FFUJ_09182			1.66				3.30	2.54	2.86	4.93
XLOC_009207	FFC1_09204	FFUJ_09181	uncharacterized protein FFUJ_09181							5.01	5.64		8.07
XLOC_009804	FFC1_09206	FFUJ_09180	uncharacterized protein FFUJ_09180								1.33		2.59
XLOC_009209	FFC1_09207	FFUJ_09179	related to tryptophan dimethylallyltransferase							2.15			
XLOC_009805	FFC1_09208	FFUJ_09178	related to methyltransferase		-2.53					10.15	7.31	3.88	5.40
XLOC_009210	FFC1_09209	FFUJ_09177	uncharacterized protein FFUJ_09177							5.03			
XLOC_009211	FFC1_09213	FFUJ_09173	related to isoflavone reductase homolog A622		1.39					2.59	2.19	2.52	3.17
XLOC_009809	FFC1_09216	FFUJ_09171	uncharacterized protein FFUJ_09171							5.19	4.36	4.44	5.71
XLOC_009810	FFC1_09217	FFUJ_09170	uncharacterized protein FFUJ_09170							3.55	2.76	2.62	3.30
XLOC_009811	FFC1_09218	FFUJ_09169	uncharacterized protein FFUJ_09169							3.43	3.13	3.47	4.52
XLOC_009819	FFC1_09230	FFUJ_03804	uncharacterized protein FFUJ_03804							-3.15	-4.68	-5.41	-4.16
XLOC_009826	FFC1_09242	FFUJ_03813	related to tyrosinase precursor							5.04	6.10	3.37	
XLOC_009827	FFC1_09243	FFUJ_03814	uncharacterized protein FFUJ_03814							1.22	1.78	2.13	
XLOC_009828	FFC1_09244	FFUJ_03815	uncharacterized protein FFUJ_03815							4.24		5.27	4.60
XLOC_009829	FFC1_09245	FFUJ_03816	related to permeases-unknown function						-3.46				
XLOC_009830	FFC1_09247	FFUJ_03819	probable monoamine oxidase N								6.87		20.14
XLOC_010287	FFC1_09249	FFUJ_03821	uncharacterized protein FFUJ_03821									6.86	
XLOC_010288	FFC1_09250	FFUJ_03822	related to signal peptide protein							3.64	4.01	3.72	2.86
XLOC_009831	FFC1_09251	FFUJ_03823	related to aspartate--tRNA ligase, mitochondrial							2.48	2.43	4.23	4.30
XLOC_010289	FFC1_09254	FFUJ_03826	uncharacterized protein FFUJ_03826							3.50	3.47	3.53	3.01
XLOC_010290	FFC1_09255	FFUJ_03827	uncharacterized protein FFUJ_03827							3.45	3.13		
XLOC_010295	FFC1_09263	FFUJ_03835	uncharacterized protein FFUJ_03835										5.61
XLOC_010296	FFC1_09265	FFUJ_03836	uncharacterized protein FFUJ_03836							4.36	5.39	4.65	5.15
XLOC_010297	FFC1_09266	FFUJ_03837	related to alpha-mannosidase 1a		-0.86	-0.93				4.28	4.23	3.78	4.42
XLOC_010298	FFC1_09268	FFUJ_03839	uncharacterized protein FFUJ_03839		-1.33	-1.78					-1.06	-1.89	-2.18
XLOC_009839	FFC1_09270	FFUJ_03841	uncharacterized protein FFUJ_03841		-1.52					-1.21	-1.98	-1.79	-2.05
XLOC_010302	FFC1_09274	FFUJ_03845	uncharacterized protein FFUJ_03845							3.73	4.29	7.09	3.88
XLOC_010303	FFC1_09275	FFUJ_03846	uncharacterized protein FFUJ_03846									4.46	
XLOC_010304	FFC1_09276	FFUJ_03847	probable Na+-transporting ATPase ENA-1 (sodium P-type ATPase ENA-1)		1.05					1.59	2.24	2.52	2.38
XLOC_010305	FFC1_09277	FFUJ_03848	uncharacterized protein FFUJ_03848		1.20					5.46	6.52	6.19	7.17
XLOC_010306	FFC1_09278	FFUJ_03849	uncharacterized protein FFUJ_03849							1.79	1.48	1.94	2.97
XLOC_009841	null									4.98	5.19		
XLOC_010307	FFC1_09279									5.78	3.67	4.86	9.05
XLOC_010308	FFC1_09282	FFUJ_03852	related to beta-glucosidase							2.19	2.08	2.39	2.79
XLOC_009844	FFC1_09283	FFUJ_03853	uncharacterized protein FFUJ_03853							-2.21	-1.80		-1.56
XLOC_010310	FFC1_09285	FFUJ_03855	uncharacterized protein FFUJ_03855							4.11	4.34	4.76	4.38
XLOC_010311	FFC1_09286	FFUJ_03856	related to ERO1 protein, required for protein disulfide bond formation in the ER		0.81					2.27	2.31	2.66	1.72
XLOC_009845	FFC1_09289	FFUJ_03859	uncharacterized protein FFUJ_03859							2.11	2.00	1.87	1.64
XLOC_009846	FFC1_09291	FFUJ_03861	probable lysosomal cobalamin transporter		1.38					2.63	3.22	3.79	3.06
XLOC_010315	FFC1_09292	FFUJ_03862	uncharacterized protein FFUJ_03862							1.76	1.64	2.14	2.00
XLOC_009847	FFC1_09293	FFUJ_03863	related to alpha-1,3-mannosyltransferases							2.01	1.98	2.01	1.82
XLOC_009848	FFC1_09294	FFUJ_03864	related to cytochrome-b5 reductase, mitochondrial							2.79	3.08	3.19	
XLOC_010316	FFC1_09295	FFUJ_03865	related to P. aeruginosa hyuA and hyuB	2.05	1.61						1.76		
XLOC_009850	FFC1_09299	FFUJ_03869	related to monophenol monooxygenase (tyrosinase)							4.71			
XLOC_010333	FFC1_09331	FFUJ_03900	related to proteoglycan						-1.40	-8.83	-9.50	-8.37	-7.88

XLOC_009868	FFC1_09332	FFUJ_03901	uncharacterized protein FFUJ_03901							-6.04	-7.23	-6.07	-5.17
XLOC_009869	FFC1_09333	FFUJ_03902	related to light induced alcohol dehydrogenase Bli-4							12.36	8.07	10.05	11.17
XLOC_009870	FFC1_09334	FFUJ_03903	related to sugar transport protein STL1							7.33	8.47	8.47	8.18
XLOC_009875	FFC1_09339			-1.32	-3.06	-3.16				3.65	2.66		
XLOC_010336	FFC1_09343									5.44	6.47	5.41	6.44
XLOC_009878	FFC1_09347									6.10	5.77	4.56	5.12
XLOC_010358	FFC1_09380	FFUJ_03909	uncharacterized protein FFUJ_03909								-1.53	-2.23	
XLOC_009894	FFC1_09381	FFUJ_03910	related to nicotinamide mononucleotide permease							-1.29	-3.12	-2.36	-2.16
XLOC_010359	FFC1_09382	FFUJ_03911	uncharacterized protein FFUJ_03911							-2.94	-2.30	-2.64	-1.95
XLOC_010360	FFC1_09383	FFUJ_03912	uncharacterized protein FFUJ_03912							-1.43	-2.39	-2.31	
XLOC_010361	FFC1_09385	FFUJ_03914	related to TFB3-TFIIH subunit (transcription/repair factor)							1.93	1.75	2.22	2.28
XLOC_010362	FFC1_09387	FFUJ_03916	uncharacterized protein FFUJ_03916							2.72	2.68	2.62	2.50
XLOC_010363	FFC1_09388	FFUJ_03917	related to mannosylphosphorylation protein MNN4							3.59	3.11	3.00	2.29
XLOC_009897	FFC1_09389	FFUJ_03918	related to endoplasmic reticulum retention receptor							2.79	2.72	2.41	2.67
XLOC_009898	FFC1_09391	FFUJ_03920	uncharacterized protein FFUJ_03920			2.88					3.82	6.68	7.38
XLOC_010365	FFC1_09392	FFUJ_03921	uncharacterized protein FFUJ_03921							4.77		6.55	6.93
XLOC_009899	FFC1_09393	FFUJ_03922	related to periplasmic beta-glucosidase/beta-xylosidase precursor		1.24					1.64	2.01	2.40	2.66
XLOC_010366	FFC1_09396	FFUJ_03925	probable Kex protein							2.04	2.25	1.88	1.82
XLOC_010367	FFC1_09397	FFUJ_03926	probable phosphate transport protein MIR1	1.82	1.91					3.60	3.90	4.65	3.54
XLOC_009903	FFC1_09398	FFUJ_03927	uncharacterized protein FFUJ_03927							3.83	3.19	3.11	
XLOC_009904	FFC1_09399	FFUJ_03928	uncharacterized protein FFUJ_03928		1.24	1.61				4.78	4.51	5.77	5.84
XLOC_010368	FFC1_09401									2.86	1.83		
XLOC_010371	FFC1_09407	FFUJ_03937	probable manganese transport protein							-2.45	-2.89	-2.92	-2.63
XLOC_010372	FFC1_09408	FFUJ_03938	uncharacterized protein FFUJ_03938							-1.32	-2.80	-2.17	
XLOC_009910	FFC1_09414	FFUJ_03943	related to hydroxyquinol-1,2-dioxygenase									5.35	
XLOC_009914	FFC1_09419	FFUJ_03947	uncharacterized protein FFUJ_03947							2.92	3.39	3.44	
XLOC_009915	FFC1_09425	FFUJ_03953	uncharacterized protein FFUJ_03953							-6.46	-6.94	-7.00	-5.47
XLOC_010385	FFC1_09428	FFUJ_03956	related to hydrolases or acyltransferases (alpha/beta hydrolase superfamily)								5.34		
XLOC_009918	FFC1_09431	FFUJ_03959	uncharacterized protein FFUJ_03959							6.32	4.89	3.55	5.70
XLOC_010387	FFC1_09432	FFUJ_03960	uncharacterized protein FFUJ_03960							4.60	2.69	3.00	3.46
XLOC_010388	FFC1_09433	FFUJ_03961	related to triacylglycerol lipase II precursor							3.17	3.45	1.69	1.90
XLOC_009919	FFC1_09442	FFUJ_03970	uncharacterized protein FFUJ_03970		7.05	6.24					4.98	7.89	7.30
XLOC_010398	FFC1_09445	FFUJ_03972	uncharacterized protein FFUJ_03972							5.83	6.20	5.66	5.15
XLOC_009922	FFC1_09448	FFUJ_03975	uncharacterized protein FFUJ_03975		6.72						6.31	6.60	
XLOC_009924	FFC1_09451	FFUJ_03978	related to conidial hydrophobin RodB							3.22	3.41	4.20	5.19
XLOC_010403	FFC1_09457	FFUJ_03984	fusarubin cluster-polyketide synthase						-1.10	-1.87	-2.05	-1.51	-1.62
XLOC_010407	FFC1_09462	FFUJ_03989	fusarubin cluster-transcription factor								-2.67		
XLOC_009929	FFC1_09463	FFUJ_03990	fusarubin cluster-esterase							4.64			
XLOC_010409	FFC1_09467	FFUJ_03994	related to YPC1-Alkaline Ceramidase		1.04					1.41	1.60	2.30	1.92
XLOC_009932	FFC1_09468				3.66							3.40	
XLOC_009933	FFC1_09469	FFUJ_03995	related to host-specific AK-toxin Akt2							-2.34	-2.82	-1.72	-1.59
XLOC_010413	FFC1_09475									2.44	2.32	2.29	2.27
XLOC_009939	FFC1_09477	FFUJ_04002	uncharacterized protein FFUJ_04002							-1.68	-2.52	-1.70	
XLOC_010414	FFC1_09478	FFUJ_04003	uncharacterized protein FFUJ_04003			1.88					5.16	4.57	5.40
XLOC_010418	FFC1_09482	FFUJ_04007	related to ALCOHOL DEHYDROGENASE I-ADH1			1.70				1.84	1.72	3.16	3.83
XLOC_010419	FFC1_09484	FFUJ_04009	probable protein disulfide isomerase-related protein A							3.44	3.14	3.83	3.94
XLOC_010421	FFC1_09488	FFUJ_04013	uncharacterized protein FFUJ_04013							4.61			
XLOC_009947	FFC1_09494	FFUJ_04019	uncharacterized protein FFUJ_04019							2.60			
XLOC_009948	FFC1_09495	FFUJ_04020	uncharacterized protein FFUJ_04020									-5.99	-3.11
XLOC_009949	FFC1_09497	FFUJ_04021	probable SIT1-Transporter of the bacterial siderophore ferrioxamine B		-1.96	-2.08			-2.41	-2.25	-2.05		-1.91
XLOC_010425	FFC1_09498	FFUJ_04022	uncharacterized protein FFUJ_04022							2.65	2.62		
XLOC_009950	FFC1_09499	FFUJ_04023	probable neutral amino acid permease		-1.53	-1.42				3.47	2.87	3.19	3.28
XLOC_010428	FFC1_09503	FFUJ_04027	related to pisatin demethylase / cytochrome P450 monooxygenase							6.98	6.27	6.84	6.78
XLOC_009952	FFC1_09504	FFUJ_04028	related to integral membrane protein PTH11		2.04					4.61	4.66	6.11	5.91
XLOC_009953	FFC1_09505	FFUJ_04029	uncharacterized protein FFUJ_04029							-2.43	-2.65	-2.24	
XLOC_010429	FFC1_09506	FFUJ_04030	uncharacterized protein FFUJ_04030							-4.87			-4.76
XLOC_010432	FFC1_09509	FFUJ_04033	uncharacterized protein FFUJ_04033							-3.11	-2.21	-2.32	-2.90
XLOC_010434	FFC1_09513	FFUJ_04037	related to heterokaryon incompatibility protein							3.64	4.24		6.37
XLOC_010438	FFC1_09518	FFUJ_04042	uncharacterized protein FFUJ_04042							-2.92			
XLOC_010439	FFC1_09519	FFUJ_04043	uncharacterized protein FFUJ_04043								-1.51	-3.78	
XLOC_009957	FFC1_09520	FFUJ_04044	related to transcription activator protein acu-15		-2.07						-1.31	-1.46	
XLOC_009958	FFC1_09522	FFUJ_04046	related to 3-isopropylmalate dehydrogenase										2.18
XLOC_010441	FFC1_09523	FFUJ_04047	uncharacterized protein FFUJ_04047							2.65	2.37	2.23	1.89
XLOC_010448	FFC1_09532	FFUJ_04056	related to Pdr3p							-1.39	-2.42	-2.22	
XLOC_009961	FFC1_09533	FFUJ_04057	related to monocarboxylate transporter 4							-4.80	-3.58		
XLOC_009963	FFC1_09537	FFUJ_04061	related to 2-polyprenyl-6-methoxyphenol hydroxylase and related FAD-dependent oxidoreductases		2.82							2.61	
XLOC_009964	FFC1_09539	FFUJ_04063	related to multidrug resistance protein	1.71	1.55					-3.06	-1.67	-1.61	-2.10
XLOC_009967	FFC1_09544	FFUJ_04068	related to salicylate 1-monooxygenase							-1.61	-2.69	-3.37	-1.92
XLOC_010468	FFC1_09572	FFUJ_04097	probable ketopantoate hydroxymethyltransferase		-1.47						-1.71	-2.47	-2.38
XLOC_010474	null										2.82		

XLOC_009991	FFC1_09585	FFUJ_04110	probable general amino acid permease						-2.09					
XLOC_009994	FFC1_09591	FFUJ_04116	uncharacterized protein FFUJ_04116							-2.46	-2.98	-2.83		
XLOC_010478	FFC1_09592	FFUJ_04117	probable pectate lyase 1							-2.05	-2.84	-2.91	-2.89	
XLOC_010480	FFC1_09594	FFUJ_04119	related to CRH1-family of putative glycosidases might exert a common role in cell wall organization							-1.82	-1.71	-1.64	-3.09	
XLOC_009995	FFC1_09595											4.28		
XLOC_010481	FFC1_09596	FFUJ_04121	related to sexual differentiation process protein								1.81	2.08		
XLOC_010482	FFC1_09597	FFUJ_04122	probable cross-pathway control protein			-0.72				-1.82	-1.53	-1.88	-2.18	
XLOC_010483	FFC1_09598	FFUJ_04123	uncharacterized protein FFUJ_04123	1.01						1.15	2.06	1.55		
XLOC_010000	FFC1_09605	FFUJ_04130	probable FBP1-fructose-1,6-bisphosphatase			-1.00				2.40				
XLOC_010486	FFC1_09606	FFUJ_04131	related to URE2-nitrogen catabolite repression regulator							2.40	2.07	3.47	2.09	
XLOC_010003	FFC1_09610	FFUJ_04133	uncharacterized protein FFUJ_04133		1.53					1.12	1.55	2.74	1.72	
XLOC_010006	FFC1_09617	FFUJ_04139	related to L-sorbosone dehydrogenase							-3.45	-3.45	-2.15	-2.62	
XLOC_010008	FFC1_09621	FFUJ_04143	uncharacterized protein FFUJ_04143							3.27	3.48	3.39	3.93	
XLOC_010010	FFC1_09623	FFUJ_04145	probable hydroxymethylglutaryl-CoA synthase		-0.74					-1.91	-1.77	-2.44	-1.81	
XLOC_010495	FFC1_09625	FFUJ_04147	related to acetyl-hydrolase							-2.95	-2.96	-1.94		
XLOC_010013	FFC1_09629	FFUJ_04151	uncharacterized protein FFUJ_04151							4.23	3.93	4.49	3.35	
XLOC_010017	FFC1_09637	FFUJ_04159	uncharacterized protein FFUJ_04159							2.44	2.17	2.31	2.70	
XLOC_010018	FFC1_09638	FFUJ_04160	uncharacterized protein FFUJ_04160							1.90	1.84	1.81	2.01	
XLOC_010503	FFC1_09642	FFUJ_04164	uncharacterized protein FFUJ_04164	1.17	1.08					2.15	2.62	2.60	1.48	
XLOC_010504	FFC1_09643	FFUJ_04165	related to PRM10 Pheromone-regulated protein						2.53	2.21	2.49	2.35		
XLOC_010505	FFC1_09644	FFUJ_04166	related to ADH4-alcohol dehydrogenase IV						2.33					
XLOC_010507	FFC1_09648	FFUJ_04170	related to pyruvate dehydrogenase (lipoamide) alpha chain precursor							3.22	2.71	3.19		
XLOC_010511	FFC1_09656	FFUJ_04177	related to TOK1-voltage-gated, outward-rectifying K+ channel						1.20	1.91	1.39	2.03	1.14	
XLOC_010026	FFC1_09657	FFUJ_04178	uncharacterized protein FFUJ_04178							1.73	0.97	2.04		
XLOC_010033	FFC1_09665	FFUJ_04185	uncharacterized protein FFUJ_04185							3.50	2.89	2.61		
XLOC_010034	FFC1_09666	FFUJ_04186	uncharacterized protein FFUJ_04186							2.03	2.21	2.28	1.69	
XLOC_010515	FFC1_09670	FFUJ_04190	uncharacterized protein FFUJ_04190							3.10	3.02	3.88	4.34	
XLOC_010526	FFC1_09685	FFUJ_04205	uncharacterized protein FFUJ_04205							4.16	5.12			
XLOC_010044	FFC1_09686	FFUJ_04206	related to phospholipid-translocating ATPase		-2.34	-2.81				4.81	6.84	6.06	4.96	
XLOC_010045	FFC1_09687	FFUJ_04207	related to monocarboxylate transporter 2							-3.71	-4.31	-3.78	-2.80	
XLOC_010532	FFC1_09699	FFUJ_04219	related to integral membrane protein PTH11							-6.05	-5.48	-4.73	-5.27	
XLOC_010056	FFC1_09702	FFUJ_04222	related to nitrogen metabolic regulation protein nmr		1.42					3.62	4.28	4.74	4.09	
XLOC_010533	FFC1_09703	FFUJ_04223	uncharacterized protein FFUJ_04223							2.78	2.95	3.96	4.19	
XLOC_010534	FFC1_09704	FFUJ_04224	related to soluble fumarate reductase (NADH)	0.99						1.02	2.15	1.98	1.57	
XLOC_010057	FFC1_09707	FFUJ_04227	related to protein MCH2 (monocarboxylate permease homolog)							-3.19	-2.80	-3.00	-3.29	
XLOC_010537	FFC1_09708									7.11	4.14	7.44	2.75	
XLOC_010058	FFC1_09708									8.41	4.92	8.66	3.54	
XLOC_010538	FFC1_09709	FFUJ_04228	uncharacterized protein FFUJ_04228								2.45	3.22		
XLOC_010542	FFC1_09716	FFUJ_04234	probable alkaline protease (oryzin)							2.67	2.66	2.52	2.03	
XLOC_010062	FFC1_09717	FFUJ_04235	related to O-methyltransferase							-1.31	-2.05	-2.64		
XLOC_010070	FFC1_09729	FFUJ_14404	uncharacterized protein FFUJ_14404							-2.06	-2.04	-2.69	-2.56	
XLOC_010074	FFC1_09733	FFUJ_04250	uncharacterized protein FFUJ_04250										2.01	
XLOC_010548	FFC1_09737									-3.87	-3.04	-3.91	-3.08	
XLOC_010078	FFC1_09737									-4.48		-3.70		
XLOC_010079	FFC1_09738	FFUJ_04252	uncharacterized protein FFUJ_04252							-1.39	-2.03	-1.62	-1.50	
XLOC_010080	FFC1_09739										4.58			
XLOC_010552	FFC1_09744	FFUJ_04257	uncharacterized protein FFUJ_04257		1.16					1.50	2.04	2.61	2.01	
XLOC_010553	null				4.76									
XLOC_010555	null												-2.38	
XLOC_010088	FFC1_09755	FFUJ_04268	uncharacterized protein FFUJ_04268							2.04			2.34	
XLOC_010562	FFC1_09762	FFUJ_04275	related to long-chain fatty-acid-CoA ligase							2.39	2.24	2.75		
XLOC_010099	null								6.56				-3.88	
XLOC_010571	FFC1_09777	FFUJ_04290	uncharacterized protein FFUJ_04290							2.73	2.44	2.69	2.25	
XLOC_010582	null			-6.09							-5.81			
XLOC_010597	FFC1_09806									-1.67			-2.63	
XLOC_010601	FFC1_09810	FFUJ_04327	uncharacterized protein FFUJ_04327							2.63	2.03	2.26	1.82	
XLOC_010602	FFC1_09811	FFUJ_04328	uncharacterized protein FFUJ_04328							2.63	2.22	2.32	2.07	
XLOC_010122	FFC1_09812	FFUJ_04329	related to putative multidrug transporter							2.22	2.00	2.17	1.84	
XLOC_010124	FFC1_09814											2.82		
XLOC_010125	FFC1_09815	FFUJ_04331	related to Rtm1p							5.89	6.60	7.23	3.82	
XLOC_010606	FFC1_09819	FFUJ_04335	uncharacterized protein FFUJ_04335	1.61	2.86					1.06	2.32	3.42	1.30	
XLOC_010127	FFC1_09820	FFUJ_04336	uncharacterized protein FFUJ_04336	2.04	2.47	1.15				1.81	3.59	3.90	3.07	
XLOC_010607	null										-4.69			
XLOC_010608	null											5.44	5.98	
XLOC_010128	FFC1_09821	FFUJ_04337	probable glucose-regulated protein 78 of hsp70 family		0.85	0.85				1.94	1.62	2.09	2.72	
XLOC_010129	FFC1_09822	FFUJ_04338	uncharacterized protein FFUJ_04338							1.60		2.02	1.70	
XLOC_010611	FFC1_09826	FFUJ_04342	related to oxidoreductase, FAD-binding		1.72					3.92	3.23	6.45	4.21	
XLOC_010131	FFC1_09828	FFUJ_04344	uncharacterized protein FFUJ_04344							-2.05	-2.93	-2.50	-6.15	
XLOC_010134	FFC1_09832	FFUJ_04348	related to SER3-3-phosphoglycerate dehydrogenase							-1.49	-1.35	-1.34	-2.12	
XLOC_010615	FFC1_09836	FFUJ_04352	related to dlpA protein							-1.77	-2.34	-2.09	-1.67	
XLOC_010617	FFC1_09841	FFUJ_04357	related to SCP160 protein			1.58				1.57	1.47	2.21	2.79	
XLOC_010618	FFC1_09843	FFUJ_04359	uncharacterized protein FFUJ_04359							-2.10	-2.03	-1.70		
XLOC_010619	FFC1_09844	FFUJ_04360	related to D-arabinitol 2-dehydrogenase			-1.69				1.92	2.51	1.31		

XLOC_010620	null									5.66	4.16		
XLOC_010624	FFC1_09852	FFUJ_04368	uncharacterized protein FFUJ_04368							2.65	2.67	2.06	
XLOC_010145	FFC1_09853	FFUJ_04369	uncharacterized protein FFUJ_04369							2.15	2.53	2.62	
XLOC_010148	null			2.00							3.49		
XLOC_010166	FFC1_09886	FFUJ_04402	related to AHA1-stress-regulated cochaperone		1.47	1.41			2.04	0.77			
XLOC_010645	null									3.79			
XLOC_010175	FFC1_09911	FFUJ_04425	related to NADPH-ferrihemoprotein reductase and mammalian nitric-oxide synthases							-2.51	-2.14	-2.15	-1.36
XLOC_010176	FFC1_09913	FFUJ_04427	uncharacterized protein FFUJ_04427							-1.45	-2.00	-1.88	-1.16
XLOC_010178	FFC1_09915	FFUJ_04429	uncharacterized protein FFUJ_04429							-1.85	-2.10	-2.32	-2.78
XLOC_010182	FFC1_09922	FFUJ_04435	related to monocarboxylate transporter 4							-2.73	-2.58	-2.49	-2.39
XLOC_010186	FFC1_09926	FFUJ_04440	uncharacterized protein FFUJ_04440							-2.31	-3.26	-3.15	-2.87
XLOC_010198	FFC1_09946	FFUJ_04459	probable 3-isopropylmalate dehydratase	1.46	2.19							1.93	2.68
XLOC_010199	FFC1_09950	FFUJ_04463	uncharacterized protein FFUJ_04463							-3.38	-4.08	-3.55	-2.56
XLOC_010200	FFC1_09952	FFUJ_04465	probable aflatoxin efflux pump AFLT							-1.35	-2.04	-2.02	-1.63
XLOC_010201	FFC1_09953	FFUJ_04466	uncharacterized protein FFUJ_04466							-2.80	-5.46	-3.00	
XLOC_010678	FFC1_09956	FFUJ_04469	related to sorbitol dehydrogenase							-2.16	-1.43	-1.59	-2.60
XLOC_010206	FFC1_09962	FFUJ_04474	uncharacterized protein FFUJ_04474							1.93	2.26	2.78	3.15
XLOC_010209	FFC1_09967	FFUJ_04478	uncharacterized protein FFUJ_04478							3.15	2.99	2.80	2.45
XLOC_010211	FFC1_09970	FFUJ_04481	uncharacterized protein FFUJ_04481			-1.17				3.00	2.26	2.02	2.05
XLOC_010212	FFC1_09971	FFUJ_04482	uncharacterized protein FFUJ_04482			-1.93				3.11	2.75	1.68	
XLOC_010685	FFC1_09974	FFUJ_04484	probable osmotic sensitive-2 protein (putative mitogen-activated protein (MAP) kinase homolog)	2.04	1.59					1.14	2.98	2.73	1.57
XLOC_010686	null			3.00	2.83	1.94				3.37	6.93	4.34	4.43
XLOC_010221	null									4.37			
XLOC_010706	FFC1_10001	FFUJ_04508	probable blue-light-inducible Bli-3 protein	2.20	3.85	2.05				2.24	3.98	5.49	3.83
XLOC_010708	FFC1_10003	FFUJ_04510	related to laccase precursor			-1.06				3.10	3.64	3.70	2.78
XLOC_010230	FFC1_10012	FFUJ_04519	probable histidinol-phosphate transaminase			0.86				-3.98	-3.36	-2.89	-1.49
XLOC_010716	FFC1_10013	FFUJ_04520	related to DFG5 protein							-4.09	-3.98	-3.92	-4.36
XLOC_010232	FFC1_10017	FFUJ_04525	uncharacterized protein FFUJ_04525							-2.69	-3.02	-2.52	-3.61
XLOC_010721	FFC1_10019	FFUJ_04527	uncharacterized protein FFUJ_04527							3.50	3.17	2.81	1.93
XLOC_010233	tRNA-Ile(AAT)									3.69			
XLOC_010234	FFC1_10020	FFUJ_04528	related to glucan 1,3-beta-glucosidase							6.44	6.36	6.56	4.98
XLOC_010237	FFC1_10023	FFUJ_04531	uncharacterized protein FFUJ_04531							2.90	2.52	1.96	1.33
XLOC_010238	FFC1_10024	FFUJ_04532	related to aromatic-L-amino-acid decarboxylase							6.43	5.83	8.94	7.24
XLOC_010722	FFC1_10025	FFUJ_04533	uncharacterized protein FFUJ_04533								4.49		
XLOC_010729	FFC1_10037	FFUJ_04547	uncharacterized protein FFUJ_04547							2.21	2.18	1.98	1.65
XLOC_010735	FFC1_10047	FFUJ_04556	probable ferrochelatase	3.45	2.99	1.83					3.53	3.12	2.70
XLOC_010738	FFC1_10053	FFUJ_00010	probable fatty acid synthase, alpha subunit	1.03						-2.18	-1.54	-2.28	-1.81
XLOC_010251	FFC1_10054	FFUJ_04563	probable fatty-acyl-CoA synthase, beta subunit	1.11						-2.14	-1.35	-1.96	-1.60
XLOC_010741	null											-5.76	-4.56
XLOC_010744	FFC1_10061	FFUJ_04570	probable L-lactate dehydrogenase (cytochrome)							2.13	1.63	1.87	1.78
XLOC_010254	FFC1_10063	FFUJ_04572	related to mannose-6-phosphate isomerase		1.09					3.09	3.44	3.71	2.54
XLOC_010255	null											5.51	
XLOC_010256	FFC1_10064	FFUJ_04573	uncharacterized protein FFUJ_04573							-1.64	-2.07	-1.15	-1.48
XLOC_010751	FFC1_10071	FFUJ_04580	uncharacterized protein FFUJ_04580	2.57						-2.98			-1.85
XLOC_010262	FFC1_10078	FFUJ_04587	related to KTR1-mannosyltransferase involved in n-linked and o-linked glycosylation							1.57	1.88	2.28	
XLOC_010264	FFC1_10081	FFUJ_04590	uncharacterized protein FFUJ_04590							4.33	3.52		
XLOC_010761	FFC1_10088	FFUJ_04597	uncharacterized protein FFUJ_04597			-1.24			-1.08	-1.99	-1.60	-2.20	-2.13
XLOC_010767	FFC1_10098	FFUJ_04606	related to CTI6 Cyc8-Tup1 Interacting protein			1.21				1.99	1.86	2.99	3.17
XLOC_010768	FFC1_10100	FFUJ_04608	probable DPP1-diacylglycerol pyrophosphate phosphatase			0.95						1.62	2.02
XLOC_010772	FFC1_10105	FFUJ_04613	related to L-ornithine N5-hydroxylase	1.49		0.97				-2.90	-1.51	-2.25	-2.11
XLOC_010775	FFC1_10109	FFUJ_04616	related to cellobiose dehydrogenase		1.34					1.28	1.74	2.48	2.43
XLOC_010274	FFC1_10111	FFUJ_04618	related to aldehyde dehydrogenase		1.91	2.01				1.66	2.36	3.93	3.35
XLOC_011332	FFC1_10116	FFUJ_11192	uncharacterized protein FFUJ_11192							7.80	6.22	7.59	4.56
XLOC_010780	FFC1_10117	FFUJ_11191	related to C6 transcription factor							4.28	4.16	3.74	3.67
XLOC_010782	FFC1_10120	FFUJ_11188	related to mitochondrial Fe2+ transporter MMT1 and related transporters (cation diffusion facilitator superfamily)							4.74	3.17		3.43
XLOC_011335	FFC1_10122	FFUJ_11186	related to endo-1,3-beta-glucanase							2.13	2.06	2.24	3.15
XLOC_011336	FFC1_10123	FFUJ_11185	related to monophenol monooxygenase							5.02	4.74	6.99	4.98
XLOC_011337	FFC1_10124	FFUJ_11184	uncharacterized protein FFUJ_11184							2.96		2.33	4.00
XLOC_011340	FFC1_10129	FFUJ_11179	uncharacterized protein FFUJ_11179		-0.86					2.32	1.84	1.64	1.77
XLOC_010785	FFC1_10130	FFUJ_11178	related to O-methylsterigmatocystin oxidoreductase							5.34	7.50	6.44	
XLOC_011342	FFC1_10133	FFUJ_11175	related to cocaine esterase	1.09						8.15	6.68	6.10	4.34
XLOC_010787	FFC1_10134	FFUJ_11174	related to cytosine deaminase and related metal-dependent hydrolases	1.39	1.08					7.47	7.02	6.81	4.65
XLOC_010794	FFC1_10149	FFUJ_11157	uncharacterized protein FFUJ_11157							3.00	2.37	3.23	3.43
XLOC_010795	FFC1_10150	FFUJ_11156	related to GNAT family N-acetyltransferase							-4.08	-5.02	-5.84	-6.14
XLOC_011357	FFC1_10159	FFUJ_11147	related to putative tartrate transporter							5.51	4.25		
XLOC_011359	FFC1_10161	FFUJ_11145	uncharacterized protein FFUJ_11145	1.37							2.08	1.31	
XLOC_010799	FFC1_10164	FFUJ_11142	probable general amino acid permease		-2.91						-1.45	-2.60	
XLOC_010801	FFC1_10168										-2.62		
XLOC_011363	FFC1_10169	FFUJ_11138	uncharacterized protein FFUJ_11138							2.64	1.92		

XLOC_010802	FFC1_10170	FFUJ_11137	uncharacterized protein FFUJ_11137							3.60	2.20		
XLOC_011365	FFC1_10174	FFUJ_11133	related to novobiocin biosynthesis protein novR							-2.14	-4.70	-5.15	-5.67
XLOC_010809	FFC1_10184	FFUJ_11122	uncharacterized protein FFUJ_11122		-2.23	-2.10				5.36	4.35		
XLOC_011373	FFC1_10191	FFUJ_11115	uncharacterized protein FFUJ_11115							3.66			
XLOC_011374	FFC1_10193									0.95	1.64	1.96	2.26
XLOC_011375	FFC1_10195	FFUJ_11111	uncharacterized protein FFUJ_11111							-5.92			
XLOC_011378	FFC1_10198	FFUJ_11108	uncharacterized protein FFUJ_11108		-1.03					1.77	1.26		2.21
XLOC_010816	FFC1_10200	FFUJ_11106	related to benzoylformate decarboxylase							4.24	2.11	2.86	3.36
XLOC_011382	FFC1_10203	FFUJ_11103	probable D-lactate dehydrogenase (cytochrome)								2.70	3.15	
XLOC_011384	FFC1_10207	FFUJ_11099	uncharacterized protein FFUJ_11099							5.75			
XLOC_011385	FFC1_10209	FFUJ_11097	uncharacterized protein FFUJ_11097		-4.23					6.82	5.88		
XLOC_011387	FFC1_10212										-4.73		-4.81
XLOC_010821	FFC1_10217	FFUJ_11090	related to oxidoreductase							-1.55	-2.38	-2.12	-1.35
XLOC_011395	FFC1_10221	FFUJ_11086	related to 5-oxoprolinase							-2.81	-2.41	-2.89	-2.23
XLOC_011396	FFC1_10222	FFUJ_11085	uncharacterized protein FFUJ_11085							-5.43	-5.72	-6.82	-4.50
XLOC_010822	FFC1_10223	FFUJ_11084	related to transporter protein							-3.23	-4.33	-5.12	-4.60
XLOC_011397	FFC1_10224	FFUJ_11083	related to formate transport protein							-4.43	-5.19	-4.92	-4.25
XLOC_010823	FFC1_10225	FFUJ_11082	uncharacterized protein FFUJ_11082								-1.76		-3.01
XLOC_010825	FFC1_10229	FFUJ_11078	uncharacterized protein FFUJ_11078									3.45	3.33
XLOC_010826	FFC1_10232	FFUJ_11075	uncharacterized protein FFUJ_11075							6.50	6.82	7.67	8.01
XLOC_011402	FFC1_10233	FFUJ_11074	related to arylformamidase							7.64	6.79	5.46	4.60
XLOC_011404	FFC1_10235	FFUJ_11072	related to allantoate permease								-5.42		
XLOC_010827	FFC1_10236	FFUJ_11071	probable D-lactate dehydrogenase (cytochrome)								-2.02	-4.17	
XLOC_010828	null										-4.63		
XLOC_010829	FFC1_10237									-1.52	-2.79	-3.73	
XLOC_011409	FFC1_10244	FFUJ_11065	related to phosphatidylserine decarboxylase 2							10.60	10.27	7.31	
XLOC_010833	FFC1_10245	FFUJ_11064	uncharacterized protein FFUJ_11064							-4.49	-3.67	-4.02	-2.20
XLOC_011410	FFC1_10246	FFUJ_11063	related to fructosyl amino acid oxidase							-2.46	-2.61	-3.44	
XLOC_010838	FFC1_10252	FFUJ_11057	related to DAL5-Allantoate and ureidosuccinate permease										-4.14
XLOC_010839	FFC1_10253	FFUJ_11056	uncharacterized protein FFUJ_11056							-1.89	-2.66	-3.10	
XLOC_010842	FFC1_10256	FFUJ_11053	uncharacterized protein FFUJ_11053							4.60	4.42	4.23	6.11
XLOC_011412	FFC1_10257	FFUJ_11052	related to quinone reductase						2.36		3.23	2.76	2.26
XLOC_011413	FFC1_10258	FFUJ_11051	uncharacterized protein FFUJ_11051							3.25	3.08	2.26	
XLOC_010845	FFC1_10262	FFUJ_11049	uncharacterized protein FFUJ_11049							3.10			
XLOC_011417	FFC1_10267	FFUJ_11045	related to phospholipase A2, cytosolic		2.46	1.68						3.02	2.37
XLOC_010848	FFC1_10269	FFUJ_11043	uncharacterized protein FFUJ_11043		2.15					7.58	7.27	7.01	6.88
XLOC_011419	FFC1_10270	FFUJ_11042	related to oxidoreductase		2.72	1.26				0.90		3.13	1.89
XLOC_011423	FFC1_10275	FFUJ_11037	related to endo-arabinase							2.16	2.60	1.89	
XLOC_010852	FFC1_10278									2.61	3.54	2.89	2.16
XLOC_010853	FFC1_10279									5.52	4.35		
XLOC_011425	FFC1_10282				-1.36	-1.84				3.60	2.41	1.49	
XLOC_011428	FFC1_10285									-2.42	-3.66	-4.11	-2.34
XLOC_011435	FFC1_10299									5.25			
XLOC_010872	FFC1_10319	FFUJ_11026	related to 6-hydroxy-D-nicotine oxidase							4.98	5.66	5.13	
XLOC_011447	FFC1_10320	FFUJ_11025	related to protoporphyrinogen oxidase							6.03	6.40	5.40	
XLOC_010874	FFC1_10323	FFUJ_11022	related to cell wall mannoprotein							-7.83	-6.98	-6.15	-6.82
XLOC_010877	FFC1_10332										2.12	2.75	2.34
XLOC_011457	FFC1_10337	FFUJ_11012	related to PHO89-Na+/phosphate co-transporter							8.02	9.84	9.51	8.03
XLOC_010880	FFC1_10339	FFUJ_11010	related to LYS12-homo-isocitrate dehydrogenase							2.40	3.33	2.75	1.97
XLOC_010881	FFC1_10340	FFUJ_11009	uncharacterized protein FFUJ_11009							2.49	2.53	2.34	
XLOC_010882	FFC1_10341	FFUJ_11008	uncharacterized protein FFUJ_11008								5.61		
XLOC_011459	FFC1_10346	FFUJ_11004	probable endopolygalacturonase							1.28	1.23	2.09	3.15
XLOC_011460	FFC1_10348	FFUJ_11001	uncharacterized protein FFUJ_11001										5.19
XLOC_010890	FFC1_10351	FFUJ_10998	uncharacterized protein FFUJ_10998							7.17	7.72	8.64	9.52
XLOC_010891	FFC1_10352	FFUJ_10997	uncharacterized protein FFUJ_10997							8.95	8.72	10.15	8.58
XLOC_010892	FFC1_10353	FFUJ_10996	probable NADPH2 dehydrogenase chain OYE2							10.40	9.69	10.50	10.20
XLOC_011462	FFC1_10354	FFUJ_10995	related to triacylglycerol lipase II precursor							3.20	2.82	3.81	5.23
XLOC_011463	FFC1_10355	FFUJ_10994	uncharacterized protein FFUJ_10994							1.88	1.14		2.10
XLOC_011465	FFC1_10357	FFUJ_10992	related to SPR1-exo-1,3-beta-glucanase precursor							2.37	2.10	2.81	2.38
XLOC_010893	FFC1_10358	FFUJ_10991	related to ferric reductase Fre2p									5.74	5.97
XLOC_010894	FFC1_10360	FFUJ_10989	uncharacterized protein FFUJ_10989							-2.27	-2.47	-2.75	-2.57
XLOC_010897	FFC1_10365	FFUJ_10982	uncharacterized protein FFUJ_10982								-2.32	-1.76	
XLOC_011471	FFC1_10369	FFUJ_10978	related to endochitinase							3.61	3.67	3.64	3.90
XLOC_010901	FFC1_10371	FFUJ_10976	related to ARG81-transcription factor involved in arginine metabolism		-2.09								
XLOC_010906	FFC1_10378	FFUJ_10970	related to NmrA-like family protein							2.67		2.92	
XLOC_011486	FFC1_10396	FFUJ_10952	uncharacterized protein FFUJ_10952							-8.00	-7.16	-6.89	-6.68
XLOC_011488	FFC1_10398	FFUJ_10950	related to oxidoreductase								-2.64		
XLOC_011489	FFC1_10400	FFUJ_10948	probable general amino acid permease							-3.00		-4.79	
XLOC_010914	FFC1_10401	FFUJ_10947	uncharacterized protein FFUJ_10947							-2.59	-4.66	-3.85	-2.09
XLOC_011490	FFC1_10402	FFUJ_10946	uncharacterized protein FFUJ_10946							-2.09	-2.83	-1.90	-2.67
XLOC_010915	FFC1_10403	FFUJ_10945	related to prenyl cysteine carboxyl methyltransferase						1.50		-1.63	-1.93	-3.50
XLOC_010916	FFC1_10404	FFUJ_10944	uncharacterized protein FFUJ_10944							-3.19	-3.37	-3.19	-3.65
XLOC_011491	FFC1_10406	FFUJ_10942	uncharacterized protein FFUJ_10942							-2.50	-3.94	-4.07	-3.21
XLOC_010922	null				-4.35	-4.56							-4.09
XLOC_011494	FFC1_10414	FFUJ_10934	non-ribosomal peptide synthetase			2.38				-3.43	-4.66	-3.88	-2.45
XLOC_010925	FFC1_10415	FFUJ_10933	probable enoyl-CoA hydratase precursor, mitochondrial			1.18				-1.71	-2.67	-3.10	-1.61

XLOC_011495	FFC1_10416	FFUJ_10932	related to triacylglycerol lipase II precursor						2.14	-4.30	-3.10	-4.00	-3.14
XLOC_011497	FFC1_10419	FFUJ_10929	uncharacterized protein FFUJ_10929										5.30
XLOC_011500	FFC1_10422	FFUJ_10926	uncharacterized protein FFUJ_10926							-3.08	-3.13	-3.03	-2.62
XLOC_011501	FFC1_10423	FFUJ_10925	uncharacterized protein FFUJ_10925							-2.98	-3.14	-2.80	-2.04
XLOC_010928	FFC1_10424	FFUJ_10924	uncharacterized protein FFUJ_10924							-4.66	-4.97	-5.80	-5.18
XLOC_010931	FFC1_10431	FFUJ_10916	uncharacterized protein FFUJ_10916							-3.72	-6.30	-5.53	-5.33
XLOC_010935	FFC1_10439	FFUJ_10908	related to double substrate-specificity short chain dehydrogenase/reductase 2							3.73	2.55	4.57	3.24
XLOC_011511	FFC1_10440	FFUJ_10907	related to pisatin demethylase cytochrome P450							4.81			
XLOC_011514	FFC1_10444	FFUJ_10902	uncharacterized protein FFUJ_10902								-4.71		
XLOC_010939	FFC1_10450	FFUJ_10896	related to 2,5-diketo-D-gluconic acid reductase		4.41	2.69				7.05	8.04	7.75	7.03
XLOC_010940	FFC1_10451	FFUJ_10895	related to galactinol synthase		9.80	7.05						7.83	7.15
XLOC_011522	FFC1_10456	FFUJ_10890	related to chitinase		1.49	1.04				3.50	2.90	4.51	3.49
XLOC_011523	FFC1_10457	FFUJ_10889	galactose oxidase precursor							2.07	2.51	2.69	2.69
XLOC_010943	FFC1_10461	FFUJ_10885	uncharacterized protein FFUJ_10885								-5.04		-5.51
XLOC_010944	FFC1_10465	FFUJ_10881	uncharacterized protein FFUJ_10881							-2.39	-3.91	-5.72	
XLOC_011529	FFC1_10466	FFUJ_10880	uncharacterized protein FFUJ_10880							5.69	5.24	6.73	8.15
XLOC_010945	FFC1_10467	FFUJ_10879	related to integral membrane protein							4.94	4.33	3.92	3.28
XLOC_011530	FFC1_10468	FFUJ_10878	related to peroxisomal amine oxidase (copper-containing)		-1.69					4.09	2.98		4.31
XLOC_011531	FFC1_10469	FFUJ_10877	uncharacterized protein FFUJ_10877										4.94
XLOC_011533	FFC1_10471	FFUJ_10875	uncharacterized protein FFUJ_10875			2.31					1.73	2.85	3.29
XLOC_011535	FFC1_10473	FFUJ_10874	uncharacterized protein FFUJ_10874	1.73	1.44	1.17	0.68			1.28	2.28	2.45	2.79
XLOC_011544	FFC1_10490	FFUJ_10860	related to integral membrane protein							-5.77			
XLOC_011548	FFC1_10494	FFUJ_10856	uncharacterized protein FFUJ_10856							3.24	3.01	2.42	1.92
XLOC_010955	FFC1_10495	FFUJ_10855	probable PDC1-Pyruvate decarboxylase, isozyme 1							3.45	3.04	2.75	2.84
XLOC_010956	FFC1_10496	FFUJ_10854	related to COG3602 family protein							4.52	3.42	3.88	2.30
XLOC_011551	FFC1_10499	FFUJ_10851	related to ketoreductases	1.52	1.50					3.53	3.76	4.51	3.10
XLOC_010957	FFC1_10500	FFUJ_10850	related to tol protein							6.10	5.33	4.86	4.46
XLOC_010958	FFC1_10501	FFUJ_10849	related to hexose transporter protein							2.25	2.89	2.26	
XLOC_010960	FFC1_10507	FFUJ_10843	uncharacterized protein FFUJ_10843							6.00			5.23
XLOC_011559	FFC1_10514	FFUJ_10836	related to xylosidase/arabinosidase							4.92	4.37	3.91	3.59
XLOC_010964	FFC1_10515	FFUJ_10835	related to photosystem II protein D2							3.53	3.16	3.20	3.35
XLOC_010965	FFC1_10517	FFUJ_10832	uncharacterized protein FFUJ_10832									5.65	6.51
XLOC_010966	FFC1_10518	FFUJ_10831	uncharacterized protein FFUJ_10831							4.78	3.98	6.45	
XLOC_011561	FFC1_10519	FFUJ_10830	probable neutral amino acid permease							1.90	2.18	1.88	
XLOC_010967	FFC1_10520	FFUJ_10829	uncharacterized protein FFUJ_10829							8.71	8.98	9.22	8.17
XLOC_010968	FFC1_10521	FFUJ_10828	probable DUF895 domain membrane protein							3.09	3.05	3.29	3.42
XLOC_010969	FFC1_10523	FFUJ_10826	uncharacterized protein FFUJ_10826		1.47					2.26	3.47	3.47	4.07
XLOC_011570	FFC1_10531	FFUJ_10818	probable NADPH2 dehydrogenase chain OYE2								2.80	3.44	2.47
XLOC_011574	FFC1_10541	FFUJ_10808	uncharacterized protein FFUJ_10808							9.89	7.69	9.21	9.77
XLOC_010978	FFC1_10542	FFUJ_10807	uncharacterized protein FFUJ_10807		-1.46					10.83	8.90	9.28	10.85
XLOC_010979	FFC1_10543	FFUJ_10806	related to RTM1 protein								4.82		
XLOC_011575	FFC1_10545	FFUJ_10804	related to hydroxyquinol-1,2-dioxygenase		1.07					3.87	3.62	3.29	3.97
XLOC_011579	FFC1_10550	FFUJ_10800	uncharacterized protein FFUJ_10800							6.33	6.59	7.72	6.04
XLOC_011580	FFC1_10551	FFUJ_10799	related to oxalate decarboxylase	1.28	1.84					6.70	7.38	7.07	6.78
XLOC_010982	FFC1_10552	FFUJ_10798	uncharacterized protein FFUJ_10798		-2.49	-1.80						-2.18	
XLOC_011582	FFC1_10555									7.83	8.11	7.39	8.45
XLOC_011585	FFC1_10560	FFUJ_10790	uncharacterized protein FFUJ_10790							3.62	4.57	6.64	4.92
XLOC_011588	FFC1_10564	FFUJ_10786	uncharacterized protein FFUJ_10786							3.49	3.25	3.31	3.18
XLOC_011593	FFC1_10571	FFUJ_10779	related to Staphylococcus multidrug resistance protein		-2.59	-2.56							-1.35
XLOC_010993	FFC1_10575	FFUJ_10778	uncharacterized protein FFUJ_10778							-2.22			
XLOC_011596	FFC1_10577	FFUJ_10776	related to beta-galactosidase							4.37	4.63	4.06	3.05
XLOC_011600	FFC1_10580	FFUJ_10773	uncharacterized protein FFUJ_10773										4.97
XLOC_011601	FFC1_10583	FFUJ_10770	related to transporter protein HOL1							4.09	4.25	4.26	3.90
XLOC_010997	FFC1_10584	FFUJ_10769	related to general amidase							3.91	4.12	4.31	4.04
XLOC_010999	FFC1_10586	FFUJ_10767	uncharacterized protein FFUJ_10767		1.59					3.46	3.48	4.50	7.20
XLOC_011602	FFC1_10587	FFUJ_10766	uncharacterized protein FFUJ_10766							3.87	4.50	5.54	3.44
XLOC_011603	FFC1_10588	FFUJ_10765	related to beta-galactosidase							3.88	2.95	2.54	
XLOC_011604	FFC1_10589	FFUJ_10764	related to sexual differentiation process protein isp4		-0.88	-1.48				-3.91	-3.99	-4.31	-4.44
XLOC_011000	FFC1_10595	FFUJ_10759	uncharacterized protein FFUJ_10759								-2.33		
XLOC_011610	FFC1_10598	FFUJ_10756	uncharacterized protein FFUJ_10756		1.50					1.37	1.67	3.19	2.38
XLOC_011004	FFC1_10601	FFUJ_10753	related to endopeptidase K							7.47	7.79	7.37	7.23
XLOC_011614	FFC1_10607	FFUJ_10748	uncharacterized protein FFUJ_10748							2.10		3.06	3.52
XLOC_011615	FFC1_10608	FFUJ_10747	probable iron-dependent peroxidase		3.49	1.82						3.54	4.34
XLOC_011008	FFC1_10609	FFUJ_10746	related to the plant PR-1 class of pathogen related proteins							2.64	2.61	2.72	2.67
XLOC_011009	FFC1_10611	FFUJ_10744	uncharacterized protein FFUJ_10744								4.65	5.78	5.37
XLOC_011617	FFC1_10612	FFUJ_10743	related to integral membrane protein PTH11							3.96		2.23	7.67
XLOC_011010	FFC1_10613	FFUJ_10742	related to oxidoreductase							4.12	5.15	4.76	8.14
XLOC_011014	null									-1.54	-1.39	-2.07	
XLOC_011626	FFC1_10626	FFUJ_10730	related to O-methylsterigmatocystin oxidoreductase							2.05		1.47	
XLOC_011627	FFC1_10629	FFUJ_10727	related to maltose O-acetyltransferase							-1.51	-1.89	-2.27	-2.00
XLOC_011628	FFC1_10630	FFUJ_10726	uncharacterized protein FFUJ_10726							3.48	2.97	3.54	2.53
XLOC_011632	FFC1_10638	FFUJ_10718	related to cocaine esterase							4.70		4.77	
XLOC_011635	FFC1_10643	FFUJ_10713	related to STB5-transcription factor							5.46		5.97	
XLOC_011026	FFC1_10644	FFUJ_10712	related to DHA14-like major facilitator efflux transporter (MFS transporter)							1.84	1.68	2.98	2.33
XLOC_011637	FFC1_10645	FFUJ_10711	probable mfs-multidrug-resistance transporter		1.98					4.83	5.95	6.25	4.37

XLOC_011029	FFC1_10648	FFUJ_10709	related to methyltransferase		-3.21							-3.07	
XLOC_011030	FFC1_10649	FFUJ_10708	uncharacterized protein FFUJ_10708							6.74	5.33	6.01	5.66
XLOC_011032	FFC1_10652	FFUJ_10705	uncharacterized protein FFUJ_10705		2.46							5.09	
XLOC_011035	FFC1_10657	FFUJ_10702	related to isoamyl alcohol oxidase							3.81		2.92	
XLOC_011037	FFC1_10659	FFUJ_10700	uncharacterized protein FFUJ_10700		-1.83	-3.00				3.00			
XLOC_011642	FFC1_10660	FFUJ_10699	related to DFG5 protein							-5.05	-7.07	-4.95	-4.64
XLOC_011038	FFC1_10664									2.41	2.71	2.98	3.05
XLOC_011039	FFC1_10665									2.44	3.90		3.56
XLOC_011646	FFC1_10666	FFUJ_10694	uncharacterized protein FFUJ_10694							5.22		5.10	5.37
XLOC_011647	FFC1_10667	FFUJ_10693	related to tol protein							3.13	2.37	3.35	3.98
XLOC_011648	FFC1_10668	FFUJ_10692	related to NADH oxidase		1.48					7.87	7.34	5.83	4.51
XLOC_011649	FFC1_10669	FFUJ_10691	related to maackiain detoxification protein 1							6.01	5.26	6.68	6.16
XLOC_011040	FFC1_10670	FFUJ_10690	related to monosaccharide transporter									2.96	
XLOC_011654	FFC1_10678	FFUJ_10682	related to O-methylsterigmatocystin oxidoreductase							9.62	7.50	6.17	9.72
XLOC_011655	FFC1_10679	FFUJ_10681	uncharacterized protein FFUJ_10681							6.86		5.94	6.34
XLOC_011658	FFC1_10681	FFUJ_10679	probable alpha-glucosidase (maltase)							-1.14	-2.07	-1.67	-1.23
XLOC_011044	FFC1_10682	FFUJ_10678	related to hexose transporter protein										-2.90
XLOC_011661	FFC1_10685	FFUJ_10675	related to non-ribosomal peptide synthetase							-2.80	-2.98	-3.18	-4.56
XLOC_011665	FFC1_10691	FFUJ_10669	related to transcriptional activator Mut3p							3.01	2.53	3.06	1.74
XLOC_011047	FFC1_10692	FFUJ_10668	probable glycine/D-amino acid oxidases (deaminating)							3.75	6.90	6.00	
XLOC_011048	FFC1_10693	FFUJ_10667	related to nucleoside-diphosphate-sugar epimerase							2.94	3.00	4.79	4.32
XLOC_011666	FFC1_10695	FFUJ_10665	related to salicylate 1-monooxygenase							4.27	4.79	6.35	5.31
XLOC_011672	FFC1_10703	FFUJ_10658	related to microcin C7 self-immunity protein mccF		-1.68						-1.17	-2.16	
XLOC_011054	FFC1_10708	FFUJ_10654	related to hydroxyquinol-1,2-dioxygenase							2.34		1.68	2.39
XLOC_011677	FFC1_10713	FFUJ_10649	related to toxD gene							-1.42	-2.81	-2.15	-1.75
XLOC_011062	FFC1_10717	FFUJ_10645	related to reductases		2.03								
XLOC_011063	FFC1_10718	FFUJ_10644	uncharacterized protein FFUJ_10644							2.09	2.15	2.59	3.76
XLOC_011680	FFC1_10720	FFUJ_10642	related to integral membrane protein pth11							-1.90	-1.88	-2.56	-1.96
XLOC_011065	FFC1_10721	FFUJ_10641	related to triacylglycerol lipase V precursor							-2.11	-1.79	-1.90	-1.28
XLOC_011066	FFC1_10725	FFUJ_10638	uncharacterized protein FFUJ_10638							-5.47	-5.07	-4.88	-7.31
XLOC_011067	FFC1_10726	FFUJ_10637	uncharacterized protein FFUJ_10637							1.37		1.06	2.10
XLOC_011685	FFC1_10730	FFUJ_10633	uncharacterized protein FFUJ_10633							3.19		4.82	4.35
XLOC_011686	FFC1_10731	FFUJ_10632	related to ankyrin							1.88	1.11	2.33	1.68
XLOC_011070	FFC1_10732	FFUJ_10631	uncharacterized protein FFUJ_10631							2.92	2.23	2.83	2.20
XLOC_011071	FFC1_10734	FFUJ_10629	uncharacterized protein FFUJ_10629							4.75	3.69		2.86
XLOC_011078	FFC1_10744	FFUJ_10619	uncharacterized protein FFUJ_10619									5.03	
XLOC_011693	FFC1_10745	FFUJ_10618	related to dihydroflavonol-4-reductases		1.84					2.57	2.59	4.25	3.25
XLOC_011082	FFC1_10749	FFUJ_10614	related to dihydrodipicolinate synthase							5.71			5.78
XLOC_011086	FFC1_10754	FFUJ_10609	related to C4-dicarboxylate transport protein mae1							5.42			
XLOC_011091	FFC1_10762	FFUJ_10602	related to methyltransferase LaeA-like	-2.52	-4.05	-2.76				8.95	6.44		6.29
XLOC_011092	FFC1_10763	FFUJ_10601	uncharacterized protein FFUJ_10601							5.27			6.02
XLOC_011094	FFC1_10766	FFUJ_10599	related to cellulose binding protein CEL1							4.31	4.41	4.44	4.84
XLOC_011700	FFC1_10768	FFUJ_10597	uncharacterized protein FFUJ_10597		-1.66	-2.34				7.48	7.62	5.76	7.16
XLOC_011096	FFC1_10769	FFUJ_10596	probable alpha-glucuronidase precursor								5.70		
XLOC_011098	FFC1_10772	FFUJ_10593	uncharacterized protein FFUJ_10593		-2.00					1.19			
XLOC_011099	FFC1_10773	FFUJ_10592	related to flavoprotein							7.44	6.95	7.38	7.28
XLOC_011100	FFC1_10774	FFUJ_10591	related to integral membrane protein							3.02	3.48		
XLOC_011704	FFC1_10779	FFUJ_10586	uncharacterized protein FFUJ_10586							-5.98	-6.36	-4.86	-4.91
XLOC_011108	FFC1_10787	FFUJ_10578	uncharacterized protein FFUJ_10578							3.82	3.82	3.89	3.07
XLOC_011713	FFC1_10798	FFUJ_10567	uncharacterized protein FFUJ_10567										4.01
XLOC_011714	FFC1_10801	FFUJ_10564	uncharacterized protein FFUJ_10564							-2.42	-3.30	-3.92	-2.04
XLOC_011117	FFC1_10802	FFUJ_10563	related to interferon-regulated resistance GTP-binding protein		-1.86						-1.54	-2.91	
XLOC_011120	FFC1_10807	FFUJ_10558	probable developmental regulator flbA							-1.70	-2.16	-2.00	-2.30
XLOC_011122	FFC1_10810	FFUJ_10555	related to GPI anchored protein							3.00	2.44	2.79	2.02
XLOC_011720	FFC1_10811	FFUJ_10554	related to glyoxalase family protein							-3.35	-2.93	-2.07	-2.61
XLOC_011127	FFC1_10816	FFUJ_10549	related to adenine phosphoribosyltransferase							4.23	6.42	3.45	6.81
XLOC_011725	FFC1_10823	FFUJ_10542	related to tetracycline resistance proteins							-2.29	-2.25		
XLOC_011726	FFC1_10824	FFUJ_10541	uncharacterized protein FFUJ_10541		-2.11					1.78			
XLOC_011135	FFC1_10828	FFUJ_10538	uncharacterized protein FFUJ_10538							4.79			
XLOC_011727	FFC1_10829	FFUJ_10537	related to dis1-suppressing protein kinase dsk1							4.93			
XLOC_011136	FFC1_10830	FFUJ_10536	uncharacterized protein FFUJ_10536										4.24
XLOC_011728	FFC1_10831	FFUJ_10535	related to peroxisomal short-chain alcohol dehydrogenase								2.25		
XLOC_011138	FFC1_10834	FFUJ_10532	uncharacterized protein FFUJ_10532							1.56	2.42	2.28	
XLOC_011139	FFC1_10835	FFUJ_10531	probable endochitinase							6.35	8.35	8.08	7.48
XLOC_011731	FFC1_10838	FFUJ_10528	uncharacterized protein FFUJ_10528							2.46	1.92	2.66	3.33
XLOC_011732	FFC1_10839	FFUJ_10527	related to integral membrane protein PTH11							5.16	5.61	5.26	4.19
XLOC_011736	FFC1_10846	FFUJ_10520	related to dienelactone hydrolase and related enzymes	0.83	1.08					3.28	3.73	4.17	3.15
XLOC_011145	FFC1_10847	FFUJ_10519	related to aflatoxin efflux pump AFLT							4.19	5.62	3.66	7.09
XLOC_011146	FFC1_10848	FFUJ_10518	probable beta-glucosidase 1 precursor							3.34	4.45	2.90	
XLOC_011737	FFC1_10850	FFUJ_10516	related to O-methyltransferase B		-4.82								
XLOC_011149	FFC1_10852	FFUJ_10514	uncharacterized protein FFUJ_10514		1.07	1.30				6.73	6.41	9.18	8.86
XLOC_011738	FFC1_10853	FFUJ_10513	uncharacterized protein FFUJ_10513							10.00	9.03	8.78	7.55
XLOC_011150	null									8.42	6.83	7.90	6.61
XLOC_011739	FFC1_10854	FFUJ_10512	related to hydrolases or acyltransferases (alpha/beta hydrolase superfamily)		1.11					6.73	7.26	7.41	7.25

XLOC_011152	FFC1_10856	FFUJ_10510	related to isotrichodermin C-15 hydroxylase (cytochrome P-450 monooxygenase CYP65A1)								4.97	4.94	
XLOC_011155	FFC1_10861	FFUJ_10505	uncharacterized protein FFUJ_10505		6.74							3.84	
XLOC_011156	FFC1_10862	FFUJ_10504	uncharacterized protein FFUJ_10504							2.16	2.42	1.99	1.72
XLOC_011158	FFC1_10864	FFUJ_10502	uncharacterized protein FFUJ_10502		1.90					5.97	4.33	7.79	4.11
XLOC_011159	FFC1_10865	FFUJ_10501	related to triacylglycerol lipase V precursor		3.52	3.14						7.82	7.67
XLOC_011160	FFC1_10866	FFUJ_10500	uncharacterized protein FFUJ_10500									5.48	
XLOC_011747	FFC1_10867	FFUJ_10499	uncharacterized protein FFUJ_10499		3.08						5.00	6.99	6.14
XLOC_011748	FFC1_10868	FFUJ_10498	uncharacterized protein FFUJ_10498									6.10	5.96
XLOC_011749	FFC1_10869				3.60	3.72						6.90	7.25
XLOC_011161	FFC1_10870	FFUJ_10497	uncharacterized protein FFUJ_10497		1.35	1.48				5.94	5.53	6.61	6.42
XLOC_011750	FFC1_10871	FFUJ_10496	related to glutamine rich protein, nitrogen starvation-induced							4.04	3.77	4.03	3.87
XLOC_011751	FFC1_10872	FFUJ_10495	related to pathway-specific regulatory protein nit-4							5.11	5.08	5.54	4.66
XLOC_011163	FFC1_10874	FFUJ_10493	related to putative tartrate transporter							2.99	2.99	2.63	3.02
XLOC_011164	FFC1_10875	FFUJ_10492	related to transporter protein							4.91		6.11	2.82
XLOC_011752	FFC1_10876	FFUJ_10491	related to LSB3-possible role in the regulation of actin cytoskeletal organization		1.46					3.57	3.39	4.29	2.61
XLOC_011165	FFC1_10877	FFUJ_10490	related to aminopeptidase			-1.70				2.33		1.88	
XLOC_011757	FFC1_10886									2.57			
XLOC_011759	FFC1_10889				-2.17	-2.25				-1.63	-2.78	-3.39	-2.68
XLOC_011762	FFC1_10898	FFUJ_10471	related to binuclear zinc cluster transcription factor that regulates the ratio between aurofusarin and rubrofusarin biosynthesis							-1.45	-1.92	-2.26	-1.35
XLOC_011179	FFC1_10903	FFUJ_10466	related to Auxin Efflux Carrier superfamily		3.27						6.04	7.36	6.25
XLOC_011770	FFC1_10911	FFUJ_10458	probable endothiapepsin precursor							5.64	6.34	7.44	5.18
XLOC_011184	FFC1_10912	FFUJ_10457	related to nitrate assimilation regulatory protein nirA							3.51	3.36	4.50	3.77
XLOC_011185	FFC1_10913	FFUJ_10456	related to chloroperoxidase		1.99					5.68	4.71	4.89	7.66
XLOC_011188	FFC1_10916	FFUJ_10453	uncharacterized protein FFUJ_10453		2.67	1.98				6.67	5.68	7.48	9.70
XLOC_011771	FFC1_10917	FFUJ_10452	related to 3-oxoacyl			1.63				2.75	3.36	3.85	4.53
XLOC_011773	FFC1_10919	FFUJ_10450	related to integral membrane protein PTH11							2.05	2.62	2.01	2.07
XLOC_011189	FFC1_10920	FFUJ_10449	related to alcohol oxidase							2.22	2.25	1.89	1.81
XLOC_011190	FFC1_10922	FFUJ_10447	uncharacterized protein FFUJ_10447								1.81		2.51
XLOC_011197	FFC1_10934	FFUJ_10439	uncharacterized protein FFUJ_10439							-7.73	-7.08		
XLOC_011198	FFC1_10935	FFUJ_10438	uncharacterized protein FFUJ_10438							-5.03	-5.62	-4.20	-2.76
XLOC_011786	FFC1_10945	FFUJ_10431	related to peptide transporter							-4.79	-4.50	-5.38	-7.89
XLOC_011203	FFC1_10948	FFUJ_10428	probable cutinase 1 precursor							-9.24	-7.91	-7.92	-7.57
XLOC_011789	FFC1_10950	FFUJ_10426	uncharacterized protein FFUJ_10426							-2.59	-2.80		
XLOC_011790	FFC1_10952	FFUJ_10423	uncharacterized protein FFUJ_10423									3.60	
XLOC_011209	null				2.58					4.80	4.18	8.26	7.07
XLOC_011216	FFC1_10970	FFUJ_10407	related to glucan 1,3-beta-glucosidase							4.56	5.31	4.30	4.45
XLOC_011220	FFC1_10975	FFUJ_10402	related to tol protein							-4.32			
XLOC_011224	FFC1_10979									-1.89	-3.10	-2.99	
XLOC_011800	FFC1_10980	FFUJ_10398	uncharacterized protein FFUJ_10398		-2.76					9.45	8.97	6.58	7.22
XLOC_011225	FFC1_10981	FFUJ_10397	uncharacterized protein FFUJ_10397		2.18					3.72	2.25	3.19	5.10
XLOC_011226	FFC1_10982	FFUJ_10396	uncharacterized protein FFUJ_10396							-5.88	-4.95	-4.51	
XLOC_011233	FFC1_10993	FFUJ_10385	uncharacterized protein FFUJ_10385								-2.02	-2.02	-2.28
XLOC_011808	FFC1_11000	FFUJ_10378	related to lipase 1							3.02			
XLOC_011810	FFC1_11004	FFUJ_10374	methyltransferase							-3.17	-3.19	-3.14	-2.44
XLOC_011240	FFC1_11005	FFUJ_10373	related to nitrogen metabolic regulation protein nmr			2.02				-3.74	-4.17	-3.59	-1.78
XLOC_011812	FFC1_11008	FFUJ_14903	uncharacterized protein FFUJ_14903							-4.22	-3.85	-4.23	-3.92
XLOC_011242	FFC1_11009	FFUJ_10370	related to purine transporter azgA									-4.93	-6.64
XLOC_011813	FFC1_11010	FFUJ_10369	uncharacterized protein FFUJ_10369								2.01	1.97	
XLOC_011243	FFC1_11011	FFUJ_10368	uncharacterized protein FFUJ_10368									2.14	
XLOC_011244	FFC1_11012	FFUJ_10367	related to sensory transduction histidine kinase	2.40	2.93	2.13				7.19	9.61	9.08	6.04
XLOC_011814	FFC1_11013	FFUJ_10366	uncharacterized protein FFUJ_10366	1.01	1.09					4.31	3.79	4.29	3.65
XLOC_011245	FFC1_11014	FFUJ_10365	uncharacterized protein FFUJ_10365		1.17				2.15	1.59		1.35	
XLOC_011251	FFC1_11023	FFUJ_10358	related to cytochrome P450 7B1								-2.69		
XLOC_011821	FFC1_11033	FFUJ_10348	probable pectin lyase precursor							6.23	8.63	9.23	8.61
XLOC_011261	FFC1_11036	FFUJ_10344	uncharacterized protein FFUJ_10344		2.17	1.42				2.34	3.52	4.18	3.09
XLOC_011262	FFC1_11038	FFUJ_10343	related to integral membrane protein	0.98		-1.33				9.38	10.36	9.33	8.18
XLOC_011264	FFC1_11043	FFUJ_10338	related to calcium-independent phospholipase A2		-2.59					3.95			
XLOC_011265	FFC1_11044	FFUJ_10337	uncharacterized protein FFUJ_10337							4.01			
XLOC_011267	FFC1_11049	FFUJ_10332	uncharacterized protein FFUJ_10332							-4.62	-5.47	-4.93	-2.34
XLOC_011268	FFC1_11050	FFUJ_10331	related to neutral amino acid permease							2.40	1.86	2.10	
XLOC_011833	FFC1_11054	FFUJ_10327	uncharacterized protein FFUJ_10327							3.51	2.75	2.62	
XLOC_011834	FFC1_11055	FFUJ_10326	uncharacterized protein FFUJ_10326								-1.94	-2.15	
XLOC_011271	FFC1_11056	FFUJ_10325	uncharacterized protein FFUJ_10325							-3.25	-5.38	-5.93	-4.14
XLOC_011272	FFC1_11057	FFUJ_10324	uncharacterized protein FFUJ_10324							-3.18	-5.48		
XLOC_011274	FFC1_11060	FFUJ_10321	probable alcohol dehydrogenase homolog Bli-4		3.24					5.62	5.42	4.58	6.01
XLOC_011277	FFC1_11063	FFUJ_10318	uncharacterized protein FFUJ_10318							1.90		2.10	1.75
XLOC_011278	FFC1_11065	FFUJ_10316	uncharacterized protein FFUJ_10316		2.21							2.91	
XLOC_011838	FFC1_11066	FFUJ_10315	OrfE-unknown, trichothecene gene cluster							2.43	1.93	2.43	1.84
XLOC_011839	FFC1_11069	FFUJ_10313	related to toxD gene							5.32	4.45	4.67	2.77
XLOC_011285	FFC1_11075	FFUJ_10307	choline permease								2.14		
XLOC_011288	FFC1_11084	FFUJ_10299	probable cytochrome P450 monooxygenase (lovA)			-3.69				3.52			
XLOC_011289	FFC1_11085	FFUJ_10298	uncharacterized protein FFUJ_10298			-1.73							-3.62

XLOC_011847	FFC1_11086	FFUJ_10297	acetylesterase, trichothecene gene cluster							4.37	5.89	4.94	4.95
XLOC_011290	FFC1_11088	FFUJ_10295	related to glucan 1,3-beta-glucosidase							2.11	2.05	2.58	2.08
XLOC_011291	FFC1_11091	FFUJ_10292	uncharacterized protein FFUJ_10292									4.96	
XLOC_011853	FFC1_11097	FFUJ_10286	uncharacterized protein FFUJ_10286							2.45			1.84
XLOC_011295	FFC1_11098	FFUJ_10285	related to ankyrin										2.58
XLOC_011854	FFC1_11099	FFUJ_10284	uncharacterized protein FFUJ_10284								-2.96		
XLOC_011855	FFC1_11100	FFUJ_10283	related to ankyrin								-4.73		
XLOC_011856	FFC1_11101	FFUJ_10282	uncharacterized protein FFUJ_10282		-2.31						-2.14	-2.47	
XLOC_011296	FFC1_11102	FFUJ_10281	related to ankyrin							-3.52	-5.46	-3.11	-4.66
XLOC_011300	FFC1_11110	FFUJ_10273	uncharacterized protein FFUJ_10273		1.65					2.83	3.41	4.03	
XLOC_011861	FFC1_11111	FFUJ_10272	related to oxidoreductase, short chain dehydrogenase/reductase family		1.22					1.83	1.62	2.72	
XLOC_011863	FFC1_11115	FFUJ_10270	monooxygenase							3.66	3.68	3.19	2.53
XLOC_011866	FFC1_11121	FFUJ_10259	related to tetracycline efflux protein (otrb)			0.93				-3.88	-3.45	-2.89	
XLOC_011308	FFC1_11123	FFUJ_10257	putative NADH cytb-reductase							7.98	6.90	7.89	5.76
XLOC_011309	FFC1_11124	FFUJ_10256	related to 3-hydroxybutyryl-CoA dehydrogenase		0.92					5.57	5.11	6.38	5.44
XLOC_011868	FFC1_11125	FFUJ_10255	uncharacterized protein FFUJ_10255							-6.19	-6.16	-5.66	
XLOC_011310	FFC1_11127	FFUJ_10253	uncharacterized protein FFUJ_10253							-4.83	-6.77	-7.01	-8.88
XLOC_011312	FFC1_11134									-7.06	-8.94	-8.39	-7.61
XLOC_011313	FFC1_11135	FFUJ_10245	uncharacterized protein FFUJ_10245									-5.85	
XLOC_011876	FFC1_11138									4.15		2.12	
XLOC_011877	FFC1_11139	FFUJ_10242	related to peroxisomal short-chain alcohol dehydrogenase							4.79	4.58		
XLOC_011315	FFC1_11140	FFUJ_10241	related to scytalone dehydratase							5.32			
XLOC_011879	FFC1_11142	FFUJ_10239	related to integral membrane protein PTH11							3.81			
XLOC_011316	FFC1_11144	FFUJ_10237	related to alkaline protease (oryzin)		-2.59					8.91	9.70	6.85	7.79
XLOC_011317	FFC1_11147	FFUJ_10235	related to NPP1 domain protein						-3.25	-10.09	-9.51	-8.21	-6.31
XLOC_011318	FFC1_11148	FFUJ_10234	related to beta-mannosidase	-2.07	-2.30					3.31	2.96		
XLOC_011887	FFC1_11155	FFUJ_10227	related to feruloyl esterase B precursor							5.43		6.47	
XLOC_011321	FFC1_11156									6.45	5.57	6.62	6.28
XLOC_011888	FFC1_11160	FFUJ_10222	uncharacterized protein FFUJ_10222									2.13	
XLOC_011889	FFC1_11162	FFUJ_10220	related to formaldehyde dehydrogenase									3.61	2.89
XLOC_011327	FFC1_11164	FFUJ_10218	uncharacterized protein FFUJ_10218							3.41	3.40	3.66	2.94
XLOC_011328	FFC1_11165	FFUJ_10217	uncharacterized protein FFUJ_10217		2.17	2.45				3.93	4.70	6.48	6.36
XLOC_011331	FFC1_11173	FFUJ_10209	related to cutinase transcription factor 1 beta									3.94	3.50
XLOC_011899	FFC1_11181	FFUJ_13456	related to ABC transporter							4.92		5.84	
XLOC_011900	FFC1_11182	FFUJ_14074	related to gluconate 5-dehydrogenase							5.68	5.53	6.32	
XLOC_011901	FFC1_11183	FFUJ_14073	uncharacterized protein FFUJ_14073							4.68	4.62	6.22	7.50
XLOC_012379	FFC1_11184	FFUJ_14072	uncharacterized protein FFUJ_14072		-1.81					-1.05	-1.46	-2.16	
XLOC_011902	FFC1_11185	FFUJ_14071	related to chitin synthase/hyaluronan synthase (glycosyltransferases)		-2.12					-1.34	-1.88	-2.47	
XLOC_012380	FFC1_11188	FFUJ_14068	uncharacterized protein FFUJ_14068		-1.51					-1.56	-2.40	-2.36	-1.17
XLOC_012382	FFC1_11190	FFUJ_14066	uncharacterized protein FFUJ_14066								-4.64	-5.27	
XLOC_011910	FFC1_11198	FFUJ_14059	related to multidrug resistance protein fnx1							5.69	5.70		
XLOC_011911	FFC1_11200	FFUJ_14057	related to 2,4-dihydroxyhept-2-ene-1,7-dioic acid aldolase							4.68			
XLOC_011912	FFC1_11201	FFUJ_14056	probable demethylmenaquinone methyltransferase							6.91	4.92	5.63	6.51
XLOC_011914	FFC1_11204	FFUJ_14053	uncharacterized protein FFUJ_14053							2.71	2.07		4.29
XLOC_012387	FFC1_11205	FFUJ_14052	uncharacterized protein FFUJ_14052							9.24	7.68	8.03	8.69
XLOC_011915	FFC1_11206	FFUJ_14051	uncharacterized protein FFUJ_14051							7.16	7.22	7.73	7.78
XLOC_011916	FFC1_11207	FFUJ_14050	uncharacterized protein FFUJ_14050						-2.70	1.72	1.62	1.46	3.32
XLOC_011917	FFC1_11208	FFUJ_14049	related to carboxypeptidase							2.99	2.19	2.57	
XLOC_012388	FFC1_11209	FFUJ_14048	uncharacterized protein FFUJ_14048										-2.88
XLOC_012390	FFC1_11212	FFUJ_14045	probable alpha-galactosidase C precursor		1.56					2.70	2.44	2.65	
XLOC_012391	FFC1_11214	FFUJ_14043	related to isoamyl alcohol oxidase										-3.54
XLOC_012393	FFC1_11219	FFUJ_14038	related to aryl-alcohol dehydrogenases							4.06			
XLOC_011925	FFC1_11223	FFUJ_14034	related to dihydrodipicolinate synthetase							3.16			
XLOC_012395	FFC1_11227	FFUJ_14030	uncharacterized protein FFUJ_14030							-7.66	-9.10	-7.52	-7.95
XLOC_011936	FFC1_11241	FFUJ_14017	related to GTT1-glutathione S-transferase							5.32	4.37	5.75	3.87
XLOC_011937	FFC1_11242	FFUJ_14016	related to bacterial leucyl aminopeptidase								7.10	6.72	
XLOC_011939	FFC1_11244	FFUJ_14014	uncharacterized protein FFUJ_14014							5.03		3.36	2.86
XLOC_011940	FFC1_11245	FFUJ_14013	uncharacterized protein FFUJ_14013			-1.50				-1.54	-2.13	-2.42	-2.14
XLOC_012402	FFC1_11246	FFUJ_14012	related to monophenol monooxygenase							-3.28	-2.65	-2.82	-3.99
XLOC_011943	FFC1_11253	FFUJ_14006	uncharacterized protein FFUJ_14006							5.93	5.97	4.54	
XLOC_011946	FFC1_11256	FFUJ_14003	related to trihydrophobin precursor							5.43	5.00	6.77	6.84
XLOC_011948	FFC1_11260	FFUJ_13999	related to monocarboxylate transporter							2.22		2.51	
XLOC_012411	FFC1_11264	FFUJ_13996	uncharacterized protein FFUJ_13996							-4.55	-5.17	-6.67	-2.31
XLOC_011949	FFC1_11265	FFUJ_13995	probable neutral amino acid permease							-6.37	-6.51	-7.10	-7.59
XLOC_011950	FFC1_11266	FFUJ_13994	related to C6 zink-finger protein PRO1A							-4.68	-5.94	-5.27	-4.63
XLOC_012413	FFC1_11268	FFUJ_13992	uncharacterized protein FFUJ_13992		1.36					3.73	3.45	5.03	3.73
XLOC_011952	FFC1_11273	FFUJ_13988	uncharacterized protein FFUJ_13988							3.65	2.26	1.97	
XLOC_011954	FFC1_11277	FFUJ_13984	related to Tripeptidyl-peptidase I precursor		-0.98					-1.65	-1.74	-2.57	
XLOC_012419	FFC1_11279	FFUJ_13982	related to GABA transport protein							1.51	1.77	1.07	2.44
XLOC_012420	FFC1_11280	FFUJ_13981	uncharacterized protein FFUJ_13981		-1.34					3.03	2.91	2.11	3.58
XLOC_012421	FFC1_11281	FFUJ_13980	uncharacterized protein FFUJ_13980							2.31	2.43	1.65	2.50
XLOC_011956	null									7.71	7.80	4.74	7.11
XLOC_011957	null									8.45	7.43	5.70	7.68
XLOC_011958	null									6.96	7.66	7.26	7.45
XLOC_011959	FFC1_11282	FFUJ_13979	uncharacterized protein FFUJ_13979							6.24	5.86	5.39	6.71
XLOC_011960	FFC1_11283	FFUJ_13978	uncharacterized protein FFUJ_13978							6.72	6.21	5.32	8.29
XLOC_011961	FFC1_11286	FFUJ_13975	uncharacterized protein FFUJ_13975		-1.99					-1.23	-1.88	-2.51	
XLOC_012425	FFC1_11290	FFUJ_13971	related to polysaccharide deacetylase							5.90			

XLOC_012426	FFC1_11292	FFUJ_13969	related to trans-aconitate 3-methyltransferase							5.34			
XLOC_011965	FFC1_11293	FFUJ_13968	uncharacterized protein FFUJ_13968							-5.92	-6.63	-6.18	-5.98
XLOC_011966	FFC1_11294	FFUJ_13967	related to integral membrane protein										4.19
XLOC_012427	FFC1_11295	FFUJ_13966	uncharacterized protein FFUJ_13966							-3.02	-5.81	-6.36	-2.62
XLOC_011968	FFC1_11297	FFUJ_13964	related to alcohol/sorbitol dehydrogenase							9.83	6.66	5.25	
XLOC_012428	FFC1_11298	FFUJ_13963	related to bikaverin cluster-transcription factor							2.86	5.08	4.89	4.03
XLOC_011969	FFC1_11299	FFUJ_13962	related to fluconazole resistance protein							5.63			
XLOC_011976	FFC1_11309	FFUJ_13952	uncharacterized protein FFUJ_13952									-2.68	
XLOC_012434	FFC1_11315	FFUJ_13945	uncharacterized protein FFUJ_13945							-2.69	-3.44	-4.96	-4.45
XLOC_011981	FFC1_11316	FFUJ_13944	uncharacterized protein FFUJ_13944							-1.70	-3.34	-4.84	
XLOC_012442	FFC1_11327	FFUJ_13934	uncharacterized protein FFUJ_13934							7.93	7.66	7.61	7.68
XLOC_012443	FFC1_11328									7.37	7.25	7.09	6.86
XLOC_012444	FFC1_11329	FFUJ_13933	probable ATP dependent RNA helicase							3.35	2.69	2.72	1.82
XLOC_012446	FFC1_11332	FFUJ_13930	uncharacterized protein FFUJ_13930										2.47
XLOC_011996	FFC1_11351	FFUJ_13339	related to multidrug resistance-associated protein		1.92								-2.69
XLOC_012455	FFC1_11352	FFUJ_13911	probable monooxygenase									3.04	
XLOC_011997	FFC1_11353	FFUJ_13910	probable NADH cytb-reductase							4.86			
XLOC_011999	FFC1_11355	FFUJ_13908	probable saccharopine dehydrogenase (NAD, L-lysine-forming)							-4.65	-5.24		
XLOC_012456	FFC1_11356	FFUJ_13907	related to allantoate permease							-5.51			
XLOC_012001	FFC1_11359	FFUJ_13902	related to dihydroxyacetone kinase							2.05	2.91	4.77	
XLOC_012458	FFC1_11360	FFUJ_13901	related to beta transducin-like protein							3.39	3.15	3.57	3.22
XLOC_012459	FFC1_11361	FFUJ_13900	related to ECM32-DNA dependent ATPase/DNA helicase B							6.72	6.17	6.61	6.56
XLOC_012002	FFC1_11362	FFUJ_13899	uncharacterized protein FFUJ_13899							3.32	2.92	2.92	3.46
XLOC_012003	FFC1_11363	FFUJ_13898	related to lysophosphatidic acid acyltransferase endophilin/SH3GL, involved in synaptic vesicle formation							1.80	2.06	1.33	1.43
XLOC_012004	FFC1_11364	FFUJ_13897	related to cyclin CCL1							2.30	2.23	2.24	2.02
XLOC_012005	FFC1_11365	FFUJ_13896	related to TGF beta induced protein ig-h3 precursor		1.82					1.23	1.20	2.94	2.49
XLOC_012460	FFC1_11366	FFUJ_13895	uncharacterized protein FFUJ_13895							2.92	2.52	3.53	3.89
XLOC_012463	FFC1_11373	FFUJ_13888	related to ECM14-involved in cell wall biogenesis and architecture							5.32	7.06	6.33	
XLOC_012464	FFC1_11374	FFUJ_13887	probable succinyl-CoA 3-ketoacid-coenzyme A transferase, mitochondrial precursor							2.76	2.53	3.07	2.64
XLOC_012465	FFC1_11375	FFUJ_13886	probable MUP1-High affinity methionine permease							3.93	3.43	2.97	3.97
XLOC_012012	FFC1_11380	FFUJ_13881	uncharacterized protein FFUJ_13881		1.45					3.92	4.16	5.26	4.67
XLOC_012013	FFC1_11381	FFUJ_13880	related to phosphatidylserine decarboxylase 2							10.96	8.76	10.17	8.49
XLOC_012014	FFC1_11382	FFUJ_13879	uncharacterized protein FFUJ_13879							4.47	5.14	7.40	7.58
XLOC_012468	FFC1_11383	FFUJ_13878	uncharacterized protein FFUJ_13878							4.80	5.74	5.96	5.22
XLOC_012470	FFC1_11387	FFUJ_13874	uncharacterized protein FFUJ_13874									2.55	2.29
XLOC_012471	FFC1_11388	FFUJ_13873	uncharacterized protein FFUJ_13873							5.01	2.88	6.27	
XLOC_012473	FFC1_11390	FFUJ_13871	uncharacterized protein FFUJ_13871							2.51	1.86	1.95	2.30
XLOC_012017	FFC1_11391	FFUJ_13870	uncharacterized protein FFUJ_13870							6.87	5.63	6.52	6.49
XLOC_012474	FFC1_11392	FFUJ_13869	uncharacterized protein FFUJ_13869							7.81	7.27	6.21	6.19
XLOC_012025	FFC1_11408	FFUJ_13853	uncharacterized protein FFUJ_13853		-2.71	-1.72				3.10	2.37		
XLOC_012483	FFC1_11409	FFUJ_13852	uncharacterized protein FFUJ_13852							3.10	2.13	1.63	
XLOC_012030	null										4.61		
XLOC_012032	FFC1_11418	FFUJ_13844	uncharacterized protein FFUJ_13844								1.02	1.67	2.62
XLOC_012492	FFC1_11427	FFUJ_13836	probable ammonium transporter MEPa							-2.96	-2.67	-3.39	
XLOC_012039	FFC1_11432	FFUJ_13831	uncharacterized protein FFUJ_13831							3.12	2.97	3.03	2.27
XLOC_012495	null									3.24	2.58	3.13	
XLOC_012496	FFC1_11433	FFUJ_13830	uncharacterized protein FFUJ_13830							2.56	2.58	2.42	1.92
XLOC_012497	null												-4.84
XLOC_012498	FFC1_11434	FFUJ_13829	uncharacterized protein FFUJ_13829							3.17	2.48	2.51	1.79
XLOC_012499	FFC1_11435	FFUJ_13828	uncharacterized protein FFUJ_13828							5.08	6.82	5.59	7.65
XLOC_012504	FFC1_11449	FFUJ_13814	uncharacterized protein FFUJ_13814			-0.80				6.60	6.53	6.37	5.12
XLOC_012508	FFC1_11456	FFUJ_13807	related to 5`-nucleotidase precursor								2.19	2.12	
XLOC_012512	FFC1_11463	FFUJ_13800	related to dihydrodipicolinate synthase								-1.30	-1.87	-2.10
XLOC_012056	FFC1_11465	FFUJ_13798	uncharacterized protein FFUJ_13798							6.04		5.35	
XLOC_012060	FFC1_11471	FFUJ_13792	probable dihydroxy-acid dehydratase		0.75				-1.50			0.85	2.06
XLOC_012069	FFC1_11487	FFUJ_13776	uncharacterized protein FFUJ_13776							7.69	7.03	4.95	5.24
XLOC_012073	FFC1_11493	FFUJ_13770	uncharacterized protein FFUJ_13770							-2.35	-2.61	-1.84	-2.28
XLOC_012075	FFC1_11494	FFUJ_13769	uncharacterized protein FFUJ_13769							-3.56	-4.92	-7.11	-3.28
XLOC_012526	FFC1_11495	FFUJ_13768	related to vegetatible incompatibility protein HET-E-1							2.70	2.00	1.65	
XLOC_012076	FFC1_11496	FFUJ_13767	probable alcohol dehydrogenase I-ADH1							-1.27	-1.59	-1.71	-2.96
XLOC_012529	FFC1_11499	FFUJ_13764	related to integral membrane protein										4.91
XLOC_012079	FFC1_11501	FFUJ_13762	related to neutral amino acid permease							3.83			
XLOC_012084	FFC1_11508	FFUJ_13755	uncharacterized protein FFUJ_13755							1.68	1.90	2.04	
XLOC_012533	FFC1_11509	FFUJ_13754	related to diacylglycerol pyrophosphate phosphatase DPP1		1.51					4.72	4.87	5.33	2.90
XLOC_012534	FFC1_11510	FFUJ_13753	uncharacterized protein FFUJ_13753							1.54	1.41	2.05	1.83
XLOC_012535	null									-2.74			
XLOC_012085	FFC1_11512	FFUJ_13751	uncharacterized protein FFUJ_13751		3.51	3.35				3.94	5.06	5.89	7.31
XLOC_012538	FFC1_11517	FFUJ_13747	uncharacterized protein FFUJ_13747							5.77	5.81	5.97	5.60
XLOC_012539	FFC1_11519	FFUJ_13745	probable heat shock protein 80		1.67				1.37	2.98	2.10	1.96	3.01
XLOC_012540	FFC1_11520	FFUJ_13744	uncharacterized protein FFUJ_13744									2.37	
XLOC_012544	FFC1_11529	FFUJ_13735	uncharacterized protein FFUJ_13735							2.43	1.34	1.32	
XLOC_012545	null												3.63
XLOC_012549	FFC1_11532	FFUJ_13733	uncharacterized protein FFUJ_13733							3.92	2.64	5.02	1.92
XLOC_012099	null											-1.86	-2.31

XLOC_012102	FFC1_11536	FFUJ_13729	related to phosphatidylserine decarboxylase 2	1.13	1.79					2.70	3.23	3.75	
XLOC_012556	FFC1_11543	FFUJ_12120	related to integral membrane protein						-4.11	2.79	2.69	3.81	5.36
XLOC_012557	FFC1_11544	FFUJ_12121	uncharacterized protein FFUJ_12121		-1.75	-2.28			-2.08	2.17	1.80		1.98
XLOC_012113	FFC1_11563	FFUJ_12140	uncharacterized protein FFUJ_12140							3.95			
XLOC_012570	FFC1_11565	FFUJ_12142	related to DUF1338 domain protein			-1.89				-1.29	-1.87	-3.16	-3.44
XLOC_012571	FFC1_11566	FFUJ_12143	probable aldehyde dehydrogenase			-2.95							
XLOC_012572	FFC1_11569	FFUJ_12146	uncharacterized protein FFUJ_12146	0.87	0.96					3.08	3.70	3.95	1.96
XLOC_012117	FFC1_11570	FFUJ_12147	uncharacterized protein FFUJ_12147	0.85						1.67	2.72	2.43	1.58
XLOC_012573	FFC1_11571	FFUJ_12148	uncharacterized protein FFUJ_12148									3.54	4.97
XLOC_012126	FFC1_11584	FFUJ_12161	uncharacterized protein FFUJ_12161							2.33	2.36	2.33	2.33
XLOC_012127	FFC1_11585									5.96	4.94	5.35	5.76
XLOC_012132	FFC1_11597	FFUJ_12171	uncharacterized protein FFUJ_12171							2.57	2.52	2.59	2.93
XLOC_012591	FFC1_11598	FFUJ_12172	uncharacterized protein FFUJ_12172							8.26	8.18	7.78	8.91
XLOC_012133	FFC1_11600	FFUJ_12174	related to G protein coupled receptor like protein		-2.24	-1.93							
XLOC_012602	FFC1_11615	FFUJ_12189	related to malate dehydrogenase							5.80	5.13	4.62	3.91
XLOC_012604	FFC1_11618	FFUJ_12192	related to NNT1 Putative nicotinamide N-methyltransferase, has a role in rDNA silencing and in lifespan determination							-2.19	-2.14	-2.06	-1.09
XLOC_012141	null									5.77		3.33	
XLOC_012147	FFC1_11636	FFUJ_12208	probable class I alpha mannosidase		-1.22					-0.99	-1.34	-2.06	-0.93
XLOC_012170	FFC1_11680	FFUJ_12256	related to TMS1 protein							2.43	2.27	2.65	2.32
XLOC_012638	FFC1_11681	FFUJ_12257	uncharacterized protein FFUJ_12257							2.96	2.44	2.70	2.29
XLOC_012171	null									5.94		5.24	
XLOC_012183	FFC1_11698	FFUJ_14913	uncharacterized protein FFUJ_14913	3.32	3.26	2.92					3.00	3.09	2.89
XLOC_012190	FFC1_11705	FFUJ_12279	probable chitin synthase D		1.46					1.15	1.70	2.27	1.90
XLOC_012191	FFC1_11706	FFUJ_12280	probable heat shock protein Hsp88							3.42	3.11	3.51	3.64
XLOC_012206	FFC1_11727	FFUJ_12300	related to phospholipase A2, cytosolic	1.46	1.69					1.18	1.99	2.36	
XLOC_012656	FFC1_11731	FFUJ_12304	uncharacterized protein FFUJ_12304		1.61	1.60				5.49	4.12	5.03	5.37
XLOC_012210	FFC1_11732	FFUJ_12305	probable bifunctional P-450:NADPH-P450 reductase							3.45	2.78	2.74	2.70
XLOC_012211	FFC1_11733	FFUJ_12306	related to phospholipase D							2.46	2.22	2.12	1.84
XLOC_012657	FFC1_11735	FFUJ_12308	related to triacylglycerol lipase		1.08					1.34	1.52	2.04	1.35
XLOC_012213	FFC1_11736	FFUJ_12309	related to aspartate-tRNA ligase, cytosolic							3.91	3.96	3.94	3.07
XLOC_012214	FFC1_11737									3.87	5.72	5.39	5.49
XLOC_012661	FFC1_11741	FFUJ_12312	uncharacterized protein FFUJ_12312							-2.02	-1.95		
XLOC_012216	FFC1_11742	FFUJ_12313	probable sulfate permease II							3.14	2.08	1.98	3.09
XLOC_012217	FFC1_11743	FFUJ_12314	related to ADH7-NADP(H)-dependent alcohol dehydrogenase		1.48					2.64	3.79	3.98	1.90
XLOC_012218	FFC1_11744									4.92	4.73	4.07	3.27
XLOC_012662	FFC1_11745	FFUJ_14911	uncharacterized protein FFUJ_14911							5.53			
XLOC_012220	FFC1_11747	FFUJ_12317	uncharacterized protein FFUJ_12317								-2.25		
XLOC_012666	FFC1_11755	FFUJ_12325	related to aldehyde dehydrogenase (NAD+), mitochondrial							4.40			
XLOC_012225	FFC1_11757	FFUJ_12327	uncharacterized protein FFUJ_12327								-3.90	-2.78	-2.76
XLOC_012674	FFC1_11764	FFUJ_12332	uncharacterized protein FFUJ_12332							-2.54	-2.72	-4.69	-3.99
XLOC_012229	FFC1_11771	FFUJ_12338	uncharacterized protein FFUJ_12338			-2.08				5.52	3.41	3.94	5.06
XLOC_012230	FFC1_11772	FFUJ_12339	related to serine protease		-1.17	-1.78				3.29	2.64	2.25	2.21
XLOC_012679	FFC1_11773	FFUJ_12340	probable endoglucanase IV precursor								5.34		4.68
XLOC_012231	FFC1_11774	FFUJ_12341	uncharacterized protein FFUJ_12341		-4.97								2.63
XLOC_012682	FFC1_11779	FFUJ_12346	uncharacterized protein FFUJ_12346							3.80	3.23	3.96	4.39
XLOC_012683	FFC1_11780	FFUJ_12347	uncharacterized protein FFUJ_12347							3.71	3.87	3.86	3.58
XLOC_012236	FFC1_11793	FFUJ_12360	related to gamma hydroxybutyrate dehydrogenase							-2.34	-2.64	-2.73	
XLOC_012695	FFC1_11794	FFUJ_12361	related to 4-hydroxybenzoate transporter							3.16	2.09	2.04	2.04
XLOC_012237	FFC1_11796	FFUJ_12363	probable methionine synthase, vitamin-b12 independent							-1.88	-2.88	-2.94	-2.01
XLOC_012241	FFC1_11800	FFUJ_12367	uncharacterized protein FFUJ_12367							2.53	2.19	2.98	2.96
XLOC_012698	FFC1_11801	FFUJ_12368	uncharacterized protein FFUJ_12368									5.83	5.82
XLOC_012701	FFC1_11807	FFUJ_12374	uncharacterized protein FFUJ_12374									5.21	5.77
XLOC_012250	FFC1_11818	FFUJ_12385	uncharacterized protein FFUJ_12385							2.51	3.20	3.80	3.38
XLOC_012251	FFC1_11820	FFUJ_12387	uncharacterized protein FFUJ_12387								4.99	5.06	2.70
XLOC_012712	null									3.66	2.15	2.31	
XLOC_012254	null									3.73	2.11	2.30	
XLOC_012255	FFC1_11826	FFUJ_12393	related to FCP1-TFIIF interacting component of CTD phosphatase							2.57	2.25	2.30	
XLOC_012256	FFC1_11827	FFUJ_12394	related to alcohol dehydrogenase homolog Bli-4							3.86	2.79	5.41	5.13
XLOC_012714	FFC1_11830	FFUJ_12397	uncharacterized protein FFUJ_12397							3.68	4.33	5.82	7.02
XLOC_012718	FFC1_11837	FFUJ_12404	related to lipase/acylhydrolase			-1.31				-2.70	-3.04	-3.06	-4.47
XLOC_012722	FFC1_11842	FFUJ_12409	probable isoamyl alcohol oxidase							-3.10	-3.46	-3.75	-3.38
XLOC_012264	FFC1_11843	FFUJ_12410	related to integral membrane protein PTH11							-2.94	-2.90	-2.71	-3.85
XLOC_012723	FFC1_11844	FFUJ_12411	related to CCC1 protein (involved in calcium homeostasis)		2.37					1.11	1.76	3.10	
XLOC_012265	FFC1_11846	FFUJ_12413	related to dopamine-responsive protein								-2.20		-4.29
XLOC_012725	FFC1_11847	FFUJ_12414	uncharacterized protein FFUJ_12414	3.98	3.68					4.91	8.89	8.50	8.11
XLOC_012266	FFC1_11848	FFUJ_12415	uncharacterized protein FFUJ_12415							6.36	7.37	4.32	6.11
XLOC_012731	FFC1_11854				-2.38					3.67	2.18		
XLOC_012268	FFC1_11855	FFUJ_12424	uncharacterized protein FFUJ_12424							2.20	1.88	2.02	
XLOC_012732	FFC1_11856	FFUJ_12425	uncharacterized protein FFUJ_12425							4.03	3.00	3.52	2.83
XLOC_012735	FFC1_11861	FFUJ_12430	uncharacterized protein FFUJ_12430							2.76	2.86	2.46	2.11
XLOC_012738	FFC1_11866	FFUJ_12434	uncharacterized protein FFUJ_12434							2.97	2.43	2.53	2.25
XLOC_012273	FFC1_11867	FFUJ_12435	uncharacterized protein FFUJ_12435		7.60	4.92						6.72	8.41
XLOC_012739	FFC1_11869	FFUJ_12437	related to cytosine deaminase and related metal-dependent hydrolases	1.41	1.85					3.94	4.46	4.75	2.11
XLOC_012276	FFC1_11871	FFUJ_12439	uncharacterized protein FFUJ_12439								2.14	3.48	
XLOC_012277	FFC1_11872	FFUJ_12440	related to E.coli galactoside O-acetyltransferase							5.04	7.58	5.12	3.79

XLOC_012278	FFC1_11873	FFUJ_12441	uncharacterized protein FFUJ_12441							8.44	6.84	5.74	5.56
XLOC_012740	FFC1_11874	FFUJ_12442	uncharacterized protein FFUJ_12442							-2.95	-2.71	-2.57	-1.67
XLOC_012279	FFC1_11875	FFUJ_12443	uncharacterized protein FFUJ_12443							-5.37	-6.14		-3.30
XLOC_012741	FFC1_11876	FFUJ_12444	uncharacterized protein FFUJ_12444		1.32					3.00	3.45	3.53	1.56
XLOC_012745	FFC1_11885	FFUJ_12453	uncharacterized protein FFUJ_12453							4.02	2.09	2.78	
XLOC_012747	FFC1_11887	FFUJ_14908	uncharacterized protein FFUJ_14908						-2.43	-4.76	-5.91	-5.60	-2.93
XLOC_012750	FFC1_11892	FFUJ_12459	related to major facilitator (MFS1) transporter							2.30			
XLOC_012751	FFC1_11893	FFUJ_12460	uncharacterized protein FFUJ_12460							6.25	6.46	6.95	6.80
XLOC_012287	FFC1_11894	FFUJ_12461	related to ankyrin 3							6.05	7.29	6.35	8.40
XLOC_012288	FFC1_11895	FFUJ_12462	uncharacterized protein FFUJ_12462			-1.78				3.42	2.73	2.32	
XLOC_012292	FFC1_11901	FFUJ_12468	uncharacterized protein FFUJ_12468	-1.69	-2.51	-3.22				5.95	5.86	3.92	
XLOC_012294	FFC1_11903	FFUJ_12470	uncharacterized protein FFUJ_12470			-2.11				-1.61	-1.55	-2.74	-2.73
XLOC_012296	FFC1_11905	FFUJ_12472	uncharacterized protein FFUJ_12472							-5.21			-3.93
XLOC_012297	FFC1_11906	FFUJ_12473	uncharacterized protein FFUJ_12473							-4.52	-4.25	-5.15	-6.61
XLOC_012754	FFC1_11907	FFUJ_12474	related to AIF1 Apoptosis-Inducing Factor	1.50	1.37					-1.54			-2.36
XLOC_012300	FFC1_11914	FFUJ_12481	uncharacterized protein FFUJ_12481							2.29			
XLOC_012302	FFC1_11916	FFUJ_12483	related to methyltransferase							2.05	1.98	1.89	2.39
XLOC_012303	FFC1_11918	FFUJ_12485	related to methyltransferase		-1.57						-1.49	-2.27	
XLOC_012310	FFC1_11931	FFUJ_12496	related to integral membrane protein PTH11						-1.09	-4.77	-3.88	-3.40	-3.19
XLOC_012773	FFC1_11935	FFUJ_12500	uncharacterized protein FFUJ_12500							-5.41	-5.12		
XLOC_012315	FFC1_11939				-2.95							-2.58	
XLOC_012776	FFC1_11945	FFUJ_12509	related to fusarubin cluster-esterase							4.31	5.49	4.13	3.96
XLOC_012779	FFC1_11948	FFUJ_12512	uncharacterized protein FFUJ_12512							-1.67	-3.69	-4.71	-3.90
XLOC_012320	FFC1_11949	FFUJ_12513	uncharacterized protein FFUJ_12513								-4.12	-5.06	
XLOC_012780	FFC1_11950	FFUJ_12514	uncharacterized protein FFUJ_12514								-3.06	-3.77	
XLOC_012322	FFC1_11954	FFUJ_12518	probable hydroxyquinol-1,2-dioxygenase							5.69	4.41	4.35	3.29
XLOC_012323	FFC1_11956	FFUJ_12520	related to phenol hydroxylase							4.87	5.76	4.78	4.78
XLOC_012328	FFC1_11961	FFUJ_12525	uncharacterized protein FFUJ_12525							-3.90	-5.21	-6.65	-3.14
XLOC_012338	FFC1_11972	FFUJ_12535	related to short-chain alcohol dehydrogenase							5.59	4.85		5.39
XLOC_012788	FFC1_11973	FFUJ_12536	related to pathway-specific regulatory protein							4.78	4.24	4.13	3.97
XLOC_012339	FFC1_11974	FFUJ_12537	related to 4-carboxymuconolactone decarboxylase family protein							6.49	4.99	3.75	6.46
XLOC_012789	FFC1_11975	FFUJ_12538	related to muconate cycloisomerase I							5.84	4.85		
XLOC_012794	FFC1_11979								-1.89	-3.77	-3.36	-2.82	-2.24
XLOC_012799	FFC1_11985	FFUJ_12548	related to quinate transport protein							3.76	2.94	2.13	
XLOC_012341	FFC1_11986	FFUJ_12549	related to putative tartrate transporter							-4.39	-5.60	-5.73	-3.87
XLOC_012344	FFC1_11989									-6.29	-6.27	-4.05	-4.79
XLOC_012345	FFC1_11990	FFUJ_12552	uncharacterized protein FFUJ_12552							-5.22	-6.48	-5.46	-5.19
XLOC_012801	FFC1_11992	FFUJ_12554	uncharacterized protein FFUJ_12554							-5.78	-8.76	-6.65	-6.39
XLOC_012802	FFC1_11993	FFUJ_12555	uncharacterized protein FFUJ_12555							-1.64	-1.97	-3.31	
XLOC_012352	FFC1_12000									4.19			
XLOC_012810	FFC1_12005	FFUJ_12564	related to transmembrane transporter Liz1p							-4.44	-4.24	-5.43	-2.53
XLOC_012811	FFC1_12006	FFUJ_12565	related to monocarboxylate transporter 4							-1.45	-2.17	-2.07	
XLOC_012358	FFC1_12011	FFUJ_12570	uncharacterized protein FFUJ_12570										-4.59
XLOC_012814	FFC1_12012	FFUJ_12571	related to aminopeptidase Y precursor, vacuolar									4.84	5.52
XLOC_012360	FFC1_12014	FFUJ_12573	uncharacterized protein FFUJ_12573								-1.74	-2.26	
XLOC_012361	FFC1_12015	FFUJ_12574	uncharacterized protein FFUJ_12574							-2.96	-2.98	-2.95	-2.28
XLOC_012816	FFC1_12016									5.34	5.12	5.04	3.87
XLOC_012362	null				1.33					2.33	2.93	3.70	2.26
XLOC_012366	FFC1_12024	FFUJ_12582	uncharacterized protein FFUJ_12582									4.20	
XLOC_012368	FFC1_12027	FFUJ_12585	related to pentalenene synthase							-4.14	-6.82	-5.61	-3.63
XLOC_012369	FFC1_12028	FFUJ_12586	probable glucan 1,4-alpha-glucosidase							-1.28	-2.43	-3.01	-1.35
XLOC_012372	FFC1_12032	FFUJ_12589	uncharacterized protein FFUJ_12589		-2.48								
XLOC_012825	FFC1_12033	FFUJ_12590	related to D-arabinitol 2-dehydrogenase									-4.28	
XLOC_012374	FFC1_12035	FFUJ_12592	uncharacterized protein FFUJ_12592							-3.93	-7.08	-5.04	-4.00
XLOC_012828	FFC1_12039	FFUJ_12596	uncharacterized protein FFUJ_12596						-1.76	-2.77	-4.38	-4.25	-3.54
XLOC_013334	FFC1_12049	FFUJ_12101	probable sugar transporter							4.70			
XLOC_013336	FFC1_12051	FFUJ_12099	probable beta-glucosidase										2.77
XLOC_013349	null										-2.36		
XLOC_013351	FFC1_12077	FFUJ_12074	polyketide synthase							-6.46	-5.64		
XLOC_012852	FFC1_12088	FFUJ_12064	related to acetate regulatory DNA binding protein FacB								5.41		
XLOC_013360	FFC1_12094	FFUJ_12058	uncharacterized protein FFUJ_12058							5.25			
XLOC_012865	FFC1_12110	FFUJ_12043	related to transcriptional activator Mut3p							6.11			
XLOC_012866	FFC1_12112	FFUJ_12041	related to bifunctional 4-hydroxyphenylacetate degradation enzyme							4.37	5.24	3.93	
XLOC_013371	FFC1_12120	FFUJ_12032	related to antifungal protein		-2.79	-3.96				9.33	7.21	6.39	4.53
XLOC_013372	FFC1_12121	FFUJ_12031	uncharacterized protein FFUJ_12031		-2.18	-1.86				7.25	5.48	3.57	4.72
XLOC_012870	FFC1_12124	FFUJ_12029	related to triacylglycerol lipase 2							3.09	3.00	3.92	4.84
XLOC_012871	FFC1_12128	FFUJ_12025	related to protein MCH2 (monocarboxylate permease homolog)							-2.06	-1.96	-1.69	
XLOC_012873	FFC1_12132									2.75	2.24	1.93	
XLOC_012874	FFC1_12133									-3.57	-4.96	-4.46	-3.91
XLOC_012878	FFC1_12138	FFUJ_12015	related to monooxygenase								-1.71	-2.85	
XLOC_012880	FFC1_12142	FFUJ_12011	uncharacterized protein FFUJ_12011							5.47			
XLOC_013383	FFC1_12143	FFUJ_12010	related to benzoate 4-monooxygenase cytochrome P450							3.93	4.66	3.56	
XLOC_012881	FFC1_12144	FFUJ_12009	uncharacterized protein FFUJ_12009							8.11	8.54	8.06	8.22
XLOC_012882	FFC1_12145									5.71	5.09	5.12	5.47
XLOC_013384	FFC1_12146	FFUJ_12007	uncharacterized protein FFUJ_12007							6.14			
XLOC_013385	FFC1_12147	FFUJ_12006	related to TRI13-cytochrome P450							5.86	5.60		5.84
XLOC_012888	FFC1_12155	FFUJ_11999	uncharacterized protein FFUJ_11999							5.58	5.00		5.28
XLOC_013389	FFC1_12159	FFUJ_11995	uncharacterized protein FFUJ_11995							-2.32	-2.88	-2.45	-2.66

XLOC_012891	FFC1_12160	FFUJ_11994	probable branched-chain amino acids aminotransferase							-4.08	-5.29	-4.35	-3.30
XLOC_012892	FFC1_12161	FFUJ_11993	uncharacterized protein FFUJ_11993							-2.49	-3.46	-3.00	-1.99
XLOC_012893	FFC1_12162	FFUJ_11992	uncharacterized protein FFUJ_11992								-5.49		
XLOC_012896	FFC1_12166	FFUJ_11988	related to aminopeptidase Y precursor, vacuolar							7.92	8.21	5.42	4.80
XLOC_013392	FFC1_12168	FFUJ_11986	uncharacterized protein FFUJ_11986							-3.31	-4.04	-3.42	-3.84
XLOC_012899	FFC1_12172	FFUJ_11982	uncharacterized protein FFUJ_11982								-2.66	-1.80	
XLOC_012901	FFC1_12174	FFUJ_11980	related to vacuolar membrane protein HMT1						-3.07	-3.74	-2.53	-2.17	-2.13
XLOC_013395	FFC1_12176	FFUJ_11978	related to 6-phosphogluconate dehydrogenase	1.93	2.14					4.04	4.92	5.73	3.20
XLOC_012902	FFC1_12177	FFUJ_11977	uncharacterized protein FFUJ_11977								4.22		5.15
XLOC_013396	FFC1_12178	FFUJ_11976	related to glucose dehydrogenase							4.93	5.69	6.03	5.91
XLOC_012904	FFC1_12182	FFUJ_10047	probable ABC1 transport protein							1.90	2.39	2.12	1.91
XLOC_012907	FFC1_12187	FFUJ_11968	related to phospholipid-translocating ATPase							2.89			
XLOC_013404	FFC1_12192	FFUJ_11963	related to 2`-hydroxyisoflavone reductase							6.54	5.61	6.31	
XLOC_012911	FFC1_12194	FFUJ_11961	uncharacterized protein FFUJ_11961								4.90	7.55	5.32
XLOC_012912	FFC1_12196	FFUJ_11959	uncharacterized protein FFUJ_11959							2.43	2.09		
XLOC_013406	FFC1_12197	FFUJ_11958	probable NADPH2 dehydrogenase chain OYE2							5.92	5.21	5.26	5.67
XLOC_013407	FFC1_12202	FFUJ_11953	uncharacterized protein FFUJ_11953									4.14	
XLOC_012919	FFC1_12207	FFUJ_11948	uncharacterized protein FFUJ_11948							6.61	6.36	6.65	6.93
XLOC_013410	FFC1_12208	FFUJ_11947	uncharacterized protein FFUJ_11947							5.82	4.20	2.69	
XLOC_012920	FFC1_12209	FFUJ_11946	uncharacterized protein FFUJ_11946							3.04	2.78	2.51	2.31
XLOC_012921	FFC1_12210	FFUJ_11945	probable hexokinase		2.03								-1.75
XLOC_013418	FFC1_12226	FFUJ_11930	uncharacterized protein FFUJ_11930							-1.34	-2.62	-3.41	-2.36
XLOC_012933	FFC1_12232	FFUJ_11924	uncharacterized protein FFUJ_11924							2.25			3.68
XLOC_013422	FFC1_12235	FFUJ_11921	related to pisatin demethylase / cytochrome P450 monooxygenase			1.50				6.34	9.56	7.31	10.42
XLOC_012935	FFC1_12236	FFUJ_11920	related to integral membrane protein		1.31	1.40				9.34	9.88	9.60	10.88
XLOC_012936	FFC1_12238	FFUJ_11917	uncharacterized protein FFUJ_11917							3.66	4.81	3.34	3.91
XLOC_013425	FFC1_12242	FFUJ_11913	uncharacterized protein FFUJ_11913							-1.83	-1.73	-2.22	-1.88
XLOC_013427	FFC1_12245	FFUJ_11910	related to Carboxypeptidase 2		-3.56					7.08	5.98		
XLOC_012941	FFC1_12247	FFUJ_11908	probable BRT1 protein, down-regulated by mating factor B								1.92	2.20	
XLOC_013428	FFC1_12248	FFUJ_11907	related to D-amino acid oxidase	2.84							2.84	2.60	
XLOC_012942	FFC1_12249	FFUJ_11906	probable 2-dehydropantoate 2-reductase family protein	3.04							2.99		
XLOC_013430	FFC1_12254	FFUJ_11902	uncharacterized protein FFUJ_11902									5.33	
XLOC_012946	FFC1_12255	FFUJ_11901	uncharacterized protein FFUJ_11901							2.71	3.63	3.49	2.13
XLOC_013431	FFC1_12256	FFUJ_11900	uncharacterized protein FFUJ_11900	1.68	2.09					4.66	5.08	5.90	5.05
XLOC_013432	FFC1_12257	FFUJ_11899	uncharacterized protein FFUJ_11899								2.14	1.91	2.36
XLOC_013433	FFC1_12258	FFUJ_11898	related to dlpA protein	2.80	2.95					4.89	6.74	7.76	
XLOC_012949	FFC1_12261	FFUJ_11895	uncharacterized protein FFUJ_11895							2.79	3.83	2.13	
XLOC_013438	FFC1_12270	FFUJ_11886	uncharacterized protein FFUJ_11886								-2.91		
XLOC_013442	FFC1_12279	FFUJ_11877	uncharacterized protein FFUJ_11877	5.50	6.39	6.11				4.70	5.93	8.60	7.55
XLOC_012959	FFC1_12280	FFUJ_11876	uncharacterized protein FFUJ_11876	2.39	2.75	2.99						3.16	2.32
XLOC_012963	FFC1_12286	FFUJ_11871	related to stress response protein rds1p							7.35	6.69	7.08	7.56
XLOC_012965	FFC1_12288	FFUJ_11869	related to tyrosinase precursor (monophenol monooxygenase)							5.19			
XLOC_013449	FFC1_12294	FFUJ_11862	uncharacterized protein FFUJ_11862							-2.07	-2.54	-1.95	-1.80
XLOC_012967	FFC1_12295	FFUJ_11861	related to nitric-oxide synthase, salivary gland		-1.18	-1.27				-1.24	-1.75	-2.30	-1.42
XLOC_012969	FFC1_12297	FFUJ_11858	uncharacterized protein FFUJ_11858							-2.23	-1.85	-3.02	-2.55
XLOC_012972	FFC1_12301	FFUJ_11854	uncharacterized protein FFUJ_11854							5.96	6.31	4.61	
XLOC_013452	FFC1_12303	FFUJ_11852	related to feruloyl esterase B precursor							5.35			
XLOC_012973	FFC1_12304	FFUJ_11851	related to short chain dehydrogenase		1.14					1.46	1.68	2.46	1.65
XLOC_013454	FFC1_12305	FFUJ_11850	uncharacterized protein FFUJ_11850							-2.00	-2.62	-2.94	-2.53
XLOC_013457	FFC1_12309	FFUJ_11846	related to thioredoxin		2.15	1.26				2.93	2.86	3.85	2.78
XLOC_013458	FFC1_12310	FFUJ_11845	uncharacterized protein FFUJ_11845									5.45	5.50
XLOC_012977	FFC1_12317									-1.46	-2.25	-2.01	-1.90
XLOC_013464	FFC1_12318	FFUJ_11838	related to integral membrane protein							3.40	2.60	2.83	3.16
XLOC_012978	FFC1_12319	FFUJ_11837	related to pisatin demethylase cytochrome P450							8.86	8.49	7.12	8.39
XLOC_013466	FFC1_12321	FFUJ_11835	uncharacterized protein FFUJ_11835							9.66	9.43	8.78	10.56
XLOC_013467	FFC1_12323	FFUJ_11833	uncharacterized protein FFUJ_11833							5.01			
XLOC_012981	null										-5.39		
XLOC_012982	FFC1_12328	FFUJ_11828	uncharacterized protein FFUJ_11828							-1.74	-1.69	-1.62	-2.01
XLOC_013472	FFC1_12329	FFUJ_11827	related to sugar transport protein STP1									5.51	
XLOC_013473	FFC1_12330	FFUJ_11826	related to putative transporter SEO1	1.65	1.76					5.50	4.72	5.74	5.24
XLOC_013475	FFC1_12332	FFUJ_11824	uncharacterized protein FFUJ_11824							8.86	11.32	9.25	9.00
XLOC_013476	FFC1_12333	FFUJ_11823	related to ethionine resistance protein							2.99	5.07	5.73	3.72
XLOC_012985	FFC1_12339	FFUJ_11817	related to neutral amino acid permease							2.94	1.78	1.98	1.58
XLOC_013480	FFC1_12340	FFUJ_11816	uncharacterized protein FFUJ_11816							-2.23	-1.98	-1.99	-2.11
XLOC_013481	FFC1_12341	FFUJ_11815	related to Glutathione S-transferase II		2.71	2.50			4.74	3.20	2.65	2.63	
XLOC_013483	FFC1_12342	FFUJ_11814	related to dehydrogenase							-2.46	-2.52	-3.10	-2.07
XLOC_012986	FFC1_12343	FFUJ_11813	related to BDH1-stereospecific (2R, 3R)-2,3-butanediol dehydrogenase							-3.09	-3.27	-2.91	-2.91
XLOC_013484	FFC1_12344	FFUJ_11812	uncharacterized protein FFUJ_11812							5.13	5.09	4.69	2.61
XLOC_012987	FFC1_12345	FFUJ_11811	uncharacterized protein FFUJ_11811			-1.05				4.82	4.73	4.62	4.61
XLOC_012988	FFC1_12348	FFUJ_11808	uncharacterized protein FFUJ_11808							4.86	4.39	3.63	
XLOC_013489	FFC1_12352	FFUJ_11804	related to HSP30 heat shock protein Yro1p	3.55	8.34	8.28				2.57	5.24	6.67	8.78
XLOC_013490	FFC1_12353	FFUJ_11803	probable phytoene dehydrogenase AL-1 (carotenoid biosynthesis protein al-1)	3.46	6.36	5.06			3.25	2.68	5.35	6.79	4.51
XLOC_013491	FFC1_12354	FFUJ_11802	probable geranylgeranyl-diphosphate geranylgeranyltransferase (AL-2)	3.66	6.54	5.36			3.61	2.10	5.28	6.27	3.87

XLOC_012990	FFC1_12355	FFUJ_11801	related to lignostilbene alphabeta-dioxygenase I	5.76	8.77	7.50					8.62	7.71	8.31
XLOC_013493	FFC1_12357	FFUJ_11799	related to dihydrodipicolinate synthase						-2.63				
XLOC_013494	FFC1_12358	FFUJ_11798	related to fructosyl amino acid oxidase									3.78	4.30
XLOC_013496	FFC1_12361	FFUJ_11795	related to pyrroline-5-carboxylate reductase							4.42			
XLOC_012994	FFC1_12369	FFUJ_11787	uncharacterized protein FFUJ_11787							-3.46	-6.07	-5.30	
XLOC_013504	FFC1_12371	FFUJ_11786	related to methyltransferase		-1.93	-3.05				6.40	6.11		
XLOC_012995	FFC1_12373	FFUJ_11784	related to tol protein							5.82	4.62		
XLOC_013506	FFC1_12374	FFUJ_11783	uncharacterized protein FFUJ_11783								-2.73		
XLOC_012998	FFC1_12377	FFUJ_11780	uncharacterized protein FFUJ_11780							2.90	5.31	4.14	6.74
XLOC_013507	FFC1_12378	FFUJ_11779	uncharacterized protein FFUJ_11779							2.21	1.58	2.92	2.60
XLOC_012999	FFC1_12379	FFUJ_11778	related to cercosporin resistance protein							3.10	2.86	3.40	2.97
XLOC_013000	FFC1_12380	FFUJ_11777	uncharacterized protein FFUJ_11777							5.56	5.11	6.91	6.80
XLOC_013002	FFC1_12382	FFUJ_11775	uncharacterized protein FFUJ_11775							-2.05	-2.38		
XLOC_013003	FFC1_12383	FFUJ_11774	uncharacterized protein FFUJ_11774							-3.62	-4.45	-2.58	-2.57
XLOC_013004	FFC1_12384	FFUJ_11773	uncharacterized protein FFUJ_11773										5.24
XLOC_013005	FFC1_12385	FFUJ_11772	related to alpha-L-arabinofuranosidase II precursor							5.01	5.84	4.56	5.26
XLOC_013007	FFC1_12387	FFUJ_11770	uncharacterized protein FFUJ_11770							-2.06	-2.19	-2.46	-2.47
XLOC_013510	FFC1_12390	FFUJ_11767	uncharacterized protein FFUJ_11767							3.98	5.00	5.21	3.78
XLOC_013011	FFC1_12402	FFUJ_11755	uncharacterized protein FFUJ_11755								-2.38		
XLOC_013014	FFC1_12406	FFUJ_11751	uncharacterized protein FFUJ_11751									2.28	
XLOC_013016	FFC1_12408	FFUJ_11749	related to neutral amino acid permease							1.79	1.47	2.03	1.89
XLOC_013520	FFC1_12410	FFUJ_11747	uncharacterized protein FFUJ_11747							4.31	3.28	4.29	3.49
XLOC_013526	FFC1_12419	FFUJ_01705	related to P-type ATPase							4.92	5.84	4.03	5.64
XLOC_013532	FFC1_12430	FFUJ_11727	related to small s protein							2.64	2.61	2.89	
XLOC_013027	FFC1_12433	FFUJ_11724	related to Y.lipolytica GPR1 protein and Fun34p							5.66	2.77	4.11	2.40
XLOC_013031	FFC1_12440	FFUJ_11717	uncharacterized protein FFUJ_11717							4.58	5.61	3.91	5.09
XLOC_013032	FFC1_12441	FFUJ_11716	uncharacterized protein FFUJ_11716	1.06	2.44	2.08				1.75	1.95	2.84	2.24
XLOC_013537	FFC1_12443	FFUJ_11714	probable carbonic anhydrase							4.99	5.49	3.33	
XLOC_013538	FFC1_12444	FFUJ_11713	related to nonphototropic hypocotyl protein 1		3.17	2.35				2.18	3.06	5.40	4.38
XLOC_013543	FFC1_12451									3.79	2.85	3.67	
XLOC_013039	FFC1_12455										5.05	5.10	6.83
XLOC_013040	FFC1_12456	FFUJ_11705	related to lipid binding protein Tfs1p							1.95		3.11	3.33
XLOC_013544	FFC1_12457	FFUJ_11704	probable endopeptidase K							4.07	3.78	3.80	
XLOC_013041	FFC1_12461	FFUJ_11700	uncharacterized protein FFUJ_11700										2.14
XLOC_013043	FFC1_12463	FFUJ_11698	uncharacterized protein FFUJ_11698	2.27	3.65	3.57					2.46	4.37	5.07
XLOC_013044	FFC1_12464	FFUJ_11697	uncharacterized protein FFUJ_11697			1.24				2.77	2.87	3.72	4.63
XLOC_013045	FFC1_12465	FFUJ_11696	uncharacterized protein FFUJ_11696							1.81	1.45	2.05	3.37
XLOC_013046	FFC1_12466	FFUJ_11695	uncharacterized protein FFUJ_11695							6.34	6.35	8.06	6.13
XLOC_013549	FFC1_12467	FFUJ_11694	uncharacterized protein FFUJ_11694							3.58	3.04	3.88	3.73
XLOC_013048	FFC1_12469	FFUJ_11693	related to putative tartrate transporter			2.48				5.39	5.37	7.20	8.02
XLOC_013050	FFC1_12471	FFUJ_11691	uncharacterized protein FFUJ_11691							9.27	7.84	8.33	9.73
XLOC_013550	FFC1_12472	FFUJ_11690	uncharacterized protein FFUJ_11690							4.66	4.84	4.72	4.55
XLOC_013052	FFC1_12475	FFUJ_11687	uncharacterized protein FFUJ_11687							8.43	8.06	8.05	7.87
XLOC_013053	FFC1_12476	FFUJ_11686	related to diacylglycerol pyrophosphate phosphatase DPP1							8.46	8.22	8.54	7.10
XLOC_013552	FFC1_12477	FFUJ_11685	uncharacterized protein FFUJ_11685							5.28	4.74	5.24	4.05
XLOC_013553	FFC1_12479	FFUJ_11683	uncharacterized protein FFUJ_11683			-1.88				2.59	1.77		
XLOC_013556	FFC1_12484	FFUJ_11678	related to glutamate carboxypeptidase II							2.11	2.80	3.15	1.76
XLOC_013558	FFC1_12487	FFUJ_11675	probable DUR3-Urea permease							3.05		1.86	
XLOC_013062	FFC1_12492	FFUJ_11670	uncharacterized protein FFUJ_11670							2.95	3.67		2.07
XLOC_013560	FFC1_12493	FFUJ_11669	uncharacterized protein FFUJ_11669							2.42	2.44	2.41	3.19
XLOC_013561	FFC1_12494	FFUJ_11668	uncharacterized protein FFUJ_11668							3.00	2.65	2.52	2.18
XLOC_013063	FFC1_12495	FFUJ_11667	uncharacterized protein FFUJ_11667							2.76	1.81	2.86	1.77
XLOC_013064	FFC1_12496	FFUJ_11666	uncharacterized protein FFUJ_11666			1.46				2.42	2.27	3.68	4.27
XLOC_013065	FFC1_12497	FFUJ_11665	uncharacterized protein FFUJ_11665			1.39				3.82	3.00	4.49	3.92
XLOC_013562	FFC1_12498	FFUJ_11664	related to multidrug resistance protein		1.42	1.80				2.59	2.64	4.23	3.94
XLOC_013066	FFC1_12499	FFUJ_11663	uncharacterized protein FFUJ_11663			1.73				2.24	2.32	3.25	3.47
XLOC_013067	FFC1_12502	FFUJ_11660	related to SPS19-peroxisomal 2,4-dienoyl-CoA reductase			2.16				4.63	6.75	6.74	4.97
XLOC_013565	FFC1_12503	FFUJ_11659	related to dityrosine transporter	2.30	1.64					4.86	6.10	4.24	2.35
XLOC_013068	FFC1_12504	FFUJ_11658	uncharacterized protein FFUJ_11658	2.10	1.64					1.16	2.83	1.71	
XLOC_013070	FFC1_12507	FFUJ_11655	uncharacterized protein FFUJ_11655			1.19				-3.16	-4.09	-3.81	-3.00
XLOC_013071	FFC1_12508	FFUJ_11654	related to sedoheptulose-1,7-bisphosphatase							-2.04	-2.52	-2.18	-1.52
XLOC_013073	FFC1_12512	FFUJ_11650	uncharacterized protein FFUJ_11650						-1.35	-3.50	-4.58	-3.38	-2.12
XLOC_013570	FFC1_12514	FFUJ_11648	uncharacterized protein FFUJ_11648							3.16	2.94	3.43	
XLOC_013571	FFC1_12515	FFUJ_11647	related to triacylglycerol lipase							4.16	4.65	3.28	
XLOC_013572	FFC1_12517	FFUJ_11645	related to fructosyl amino acid oxidase							3.42	2.86	3.50	4.49
XLOC_013575	FFC1_12522	FFUJ_11640	probable lysine permease							3.45	4.12	3.15	
XLOC_013576	FFC1_12523	FFUJ_11639	related to Dal5p							-7.87	-8.75	-8.11	-8.52
XLOC_013577	FFC1_12524	FFUJ_11638	uncharacterized protein FFUJ_11638							-4.42	-5.93	-6.16	-5.86
XLOC_013578	FFC1_12525	FFUJ_11637	related to hydrolases or acyltransferases (alpha/beta hydrolase superfamily)							-2.76	-3.52	-3.22	-2.97
XLOC_013579	FFC1_12526	FFUJ_11636	uncharacterized protein FFUJ_11636							-4.99			
XLOC_013078	FFC1_12529	FFUJ_11633	uncharacterized protein FFUJ_11633							7.54	7.40	8.60	6.00
XLOC_013581	FFC1_12530	FFUJ_11632	probable pectinesterase precursor			-1.37				4.21	2.99	3.10	3.23
XLOC_013582	FFC1_12531	FFUJ_11631	uncharacterized protein FFUJ_11631							6.04	6.22	6.79	6.09
XLOC_013583	FFC1_12532	FFUJ_11630	uncharacterized protein FFUJ_11630							4.28		2.52	
XLOC_013081	FFC1_12544	FFUJ_11618	related to flavin-containing monooxygenase			2.35				5.00	5.03	4.99	7.48
XLOC_013594	FFC1_12545	FFUJ_07335	probable Chitin Synthase 1 (chs-1)							3.66	3.31	2.79	2.41
XLOC_013082	FFC1_12546									5.76	6.05		7.01
XLOC_013595	FFC1_12547	FFUJ_11616	related to QDE3 protein (involved in gene silencing)							2.89	2.44	2.28	2.21
XLOC_013083	FFC1_12548	FFUJ_11615	uncharacterized protein FFUJ_11615		2.33					3.22	2.75	4.61	3.93

XLOC_013597	FFC1_12551	FFUJ_11612	probable cytochrome P450 55A2									3.45	
XLOC_013085	null										3.39	4.68	
XLOC_013086	FFC1_12552	FFUJ_11611	uncharacterized protein FFUJ_11611								2.12	3.05	
XLOC_013598	FFC1_12554	FFUJ_11609	uncharacterized protein FFUJ_11609							-2.28	-2.89	-2.71	-3.12
XLOC_013602	FFC1_12560	FFUJ_11604	uncharacterized protein FFUJ_11604										6.32
XLOC_013603	FFC1_12561	FFUJ_11603	uncharacterized protein FFUJ_11603			-1.40				6.92	6.03	6.93	5.07
XLOC_013091	FFC1_12562	FFUJ_11602	uncharacterized protein FFUJ_11602							1.82	1.62	2.04	1.66
XLOC_013096	FFC1_12568	FFUJ_11597	uncharacterized protein FFUJ_11597							5.07	5.43		
XLOC_013606	FFC1_12569	FFUJ_11596	related to TfdA family oxidoreductase							5.44			
XLOC_013607	FFC1_12574	FFUJ_11591	uncharacterized protein FFUJ_11591		-1.14					3.05	1.99	1.26	2.56
XLOC_013101	FFC1_12575	FFUJ_11590	related to calcium-independent phospholipase A2							2.98	2.06	1.88	2.49
XLOC_013612	FFC1_12584	FFUJ_14932	uncharacterized protein FFUJ_14932							6.68	6.84	6.77	5.46
XLOC_013107	FFC1_12585	FFUJ_11581	uncharacterized protein FFUJ_11581							6.49	4.93	8.11	8.16
XLOC_013613	FFC1_12588	FFUJ_11578	uncharacterized protein FFUJ_11578							-1.71	-3.45	-5.20	
XLOC_013614	FFC1_12589	FFUJ_11577	related to guanine deaminase							2.58	2.19	2.72	2.74
XLOC_013110	FFC1_12590	FFUJ_11576	uncharacterized protein FFUJ_11576							1.30		1.93	2.48
XLOC_013615	FFC1_12591	FFUJ_11575	related to wound-inducible protein AWI 31							4.10	4.24	6.02	4.89
XLOC_013112	FFC1_12594	FFUJ_11572	uncharacterized protein FFUJ_11572							4.21	3.87		
XLOC_013617	FFC1_12595	FFUJ_11571	related to Cytochrome P450 3A5							-1.28	-2.16	-2.11	
XLOC_013618	FFC1_12596	FFUJ_11570	uncharacterized protein FFUJ_11570		-1.45	-1.46				-0.96	-1.94	-2.48	-1.47
XLOC_013113	null									-2.22	-3.84	-6.64	-5.10
XLOC_013619	FFC1_12597	FFUJ_11569	related to 4-coumarate--CoA ligase		-2.05	-1.16			-1.67	-4.03	-4.95	-5.41	-3.51
XLOC_013114	null										-4.99		
XLOC_013116	FFC1_12599	FFUJ_11567	related to estradiol 17 beta-dehydrogenase							2.62	2.87	3.89	
XLOC_013117	FFC1_12600					-1.22				3.06	2.52	1.89	
XLOC_013622	FFC1_12604	FFUJ_11562	related to PHO11-secreted acid phosphatase	3.84	4.51	1.90				7.87	9.25	8.10	7.05
XLOC_013623	FFC1_12605	FFUJ_11561	uncharacterized protein FFUJ_11561										5.32
XLOC_013120	FFC1_12612	FFUJ_11554	related to L-fucose permease							6.72	8.38	5.29	6.85
XLOC_013629	FFC1_12615	FFUJ_11551	probable MNN2-type II membrane protein							2.04	1.64	1.64	1.67
XLOC_013630	FFC1_12616	FFUJ_11550	uncharacterized protein FFUJ_11550							2.06	1.35	1.92	2.09
XLOC_013631	FFC1_12617	FFUJ_11549	related to aromatic-L-amino-acid decarboxylase							-3.22	-3.72	-3.61	-2.12
XLOC_013632	FFC1_12618	FFUJ_11548	uncharacterized protein FFUJ_11548							-2.22	-3.17	-2.10	-1.37
XLOC_013122	FFC1_12619	FFUJ_11547	probable lactonohydrolase							-0.87	-2.41	-1.61	
XLOC_013637	FFC1_12625	FFUJ_11542	related to DNA repair exonuclease SIA1		1.24					3.80	4.06	4.54	3.42
XLOC_013125	FFC1_12626	FFUJ_11541	uncharacterized protein FFUJ_11541							2.56			
XLOC_013126	FFC1_12627	FFUJ_11540	uncharacterized protein FFUJ_11540									5.04	
XLOC_013129	FFC1_12630	FFUJ_11537	uncharacterized protein FFUJ_11537									4.22	4.36
XLOC_013640	FFC1_12632	FFUJ_11535	uncharacterized protein FFUJ_11535		1.49						0.98	2.05	0.80
XLOC_013130	FFC1_12633	FFUJ_11534	uncharacterized protein FFUJ_11534							4.73	5.25	5.88	
XLOC_013642	FFC1_12635	FFUJ_11532	related to alpha-glucoside transport protein							4.11			
XLOC_013645	FFC1_12639	FFUJ_11528	uncharacterized protein FFUJ_11528							6.47	8.16	6.77	6.36
XLOC_013140	FFC1_12652	FFUJ_11521	related to long-chain-fatty-acid--CoA ligase							-1.94	-2.59	-2.90	
XLOC_013652	FFC1_12654	FFUJ_11519	uncharacterized protein FFUJ_11519							-1.25	-2.23	-1.78	-2.02
XLOC_013141	FFC1_12655	FFUJ_11518	related to putative multidrug transporter							-2.40	-3.98	-2.34	-3.65
XLOC_013146	FFC1_12664	FFUJ_11510	related to polyamine oxidase precursor							2.26	1.95	2.08	
XLOC_013147	FFC1_12665	FFUJ_11509	related to DNA repair exonuclease SIA1							2.29	4.33	3.53	2.32
XLOC_013148	FFC1_12666	FFUJ_11508	uncharacterized protein FFUJ_11508			1.24				7.78	7.89	8.58	8.19
XLOC_013149	FFC1_12667	FFUJ_11507	related to nitrate assimilation regulatory protein nirA							2.46	2.33	2.83	1.61
XLOC_013150	FFC1_12668	FFUJ_11506	uncharacterized protein FFUJ_11506		1.76					2.97	2.21	4.66	2.53
XLOC_013151	FFC1_12669	FFUJ_11505	uncharacterized protein FFUJ_11505		2.41	1.36			2.43	4.95	4.78	5.44	3.91
XLOC_013154	null									3.26	2.45	2.05	3.56
XLOC_013161	FFC1_12680	FFUJ_11494	uncharacterized protein FFUJ_11494							6.94	4.09	7.52	
XLOC_013162	FFC1_12681	FFUJ_11493	uncharacterized protein FFUJ_11493		2.45							2.51	
XLOC_013166	FFC1_12685	FFUJ_11489	related to endo-1,3-beta-glucanase										5.81
XLOC_013168	FFC1_12687	FFUJ_11487	related to ankyrin							5.23	7.18	5.24	5.48
XLOC_013169	FFC1_12688	FFUJ_11486	probable Cyanamide hydratase							6.60	5.08	6.22	
XLOC_013662	FFC1_12689	FFUJ_11485	uncharacterized protein FFUJ_11485		3.49	4.38						6.93	4.08
XLOC_013171	FFC1_12691	FFUJ_11483	related to quinate transport protein		1.68	2.35				-1.78	-1.70		
XLOC_013667	FFC1_12694	FFUJ_11480	uncharacterized protein FFUJ_11480			-2.02				3.18			
XLOC_013669	FFC1_12696	FFUJ_11478	probable potassium transporter TRK-1							-2.57	-2.98	-2.68	-1.68
XLOC_013672	FFC1_12699	FFUJ_11475	uncharacterized protein FFUJ_11475		2.37						1.45		
XLOC_013674	FFC1_12701	FFUJ_11473	related to spore coat protein SP96 precursor							1.92	2.10	1.99	
XLOC_013172	FFC1_12702	FFUJ_11472	probable catalase isozyme P	1.13	2.30					4.51	5.90	6.63	5.11
XLOC_013176	FFC1_12703	FFUJ_11471	uncharacterized protein FFUJ_11471							4.93	6.61	7.28	5.38
XLOC_013675	FFC1_12704	FFUJ_11470	related to channel proteins							2.19	4.44	4.68	
XLOC_013677	FFC1_12705	FFUJ_11469	related to thermoresistant gluconokinase		1.82	0.99				2.78	3.00	3.53	3.01
XLOC_013178	FFC1_12706									2.85			2.76
XLOC_013181	FFC1_12715	FFUJ_11460	related to aminotriazole resistance protein							1.86	1.91	2.16	1.75
XLOC_013182	FFC1_12716	FFUJ_11459	related to hydroxylase							2.89	2.05	3.90	2.66
XLOC_013183	FFC1_12717	FFUJ_11458	related to 7alpha-cephem-methoxylase P8 chain							2.93	2.36	3.52	2.84
XLOC_013684	FFC1_12718	FFUJ_11457	uncharacterized protein FFUJ_11457								4.97	6.07	6.72
XLOC_013194	null									4.76			
XLOC_013195	FFC1_12735	FFUJ_11440	related to ADH2-alcohol dehydrogenase II							5.83	4.43	4.25	4.01
XLOC_013196	FFC1_12736	FFUJ_11439	related to protein LAC1							-1.81	-2.33	-2.92	-2.35
XLOC_013197	FFC1_12737	FFUJ_11438	probable catalase 2							2.29	2.14	2.03	2.98
XLOC_013696	FFC1_12745	FFUJ_11430	related to tripeptidyl-peptidase I								-2.56		-1.96
XLOC_013697	FFC1_12747	FFUJ_11428	uncharacterized protein FFUJ_11428							-5.67	-8.68	-7.75	-6.69
XLOC_013202	null										-4.90		

XLOC_013698	null									4.07	6.51		
XLOC_013203	FFC1_12748	FFUJ_11427	uncharacterized protein FFUJ_11427		-2.11	-1.90				3.40	2.18		
XLOC_013699	FFC1_12750	FFUJ_11425	uncharacterized protein FFUJ_11425							3.38	1.94	2.40	2.34
XLOC_013206	FFC1_12751	FFUJ_11424	probable ADP-ribosylation factor							2.20		1.76	
XLOC_013208	FFC1_12753	FFUJ_11422	uncharacterized protein FFUJ_11422							2.27	2.21	1.79	
XLOC_013209	FFC1_12754	FFUJ_11421	related to NADPH-dependent aldehyde reductase							4.64	5.65	5.99	4.24
XLOC_013210	FFC1_12755	FFUJ_11420	related to lipase 1							1.64		2.44	
XLOC_013701	FFC1_12758										-1.69	-2.44	-4.66
XLOC_013703	FFC1_12762	FFUJ_11412	uncharacterized protein FFUJ_11412						-2.29	-1.90	-2.65	-3.70	
XLOC_013706	FFC1_12765	FFUJ_11410	probable lactonohydrolase							-1.28	-1.65	-2.44	
XLOC_013214	FFC1_12766	FFUJ_11409	uncharacterized protein FFUJ_11409							-1.12	-1.60	-2.01	
XLOC_013708	FFC1_12770	FFUJ_11405	uncharacterized protein FFUJ_11405		-5.09					5.76			
XLOC_013710	FFC1_12774	FFUJ_11400	related to 3-oxoacyl							-2.32	-2.20	-2.18	-1.86
XLOC_013222	FFC1_12779	FFUJ_11396	uncharacterized protein FFUJ_11396							-2.18	-2.56	-2.57	-2.90
XLOC_013228	FFC1_12787	FFUJ_11388	uncharacterized protein FFUJ_11388										4.05
XLOC_013232	FFC1_12791	FFUJ_11384	uncharacterized protein FFUJ_11384							2.24	1.25		
XLOC_013233	FFC1_12792	FFUJ_11383	related to tol protein							-2.52	-3.44	-3.49	
XLOC_013717	FFC1_12798	FFUJ_11377	related to vacuolar membrane protein HMT1 (heavy metal tolerance protein)							3.18	3.11	3.44	3.19
XLOC_013238	null									4.01			
XLOC_013239	FFC1_12799	FFUJ_11376	uncharacterized protein FFUJ_11376							7.06	5.03	6.11	6.75
XLOC_013240	FFC1_12800	FFUJ_11375	uncharacterized protein FFUJ_11375							7.00	7.87	9.61	8.80
XLOC_013241	FFC1_12801	FFUJ_11374	uncharacterized protein FFUJ_11374							6.28	6.89	7.80	7.62
XLOC_013718	FFC1_12802	FFUJ_11373	uncharacterized protein FFUJ_11373									6.35	6.22
XLOC_013719	FFC1_12803	FFUJ_11372	uncharacterized protein FFUJ_11372										5.75
XLOC_013720	FFC1_12804	FFUJ_11371	related to esterase/lipase							-2.37	-3.15		
XLOC_013722	FFC1_12806	FFUJ_11369	related to CLC chloride channel protein								4.80	4.77	
XLOC_013243	FFC1_12808	FFUJ_11367	probable alpha-L-arabinofuranosidase								3.46	3.81	3.91
XLOC_013723	FFC1_12809	FFUJ_11366	related to sulfonate dioxygenase							4.58	5.26		5.33
XLOC_013726	FFC1_12812	FFUJ_11363	related to heterokaryon incompatibility protein het-6									6.50	6.68
XLOC_013729	FFC1_12816	FFUJ_11359	related to ketoreductases		1.79					2.65	2.93	4.53	2.73
XLOC_013245	FFC1_12818	FFUJ_11357	uncharacterized protein FFUJ_11357							-1.98	-2.69	-2.22	-2.19
XLOC_013733	FFC1_12823	FFUJ_11352	related to methyltransferase		-1.96	-1.63				5.39	4.30	3.02	2.97
XLOC_013735	FFC1_12826	FFUJ_11349	related to large-conductance mechanosensitive channel							5.72	4.60	3.86	
XLOC_013251	FFC1_12827	FFUJ_11348	related to 2-polyprenyl-6-methoxyphenol hydroxylase and related FAD-dependent oxidoreductases							2.64	2.26		
XLOC_013263	FFC1_12851	FFUJ_11325	related to SUR1-required for mannosylation of sphingolipids		-1.42					-1.47	-2.21	-2.56	-2.34
XLOC_013749	FFC1_12852	FFUJ_11324	related to aromatic-L-amino-acid decarboxylase							-1.23	-1.69	-2.15	
XLOC_013750	FFC1_12853	FFUJ_11323	uncharacterized protein FFUJ_11323							-2.21	-1.97	-1.87	-2.67
XLOC_013752	FFC1_12858	FFUJ_11315	related to small s protein							6.68	5.76	5.66	4.05
XLOC_013755	FFC1_12864	FFUJ_11309	uncharacterized protein FFUJ_11309							-6.53	-6.74	-7.01	-8.04
XLOC_013270	FFC1_12865	FFUJ_11308	DAN4-Cell wall mannoprotein, expressed under anaerobic conditions, completely repressed during aerobic growth							-4.18	-6.14	-5.33	-4.61
XLOC_013764	FFC1_12878	FFUJ_11295	related to integral membrane protein PTH11							2.90	2.26	2.05	2.18
XLOC_013275	FFC1_12879	FFUJ_11294	related to O-methyltransferase B		-1.42					6.55	5.43	4.39	4.66
XLOC_013276	FFC1_12883	FFUJ_11290	probable permeases							5.22			
XLOC_013769	FFC1_12889	FFUJ_11285	uncharacterized protein FFUJ_11285									5.63	
XLOC_013771	FFC1_12893	FFUJ_11281	uncharacterized protein FFUJ_11281							-4.13	-8.58	-4.87	-4.59
XLOC_013283	FFC1_12894	FFUJ_11280	uncharacterized protein FFUJ_11280							-7.09	-5.64	-6.80	-4.47
XLOC_013288	FFC1_12904	FFUJ_11269	uncharacterized protein FFUJ_11269							-3.38	-4.24	-6.05	-3.60
XLOC_013289	FFC1_12905	FFUJ_11268	probable carboxy-cis,cis-muconate cyclase							4.49			
XLOC_013291	FFC1_12907	FFUJ_11266	uncharacterized protein FFUJ_11266							2.83	2.82	4.26	4.93
XLOC_013778	FFC1_12911	FFUJ_11263	uncharacterized protein FFUJ_11263							3.09	1.64	3.14	3.60
XLOC_013294	FFC1_12916	FFUJ_11259	uncharacterized protein FFUJ_11259							5.16	4.61	5.27	4.69
XLOC_013783	FFC1_12917	FFUJ_11258	related to 1-acyldihydroxyacetone-phosphate reductase										5.00
XLOC_013296	FFC1_12919	FFUJ_11256	uncharacterized protein FFUJ_11256							-8.74	-8.37	-7.52	-7.81
XLOC_013784	FFC1_12920	FFUJ_11255	uncharacterized protein FFUJ_11255							8.67	8.63	7.99	8.20
XLOC_013786	FFC1_12923	FFUJ_11253	related to glucose/galactose transporter							-3.94	-2.16	-3.84	-3.09
XLOC_013299	FFC1_12925	FFUJ_11251	uncharacterized protein FFUJ_11251		-1.31	-1.24				-0.82	-1.72	-2.07	-1.99
XLOC_013787	FFC1_12930	FFUJ_11246	related to cocaine esterase							6.42	2.89		
XLOC_013791	FFC1_12935	FFUJ_11241	uncharacterized protein FFUJ_11241							3.68			
XLOC_013306	FFC1_12938	FFUJ_11239	related to aldehyde-alcohol dehydrogenase							2.00	1.69	2.07	1.56
XLOC_013794	FFC1_12943	FFUJ_11234	related to integral membrane protein PTH11							4.39	3.47	2.89	3.09
XLOC_013311	FFC1_12944	FFUJ_11233	related to 15-hydroxyprostaglandin dehydrogenase		-1.14					2.34	1.55		
XLOC_013312	FFC1_12945	FFUJ_11232	related to secretory lipase							9.54	9.06	8.21	9.72
XLOC_013795	FFC1_12946	FFUJ_11231	uncharacterized protein FFUJ_11231							6.84	6.26	6.65	6.99
XLOC_013796	FFC1_12947	FFUJ_11230	related to TRI13-cytochrome P450							6.07	5.18	3.81	5.06
XLOC_013798	FFC1_12951	FFUJ_11226	uncharacterized protein FFUJ_11226									2.75	2.20
XLOC_013316	FFC1_12952	FFUJ_11225	related to amidohydrolase AmhX										2.93
XLOC_013317	FFC1_12953	FFUJ_11224	related to allantoate permease			4.27						2.78	4.38
XLOC_013318	FFC1_12954	FFUJ_11223	uncharacterized protein FFUJ_11223	1.96	3.05	4.57						2.41	3.73
XLOC_013799	FFC1_12955	FFUJ_11222	uncharacterized protein FFUJ_11222	1.82	2.41	3.85				-1.32		1.24	3.18
XLOC_013800	FFC1_12956	FFUJ_11221	uncharacterized protein FFUJ_11221							-5.30	-5.98	-3.58	-3.27
XLOC_013322	FFC1_12963	FFUJ_11214	related to ankyrin 3		1.04	2.07				3.53	3.04	4.31	4.72
XLOC_013804	FFC1_12964	FFUJ_11213	related to ketoreductase							3.62	2.73	3.20	3.97
XLOC_013805	FFC1_12965	FFUJ_11212	related to DUF1338 domain protein							5.94			

XLOC_013323	FFC1_12966	FFUJ_11211	related to novobiocin biosynthesis protein novR							5.32			
XLOC_013806	FFC1_12967	FFUJ_11210	uncharacterized protein FFUJ_11210							2.65			
XLOC_013324	FFC1_12968	FFUJ_11209	related to glycerate-and formate-dehydrogenases							2.43	1.45	2.52	
XLOC_013809	FFC1_12973	FFUJ_11205	related to Alpha-N-acetylgalactosaminidase precursor							7.22	6.48	6.43	4.63
XLOC_013327	FFC1_12974	FFUJ_11204	related to alpha-glucoside transport protein								6.88		
XLOC_013810	FFC1_12975	FFUJ_11203	related to O-methylsterigmatocystin oxidoreductase		-2.79					2.19			
XLOC_013329	FFC1_12977	FFUJ_11201	uncharacterized protein FFUJ_11201								1.80	2.35	1.92
XLOC_014179	FFC1_12982	FFUJ_04654	related to 2-polyprenyl-6-methoxyphenol hydroxylase and related FAD-dependent oxidoreductases		5.20	3.71					2.81	5.23	2.96
XLOC_013815	FFC1_12989	FFUJ_04661	uncharacterized protein FFUJ_04661							-1.39	-1.57	-2.26	-1.34
XLOC_014186	FFC1_12995	FFUJ_04669	related to helicase-like transcription factor		2.77	1.15						3.39	1.80
XLOC_014187	FFC1_12996	FFUJ_04670	uncharacterized protein FFUJ_04670		1.55	1.70				7.62	7.02	7.27	
XLOC_013819	FFC1_12997	FFUJ_04671	uncharacterized protein FFUJ_04671	0.76	1.33	1.32				2.92	2.95	3.73	2.36
XLOC_014188	FFC1_12998	FFUJ_04672	uncharacterized protein FFUJ_04672	1.65	1.78					8.03	7.53	7.54	6.30
XLOC_014190	FFC1_13003	FFUJ_04677	uncharacterized protein FFUJ_04677							-2.66	-3.12	-3.50	-2.34
XLOC_014194	FFC1_13013	FFUJ_04686	uncharacterized protein FFUJ_04686							-3.63	-3.31	-1.96	-3.08
XLOC_013832	null										-2.83		
XLOC_013845	FFC1_13035	FFUJ_04707	uncharacterized protein FFUJ_04707							5.60	5.29	5.55	5.52
XLOC_013859	null									2.32			
XLOC_014213	FFC1_13061	FFUJ_04733	uncharacterized protein FFUJ_04733		0.92					-2.12	-1.87	-1.48	-2.24
XLOC_014216	FFC1_13065	FFUJ_04737	related to heat shock protein MDJ1		1.24					2.00	1.87	2.59	2.11
XLOC_014217	FFC1_13066	FFUJ_04738	uncharacterized protein FFUJ_04738							2.48	2.36	2.46	2.35
XLOC_013863	FFC1_13067	FFUJ_04739	related to C2H2 zinc finger protein							3.27	2.73	2.61	2.77
XLOC_013865	FFC1_13071	FFUJ_04743	related to mixed-linked glucanase precursor MLG1			-1.20				3.13	2.94	2.42	2.35
XLOC_013866	FFC1_13073	FFUJ_04745	related to IST2 protein		0.76					2.00	2.28	2.39	1.95
XLOC_014226	FFC1_13086	FFUJ_04757	uncharacterized protein FFUJ_04757	1.46	2.24					3.68	3.99	4.55	3.30
XLOC_013885	FFC1_13103	FFUJ_04774	related to DUF domain protein							-0.83	-2.05	-2.36	-2.36
XLOC_013887	FFC1_13107	FFUJ_04778	uncharacterized protein FFUJ_04778							3.64	3.25	3.67	2.61
XLOC_014237	FFC1_13108	FFUJ_04779	uncharacterized protein FFUJ_04779		0.99					-2.85	-1.45	-2.00	-2.51
XLOC_013888	FFC1_13109									-2.14		-1.50	-1.47
XLOC_014239	FFC1_13113	FFUJ_04782	uncharacterized protein FFUJ_04782									-1.67	-2.92
XLOC_014242	FFC1_13118	FFUJ_04787	uncharacterized protein FFUJ_04787							-1.29	-2.22	-2.33	-2.29
XLOC_013902	FFC1_13134	FFUJ_04800	probable 4-alpha-glucanotransferase / amylo-1,6-glucosidase (glycogen-debranching enzyme)	1.03	1.78						1.24	2.11	
XLOC_013903	FFC1_13138	FFUJ_04804	uncharacterized protein FFUJ_04804		4.14							4.96	6.56
XLOC_013907	null									4.22	3.87		
XLOC_013908	FFC1_13144	FFUJ_04810	uncharacterized protein FFUJ_04810		2.01	1.59			1.43	1.87	1.92	2.67	2.05
XLOC_014257	FFC1_13145	FFUJ_04811	related to G protein coupled receptor like protein		1.91	2.41				4.97	5.32	6.80	8.10
XLOC_013914	FFC1_13155	FFUJ_04821	related to flavin oxidoreductase							2.66	2.63	2.59	1.55
XLOC_014269	FFC1_13167	FFUJ_04833	related to CHIP protein (carboxyl terminus of Hsc70-interacting protein)							2.87	2.11	2.15	2.28
XLOC_014270	FFC1_13168	FFUJ_04834	related to benzoate 4-monooxygenase cytochrome P450							3.54	2.81	2.35	3.01
XLOC_014285	FFC1_13193	FFUJ_04859	related to phospholipid-translocating ATPase							-2.29	-1.51		
XLOC_014288	null											-3.47	
XLOC_014290	FFC1_13200	FFUJ_04865	related to fungal transcriptional regulatory protein							-1.51	-1.81	-1.55	-2.10
XLOC_014293	FFC1_13202	FFUJ_04867	probable uracil permease			-1.42				-3.81	-3.43	-4.15	-4.48
XLOC_014299	FFC1_13211	FFUJ_04876	related to Zn-finger protein							3.51	3.13	3.99	2.95
XLOC_013936	null											6.92	
XLOC_014300	FFC1_13212	FFUJ_04877	uncharacterized protein FFUJ_04877		1.87					1.56	1.71	2.72	1.41
XLOC_014304	FFC1_13220	FFUJ_04885	uncharacterized protein FFUJ_04885							-1.53	-1.70	-2.50	-1.78
XLOC_013947	FFC1_13230	FFUJ_04895	probable proline-tRNA ligase							-2.46	-2.40	-2.51	-1.63
XLOC_014311	FFC1_13237	FFUJ_04902	related to GAL4-like transcriptional activator							4.79	7.17	3.36	4.12
XLOC_013951	null									-4.39			
XLOC_014312	FFC1_13238									-1.61	-2.31		-2.33
XLOC_014314	FFC1_13241	FFUJ_04906	related to allantoate permease							3.46	2.53	2.15	
XLOC_013961	FFC1_13261	FFUJ_04925	uncharacterized protein FFUJ_04925							-2.73	-4.95	-3.45	
XLOC_014330	FFC1_13266	FFUJ_04931	probable norsolorinic acid reductase		1.20					1.98	2.57	4.04	3.48
XLOC_014338	FFC1_13277	FFUJ_04942	related to protein kinase NPR1							2.42	2.83	2.64	2.44
XLOC_013969	FFC1_13281	FFUJ_04946	uncharacterized protein FFUJ_04946							-2.07	-1.86	-1.78	
XLOC_014342	FFC1_13282	FFUJ_04947	related to brt1 protein							-4.37	-3.98	-3.11	-2.81
XLOC_014344	FFC1_13284	FFUJ_04949	related to methyltransferase							-3.56	-2.99	-2.98	-2.22
XLOC_013970	FFC1_13286	FFUJ_14890	uncharacterized protein FFUJ_14890							2.72	2.01	1.88	
XLOC_013971	FFC1_13287	FFUJ_04951	related to coxI translation protein CYA5		1.17	1.07				2.70	3.04	3.43	2.92
XLOC_014348	FFC1_13295	FFUJ_04958	uncharacterized protein FFUJ_04958							1.87	1.95	2.12	1.38
XLOC_014349	null									2.69	1.93	3.48	4.76
XLOC_014350	FFC1_13296	FFUJ_04959	uncharacterized protein FFUJ_04959	1.76	1.73			1.57		3.00	3.54	3.16	2.32
XLOC_014358	FFC1_13308	FFUJ_04971	uncharacterized protein FFUJ_04971							-1.99	-2.19	-2.18	-1.38
XLOC_014359	null									-3.34			
XLOC_014364	FFC1_13316	FFUJ_04978	uncharacterized protein FFUJ_04978		0.87					1.00	0.79	1.94	2.08
XLOC_013984	null									-1.54	-2.08	-1.79	
XLOC_013989	FFC1_13325	FFUJ_04986	related to SNARE binding protein		1.15					1.22	1.31	2.17	1.79
XLOC_014368	FFC1_13326	FFUJ_04987	related to methyltransferase involved in pre-rRNA cleavage							1.01	1.44	2.23	2.18
XLOC_014370	FFC1_13330	FFUJ_04991	related to helicase-like transcription factor protein							2.12	1.86	1.57	
XLOC_014371	null									3.07	2.17		

XLOC_013996	FFC1_13338	FFUJ_04998	uncharacterized protein FFUJ_04998							2.92	2.93	2.35	2.35
XLOC_014002	FFC1_13347	FFUJ_05006	related to cytochrome p450							-2.39	-4.25		
XLOC_014003	FFC1_13348	FFUJ_05007	related to purine-cytosine permease							6.59	6.74	6.05	
XLOC_014379	FFC1_13349	FFUJ_05008	related to riboflavin biosynthesis protein RIB7		0.93					2.28	3.65	3.56	2.97
XLOC_014384	FFC1_13356	FFUJ_05015	uncharacterized protein FFUJ_05015							-1.58	-1.63	-2.18	-2.05
XLOC_014006	null												-3.10
XLOC_014007	FFC1_13357	FFUJ_05016	uncharacterized protein FFUJ_05016							-2.29	-0.96	-2.14	-2.24
XLOC_014014	FFC1_13364	FFUJ_05023	related to ferroportin 1		-1.04					-1.42	-1.75	-2.10	-1.36
XLOC_014022	FFC1_13378	FFUJ_05037	related to spherulin 1A precursor							-1.74	-2.12	-3.76	
XLOC_014035	FFC1_13397									4.34	6.12	5.91	6.05
XLOC_014401	FFC1_13398	FFUJ_05055	uncharacterized protein FFUJ_05055		-0.89	-0.96				2.03	1.44	1.07	
XLOC_014402	FFC1_13399	FFUJ_05056	related to acetate regulatory DNA binding protein FacB		-1.27	-1.82						-2.23	
XLOC_014404	FFC1_13401	FFUJ_05057	uncharacterized protein FFUJ_05057		-1.32					-1.84	-2.62	-3.04	-2.35
XLOC_014038	FFC1_13406	FFUJ_05061	uncharacterized protein FFUJ_05061							1.76	1.41	2.55	
XLOC_014039	FFC1_13407	FFUJ_05062	related to 3-phytase precursor								-2.12		
XLOC_014044	FFC1_13411	FFUJ_05066	uncharacterized protein FFUJ_05066							-4.89		-4.03	-5.98
XLOC_014418	FFC1_13427	FFUJ_05082	uncharacterized protein FFUJ_05082		1.85					3.05	3.69	4.52	3.45
XLOC_014420	FFC1_13429	FFUJ_05084	related to integral membrane protein							-3.43	-3.05	-3.31	-3.77
XLOC_014421	FFC1_13431	FFUJ_05086	uncharacterized protein FFUJ_05086										2.81
XLOC_014422	FFC1_13432	FFUJ_05087	uncharacterized protein FFUJ_05087							2.20	1.74	2.47	1.82
XLOC_014424	FFC1_13435	FFUJ_05090	uncharacterized protein FFUJ_05090							2.64	2.78	2.25	3.62
XLOC_014425	FFC1_13436									2.89	2.81	2.37	3.28
XLOC_014056	null									4.28			
XLOC_014057	FFC1_13438	FFUJ_05092	related to dihydrodipicolinate synthase							2.34			
XLOC_014427	FFC1_13440	FFUJ_05094	uncharacterized protein FFUJ_05094			5.78							4.93
XLOC_014428	FFC1_13442	FFUJ_05096	related to low-affinity hexose transporter HXT3								1.53		2.04
XLOC_014430	FFC1_13444									2.43			
XLOC_014433	FFC1_13450	FFUJ_05104	related to sentrin-specific protease SENP8 (SUMO-specific protease)							3.04	3.54	3.18	2.38
XLOC_014434	null									3.44	5.46	3.84	3.02
XLOC_014435	FFC1_13451				1.09					4.16	3.51	4.46	3.54
XLOC_014436	FFC1_13452	FFUJ_05105	uncharacterized protein FFUJ_05105							3.23	3.24	3.46	2.92
XLOC_014062	FFC1_13453	FFUJ_05106	uncharacterized protein FFUJ_05106							1.54	1.75	2.15	1.26
XLOC_014063	FFC1_13454	FFUJ_05107	probable glycerol-3-phosphate dehydrogenase (NAD)							5.72	5.67	5.88	6.48
XLOC_014440	FFC1_13463	FFUJ_05115	related to alpha/beta hydrolase		1.75					0.76	1.82	2.50	1.02
XLOC_014441	FFC1_13465	FFUJ_05117	uncharacterized protein FFUJ_05117							-1.75	-2.41	-2.10	-2.51
XLOC_014070	FFC1_13466	FFUJ_05118	related to chitinase							-4.04	-4.39	-4.68	-4.59
XLOC_014444	FFC1_13474	FFUJ_05126	uncharacterized protein FFUJ_05126							-3.38	-3.58	-2.21	
XLOC_014076	FFC1_13475	FFUJ_05127	uncharacterized protein FFUJ_05127		2.42	2.85				5.01		6.39	8.03
XLOC_014077	FFC1_13476	FFUJ_05128	probable CTT1-catalase T, cytosolic		3.16	2.53				6.07	6.36	6.59	7.09
XLOC_014445	FFC1_13477	FFUJ_05129	uncharacterized protein FFUJ_05129		1.92					2.79	2.77	3.29	4.10
XLOC_014446	FFC1_13478	FFUJ_05130	related to branched-chain amino acid aminotransferase		1.64							2.11	2.57
XLOC_014448	null										4.89		6.36
XLOC_014078	FFC1_13482	FFUJ_05134	related to acyl-CoA dehydrogenase, medium-chain specific, mitochondrial precursor		1.79	2.33							
XLOC_014081	FFC1_13485	FFUJ_05136	uncharacterized protein FFUJ_05136							4.50			
XLOC_014455	FFC1_13495	FFUJ_05146	related to quinate transport protein							-2.06	-1.95	-1.73	
XLOC_014089	FFC1_13498	FFUJ_05149	uncharacterized protein FFUJ_05149							7.09			
XLOC_014459	FFC1_13502	FFUJ_05153	probable threonine synthase							-2.23	-1.57	-1.27	
XLOC_014091	FFC1_13503	FFUJ_05154	uncharacterized protein FFUJ_05154							-5.05	-4.84	-4.42	-5.26
XLOC_014102	FFC1_13524	FFUJ_05173	related to glutathione S-transferase PM239X14									5.37	
XLOC_014106	FFC1_13531	FFUJ_05180	uncharacterized protein FFUJ_05180							4.91		5.37	5.01
XLOC_014107	FFC1_13532	FFUJ_05181	related to interferon-regulated resistance GTP-binding protein							3.74	4.25	4.00	3.14
XLOC_014474	FFC1_13533	FFUJ_05182	uncharacterized protein FFUJ_05182									4.66	3.21
XLOC_014108	FFC1_13534	FFUJ_05183	related to PNG1-protein with de-N-glycosylation function (N-glycanase)							5.20	5.19	4.27	3.65
XLOC_014109	FFC1_13535	FFUJ_06979	uncharacterized protein FFUJ_06979							4.24	3.65	3.54	3.28
XLOC_014110	FFC1_13536	FFUJ_05185	uncharacterized protein FFUJ_05185							5.50	5.41	5.43	5.38
XLOC_014114	FFC1_13540	FFUJ_05189	related to RTA1-involved in 7-aminocholesterol resistance							-2.13	-1.72	-2.09	-2.50
XLOC_014117	FFC1_13543	FFUJ_05191	uncharacterized protein FFUJ_05191							-2.68	-1.66	-2.01	-2.26
XLOC_014120	FFC1_13548	FFUJ_05196	uncharacterized protein FFUJ_05196							2.00	1.79	1.69	1.68
XLOC_014121	FFC1_13549	FFUJ_05197	uncharacterized protein FFUJ_05197							6.55	5.29	6.24	5.98
XLOC_014478	FFC1_13550	FFUJ_05198	related to putative tartrate transporter		1.77	1.75				5.99	5.09	5.50	5.06
XLOC_014128	FFC1_13560	FFUJ_05208	probable delta(24)-sterol c-methyltransferase (ERG6)							1.61	2.88		
XLOC_014485	FFC1_13570	FFUJ_05218	uncharacterized protein FFUJ_05218							3.22	3.69		
XLOC_014135	FFC1_13571	FFUJ_05219	uncharacterized protein FFUJ_05219							2.47	2.06	1.96	1.52
XLOC_014136	FFC1_13572	FFUJ_05220	uncharacterized protein FFUJ_05220							2.38	2.51	1.71	1.40
XLOC_014486	FFC1_13573	FFUJ_05221	related to NUDIX domain							3.83			
XLOC_014137	FFC1_13574	FFUJ_05222	uncharacterized protein FFUJ_05222							4.64	4.11	5.90	3.14
XLOC_014489	FFC1_13577	FFUJ_05225	uncharacterized protein FFUJ_05225							6.87	4.58	7.28	7.22
XLOC_014490	FFC1_13579	FFUJ_05227	uncharacterized protein FFUJ_05227							5.03	3.83		
XLOC_014145	FFC1_13591	FFUJ_05239	related to integral membrane protein pth11	1.30						7.18	8.50	7.15	6.49
XLOC_014147	FFC1_13594	FFUJ_05242	uncharacterized protein FFUJ_05242										-2.03
XLOC_014498	FFC1_13595	FFUJ_05243	uncharacterized protein FFUJ_05243							-1.82	-3.31	-4.32	
XLOC_014499	FFC1_13596	FFUJ_05244	probable rAsp f 9 allergen							-3.15	-3.53	-4.53	-5.33
XLOC_014500	FFC1_13597	FFUJ_05245	uncharacterized protein FFUJ_05245							-3.62	-3.68	-3.47	-4.77
XLOC_014501	FFC1_13598	FFUJ_05246	related to ARCA protein							-2.99	-2.74	-3.45	-3.86
XLOC_014150	FFC1_13606	FFUJ_05257	uncharacterized protein FFUJ_05257							2.11	1.74	3.34	
XLOC_014509	FFC1_13609										5.05		

XLOC_014152	FFC1_13610				-2.33					3.50			
XLOC_014157	FFC1_13620	FFUJ_05269	related to monooxigenase			-2.15				4.14	4.37	5.93	5.11
XLOC_014164	FFC1_13629	FFUJ_05280	related to 6-phosphogluconate dehydrogenase		3.63						3.05	3.53	
XLOC_014524	FFC1_13639	FFUJ_05289	related to delta-12 fatty acid desaturase	0.88						-2.26	-1.38	-2.18	-1.69
XLOC_014525	FFC1_13640	FFUJ_05290	uncharacterized protein FFUJ_05290							-3.57	-3.85	-4.26	-5.27
XLOC_014526	FFC1_13641	FFUJ_05291	uncharacterized protein FFUJ_05291							-3.11	-2.74	-4.42	-4.86
XLOC_014532	FFC1_13648	FFUJ_05298	related to transforming acidic coiled-coil containing protein 3							2.06	1.73	2.35	
XLOC_014533	FFC1_13649	FFUJ_05299	related to E3 ubiquitin ligase		1.32					1.22	1.47	2.41	2.25
XLOC_014536	FFC1_13652	FFUJ_05302	uncharacterized protein FFUJ_05302							-2.74	-2.42	-2.20	-3.03
XLOC_014537	FFC1_13654	FFUJ_05304	uncharacterized protein FFUJ_05304							-3.55	-3.33	-3.69	-3.39
XLOC_014172	FFC1_13659	FFUJ_05308	related to MFS transporter	-1.83	-3.03	-2.36				3.76	1.84		2.60
XLOC_014931	FFC1_13672	FFUJ_09161	related to lactose regulatory protein		-2.34					3.31			
XLOC_014935	FFC1_13679	FFUJ_09154	uncharacterized protein FFUJ_09154							-3.98	-5.18		
XLOC_014940	FFC1_13688	FFUJ_09146	uncharacterized protein FFUJ_09146							3.01	3.02	3.28	
XLOC_014942	FFC1_13691	FFUJ_09142	uncharacterized protein FFUJ_09142								2.39	2.41	
XLOC_014943	FFC1_13692	FFUJ_09141	uncharacterized protein FFUJ_09141		1.25					1.89	2.92	3.75	1.94
XLOC_014556	FFC1_13693	FFUJ_09140	related to protocatechuate 3,4-dioxygenase beta subunit							6.33	6.44	5.14	6.23
XLOC_014947	FFC1_13698	FFUJ_09135	uncharacterized protein FFUJ_09135							-3.14	-3.93		
XLOC_014948	FFC1_13699	FFUJ_09134	uncharacterized protein FFUJ_09134							-4.05	-6.10	-3.12	
XLOC_014952	FFC1_13705	FFUJ_09129	uncharacterized protein FFUJ_09129							10.84	10.11	10.92	9.56
XLOC_014953	null									5.80	5.58	5.93	
XLOC_014560	FFC1_13706	FFUJ_09128	uncharacterized protein FFUJ_09128							9.68	9.33	9.22	9.18
XLOC_014957	FFC1_13712	FFUJ_09122	uncharacterized protein FFUJ_09122							4.84			
XLOC_014564	FFC1_13713	FFUJ_09121	related to 5-carboxyvanillate decarboxylase							7.37	7.19	6.57	5.55
XLOC_014958	FFC1_13714	FFUJ_09120	related to 4-hydroxybenzoate transporter		3.76	3.80				5.75	3.96	6.98	6.84
XLOC_014565	FFC1_13715	FFUJ_09119	related to flavin-containing amine oxidasedehydrogenase	4.45	6.44	3.89				3.96	6.64	7.08	5.25
XLOC_014567	FFC1_13717	FFUJ_09117	related to quinate transport protein								2.26		
XLOC_014959	FFC1_13718	FFUJ_09116	uncharacterized protein FFUJ_09116							5.78	2.48		
XLOC_014569	FFC1_13720	FFUJ_09114	related to glu/asp-tRNA amidotransferase subunit A							2.72	1.54	1.62	
XLOC_014573	FFC1_13724	FFUJ_09110	related to alcohol dehydrogenase homolog Bli-4							4.14			4.46
XLOC_014961	FFC1_13730	FFUJ_09104	related to KES1-involved in ergosterol biosynthesis							2.07	1.79	1.98	2.45
XLOC_014963	FFC1_13738	FFUJ_09096	related to tryptophan 2,3 dioxygenase								6.59	6.95	4.91
XLOC_014964	FFC1_13739	FFUJ_09095	related to homoserine acetyltransferase family protein							3.62	3.29	2.13	
XLOC_014585	FFC1_13740	FFUJ_09094	probable formamidase							2.97	2.09		
XLOC_014586	FFC1_13742	FFUJ_09092	related to multidrug resistance protein							-1.25	-2.51	-2.22	-2.66
XLOC_014588	FFC1_13744	FFUJ_09090	uncharacterized protein FFUJ_09090							4.05			
XLOC_014593	FFC1_13750	FFUJ_09084	uncharacterized protein FFUJ_09084							5.90	3.86	3.80	4.27
XLOC_014598	FFC1_13755	FFUJ_09079	uncharacterized protein FFUJ_09079								4.82	5.28	
XLOC_014973	FFC1_13768	FFUJ_09069	related to integral membrane protein		-1.08	-0.94				4.69	4.68	3.97	4.40
XLOC_014605	FFC1_13769	FFUJ_09068	related to 6-hydroxy-d-nicotine oxidase							2.50	2.25	1.94	3.19
XLOC_014976	FFC1_13773	FFUJ_09064	probable maltose permease (MalP)						2.67	3.00	3.05	1.62	
XLOC_014607	FFC1_13774	FFUJ_09063	probable alpha-glucosidase (maltase)							3.11			
XLOC_014608	FFC1_13775	FFUJ_09062	related to RBTMx2 protein							3.81	2.63		
XLOC_014977	FFC1_13776	FFUJ_09061	uncharacterized protein FFUJ_09061							8.42	5.33	5.96	5.52
XLOC_014611	FFC1_13779	FFUJ_09058	related to neutral amino acid permease			-1.65				4.78	3.50	4.75	3.80
XLOC_014614	FFC1_13783	FFUJ_09054	related to dis1-suppressing protein kinase dsk1							-1.82	-2.68		
XLOC_014980	FFC1_13785	FFUJ_09052	uncharacterized protein FFUJ_09052							-4.24		-4.03	
XLOC_014998	FFC1_13827	FFUJ_09011	uncharacterized protein FFUJ_09011							-1.44	-2.37	-2.31	-1.71
XLOC_014640	FFC1_13830	FFUJ_09008	related to triacylglycerol lipase V precursor		1.58	1.79				2.98	2.21	3.78	3.89
XLOC_015000	FFC1_13832	FFUJ_09006	related to NonF protein, involved in nonactin biosynthesis		1.42				1.67	2.20	1.99	2.15	1.33
XLOC_015003	FFC1_13837	FFUJ_09001	uncharacterized protein FFUJ_09001						2.44	2.57	2.01		
XLOC_015004	FFC1_13838	FFUJ_09000	uncharacterized protein FFUJ_09000							3.15	3.35	3.10	2.82
XLOC_015005	FFC1_13839	FFUJ_08999	uncharacterized protein FFUJ_08999							2.07	1.97	1.97	1.67
XLOC_015014	FFC1_13851	FFUJ_08987	probable UV-endonuclease UVE-1	0.98	1.75	1.74				2.08	2.88	3.73	3.49
XLOC_014651	FFC1_13854	FFUJ_08984	uncharacterized protein FFUJ_08984							4.66	3.99	4.75	4.60
XLOC_014652	null										1.73	2.75	1.88
XLOC_014653	FFC1_13855	FFUJ_08983	related to Glc8 protein							2.50	2.09	2.38	1.93
XLOC_015016	FFC1_13856	FFUJ_08982	Long chronological lifespan protein 2			1.07				1.75	1.72	2.44	2.76
XLOC_014656	FFC1_13859	FFUJ_08979	uncharacterized protein FFUJ_08979							2.50	1.70		
XLOC_014657	FFC1_13860	FFUJ_08978	uncharacterized protein FFUJ_08978		0.92					5.54	4.77	4.84	3.33
XLOC_015017	FFC1_13861	FFUJ_08977	uncharacterized protein FFUJ_08977							4.62	4.81	4.69	6.71
XLOC_014658	FFC1_13862	FFUJ_08976	uncharacterized protein FFUJ_08976							1.86	1.40	1.65	2.07
XLOC_015018	FFC1_13864	FFUJ_08974	uncharacterized protein FFUJ_08974							3.13	2.09		
XLOC_014663	null										4.97		
XLOC_015022	FFC1_13872	FFUJ_08966	uncharacterized protein FFUJ_08966		0.97					1.99	2.23	2.51	2.34
XLOC_014674	FFC1_13891	FFUJ_08950	uncharacterized protein FFUJ_08950		2.06					1.66	2.01	2.96	1.80
XLOC_014683	FFC1_13902	FFUJ_08939	related to protein tyrosine phosphatase							3.68	2.73	2.68	2.47
XLOC_014685	FFC1_13905	FFUJ_08936	related to Sms-3 endoribonuclease Dicer (EC 3.1.26.-) (Helicase with RNase motif)								1.58	2.08	2.20
XLOC_014687	FFC1_13909	FFUJ_08932	probable sulfonate biosynthesis enzyme							5.58	5.51	5.57	4.95
XLOC_014688	FFC1_13910	FFUJ_08931	related to short-chain alcohol dehydrogenase		2.22					3.85	4.21	4.43	3.24
XLOC_014695	FFC1_13918	FFUJ_08923	uncharacterized protein FFUJ_08923							-1.38	-1.61	-2.19	-1.48
XLOC_015041	FFC1_13921	FFUJ_08920	uncharacterized protein FFUJ_08920			-1.18				10.08	9.39	10.46	8.08
XLOC_014697	FFC1_13922	FFUJ_08919	related to beta-1,4-mannosyl-glycoprotein 4-beta-N-acetylglucosaminyltransferase		-0.83					5.18	4.51	4.34	3.42
XLOC_014698	FFC1_13925	FFUJ_08916	related to pisatin demethylase		2.21					6.13	7.02	8.24	7.55

XLOC_015045	FFC1_13927	FFUJ_08914	uncharacterized protein FFUJ_08914			-2.08				3.89	4.91	5.57	6.60
XLOC_014703	FFC1_13936	FFUJ_08904	uncharacterized protein FFUJ_08904							3.72	1.96		
XLOC_015050	FFC1_13937	FFUJ_08903	uncharacterized protein FFUJ_08903							3.61	2.43	2.23	
XLOC_015053	FFC1_13940	FFUJ_08900	probable beta-glucosidase precursor									-2.71	
XLOC_015054	null									4.90			
XLOC_015061	FFC1_13949	FFUJ_08895	related to transcriptional activator acu-15		1.15					1.26	1.42	2.25	1.03
XLOC_015062	FFC1_13953	FFUJ_08891	uncharacterized protein FFUJ_08891							6.75	5.37	5.41	
XLOC_014710	FFC1_13954	FFUJ_08890	uncharacterized protein FFUJ_08890							5.94			5.06
XLOC_015066	FFC1_13961	FFUJ_08883	probable aromatic ring-opening dioxygenase family protein							4.33			
XLOC_014714	FFC1_13962	FFUJ_08882	related to transcription factor Pig1p							4.79	4.15	3.53	5.78
XLOC_015067	FFC1_13963	FFUJ_08881	related to cyanovirin-N family protein		-1.34					2.70	1.77		2.49
XLOC_015068	FFC1_13964	FFUJ_08880	related to HOL1 protein									-2.42	
XLOC_014715	FFC1_13967	FFUJ_08877	related to methyltransferase		-2.14	-2.16							
XLOC_014716	FFC1_13969	FFUJ_08875	uncharacterized protein FFUJ_08875	-2.23	-3.62	-4.81				7.71	5.48		
XLOC_014717	FFC1_13970	FFUJ_08874	uncharacterized protein FFUJ_08874			-1.60				5.95	5.98	6.05	5.28
XLOC_015073	FFC1_13971	FFUJ_08873	uncharacterized protein FFUJ_08873							-0.85	-1.69	-2.05	-1.56
XLOC_015075	FFC1_13975	FFUJ_08869	related to protein-tyrosine phosphatase							2.81	2.56	2.57	2.62
XLOC_014722	FFC1_13978	FFUJ_08866	related to D-arabinitol 2-dehydrogenase							5.73	4.63	3.66	2.72
XLOC_015077	FFC1_13979	FFUJ_08865	uncharacterized protein FFUJ_08865		1.87					3.62		4.40	
XLOC_015078	FFC1_13981	FFUJ_08863	related to magnesium dependent phosphatase							2.22	1.57	1.85	1.84
XLOC_015079	FFC1_13984	FFUJ_08860	related to L-lactate dehydrogenase (cytochrome)							-2.13	-2.19	-2.28	-2.08
XLOC_014731	FFC1_13993	FFUJ_09699	related to Ca2+-transporting ATPase							1.74	2.05	1.67	
XLOC_015090	FFC1_14000	FFUJ_08844	related to protein RIS1							2.02		2.61	3.22
XLOC_015091	FFC1_14001	FFUJ_08843	related to P.aeruginosa anthranilate synthase component II							1.58	1.44	2.22	2.41
XLOC_014742	FFC1_14015	FFUJ_08829	uncharacterized protein FFUJ_08829							2.22	1.71	1.58	1.58
XLOC_014743	null									6.40			
XLOC_014748	FFC1_14024	FFUJ_08820	uncharacterized protein FFUJ_08820							4.05	3.10	3.59	3.19
XLOC_014754	FFC1_14032	FFUJ_08812	uncharacterized protein FFUJ_08812								-1.95		-3.65
XLOC_014760	FFC1_14046	FFUJ_08799	related to chitin binding protein							6.76	8.31	8.13	8.91
XLOC_014761	FFC1_14047	FFUJ_08798	related to lactose regulatory protein							-0.97	-1.05	-1.36	-2.44
XLOC_014762	FFC1_14048	FFUJ_08797	related to Mx protein							3.83	3.78	3.06	2.32
XLOC_015122	FFC1_14063	FFUJ_08783	related to TAD2-tRNA-specific adenosine deaminase 2							4.05	2.09		
XLOC_015123	FFC1_14064	FFUJ_08782	uncharacterized protein FFUJ_08782							3.43	2.68	2.72	2.11
XLOC_014771	FFC1_14065	FFUJ_08781	uncharacterized protein FFUJ_08781							2.12	1.77	1.85	1.37
XLOC_014774	null										-2.90		
XLOC_015128	FFC1_14073	FFUJ_08773	uncharacterized protein FFUJ_08773		-1.25					-2.68	-3.06	-3.62	-2.14
XLOC_014779	null									-1.64	-2.20	-3.04	-4.54
XLOC_014783	FFC1_14086	FFUJ_08760	probable threonine aldolase			-2.03							-1.46
XLOC_014784	FFC1_14087	FFUJ_08759	related to trehalase precursor			-2.86				0.78	1.47		-1.00
XLOC_015143	FFC1_14099	FFUJ_08747	related to PET8 protein, member of the mitochondrial carrier (MCF) family		1.95					2.47	2.33	3.27	2.25
XLOC_014789	FFC1_14101	FFUJ_08745	probable succinate dehydrogenase (ubiquinone) iron-sulfur protein precursor		1.92	1.00				0.81	1.40	2.05	2.08
XLOC_014792	FFC1_14105	FFUJ_08741	uncharacterized protein FFUJ_08741									-4.76	
XLOC_015149	FFC1_14112	FFUJ_08734	uncharacterized protein FFUJ_08734		2.19					-1.27			
XLOC_015153	FFC1_14119									-3.38			
XLOC_015156	FFC1_14127	FFUJ_08722	related to ATP-binding cassette protein							5.98	3.73	5.87	4.95
XLOC_014808	FFC1_14134	FFUJ_08716	uncharacterized protein FFUJ_08716		1.29					2.49	2.27	3.28	2.84
XLOC_015163	FFC1_14140	FFUJ_08710	uncharacterized protein FFUJ_08710							3.58	3.75	4.08	5.31
XLOC_015166	FFC1_14146	FFUJ_08705	probable GAP1-General amino acid permease										-2.11
XLOC_015171	FFC1_14156	FFUJ_08695	uncharacterized protein FFUJ_08695									4.46	
XLOC_015173	null										-4.56	-5.05	
XLOC_014822	FFC1_14163									-2.96	-4.05	-5.08	
XLOC_015177	FFC1_14165	FFUJ_08687	probable UGA1-4-aminobutyrate aminotransferase (GABA transaminase)							-3.12	-2.09	-1.83	-3.13
XLOC_014831	FFC1_14183	FFUJ_08669	related to cell cycle progression protein							-2.07	-2.21	-2.00	-1.84
XLOC_014834	null												-4.06
XLOC_015192	FFC1_14188	FFUJ_08665	uncharacterized protein FFUJ_08665									2.11	1.51
XLOC_015197	FFC1_14195	FFUJ_08659	related to pH signal transduction protein PalH							2.67	2.50	2.54	1.75
XLOC_015201	null									5.05			
XLOC_014848	FFC1_14217	FFUJ_08637	related to nitrate assimilation regulatory protein nirA							2.48	2.37	1.66	
XLOC_014857	FFC1_14233	FFUJ_08621	uncharacterized protein FFUJ_08621		2.47	1.49				1.63	1.85	3.82	3.15
XLOC_014862	FFC1_14243	FFUJ_08611	uncharacterized protein FFUJ_08611	-0.67	-1.45	-1.72				6.09	4.92	3.90	4.98
XLOC_014863	FFC1_14245	FFUJ_08609	probable heat shock protein HSP104 (endopeptidase Clp ATP-binding chain HSP104)		1.57	1.66				5.34	4.84	4.97	5.58
XLOC_014867	null										4.29	2.56	2.66
XLOC_014868	FFC1_14251	FFUJ_08605	uncharacterized protein FFUJ_08605	1.30		1.18				1.69	3.27	2.36	2.39
XLOC_015227	FFC1_14252											4.46	
XLOC_014874	FFC1_14266	FFUJ_08591	uncharacterized protein FFUJ_08591		-1.04	-1.41				3.10	3.18	2.46	2.20
XLOC_014876	null										5.56		
XLOC_014877	FFC1_14269	FFUJ_08588	uncharacterized protein FFUJ_08588							4.38	4.36	4.18	2.87
XLOC_014882	FFC1_14276	FFUJ_08581	uncharacterized protein FFUJ_08581		1.84							2.13	1.35
XLOC_014889	FFC1_14286	FFUJ_08571	uncharacterized protein FFUJ_08571			-1.63				2.90	2.26	1.70	
XLOC_015246	FFC1_14296	FFUJ_08561	probable phenylalanine--tRNA ligase alpha chain							-2.15	-1.71	-1.89	-1.26
XLOC_015267	FFC1_14335	FFUJ_08523	uncharacterized protein FFUJ_08523		1.83	1.29				0.80	1.10	2.31	1.70
XLOC_014922	FFC1_14349	FFUJ_08509	related to ferric-chelate reductase							2.16	2.12	2.20	1.71
XLOC_015511	FFC1_14380	FFUJ_08065	related to pisatin demethylase							2.27			
XLOC_015285	FFC1_14381	FFUJ_08066	probable acyl-CoA dehydrogenase			-3.41				3.56			
XLOC_015289	FFC1_14388	FFUJ_08073	related to xylosidase/glycosyl hydrolase										3.23

XLOC_015292	FFC1_14393	FFUJ_08078	related to ARO80-positive transcription regulator of ARO9 and ARO10							2.32			
XLOC_015517	FFC1_14394	FFUJ_08079	related to oxidoreductase							-1.24			-2.48
XLOC_015294	FFC1_14396	FFUJ_08081	probable 2-haloalkanoic acid dehalogenase							-2.32		-2.00	-2.42
XLOC_015518	FFC1_14397	FFUJ_08082	related to fungal specific transcription factor							-2.21	-2.67	-1.43	-1.39
XLOC_015295	FFC1_14398	FFUJ_08083	uncharacterized protein FFUJ_08083		2.76	2.66						4.40	3.89
XLOC_015296	FFC1_14399	FFUJ_08084	related to 3-(3-Hydroxyphenyl)propionate 2-hydroxylase		2.32	2.06				2.86	3.63	6.96	5.05
XLOC_015519	FFC1_14400	FFUJ_08085	related to triacylglycerol lipase II precursor		2.26							8.05	7.41
XLOC_015520	FFC1_14401	FFUJ_08086	related to heat shock protein 30								6.59		6.09
XLOC_015297	FFC1_14402	FFUJ_08087	uncharacterized protein FFUJ_08087							4.83	4.51	7.15	5.59
XLOC_015521	FFC1_14403	FFUJ_08088	uncharacterized protein FFUJ_08088		1.83					2.77	2.12	4.48	3.62
XLOC_015522	FFC1_14404	FFUJ_08089	uncharacterized protein FFUJ_08089							-5.68	-7.23	-4.85	-5.39
XLOC_015299	FFC1_14407	FFUJ_08092	uncharacterized protein FFUJ_08092							-2.01	-3.13	-2.78	-2.41
XLOC_015300	FFC1_14408				-1.31	-2.46			-1.78	-1.81	-2.12	-2.57	-2.49
XLOC_015301	FFC1_14409	FFUJ_08094	uncharacterized protein FFUJ_08094							3.36	3.23	2.15	4.09
XLOC_015525	FFC1_14414	FFUJ_08099	related to choline dehydrogenase							5.00		5.52	5.52
XLOC_015526	FFC1_14415	FFUJ_08100	related to flavin-containing monooxygenase							5.78	4.18	6.00	3.94
XLOC_015527	FFC1_14416	FFUJ_08101	related to acyl-CoA transferases/carnitine dehydratase		1.32					3.30	3.65	3.82	3.94
XLOC_015306	FFC1_14419	FFUJ_08104	probable bifunctional P-450:NADPH-P450 reductase									2.57	
XLOC_015307	FFC1_14420				2.58						2.12	3.10	
XLOC_015529	FFC1_14422	FFUJ_08106	probable general amino acid permease							4.89			
XLOC_015530	FFC1_14423	FFUJ_08107	related to transcription activator protein acu-15									-2.88	
XLOC_015532	FFC1_14425	FFUJ_08109	related to dehydrogenases with different specificities (related to short-chain alcohol dehydrogenases)							5.47		3.57	6.65
XLOC_015309	FFC1_14426	FFUJ_08110	uncharacterized protein FFUJ_08110							5.51	5.82	7.08	5.60
XLOC_015533	FFC1_14427	FFUJ_08111	uncharacterized protein FFUJ_08111							4.96			
XLOC_015534	FFC1_14430	FFUJ_12008	related to non-ribosomal peptide synthetase		1.06	1.00				9.43	7.98	9.75	9.08
XLOC_015312	FFC1_14431			1.38	1.61	1.41				8.05	8.81	8.71	8.40
XLOC_015313	FFC1_14432	FFUJ_08115	related to peroxisomal amine oxidase (copper-containing)							5.77	5.92	5.84	6.17
XLOC_015314	FFC1_14434	FFUJ_08117	related to HOL1 protein							4.96			
XLOC_015536	FFC1_14435	FFUJ_08118	uncharacterized protein FFUJ_08118		-1.59					4.92	4.24	2.38	5.82
XLOC_015537	FFC1_14438	FFUJ_08121	related to lipase/esterase							2.69	2.56	3.02	2.80
XLOC_015539	FFC1_14441	FFUJ_08124	related to 15-hydroxyprostaglandin dehydrogenase							6.31	9.96	7.73	7.65
XLOC_015318	FFC1_14442	FFUJ_08125	related to decarboxylase DEC1							6.51	5.85	6.01	5.99
XLOC_015540	FFC1_14443	FFUJ_08126	related to D-arabinitol 2-dehydrogenase							8.34	8.55	8.54	8.13
XLOC_015319	FFC1_14444	FFUJ_08127	related to TRI13-cytochrome P450							9.41	9.72	9.26	8.90
XLOC_015320	FFC1_14445	FFUJ_08128	related to UPC2-regulatory protein involved in control of sterol uptake								2.46	2.37	
XLOC_015321	FFC1_14446	FFUJ_08129	related to DUF124 domain protein							4.25	4.12	4.68	5.50
XLOC_015541	FFC1_14447	FFUJ_08130	uncharacterized protein FFUJ_08130								6.23		
XLOC_015322	FFC1_14449	FFUJ_08132	related to toxD gene							1.86	2.15	2.76	1.77
XLOC_015324	FFC1_14453	FFUJ_08137	uncharacterized protein FFUJ_08137							8.73	8.47	9.42	7.31
XLOC_015327	FFC1_14459	FFUJ_08143	related to pisatin demethylase								-3.51		
XLOC_015548	FFC1_14460	FFUJ_08144	uncharacterized protein FFUJ_08144								-4.75		
XLOC_015328	FFC1_14465	FFUJ_08149	related to 6-hydroxy-D-nicotine oxidase							-2.40	-2.26	-2.57	-2.47
XLOC_015329	FFC1_14466	FFUJ_08150	uncharacterized protein FFUJ_08150							-2.13	-2.58	-2.24	-1.27
XLOC_015557	FFC1_14474	FFUJ_08158	related to KP4 killer toxin		-4.50					3.23			
XLOC_015558	FFC1_14475	FFUJ_08159	uncharacterized protein FFUJ_08159							-2.61	-3.23	-3.31	-2.70
XLOC_015333	FFC1_14476	FFUJ_08160	related to 3-oxoacyl							-3.07	-4.52	-4.94	-4.33
XLOC_015335	FFC1_14479	FFUJ_08163	uncharacterized protein FFUJ_08163							3.30	2.80		
XLOC_015561	FFC1_14481	FFUJ_08165	uncharacterized protein FFUJ_08165							-5.54	-6.98	-5.38	-4.80
XLOC_015336	FFC1_14482	FFUJ_08166	related to integral membrane protein PTH11									-4.49	-2.49
XLOC_015337	FFC1_14483	FFUJ_08167	related to TAM domain methyltransferase		-1.80	-1.63				5.00	4.02	2.88	3.25
XLOC_015338	FFC1_14485	FFUJ_08169	related to polyamine oxidase precursor							-1.75	-2.49		
XLOC_015563	FFC1_14486	FFUJ_08170	uncharacterized protein FFUJ_08170							-2.45	-4.74		
XLOC_015339	FFC1_14487	FFUJ_08171	uncharacterized protein FFUJ_08171							-5.08	-4.82		
XLOC_015342	FFC1_14492	FFUJ_08176	related to nitrate assimilation regulatory protein nirA								-5.10	-5.08	-5.38
XLOC_015568	FFC1_14495	FFUJ_08179	related to integral membrane protein PTH11							-5.34	-5.69	-5.56	-6.01
XLOC_015570	FFC1_14497	FFUJ_08181	related to TAM domain methyltransferase		-1.09	-1.10				3.30	2.39	2.08	2.25
XLOC_015346	FFC1_14502	FFUJ_08190	related to dipeptidyl aminopeptidase B								6.46		6.22
XLOC_015579	FFC1_14512	FFUJ_08199	uncharacterized protein FFUJ_08199									6.29	4.85
XLOC_015581	FFC1_14514	FFUJ_08201	uncharacterized protein FFUJ_08201		1.94	1.58					0.94	3.08	3.13
XLOC_015350	FFC1_14515	FFUJ_08202	uncharacterized protein FFUJ_08202		1.56					2.11	2.00	3.64	2.55
XLOC_015582	FFC1_14516	FFUJ_08203	uncharacterized protein FFUJ_08203							1.85	1.37	2.35	1.31
XLOC_015583	FFC1_14517	FFUJ_08204	uncharacterized protein FFUJ_08204							6.42	5.70	5.30	5.31
XLOC_015584	FFC1_14518	FFUJ_08205	related to DUF1479 domain protein							3.68	2.62	3.48	2.18
XLOC_015355	FFC1_14530	FFUJ_08217	related to linoleate diol synthase		2.79	2.30				3.46	1.68	4.43	4.59
XLOC_015356	FFC1_14532									-5.36			
XLOC_015595	FFC1_14540	FFUJ_08227	related to helicase-like transcription factor protein							2.85	2.99	3.51	
XLOC_015599	FFC1_14546	FFUJ_08234	related to GNT1 alphaN-acetylglucosamine transferase K. lactis		-1.94	-1.82				4.65	4.69		
XLOC_015363	FFC1_14547	FFUJ_08235	uncharacterized protein FFUJ_08235							5.16			
XLOC_015364	FFC1_14548	FFUJ_08236	related to beta-N-hexosaminidase		-2.38	-2.68				5.15	6.01	5.87	
XLOC_015602	FFC1_14551	FFUJ_08240	probable homoaconitase precursor		1.47	1.27							2.15

XLOC_015369	FFC1_14563	FFUJ_08252	related to GNT1 alphaN-acetylglucosamine transferase K. lactis								-1.03	-2.10	-2.58
XLOC_015610	FFC1_14564	FFUJ_08253	related to emopamil-binding protein							2.91	2.89	2.23	1.90
XLOC_015373	FFC1_14572	FFUJ_08261	related to A.gambiae ATP-binding-cassette protein							1.39	1.49	1.57	2.12
XLOC_015615	FFC1_14574										4.97		6.53
XLOC_015619	FFC1_14582	FFUJ_08271	probable saccharopine dehydrogenase (NAD, L-lysine-forming)							-2.11	-1.60		
XLOC_015378	FFC1_14583	FFUJ_08272	uncharacterized protein FFUJ_08272	2.98	6.83	3.20					2.78	6.30	4.34
XLOC_015623	FFC1_14589	FFUJ_08278	related to allantoate transport protein							-2.04	-2.50	-2.48	-1.02
XLOC_015383	FFC1_14595	FFUJ_08284	probable DUR1,2-urea amidolyase									2.92	
XLOC_015387	FFC1_14602	FFUJ_08290	related to stomatin		-1.17	-1.51					-1.54	-2.49	-3.55
XLOC_015643	FFC1_14618	FFUJ_08306	uncharacterized protein FFUJ_08306							-2.49	-3.31	-2.33	-1.83
XLOC_015394	FFC1_14619	FFUJ_08307	related to positive activator of transcription							-1.43	-2.12	-2.75	-1.91
XLOC_015395	FFC1_14622	FFUJ_08309	NAAP-1 amino acid permease NAAP1				-1.01	-1.43	-3.16				
XLOC_015397	FFC1_14624											-3.93	
XLOC_015647	FFC1_14625										4.88		
XLOC_015398	null									-5.96		-3.42	-2.80
XLOC_015399	null									-2.06	-1.67	-3.04	-2.38
XLOC_015404	FFC1_14631				1.73	1.73				1.62	1.26	2.34	1.74
XLOC_015405	FFC1_14632	FFUJ_08316	related to fructosamine-3-kinase		0.86					3.15	2.99	3.97	3.64
XLOC_015650	FFC1_14635	FFUJ_08319	probable cytochrome c		1.92	1.19				1.78	1.43	1.90	2.26
XLOC_015412	FFC1_14644	FFUJ_08327	uncharacterized protein FFUJ_08327		2.81					5.07	6.26	5.17	5.92
XLOC_015669	FFC1_14668	FFUJ_08351	related to transcription factor 25							2.46	2.02	2.63	2.58
XLOC_015672	FFC1_14672	FFUJ_08355	uncharacterized protein FFUJ_08355							-2.73	-1.88	-2.79	-3.67
XLOC_015673	FFC1_14675	FFUJ_08358	uncharacterized protein FFUJ_08358							-2.07	-2.18	-2.31	-2.46
XLOC_015426	FFC1_14676	FFUJ_08359	uncharacterized protein FFUJ_08359							-2.65	-3.01	-3.30	-2.91
XLOC_015427	FFC1_14678	FFUJ_08361	uncharacterized protein FFUJ_08361							1.81	2.15	1.90	1.78
XLOC_015678	FFC1_14684	FFUJ_08367	uncharacterized protein FFUJ_08367		-0.95	-1.35				3.24	3.09	1.69	1.64
XLOC_015680	FFC1_14685	FFUJ_08368	related to cytosine/adenosine deaminases							1.23		1.62	2.54
XLOC_015688	FFC1_14697	FFUJ_08380	related to fluconazole resistance protein (FLU1)							-1.57	-1.35	-1.48	-2.16
XLOC_015438	FFC1_14701	FFUJ_08384	related to stress protein ORP150							2.84	2.53	3.35	3.95
XLOC_015439	FFC1_14702	FFUJ_08385	related to aspartic proteinase precursor			1.90				5.70	4.93	5.81	7.17
XLOC_015694	FFC1_14709	FFUJ_08390	uncharacterized protein FFUJ_08390							-1.81	-2.42	-1.42	-1.20
XLOC_015697	FFC1_14714	FFUJ_08395	probable MFS transporter							-1.71	-1.57	-2.04	
XLOC_015699	FFC1_14716	FFUJ_08397	related to NADPH oxidase 1		-1.11	-1.57				-2.46	-2.77	-3.19	-3.46
XLOC_015703	FFC1_14720									-1.32	-1.97	-1.96	-2.11
XLOC_015711	FFC1_14733	FFUJ_08412	probable acyl-CoA dehydrogenase							3.13	2.57	2.76	
XLOC_015715	FFC1_14737									2.51	2.47	2.08	
XLOC_015452	FFC1_14738	FFUJ_08416	uncharacterized protein FFUJ_08416							1.95	2.16	2.84	3.64
XLOC_015722	FFC1_14749	FFUJ_08425	related to laccase 2							5.02			
XLOC_015459	FFC1_14755	FFUJ_08431	related to isoflavone reductase homolog P3							-1.55	-1.74	-2.11	
XLOC_015727	FFC1_14756	FFUJ_08432	probable brt1 protein								-1.33	-1.76	-2.64
XLOC_015461	FFC1_14759	FFUJ_08435	related to beta transducin-like protein							1.27	1.03	2.34	2.23
XLOC_015462	FFC1_14760	FFUJ_08436	uncharacterized protein FFUJ_08436		1.08					2.26	2.04	3.20	3.06
XLOC_015729	FFC1_16048									2.83	2.86	2.81	3.38
XLOC_015469	FFC1_14776	FFUJ_08451	uncharacterized protein FFUJ_08451	1.73	2.34					1.48	2.97	3.32	1.96
XLOC_015471	null									4.85			
XLOC_015472	null											-5.02	
XLOC_015743	FFC1_14783	FFUJ_08458	related to actin cytoskeleton organization and biogenesis	0.78	0.77					2.76	3.36	2.98	1.88
XLOC_015476	FFC1_14787	FFUJ_08461	uncharacterized protein FFUJ_08461							6.12	5.69	6.91	6.77
XLOC_015478	FFC1_14789	FFUJ_08463	probable alpha-glucoside transport protein							-2.48	-1.96	-2.15	
XLOC_015491	FFC1_14816	FFUJ_08489	probable isoleucine--tRNA ligase							-2.16	-1.97	-1.92	-1.21
XLOC_015763	FFC1_14829									4.50	4.93	4.70	
XLOC_015764	FFC1_14830	FFUJ_02106	uncharacterized protein FFUJ_02106			-2.66				3.65		2.60	
XLOC_015765	FFC1_14831	FFUJ_02107	probable aspartate kinase			-2.20				4.67	4.54	3.94	
XLOC_015968	FFC1_14832	FFUJ_02108	uncharacterized protein FFUJ_02108							5.62	5.47	5.22	
XLOC_015766	FFC1_14833					-1.23				4.82			
XLOC_015969	FFC1_14834											1.93	3.47
XLOC_015970	FFC1_14835	FFUJ_01804	uncharacterized protein FFUJ_01804							2.64	2.39	3.05	1.90
XLOC_015768	FFC1_14837	FFUJ_02112	related to zinc-binding dehydrogenase							10.41	8.54	8.60	7.85
XLOC_015971	FFC1_14838	FFUJ_02113	probable reductase RED1		-0.86	-2.46				2.64	2.52	1.87	
XLOC_015972	FFC1_14839	FFUJ_02114	probable O-acetylhomoserine (thiol)-lyase		-1.00	-2.86				3.47			
XLOC_015769	FFC1_14840	FFUJ_02115	related to nonribosomal peptide synthetase MxcG (component of the myxochelin iron transport regulon)		-1.18	-2.92					3.67		
XLOC_015770	FFC1_14841	FFUJ_02116	probable L-lactate dehydrogenase (cytochrome)		-1.05	-1.99				2.91	2.72	1.95	
XLOC_015771	FFC1_14842	FFUJ_02117	uncharacterized protein FFUJ_02117							6.32	5.36	5.06	5.33
XLOC_015973	FFC1_14842	FFUJ_02117	uncharacterized protein FFUJ_02117							6.09	5.28	4.88	5.15
XLOC_015974	FFC1_14843	FFUJ_02118	probable mfs-multidrug-resistance transporter							4.64	4.68	4.32	3.99
XLOC_015772	FFC1_14844	FFUJ_02119	related to cutinase transcription factor 1 beta							3.75	3.78	3.30	3.01
XLOC_015975	FFC1_14846	FFUJ_02121	uncharacterized protein FFUJ_02121							4.84	4.97	5.22	5.88
XLOC_015774	FFC1_14847	FFUJ_02122	uncharacterized protein FFUJ_02122							4.26	6.32	5.17	6.24
XLOC_015976	FFC1_14848	FFUJ_02123	related to IBR finger domain protein								2.56	3.06	3.63
XLOC_015977	FFC1_14849	FFUJ_02124	uncharacterized protein FFUJ_02124							5.77	4.89	5.77	6.77
XLOC_015978	FFC1_14850	FFUJ_02125	related to linoleate diol synthase			-2.60				7.11	6.12	4.92	
XLOC_015780	FFC1_14857	FFUJ_02135	related to Pseudomonas L-fucose dehydrogenase							3.53	3.27		
XLOC_015980	FFC1_14858	FFUJ_02136	probable L-alanine-DL-glutamate epimerase and related enzymes of enolase superfamily							6.70	6.01	7.03	5.00
XLOC_015982	FFC1_14862	FFUJ_02140	uncharacterized protein FFUJ_02140							4.72			

XLOC_015783	FFC1_14864	FFUJ_02142	related to beta transducin-like protein							3.06			
XLOC_015985	FFC1_14868	FFUJ_02148	related to glu/asp-tRNA amidotransferase subunit A	2.37	1.88					3.02	5.40	4.03	
XLOC_015986	FFC1_14870	FFUJ_02150	uncharacterized protein FFUJ_02150		0.89					-1.87	-2.22	-1.03	
XLOC_015988	FFC1_14874	FFUJ_02154	related to pisatin demethylase							1.84		1.97	3.15
XLOC_015989	FFC1_14875	FFUJ_02155	related to transaminase type I							2.67			
XLOC_015791	FFC1_14883	FFUJ_02163	related to 5-carboxyvanillate decarboxylase							2.81	4.30	5.00	2.75
XLOC_015995	FFC1_14884	FFUJ_02164	probable acyl-CoA dehydrogenase							6.11	6.44	6.28	5.73
XLOC_015792	FFC1_14885	FFUJ_02165	related to 3-oxoacyl-(acyl carrier protein) reductase							6.92	6.46	7.22	7.21
XLOC_015996	FFC1_14886	FFUJ_02166	related to 4-coumarate-CoA ligase							6.29	6.40	6.23	4.90
XLOC_015793	FFC1_14889	FFUJ_02169	uncharacterized protein FFUJ_02169							8.53	5.37	3.88	
XLOC_015797	FFC1_14896	FFUJ_02176	uncharacterized protein FFUJ_02176							1.87	2.20	2.16	2.19
XLOC_016003	FFC1_14900	FFUJ_02180	related to methyltransferase		-2.06					1.18			
XLOC_015801	FFC1_14906	FFUJ_02186	uncharacterized protein FFUJ_02186							4.83	4.48	5.69	
XLOC_015804	FFC1_14911	FFUJ_02191	uncharacterized protein FFUJ_02191							-1.59			-2.24
XLOC_015805	FFC1_14912	FFUJ_02192	probable bifunctional P-450:NADPH-P450 reductase	1.94	1.38					-1.51			-3.05
XLOC_016010	FFC1_14913	FFUJ_02193	related to DAL5-Allantoate and ureidosuccinate permease								-2.29		-3.44
XLOC_015809	FFC1_14919	FFUJ_02199	uncharacterized protein FFUJ_02199			-3.15				2.97			
XLOC_016014	FFC1_14922	FFUJ_02202	uncharacterized protein FFUJ_02202							3.35	2.92	2.55	3.48
XLOC_016015	FFC1_14925	FFUJ_02205	related to galactinol synthase	2.78	1.93					4.10	7.38	8.66	6.72
XLOC_016017	FFC1_14929	FFUJ_02209	uncharacterized protein FFUJ_02209										2.43
XLOC_016019	FFC1_14933	FFUJ_02213	related to sugar transport protein STL1							7.70	4.88	4.19	3.55
XLOC_015817	FFC1_14936	FFUJ_02216	probable catalase isozyme P		2.38								
XLOC_016022	FFC1_14939									3.89	3.87	3.75	4.07
XLOC_015820	FFC1_14940	FFUJ_02220	uncharacterized protein FFUJ_02220							6.86	5.07	6.09	6.39
XLOC_015821	FFC1_14941	FFUJ_02221	related to C.carbonum toxD protein							2.12	1.80	2.45	1.32
XLOC_016023	FFC1_14942	FFUJ_02222	uncharacterized protein FFUJ_02222							9.65	10.00	9.73	8.93
XLOC_016024	FFC1_14943	FFUJ_02223	uncharacterized protein FFUJ_02223							5.77	5.75	5.52	4.54
XLOC_015822	FFC1_14944	FFUJ_02224	related to multidrug resistant protein							10.00	10.46	9.36	9.08
XLOC_015826	FFC1_14951	FFUJ_02232	uncharacterized protein FFUJ_02232									5.50	
XLOC_016029	FFC1_14955	FFUJ_02237	related to monocarboxylate transporter 2							2.52	2.22	2.80	2.60
XLOC_015829	FFC1_14957	FFUJ_02239	probable acyl-CoA transferases/carnitine dehydratase							2.15	1.64	2.78	3.71
XLOC_015831	FFC1_14961	FFUJ_02243	related to triacylglycerol lipase V precursor							3.22	2.53	2.99	
XLOC_016036	FFC1_14971	FFUJ_02254	related to chitinase		-2.90					2.13			
XLOC_016037	FFC1_14973	FFUJ_02256	related to methyltransferase	-0.97	-1.97	-2.28				5.37	3.85	3.48	7.64
XLOC_016038	FFC1_14974	FFUJ_02257	related to toxD protein							3.18	3.39	2.90	
XLOC_015839	FFC1_14975	FFUJ_02258	uncharacterized protein FFUJ_02258							-5.32	-6.73	-6.96	-6.27
XLOC_015842	FFC1_14979	FFUJ_02262	uncharacterized protein FFUJ_02262							5.22	5.59		
XLOC_015847	FFC1_14983	FFUJ_02264	related to permease of the major facilitator superfamily							-2.29	-2.59	-2.73	-1.77
XLOC_016040	FFC1_14984	FFUJ_02265	uncharacterized protein FFUJ_02265							-1.35	-2.19	-2.18	
XLOC_016049	FFC1_14998	FFUJ_02278	probable alpha-L-arabinofuranosidase precursor							-3.06			-3.10
XLOC_016051	FFC1_15002	FFUJ_02279	uncharacterized protein FFUJ_02279	0.86		-1.34				3.19	4.49	3.56	3.49
XLOC_016053	FFC1_15004	FFUJ_02281	probable laccase precursor								-5.02		
XLOC_015855	FFC1_15005	FFUJ_02282	related to ROT2-glucosidase II, catalytic subunit							-6.30	-6.14		
XLOC_016054	FFC1_15007	FFUJ_02284	related to tol protein	-1.10	-1.93					2.34	1.02		1.81
XLOC_015857	FFC1_15008	FFUJ_02285	uncharacterized protein FFUJ_02285		-1.09					7.36	6.02	5.92	7.42
XLOC_015858	FFC1_15009												4.67
XLOC_015859	FFC1_15010	FFUJ_02286	related to heterokaryon incompatibility protein het-6								2.00		3.78
XLOC_016056	FFC1_15012	FFUJ_02288	uncharacterized protein FFUJ_02288							5.65	5.56	6.83	6.89
XLOC_015860	FFC1_15014	FFUJ_02290	uncharacterized protein FFUJ_02290							4.17	6.23	5.15	6.97
XLOC_016058	FFC1_15015	FFUJ_02291	uncharacterized protein FFUJ_02291							10.26	9.45	7.19	7.79
XLOC_015861	FFC1_15017	FFUJ_02293	uncharacterized protein FFUJ_02293							-2.21	-1.22	-1.75	-2.10
XLOC_015863	FFC1_15019	FFUJ_02295	probable transcriptional regulator		2.45						2.16	2.81	
XLOC_015864	FFC1_15020	FFUJ_02296	related to tol protein							3.40			
XLOC_015867	FFC1_15023	FFUJ_02299	uncharacterized protein FFUJ_02299							2.04	2.27	1.64	1.98
XLOC_016060	FFC1_15025	FFUJ_02301	uncharacterized protein FFUJ_02301		5.54	3.31						7.61	4.07
XLOC_015869	FFC1_15026	FFUJ_02302	related to pentafunctional arom polypeptide		6.27								
XLOC_015875	FFC1_15037	FFUJ_02313	related to ankyrin							6.24	6.67	5.63	5.55
XLOC_015876	FFC1_15039	FFUJ_02315	related to seed maturation protein pm25		1.71					3.35	3.24	4.24	3.18
XLOC_015878	FFC1_15041	FFUJ_02318	related to RF2 protein							-4.88	-4.78	-4.70	-5.24
XLOC_016070	FFC1_15047	FFUJ_02324	uncharacterized protein FFUJ_02324							4.41	3.98	6.18	4.78
XLOC_016071	FFC1_15048	FFUJ_02325	related to oxidoreductase CipA-like							4.01	3.89	6.33	4.59
XLOC_016072	FFC1_15049	FFUJ_02326	uncharacterized protein FFUJ_02326							2.95	3.29	4.81	3.63
XLOC_016073	FFC1_15050	FFUJ_02327	related to Staphylococcus multidrug resistance protein	0.76	0.90					2.90	3.77	3.74	2.21
XLOC_016074	FFC1_15051	FFUJ_02328	related to ethanolamine kinase							4.01	3.79	3.57	2.72
XLOC_015881	FFC1_15052	FFUJ_02329	related to CAR2-ornithine aminotransferase		1.35					2.83	2.59	4.74	2.54
XLOC_016076	FFC1_15055	FFUJ_02332	uncharacterized protein FFUJ_02332							6.17			5.94
XLOC_016077	FFC1_15056	FFUJ_02333	related to lactose permease						1.52	3.29	2.03	1.60	1.29
XLOC_016078	FFC1_15058	FFUJ_02335	uncharacterized protein FFUJ_02335							3.46	2.85	3.23	2.84
XLOC_015887	FFC1_15062	FFUJ_02339	uncharacterized protein FFUJ_02339										5.68
XLOC_015888	FFC1_15063	FFUJ_02340	related to hydroxylase			2.28				5.23	4.98	4.27	7.66
XLOC_016080	FFC1_15064	FFUJ_02341	uncharacterized protein FFUJ_02341							2.02	1.74	1.54	
XLOC_015891	FFC1_15068									4.86		5.63	5.99
XLOC_016082	FFC1_15069									6.36	7.12	7.79	6.20
XLOC_015892	FFC1_15070	FFUJ_02346	related to multidrug resistant protein	2.04	2.34					3.18	2.80		
XLOC_016084	FFC1_15072	FFUJ_02348	related to ABC transporter							3.74	4.69	4.51	5.18

XLOC_015893	FFC1_15073	FFUJ_02349	related to transcription co-repressor GAL80							9.49	8.91	9.41	9.34
XLOC_016085	FFC1_15074	FFUJ_02350	related to thioredoxin reductase							5.64		6.60	7.58
XLOC_016086	FFC1_15075	FFUJ_02351	related to TGL4-triacylglycerol lipase							3.13	2.89	2.29	2.65
XLOC_015894	FFC1_15076	FFUJ_02352	related to YRO2 protein							5.19	5.36	5.08	5.35
XLOC_016088	FFC1_15078	FFUJ_02354	related to Transcriptional activator of proteases prtT								-1.26		-2.09
XLOC_016090	FFC1_15081	FFUJ_02357	uncharacterized protein FFUJ_02357							4.92			
XLOC_016093	FFC1_15091	FFUJ_02366	uncharacterized protein FFUJ_02366		-1.69	-1.88				2.11			
XLOC_015904	FFC1_15093	FFUJ_02368	uncharacterized protein FFUJ_02368							2.08	1.50	2.36	1.64
XLOC_015905	FFC1_15094	FFUJ_02369	related to BCS1 protein precursor							2.40	2.63	3.55	3.14
XLOC_016094	FFC1_15095	FFUJ_02370	related to alpha-L-arabinofuranosidase 1							3.92			
XLOC_016099	FFC1_15103	FFUJ_02378	probable PRX1-mitochondrial isoform of thioredoxin peroxidase		-1.08					-1.50	-2.44	-3.21	-1.32
XLOC_015910	FFC1_15104	FFUJ_02379	uncharacterized protein FFUJ_02379			-1.60				3.76	3.80	3.36	2.58
XLOC_016100	FFC1_15105	FFUJ_02380	uncharacterized protein FFUJ_02380							-8.12		-6.11	-6.20
XLOC_015916	FFC1_15114	FFUJ_02389	related to high affinity methionine permease							2.82	2.36	2.42	2.52
XLOC_015917	FFC1_15115	FFUJ_02390	uncharacterized protein FFUJ_02390								-6.45	-6.57	-6.01
XLOC_016111	FFC1_15125	FFUJ_02400	related to purine nucleoside permease		1.43	1.35				3.91	4.16	5.92	5.88
XLOC_015921	FFC1_15126	FFUJ_02401	probable calcium P-type ATPase							2.06	2.12	1.74	1.74
XLOC_016113	FFC1_15128	FFUJ_02403	related to STE6-`Full-size` ABC transporter responsible for export of the `a` factor mating pheromon							2.48	1.65	2.55	1.95
XLOC_015924	FFC1_15133	FFUJ_02408	probable DUF757 domain protein							3.17	2.94	3.77	3.38
XLOC_016119	FFC1_15140	FFUJ_02414	uncharacterized protein FFUJ_02414							-2.45	-2.28	-2.35	
XLOC_015929	FFC1_15141	FFUJ_02415	uncharacterized protein FFUJ_02415								-3.00		
XLOC_015940	FFC1_15155	FFUJ_02429	uncharacterized protein FFUJ_02429	0.82	1.15					1.53	1.98	2.33	1.06
XLOC_015943	FFC1_15157	FFUJ_02431	uncharacterized protein FFUJ_02431		1.20					1.18	1.43	2.06	2.10
XLOC_015944	FFC1_15159	FFUJ_02433	uncharacterized protein FFUJ_02433		-1.16			3.44	2.03	1.42		-3.19	-1.67
XLOC_016127	FFC1_15164									10.64	8.04	11.66	
XLOC_016142	null											-4.42	-3.75
XLOC_015963	null									-2.09			
XLOC_016146	FFC1_15198	FFUJ_04649	related to RNA-3`-phosphate cyclase 1							-2.15	-2.47	-2.14	-2.28
XLOC_016149	FFC1_15201	FFUJ_04652	related to endoglucanase B							2.72	2.67	2.55	
XLOC_016337	FFC1_15202	FFUJ_12598	uncharacterized protein FFUJ_12598							6.50	6.24	7.07	8.55
XLOC_016338	FFC1_15203	FFUJ_12599	uncharacterized protein FFUJ_12599							1.79	1.70	2.75	2.75
XLOC_016339	FFC1_15205	FFUJ_12601	related to hydrolases or acyltransferases (alpha/beta hydrolase superfamily)									4.32	
XLOC_016342	FFC1_15206	FFUJ_12602	uncharacterized protein FFUJ_12602							3.01	2.51	4.21	4.41
XLOC_016343	FFC1_15207	FFUJ_12603	related to aliphatic nitrilase							2.77			
XLOC_016344	FFC1_15208	FFUJ_12604	related to glycosyl hydrolase family 43 protein							4.85		6.75	
XLOC_016348	FFC1_15213	FFUJ_12607	related to GNAT family acetyltransferase							-2.23	-2.42	-1.92	-2.31
XLOC_016162	FFC1_15222	FFUJ_12614	uncharacterized protein FFUJ_12614									-1.49	-2.08
XLOC_016355	FFC1_15229	FFUJ_12620	related to endo-1,4-beta-xylanase							-8.78	-8.27	-9.06	-8.04
XLOC_016166	FFC1_15230	FFUJ_12621	related to cellulose binding protein CEL1								-2.56		
XLOC_016361	FFC1_15238	FFUJ_12629	probable inosine triphosphate pyrophosphatase							-5.80	-4.25		
XLOC_016170	FFC1_15243	FFUJ_12634	related to pisatin demethylase (cytochrome P450)							1.92	1.58	1.83	2.87
XLOC_016365	FFC1_15245	FFUJ_12636	related to integral membrane protein								-2.39		
XLOC_016175	FFC1_15250	FFUJ_12641	related to Rossmann fold nucleotide-binding protein								5.16		2.80
XLOC_016176	FFC1_15251	FFUJ_12642	uncharacterized protein FFUJ_12642							5.74		5.81	5.79
XLOC_016177	FFC1_15252	FFUJ_12643	probable hydrolases of the alpha/beta superfamily							5.56	6.02	6.45	7.61
XLOC_016180	FFC1_15255	FFUJ_12646	related to transcriptional activator Mut3p							4.28			
XLOC_016367	FFC1_15257	FFUJ_12648	uncharacterized protein FFUJ_12648							5.07			
XLOC_016182	FFC1_15259	FFUJ_12650	related to quinate transport protein							4.76			
XLOC_016369	FFC1_15260	FFUJ_12651	uncharacterized protein FFUJ_12651	2.92	3.19	3.34					2.28	3.19	1.34
XLOC_016370	FFC1_15262	FFUJ_12653	uncharacterized protein FFUJ_12653		-4.93								
XLOC_016374	FFC1_15271	FFUJ_12662	related to phenol 2-monooxygenase							5.16		3.42	5.26
XLOC_016375	FFC1_15272	FFUJ_12663	related to integral membrane protein										2.07
XLOC_016189	FFC1_15273	FFUJ_12664	uncharacterized protein FFUJ_12664							2.52	1.93		
XLOC_016376	FFC1_15274	FFUJ_12665	related to thioredoxin							-4.04	-4.94		
XLOC_016191	FFC1_15277	FFUJ_12668	related to 5-carboxyvanillate decarboxylase		0.96					2.22	1.87	2.06	
XLOC_016193	FFC1_15280	FFUJ_12671	related to ketoreductases							4.52	4.17	5.02	3.87
XLOC_016379	FFC1_15283	FFUJ_12674	probable beta-glucosidase precursor							-3.33	-6.85	-6.20	-7.49
XLOC_016197	FFC1_15288	FFUJ_12679	uncharacterized protein FFUJ_12679									4.73	
XLOC_016384	FFC1_15289	FFUJ_12680	related to steroid monooxygenase										6.41
XLOC_016198	FFC1_15290	FFUJ_12681	related to maltose permease										4.77
XLOC_016385	FFC1_15291	FFUJ_12682	uncharacterized protein FFUJ_12682							2.17	1.56		1.72
XLOC_016199	FFC1_15292	FFUJ_12683	FOX-2 multifunctional beta-oxidation protein							2.27	1.19	1.59	
XLOC_016201	FFC1_15294	FFUJ_12685	uncharacterized protein FFUJ_12685							3.40	3.50	4.10	4.24
XLOC_016202	FFC1_15295	FFUJ_12686	related to ADH2-alcohol dehydrogenase II							4.47	4.79	8.59	6.14
XLOC_016204	FFC1_15297	FFUJ_12688	probable subtilisin-like serine protease							7.60	7.90	8.25	7.60
XLOC_016386	FFC1_15298	FFUJ_12689	related to laccase 2									5.68	
XLOC_016206	FFC1_15300	FFUJ_12691	uncharacterized protein FFUJ_12691							4.72			3.99
XLOC_016208	FFC1_15303	FFUJ_12693	related to reductases		2.72							2.63	
XLOC_016211	FFC1_15307	FFUJ_12696	uncharacterized protein FFUJ_12696							2.25	2.53		4.01
XLOC_016213	FFC1_15310	FFUJ_12699	uncharacterized protein FFUJ_12699		1.84					2.89	3.34	4.78	3.88
XLOC_016215	FFC1_15312	FFUJ_12701	related to methyltransferase							6.79	2.81	4.36	4.53
XLOC_016390	FFC1_15313	FFUJ_12702	related to NADPH-dependent aldehyde reductase							-3.24	-4.01	-3.93	-2.60
XLOC_016217	FFC1_15315									4.10	4.80	4.08	4.25
XLOC_016220	FFC1_15321	FFUJ_12709	related to n-alkane-inducible cytochrome P450							9.62	7.04	7.30	5.40

XLOC_016393	FFC1_15322	FFUJ_12710	uncharacterized protein FFUJ_12710							6.42		2.63	
XLOC_016221	FFC1_15323	FFUJ_12711	related to cytochrome P450 monooxigenase							3.77	2.53	2.39	2.96
XLOC_016394	FFC1_15324	FFUJ_12712	trichodiene oxygenase							4.14	5.67	6.40	
XLOC_016222	FFC1_15325	FFUJ_12713	uncharacterized protein FFUJ_12713							5.52	6.46		
XLOC_016225	FFC1_15328	FFUJ_12717	related to NADH oxidase									4.20	
XLOC_016226	FFC1_15333	FFUJ_12721	uncharacterized protein FFUJ_12721							-2.40	-2.91	-2.78	-1.96
XLOC_016398	FFC1_15334	FFUJ_12722	probable alpha-N-arabinofuranosidase / alpha-L-arabinofuranosidase							2.04		2.95	3.17
XLOC_016400	FFC1_15338									2.97	2.65	2.70	2.46
XLOC_016238	FFC1_15356	FFUJ_12743	related to monooxigenase							5.11			
XLOC_016411	FFC1_15364	FFUJ_12751	uncharacterized protein FFUJ_12751							3.38	3.69	2.76	
XLOC_016244	FFC1_15365	FFUJ_12752	related to alcohol dehydrogenase							3.84	4.96	3.67	3.49
XLOC_016416	FFC1_15373	FFUJ_12761	uncharacterized protein FFUJ_12761									5.62	
XLOC_016417	FFC1_15376	FFUJ_12764	related to cupin domain protein							5.79	5.06		
XLOC_016250	FFC1_15377	FFUJ_12765	uncharacterized protein FFUJ_12765							5.20		4.39	
XLOC_016253	FFC1_15381	FFUJ_12769	related to phenol 2-monooxygenase							3.45	2.59	2.83	2.06
XLOC_016254	FFC1_15382	FFUJ_12770	related to benzoate 4-monooxygenase cytochrome P450							6.12	5.12	6.22	
XLOC_016255	FFC1_15383	FFUJ_12771	related to 6-hydroxy-d-nicotine oxidase		2.07	2.28				7.42	5.74	7.94	7.92
XLOC_016258	FFC1_15389	FFUJ_12777	uncharacterized protein FFUJ_12777							4.74	5.00	4.96	
XLOC_016423	FFC1_15392	FFUJ_12780	related to xyloglucan endo-transglycosylase-like protein							-2.29	-2.85	-6.14	-6.03
XLOC_016424	FFC1_15393	FFUJ_12781	related to Vi polysaccharide biosynthesis protein vipA/tviB								-2.57		
XLOC_016262	FFC1_15397	FFUJ_12785	uncharacterized protein FFUJ_12785							6.58	5.88	5.48	5.83
XLOC_016266	FFC1_15404	FFUJ_12793	uncharacterized protein FFUJ_12793								5.01	6.71	
XLOC_016430	FFC1_15405	FFUJ_12794	uncharacterized protein FFUJ_12794							7.79	8.44	9.47	8.14
XLOC_016267	FFC1_15406	FFUJ_12795	related to ADH7-NADP(H)-dependent alcohol dehydrogenase		1.80					6.64	7.65	9.83	7.07
XLOC_016431	FFC1_15407	FFUJ_12796	related to alcohol dehydrogenase homolog Bli-4		1.48					1.25	1.56	2.15	
XLOC_016432	FFC1_15408	FFUJ_12797	probable 2-polyprenyl-6-methoxyphenol hydroxylase and related FAD-dependent oxidoreductases									3.42	
XLOC_016269	FFC1_15410	FFUJ_12799	uncharacterized protein FFUJ_12799								-1.75	-2.26	
XLOC_016437	FFC1_15417	FFUJ_12806	uncharacterized protein FFUJ_12806							6.83	6.17	6.34	8.87
XLOC_016438	FFC1_15419	FFUJ_12808	related to bifunctional 4-hydroxyphenylacetate degradation enzyme							4.13	3.60	3.98	
XLOC_016273	FFC1_15420	FFUJ_12809	related to 2,3-dihydroxybiphenyl-1,2-dioxygenase							4.11	3.17	3.79	
XLOC_016443	FFC1_15429	FFUJ_12818	related to ferric-chelate reductase							-4.45	-4.88	-5.32	-4.97
XLOC_016450	FFC1_15441	FFUJ_12830	uncharacterized protein FFUJ_12830							4.32			
XLOC_016285	FFC1_15448	FFUJ_12847	related to pisatin demethylase (cytochrome P450)							6.26	4.62	3.14	4.55
XLOC_016455	FFC1_15449	FFUJ_12845	uncharacterized protein FFUJ_12845							5.71	2.78	2.90	
XLOC_016286	FFC1_15451	FFUJ_12843	uncharacterized protein FFUJ_12843							2.32			
XLOC_016460	FFC1_15455	FFUJ_12838	uncharacterized protein FFUJ_12838							5.65	2.67		3.68
XLOC_016287	FFC1_15456	FFUJ_12837	related to thermostable alkaline protease precursor							3.32			
XLOC_016288	FFC1_15457	FFUJ_12836	uncharacterized protein FFUJ_12836							-4.09	-5.28		
XLOC_016461	FFC1_15458	FFUJ_12835	ATH1-Acid trehalase, vacuolar	-4.74						5.30			
XLOC_016467	FFC1_15469	FFUJ_12863	related to tol protein							-5.22	-5.71	-3.17	-6.52
XLOC_016469	FFC1_15471	FFUJ_12865	probable feruloyl esterase B precursor (subclass of the carboxylic acid esterases)							4.67			
XLOC_016473	FFC1_15478	FFUJ_12874	uncharacterized protein FFUJ_12874							-1.51	-2.54	-1.97	-1.83
XLOC_016474	FFC1_15479	FFUJ_12875	uncharacterized protein FFUJ_12875							-1.72	-2.55	-2.25	-2.16
XLOC_016475	FFC1_15480	FFUJ_12876	uncharacterized protein FFUJ_12876							-3.52	-5.15	-3.43	
XLOC_016301	FFC1_15485	FFUJ_12881	uncharacterized protein FFUJ_12881							5.46			
XLOC_016478	FFC1_15488	FFUJ_12884	uncharacterized protein FFUJ_12884							-3.31	-3.10	-2.27	-2.65
XLOC_016479	null									-7.61		-7.20	
XLOC_016480	FFC1_15489	FFUJ_12885	uncharacterized protein FFUJ_12885							-6.05	-4.61	-5.01	
XLOC_016304	FFC1_15490	FFUJ_12886	uncharacterized protein FFUJ_12886		-4.44					2.92			
XLOC_016482	FFC1_15495	FFUJ_12891	probable glucan 1,3-beta-glucosidase		-1.60	-1.98			-2.73	-1.22	-1.65	-1.54	
XLOC_016308	FFC1_15496	FFUJ_12892	related to chitinase		-1.67	-1.54			-2.73	-0.89	-1.41	-1.35	
XLOC_016314	FFC1_15504	FFUJ_12901	related to ankyrin							5.93	2.10		
XLOC_016315	FFC1_15505									-6.15	-4.76	-5.69	-6.28
XLOC_016485	FFC1_15506	FFUJ_12903	uncharacterized protein FFUJ_12903							-6.76	-6.18	-5.64	-6.58
XLOC_016487	FFC1_15510	FFUJ_12905	uncharacterized protein FFUJ_12905						-1.12	2.10	2.47	2.47	2.37
XLOC_016488	FFC1_15511	FFUJ_12906	uncharacterized protein FFUJ_12906						-0.97	2.27	2.20	2.43	2.80
XLOC_016318	FFC1_15512	FFUJ_12907	related to beta-1,3-glucan binding protein			-1.21				2.95	3.04	3.40	3.96
XLOC_016320	FFC1_15514	FFUJ_12909	uncharacterized protein FFUJ_12909							-7.10	-9.36	-8.81	-9.38
XLOC_016490	FFC1_15516	FFUJ_12911	probable benzoate 4-monooxygenase cytochrome P450			-1.97				8.91	9.25	7.59	6.65
XLOC_016321	FFC1_15517	FFUJ_12912	related to gibberellin 20-oxidase			-2.65				12.19	11.49	10.33	9.66
XLOC_016491	FFC1_15518	FFUJ_12913	uncharacterized protein FFUJ_12913			-2.79				11.63	10.15	11.62	10.83
XLOC_016492	FFC1_15519	FFUJ_12914	related to monocarboxylate transporter			-2.66				9.21	9.48	8.70	6.67
XLOC_016322	FFC1_15520	FFUJ_12915	related to nonribosomal peptide synthetase MxcG			-2.52				11.98	13.50	10.15	8.11
XLOC_016500	FFC1_15532										5.09		
XLOC_016501	FFC1_15533	FFUJ_12925	uncharacterized protein FFUJ_12925							3.55	3.10	3.88	3.04
XLOC_016328	FFC1_15535	FFUJ_12927	uncharacterized protein FFUJ_12927								-2.02	-1.81	
XLOC_016506	FFC1_15542	FFUJ_12935	probable uracil permease						-2.32	-5.66	-6.32	-4.42	-5.26
XLOC_016507	FFC1_15544	FFUJ_12937	uncharacterized protein FFUJ_12937								-2.76	-2.14	-3.39
XLOC_016333	FFC1_15545	FFUJ_12938	related to transcription activator protein acu-15							-2.35	-3.85	-4.54	-2.63
XLOC_016511	FFC1_15550	FFUJ_12943	probable alpha-glucuronidase precursor										-2.96
XLOC_016518	FFC1_15559									8.55	9.33	8.74	8.44
XLOC_016519	FFC1_15560										5.94	5.53	5.40

XLOC_016520	FFC1_15561									11.69	10.02	9.38	10.68
XLOC_016630	FFC1_15571									5.14		5.85	6.40
XLOC_016537	FFC1_15593										4.61		
XLOC_016644	FFC1_15606									9.00	6.39	7.47	9.28
XLOC_016645	FFC1_15607	FFUJ_14134	related to tol protein								5.08		
XLOC_016647	FFC1_15609									7.31	6.73	6.13	7.40
XLOC_016548	FFC1_15610									10.73	9.15	10.75	8.94
XLOC_016648	FFC1_15611									6.17	5.90	5.79	5.77
XLOC_016549	FFC1_15612									8.25	8.58	8.26	8.24
XLOC_016550	FFC1_15613											5.03	
XLOC_016551	FFC1_15614									7.97	8.10	8.22	8.48
XLOC_016552	FFC1_15615									8.84	8.19	8.39	8.64
XLOC_016652	FFC1_15624									5.90	4.82	5.62	6.16
XLOC_016653	FFC1_15626	FFUJ_14238	uncharacterized protein FFUJ_14238							8.86	8.85	9.38	10.76
XLOC_016656	FFC1_15630	FFUJ_14234	uncharacterized protein FFUJ_14234							5.77	6.73	6.04	7.13
XLOC_016560	FFC1_15631									7.22	6.48	5.76	7.18
XLOC_016567	FFC1_15641	FFUJ_14227	uncharacterized protein FFUJ_14227							6.76	6.38	7.53	7.66
XLOC_016569	FFC1_15643	FFUJ_14225	uncharacterized protein FFUJ_14225							6.78	6.51	5.07	7.13
XLOC_016571	FFC1_15646	FFUJ_14223	uncharacterized protein FFUJ_14223							7.95	7.25	6.54	7.41
XLOC_016662	FFC1_15648	FFUJ_14221	uncharacterized protein FFUJ_14221							5.77		5.51	6.38
XLOC_016575	FFC1_15653	FFUJ_14216	uncharacterized protein FFUJ_14216							5.12		5.23	
XLOC_016576	FFC1_15654	FFUJ_14215	uncharacterized protein FFUJ_14215							5.25		5.26	5.87
XLOC_016665	FFC1_15656	FFUJ_14213	probable uracil permease							6.58	5.39	5.53	6.46
XLOC_016577	FFC1_15657	FFUJ_14212	related to oxidoreductase										5.23
XLOC_016666	FFC1_15658									7.27	7.28	7.07	7.70
XLOC_016578	FFC1_15659	FFUJ_14211	uncharacterized protein FFUJ_14211							6.09	6.67	6.71	6.75
XLOC_016580	FFC1_15661	FFUJ_14209	uncharacterized protein FFUJ_14209							9.88	9.90	9.62	9.11
XLOC_016667	FFC1_15662									9.40	9.75	9.14	8.04
XLOC_016668	FFC1_15663	FFUJ_14208	uncharacterized protein FFUJ_14208			-1.55				9.42	9.69	9.18	8.02
XLOC_016669	FFC1_15664	FFUJ_14207	uncharacterized protein FFUJ_14207							8.71	8.89	8.72	7.24
XLOC_016581	FFC1_15665	FFUJ_14206	uncharacterized protein FFUJ_14206							6.60	5.43	6.31	5.57
XLOC_016671	null									6.64	6.27	5.15	6.44
XLOC_016582	FFC1_15667	FFUJ_14205	uncharacterized protein FFUJ_14205							8.19	7.77	7.65	7.79
XLOC_016583	FFC1_15668	FFUJ_14204	uncharacterized protein FFUJ_14204							5.43	5.69	5.92	5.56
XLOC_016672	FFC1_15669	FFUJ_14203	uncharacterized protein FFUJ_14203							7.99	7.52	7.57	7.88
XLOC_016585	FFC1_15671	FFUJ_14201	uncharacterized protein FFUJ_14201							6.30	6.16	6.21	6.63
XLOC_016680	FFC1_15687	FFUJ_14186	uncharacterized protein FFUJ_14186							4.64		5.13	4.91
XLOC_016594	FFC1_15688	FFUJ_14185	uncharacterized protein FFUJ_14185							9.96	11.26	10.42	13.61
XLOC_016595	FFC1_15690									5.70			
XLOC_016685	FFC1_15696	FFUJ_14180	uncharacterized protein FFUJ_14180							10.53	9.48	10.86	11.03
XLOC_016686	FFC1_15697	FFUJ_14179	uncharacterized protein FFUJ_14179							11.61	11.58	10.18	11.04
XLOC_016687	null									8.14	8.17	8.49	8.44
XLOC_016605	FFC1_15708	FFUJ_14165	uncharacterized protein FFUJ_14165							6.63	6.20	5.92	7.18
XLOC_016607	FFC1_15711					-5.27				5.75	4.58		
XLOC_016611	FFC1_15720	FFUJ_14154	related to NADPH-dependent beta-ketoacyl reductase (rhlG)							5.10	5.85		5.68
XLOC_016614	FFC1_15723	FFUJ_14151	uncharacterized protein FFUJ_14151							6.39	6.21	5.70	5.07
XLOC_016615	FFC1_15724	FFUJ_14150	uncharacterized protein FFUJ_14150									4.77	
XLOC_016616	FFC1_15725	FFUJ_14149	uncharacterized protein FFUJ_14149							6.12	5.61		5.99
XLOC_016617	FFC1_15726	FFUJ_14148	uncharacterized protein FFUJ_14148							8.61	7.72	7.29	8.39
XLOC_016697	FFC1_15727	FFUJ_14147	uncharacterized protein FFUJ_14147							5.12	4.68	5.12	
XLOC_016619	FFC1_15729	FFUJ_14146	uncharacterized protein FFUJ_14146							7.17	8.41	8.94	9.92
XLOC_016620	FFC1_15732	FFUJ_14143	uncharacterized protein FFUJ_14143							9.24	8.90	8.66	8.99
XLOC_016700	FFC1_15733	FFUJ_14142	uncharacterized protein FFUJ_14142		-1.50					7.77	7.29	6.15	7.51
XLOC_016701	FFC1_15737	FFUJ_14138	uncharacterized protein FFUJ_14138							8.49	7.86	7.63	7.66
XLOC_016624	FFC1_15738	FFUJ_14137	uncharacterized protein FFUJ_14137							8.71	8.54	9.29	8.11
FFC1_15748	FFC1_15748									6.20	7.11	6.81	6.50
FFC1_15749	FFC1_15749									6.89	7.96	7.05	7.68
FFC1_15750	FFC1_15750									7.05	6.55	6.95	7.62
FFC1_15751	FFC1_15751									4.50	3.24	4.64	
FFC1_15758	FFC1_15758									-5.38	-5.07		
FFC1_15759	FFC1_15759										-4.51		
FFC1_15762	FFC1_15762									-3.77	-6.24		
FFC1_15770	FFC1_15770									5.39	5.70	4.96	5.11
FFC1_15773	FFC1_15773									-2.27	-2.46	-2.56	-2.48
FFC1_15775	FFC1_15775									4.05	3.91	4.31	2.29
FFC1_15778	FFC1_15778										-2.80		
FFC1_15780	FFC1_15780									3.05			
FFC1_15786	FFC1_15786									-1.67	-1.95	-3.56	-1.82
FFC1_15790	FFC1_15790				-1.92					-1.29	-1.63	-2.96	
FFC1_15796	FFC1_15796									5.35			
FFC1_15800	FFC1_15800									5.28			
FFC1_15803	FFC1_15803									4.51	4.70	5.05	3.60
FFC1_15805	FFC1_15805									5.86	5.18	5.78	4.88
FFC1_15806	FFC1_15806									4.27	3.59	4.88	
FFC1_15815	FFC1_15815									-1.94	-3.05	-3.45	
FFC1_15817	FFC1_15817									5.44			
FFC1_15826	FFC1_15826										5.90	6.06	
FFC1_15827	FFC1_15827				1.66				2.08			1.18	
FFC1_15829	FFC1_15829									3.44	2.78	2.76	2.70
FFC1_15830	FFC1_15830									3.14	2.15		
FFC1_15831	FFC1_15831									8.18	7.34	8.62	4.91
FFC1_15832	FFC1_15832									2.83	5.55	5.25	4.77
FFC1_15833	FFC1_15833											5.62	
FFC1_15848	FFC1_15848									5.69	4.06		5.40
FFC1_15849	FFC1_15849				-3.32	-3.85				5.71	4.94		
FFC1_15850	FFC1_15850				-1.89	-2.38				3.95	3.36	4.12	3.92
FFC1_15854	FFC1_15854									4.68	5.06	5.71	
FFC1_15861	FFC1_15861									1.99	2.74	3.22	3.01

FFC1_15863	FFC1_15863			1.77	3.11					3.40	4.07	6.08	1.96
FFC1_15864	FFC1_15864			1.89	1.99						2.11	2.21	
FFC1_15873	FFC1_15873				-2.03					2.79	1.91		
FFC1_15874	FFC1_15874									4.30			
FFC1_15880	FFC1_15880									-4.32	-5.43	-5.17	
FFC1_15888	FFC1_15888										-2.32	-2.79	-1.73
FFC1_15890	FFC1_15890				7.55							6.44	
FFC1_15892	FFC1_15892									3.56			
FFC1_15894	FFC1_15894									3.22	2.50	2.29	2.46
FFC1_15895	FFC1_15895									4.54	4.56	2.74	4.38
FFC1_15896	FFC1_15896									2.02	2.05	2.37	2.43
FFC1_15897	FFC1_15897									1.66	1.75	1.85	2.13
FFC1_15898	FFC1_15898									2.45	2.27	2.53	2.76

Table S4. Total differentially expressed genes included in the third chapter RNA-seq analysis, corresponding to the study of the effect of *cryD* deletion (Cuffdiff with p<0.05 after correction), including the differential fold change for each of the comparisons analyzed.

Probe	C95	IMI	Description	Log2 FC (WT0 WT60)	Log2 FC (CRY0 CRY60)	Log2 FC (WT0 CRY0)	Log2 FC (WT60 CRY60)
XLOC_005055	FFC1_04237	FFUJ_05732	related to deoxyribodipyrimidine photo-lyase	8.88		6.36	-2.33
XLOC_012990	FFC1_12355	FFUJ_11801	related to lignostilbene alphabeta-dioxygenase I	8.36			1.68
XLOC_013489	FFC1_12352	FFUJ_11804	related to HSP30 heat shock protein Yro1p	8.20	10.20		1.98
XLOC_012273	FFC1_11867	FFUJ_12435	hypothetical protein FOXB_05815	6.99			2.74
XLOC_015378	FFC1_14583	FFUJ_08272		6.79	8.36		
XLOC_013491	FFC1_12354	FFUJ_11802	probable geranylgeranyl-diphosphate geranylgeranyltransferase (AL-2)	6.51	8.11		
XLOC_014565	FFC1_13715	FFUJ_09119		6.39	8.03		2.15
XLOC_013490	FFC1_12353	FFUJ_11803	probable phytoene dehydrogenase AL-1 (carotenoid biosynthesis protein al-1)	6.34	7.99		
XLOC_013442	FFC1_12279	FFUJ_11877	uncharacterized protein FFC1_12279	6.23	6.21		
XLOC_009739	FFC1_09074	FFUJ_09320	related to Rds1 protein	5.78	8.07		
XLOC_004390	FFC1_04443	FFUJ_05934	uncharacterized protein LW93_1076	5.33	4.43	1.96	
XLOC_007793	FFC1_07843	FFUJ_03408	probable gibberellin biosynthesis-related	5.27	4.85		1.30
XLOC_005225	FFC1_04568	FFUJ_06055	probable vivid PAS protein VVD	5.18	4.58		
XLOC_001436	FFC1_00478	FFUJ_00436	probable deoxyribodipyrimidine photo-lyase PHR	5.18	6.52		
XLOC_002308	FFC1_02122	FFUJ_01993	probable organic hydroperoxide resistance protein	4.99	7.15		
XLOC_001804	FFC1_01162	FFUJ_01088	related to short-chain alcohol dehydrogenase	4.96	5.47		
XLOC_014179	FFC1_12982	FFUJ_04654	related to 2-polyprenyl-6-methoxyphenol hydroxylase and related FAD-dependent oxidoreductases	4.94			1.89
XLOC_000761	FFC1_01379	FFUJ_01292	conidiation-specific expression protein	4.53	6.30		
XLOC_013622	FFC1_12604	FFUJ_11562	related to PHO11-secreted acid phosphatase	4.51	2.26	2.39	
XLOC_002988	FFC1_03389	FFUJ_07815	related to anthranilate synthase component II	4.50	5.04		1.59
XLOC_010939	FFC1_10450	FFUJ_10896	related to 2,5-diketo-D-gluconic acid reductase	4.41	6.76		
XLOC_003325	FFC1_02494	FFUJ_06962	probable maltase	4.32		3.55	
XLOC_003905	FFC1_03584	FFUJ_08004	related to linoleate diol synthase	4.30			-2.11
XLOC_004125	FFC1_04003	FFUJ_02574	probable ATP-binding multidrug cassette transport protein	4.29	3.96		
XLOC_007821	FFC1_07888	FFUJ_03452	related to xylulose-5-phosphate/fructose-6-phosphate phosphoketolase	4.12	2.85	2.20	
XLOC_003205	FFC1_02249	FFUJ_06731	uncharacterized protein FFUJ_06731	4.05			
XLOC_000031	FFC1_00066	FFUJ_00034	related to vegetatible incompatibility protein HET-E-1	3.88	3.54		
XLOC_005384	FFC1_04836	FFUJ_06304	probable glucose repressible protein Grg1	3.85	2.97	1.61	
XLOC_004690	FFC1_05009	FFUJ_06474	related to Cu-binding metallothionein	3.82		2.02	
XLOC_010706	FFC1_10001	FFUJ_04508	protein bli-3	3.82	3.37		
XLOC_012725	FFC1_11847	FFUJ_12414	uncharacterized protein FFUJ_12414	3.71			
XLOC_014958	FFC1_13714	FFUJ_09120	related to 4-hydroxybenzoate transporter	3.64	5.08		1.57
XLOC_002475	FFC1_02450	FFUJ_06923	probable MNN4-regulates the mannosylphosphorylation	3.63	2.47	1.84	
XLOC_002534	FFC1_02565	FFUJ_07032	uncharacterized protein FFB20_00222	3.60	2.42	1.96	
XLOC_002806	FFC1_03075	FFUJ_07515	related to arabinose 5-phosphate isomerase	3.60	4.37		
XLOC_013043	FFC1_12463	FFUJ_11698	Glutamyl endopeptidase	3.60	3.39		
XLOC_008535	FFC1_07854	FFUJ_03418	uncharacterized protein FFUJ_03418	3.58	8.55		6.08
XLOC_005917	FFC1_05867	FFUJ_14510	uncharacterized protein LW93_9960	3.56	3.19		
XLOC_008552	FFC1_07887	FFUJ_03451	Catalase-1	3.53	2.13	2.09	
XLOC_012085	FFC1_11512	FFUJ_13751	uncharacterized protein FFUJ_13751	3.52	3.61	1.76	1.87
XLOC_003553	FFC1_02904	FFUJ_07351	related to mfs-multidrug-resistance transporter	3.52	4.69		2.67
XLOC_006510	FFC1_05394		probable GPI anchored protein	3.52			
XLOC_007791	FFC1_07841		Vegetative catalase	3.50			
XLOC_011615	FFC1_10608	FFUJ_10747	iron-dependent peroxidase	3.50	3.84		
XLOC_000174	FFC1_00338	FFUJ_00295	conidiation-specific protein 10	3.41	3.67		1.30
XLOC_009744	FFC1_09084	FFUJ_09310	related to NmrA-like family protein	3.40			
XLOC_004157	FFC1_04063	FFUJ_05570	uncharacterized protein LW94_9711	3.39		2.27	
XLOC_009704	FFC1_09009	FFUJ_09382	related to lactate 2-monooxygenase	3.36	2.21	1.61	
XLOC_002525	FFC1_02544	FFUJ_07011	uncharacterized protein FFUJ_07011	3.36			
XLOC_014164	FFC1_13629	FFUJ_05280	related to 6-phosphogluconate dehydrogenase	3.34			
XLOC_007884	FFC1_08012	FFUJ_03574	Speckle-type POZ protein-like protein	3.33	3.29		
XLOC_011159	FFC1_10865	FFUJ_10501	related to triacylglycerol lipase V precursor	3.32			
XLOC_013662	FFC1_12689	FFUJ_11485	uncharacterized protein FFUJ_11485	3.29			
XLOC_002378	FFC1_02264	FFUJ_06745	bikaverin cluster-transcription factor enhancer	3.28	2.89		
XLOC_012183	FFC1_11698	FFUJ_14913	uncharacterized protein FFUJ_14913	3.26	3.26		
XLOC_009932	FFC1_09468		host-specific AK-toxin Akt2	3.24			
XLOC_005295	FFC1_04679	FFUJ_06163	amidophosphoribosyltransferase	3.23	4.09		
XLOC_000421	FFC1_00754	FFUJ_00691	hypothetical protein FVEG_00634	3.21		2.20	
XLOC_016369	FFC1_15260	FFUJ_12651	uncharacterized protein FFB20_05554	3.20	2.32		
XLOC_009130	FFC1_09056	FFUJ_09337	uncharacterized protein FFUJ_09337	3.19	4.82		1.83
XLOC_014077	FFC1_13476	FFUJ_05128	probable CTT1-catalase T, cytosolic	3.19	4.19		
XLOC_016822	FFC1_15863			3.18		2.29	
XLOC_013538	FFC1_12444	FFUJ_11713	related to nonphototropic hypocotyl protein 1	3.18	3.24		
XLOC_011274	FFC1_11060	FFUJ_10321	probable alcohol dehydrogenase homolog Bli-4	3.16			2.74
XLOC_004256	FFC1_04236	FFUJ_09492	related to alpha-1,3-mannosyltransferase	3.15		4.39	1.60

XLOC_003571	FFC1_02940	FFUJ_07384	tubulin gamma chain	3.14		1.70	
XLOC_011179	FFC1_10903	FFUJ_10466	related to Auxin Efflux Carrier superfamily	3.12	4.05		
XLOC_011749	FFC1_10869		serine threonine- phosphatase 6 regulatory ankyrin repeat subunit a	3.12			
XLOC_000200	FFC1_00380	FFUJ_00337	probable catechol O-methyltransferase	3.11	4.42		2.18
XLOC_005258	FFC1_04610	FFUJ_06096	uncharacterized protein FFUJ_06096	3.08	3.11		
XLOC_001482	FFC1_00549	FFUJ_00502	Putative methyltransferase C70.08c	3.06		2.47	
XLOC_013318	FFC1_12954	FFUJ_11223	lysozyme	3.01	2.67		
XLOC_010735	FFC1_10047	FFUJ_04556	probable ferrochelatase	2.99	2.89		
XLOC_004742	FFC1_05110	FFUJ_06572	putative pathogenicity protein	2.99			
XLOC_008529	FFC1_07840	FFUJ_03406	Isoflavone reductase like protein IRL	2.98	3.01		
XLOC_006226	FFC1_06444	FFUJ_13183	related to CYTOCHROME B561	2.96	2.68		
XLOC_011244	FFC1_11012	FFUJ_10367	related to sensory transduction histidine kinase	2.94	4.91		1.65
XLOC_002770	FFC1_03014	FFUJ_07454	uncharacterized protein FPRO_08028	2.91			
XLOC_010606	FFC1_09819	FFUJ_04335	uncharacterized protein FFB20_03227	2.88	4.15		2.43
XLOC_010686	-			2.85			
XLOC_007766	FFC1_07793	FFUJ_03361	probable 2-isopropylmalalate synthase	2.84			
XLOC_009709	FFC1_09015	FFUJ_14904	related to serum paraoxonase/arylesterase family protein	2.84	3.38		
XLOC_009963	FFC1_09537	FFUJ_04061	related to 2-polyprenyl-6-methoxyphenol hydroxylase and related FAD-dependent oxidoreductases	2.83	4.40		1.72
XLOC_007080	FFC1_06476	FFUJ_13152	uncharacterized protein FFUJ_13152	2.83	2.62		
XLOC_003201	FFC1_02241	FFUJ_06723	related to transcriptional activator Mut3p	2.80			
XLOC_015412	FFC1_14644	FFUJ_08327		2.79	4.53		2.04
XLOC_013433	FFC1_12258	FFUJ_11898	related to dlpA protein	2.79			
XLOC_011747	FFC1_10867	FFUJ_10499	uncharacterized protein FFE2_09483	2.78			
XLOC_015355	FFC1_14530	FFUJ_08217	related to linoleate diol synthase	2.77			
XLOC_014186	FFC1_12995	FFUJ_04669	related to helicase-like transcription factor	2.77	2.88		
XLOC_004002	FFC1_03757	FFUJ_14280	related to neutral amino acid permease	2.77		3.39	
XLOC_005915	FFC1_05864	FFUJ_14513	related to nitrate reductase	2.76		2.22	
XLOC_002628	FFC1_02742	FFUJ_07199	calcofluor white hypersensitive protein	2.73			
XLOC_001060	FFC1_01905	FFUJ_01785	uncharacterized protein LW93_11437	2.73	4.94		2.10
XLOC_007875	FFC1_07995	FFUJ_03556	related to haloacetate dehalogenase H-1	2.73			
XLOC_016208	FFC1_15303	FFUJ_12693	related to reductases	2.73	3.84		1.61
XLOC_011419	FFC1_10270	FFUJ_11042	related to oxidoreductase	2.72	3.42		1.73
XLOC_004025	FFC1_03793		related to kinesin light chain	2.72			
XLOC_015295	FFC1_14398	FFUJ_08083	uncharacterized protein FFUJ_08083	2.71			
XLOC_005905	FFC1_05848	FFUJ_14529	uncharacterized protein FFUJ_14529	2.70		1.88	
XLOC_004373	FFC1_04417	FFUJ_05908	pirin (iron-binding nuclear protein)	2.70			
XLOC_013481	FFC1_12341	FFUJ_11815	related to Glutathione S-transferase II	2.70	2.56		
XLOC_004810	FFC1_05236	FFUJ_06684	related to Zn(II)2Cys6 transcriptional activator	2.69			
XLOC_012959	FFC1_12280	FFUJ_11876	uncharacterized protein FFFS_11390	2.69	3.31		
XLOC_011188	FFC1_10916	FFUJ_10453	uncharacterized protein FFC1_10916	2.68	2.37		
XLOC_000506	-			2.68			
XLOC_007073	FFC1_06466	FFUJ_13161	related to YER185w, Rta1p	2.67	4.08		
XLOC_000710	FFC1_01292	FFUJ_01212	benzodiazapine receptor	2.67	2.66		
XLOC_009044	FFC1_08876	FFUJ_09512	uncharacterized protein FFUJ_09512	2.67			
XLOC_007842	FFC1_07919	FFUJ_03481	related to flavin oxidoreductase	2.66	3.20		
XLOC_007284	FFC1_06910	FFUJ_02524	related to glutamic acid decarboxylase	2.65			2.20
XLOC_003098	FFC1_03596	FFUJ_08014	S-(hydroxymethyl)glutathione dehydrogenase/alcohol dehydrogenase	2.65	3.43		
XLOC_002379	FFC1_02266	FFUJ_06747	bikaverin cluster-efflux pump	2.64	2.63		
XLOC_000643	FFC1_01167	FFUJ_01091	related to hxB protein	2.61	2.23		
XLOC_007331	FFC1_06993	FFUJ_02606	related to finger protein AZF1	2.59	3.16		
XLOC_004740	FFC1_05108	FFUJ_06570	AhpC/TSA family thioredoxin peroxidase	2.59	2.35		
XLOC_007939	FFC1_08118	FFUJ_03675	related to hexose transporter protein	2.58			
XLOC_015307	FFC1_14420		Zn(2)-Cys(6) zinc finger domain protein	2.57	2.77		
XLOC_013162	FFC1_12681	FFUJ_11493	uncharacterized protein Y057_11016	2.57			
XLOC_003580	FFC1_02952	FFUJ_07396	related to mismatched base pair and cruciform dna recognition protein	2.54			
XLOC_016266	FFC1_15404	FFUJ_12793	uncharacterized protein Y057_8557	2.53			
XLOC_008443	FFC1_07693	FFUJ_03267	related to DUF1295 domain protein	2.52	3.42		
XLOC_001913	FFC1_01383	FFUJ_01296	related to glycosyl hydrolase, family 15	2.52	2.81		1.29
XLOC_010127	FFC1_09820	FFUJ_04336	uncharacterized protein LW93_14147	2.51	2.26		
XLOC_004939	FFC1_04012	FFUJ_05524	uncharacterized protein FFUJ_05524	2.49	3.88		2.46
XLOC_011209	-			2.48			
XLOC_001975	FFC1_01486	FFUJ_01396	related to mitochondrial integral membrane protein	2.48	2.42		
XLOC_000454	FFC1_00820	FFUJ_00756	related to UDP-glucuronosyltransferase 2C1 microsomal	2.47	3.44		2.08
XLOC_013799	FFC1_12955	FFUJ_11222	uncharacterized protein FFB14_11372	2.47	2.54		
XLOC_005897	FFC1_05833	FFUJ_14546	Uncharacterized protein LW93_9926	2.47	5.52		2.75
XLOC_015579	FFC1_14512	FFUJ_08199		2.47			
XLOC_011417	FFC1_10267	FFUJ_11045	related to phospholipase A2, cytosolic	2.46	4.29		1.86
XLOC_014857	FFC1_14233	FFUJ_08621		2.46	2.44		
XLOC_012251	FFC1_11820	FFUJ_12387	P450 monooxygenase AflN	2.45			
XLOC_002708	FFC1_02905	FFUJ_07352	geranylgeranyl pyrophosphate synthase	2.45	3.04		
XLOC_003123	FFC1_03652	FFUJ_14380	uncharacterized protein Y057_11858	2.45			
XLOC_007384	FFC1_07083	FFUJ_02691	probable glucose repressible protein Grg1	2.45	3.19		2.10
XLOC_003011	FFC1_03428	FFUJ_07852	signal peptide-containing protein	2.45	2.30		

XLOC_015863	FFC1_15019	FFUJ_02295	probable transcriptional regulator	2.44			
XLOC_013032	FFC1_12441	FFUJ_11716	Putative transcriptional regulatory protein C3C7.04	2.44	2.47		
XLOC_013151	FFC1_12669	FFUJ_11505	uncharacterized protein FFUJ_11505	2.43			
XLOC_008372	FFC1_07580	FFUJ_03157	related to protein involved in cell growth	2.43			
XLOC_008869	FFC1_08520	FFUJ_09849	uncharacterized protein FFUJ_09849	2.43	2.39		
XLOC_008668	FFC1_08117	FFUJ_03674	related to OrfH, unknown gene in trichothecene gene cluster	2.42			
XLOC_005815	FFC1_05684	FFUJ_14683	uncharacterized protein FFUJ_14683	2.42	2.16		
XLOC_001890	FFC1_01340	FFUJ_01259	uncharacterized protein FFC1_01340	2.42			
XLOC_001597	FFC1_00790	FFUJ_00727	uncharacterized protein FFUJ_00727	2.41			
XLOC_003124	FFC1_03653	FFUJ_14379	uncharacterized protein LW94_9307	2.40			
XLOC_003405	FFC1_02656	FFUJ_07115	uncharacterized protein FFUJ_07115	2.39			
XLOC_004420	FFC1_04494	FFUJ_05984	uncharacterized protein LW94_11934	2.38	1.70		
XLOC_015817	FFC1_14936	FFUJ_02216	catalase	2.38			
XLOC_004878	FFC1_03883	FFUJ_05402	uncharacterized protein FFB20_05856	2.37	3.22		1.85
XLOC_006087	FFC1_06179	FFUJ_13436	related to quinate transport protein	2.37	3.61		
XLOC_012723	FFC1_11844	FFUJ_12411	related to CCC1 protein (involved in calcium homeostasis)	2.36			
XLOC_011032	FFC1_10652	FFUJ_10705	uncharacterized protein FFUJ_10705	2.35	3.98		2.39
XLOC_015469	FFC1_14776	FFUJ_08451	uncharacterized protein Y057_701	2.34	1.58		
XLOC_006175	FFC1_06346	FFUJ_13276	related to LEA domain protein	2.33	2.22		
XLOC_013083	FFC1_12548	FFUJ_11615	uncharacterized protein FFUJ_11615	2.32	2.76		
XLOC_003808	FFC1_03399	FFUJ_07825	uncharacterized protein LW93_12912	2.31			
XLOC_015296	FFC1_14399	FFUJ_08084	related to 3-(3-Hydroxyphenyl)propionate 2-hydroxylase	2.31			
XLOC_007189	FFC1_06707		related to HNM1-Choline permease	2.31			
XLOC_004107	FFC1_03970	FFUJ_05482		2.31		1.50	
XLOC_013172	FFC1_12702	FFUJ_11472	related to nitrate reductase [NADPH]	2.31	2.35		
XLOC_001304	FFC1_00184	FFUJ_00148	related to nucleoside-diphosphate-sugar epimerase	2.31	2.44		
XLOC_014076	FFC1_13475	FFUJ_05127		2.31			
XLOC_015892	FFC1_15070	FFUJ_02346	related to multidrug resistant protein	2.30	1.43		
XLOC_003333	FFC1_02509	FFUJ_06977	related to DUF1264 domain protein	2.29	1.87		
XLOC_015519	FFC1_14400	FFUJ_08085		2.28	1.81		-1.60
XLOC_003338	FFC1_02520	FFUJ_06987	alcohol dehydrogenase	2.28	2.08		
XLOC_005984	-			2.28			
XLOC_002855	FFC1_03162	FFUJ_07599	sterol O-acyltransferase	2.27		1.68	
XLOC_007890	FFC1_08023	FFUJ_03586	uncharacterized protein Y057_6537	2.27	4.84		2.66
XLOC_009094	FFC1_08978	FFUJ_09413	csbdlike domain-containing protein	2.26	1.81		
XLOC_006104	FFC1_06211	FFUJ_13406	uncharacterized protein FFUJ_13406	2.26			
XLOC_014674	FFC1_13891	FFUJ_08950	uncharacterized protein FFUJ_08950	2.26			
XLOC_008036	FFC1_06967	FFUJ_02582	probable succinate dehydrogenase (ubiquinone) flavoprotein precursor, mitochondrial	2.25	2.82		
XLOC_009327	FFC1_08370	FFUJ_09993	related to PMR1-Ca++-transporting P-type ATPase located in Golgi	2.24			
XLOC_014226	FFC1_13086	FFUJ_04757	cytosceleton binding protein	2.24	1.68		
XLOC_009898	FFC1_09391	FFUJ_03920	uncharacterized protein FFE2_02514	2.24			
XLOC_005292	FFC1_04676	FFUJ_06160	related to short chain dehydrogenase	2.23	3.63		1.74
XLOC_013672	FFC1_12699	FFUJ_11475	uncharacterized protein Y057_11035	2.23			
XLOC_007631	FFC1_07528	FFUJ_03105	related to deoxyribodipyrimidine photo-lyase PHR	2.22	3.48		
XLOC_014688	FFC1_13910	FFUJ_08931	related to short-chain alcohol dehydrogenase	2.21	2.32		
XLOC_009234	FFC1_08194	FFUJ_10166	uncharacterized protein FFUJ_10166	2.21			
XLOC_015149	FFC1_14112	FFUJ_08734	uncharacterized protein FFUJ_08734	2.20			
XLOC_009416	FFC1_08524	FFUJ_09845	related to putative transmembrane protein	2.20	2.14		
XLOC_009547	FFC1_08741	FFUJ_09643	related to protein involved in biosynthesis of mitomycin antibiotics/polyketide fumonisin	2.20			
XLOC_005068	FFC1_04271	FFUJ_12086	related to ATP-binding multidrug cassette transport protein	2.20			
XLOC_002508	FFC1_02515		uncharacterized protein FFM5_05641	2.19			
XLOC_011328	FFC1_11165	FFUJ_10217	uncharacterized protein FFUJ_10217	2.19			-1.31
XLOC_007208	FFC1_06747		related to peroxisomal amine oxidase (copper-containing)	2.18			
XLOC_011261	FFC1_11036	FFUJ_10344	uncharacterized protein Y057_7602	2.18	2.15		
XLOC_010198	FFC1_09946	FFUJ_04459	3-isopropylmalate dehydratase	2.18			
XLOC_010848	FFC1_10269	FFUJ_11043	uncharacterized protein FFC1_10269	2.18	1.61		
XLOC_000507	FFC1_00913	FFUJ_00845	uncharacterized protein FFUJ_00845	2.17	1.89		
XLOC_002017	FFC1_01589	FFUJ_01494	related to transcriptional repressor	2.17			
XLOC_004918	FFC1_03969	FFUJ_05481	related to aldo-keto reductase family protein	2.17		1.59	
XLOC_011225	FFC1_10981	FFUJ_10397	uncharacterized protein Y057_15039	2.17			
XLOC_014698	FFC1_13925	FFUJ_08916	related to pisatin demethylase	2.16			
XLOC_000824	FFC1_01506	FFUJ_01415	related to zinc-binding protein	2.16			
XLOC_013457	FFC1_12309	FFUJ_11846	related to thioredoxin	2.15	2.17		
XLOC_002599	FFC1_02678	FFUJ_07137	predicted protein [	2.15			
XLOC_003350	FFC1_02545	FFUJ_07012	related to hydrolases or acyltransferases (alpha/beta hydrolase superfamily)	2.15			
XLOC_002271	FFC1_02055	FFUJ_01929	related to UDPglucose 4-epimerase	2.15			
XLOC_011278	FFC1_11065	FFUJ_10316	uncharacterized protein Y057_7535	2.14			
XLOC_000364	FFC1_00658	FFUJ_00601	uncharacterized protein FFUJ_00601	2.14			
XLOC_013395	FFC1_12176	FFUJ_11978	related to 6-phosphogluconate dehydrogenase	2.14		1.60	
XLOC_006006	FFC1_06040	FFUJ_13569	related to subtilisin-like serine protease	2.14	3.09		
XLOC_009750	FFC1_09095	FFUJ_09299	related to monoamine oxidase N	2.13	2.10		
XLOC_003351	FFC1_02546	FFUJ_07013	related to 6-hydroxy-D-nicotine oxidase	2.13			
XLOC_001891	FFC1_01341		uncharacterized protein FFE2_01347	2.12			

XLOC_002890	FFC1_03224	FFUJ_07659	related to the plant PR-1 class of pathogen related proteins	2.10		1.51	
XLOC_000536	FFC1_00973	FFUJ_00904	related to Cupin domain protein	2.10			-1.80
XLOC_009129	FFC1_09055	FFUJ_09338	uncharacterized protein FFUJ_09338	2.10	2.47		
XLOC_001780	FFC1_01125	FFUJ_01051	uncharacterized protein Y057_14727	2.09			
XLOC_007896	FFC1_08039	FFUJ_03599	related to N-carbamoyl-L-amino acid hydrolase	2.09		1.95	
XLOC_002084	FFC1_01714	FFUJ_01607	minor allergen Alt a 7	2.08	1.76		
XLOC_001698	FFC1_00971	FFUJ_00902	uncharacterized protein FFE2_00976	2.07			
XLOC_003004	FFC1_03419	FFUJ_07843	related to integral membrane protein PTH11	2.07	1.89		
XLOC_009117	FFC1_09034	FFUJ_09358	probable general amidase	2.07	3.63		
XLOC_016255	FFC1_15383	FFUJ_12771	related to 6-hydroxy-d-nicotine oxidase	2.06			
XLOC_005317	FFC1_04714	FFUJ_06194	glutathione s-transferase	2.06			
XLOC_012941	FFC1_12247	FFUJ_11908	probable BRT1 protein, down-regulated by mating factor B	2.04			
XLOC_001331	FFC1_00245	FFUJ_00204	related to endo-polygalacturonase 6	2.04			
XLOC_007085	FFC1_06487	FFUJ_13141	related to SGT1 protein	2.04			
XLOC_012921	FFC1_12210	FFUJ_11945	Hexokinase	2.04		2.43	
XLOC_013014	FFC1_12406	FFUJ_11751	hypothetical protein FOXG_12212	2.03			
XLOC_011062	FFC1_10717	FFUJ_10645	related to reductases	2.03			
XLOC_016823	FFC1_15864			2.03			
XLOC_004934	FFC1_04002	FFUJ_05514	uncharacterized protein FFUJ_05514	2.03			
XLOC_013908	FFC1_13144	FFUJ_04810	nad dependent epimerase dehydratase family protein	2.03			
XLOC_006366	FFC1_06708		copper amine oxidase 1	2.02			
XLOC_007790	FFC1_07838	FFUJ_03404	alcohol dehydrogenase	2.02			
XLOC_009952	FFC1_09504	FFUJ_04028	related to integral membrane protein PTH11	2.02	2.90		
XLOC_008177	FFC1_07221	FFUJ_02814	uncharacterized protein FFUJ_02814	2.02	2.56		
XLOC_004464	FFC1_04569	FFUJ_06056	related to DNA repair protein MMS21	2.01	2.71		
XLOC_002265	FFC1_02042	FFUJ_01915	alcohol dehydrogenase (NADP+)	2.01			
XLOC_004419	FFC1_04493	FFUJ_05983	uncharacterized protein FFB20_02527	2.01			
XLOC_004618	FFC1_04872	FFUJ_06338	related to ABC1 transport protein	2.00			
XLOC_016015	FFC1_14925	FFUJ_02205	related to galactinol synthase	2.00			
XLOC_001367	FFC1_00317	FFUJ_00275	related to DUF636 domain protein	1.97	2.35		
XLOC_009536	FFC1_08722	FFUJ_09661	uncharacterized protein LW93_13615	1.97			
XLOC_011185	FFC1_10913	FFUJ_10456	related to chloroperoxidase	1.97			
XLOC_010490	FFC1_09615	FFUJ_04138	related to benzoate-para-hydroxylase (cytochrome P450)	1.97			
XLOC_008889	FFC1_08564	FFUJ_09807	uncharacterized protein FFUJ_09807	1.97			
XLOC_015581	FFC1_14514	FFUJ_08201		1.97			-1.30
XLOC_006879	FFC1_06098	FFUJ_13514	ornithine carbamoyltransferase, mitochondrial	1.96			
XLOC_009740	FFC1_09077	FFUJ_09317	probable RCO3 glucose transporter	1.95			
XLOC_002466	FFC1_02433	FFUJ_06907	related to dehydroshikimate dehydratase	1.95	2.66		1.39
XLOC_004926	FFC1_03982	FFUJ_05494	related to GNAT family acetyltransferase	1.94			
XLOC_015143	FFC1_14099	FFUJ_08747	related to PET8 protein, member of the mitochondrial carrier (MCF) family	1.94			
XLOC_005778	FFC1_05603	FFUJ_14760	related to acid phosphatase	1.94	1.74		
XLOC_011637	FFC1_10645	FFUJ_10711	probable mfs-multidrug-resistance transporter	1.94			
XLOC_014789	FFC1_14101	FFUJ_08745	succinate dehydrogenase [ubiquinone] iron-sulfur subunit, mitochondrial	1.94	2.58		
XLOC_014652	-			1.94			
XLOC_014737	FFC1_14006	FFUJ_08838	related to proliferation associated SNF2-like protein	1.93	2.97		
XLOC_013428	FFC1_12248	FFUJ_11907	related to D-amino acid oxidase	1.93			
XLOC_000145	FFC1_00272	FFUJ_00230	GTP-binding rho3	1.93			
XLOC_005486	FFC1_05034	FFUJ_06497	related to transmembrane transporter Liz1p	1.93			
XLOC_003434	FFC1_02708	FFUJ_07165	related to galactinol synthase	1.92	3.54		1.95
XLOC_002551	FFC1_02595		uncharacterized protein FFM5_05560	1.92	1.63		
XLOC_010099	-			1.92			
XLOC_011996	FFC1_11351	FFUJ_13339	related to multidrug resistance-associated protein	1.92			
XLOC_014445	FFC1_13477	FFUJ_05129	branched-chain amino acid aminotransferase	1.92			
XLOC_006195	-			1.91	1.91		
XLOC_016344	FFC1_15208	FFUJ_12604	related to glycosyl hydrolase family 43 protein	1.90			
XLOC_013976	FFC1_13294	FFUJ_04957	related to pathogenesis-related protein NtPRp27	1.90			
XLOC_005195	FFC1_04514	FFUJ_06003	predicted protein [	1.90			
XLOC_015650	FFC1_14635	FFUJ_08319	cytochrome c	1.90	1.75		
XLOC_013129	FFC1_12630	FFUJ_11537	nadp-binding domain-containing	1.90			
XLOC_010274	FFC1_10111	FFUJ_04618	related to aldehyde dehydrogenase	1.90			
XLOC_001764	FFC1_01090	FFUJ_01016	related to meiotic expression up-regulated protein 14	1.89	1.76		
XLOC_004004	FFC1_03760	FFUJ_14277	related to 2`-hydroxyisoflavone reductase	1.89			
XLOC_005420	FFC1_04908	FFUJ_06373	uncharacterized protein FFUJ_06373	1.89			
XLOC_014257	FFC1_13145	FFUJ_04811	related to G protein coupled receptor like protein	1.89			
XLOC_003729	FFC1_03238	FFUJ_07673	uncharacterized protein FFUJ_07673	1.89	2.37		
XLOC_006100	FFC1_06206	FFUJ_13411	uncharacterized protein FFUJ_13411	1.89			
XLOC_015077	FFC1_13979	FFUJ_08865		1.89			
XLOC_007834	FFC1_07906	FFUJ_03469	related to integral membrane protein PTH11	1.89	1.97		
XLOC_001129	FFC1_02051	FFUJ_01925	uncharacterized protein FFC1_02051	1.89			-1.97
XLOC_000288	FFC1_00538	FFUJ_00492	related to nitrogen permease regulator	1.88	2.57		
XLOC_010367	FFC1_09397	FFUJ_03926	probable phosphate transport protein MIR1	1.88		1.68	
XLOC_013242	FFC1_12807	FFUJ_11368	related to epoxide hydrolase	1.88			
XLOC_004663	FFC1_04951	FFUJ_06418	uncharacterized protein FFUJ_06418	1.88			
XLOC_015985	FFC1_14868	FFUJ_02148	related to glu/asp-tRNA amidotransferase subunit A	1.88		2.75	
XLOC_002914	FFC1_03269	FFUJ_07699	uncharacterized protein Y057_8326	1.87	2.12		

XLOC_011158	FFC1_10864	FFUJ_10502	Putative competence-damage inducible protein	1.87			
XLOC_005217	FFC1_04559	FFUJ_06046	related to nucleoside-diphosphate-sugar epimerases	1.87			
XLOC_012739	FFC1_11869	FFUJ_12437	related to cytosine deaminase and related metal-dependent hydrolases	1.86			
XLOC_000257	FFC1_00469	FFUJ_00427	malate dehydrogenase (oxaloacetate-decarboxylating)	1.86	1.67		
XLOC_014300	FFC1_13212	FFUJ_04877	Mitochondrial fission process protein 1	1.86			
XLOC_008044	-			1.86	1.72		
XLOC_006750	FFC1_05865	FFUJ_14512	reductase	1.86	1.59		
XLOC_013431	FFC1_12256	FFUJ_11900	uncharacterized protein FFB14_10692	1.86		1.62	
XLOC_011693	FFC1_10745	FFUJ_10618	related to dihydroflavonol-4-reductases	1.85			
XLOC_001130	FFC1_02053	FFUJ_01927	uncharacterized protein FFUJ_01927	1.85			
XLOC_014418	FFC1_13427	FFUJ_05082	uncharacterized protein FFUJ_05082	1.85	3.69		1.94
XLOC_005300	FFC1_04688		uncharacterized protein FFB20_02443	1.85			
XLOC_014882	FFC1_14276	FFUJ_08581	uncharacterized protein Y057_12343	1.85			
XLOC_008046	-			1.84			
XLOC_005618	FFC1_05304		related to dehydrogenases and related proteins	1.84			
XLOC_016213	FFC1_15310	FFUJ_12699	uncharacterized protein Y057_1964	1.84			
XLOC_015521	FFC1_14403	FFUJ_08088	uncharacterized protein FFUJ_08088	1.84			
XLOC_003433	FFC1_02705	FFUJ_07162	acyl-CoA dehydrogenase	1.84			
XLOC_004168	FFC1_04079	FFUJ_05585	gluconate 5-dehydrogenase	1.84	3.53		2.21
XLOC_015267	FFC1_14335	FFUJ_08523		1.84	2.02		
XLOC_001621	FFC1_00841	FFUJ_00777	Early meiotic induction protein 1	1.84			-1.30
XLOC_009517	FFC1_08693	FFUJ_09690	amidase	1.84			
XLOC_009086	FFC1_08953	FFUJ_09438	uncharacterized protein Y057_9952	1.83			
XLOC_011325	FFC1_11161	FFUJ_10221	probable flavohemoglobin	1.83		2.85	2.35
XLOC_011580	FFC1_10551	FFUJ_10799	related to oxalate decarboxylase	1.83			
XLOC_013677	FFC1_12705	FFUJ_11469	shikimate kinase	1.83			
XLOC_013048	FFC1_12469	FFUJ_11693	related to putative tartrate transporter	1.83			
XLOC_014188	FFC1_12998	FFUJ_04672	hypothetical protein FSPOR_7648	1.83			
XLOC_003421	FFC1_02685	FFUJ_07144	related to UPF0591 membrane protein C15E1.02c	1.82			
XLOC_003838	FFC1_03450	FFUJ_07874	related to ketoreductases	1.82	1.93		
XLOC_013081	FFC1_12544	FFUJ_11618	related to flavin-containing monooxygenase	1.82			
XLOC_007068	FFC1_06459	FFUJ_13168	related to Mechanosensitive ion channel family	1.82			
XLOC_014337	FFC1_13276	FFUJ_04941	hsp10-like protein	1.81			
XLOC_000419	FFC1_00749	FFUJ_00686	TDG/mug DNA glycosylase	1.81			
XLOC_004667	FFC1_04958	FFUJ_06424	uncharacterized protein Y057_10009	1.81			-1.72
XLOC_003391	FFC1_02630	FFUJ_07093	peptidyl-prolyl cis-trans isomerase D	1.81			
XLOC_012005	FFC1_11365	FFUJ_13896	related to TGF beta induced protein ig-h3 precursor	1.81	4.25		
XLOC_006196	FFC1_06380	FFUJ_13245	probable period clock protein FRQ	1.80	1.75		
XLOC_005657	FFC1_05383		related to Het-c protein	1.80			
XLOC_014641	FFC1_13831	FFUJ_09007	alcohol dehydrogenase (NADP+)	1.79	4.37		2.75
XLOC_012102	FFC1_11536	FFUJ_13729	phosphatidylserine decarboxylase	1.79			
XLOC_013902	FFC1_13134	FFUJ_04800	probable 4-alpha-glucanotransferase / amylo-1,6-glucosidase (glycogen-debranching enzyme)	1.79	2.20		
XLOC_013243	FFC1_12808	FFUJ_11367	probable alpha-L-arabinofuranosidase	1.79			
XLOC_014078	FFC1_13482	FFUJ_05134	related to acyl-CoA dehydrogenase, medium-chain specific, mitochondrial precursor	1.78			
XLOC_003862	FFC1_03492	FFUJ_07916	related to glutathione S-transferase	1.78	2.60		
XLOC_013729	FFC1_12816	FFUJ_11359	related to ketoreductases	1.78			
XLOC_004333	FFC1_04354	FFUJ_05845	uncharacterized protein Y057_3486	1.78			
XLOC_016267	FFC1_15406	FFUJ_12795	related to ADH7-NADP(H)-dependent alcohol dehydrogenase	1.77			
XLOC_015014	FFC1_13851	FFUJ_08987	probable UV-endonuclease UVE-1	1.77			
XLOC_013597	FFC1_12551	FFUJ_11612	probable cytochrome P450 55A2	1.77			
XLOC_006531	FFC1_05437		Uncharacterized protein LW94_992	1.77			
XLOC_009114	FFC1_09024	FFUJ_09368	related to isoamyl alcohol oxidase	1.76			
XLOC_016430	FFC1_15405	FFUJ_12794	uncharacterized protein FFB20_05485	1.76			
XLOC_014440	FFC1_13463	FFUJ_05115	related to alpha/beta hydrolase	1.76			
XLOC_008884	FFC1_08557	FFUJ_09813	uncharacterized protein FFUJ_09813	1.76			
XLOC_007983	FFC1_06879	FFUJ_02494	related to FK506 suppressor Sfk1	1.75			
XLOC_002496	FFC1_02490	FFUJ_06959	related to metallo-beta-lactamase family protein	1.75	1.78		
XLOC_014478	FFC1_13550	FFUJ_05198	related to putative tartrate transporter	1.75			-1.63
XLOC_003100	FFC1_03599	FFUJ_08017	related to monocarboxylate transporter 4	1.75			
XLOC_016319	FFC1_15513	FFUJ_14324	related to acid phosphatase precursor (pH 6-optimum acid phosphatase)	1.75			
XLOC_008881	FFC1_08552	FFUJ_09818	mitochondrial carrier	1.75			
XLOC_010144	FFC1_09851	FFUJ_04367	related to M.capricolum transcription repressor	1.75	2.12		
XLOC_013150	FFC1_12668	FFUJ_11506	putative antibiotic biosynthesis protein	1.74			
XLOC_008962	FFC1_08709	FFUJ_09674	alcohol dehydrogenase (NADP+)	1.74	1.47		
XLOC_003974	FFC1_03709	FFUJ_14325	related to dTDP-glucose 4,6-dehydratase	1.74			
XLOC_013473	FFC1_12330	FFUJ_11826	putative transporter SEO1	1.74			
XLOC_004615	FFC1_04866		ATP-binding cassette, subfamily G (WHITE), member 2, PDR	1.74			
XLOC_015404	FFC1_14631		hypothetical protein FNYG_05403	1.74			
XLOC_010611	FFC1_09826	FFUJ_04342	related to oxidoreductase, FAD-binding	1.73			-1.70
XLOC_010751	FFC1_10071	FFUJ_04580	Uncharacterized protein Y057_6006	1.73			
XLOC_014350	FFC1_13296	FFUJ_04959	uncharacterized protein FFUJ_04959	1.72		1.27	
XLOC_010937	FFC1_10447	FFUJ_10899	related to fungal transcriptional regulatory protein	1.72			
XLOC_000436	FFC1_00783	FFUJ_00720	probable meiotic expression up-regulated protein 14	1.72			

XLOC_011841	FFC1_11076	FFUJ_10306	related to peroxisomal amine oxidase (copper-containing)	1.72			
XLOC_005126	FFC1_04386	FFUJ_05875	uncharacterized protein FFUJ_05875	1.71			
XLOC_015876	FFC1_15039	FFUJ_02315		1.71			
XLOC_012206	FFC1_11727	FFUJ_12300	related to phospholipase A2, cytosolic	1.71			
XLOC_008467	FFC1_07742	FFUJ_03315	uncharacterized protein FFUJ_03315	1.71			
XLOC_001465	FFC1_00526	FFUJ_00481	Arginine--tRNA ligase, cytoplasmic	1.70			
XLOC_006044	FFC1_06101	FFUJ_13511	glucoamylase	1.70			
XLOC_003791	FFC1_03357	FFUJ_07784	related to lipase/esterase	1.70			
XLOC_006661	FFC1_05682	FFUJ_14685	related to integral membrane protein PTH11	1.70			
XLOC_010599	-			1.70			
XLOC_008388	FFC1_07609	FFUJ_03185	related to members of the aldo/keto reductase family	1.69			
XLOC_011382	FFC1_10203	FFUJ_11103	probable D-lactate dehydrogenase (cytochrome)	1.69			
XLOC_005280	FFC1_04653	FFUJ_06138	uncharacterized protein FFUJ_06138	1.69	2.39		
XLOC_007084	FFC1_06484	FFUJ_13144	uncharacterized protein FFC1_06484	1.69			-1.19
XLOC_008047	-			1.69			
XLOC_000796	FFC1_01459	FFUJ_01372	uncharacterized protein FFE2_01464	1.69			
XLOC_001726	-			1.69			
XLOC_007332	FFC1_06995	FFUJ_02608	elongator complex protein 2	1.68	1.67		
XLOC_001408	FFC1_00419	FFUJ_00375	uncharacterized protein Y057_1452	1.68			
XLOC_015032	FFC1_13892	FFUJ_08949	transcription factor	1.68			
XLOC_012767	FFC1_11930	FFUJ_12495	related to triacylglycerol lipase II precursor	1.68			
XLOC_001813	FFC1_01180	FFUJ_01103	related to papaya ringspot virus polyprotein	1.68			
XLOC_008043	FFC1_06973	FFUJ_02588	uncharacterized protein FFUJ_02588	1.67			
XLOC_008045	FFC1_06974	FFUJ_02589	uncharacterized protein FFUJ_02589	1.67			
XLOC_000437	FFC1_00785	FFUJ_00722	related to RAD13	1.67	1.66		
XLOC_002987	FFC1_03388	FFUJ_07814	4,5-DOPA dioxygenase extradiol-like protein	1.66			
XLOC_016743	FFC1_15827			1.66			
XLOC_014449	FFC1_13480	FFUJ_05132	Ribosome assembly protein 4	1.66			
XLOC_002266	FFC1_02044	FFUJ_01917	uncharacterized protein FFC1_02044	1.66			
XLOC_011300	FFC1_11110	FFUJ_10273	uncharacterized protein Y057_1070	1.66			
XLOC_000642	FFC1_01166	FFUJ_01090	related to cytosolic Cu/Zn superoxide dismutase	1.66	1.70		
XLOC_005916	FFC1_05866	FFUJ_14511	probable CDP-alcohol phosphatidyltransferase	1.65			
XLOC_013171	FFC1_12691	FFUJ_11483	related to quinate transport protein	1.65			
XLOC_001121	FFC1_02036	FFUJ_01909	uncharacterized protein FFUJ_01909	1.65			
XLOC_008632	FFC1_08038	FFUJ_03598	related to allantoate transport protein	1.65			
XLOC_014372	FFC1_13333	FFUJ_04994	hsp70-like protein	1.65			
XLOC_013068	FFC1_12504	FFUJ_11658	Zinc finger protein zas1	1.65			
XLOC_005135	FFC1_04403	FFUJ_05894	related to ATP-dependent RNA helicase	1.65			
XLOC_014446	FFC1_13478	FFUJ_05130	related to branched-chain amino acid aminotransferase	1.64			
XLOC_007096	FFC1_06505	FFUJ_13123	related to triacylglycerol lipase V precursor	1.64			
XLOC_009509	FFC1_08675	FFUJ_09706	related to dehydrogenases with different specificities (related to short-chain alcohol dehydrogenases)	1.64			
XLOC_015351	FFC1_14521	FFUJ_08208	homocitrate synthase, mitochondrial	1.64			
XLOC_005032	FFC1_04185	FFUJ_05684	mating type protein MAT1-2-3	1.64			
XLOC_008374	FFC1_07582	FFUJ_03159	uncharacterized protein LW93_1912	1.64			
XLOC_016337	FFC1_15202	FFUJ_12598	glutathione-dependent formaldehyde-activating, gfa	1.63			
XLOC_005299	FFC1_04687	FFUJ_06170	mfs monocarboxylate transporter	1.63			
XLOC_009582	FFC1_08806	FFUJ_09580	uncharacterized protein Y057_8033	1.63	1.61		
XLOC_015969	FFC1_14834		related to integral membrane protein	1.62			
XLOC_003560	FFC1_02922	FFUJ_07367	related to carrier protein YMC1, mitochondrial	1.62	2.03		1.70
XLOC_013565	FFC1_12503	FFUJ_11659	related to dityrosine transporter	1.62			
XLOC_001955	FFC1_01450	FFUJ_01364	uncharacterized protein FFUJ_01364	1.62			-1.34
XLOC_008181	FFC1_07229	FFUJ_02822	related to MYND domain protein	1.62			
XLOC_014640	FFC1_13830	FFUJ_09008	related to triacylglycerol lipase V precursor	1.62			
XLOC_013241	FFC1_12801	FFUJ_11374	Kelch-like protein 4	1.62			
XLOC_007678	FFC1_07610	FFUJ_03186	mss4-like protein	1.61			
XLOC_012656	FFC1_11731	FFUJ_12304	uncharacterized protein FFM5_13329	1.61			
XLOC_014187	FFC1_12996	FFUJ_04670	hypothetical protein FOXG_08226	1.61			
XLOC_010825	FFC1_10229	FFUJ_11078	uncharacterized protein FFUJ_11078	1.61			
XLOC_001126	FFC1_02046	FFUJ_01919	uncharacterized protein FFC1_02046	1.61			
XLOC_007196	FFC1_06721	FFUJ_05323	related to hydroxylase	1.61			
XLOC_002346	FFC1_02194	FFUJ_02062	uncharacterized protein Y057_10557	1.61			
XLOC_002309	FFC1_02125	FFUJ_01996	related to C4-dicarboxylate transport protein mae1	1.61			
XLOC_004987	-			1.61			
XLOC_010999	FFC1_10586	FFUJ_10767	uncharacterized protein Y057_382	1.61			
XLOC_010316	FFC1_09295	FFUJ_03865	related to P. aeruginosa hyuA and hyuB	1.60		2.32	
XLOC_007276	FFC1_06896	FFUJ_02510	CMGC/CDK protein kinase	1.60			
XLOC_015312	FFC1_14431	FFUJ_08114	related to multidrug resistance protein	1.60			
XLOC_003900	FFC1_03575	FFUJ_07995	endoglucanase type K	1.60			
XLOC_010685	FFC1_09974	FFUJ_04484	CMGC/MAPK/P38 protein kinase	1.59			
XLOC_001468	FFC1_00527		uncharacterized protein FFNC_00531	1.58			
XLOC_009480	-			1.58			
XLOC_010196	FFC1_09944	FFUJ_04458	uncharacterized protein FFB20_03353	1.57			
XLOC_009363	FFC1_08421	FFUJ_09944	Fe-Mn family superoxide dismutase	1.57			
XLOC_002650	FFC1_02796	FFUJ_07247	aconitate hydratase, mitochondrial	1.57			
XLOC_003020	FFC1_03454	FFUJ_07878	histone H3like centromeric protein cse-4	1.57			
XLOC_015350	FFC1_14515	FFUJ_08202	uncharacterized protein FFE2_12529	1.57			-1.39

XLOC_006227	FFC1_06445	FFUJ_13182	related to two-component histidine kinase chk-1	1.57			
XLOC_004401	FFC1_04462	FFUJ_05953	uncharacterized protein Y057_12842	1.56			
XLOC_015192	FFC1_14188	FFUJ_08665	uncharacterized protein FFUJ_08665	1.56			
XLOC_004549	FFC1_04744	FFUJ_06223	related to bacterial aminoglycoside acetyltransferase regulators	1.56			
XLOC_012390	FFC1_11212	FFUJ_14045	probable alpha-galactosidase C precursor	1.56			
XLOC_002960	FFC1_03348	FFUJ_07776	related to Acyl-coenzyme A:6-aminopenicillanic-acid-acyltransferase 40 kDa form	1.55			
XLOC_001725	-			1.55			
XLOC_004348	FFC1_04377	FFUJ_05866	related to stilbene synthase 2	1.55	2.81		
XLOC_009347	FFC1_08399		uncharacterized protein FFC1_08399	1.54			
XLOC_004811	FFC1_05237	FFUJ_06685	uncharacterized protein FFUJ_06685	1.54			
XLOC_008042	FFC1_06972	FFUJ_02587	uncharacterized protein FMAN_04136	1.54			
XLOC_008130	FFC1_07142	FFUJ_02744	uncharacterized protein FFNC_12095	1.54			
XLOC_010003	FFC1_09610	FFUJ_04133	complex i intermediate-associated 30	1.54	1.78		
XLOC_005220	FFC1_04562	FFUJ_06049	related to sarcosine oxidase	1.53	2.46		
XLOC_012940	FFC1_12246	FFUJ_11909	uncharacterized protein FFB20_00807	1.53		2.67	
XLOC_016082	FFC1_15069			1.53			
XLOC_015617	FFC1_14580	FFUJ_08269		1.53	2.26		
XLOC_014018	FFC1_13369	FFUJ_05028	related to Lactobacillus putative histidine protein kinase SppK	1.53			
XLOC_009715	FFC1_09025	FFUJ_09367	related to serum paraoxonase/arylesterase	1.53			
XLOC_016745	FFC1_15832			1.52			
XLOC_011685	FFC1_10730	FFUJ_10633	uncharacterized protein FFUJ_10633	1.52			
XLOC_011522	FFC1_10456	FFUJ_10890	related to chitinase	1.52			
XLOC_005882	FFC1_05807	FFUJ_14569	related to hydrolase related to dienelactone hydrolase	1.52			
XLOC_009964	FFC1_09539	FFUJ_04063	related to multidrug resistance protein	1.52			
XLOC_002506	FFC1_02513	FFUJ_06981	related to myo-inositol transport protein ITR1	1.52			
XLOC_009297	FFC1_08319	FFUJ_10045	uncharacterized protein FFUJ_10045	1.51	2.17		
XLOC_003852	FFC1_03479	FFUJ_07903	uncharacterized protein FFUJ_07903	1.51			
XLOC_012533	FFC1_11509	FFUJ_13754	related to diacylglycerol pyrophosphate phosphatase DPP1	1.51			
XLOC_004339	FFC1_04361	FFUJ_05852	uncharacterized protein FFUJ_05852	1.51			
XLOC_011551	FFC1_10499	FFUJ_10851	related to ketoreductases	1.51		1.99	
XLOC_013086	FFC1_12552	FFUJ_11611	related to DUF323 domain protein	1.50		2.03	
XLOC_006765	FFC1_05894	FFUJ_13708	related to pathway-specific regulatory protein nit-4	1.50			
XLOC_009591	FFC1_08814	FFUJ_09572	related to sexual differentiation and meiosis protein ste20	1.50	2.11		
XLOC_016431	FFC1_15407	FFUJ_12796		1.50			
XLOC_003353	FFC1_02548	FFUJ_07015	related to COQ2-para-hydroxybenzoate--polyprenyltransferase	1.50			
XLOC_011579	FFC1_10550	FFUJ_10800	uncharacterized protein FFB20_02249	1.50	2.47		
XLOC_011610	FFC1_10598	FFUJ_10756	uncharacterized protein LW93_051	1.49			
XLOC_010969	FFC1_10523	FFUJ_10826	uncharacterized protein FFUJ_10826	1.49			
XLOC_011648	FFC1_10668	FFUJ_10692	related to NADH oxidase	1.49	1.89		
XLOC_002123	FFC1_01789	FFUJ_01678	uncharacterized protein FFUJ_01678	1.49			
XLOC_012549	FFC1_11532	FFUJ_13733	uncharacterized protein FFUJ_13733	1.49			
XLOC_015586	FFC1_14520	FFUJ_08207		1.49		1.69	1.11
XLOC_006935	FFC1_06212	FFUJ_13405	pirin (iron-binding nuclear protein)	1.49			
XLOC_013640	FFC1_12632	FFUJ_11535	uncharacterized protein FFUJ_11535	1.48			
XLOC_000859	FFC1_01557	FFUJ_01463	related to RNA binding protein	1.48			
XLOC_002262	FFC1_02034	FFUJ_01907	uncharacterized protein FFUJ_01907	1.48			
XLOC_007334	FFC1_06999	FFUJ_02612	hsp70-like protein	1.48			
XLOC_015372	FFC1_14571	FFUJ_08260	allantoinase	1.48			
XLOC_011752	FFC1_10876	FFUJ_10491	related to LSB3-possible role in the regulation of actin cytoskeletal organization	1.48			
XLOC_009233	FFC1_08193	FFUJ_10167	serine/threonine protein kinase	1.47			
XLOC_004580	FFC1_04804	FFUJ_06275	carboxymethylenebutenolidase	1.47			
XLOC_006250	FFC1_06503	FFUJ_13125	related to acetylhydrolase	1.47			
XLOC_004250	FFC1_04224	FFUJ_05719	related to small unique nuclear receptor co-repressor	1.47			
XLOC_003839	FFC1_03451	FFUJ_07875	related to P.aeruginosa regulatory protein mmsR	1.47			
XLOC_004905	FFC1_03944	FFUJ_05459	uncharacterized protein FFNC_14721	1.47			
XLOC_013826	FFC1_13008	FFUJ_04682	related to Fe-S oxidoreductase	1.47			
XLOC_010166	FFC1_09886	FFUJ_04402	related to AHA1-stress-regulated cochaperone	1.47			
XLOC_012217	FFC1_11743	FFUJ_12314	related to ADH7-NADP(H)-dependent alcohol dehydrogenase	1.46			
XLOC_008976	FFC1_08747	FFUJ_09637	related to ASTRA-associated protein 1	1.46			
XLOC_015602	FFC1_14551	FFUJ_08240	probable homoaconitase precursor	1.46			
XLOC_012012	FFC1_11380	FFUJ_13881	uncharacterized protein Y057_12185	1.46			
XLOC_007874	FFC1_07994	FFUJ_03555	uncharacterized protein FFUJ_03555	1.46			
XLOC_004255	FFC1_04234	FFUJ_05729	uncharacterized protein FFUJ_05729	1.46	1.94		
XLOC_001817	FFC1_01187	FFUJ_01109	uncharacterized protein FFUJ_01109	1.46	1.79		
XLOC_008485	FFC1_07770	FFUJ_03339	uncharacterized protein FFUJ_03339	1.46			
XLOC_011535	FFC1_10473	FFUJ_10874	GATA zinc finger domain-containing protein 10	1.46			
XLOC_006949	FFC1_06242	FFUJ_13376	related to thioredoxin	1.45			
XLOC_012245	FFC1_11809	FFUJ_12376	related to dehydrogenases with different specificities (related to short-chain alcohol dehydrogenases)	1.45		1.34	
XLOC_015439	FFC1_14702	FFUJ_08385	related to aspartic proteinase precursor	1.45			
XLOC_002981	FFC1_03379	FFUJ_07805	NADH dehydrogenase	1.45			
XLOC_012190	FFC1_11705	FFUJ_12279	probable chitin synthase D	1.45			

XLOC_000821	FFC1_01502	FFUJ_01412	uncharacterized protein FFUJ_01412	1.45			
XLOC_001850	FFC1_01261	FFUJ_01183	uncharacterized protein FFUJ_01183	1.45			
XLOC_013596	FFC1_12549	FFUJ_11614	uncharacterized protein Y057_9882	1.44			
XLOC_004496	FFC1_04640	FFUJ_06126	related to dithiol-disulfide isomerase involved in polyketide biosynthesis	1.44			
XLOC_014534	FFC1_13650	FFUJ_05300		1.44	1.99		
XLOC_016111	FFC1_15125	FFUJ_02400	related to purine nucleoside permease	1.44			-1.58
XLOC_006063	FFC1_06135	FFUJ_13479	heat shock protein 60	1.44			
XLOC_002251	FFC1_02014	FFUJ_01887	predicted protein [	1.44	5.86		4.81
XLOC_015431	FFC1_14689	FFUJ_08372		1.44			
XLOC_014447	FFC1_13479	FFUJ_05131	trehalose 6-phosphate synthase	1.44			
XLOC_010056	FFC1_09702	FFUJ_04222	related to nitrogen metabolic regulation protein nmr	1.44			
XLOC_004967	FFC1_04070	FFUJ_05576	related to NAM7-nonsense-mediated mRNA decay protein	1.43			
XLOC_004340	FFC1_04363	FFUJ_05854	uncharacterized protein FFC1_04363	1.43			
XLOC_007094	FFC1_06501	FFUJ_13127	related to carboxyphosphonoenolpyruvate phosphonomutase-like protein	1.43			
XLOC_007795	FFC1_07847	FFUJ_03411	Transforming growth factor-beta-induced protein ig-h3	1.43			
XLOC_008925	FFC1_08628	FFUJ_09747	related to 26S proteasome subunit RPN4	1.43			
XLOC_002965	FFC1_03356	FFUJ_07783	related to pisatin demethylase	1.43			
XLOC_011243	FFC1_11011	FFUJ_10368	uncharacterized protein FFUJ_10368	1.43			
XLOC_000969	FFC1_01757	FFUJ_01647	related to putative plasma membrane protein YRO2	1.42			
XLOC_011412	FFC1_10257	FFUJ_11052	related to quinone reductase	1.42			
XLOC_001444	FFC1_00492	FFUJ_00450	uncharacterized protein FFUJ_00450	1.42			
XLOC_015258	FFC1_14322	FFUJ_08536	ph protein	1.42			
XLOC_011516	FFC1_10446	FFUJ_10900	related to nonribosomal peptide synthetase MxcG	1.42	2.36		
XLOC_006417	FFC1_06800		related to purine-cytosine permease	1.42			
XLOC_000279	FFC1_00513	FFUJ_00469	related to beta-glucosidase	1.42			
XLOC_013562	FFC1_12498	FFUJ_11664	related to multidrug resistance protein	1.42			
XLOC_014122	FFC1_13551	FFUJ_05199	related to transcription activator protein acu-15	1.42			
XLOC_012095	FFC1_11525	FFUJ_13739	related to type-III integral membrane protein, involved in copper and iron homeostasis	1.41			
XLOC_008966	FFC1_08721	FFUJ_09662	related to XAP-5 protein	1.41			
XLOC_008091	FFC1_07071	FFUJ_02679	uncharacterized protein FFUJ_02679	1.41			
XLOC_004362	FFC1_04396	FFUJ_05887	related to phytochrome	1.41	1.85		
XLOC_001463	FFC1_00524	FFUJ_00479	stress-induced-phosphoprotein 1	1.40			
XLOC_015000	FFC1_13832	FFUJ_09006		1.40			
XLOC_013991	FFC1_13327	FFUJ_04988	related to UPC2-regulatory protein involved in control of sterol uptake	1.40	1.79		
XLOC_003445	FFC1_02724	FFUJ_07181	plasma membrane proteolipid 3	1.40			
XLOC_011888	FFC1_11160	FFUJ_10222	uncharacterized protein FFUJ_10222	1.40			
XLOC_005361	FFC1_04791		uncharacterized protein FFM5_03343	1.40			
XLOC_002254	FFC1_02018	FFUJ_01891	uncharacterized protein FFUJ_01891	1.40			
XLOC_015138	FFC1_14092	FFUJ_08754	probable aflatoxin efflux pump AFLT	1.40			
XLOC_009446	FFC1_08571	FFUJ_01057	related to multidrug resistance protein	1.39			
XLOC_002760	FFC1_02998	FFUJ_07441	related to GIP3 Glc7-interacting protein whose overexpression relocalizes Glc7p from the nucleus	1.39			
XLOC_005949	FFC1_05925	FFUJ_13678	aconitate hydratase, mitochondrial	1.39			
XLOC_006660	FFC1_05681	FFUJ_14686	related to monooxigenase	1.39			
XLOC_000248	FFC1_00454	FFUJ_00412	related to growth hormone inducible transmembrane protein	1.39			
XLOC_012413	FFC1_11268	FFUJ_13992	uncharacterized protein FFC1_11268	1.39			
XLOC_009211	FFC1_09213	FFUJ_09173	related to isoflavone reductase homolog A622	1.39			
XLOC_007940	FFC1_08119	FFUJ_03676	related to beta-galactosidase	1.39			
XLOC_003539	FFC1_02884	FFUJ_07332	threonine dehydratase	1.39			
XLOC_015805	FFC1_14912	FFUJ_02192	probable bifunctional P-450:NADPH-P450 reductase	1.39		1.37	
XLOC_000261	FFC1_00474	FFUJ_00432	uncharacterized protein LW93_2490	1.38			
XLOC_003692	FFC1_03174	FFUJ_07608	probable brefeldin A resistance protein	1.38			
XLOC_010075	FFC1_09734		uncharacterized protein FFM5_04418	1.38			
XLOC_010476	FFC1_09589	FFUJ_04114	uncharacterized protein Y057_9535	1.38			
XLOC_003671	FFC1_03132	FFUJ_07570	ATPase get3	1.38			
XLOC_015297	FFC1_14402	FFUJ_08087	uncharacterized protein FFE2_12643	1.37			
XLOC_002743	FFC1_02969	FFUJ_07412	Putative peptidase yqhT	1.37			
XLOC_006834	FFC1_06013	FFUJ_13596	uncharacterized protein Y057_3565	1.37			
XLOC_001724	FFC1_01024	FFUJ_00951	related to CAF120 CCR4 Associated Factor 120 kDa	1.37			
XLOC_011161	FFC1_10870	FFUJ_10497	uncharacterized protein FFUJ_10497	1.37			
XLOC_002495	FFC1_02489	FFUJ_06958	uncharacterized protein Y057_14945	1.37			
XLOC_012754	FFC1_11907	FFUJ_12474	related to AIF1 Apoptosis-Inducing Factor	1.37		1.28	
XLOC_014810	FFC1_14136	FFUJ_08714		1.37	1.71		
XLOC_009846	FFC1_09291	FFUJ_03861	probable lysosomal cobalamin transporter	1.37			
XLOC_003759	FFC1_03290	FFUJ_07719	related to Putative dioxygenase C576.01c	1.36			-2.86
XLOC_003836	FFC1_03448	FFUJ_07872	probable membrane-bound O-acyltransferase domain-containing protein 5	1.36			
XLOC_006130	FFC1_06255	FFUJ_13363	DnaJ like subfamily B member 4	1.36			
XLOC_014126	FFC1_13557	FFUJ_05205	related to polyadenylate-binding protein	1.36			
XLOC_001333	FFC1_00249	FFUJ_00208	related to tetracycline resistance protein (probable transport protein)	1.36			
XLOC_011348	FFC1_10145	FFUJ_11163	related to purine-cytosine permease	1.36			

XLOC_014556	FFC1_13693	FFUJ_09140	related to protocatechuate 3,4-dioxygenase beta subunit	1.36			
XLOC_013819	FFC1_12997	FFUJ_04671	Uncharacterized protein LW93_10538	1.35			
XLOC_010505	FFC1_09644	FFUJ_04166	hydroxyacid-oxoacid transhydrogenase	1.35			
XLOC_001700	FFC1_00974	FFUJ_00905	uncharacterized protein LW93_2341	1.35			-1.39
XLOC_006121	FFC1_06240	FFUJ_13378	uncharacterized protein FFUJ_13378	1.35			
XLOC_010657	FFC1_09916	FFUJ_04430	uncharacterized protein LW93_14052	1.34			
XLOC_003519	FFC1_02851	FFUJ_07302	related to pall protein	1.34	1.83		
XLOC_011285	FFC1_11075	FFUJ_10307	choline permease	1.34			
XLOC_013564	FFC1_12501	FFUJ_11661	uncharacterized protein FFM5_10663	1.34			
XLOC_009346	FFC1_08398	FFUJ_09966	uncharacterized protein FFUJ_09966	1.34			
XLOC_003851	FFC1_03477	FFUJ_07901	condensin complex subunit 3	1.34			-1.16
XLOC_015527	FFC1_14416	FFUJ_08101	related to acyl-CoA transferases/carnitine dehydratase	1.34			
XLOC_011517	FFC1_10448	FFUJ_10898	related to multidrug resistance protein	1.34	2.27		
XLOC_011210	FFC1_10958	FFUJ_10418	probable potassium channel beta subunit protein	1.34			
XLOC_014837	FFC1_14190	FFUJ_08663	cell division control protein 48	1.34			
XLOC_015881	FFC1_15052	FFUJ_02329	related to CAR2-ornithine aminotransferase	1.33			
XLOC_014238	FFC1_13111	FFUJ_04780	lon protease like 2, peroxisomal	1.33			
XLOC_014533	FFC1_13649	FFUJ_05299	related to E3 ubiquitin ligase	1.33			
XLOC_000127	FFC1_00248	FFUJ_00207	related to arsenic resistance protein ArsH	1.33			
XLOC_014650	FFC1_13853	FFUJ_03847	probable ENA5-Plasma membrane P-type ATPase involved in Na+ and Li+ efflux	1.33			
XLOC_010092	FFC1_09764	FFUJ_04277	uncharacterized protein FFUJ_04277	1.33			
XLOC_008530	FFC1_07844	FFUJ_03409	uncharacterized protein Y057_6569	1.33			
XLOC_015692	FFC1_14705	FFUJ_08387	related to aquaporin	1.33			
XLOC_015241	FFC1_14283	FFUJ_08574		1.33			
XLOC_005512	FFC1_05079	FFUJ_06541	related to PRLI-interacting factor K	1.33			
XLOC_001580	FFC1_00757	FFUJ_00694	uncharacterized protein FFE2_00761	1.32			
XLOC_007640	FFC1_07541	FFUJ_03119	cell division cycle protein 37	1.32			
XLOC_012741	FFC1_11876	FFUJ_12444	22kda glyco	1.32			
XLOC_010775	FFC1_10109	FFUJ_04616	choline dehydrogenase	1.32			
XLOC_012597	FFC1_11608	FFUJ_12182	related to oxidoreductase related to nitroreductase	1.32			
XLOC_004296	FFC1_04300	FFUJ_05794	uncharacterized protein Y057_3431	1.32			
XLOC_002091	FFC1_01728	FFUJ_01621	related to rna-binding protein fus/tls	1.32			
XLOC_007580	FFC1_07436	FFUJ_03019	Putative 28.5 kDa protein in 7S RNA 5'region	1.32			
XLOC_014796	FFC1_14113	FFUJ_08733	ATP synthase mitochondrial F1 complex assembly factor 1	1.31			
XLOC_000289	FFC1_00540	FFUJ_00494	succinate dehydrogenase (ubiquinone) membrane anchor subunit	1.31			
XLOC_014354	FFC1_13301	FFUJ_04964	lon protease like, mitochondrial	1.31			
XLOC_007836	FFC1_07909	FFUJ_03471	related to ACB 4-hydroxyacetophenone monooxygenase	1.31		1.39	
XLOC_012911	FFC1_12194	FFUJ_11961	Uncharacterized protein LW94_4703	1.31			
XLOC_015159	FFC1_14135	FFUJ_08715		1.31			
XLOC_001953	FFC1_01444	FFUJ_01358	related to SLS1 protein precursor	1.31			
XLOC_008078	FFC1_07041	FFUJ_02652	cutinase transcription factor 1 beta	1.31			
XLOC_013067	FFC1_12502	FFUJ_11660	related to SPS19-peroxisomal 2,4-dienoyl-CoA reductase	1.31			
XLOC_002124	FFC1_01790	FFUJ_01679	zinc finger protein	1.30			
XLOC_001459	FFC1_00518	FFUJ_00474	related to monooxygenase	1.30			
XLOC_009635	FFC1_08884	FFUJ_09505	uncharacterized protein FFUJ_09505	1.30			
XLOC_008000	FFC1_06902	FFUJ_02516	uncharacterized protein FFUJ_02516	1.30			
XLOC_000222	FFC1_00413	FFUJ_00369	related to nicotinate phosphoribosyltransferase	1.30			
XLOC_009006	-			1.30			
XLOC_001793	FFC1_01145	FFUJ_01071	related to putative sterigmatocystin biosynthesis lipase/esterase STCI	1.30			-1.56
XLOC_012702	FFC1_11808	FFUJ_12375	Isoflavone reductase like protein IRL	1.30			
XLOC_002555	FFC1_02602	FFUJ_07065	uncharacterized protein FFUJ_07065	1.30			
XLOC_009354	FFC1_08406	FFUJ_09959	GTP cyclohydrolase II	1.30			
XLOC_004353	FFC1_04385	FFUJ_05874	cytochrome c heme lyase	1.29			
XLOC_000268	FFC1_00489	FFUJ_00447	related to DUF1275 domain protein	1.29			
XLOC_012935	FFC1_12236	FFUJ_11920	related to integral membrane protein	1.29			
XLOC_000173	FFC1_00336	FFUJ_00293	related to multidrug resistant protein	1.29			
XLOC_005991	FFC1_06010	FFUJ_13599	related to nuclear pore membrane protein POM152	1.29			
XLOC_012208	FFC1_11730	FFUJ_12303	uncharacterized protein FFB20_10100	1.29			
XLOC_000534	FFC1_00970	FFUJ_00901	related to dehydrogenases and related proteins	1.29			
XLOC_012540	FFC1_11520	FFUJ_13744	molecular chaperone	1.29			
XLOC_011268	FFC1_11050	FFUJ_10331	related to neutral amino acid permease	1.28			
XLOC_001464	FFC1_00525	FFUJ_00480	arginyl-tRNA synthetase	1.28			
XLOC_005695	FFC1_05449		related to short chain dehydrogenase/reductase family protein	1.28			
XLOC_002549	FFC1_02592	FFUJ_07056	uncharacterized protein FFUJ_07056	1.28			
XLOC_002666	FFC1_02823	FFUJ_07274	uncharacterized protein FFUJ_07274	1.28			
XLOC_002925	FFC1_03287	FFUJ_07717	related to spherulin 1B precursor	1.28			
XLOC_004365	FFC1_04402	FFUJ_05893	phosphoenolpyruvate carboxykinase	1.28			
XLOC_013612	FFC1_12584	FFUJ_14932	uncharacterized protein FFUJ_14932	1.28		2.28	
XLOC_010418	FFC1_09482	FFUJ_04007	related to ALCOHOL DEHYDROGENASE I-ADH1	1.28			
XLOC_010826	FFC1_10232	FFUJ_11075	phosphotransferase family protein	1.27			
XLOC_003771	FFC1_03319	FFUJ_07745	uncharacterized protein FFUJ_07745	1.27			
XLOC_003453	FFC1_02741	FFUJ_07198	Meiotically up-regulated protein 65 protein	1.27			

XLOC_004528	FFC1_04705	FFUJ_06185	related to ubiquinol--cytochrome-c reductase assembly factor	1.27			
XLOC_014808	FFC1_14134	FFUJ_08716	Insulin-induced protein 2 protein	1.27			
XLOC_014638	FFC1_13823	FFUJ_09015	related to transporter protein HOL1	1.26			
XLOC_014068	FFC1_13462	FFUJ_05114	related to PHM7-similarity to A.thaliana hyp1 protein	1.26	1.63		
XLOC_004540	FFC1_04727	FFUJ_06207	D-arabinono-1,4-lactone oxidase	1.26			
XLOC_001944	FFC1_01431	FFUJ_01344	Nucleoporin NUP120	1.26			
XLOC_004512	FFC1_04671	FFUJ_06155	predicted protein	1.26			
XLOC_004935	FFC1_04006	FFUJ_05518	related to lysophospholipase (lpl)	1.26			
XLOC_000027	FFC1_00058	FFUJ_00026	uncharacterized protein FFUJ_00026	1.26			
XLOC_003815	FFC1_03410	FFUJ_07835	related to FMP27 Found in Mitochondrial Proteome	1.26			
XLOC_000736	FFC1_01332	FFUJ_01251	uncharacterized protein Y057_14069	1.26			
XLOC_009596	FFC1_08824	FFUJ_09562	NAD-specific glutamate dehydrogenase	1.26			
XLOC_014826	FFC1_14171	FFUJ_08681	related to calmodulin-binding protein kinase	1.26			
XLOC_003837	FFC1_03449	FFUJ_07873	GDP-mannose transporter	1.25			
XLOC_008922	FFC1_08625	FFUJ_09750	DNA-directed RNA polymerase I subunit RPA1	1.25			
XLOC_001391	FFC1_00364	FFUJ_00322	related to ketoreductases	1.25			
XLOC_001481	FFC1_00548	FFUJ_00501	related to WSS1 Protein involved in sister chromatid separation and segregation	1.25			
XLOC_008395	FFC1_07624	FFUJ_03200	related to UTP10-U3 snoRNP protein	1.25			
XLOC_014943	FFC1_13692	FFUJ_09141	uncharacterized protein Y057_13071	1.25			
XLOC_008872	FFC1_08529	FFUJ_09840	uncharacterized protein FFUJ_09840	1.25			
XLOC_009904	FFC1_09399	FFUJ_03928	uncharacterized protein Y057_5031	1.25			
XLOC_001437	FFC1_00480	FFUJ_00438	Forkhead box protein O4	1.24			
XLOC_015526	FFC1_14415	FFUJ_08100	related to flavin-containing monooxygenase	1.24			
XLOC_012287	FFC1_11894	FFUJ_12461	related to ankyrin 3	1.24			
XLOC_008829	FFC1_08445	FFUJ_09921	related to TEA1-TY1 enhancer activator	1.24			
XLOC_001667	FFC1_00920	FFUJ_00851	related to allantoate permease	1.23			
XLOC_004986	FFC1_04101	FFUJ_05605	related to sterol glucosyltransferase	1.23			
XLOC_012784	FFC1_11955	FFUJ_12519	related to Put3p and to hypothetical protein YJL206c	1.23			
XLOC_004912	FFC1_03956	FFUJ_05468	uncharacterized protein Y057_13877	1.23			
XLOC_011861	FFC1_11111	FFUJ_10272	related to oxidoreductase, short chain dehydrogenase/reductase family	1.23			
XLOC_013637	FFC1_12625	FFUJ_11542	related to DNA repair exonuclease SIA1	1.23	2.59		
XLOC_010533	FFC1_09703	FFUJ_04223	Phosphotransferase	1.23			
XLOC_002514	FFC1_02525	FFUJ_06991	uncharacterized protein Y057_8787	1.23			
XLOC_014216	FFC1_13065	FFUJ_04737	molecular chaperone DnaJ	1.23			
XLOC_009899	FFC1_09393	FFUJ_03922	related to periplasmic beta-glucosidase/beta-xylosidase precursor	1.23			
XLOC_010767	FFC1_10098	FFUJ_04606	related to CTI6 Cyc8-Tup1 Interacting protein	1.22			
XLOC_003589	FFC1_02970	FFUJ_07413	uncharacterized protein FFUJ_07413	1.22			
XLOC_000860	FFC1_01560	FFUJ_01466	OPA3-like protein	1.22			
XLOC_004822	FFC1_03792		ATP-nad kinase	1.22			
XLOC_003879	FFC1_03533	FFUJ_07956	acyl-CoA thioester hydrolase	1.22			
XLOC_001592	FFC1_00781	FFUJ_00718	related to endoplasmic reticulum 25 kDa transmembrane protein	1.22			
XLOC_014330	FFC1_13266	FFUJ_04931	alcohol dehydrogenase	1.22			
XLOC_001873	FFC1_01298	FFUJ_01217	probable DNA repair protein MUS-42	1.21			
XLOC_007835	FFC1_07908		related to ACB 4-hydroxyacetophenone monooxygenase	1.21			
XLOC_005977	FFC1_05983	FFUJ_13626	probable aflatoxin efflux pump AFLT	1.21			
XLOC_005694	FFC1_05448		uncharacterized protein FFB20_04031	1.21			
XLOC_000890	FFC1_01609	FFUJ_01512	related to transcription activator protein acu-15	1.21			
XLOC_005993	FFC1_06014	FFUJ_13595	related to transcription factor BOM	1.21			
XLOC_000482	FFC1_00866	FFUJ_00801	probable glucosidase I	1.21			
XLOC_002668	FFC1_02824	FFUJ_07275	DUF636 domain protein	1.21			
XLOC_008748	FFC1_08266	FFUJ_10095	related to DUF1295 domain protein	1.21			
XLOC_011771	FFC1_10917	FFUJ_10452	related to 3-oxoacyl-[acyl-carrier-protein] reductase	1.21			
XLOC_010305	FFC1_09277	FFUJ_03848	hypothetical protein FVEG_03570	1.20			
XLOC_006145	FFC1_06284	FFUJ_13335	related to SYG1 protein	1.20			
XLOC_009082	FFC1_08943	FFUJ_09448	related to heterokaryon incompatibility protein (het-6OR allele)	1.20			
XLOC_013971	FFC1_13287	FFUJ_04951	related to coxI translation protein CYA5	1.20			
XLOC_005981	FFC1_05994	FFUJ_13615	uncharacterized protein FFUJ_13615	1.20			
XLOC_006987	FFC1_06310	FFUJ_13310	3-isopropylmalate dehydrogenase	1.19			
XLOC_003625	FFC1_03049	FFUJ_07488	uncharacterized protein FFUJ_07488	1.19			
XLOC_000789	FFC1_01447	FFUJ_01361	uncharacterized protein FFUJ_01361	1.19			
XLOC_006336	FFC1_06653	FFUJ_12988	uncharacterized protein LW93_8207	1.19			
XLOC_002550	FFC1_02594	FFUJ_07058	related to SCJ1 protein	1.19			
XLOC_004588	FFC1_04818	FFUJ_06288	related to cytoplasmic Zn-finger protein BRAP2 (BRCA1 associated protein)	1.19			
XLOC_002884	FFC1_03209	FFUJ_07643	related to DNA damage response protein	1.18			
XLOC_015943	FFC1_15157	FFUJ_02431	uncharacterized protein FFUJ_02431	1.18			
XLOC_005427	FFC1_04922	FFUJ_06388	probable xanthine phosphoribosyl transferase	1.18			
XLOC_003801	FFC1_03380	FFUJ_07806	related to myosin heavy chain proteins	1.18			
XLOC_003323	FFC1_02491	FFUJ_06960	uncharacterized protein FFUJ_06960	1.18			
XLOC_008014	FFC1_06923	FFUJ_02537	protein phosphatase 5	1.18			
XLOC_015924	FFC1_15133	FFUJ_02408	probable DUF757 domain protein	1.18			

XLOC_016092	FFC1_15089	FFUJ_02364	related to transaldolase	1.17		3.54	
XLOC_004178	FFC1_04098	FFUJ_05604	uncharacterized protein FFUJ_05604	1.17			
XLOC_015309	FFC1_14426	FFUJ_08110		1.17			
XLOC_010552	FFC1_09744	FFUJ_04257	uncharacterized protein FFUJ_04257	1.17			
XLOC_012608	FFC1_11622	FFUJ_12196	uncharacterized protein FFUJ_12196	1.17			
XLOC_002964	FFC1_03355	FFUJ_07782	related to pisatin demethylase	1.17			
XLOC_015061	FFC1_13949	FFUJ_08895	related to transcriptional activator acu-15	1.17			
XLOC_002730	FFC1_02947	FFUJ_07391	uncharacterized protein Y057_7487	1.16			
XLOC_006241	FFC1_06481	FFUJ_13147	uncharacterized protein Y057_521	1.16			
XLOC_006449	FFC1_05291		uncharacterized protein FFNC_08564	1.16			
XLOC_003097	FFC1_03595	FFUJ_08013	related to putidaredoxin reductase	1.16			
XLOC_013989	FFC1_13325	FFUJ_04986	related to SNARE binding protein	1.16			
XLOC_004291	FFC1_04293	FFUJ_05787	probable novel protein of ras superfamily KREV-1	1.16	1.92		
XLOC_016150	FFC1_15204	FFUJ_12600	related to fluconazole resistance protein (FLU1)	1.16			-1.62
XLOC_008293	FFC1_07435	FFUJ_03018	uncharacterized protein FFUJ_03018	1.16			
XLOC_016070	FFC1_15047	FFUJ_02324		1.16			
XLOC_000999	FFC1_01806	FFUJ_01693	uncharacterized protein FFNC_11854	1.15			
XLOC_013639	FFC1_12631	FFUJ_11536	related to nitrate assimilation regulatory protein nirA	1.15			
XLOC_002396	FFC1_02301	FFUJ_06781	related to alcohol dehydrogenase, class C	1.15	2.91		
XLOC_002769	FFC1_03013	FFUJ_07453	related to integral membrane protein	1.15			
XLOC_012973	FFC1_12304	FFUJ_11851	related to short chain dehydrogenase	1.15			
XLOC_016799	FFC1_15828			1.15			
XLOC_016072	FFC1_15049	FFUJ_02326	uncharacterized protein FFUJ_02326	1.14			
XLOC_011919	FFC1_11213	FFUJ_14044	related to cytosine deaminase	1.14	2.24		
XLOC_014210	FFC1_13053	FFUJ_04725	probable 3^-phosphoadenosine 5^-phosphosulfate sulfotransferase (PAPS reductase)/FAD synthetase and related enzymes	1.14	1.85		
XLOC_015920	FFC1_15124	FFUJ_02399	IKS protein kinase	1.14			
XLOC_005253	FFC1_04604	FFUJ_06089	ubiquitin-protein ligase E3 C	1.14			
XLOC_010252	FFC1_10055	FFUJ_04564	guanine deaminase	1.14			
XLOC_007923	FFC1_08086	FFUJ_03646	archaeal flagellin N-terminal-like domain-containing protein	1.14			
XLOC_003714	FFC1_03214	FFUJ_07648	alcohol dehydrogenase	1.13			
XLOC_003304	FFC1_02449	FFUJ_06922	related to vacuolar protein sorting-associated protein VPS13	1.13			
XLOC_013964	FFC1_13268	FFUJ_04933	squalene monooxygenase	1.13			
XLOC_015401	FFC1_14628	FFUJ_08313	related to Fe/S cluster assembly protein ISA1	1.13			
XLOC_002209	FFC1_01946	FFUJ_01821	related to IQ calmodulin-binding motif domain protein	1.13			
XLOC_015160	FFC1_14137	FFUJ_08713		1.13			
XLOC_008431	FFC1_07678	FFUJ_03253	Fungal specific transcription factor, putative	1.13			
XLOC_014758	FFC1_14044	FFUJ_08801	hydrolase-HD superfamily protein	1.13			
XLOC_002687	FFC1_02860	FFUJ_07310	related to transcription factor atf1+	1.13			
XLOC_004976	FFC1_04082	FFUJ_05588	uncharacterized protein FFUJ_05588	1.12			
XLOC_014435	FFC1_13451			1.12			
XLOC_015940	FFC1_15155	FFUJ_02429	predicted protein	1.12			
XLOC_001475	FFC1_00537	FFUJ_00491	related to ubiquitin-like protein DSK2	1.12			
XLOC_001021	FFC1_01841	FFUJ_01726	transcription factor	1.12			
XLOC_013476	FFC1_12333	FFUJ_11823	related to ethionine resistance protein	1.12			
XLOC_009077	FFC1_08930	FFUJ_09461	related to histidine triad protein	1.12			
XLOC_005250	FFC1_04600	FFUJ_06085	related to fructosyl amino acid oxidase	1.12			
XLOC_009481	FFC1_08629	FFUJ_09746	probable PENTAFUNCTIONAL AROM POLYPEPTIDE	1.12			
XLOC_015580	FFC1_14513	FFUJ_08200	related to glomerulosclerosis protein Mpv17	1.12		1.41	
XLOC_014544	FFC1_13667	FFUJ_05316		1.12			
XLOC_015462	FFC1_14760	FFUJ_08436		1.11			
XLOC_013876	-			1.11			
XLOC_009355	FFC1_08407	FFUJ_09958	predicted protein [	1.11			
XLOC_011814	FFC1_11013	FFUJ_10366	uncharacterized protein FFUJ_10366	1.11		1.22	
XLOC_013236	FFC1_12795	FFUJ_11380	bet v1-like protein	1.11	1.72		
XLOC_006671	FFC1_05703	FFUJ_14665	related to trans-aconitate 3-methyltransferase	1.11			
XLOC_015225	FFC1_14246	FFUJ_08608	related to transcription factor	1.11			
XLOC_002791	FFC1_03051	FFUJ_07490	uncharacterized protein FFUJ_07490	1.10			
XLOC_011739	FFC1_10854	FFUJ_10512	related to hydrolases or acyltransferases (alpha/beta hydrolase superfamily)	1.10			
XLOC_004728	FFC1_05082	FFUJ_06544	Beta-lactamase-like protein	1.10			
XLOC_014407	FFC1_13405	FFUJ_05060	salicylate hydroxylase	1.10			
XLOC_013728	FFC1_12814	FFUJ_11361	uncharacterized protein FFUJ_11361	1.10			
XLOC_000866	FFC1_01569	FFUJ_01475	glucose-6-phosphate 1-dehydrogenase	1.10			
XLOC_009802	FFC1_09202	FFUJ_09183	uncharacterized protein FFUJ_09183	1.10	2.56		2.72
XLOC_013053	FFC1_12476	FFUJ_11686	related to diacylglycerol pyrophosphate phosphatase DPP1	1.10			
XLOC_001312	FFC1_00199	FFUJ_00164	cardiolipin synthase	1.10			
XLOC_012699	FFC1_11803	FFUJ_12370	predicted protein [	1.10			
XLOC_010260	FFC1_10075	FFUJ_04584	uncharacterized protein FFUJ_04584	1.10			
XLOC_001234	FFC1_00041		Uncharacterized protein Y057_8058	1.10			
XLOC_004279	FFC1_04272	FFUJ_05767	related to transcriptional activator Mut3p	1.10			
XLOC_010254	FFC1_10063	FFUJ_04572	phosphomannose isomerase type I	1.09			
XLOC_001874	FFC1_01301	FFUJ_01220	related to TPC1-mitochondrial transport protein	1.09			
XLOC_004727	FFC1_05081	FFUJ_06543	related to Pseudomonas L-fucose dehydrogenase	1.09			
XLOC_002611	FFC1_02706	FFUJ_07163	related to anon-37cs protein	1.09			

XLOC_010787	FFC1_10134	FFUJ_11174	related to cytosine deaminase and related metal-dependent hydrolases	1.09			
XLOC_011736	FFC1_10846	FFUJ_10520	related to dienelactone hydrolase and related enzymes	1.09			
XLOC_013147	FFC1_12665	FFUJ_11509	related to DNA repair exonuclease SIA1	1.09			
XLOC_010964	FFC1_10515	FFUJ_10835	related to photosystem II protein D2	1.09			
XLOC_012116	FFC1_11568	FFUJ_12145	related to arylamine N-acetyltransferase	1.09		1.75	
XLOC_013065	FFC1_12497	FFUJ_11665	uncharacterized protein FFUJ_11665	1.09			
XLOC_009282	FFC1_08290	FFUJ_10073	probable DFG5 protein	1.09			
XLOC_014815	FFC1_14149	FFUJ_08702	related to Ycf1p, Yor1p, rat organic anion transporter	1.08			
XLOC_013066	FFC1_12499	FFUJ_11663	uncharacterized protein FFUJ_11663	1.08			
XLOC_012302	FFC1_11916	FFUJ_12483	related to methyltransferase	1.08			
XLOC_015231	FFC1_14259	FFUJ_08598	related to methyltransferase	1.08			
XLOC_005985	FFC1_05998	FFUJ_13611	related to transcription factor Ask10p	1.08			
XLOC_008578	FFC1_07946	FFUJ_03508	Protein PNS1	1.08			
XLOC_008487	FFC1_07772	FFUJ_03341	uncharacterized protein FFUJ_03341	1.08			
XLOC_015582	FFC1_14516	FFUJ_08203		1.08			
XLOC_010973	FFC1_10534	FFUJ_10815	related to PET8 protein, member of the mitochondrial carrier (MCF) family	1.08			
XLOC_015626	FFC1_14593	FFUJ_08282		1.08	1.93		
XLOC_010731	FFC1_10039	FFUJ_04548	uncharacterized protein LW93_13936	1.08	1.53		
XLOC_007031	FFC1_06397	FFUJ_13229	probable beta (1-3) glucanosyltransferase	1.08			
XLOC_010503	FFC1_09642	FFUJ_04164	uncharacterized protein FFUJ_04164	1.08			
XLOC_015931	FFC1_15142	FFUJ_02416	related to nitrate reductase	1.08			
XLOC_014722	FFC1_13978	FFUJ_08866	related to D-arabinitol 2-dehydrogenase	1.08		2.10	
XLOC_001106	FFC1_02007	FFUJ_01879	probable ATP dependent RNA helicase	1.08			
XLOC_011575	FFC1_10545	FFUJ_10804	related to hydroxyquinol-1,2-dioxygenase	1.07			
XLOC_001041	FFC1_01880	FFUJ_01764	probable ribosomal RNA-processing protein 12	1.07			
XLOC_009615	FFC1_08853	FFUJ_09533	protein phosphatase	1.07			
XLOC_007291	FFC1_06925	FFUJ_02539	atypical/ABC1/ABC1-A protein kinase	1.07			
XLOC_012657	FFC1_11735	FFUJ_12308	related to triacylglycerol lipase	1.07			
XLOC_003354	FFC1_02551	FFUJ_07018	cytochrome c heme-lyase	1.06			
XLOC_015076	FFC1_13976	FFUJ_08868	related to uncharacterized integral membrane protein	1.06			
XLOC_011420	FFC1_10271	FFUJ_11041	related to C6 finger domain protein	1.06			
XLOC_000770	FFC1_01405	FFUJ_01318	related to dual specificity protein phosphatase	1.06			
XLOC_003352	FFC1_02547	FFUJ_07014	related to aerobactin siderophore biosynthesis protein iucB	1.06			
XLOC_015406	FFC1_14634	FFUJ_08318	related to nuclear VCP-like protein	1.06			
XLOC_016796	FFC1_15824			1.06			
XLOC_015001	FFC1_13833	FFUJ_09005		1.06			
XLOC_003578	FFC1_02949	FFUJ_07393	ribonucleoprotein-associated protein	1.06			
XLOC_005344	FFC1_04765	FFUJ_06242	3-oxoacyl-[acyl-carrier protein] reductase	1.06			
XLOC_009556	FFC1_08759	FFUJ_09627	elongation factor 3	1.06			
XLOC_000740	FFC1_01339	FFUJ_01258	uncharacterized protein FPRN_00840	1.06			
XLOC_005599	FFC1_05267		Uncharacterized protein Y057_9255	1.06			
XLOC_007463	FFC1_07230	FFUJ_02823	6-phosphogluconolactonase	1.06			
XLOC_014731	FFC1_13993	FFUJ_09699	potassium/sodium efflux P-type ATPase, fungal-type	1.06			
XLOC_008203	FFC1_07263	FFUJ_02854	related to PET127	1.06			
XLOC_016740	FFC1_15820			1.06		1.34	
XLOC_010747	FFC1_10065	FFUJ_04574	Sterol regulatory element-binding protein ECM22	1.06			
XLOC_001053	FFC1_01895	FFUJ_01775	adenosine deaminase	1.06			
XLOC_013322	FFC1_12963	FFUJ_11214	related to ankyrin 3	1.05			
XLOC_015534	FFC1_14430	FFUJ_08113	related to non-ribosomal peptide synthetase	1.05			
XLOC_006913	FFC1_06172	FFUJ_13443	related to Rossmann fold nucleotide-binding protein	1.05		1.41	
XLOC_014566	FFC1_13716	FFUJ_09118	probable GAP1-General amino acid permease	1.05			
XLOC_011720	FFC1_10811	FFUJ_10554	prolyl oligopeptidase	1.05		2.34	2.03
XLOC_013050	FFC1_12471	FFUJ_11691	uncharacterized protein FFC1_12471	1.05			
XLOC_003069	FFC1_03541	FFUJ_07962	related to beta-carotene 15,15`-dioxygenase	1.05			
XLOC_006174	FFC1_06345	FFUJ_13277	uncharacterized protein FFUJ_13277	1.05			
XLOC_008265	FFC1_07383	FFUJ_02971	related to fatty acid elongation protein	1.05		1.58	
XLOC_010419	FFC1_09484	FFUJ_04009	probable protein disulfide isomerase-related protein A	1.04			
XLOC_002105	FFC1_01750	FFUJ_01640	glutamate synthase [NADPH]	1.04			
XLOC_014121	FFC1_13549	FFUJ_05197		1.04			
XLOC_011149	FFC1_10852	FFUJ_10514	uncharacterized protein FFUJ_10514	1.04			
XLOC_004988	FFC1_04102	FFUJ_05606	uncharacterized protein FFUJ_05606	1.04			
XLOC_002645	FFC1_02783	FFUJ_07236	NADH-ubiquinone oxidoreductase 19.3 kDa subunit, mitochondrial	1.04	1.53		
XLOC_010074	FFC1_09733	FFUJ_04250	uncharacterized protein FFUJ_04250	1.04			
XLOC_002882	FFC1_03207	FFUJ_07641	related to mitochondrial import protein MPI1 precursor	1.04			
XLOC_015403	FFC1_14630	FFUJ_08315	succinyl-CoA ligase [GDP-forming] subunit beta, mitochondrial	1.04			
XLOC_006527	FFC1_05429		related to NADPH oxidase homolog 1	1.04			
XLOC_016732	FFC1_15803			1.03			
XLOC_003649	FFC1_03092		Chaperone protein DnaJ 2	1.03			
XLOC_008817	FFC1_08420	FFUJ_09945	uncharacterized protein FFUJ_09945	1.03			
XLOC_001980	FFC1_01498	FFUJ_04517	carbamoyl-phosphate synthase arginine-specific large chain	1.03			
XLOC_010066	FFC1_09722	FFUJ_04240	related to C-term. of A.nidulans regulatory protein (qutR)	1.03			
XLOC_015584	FFC1_14518	FFUJ_08205		1.03			
XLOC_010504	FFC1_09643	FFUJ_04165	related to PRM10 Pheromone-regulated protein	1.03			

XLOC_003505	FFC1_02822	FFUJ_07273	multiprotein-bridging factor 1	1.03			
XLOC_016338	FFC1_15203	FFUJ_12599	uncharacterized protein FFUJ_12599	1.03		-1.76	-1.82
XLOC_015905	FFC1_15094	FFUJ_02369	related to BCS1 protein precursor	1.03			
XLOC_004637	FFC1_04909	FFUJ_06374	uncharacterized protein Y057_10057	1.03			
XLOC_003145	FFC1_03684	FFUJ_14350	Pectate lyase E	1.03			
XLOC_001522	FFC1_00641	FFUJ_00585	related to mitochondrial hypoxia responsive domain protein	1.02			
XLOC_004573	FFC1_04794	FFUJ_06265	uncharacterized protein FFUJ_06265	1.02			
XLOC_004413	FFC1_04485		uncharacterized protein FFE2_05159	1.02			
XLOC_001474	FFC1_00536	FFUJ_00490	NADPH2:quinone reductase	1.02			
XLOC_005939	FFC1_05902		uncharacterized protein FFUJ_13700	1.02			
XLOC_015031	FFC1_13890	FFUJ_08951	related to cytochrome b-large subunit	1.02			
XLOC_010304	FFC1_09276	FFUJ_03847	potassium/sodium efflux P-type ATPase, fungal-type	1.02			
XLOC_004425	FFC1_04505	FFUJ_05994	uncharacterized protein Y057_12980	1.02			
XLOC_006238	FFC1_06477	FFUJ_13151	related to DUF967 domain protein	1.02			
XLOC_005177	FFC1_04484	FFUJ_05975	palmitoyltransferase ERF2	1.02			
XLOC_012201	FFC1_11720	FFUJ_12293	chitin synthase	1.02			
XLOC_015959	FFC1_15187	FFUJ_04638	ribonucleotide reductase inhibitor	1.01			
XLOC_010409	FFC1_09467	FFUJ_03994	related to YPC1-Alkaline Ceramidase	1.01			
XLOC_001636	FFC1_00865	FFUJ_00800	undecaprenyl diphosphate synthase	1.01			
XLOC_002920	FFC1_03277	FFUJ_07707	related to WD repeat-containing protein 44	1.01			
XLOC_013183	FFC1_12717	FFUJ_11458	related to 7alpha-cephem-methoxylase P8 chain	1.01			
XLOC_001371	FFC1_00326	FFUJ_00283	Isoflavone reductase like protein	1.01			
XLOC_003033	FFC1_03478	FFUJ_07902	related to nucleolar protein NOP4 (NOP77)	1.01			
XLOC_002596	FFC1_02670	FFUJ_07129	probable protein involved in intramitochondrial protein sorting	1.01			
XLOC_015022	FFC1_13872	FFUJ_08966	Putative Rho-GTPase-activating protein 6	1.01			
XLOC_012247	FFC1_11811	FFUJ_12378	NADH-ubiquinone oxidoreductase 23 kDa subunit, mitochondrial	1.01			
XLOC_008879	FFC1_08544	FFUJ_09826	elongator complex protein 1	1.01			
XLOC_016135	FFC1_15176	FFUJ_04628		1.01	1.49		
XLOC_013844	FFC1_13033	FFUJ_04705	related to cell wall protein cwl1	1.01			
XLOC_000478	FFC1_00856	FFUJ_00792	probable methyltransferase	1.01			
XLOC_000321	FFC1_00595	FFUJ_00543	related to manganese resistance protein	1.00			
XLOC_011457	FFC1_10337	FFUJ_11012	related to PHO89-Na+/phosphate co-transporter	1.00		-1.63	-1.97
XLOC_010617	FFC1_09841	FFUJ_04357	related to SCP160 protein	1.00			
XLOC_001888	FFC1_01336	FFUJ_01255	related to cercosporin resistance protein	1.00			
XLOC_002624	FFC1_02734	FFUJ_07191	uncharacterized protein FFB14_02172	-1.00			
XLOC_005634	FFC1_05339		related to methyltransferase	-1.00			
XLOC_008514	FFC1_07810	FFUJ_03378	alcohol dehydrogenase (NADP+)	-1.01		1.60	
XLOC_000662	FFC1_01201	FFUJ_01123	uncharacterized protein FFUJ_01123	-1.01			
XLOC_010656	FFC1_09912	FFUJ_04426	uncharacterized protein FFNC_05186	-1.01			
XLOC_014818	FFC1_14152	FFUJ_08699	related to macrophage erythroblast attacher	-1.01			
XLOC_012131	FFC1_11594	FFUJ_12168	related to putative trehalase	-1.01			
XLOC_013293	FFC1_12910	FFUJ_11264	Putative ATPase YjoB	-1.01			
XLOC_000054	FFC1_00115	FFUJ_00082	uncharacterized protein FFC1_00115	-1.01			
XLOC_000412	FFC1_00738	FFUJ_00675	Protein PLANT CADMIUM RESISTANCE 3	-1.01			
XLOC_002353	FFC1_02206	FFUJ_02075	related to Virulence protein STM3117	-1.01			
XLOC_007121	FFC1_06548	FFUJ_13083	acid phosphatase	-1.01			
XLOC_000981	FFC1_01776	FFUJ_01665	uncharacterized protein FFUJ_01665	-1.01			
XLOC_006530	FFC1_05436		probable amino acid transporters	-1.02			
XLOC_011741	FFC1_10857	FFUJ_10509	uncharacterized protein Y057_6280	-1.02			
XLOC_014293	FFC1_13202	FFUJ_04867	NCS1 family nucleobase:cation symporter-1	-1.02			
XLOC_014050	FFC1_13421	FFUJ_05076	1-aminocyclopropane-1-carboxylate deaminase	-1.02	-2.03		
XLOC_014874	FFC1_14266	FFUJ_08591		-1.02			
XLOC_001715	FFC1_01004	FFUJ_00932	related to S.pombe beta-transducin	-1.02		-1.26	
XLOC_010953	FFC1_10486	FFUJ_10862	related to multidrug transporter	-1.02			
XLOC_008738	FFC1_08247	FFUJ_10116	uncharacterized protein FFUJ_10116	-1.02			
XLOC_011960	FFC1_11283	FFUJ_13978	DUF221 domain-containing protein	-1.02			
XLOC_015957	FFC1_15184	FFUJ_04635	Glucose-repressible alcohol dehydrogenase transcriptional effector	-1.02			
XLOC_011940	FFC1_11245	FFUJ_14013	Flocculation protein FLO9	-1.02			
XLOC_000661	FFC1_01200	FFUJ_01122	related to alpha-methylacyl-coa racemase	-1.03			
XLOC_003117	FFC1_03642	FFUJ_08057	uncharacterized protein Y057_11848	-1.03			
XLOC_010529	FFC1_09695	FFUJ_04215	related to NPL3-nucleolar protein	-1.03			
XLOC_015140	FFC1_14096	FFUJ_08750	adenosylhomocysteinase	-1.03			
XLOC_001212	FFC1_00006	FFUJ_00005	isoamyl alcohol oxidase	-1.03			
XLOC_004406	FFC1_04473	FFUJ_05963	uncharacterized protein Y057_13010	-1.03			
XLOC_011378	FFC1_10198	FFUJ_11108	uncharacterized protein FFC1_10198	-1.03			
XLOC_009311	FFC1_08346	FFUJ_10017	related to Carboxymuconolactone decarboxylase	-1.03			
XLOC_002160	FFC1_01864	FFUJ_01748	kinetochore protein SPC25	-1.03			
XLOC_003976	FFC1_03712	FFUJ_14322	bys1 protein	-1.03			1.57
XLOC_008095	FFC1_07077	FFUJ_02685	related to acid phosphatase	-1.03			
XLOC_000276	FFC1_00503	FFUJ_00461	membrane-associating domain-containing protein	-1.04			
XLOC_000955	FFC1_01725	FFUJ_01618	uncharacterized protein LW94_6306	-1.04			
XLOC_006752	-			-1.04			
XLOC_000300	FFC1_00561	FFUJ_00513	probable peroxisome assembly protein	-1.04			
XLOC_015352	FFC1_14524	FFUJ_08211	related to capsular associated protein (CAP10)	-1.04			

XLOC_006512	FFC1_05400		related to general amidase	-1.04			
XLOC_011829	FFC1_11046	FFUJ_10335	related to small s protein	-1.04			
XLOC_000048	FFC1_00100	FFUJ_00068	related to small s protein	-1.04			
XLOC_008134	FFC1_07148	FFUJ_02750	uncharacterized protein LW93_7447	-1.05			
XLOC_001344	FFC1_00282	FFUJ_00240	Trans-aconitate 2-methyltransferase	-1.05			
XLOC_006682	FFC1_05722	FFUJ_14647	uncharacterized protein FFUJ_14647	-1.05			
XLOC_005085	FFC1_04303	FFUJ_05797	related to trichodiene oxygenase cytochrome P450	-1.05			
XLOC_004330	FFC1_04349	FFUJ_05841	glycine cleavage system H protein	-1.05			
XLOC_003302	FFC1_02447	FFUJ_06921	CNT family concentrative nucleoside transporter	-1.05			
XLOC_009976	FFC1_09560	FFUJ_04085	hypothetical protein FPRO05_09861	-1.05			
XLOC_013061	FFC1_12491	FFUJ_11671	uncharacterized protein FFUJ_11671	-1.05			
XLOC_009106	FFC1_09001	FFUJ_09390	related to aldehyde reductase II	-1.05			
XLOC_001342	FFC1_00278	FFUJ_00236	2-methylcitrate synthase, mitochondrial	-1.05			
XLOC_015770	FFC1_14841	FFUJ_02116	probable L-lactate dehydrogenase (cytochrome)	-1.05			
XLOC_013417	FFC1_12225	FFUJ_11931	uncharacterized protein FFUJ_11931	-1.05			
XLOC_005107	FFC1_04347	FFUJ_05839	related to C6 transcription factor	-1.05			
XLOC_013017	FFC1_12409	FFUJ_11748	probable DFG5 protein	-1.05			
XLOC_013749	FFC1_12852	FFUJ_11324	aromatic-L-amino-acid decarboxylase	-1.06			
XLOC_008447	FFC1_07702	FFUJ_03276	spectrin beta chain	-1.06			
XLOC_012977	FFC1_12317		uncharacterized protein FFC1_12317	-1.06			
XLOC_005572	FFC1_05199	FFUJ_06649	related to 3-oxoacyl-[acyl-carrier-protein] reductase	-1.06			
XLOC_013667	FFC1_12694	FFUJ_11480	Mannose-specific lectin	-1.06			1.41
XLOC_001496	FFC1_00575	FFUJ_00526	related to STB5-SIN3 binding protein	-1.06			
XLOC_003678	FFC1_03139	FFUJ_07577	related to Zn(II)2Cys6 transcriptional activator	-1.06			
XLOC_005355	FFC1_04780	FFUJ_06259	related to sterigmatocystin 7-O-methyltransferase precursor	-1.06			
XLOC_007205	FFC1_06738		Uncharacterized protein Y057_2617	-1.06			
XLOC_008316	FFC1_07485	FFUJ_03063	uncharacterized protein FFUJ_03063	-1.06			
XLOC_014889	FFC1_14286	FFUJ_08571	uncharacterized protein FFUJ_08571	-1.07			
XLOC_014157	FFC1_13620	FFUJ_05269	related to monooxigenase	-1.07			
XLOC_011525	FFC1_10459	FFUJ_03676	beta-galactosidase	-1.07			
XLOC_003075	FFC1_03557	FFUJ_07977	related to micromolar calcium activated neutral protease 1 (capn1)	-1.07			
XLOC_007501	FFC1_07301	FFUJ_02889	related to F-box protein Fbl2	-1.07			
XLOC_013190	FFC1_12728	FFUJ_11447	related to carboxypeptidase	-1.07			
XLOC_012483	FFC1_11409	FFUJ_13852	uncharacterized protein Y057_12157	-1.07			
XLOC_004487	FFC1_04627	FFUJ_06113	related to integral membrane protein PTH11	-1.07			
XLOC_004140	FFC1_04031	FFUJ_05541	uncharacterized protein FFUJ_05541	-1.08			-1.64
XLOC_001922	FFC1_01396	FFUJ_01309	related to verprolin	-1.08			
XLOC_014717	FFC1_13970	FFUJ_08874		-1.08			
XLOC_004703	FFC1_05030	FFUJ_06495	high-affinity iron transporter	-1.08			
XLOC_005244	FFC1_04594	FFUJ_06079	related to Putative nicotinamide N-methyltransferase	-1.08			
XLOC_013581	FFC1_12530	FFUJ_11632	probable pectinesterase precursor	-1.08			
XLOC_015570	FFC1_14497	FFUJ_08181	related to TAM domain methyltransferase	-1.08			
XLOC_016099	FFC1_15103	FFUJ_02378	probable PRX1-mitochondrial isoform of thioredoxin peroxidase	-1.08			
XLOC_010095	FFC1_09769	FFUJ_04282	related to dihydrofolate reductase	-1.09			
XLOC_013607	FFC1_12574	FFUJ_11591	uncharacterized protein FFC1_12574	-1.09			
XLOC_010014	FFC1_09632	FFUJ_04154	mandelate racemase	-1.09			
XLOC_007955	FFC1_06826	FFUJ_02443	heterogeneous nuclear ribonucleoprotein g	-1.09			
XLOC_015857	FFC1_15008	FFUJ_02285	related to methyltransferase	-1.09			
XLOC_004585	FFC1_04815	FFUJ_06285	uncharacterized protein FFUJ_06285	-1.09			
XLOC_014248	FFC1_13129	FFUJ_13912	related to multidrug resistance-associated protein	-1.09			
XLOC_015705	FFC1_14722	FFUJ_08402	histone H1/5	-1.09			
XLOC_004457	FFC1_04558	FFUJ_06045	related to excitatory amino acid transporter	-1.09			
XLOC_000498	FFC1_00901	FFUJ_00833	acetyl-coenzyme A synthetase	-1.10			
XLOC_015910	FFC1_15104	FFUJ_02379	uncharacterized protein FFUJ_02379	-1.10			
XLOC_012045	FFC1_11445	FFUJ_13818	related to permease of the major facilitator superfamily	-1.10			
XLOC_014020	FFC1_13375	FFUJ_05034	acetyl-CoA C-acetyltransferase	-1.10			
XLOC_014973	FFC1_13768	FFUJ_09069	related to integral membrane protein	-1.10			
XLOC_008164	FFC1_07198	FFUJ_02793	related to a putative low-affinity copper transport protein	-1.10			
XLOC_001491	FFC1_00565	FFUJ_00517	uncharacterized protein LW93_2577	-1.10			1.94
XLOC_000619	FFC1_01115	FFUJ_01041	uncharacterized protein FFUJ_01041	-1.11			
XLOC_006381	FFC1_06739		Uncharacterized protein Y057_2618	-1.11			
XLOC_002082	FFC1_01711	FFUJ_01604	uncharacterized protein Y057_5944	-1.11			
XLOC_000051	FFC1_00106	FFUJ_00074	related to small s protein	-1.11			
XLOC_001560	FFC1_00716	FFUJ_00655	Putative J domain-containing protein C63.03	-1.11			
XLOC_015483	FFC1_14798	FFUJ_14915	uncharacterized protein FFUJ_14915	-1.11			
XLOC_013706	FFC1_12765	FFUJ_11410	gluconolactonase	-1.12			
XLOC_000172	FFC1_00331	FFUJ_00288	related to DAL5-Allantoate and ureidosuccinate permease	-1.12			
XLOC_008983	FFC1_08758	FFUJ_09628	probable carnitine transporter	-1.12			
XLOC_003713	FFC1_03212	FFUJ_07646	Autophagy-related protein 3	-1.12			
XLOC_013307	FFC1_12940	FFUJ_11237	related to aflatoxin efflux pump AFLT	-1.12			
XLOC_003442	FFC1_02718	FFUJ_07175	related to potassium channel beta subunit protein	-1.12			
XLOC_000305	FFC1_00570	FFUJ_00521	related to aldehyde dehydrogenase	-1.12			
XLOC_015699	FFC1_14716	FFUJ_08397	NADPH oxidase	-1.12			
XLOC_009639	FFC1_08898	FFUJ_09491	uncharacterized protein Y057_189	-1.13			
XLOC_016058	FFC1_15015	FFUJ_02291		-1.13	-2.79		

XLOC_015374	FFC1_14573	FFUJ_08262	related to methyltransferase	-1.13			
XLOC_011147	FFC1_10849	FFUJ_10517	probable galactose oxidase	-1.13			
XLOC_012457	FFC1_11358	FFUJ_13903	uncharacterized protein Y057_12207	-1.13			
XLOC_004231	FFC1_04194	FFUJ_05693	uncharacterized protein Y057_10822	-1.14			
XLOC_015944	FFC1_15159	FFUJ_02433	Salicylate hydroxylase	-1.14			
XLOC_005270	FFC1_04633	FFUJ_06119	alpha-D-xyloside xylohydrolase	-1.14			-1.29
XLOC_013679	FFC1_12709	FFUJ_11466	Putative oxidoreductase ordL	-1.14			
XLOC_011470	FFC1_10366	FFUJ_10981	uncharacterized protein Y057_14453	-1.14			
XLOC_001274	FFC1_00114	FFUJ_00081	related to tenascin X precursor	-1.14			
XLOC_014279	FFC1_13184	FFUJ_04850	related to tetracycline resistance proteins	-1.15			
XLOC_004114	FFC1_03988	FFUJ_05500	related to TAM domain methyltransferase	-1.15			
XLOC_001827	FFC1_01206	FFUJ_01128	uncharacterized protein FFUJ_01128	-1.15			
XLOC_013311	FFC1_12944	FFUJ_11233	related to 15-hydroxyprostaglandin dehydrogenase	-1.15			
XLOC_006390	FFC1_06750		Chymotrypsin-elastase inhibitor ixodidin	-1.15			
XLOC_005437	FFC1_04944		probable peroxin-1	-1.16			
XLOC_012730	FFC1_11853	FFUJ_12422	uncharacterized protein Y057_6722	-1.16			
XLOC_003782	FFC1_03337	FFUJ_07765	related to sporulation-specific protein Sps2p	-1.16			
XLOC_001531	FFC1_00661	FFUJ_00604	DASH complex subunit dad3	-1.16			
XLOC_015769	FFC1_14840	FFUJ_02115	related to nonribosomal peptide synthetase MxcG (component of the myxochelin iron transport regulon)	-1.16			
XLOC_003982	FFC1_03721	FFUJ_14313	probable c-14 sterol reductase ERG-3	-1.16			
XLOC_012513	FFC1_11464	FFUJ_13799	Transcriptional regulatory protein moc3	-1.16			
XLOC_012729	FFC1_11851	FFUJ_12420	related to Zn(II)2Cys6 transcriptional activator	-1.16			
XLOC_014402	FFC1_13399	FFUJ_05056	related to acetate regulatory DNA binding protein FacB	-1.17			
XLOC_009549	FFC1_08743	FFUJ_09641	uncharacterized protein LW93_13200	-1.17			
XLOC_002675	FFC1_02836	FFUJ_07287	related to DUF124 domain protein	-1.17			
XLOC_012230	FFC1_11772	FFUJ_12339	related to serine protease	-1.17			
XLOC_003594	FFC1_02981	FFUJ_07424	related to 3-oxoacyl-[acyl-carrier-protein] reductase	-1.17			
XLOC_007733	FFC1_07717	FFUJ_03290	1-phosphatidylinositol-4,5-bisphosphate phosphodiesterase 1	-1.17			
XLOC_003597	FFC1_02985	FFUJ_07428	related to phospholipid-translocating ATPase	-1.17			
XLOC_005080	FFC1_04296	FFUJ_05790	uncharacterized protein FFNC_04205	-1.17			
XLOC_009858	FFC1_09312	FFUJ_03882	Cysteine-rich transmembrane CYSTM domain	-1.17			
XLOC_005927	FFC1_05880	FFUJ_13722	probable DUF895 domain membrane protein	-1.17			
XLOC_010188	FFC1_09927	FFUJ_04441	methylenetetrahydrofolate reductase (NADPH)	-1.17			
XLOC_004148	-			-1.18			
XLOC_000577	FFC1_01034	FFUJ_00961	related to programmed cell death protein (calcium-binding protein)	-1.18			
XLOC_012967	FFC1_12295	FFUJ_11861	related to nitric-oxide synthase, salivary gland	-1.18			
XLOC_015387	FFC1_14602	FFUJ_08290	related to stomatin	-1.18			
XLOC_013617	FFC1_12595	FFUJ_11571	related to Cytochrome P450 3A5	-1.18			
XLOC_003027	FFC1_03468	FFUJ_07892	C-5 sterol desaturase	-1.18	-1.49		
XLOC_013115	FFC1_12598	FFUJ_11568	related to general amidase	-1.18			
XLOC_002012	FFC1_01575	FFUJ_01481	aromatic amino acid aminotransferase I	-1.18			
XLOC_002260	FFC1_02030	FFUJ_01903	uncharacterized protein Y057_14817	-1.19			
XLOC_000576	FFC1_01032	FFUJ_00959	related to glycine-rich RNA-binding protein	-1.19			
XLOC_004115	FFC1_03989	FFUJ_05501	related to cell wall glycosyl hydrolase YteR	-1.19			
XLOC_010619	FFC1_09844	FFUJ_04360	related to D-arabinitol 2-dehydrogenase	-1.19			
XLOC_016331	FFC1_15539	FFUJ_12932		-1.19			
XLOC_000133	FFC1_00255	FFUJ_00214	related to succinate-semialdehyde dehydrogenase	-1.19			
XLOC_008160	FFC1_07188	FFUJ_02784	Protein pob1	-1.19		-1.34	
XLOC_001584	FFC1_00764	FFUJ_00701	uncharacterized protein FFUJ_00701	-1.19			
XLOC_000189	FFC1_00366	FFUJ_00324	Uncharacterized protein LW93_4630	-1.19			
XLOC_001690	FFC1_00957	FFUJ_00888	Putative N-acetyltransferase p20	-1.19			
XLOC_016133	FFC1_15174	FFUJ_04626	related to CECR1 protein	-1.19			
XLOC_012869	FFC1_12119	FFUJ_12033	related to transcription activator protein acu-15	-1.20			
XLOC_016013	FFC1_14920	FFUJ_02200	uncharacterized protein Y057_4902	-1.20			
XLOC_011483	FFC1_10393	FFUJ_10955	related to tol protein	-1.20			
XLOC_010062	FFC1_09717	FFUJ_04235	related to O-methyltransferase	-1.20			
XLOC_007304	FFC1_06944	FFUJ_02557	related to GCP3 (gamma-tubulin complex)	-1.20			
XLOC_007251	FFC1_06842	FFUJ_02459	probable phospholipase	-1.20			
XLOC_003883	FFC1_03540	FFUJ_07961	Kinetochore protein fta4	-1.21			
XLOC_000682	FFC1_01234	FFUJ_01156	uncharacterized protein FFUJ_01156	-1.21			
XLOC_012890	FFC1_12158	FFUJ_11996	ribonucleoside-triphosphate reductase	-1.21			
XLOC_013768	FFC1_12887	FFUJ_11287	SKY1-Protein serine kinase	-1.21			
XLOC_007933	FFC1_08103	FFUJ_14419	related to beta-mannosidase	-1.22			
XLOC_003282	FFC1_02409	FFUJ_06884	probable alpha-glucosidase (MalT)	-1.22			
XLOC_002295	FFC1_02098	FFUJ_01970	related to transcription factor, SIN3 binding	-1.22			
XLOC_013124	FFC1_12624	FFUJ_11543	related to Staphylococcus multidrug resistance protein	-1.22			
XLOC_000221	FFC1_00412	FFUJ_00368	related to protein BTN1	-1.22			1.39
XLOC_006415	FFC1_06797		Uncharacterized protein Y057_7465	-1.23			
XLOC_016019	FFC1_14933	FFUJ_02213	related to sugar transport protein STL1	-1.23			
XLOC_012147	FFC1_11636	FFUJ_12208	mannosyl-oligosaccharide alpha-1,2-mannosidase	-1.23			
XLOC_016868	FFC1_15905			-1.23			
XLOC_000308	FFC1_00576	FFUJ_00527	related to flavin-containing monooxygenase	-1.23			
XLOC_015915	FFC1_15112	FFUJ_02387	uncharacterized protein Y057_13678	-1.23			
XLOC_011068	FFC1_10727	FFUJ_10636	uncharacterized protein FFUJ_10636	-1.23			

XLOC_004329	FFC1_04348	FFUJ_05840	serine hydroxymethyltransferase, mitochondrial	-1.23			
XLOC_010942	FFC1_10460	FFUJ_10886	uncharacterized protein Y057_4663	-1.23			
XLOC_004881	FFC1_03890	FFUJ_05411	related to methyltransferase	-1.24			
XLOC_007553	FFC1_07394	FFUJ_02982	uncharacterized protein FFUJ_02982	-1.24			
XLOC_016571	FFC1_15646	FFUJ_14223	predicted protein	-1.24			
XLOC_013701	FFC1_12758		related to multidrug resistant protein	-1.24			
XLOC_013867	FFC1_13074	FFUJ_04746	uncharacterized protein FFUJ_04746	-1.24			
XLOC_001152	FFC1_02099	FFUJ_01971	related to 3-oxoadipate enol-lactonase II	-1.24			
XLOC_013179	FFC1_12707	FFUJ_11468	related to neutral amino acid permease	-1.24			
XLOC_016035	FFC1_14968	FFUJ_02250	related to phthalate 4,5-dioxygenase oxygenase reductase subunit	-1.24			
XLOC_004748	FFC1_05124	FFUJ_06580	probable argonaute like post-transcriptional gene silencing protein QDE-2	-1.25			
XLOC_002455	FFC1_02410	FFUJ_06885	probable maltose permease (MalP)	-1.25			
XLOC_009320	FFC1_08357	FFUJ_10006	uncharacterized protein Y057_6017	-1.26			
XLOC_001505	FFC1_00599	FFUJ_00547	uncharacterized protein FFUJ_00547	-1.26			
XLOC_012063	FFC1_11477	FFUJ_13786	uncharacterized protein LW93_5783	-1.26			
XLOC_008550	FFC1_07884	FFUJ_03448	related to BENZOYLFORMATE DECARBOXYLASE	-1.26		-2.20	
XLOC_012567	FFC1_11560	FFUJ_12137	uncharacterized protein Y057_9311	-1.26			
XLOC_005402	FFC1_04873	FFUJ_06339	related to conserved oligomeric golgi complex component 4	-1.26			
XLOC_004607	FFC1_04851	FFUJ_06319	related to transcription factor ZMS1	-1.27			
XLOC_005675	FFC1_05413		related to cytosine deaminase and related metal-dependent hydrolases	-1.27			
XLOC_005247	FFC1_04597	FFUJ_06082	related to putative copper-activated transcription factor	-1.27			
XLOC_004072	FFC1_03905		related to subtilisin DY	-1.27			
XLOC_001554	FFC1_00704	FFUJ_00644	related to amidase (acetamidase)	-1.27			
XLOC_012293	FFC1_11902	FFUJ_12469	related to lysophospholipase	-1.27			
XLOC_012799	FFC1_11985	FFUJ_12548	related to quinate transport protein	-1.27		-1.89	
XLOC_000965	FFC1_01742	FFUJ_01632	related to myocyte-specific enhancer factor 2d	-1.27			
XLOC_011608	FFC1_10593	FFUJ_10761	related to TOB3 (member of AAA-ATPase family)	-1.27			
XLOC_007356	FFC1_07033	FFUJ_02644	uncharacterized protein FFUJ_02644	-1.27			
XLOC_005121	FFC1_04372, FFC1_04373			-1.27			
XLOC_008107	FFC1_07102	FFUJ_02707	related to integral membrane protein pth11	-1.28			
XLOC_014585	FFC1_13740	FFUJ_09094	probable formamidase	-1.28			
XLOC_004665	FFC1_04956	FFUJ_06422	related to cocaine esterase	-1.28			
XLOC_000563	FFC1_01014	FFUJ_00941	1-phosphatidylinositol phosphodiesterase	-1.28			
XLOC_015128	FFC1_14073	FFUJ_08773		-1.28	-1.60		
XLOC_011022	FFC1_10636	FFUJ_10720	related to major facilitator MirA	-1.29			
XLOC_016334	FFC1_15546	FFUJ_12939	DAL1-Allantoinase	-1.29			
XLOC_000301	FFC1_00562	FFUJ_00514	uncharacterized protein Y057_11331	-1.29			
XLOC_001680	FFC1_00940	FFUJ_00871	uncharacterized protein Y057_12574	-1.29			
XLOC_012119	FFC1_11574	FFUJ_12151	uncharacterized protein Y057_354	-1.29			
XLOC_013299	FFC1_12925	FFUJ_11251	uncharacterized protein FFUJ_11251	-1.29			
XLOC_011952	FFC1_11273	FFUJ_13988	uncharacterized protein Y057_7337	-1.30			
XLOC_010298	FFC1_09268	FFUJ_03839	uncharacterized protein FFUJ_03839	-1.30			
XLOC_005444	FFC1_04959	FFUJ_06425	uncharacterized protein Y057_10008	-1.30			
XLOC_009090	FFC1_08966	FFUJ_09425	related to tol protein	-1.31			
XLOC_015302	FFC1_14410	FFUJ_08095	related to methyltransferase	-1.31			
XLOC_012677	FFC1_11767	FFUJ_12334	uncharacterized protein Y057_10895	-1.31			
XLOC_010802	FFC1_10170	FFUJ_11137	uncharacterized protein FFUJ_11137	-1.31			
XLOC_005066	FFC1_04268	FFUJ_05763	uncharacterized protein LW94_1074	-1.31			
XLOC_014416	FFC1_13424	FFUJ_05079	pyridoxine biosynthesis protein PDX1	-1.31			
XLOC_001024	FFC1_01848	FFUJ_01733	uncharacterized protein FFNC_11812	-1.31			
XLOC_013577	FFC1_12524	FFUJ_11638	uncharacterized protein Y057_9905	-1.31			
XLOC_010760	FFC1_10085	FFUJ_04594	related to positive activator of transcription	-1.32			
XLOC_014404	FFC1_13401	FFUJ_05057	uncharacterized protein Y057_2731	-1.32			
XLOC_003935	FFC1_03633	FFUJ_08048	related to zinc finger protein	-1.32			
XLOC_006284	FFC1_06569	FFUJ_13063	related to nitrate assimilation regulatory protein nirA	-1.33			
XLOC_012989	FFC1_12351	FFUJ_11805	probable ammonium permease MEPA	-1.33	4.24	-2.92	2.65
XLOC_006470	FFC1_05324		uncharacterized protein FFB20_07930	-1.33			
XLOC_004659	FFC1_04947	FFUJ_06414	uncharacterized protein Y057_10021	-1.33			
XLOC_015300	FFC1_14408			-1.34		-1.43	
XLOC_011100	FFC1_10774	FFUJ_10591	related to integral membrane protein	-1.34			
XLOC_003991	FFC1_03739	FFUJ_14297	uncharacterized protein FFUJ_14297	-1.34			
XLOC_014548	FFC1_13677	FFUJ_09156	probable Modin	-1.34			
XLOC_011425	FFC1_10282		Uncharacterized protein Y057_14521	-1.34			
XLOC_015067	FFC1_13963	FFUJ_08881		-1.34	-2.54	1.87	
XLOC_006139	FFC1_06270	FFUJ_13348	related to acriflavine sensitivity control protein ACR-2	-1.34			
XLOC_015875	FFC1_15037	FFUJ_02313	related to ankyrin	-1.34			
XLOC_009252	FFC1_08229	FFUJ_10131	related to low-affinity hexose transporter HXT3	-1.34			
XLOC_005480	FFC1_05026	FFUJ_06490	related to 2`-hydroxyisoflavone reductase	-1.34			
XLOC_002354	FFC1_02207	FFUJ_02076	related to MFS transporter	-1.34			
XLOC_008812	FFC1_08411	FFUJ_09954	arylsulfatase	-1.35			-1.37
XLOC_004326	FFC1_04343	FFUJ_05835	choline permease	-1.36			
XLOC_001307	FFC1_00188	FFUJ_00153	related to small s protein	-1.36			
XLOC_013300	FFC1_12926	FFUJ_11250	uncharacterized protein LW94_2578	-1.36			

XLOC_003060	FFC1_03523	FFUJ_07946	probable alpha/beta fold family hydrolase	-1.36			
XLOC_012420	FFC1_11280	FFUJ_13981	uncharacterized protein FFUJ_13981	-1.36			
XLOC_013258	FFC1_12841	FFUJ_11334	Transcriptional regulatory protein moc3	-1.36			
XLOC_013553	FFC1_12479	FFUJ_11683	uracil phosphoribosyltransferase	-1.36			
XLOC_012909	FFC1_12191	FFUJ_11964	uncharacterized protein Y057_2142	-1.36			
XLOC_013493	FFC1_12357	FFUJ_11799	related to dihydrodipicolinate synthase	-1.37			
XLOC_012380	FFC1_11188	FFUJ_14068	uncharacterized protein FFUJ_14068	-1.37			
XLOC_012409	FFC1_11261	FFUJ_13998	related to amidohydrolase family protein	-1.37			
XLOC_006650	FFC1_05659	FFUJ_14708	Isoflavone reductase like protein P3	-1.37			
XLOC_007555	FFC1_07398	FFUJ_02986	p-loop containing nucleoside triphosphate hydrolase	-1.37			
XLOC_002329	FFC1_02161	FFUJ_02030	uncharacterized protein Y057_12858	-1.37	-3.01		
XLOC_013583	FFC1_12532	FFUJ_11630	Uncharacterized protein Y057_9897	-1.38			
XLOC_016132	FFC1_15173	FFUJ_04625	uncharacterized protein LW93_10496	-1.38			
XLOC_005246	FFC1_04596	FFUJ_06081	related to RNA helicase HEL117	-1.38			
XLOC_011484	FFC1_10394	FFUJ_10954	uncharacterized protein Y057_4598	-1.38			
XLOC_005410	FFC1_04886	FFUJ_06351	related to esterase	-1.38			
XLOC_010888	FFC1_10347	FFUJ_11002	related to carboxylesterase	-1.38			
XLOC_010923	FFC1_10412	FFUJ_10936	glycerol kinase	-1.39			
XLOC_007103	FFC1_06517	FFUJ_13110	uncharacterized protein FFUJ_13110	-1.39			
XLOC_012149	FFC1_11638	FFUJ_12210	Oxidoreductase NAD-binding domain-containing protein 1	-1.39			
XLOC_004568	FFC1_04783	FFUJ_06256	related to annexin XIV	-1.39			
XLOC_015741	FFC1_14780	FFUJ_08455	related to mitochondrial ribosomal protein	-1.39			
XLOC_012968	FFC1_12296	FFUJ_11859	related to methyltransferase	-1.39			
XLOC_001188	FFC1_02169	FFUJ_02038	related to tol protein	-1.39			
XLOC_015687	FFC1_14695	FFUJ_08378	5-methyltetrahydropteroyltriglutamate-homocysteine methyltransferase	-1.40			
XLOC_002805	FFC1_03073	FFUJ_07513	f-box protein	-1.40			
XLOC_013263	FFC1_12851	FFUJ_11325	related to SUR1-required for mannosylation of sphingolipids	-1.40			
XLOC_002561	FFC1_02611	FFUJ_07074	sphingolipid delta-4 desaturase	-1.40			
XLOC_005265	FFC1_04622	FFUJ_06108	rna polymerase ii transcription initiation nucleotide excision repair factor tfiih	-1.41			
XLOC_016268	FFC1_15409	FFUJ_12798		-1.41			
XLOC_002150	FFC1_01847	FFUJ_01732	NAD(P)H-dependent D-xylose reductase xyl1	-1.41	-1.45		
XLOC_006931	FFC1_06203	FFUJ_13414	uncharacterized protein Y057_826	-1.41			
XLOC_010360	FFC1_09383	FFUJ_03912	uncharacterized protein Y057_5048	-1.42			
XLOC_014144	FFC1_13590	FFUJ_05238		-1.42			
XLOC_002332	FFC1_02171	FFUJ_02040	Heterokaryon incompatibility	-1.43			
XLOC_016700	FFC1_15733	FFUJ_14142		-1.44			
XLOC_011772	FFC1_10918	FFUJ_10451	related to TPN1 Pyridoxine transporter	-1.44			
XLOC_013275	FFC1_12879	FFUJ_11294	related to O-methyltransferase B	-1.44	-1.62	1.43	
XLOC_014745	FFC1_14017	FFUJ_08827	uncharacterized protein FFUJ_08827	-1.44			
XLOC_013618	FFC1_12596	FFUJ_11570	AMP-dependent synthetase/ligase	-1.44		-1.89	
XLOC_001548	FFC1_00692	FFUJ_00634	aldehyde dehydrogenase	-1.44			
XLOC_010978	FFC1_10542	FFUJ_10807	Clavaminate synthase-like protein	-1.44			
XLOC_006633	FFC1_05629	FFUJ_14737	uncharacterized protein LW94_12438	-1.44			
XLOC_014862	FFC1_14243	FFUJ_08611	Branched-chain-amino-acid aminotransferase-like protein 2	-1.44			
XLOC_014034	FFC1_13396	FFUJ_05054	related to multidrug resistance protein	-1.44			
XLOC_014725	FFC1_13983	FFUJ_08861	alcohol dehydrogenase	-1.45			
XLOC_009323	FFC1_08360	FFUJ_10003	related to TRI7-trichothecene biosynthesis gene cluster	-1.45			
XLOC_015369	FFC1_14563	FFUJ_08252	related to GNT1 alphaN-acetylglucosamine transferase K. lactis	-1.45			
XLOC_000272	FFC1_00495	FFUJ_00453	related to acetylxylan esterase precursor	-1.45			
XLOC_016402	FFC1_15343	FFUJ_12730	GTP-binding protein YchF	-1.45			
XLOC_015365	FFC1_14552	FFUJ_08241	mesaconyl-C4 CoA hydratase	-1.45			
XLOC_001392	FFC1_00365	FFUJ_00323	Uncharacterized protein Y057_324	-1.46			
XLOC_006444	FFC1_05278		WW domain-containing oxidoreductase	-1.46			
XLOC_014086	FFC1_13493	FFUJ_05144		-1.46			
XLOC_016057	FFC1_15013	FFUJ_02289	related to Dextranase	-1.46			
XLOC_012559	FFC1_11547	FFUJ_12124	related to HNM1-Choline permease	-1.47			
XLOC_010030	FFC1_09663	FFUJ_04183	related to glucosidase II, alpha subunit	-1.47			
XLOC_007663	FFC1_07587	FFUJ_03163	uncharacterized protein FFUJ_03163	-1.48			
XLOC_002111	FFC1_01762	FFUJ_01652	related to serine protease	-1.48	-1.42		
XLOC_004947	FFC1_04029	FFUJ_05539	related to peptide transport protein	-1.48			
XLOC_016163	FFC1_15225	FFUJ_12616	related to triacylglycerol lipase II precursor	-1.49			
XLOC_007449	FFC1_07207	FFUJ_02801	related to krueppel protein	-1.49			
XLOC_010468	FFC1_09572	FFUJ_04097	3-methyl-2-oxobutanoate hydroxymethyltransferase	-1.49			
XLOC_009839	FFC1_09270	FFUJ_03841	uncharacterized protein Y057_5617	-1.49			
XLOC_006585	FFC1_05535	FFUJ_14818	related to ARG81-transcription factor involved in arginine metabolism	-1.49			
XLOC_009785	FFC1_09166	FFUJ_09219	uncharacterized protein FFUJ_09219	-1.49			
XLOC_012303	FFC1_11918	FFUJ_12485	related to methyltransferase	-1.49			
XLOC_006347	FFC1_06673	FFUJ_12968	uncharacterized protein FFC1_06673	-1.49			
XLOC_015240	FFC1_14279	FFUJ_08578	related to vesicular amine transporter	-1.49			
XLOC_005791	FFC1_05635	FFUJ_14731	uncharacterized protein FFUJ_14731	-1.49			
XLOC_004491	FFC1_04634	FFUJ_06120	related to beta-glucosidase	-1.50		-1.90	
XLOC_004723	FFC1_05073	FFUJ_06535	Transcriptional regulatory protein moc3	-1.50			
XLOC_006718	FFC1_05793	FFUJ_14580	Lysine biosynthesis regulatory protein LYS14	-1.50			

XLOC_009053	FFC1_08893	FFUJ_09496	related to extracellular cellulase CelA/allergen Asp F7-like, putative	-1.51			
XLOC_006698	FFC1_05750	FFUJ_14618	uncharacterized protein FFUJ_14618	-1.52			
XLOC_009667	FFC1_08950	FFUJ_09441	Hydroxycinnamoyl-Coenzyme A shikimate/quinate hydroxycinnamoyltransferase	-1.52			
XLOC_005481	FFC1_05027	FFUJ_06491	uncharacterized protein FFE2_04564	-1.52			
XLOC_012104	FFC1_11541	FFUJ_12118	probable cysteine synthase B	-1.53			
XLOC_001559	FFC1_00714	FFUJ_00653	uncharacterized protein FFUJ_00653	-1.53			
XLOC_010264	FFC1_10081	FFUJ_04590	uncharacterized protein FFUJ_04590	-1.54			
XLOC_016773	FFC1_15780			-1.54			
XLOC_006720	FFC1_05801	FFUJ_14573	related to monocarboxylate transporter	-1.54			1.52
XLOC_009319	FFC1_08356	FFUJ_10007	related to serine-type carboxypeptidase f precursor	-1.55		-1.69	
XLOC_012570	FFC1_11565	FFUJ_12142	related to DUF1338 domain protein	-1.55			
XLOC_004306	FFC1_04315	FFUJ_14922	hypothetical protein FGSG_13392	-1.56			
XLOC_015536	FFC1_14435	FFUJ_08118	Mg2+ transporter zinc transport protein	-1.56			
XLOC_003130	FFC1_03661	FFUJ_14372	related to tetracycline resistance proteins	-1.56			
XLOC_008641	FFC1_08061	FFUJ_03620	uncharacterized protein FFC1_08061	-1.56	-2.48		
XLOC_011504	FFC1_10429	FFUJ_10918	uncharacterized protein Y057_4631	-1.56			
XLOC_009950	FFC1_09499	FFUJ_04023	probable neutral amino acid permease	-1.56			
XLOC_006086	FFC1_06178	FFUJ_13437	uncharacterized protein LW93_8593	-1.57			
XLOC_004779	FFC1_05185	FFUJ_06635	uncharacterized protein Y057_10650	-1.57			
XLOC_016460	FFC1_15455	FFUJ_12838	uncharacterized protein FFUJ_12838	-1.58			
XLOC_013900	FFC1_13130	FFUJ_04797	related to positive effector protein GCN20	-1.58			
XLOC_002083	FFC1_01712	FFUJ_01605	F-box domain, Skp2-like protein	-1.58			
XLOC_016482	FFC1_15495	FFUJ_12891		-1.58	-2.07		
XLOC_007826	FFC1_07896	FFUJ_03460	uncharacterized protein FFB20_07315	-1.58			
XLOC_016063	FFC1_15031	FFUJ_02307	probable GTP-binding protein Drab11	-1.58			
XLOC_011672	FFC1_10703	FFUJ_10658	related to microcin C7 self-immunity protein mccF	-1.58			
XLOC_005276	FFC1_04646	FFUJ_06132	Williams-Beuren syndrome chromosomal region 27 protein	-1.58			
XLOC_010740	FFC1_10057	FFUJ_04566	related to transcription activator	-1.58			
XLOC_012294	FFC1_11903	FFUJ_12470	uncharacterized protein FFUJ_12470	-1.58		1.86	1.76
XLOC_002341	FFC1_02186	FFUJ_02054	related to methyltransferase	-1.58			
XLOC_001187	FFC1_02168	FFUJ_02037	n- gnat protein	-1.58			
XLOC_002504	FFC1_02505	FFUJ_06973	Uncharacterized protein Y057_8806	-1.59			
XLOC_004066	FFC1_03895			-1.59			
XLOC_005064	FFC1_04260	FFUJ_05755	probable C6 transcription factor	-1.60			
XLOC_008174	FFC1_07215	FFUJ_02808	uncharacterized protein FFUJ_02808	-1.60			
XLOC_009334	FFC1_08382	FFUJ_09981	uncharacterized protein Y057_10438	-1.61			
XLOC_004993	-			-1.61			
XLOC_001940	FFC1_01426	FFUJ_01339	related to aminomethyltransferase precursor (glycine cleavage system protein T)	-1.61			
XLOC_004686	FFC1_04999	FFUJ_06464	putative bifunctional phosphoglucose phosphomannose isomerase protein	-1.62			
XLOC_004826	FFC1_03797		Uncharacterized protein Y057_10531	-1.63	-1.67		
XLOC_004069	FFC1_03898	FFUJ_05419	Uncharacterized protein Y057_13927	-1.64			
XLOC_016308	FFC1_15496	FFUJ_12892	related to chitinase	-1.65	-2.28		
XLOC_003765	FFC1_03305	FFUJ_07731	related to allantoate transport protein	-1.66			
XLOC_013462	FFC1_12314	FFUJ_11841	related to ethionine resistance protein	-1.66	-2.14		
XLOC_009057	FFC1_08899	FFUJ_09490	related to TOB3 (member of AAA-ATPase family)	-1.67			
XLOC_009196	FFC1_09179		uncharacterized protein FFNC_10916	-1.67			
XLOC_002183	FFC1_01916	FFUJ_01794	related to putative multidrug transporter Mfs1.1 (major facilitator family protein)	-1.67			
XLOC_011020	FFC1_10633	FFUJ_10723	related to lipase/esterase	-1.67			
XLOC_011530	FFC1_10468	FFUJ_10878	related to peroxisomal amine oxidase (copper-containing)	-1.67		-1.96	
XLOC_010046	FFC1_09689	FFUJ_04209	probable benzoate 4-monooxygenase cytochrome P450	-1.67			
XLOC_003166	FFC1_03735	FFUJ_14300	MARVEL domain containing protein	-1.68			
XLOC_006269	FFC1_06547	FFUJ_13084	related to RBTMx2 protein	-1.68			
XLOC_010524	FFC1_09683	FFUJ_04203	related to Putative sterigmatocystin biosynthesis lipase/esterase STCI	-1.69			
XLOC_007438	FFC1_07190	FFUJ_02785	transcriptional regulatory protein Pro-1	-1.69		-1.40	
XLOC_011700	FFC1_10768	FFUJ_10597	uncharacterized protein FFUJ_10597	-1.69			
XLOC_011154	FFC1_10859	FFUJ_10507	uncharacterized protein Y057_6283	-1.69			
XLOC_003548	FFC1_02896	FFUJ_07343	thiol methyltransferase	-1.69			
XLOC_004062	FFC1_03888	FFUJ_05409	Uncharacterized protein Y057_13940	-1.69			
XLOC_012072	FFC1_11492	FFUJ_13771	related to protein TOL	-1.70			
XLOC_006335	FFC1_06650	FFUJ_12991	probable sugar transport protein STL1	-1.71			
XLOC_016093	FFC1_15091	FFUJ_02366	uncharacterized protein LW94_12588	-1.71			
XLOC_009532	FFC1_08717	FFUJ_09666	related to monocarboxylate transporter 2	-1.72	-2.58	3.06	
XLOC_001369	FFC1_00321	FFUJ_00278	lipase class 3	-1.72			
XLOC_013504	FFC1_12371	FFUJ_11786	related to methyltransferase	-1.72			
XLOC_006732	FFC1_05831	FFUJ_14548	related to Carboxypeptidase 2	-1.72			
XLOC_005676	FFC1_05415		related to general amidase	-1.72			
XLOC_011630	FFC1_10632	FFUJ_10724	uncharacterized protein Y057_2070	-1.72			
XLOC_015337	FFC1_14483	FFUJ_08167	related to TAM domain methyltransferase	-1.74			
XLOC_016811	FFC1_15850			-1.74			
XLOC_008652	FFC1_08084	FFUJ_03644	peptidase a1 protein	-1.74			
XLOC_015739	FFC1_14777	FFUJ_08452		-1.75			

XLOC_011037	FFC1_10659	FFUJ_10700	uncharacterized protein FFUJ_10700	-1.75			
XLOC_012557	FFC1_11544	FFUJ_12121	amidohydrolase ytcJ-like	-1.75			
XLOC_001368	FFC1_00319	FFUJ_00277	uncharacterized protein FFUJ_00277	-1.75		-3.31	
XLOC_015599	FFC1_14546	FFUJ_08234	related to GNT1 alphaN-acetylglucosamine transferase K. lactis	-1.76			
XLOC_006053	FFC1_06120	FFUJ_13494	related to ThiJ/PfpI family protein	-1.76			
XLOC_012417	FFC1_11274	FFUJ_13987	methylmalonate-semialdehyde dehydrogenase (acylating)	-1.76			
XLOC_002802	FFC1_03068	FFUJ_07508	cfem domain-containing protein	-1.76	-1.81		
XLOC_005604	FFC1_05279		G-protein coupled receptor 1	-1.76			
XLOC_001262	FFC1_00090	FFUJ_00057	related to lipase 2	-1.77			
XLOC_012554	FFC1_11540	FFUJ_12117	related to tetracycline efflux protein (otrb)	-1.77			
XLOC_003646	FFC1_03083	FFUJ_07522	Paxillin-like protein 1	-1.78			
XLOC_000043	FFC1_00092	FFUJ_00059	probable amino acid aldolase or racemase	-1.78			
XLOC_012300	FFC1_11914	FFUJ_12481	Putative oxidoreductase ordL	-1.79			
XLOC_002299	FFC1_02106	FFUJ_01978	related to TOB3 (member of AAA-ATPase family)	-1.79			
XLOC_012379	FFC1_11184	FFUJ_14072	glycosyltransferase family 31 protein	-1.81	-2.91		
XLOC_008839	FFC1_08459	FFUJ_09907	related to Dal5p	-1.81			
XLOC_014715	FFC1_13967	FFUJ_08877	related to methyltransferase	-1.81			
XLOC_009337	FFC1_08387	FFUJ_09977	uncharacterized protein Y057_10442	-1.82	-2.18	-3.05	-3.39
XLOC_012571	FFC1_11566	FFUJ_12143	aldehyde dehydrogenase (NAD+)	-1.82			
XLOC_000104	FFC1_00206	FFUJ_00170	Ankyrin repeat-containing domain protein	-1.82			
XLOC_011117	FFC1_10802	FFUJ_10563	related to interferon-regulated resistance GTP-binding protein	-1.82			
XLOC_014515	FFC1_13621	FFUJ_05270	related to lipase/esterase	-1.82			
XLOC_007787	FFC1_07833	FFUJ_03400	uncharacterized protein FFUJ_03400	-1.82			
XLOC_008958	FFC1_08698	FFUJ_09685	UDPglucose 6-dehydrogenase	-1.83	-1.90		
XLOC_000249	FFC1_00456	FFUJ_00414	related to TIM barrel metal-dependent hydrolase	-1.83	-2.53		
XLOC_003931	FFC1_03625	FFUJ_08040	uncharacterized protein FFNC_03082	-1.84			
XLOC_011256	FFC1_11028	FFUJ_10353	Aristolochene synthase	-1.84	-2.66	1.91	
XLOC_006885	FFC1_06108	FFUJ_13504	uncharacterized protein FFUJ_13504	-1.84			
XLOC_016180	FFC1_15255	FFUJ_12646	related to transcriptional activator Mut3p	-1.84			
XLOC_004324	FFC1_04341	FFUJ_05833	probable potassium channel beta subunit protein	-1.84	-2.35		
XLOC_012810	FFC1_12005	FFUJ_12564	related to transmembrane transporter Liz1p	-1.85			
XLOC_002911	FFC1_03258	FFUJ_07688	uncharacterized protein FFUJ_07688	-1.85			
XLOC_008954	FFC1_08689	FFUJ_09694	related to sodium-and chloride-dependent GABA transporter 1	-1.85			
XLOC_007430	FFC1_07174	FFUJ_02768	uncharacterized protein FFUJ_02768	-1.85			
XLOC_008678	FFC1_08137	FFUJ_03693	related to aldehyde dehydrogenase	-1.86			
XLOC_000041	FFC1_00089		uncharacterized protein FFE2_00092	-1.86			
XLOC_003131	FFC1_03662	FFUJ_14371	related to D-mandelate dehydrogenase	-1.87			
XLOC_009666	FFC1_08949	FFUJ_09442	uncharacterized protein FFUJ_09442	-1.87			
XLOC_013733	FFC1_12823	FFUJ_11352	related to methyltransferase	-1.89			
XLOC_016833	FFC1_15873			-1.90			
XLOC_003237	FFC1_02311	FFUJ_06789	uncharacterized protein Y057_10581	-1.90			
XLOC_008604	FFC1_07984	FFUJ_03545	related to xylosidase/arabinosidase	-1.90			
XLOC_011961	FFC1_11286	FFUJ_13975	uncharacterized protein FFNC_07792	-1.90			
XLOC_007929	FFC1_08096	FFUJ_03656	related to aspartic-type signal peptidase	-1.90			
XLOC_009957	FFC1_09520	FFUJ_04044	related to transcription activator protein acu-15	-1.91			
XLOC_001417	FFC1_00435	FFUJ_00390	uncharacterized protein Y057_1469	-1.92			
XLOC_004057	FFC1_03879	FFUJ_05398	related to monomeric sarcosine oxidase	-1.92			
XLOC_016037	FFC1_14973	FFUJ_02256	related to methyltransferase	-1.92	-2.14		
XLOC_004281	FFC1_04275	FFUJ_05770	uncharacterized protein Y057_3407	-1.93			
XLOC_009949	FFC1_09497	FFUJ_04021	probable SIT1-Transporter of the bacterial siderophore ferrioxamine B	-1.93	-2.19		
XLOC_004857	FFC1_03846	FFUJ_05366	related to beta-glucosidase	-1.93			
XLOC_000141	FFC1_00267	FFUJ_00225	probable unsaturated glucuronyl hydrolase involved in regulation of bacterial surface properties, and related proteins	-1.93			
XLOC_011098	FFC1_10772	FFUJ_10593	uncharacterized protein Y057_6191	-1.93			
XLOC_001363	FFC1_00310	FFUJ_00268	uncharacterized protein FFUJ_00268	-1.94			
XLOC_009261	FFC1_08248	FFUJ_10115	uncharacterized protein Y057_8171	-1.94			
XLOC_004095	FFC1_03946	FFUJ_05461	related to tol protein	-1.95			
XLOC_016724	FFC1_15790			-1.96			
XLOC_013203	FFC1_12748	FFUJ_11427	GATA zinc finger domain-containing protein 7	-1.96			
XLOC_012133	FFC1_11600	FFUJ_12174	related to G protein coupled receptor like protein	-1.96			
XLOC_008006	FFC1_06912	FFUJ_02526	LysM domain-containing protein	-1.97			
XLOC_009186	FFC1_09164	FFUJ_09221	related to ferric reductase Fre2p	-1.97			
XLOC_010901	FFC1_10371	FFUJ_10976	related to ARG81-transcription factor involved in arginine metabolism	-1.98			
XLOC_011726	FFC1_10824	FFUJ_10541	uncharacterized protein Y057_6245	-1.98			
XLOC_011856	FFC1_11101	FFUJ_10282	uncharacterized protein Y057_1061	-1.99			
XLOC_007429	FFC1_07172	FFUJ_02770	related to triacylglycerol lipase II precursor	-1.99			
XLOC_008968	FFC1_08726	FFUJ_09657		-1.99			
XLOC_001213	FFC1_00007	FFUJ_00006	related to cytochrom P450	-1.99			
XLOC_013619	FFC1_12597	FFUJ_11569	related to 4-coumarate--CoA ligase	-2.00			
XLOC_009829	FFC1_09245	FFUJ_03816	metal-nicotianamine transporter ysl11	-2.01		-2.02	
XLOC_004042	FFC1_03842	FFUJ_05362	probable mutanase (glucan endo-1,3-alpha-glucosidase)	-2.01	-1.99		

XLOC_008074	FFC1_07031	FFUJ_02642	related to exo-alpha-sialidase / neuraminidase	-2.01			
XLOC_004790	FFC1_05205	FFUJ_06653	uncharacterized protein FFUJ_06653	-2.02			
XLOC_012372	FFC1_12032	FFUJ_12589	uncharacterized protein Y057_12893	-2.02			
XLOC_008704	FFC1_08178	FFUJ_10181	uncharacterized protein Y057_7400	-2.04			
XLOC_004624	FFC1_04887	FFUJ_06352	probable proline racemase	-2.05			
XLOC_012503	FFC1_11443	FFUJ_13820	related to tol protein	-2.05			
XLOC_016003	FFC1_14900	FFUJ_02180	related to methyltransferase	-2.06	-2.16		
XLOC_014152	FFC1_13610			-2.06			
XLOC_014931	FFC1_13672	FFUJ_09161	related to lactose regulatory protein	-2.06			
XLOC_002910	FFC1_03254	FFUJ_07684	alpha-galactosidase a precursor	-2.07			
XLOC_010439	FFC1_09519	FFUJ_04043	Positive regulator of purine utilization	-2.07			
XLOC_011318	FFC1_11148	FFUJ_10234	related to beta-mannosidase	-2.07			
XLOC_004150	FFC1_04051	FFUJ_05559	protein kinase	-2.08			
XLOC_001820	FFC1_01196	FFUJ_01118	probable ASP3-1-L-asparaginase II	-2.09	-1.84		
XLOC_011902	FFC1_11185	FFUJ_14071	related to chitin synthase/hyaluronan synthase (glycosyltransferases)	-2.11	-2.56		
XLOC_003804	FFC1_03390	FFUJ_07816	CMGC/SRPK protein kinase	-2.12			
XLOC_016054	FFC1_15007	FFUJ_02284		-2.14			
XLOC_005801	FFC1_05658	FFUJ_14709	related to Transaldolase B	-2.17			
XLOC_008657	FFC1_08097	FFUJ_03657	uncharacterized protein FFC1_08097	-2.17			
XLOC_011264	FFC1_11043	FFUJ_10338	related to calcium-independent phospholipase A2	-2.18			
XLOC_010809	FFC1_10184	FFUJ_11122	uncharacterized protein FFUJ_11122	-2.18			
XLOC_013372	FFC1_12121	FFUJ_12031	uncharacterized protein FFUJ_12031	-2.19	-2.50		
XLOC_009523	FFC1_08703	FFUJ_09680	uncharacterized protein FFUJ_09680	-2.20			
XLOC_000004	FFC1_00008	FFUJ_00007	related to benzoate-para-hydroxylase (cytochrome P450)	-2.20			
XLOC_015364	FFC1_14548	FFUJ_08236	related to beta-N-hexosaminidase	-2.21			
XLOC_005661	FFC1_05391		Trypsin	-2.23		-4.11	-2.59
XLOC_006509	FFC1_05392		succinyl- :3-ketoacid-coenzyme a mitochondrial precursor	-2.25			
XLOC_016270	FFC1_15413	FFUJ_12802	serine/threonine kinase 16	-2.25			
XLOC_014977	FFC1_13776	FFUJ_09061		-2.25			
XLOC_003330	FFC1_02504	FFUJ_06972	uncharacterized protein Y057_8807	-2.27			
XLOC_013703	FFC1_12762	FFUJ_11412	uncharacterized protein FFUJ_11412	-2.28			
XLOC_008832	FFC1_08450	FFUJ_09916	related to L-2.3-butanediol dehydrogenase	-2.31			
XLOC_008004	FFC1_06907	FFUJ_02521	related to GNT1 alphaN-acetylglucosamine transferase K. lactis	-2.32			
XLOC_010044	FFC1_09686	FFUJ_04206	related to phospholipid-translocating ATPase	-2.33		2.67	2.93
XLOC_006731	FFC1_05830	FFUJ_14549	related to ARG8-acetylornithine aminotransferase	-2.33			
XLOC_002421	FFC1_02352	FFUJ_06828	related to multidrug resistance protein	-2.35			
XLOC_003941	FFC1_03640	FFUJ_08055	related to aminopeptidase	-2.38	-2.80		
XLOC_013810	FFC1_12975	FFUJ_11203	related to O-methylsterigmatocystin oxidoreductase	-2.38			
XLOC_006983	FFC1_06306	FFUJ_13314	related to integral membrane protein	-2.43	-2.89		
XLOC_012292	FFC1_11901	FFUJ_12468	uncharacterized protein FFUJ_12468	-2.43			
XLOC_008611	FFC1_07998	FFUJ_03559	uncharacterized protein FFUJ_03559	-2.44			
XLOC_005566	FFC1_05183	FFUJ_06633	uncharacterized protein FFUJ_06633	-2.45			
XLOC_009218	FFC1_08163	FFUJ_10195	related to phenol 2-monooxygenase	-2.45			
XLOC_012025	FFC1_11408	FFUJ_13853	uncharacterized protein Y057_12158	-2.46			
XLOC_001261	FFC1_00088		GTP binding domain	-2.46			
XLOC_010982	FFC1_10552	FFUJ_10798	uncharacterized protein LW93_094	-2.47			
XLOC_007372	FFC1_07059	FFUJ_02669	NADP-specific glutamate dehydrogenase	-2.47			
XLOC_009805	FFC1_09208	FFUJ_09178	related to methyltransferase	-2.52	-2.82		
XLOC_000017	FFC1_00035		uncharacterized protein FFC1_00035	-2.57			
XLOC_011316	FFC1_11144	FFUJ_10237	related to alkaline protease (oryzin)	-2.57			
XLOC_010799	FFC1_10164	FFUJ_11142	probable general amino acid permease	-2.61			
XLOC_011593	FFC1_10571	FFUJ_10779	related to Staphylococcus multidrug resistance protein	-2.62			
XLOC_008751	FFC1_08272	FFUJ_10091	probable amino acid permease NAAP1	-2.62			
XLOC_012315	FFC1_11939		related to S. pombe trp-asp repeat containing protein	-2.62			
XLOC_016036	FFC1_14971	FFUJ_02254	related to chitinase	-2.65			
XLOC_015166	FFC1_14146	FFUJ_08705	probable GAP1-General amino acid permease	-2.67			
XLOC_011800	FFC1_10980	FFUJ_10398	uncharacterized protein FFUJ_10398	-2.69		-2.95	
XLOC_005267	FFC1_04626	FFUJ_06112	related to alcohol oxidase	-2.69	-2.67		
XLOC_013371	FFC1_12120	FFUJ_12032	antifungal protein	-2.69	-3.94		
XLOC_013427	FFC1_12245	FFUJ_11910	related to Carboxypeptidase 2	-2.79			
XLOC_009875	FFC1_09339		uncharacterized protein FFC1_09339	-2.85			
XLOC_011029	FFC1_10648	FFUJ_10709	related to methyltransferase	-2.89			
XLOC_004070	FFC1_03900	FFUJ_05421	Protein of unknown function localised to cytoplasm	-2.98			
XLOC_014172	FFC1_13659	FFUJ_05308	related to MFS transporter	-3.03		-2.34	
XLOC_016434	FFC1_15412	FFUJ_12801	related to general amidase	-3.04			
XLOC_012666	FFC1_11755	FFUJ_12325	aldehyde dehydrogenase (NAD+)	-3.06			
XLOC_002597	FFC1_02673	FFUJ_07132	uncharacterized protein Y057_12154	-3.06			
XLOC_005819	FFC1_05693	FFUJ_14675	related to laccase precursor	-3.08			
XLOC_005521	FFC1_05098	FFUJ_06560	uncharacterized protein FFC1_05098	-3.22			
XLOC_005091	FFC1_04313	FFUJ_05807	uncharacterized protein FFUJ_05807	-3.23	-5.72		-2.72
XLOC_014716	FFC1_13969	FFUJ_08875		-3.24			
XLOC_004771	FFC1_05163	FFUJ_06616	uncharacterized protein Y057_10668	-3.42			
XLOC_009830	FFC1_09247	FFUJ_03819	probable monoamine oxidase N	-3.56			
XLOC_002471	FFC1_02444	FFUJ_06918	related to ornithine aminotransferase	-3.61			
XLOC_011091	FFC1_10762	FFUJ_10602	related to methyltransferase LaeA-like	-3.77	-2.87		

XLOC_000201	FFC1_00381	FFUJ_00338	uncharacterized protein FFC1_00381		3.34		
XLOC_004325	FFC1_04342	FFUJ_05834	probable oxidoreductase CipA-like		3.01		
XLOC_013210	FFC1_12755	FFUJ_11420	related to lipase 1		2.87		2.06
XLOC_006581	FFC1_05530	FFUJ_14823	uncharacterized protein FFM5_12969		2.79		
XLOC_014262	FFC1_13156	FFUJ_04822	Putative exonuclease V		2.56		1.77
XLOC_013182	FFC1_12716	FFUJ_11459	related to hydroxylase		2.51		
XLOC_013087	FFC1_12553	FFUJ_11610	Phenolic acid decarboxylase padC		2.50		
XLOC_009708	FFC1_09014	FFUJ_09378	uncharacterized protein LW93_470		2.37		1.49
XLOC_001028	FFC1_01856	FFUJ_01741	probable CYB2-lactate dehydrogenase cytochrome b2		2.21		2.93
XLOC_004285	FFC1_04284	FFUJ_05779	uncharacterized protein FFUJ_05779		2.17		
XLOC_011570	FFC1_10531	FFUJ_10818	probable NADPH2 dehydrogenase chain OYE2		1.93	-2.13	
XLOC_005230	FFC1_04576	FFUJ_14921	related to transcription factor Ask10p		1.91		
XLOC_014115	FFC1_13541	FFUJ_05190			1.81		1.82
XLOC_014868	FFC1_14251	FFUJ_08605	Homeobox protein PKNOX2		1.71		
XLOC_010043	FFC1_09682	FFUJ_04202	retrograde regulation protein 2		1.68		
XLOC_002976	FFC1_03372	FFUJ_07798	related to transcription factor medusa		1.65		
XLOC_007797	FFC1_07848	FFUJ_03412	uncharacterized protein FFUJ_03412		1.50		
XLOC_015609	FFC1_14562	FFUJ_08251	related to allantoate permease		-1.41		
XLOC_002093	FFC1_01731	FFUJ_01624	O-acetylhomoserine (thiol)-lyase		-1.73		
XLOC_007308	FFC1_06952	FFUJ_02565	related to phosphatase 2a inhibitor		-1.75	1.80	
XLOC_001185	FFC1_02166	FFUJ_02035	related to WSC2 Glucoamylase III (alpha-1,4-glucan-glucosidase)		-1.77		
XLOC_006711	FFC1_05780	FFUJ_14592	probable fusarubin cluster-esterase		-1.84	2.15	
XLOC_010085	FFC1_09749	FFUJ_04262	related to arylamine N-acetyltransferase		-1.87		
XLOC_006679	FFC1_05715	FFUJ_14654	related to short-chain alcohol dehydrogenase			6.52	4.52
XLOC_005831	FFC1_05717	FFUJ_14652	3-hydroxybutyrate dehydrogenase			5.76	
XLOC_009695	FFC1_08992	FFUJ_09399	uncharacterized protein FFUJ_09399			4.49	3.27
XLOC_010456	FFC1_09546	FFUJ_11292	probable ABC1 transport protein			4.09	3.92
XLOC_015917	FFC1_15115	FFUJ_02390	uncharacterized protein FFUJ_02390			3.89	3.74
XLOC_011198	FFC1_10935	FFUJ_10438	uncharacterized protein FFC1_10935			3.66	2.01
XLOC_005710	FFC1_05476	FFUJ_14874	related to ATP/GTP-binding protein			3.35	
XLOC_000074	FFC1_00150	FFUJ_00115	uncharacterized protein FFUJ_00115			3.17	2.60
XLOC_005865	FFC1_05781	FFUJ_14591	Pth11-like integral membrane protein			3.13	2.44
XLOC_011999	FFC1_11355	FFUJ_13908	probable saccharopine dehydrogenase (NAD, L-lysine-forming)			3.02	
XLOC_000075	FFC1_00152	FFUJ_00117	related to integral membrane protein PTH11			2.88	2.48
XLOC_015568	FFC1_14495	FFUJ_08179	related to integral membrane protein PTH11			2.87	
XLOC_004931	FFC1_03994	FFUJ_05506	predicted protein [			2.75	2.04
XLOC_015877	FFC1_15040	FFUJ_02316	uncharacterized protein FFB20_03135			2.70	
XLOC_016166	FFC1_15230	FFUJ_12621				2.66	
XLOC_011397	FFC1_10224	FFUJ_11083	related to formate transport protein			2.62	2.84
XLOC_010230	FFC1_10012	FFUJ_04519	Histidinol-phosphate aminotransferase			2.54	
XLOC_006279	FFC1_06563	FFUJ_13068	hypothetical protein FOXG_07583			2.51	
XLOC_004721	FFC1_05066	FFUJ_06528	related to BCS1 protein precursor			2.47	2.56
XLOC_016443	FFC1_15429	FFUJ_12818	related to ferric-chelate reductase			2.44	2.72
XLOC_009255	FFC1_08235	FFUJ_10126				2.44	1.88
XLOC_011073	FFC1_10737	FFUJ_10626	uncharacterized protein FFUJ_10626			2.43	2.95
XLOC_016365	FFC1_15245	FFUJ_12636	related to integral membrane protein			2.41	
XLOC_005458	FFC1_04988	FFUJ_06453	hypothetical protein BFJ72_g3623			2.41	
XLOC_013002	FFC1_12382	FFUJ_11775	uncharacterized protein Y057_7900			2.39	
XLOC_012874	FFC1_12133	FFUJ_12020	polyketide synthase			2.38	
XLOC_011866	FFC1_11121	FFUJ_10259	related to tetracycline efflux protein (otrb)			2.33	
XLOC_001141	FFC1_02075	FFUJ_01947	uncharacterized protein LW93_11280			2.31	
XLOC_006623	FFC1_05612		Uncharacterized protein Y057_905			2.28	
XLOC_007882	FFC1_08010	FFUJ_03572	uncharacterized protein Y057_6525			2.24	2.23
XLOC_002282	FFC1_02076	FFUJ_01948	uncharacterized protein FFM5_10375			2.17	
XLOC_000176	FFC1_00341	FFUJ_00298	related to acetyltransferase			2.16	1.91
XLOC_006996	FFC1_06329	FFUJ_13293	argininosuccinate synthase			2.14	
XLOC_013576	FFC1_12523	FFUJ_11639	related to Dal5p			2.14	
XLOC_016478	FFC1_15488	FFUJ_12884				2.13	
XLOC_010526	FFC1_09685	FFUJ_04205	uncharacterized protein LW93_14625			2.12	
XLOC_012943	FFC1_12250	FFUJ_14930	probable C6 transcription factor			2.12	
XLOC_002385	FFC1_02279	FFUJ_06760	uncharacterized protein FFUJ_06760			2.12	
XLOC_009377	FFC1_08447	FFUJ_09919	glutathione s-transferase omega 2			2.10	
XLOC_012901	FFC1_12174	FFUJ_11980	related to vacuolar membrane protein HMT1			2.09	2.17
XLOC_007167	FFC1_06660	FFUJ_12981	uncharacterized protein Y057_13448			2.08	
XLOC_001378	FFC1_00339	FFUJ_00296	uncharacterized protein FFC1_00339			2.08	
XLOC_000617	FFC1_01112	FFUJ_01038	uncharacterized protein FFUJ_01038			2.06	2.47
XLOC_011002	FFC1_10597	FFUJ_10757	related to multicopper oxidase			2.02	
XLOC_014285	FFC1_13193	FFUJ_04859	related to phospholipid-translocating ATPase			2.01	
XLOC_005614	FFC1_05292		aspartate aminotransferase			2.01	
XLOC_011499	FFC1_10421	FFUJ_10927	related to sugar transporter			1.98	
XLOC_010855	FFC1_10283		uncharacterized protein FFE2_08894			1.97	
XLOC_014500	FFC1_13597	FFUJ_05245	gnat family			1.92	
XLOC_008830	FFC1_08448	FFUJ_09918	uncharacterized protein FFUJ_09918			1.91	1.51
XLOC_016390	FFC1_15313	FFUJ_12702				1.86	2.15
XLOC_016016	FFC1_14928	FFUJ_02208	related to ankyrin			1.86	

XLOC_009084	FFC1_08944	FFUJ_09447	related to integral membrane protein pth11			1.86	1.63
XLOC_004251	FFC1_04226	FFUJ_05721	Ribosomal N-lysine methyltransferase set11			1.84	
XLOC_012076	FFC1_11496	FFUJ_13767	probable alcohol dehydrogenase I-ADH1			1.80	
XLOC_000338	FFC1_00619	FFUJ_00563	hypothetical protein FOXB_11117			1.79	
XLOC_007870	FFC1_07987	FFUJ_03548	uncharacterized protein FFE2_04402			1.79	1.42
XLOC_010928	FFC1_10424	FFUJ_10924	uncharacterized protein LW93_216			1.76	2.21
XLOC_005828	FFC1_05712	FFUJ_14657	related to endo-1,3-beta-glucanase			1.75	
XLOC_007781	FFC1_07825	FFUJ_03393	uncharacterized protein Y057_7127			1.73	
XLOC_005840	FFC1_05736	FFUJ_14634	Altered inheritance of mitochondria protein 6			1.72	
XLOC_009447	FFC1_08575	FFUJ_09796	long-chain acyl-CoA synthetase			1.69	1.20
XLOC_001290	FFC1_00151	FFUJ_00116	related to Tri201-trichothecene 3-O-acetyltransferase			1.69	1.61
XLOC_012073	FFC1_11493	FFUJ_13770	Quinone oxidoreductase 2			1.63	
XLOC_016172	FFC1_15246	FFUJ_12637	related to triacylglycerol lipase V precursor			1.62	
XLOC_007986	FFC1_06883	FFUJ_02498	aspartate kinase			1.57	
XLOC_013223	FFC1_12780	FFUJ_11395	uncharacterized protein Y057_10193			1.55	1.28
XLOC_013392	FFC1_12168	FFUJ_11986	putative phosphoglycerate mutase family protein			1.52	
XLOC_010175	FFC1_09911	FFUJ_04425	related to NADPH-ferrihemoprotein reductase and mammalian nitric-oxide synthases			1.51	
XLOC_009118	FFC1_09035	FFUJ_09357	related to integral membrane protein PTH11			1.51	
XLOC_015865	FFC1_15021	FFUJ_02297	MFS transporter, SP family, sugar:H+ symporter			1.50	1.36
XLOC_008895	FFC1_08574	FFUJ_09797	related to aerobactin siderophore biosynthesis protein iucB			1.45	1.37
XLOC_016251	FFC1_15379	FFUJ_12767	uncharacterized protein Y057_2030			1.43	
XLOC_004112	FFC1_03985	FFUJ_05497	uncharacterized protein FFUJ_05497			1.43	
XLOC_012472	FFC1_11389	FFUJ_13872	uncharacterized protein FFUJ_13872			1.42	
XLOC_009308	FFC1_08340	FFUJ_10023	uncharacterized protein FFMR_13579			1.41	
XLOC_011624	FFC1_10624	FFUJ_10732	related to hydrolase of the alpha/beta superfamily			1.41	
XLOC_003001	FFC1_03409	FFUJ_07834	hypothetical protein FOXG_10469			1.40	
XLOC_005353	FFC1_04776	FFUJ_06252	GMP synthase			1.39	
XLOC_002472	FFC1_02445	FFUJ_06919	uncharacterized protein Y057_7739			1.38	
XLOC_013246	FFC1_12819	FFUJ_11356	uncharacterized protein FFC1_12819			1.35	
XLOC_001431	FFC1_00462	FFUJ_00420	homocitrate synthase			1.32	
XLOC_001003	FFC1_01813	FFUJ_01700	argininosuccinate lyase			1.31	
XLOC_011959	FFC1_11282	FFUJ_13979	uncharacterized protein Y057_7328			-1.27	
XLOC_012233	FFC1_11778	FFUJ_12345	probable glycosylasparaginase			-1.32	-1.45
XLOC_012218	FFC1_11744		related to multidrug resistance protein			-1.32	
XLOC_006778	FFC1_05916	FFUJ_13687	related to glucanase			-1.35	-1.18
XLOC_013674	FFC1_12701	FFUJ_11473	related to spore coat protein SP96 precursor			-1.37	-1.64
XLOC_015901	FFC1_15087	FFUJ_02362	probable MSH6-DNA mismatch repair protein			-1.41	
XLOC_008339	FFC1_07521	FFUJ_03096	uncharacterized protein LW93_2021			-1.43	
XLOC_010234	FFC1_10020	FFUJ_04528	murein transglycosylase			-1.44	-1.35
XLOC_000798	FFC1_01461	FFUJ_01373	uncharacterized protein Y057_13381			-1.45	
XLOC_002706	FFC1_02901	FFUJ_07348	uncharacterized protein FFUJ_07348			-1.46	
XLOC_013865	FFC1_13071	FFUJ_04743	related to mixed-linked glucanase precursor MLG1			-1.47	-1.22
XLOC_015678	FFC1_14684	FFUJ_08367	uncharacterized protein FFUJ_08367			-1.49	
XLOC_010296	FFC1_09265	FFUJ_03836	uncharacterized protein LW93_14264			-1.49	
XLOC_015303	FFC1_14411	FFUJ_08096				-1.54	
XLOC_011270	FFC1_11052	FFUJ_10329	uncharacterized protein FFC1_11052			-1.55	-1.94
XLOC_001585	FFC1_00765	FFUJ_00702	Regulatory protein abaA			-1.56	
XLOC_002180	FFC1_01909		related to zinc finger protein odd-paired-like (opl)			-1.57	
XLOC_012882	FFC1_12145	FFUJ_12008	related to non-ribosomal peptide synthetase			-1.58	-1.21
XLOC_009809	FFC1_09216	FFUJ_09171	uncharacterized protein Y057_12826			-1.60	-1.41
XLOC_005900	FFC1_05839	FFUJ_14539	uncharacterized protein Y057_3004			-1.61	
XLOC_002248	FFC1_02010	FFUJ_01882	taurine dioxygenase			-1.63	-2.35
XLOC_002202	FFC1_01936	FFUJ_01811	Uncharacterized protein LW93_11410			-1.63	-1.95
XLOC_008743	FFC1_08258	FFUJ_10104	uncharacterized protein FFUJ_10104			-1.68	
XLOC_010997	FFC1_10584	FFUJ_10769	related to general amidase			-1.68	
XLOC_012465	FFC1_11375	FFUJ_13886	High-affinity methionine permease			-1.69	
XLOC_013582	FFC1_12531	FFUJ_11631	Uncharacterized protein Y057_9898			-1.75	-1.86
XLOC_016520	FFC1_15561		hydrophobic surface binding protein A			-1.77	-1.84
XLOC_006846	FFC1_06031	FFUJ_13578	uncharacterized protein FFUJ_13578			-1.79	
XLOC_014228	FFC1_13090	FFUJ_04761	uncharacterized protein Y057_3987			-1.87	
XLOC_004616	FFC1_04868	FFUJ_06335	related to cornifin B			-1.87	-1.63
XLOC_007860	FFC1_07954	FFUJ_03516	uncharacterized protein Y057_11253			-1.92	
XLOC_014321	FFC1_13254	FFUJ_04919	related to sporozoite surface protein 2 precursor			-1.93	-1.98
XLOC_005767	FFC1_05578	FFUJ_14774	uncharacterized protein Y057_940			-1.94	
XLOC_013750	FFC1_12853	FFUJ_11323	uncharacterized protein LW93_6855			-2.03	-2.39
XLOC_016580	FFC1_15661	FFUJ_14209				-2.19	-2.22
XLOC_013058	FFC1_12488	FFUJ_11674	related to plant PR-1 class of pathogen related proteins			-2.25	
XLOC_011523	FFC1_10457	FFUJ_10889	galactose oxidase precursor			-2.30	-2.71
XLOC_012013	FFC1_11381	FFUJ_13880	related to phosphatidylserine decarboxylase 2			-2.33	-1.80
XLOC_016669	FFC1_15664	FFUJ_14207				-2.43	-3.09
XLOC_001267	FFC1_00102	FFUJ_00070	probable aspartic proteinase precursor			-2.44	
XLOC_016667	FFC1_15662		uncharacterized protein FFE2_15851			-2.44	-2.49
XLOC_011409	FFC1_10244	FFUJ_11065	related to phosphatidylserine decarboxylase 2			-2.48	
XLOC_009924	FFC1_09451	FFUJ_03978	related to conidial hydrophobin RodB			-2.50	
XLOC_016668	FFC1_15663	FFUJ_14208				-2.66	-2.53
XLOC_014963	FFC1_13738	FFUJ_09096	related to tryptophan 2,3 dioxygenase			-2.73	

XLOC_006562	FFC1_05495	FFUJ_14856	carboxypeptidase A4			-3.10	-3.31
XLOC_015869	FFC1_15026	FFUJ_02302	related to pentafunctional arom polypeptide				4.80
XLOC_004015	FFC1_03774	FFUJ_14263	related to multidrug resistance protein				3.76
XLOC_015382	FFC1_14592	FFUJ_08281	uncharacterized protein FFUJ_08281				3.72
XLOC_005561	FFC1_05178	FFUJ_06628	related to NAD(P)H-dependent oxidoreductase				3.44
XLOC_011155	FFC1_10861	FFUJ_10505	uncharacterized protein Y057_6285				2.90
XLOC_016852	FFC1_15890			inf			2.73
XLOC_011494	FFC1_10414	FFUJ_10934	non-ribosomal peptide synthetase				2.66
XLOC_016060	FFC1_15025	FFUJ_02301	uncharacterized protein Y057_5000				2.60
XLOC_011677	FFC1_10713	FFUJ_10649	related to toxD gene				2.60
XLOC_003181	FFC1_03775	FFUJ_14262	uncharacterized protein Y057_11416				2.34
XLOC_007808	FFC1_07862	FFUJ_03426	uncharacterized protein FFM5_02610				2.29
XLOC_002145	FFC1_01839	FFUJ_01724	uncharacterized protein FFUJ_01724				2.27
XLOC_005824	FFC1_05702	FFUJ_14666	sulfite oxidase				2.21
XLOC_006670	FFC1_05701	FFUJ_14667	probable catalase isozyme P				2.17
XLOC_007255	FFC1_06850	FFUJ_02467	cyanate hydratase				2.08
XLOC_001236	FFC1_00046	FFUJ_00014	related to ferric reductase Fre2p				1.98
XLOC_010940	FFC1_10451	FFUJ_10895	related to galactinol synthase		inf		1.97
XLOC_012027	FFC1_11411	FFUJ_13851	Tripeptidyl aminopeptidase				1.95
XLOC_007169	FFC1_06662	FFUJ_12979	related to peptidase yuxL				1.94
XLOC_011240	FFC1_11005	FFUJ_10373	related to nitrogen metabolic regulation protein nmr				1.85
XLOC_001109	FFC1_02015	FFUJ_01888	tat pathway signal sequence				1.80
XLOC_011689	FFC1_10736	FFUJ_10627	uncharacterized protein FFB20_01643				1.71
XLOC_006678	FFC1_05711	FFUJ_14658	probable				1.68
XLOC_013669	FFC1_12696	FFUJ_11478	probable potassium transporter TRK-1				1.64
XLOC_015706	FFC1_14724	FFUJ_08404					1.58
XLOC_003633	FFC1_03063	FFUJ_07503	related to aldehyde dehydrogenase				1.57
XLOC_005752	FFC1_05551	FFUJ_14801	uncharacterized protein FFUJ_14801				1.51
XLOC_015672	FFC1_14672	FFUJ_08355	uncharacterized protein FFUJ_08355				1.50
XLOC_001428	FFC1_00459	FFUJ_00417	related to aquaporin				1.49
XLOC_007302	FFC1_06941	FFUJ_02554	related to nitrate assimilation regulatory protein nirA				1.38
XLOC_015623	FFC1_14589	FFUJ_08278	related to allantoate transport protein				1.35
XLOC_001458	FFC1_00517	FFUJ_00473	related to pisatin demethylase (cytochrome P450)				1.27
XLOC_006673	FFC1_05704	FFUJ_14664	related to C4-dicarboxylate transport protein mae1				1.24
XLOC_014961	FFC1_13730	FFUJ_09104					1.24
XLOC_013598	FFC1_12554	FFUJ_11609	uncharacterized protein FFUJ_11609				1.22
XLOC_008464	FFC1_07739	FFUJ_03312	Uncharacterized protein Y057_4500				1.19
XLOC_001915	FFC1_01388	FFUJ_01301	probable endochitinase				-1.15
XLOC_000233	FFC1_00429	FFUJ_00384	cell cycle checkpoint protein				-1.19
XLOC_001959	FFC1_01457	FFUJ_01370	uncharacterized protein Y057_13378				-1.20
XLOC_005329	FFC1_04735	FFUJ_06214	related to protein kinase Gin4p				-1.20
XLOC_009942	FFC1_09485	FFUJ_04010	Vacuolar protein sorting-associated protein VTA1 like protein				-1.22
XLOC_013078	FFC1_12529	FFUJ_11633	uncharacterized protein FFUJ_11633				-1.22
XLOC_016086	FFC1_15075	FFUJ_02351	related to TGL4-triacylglycerol lipase				-1.23
XLOC_015438	FFC1_14701	FFUJ_08384	hypoxia up-regulated 1				-1.23
XLOC_001351	FFC1_00292	FFUJ_00250	uncharacterized protein FFC1_00292				-1.26
XLOC_005887	FFC1_05816	FFUJ_14561	Uncharacterized protein Y057_2985				-1.30
XLOC_003243	FFC1_02323	FFUJ_06800	uncharacterized protein FFC1_02323				-1.31
XLOC_012459	FFC1_11361	FFUJ_13900	related to ECM32-DNA dependent ATPase/DNA helicase B				-1.33
XLOC_011684	FFC1_10729	FFUJ_10634	uncharacterized protein Y057_4175				-1.34
XLOC_005884	FFC1_05811	FFUJ_14565	uncharacterized protein Y057_2982				-1.43
XLOC_008974	FFC1_08740	FFUJ_09644	23S rRNA (-N6)-methyltransferase				-1.44
XLOC_003915	FFC1_03603	FFUJ_14426	uncharacterized protein FFC1_03603				-1.46
XLOC_009098	FFC1_08984	FFUJ_09407	related to rabkinesin-6				-1.50
XLOC_015610	FFC1_14564	FFUJ_08253	related to emopamil-binding protein				-1.55
XLOC_012692	FFC1_11791	FFUJ_12358	related to covalently-linked cell wall protein				-1.59
XLOC_002863	FFC1_03169		RNA-directed DNA polymerase (Reverse transcriptase)				-1.67
XLOC_005762	FFC1_05572	FFUJ_14781	related to monooxygenase				-1.69
XLOC_015654	FFC1_14645	FFUJ_08328					-1.69
XLOC_001939	FFC1_01425	FFUJ_01338	related to PPN1-vacuolar endopolyphosphatase				-1.72
XLOC_006943	FFC1_06231	FFUJ_13386	uncharacterized protein Y057_084				-1.83
XLOC_015822	FFC1_14944	FFUJ_02224	related to multidrug resistant protein				-1.84
XLOC_015041	FFC1_13921	FFUJ_08920	hypothetical protein FOPG_12929				-1.95
XLOC_003989	FFC1_03733	FFUJ_14302	related to uracil permease				-2.09
XLOC_011529	FFC1_10466	FFUJ_10880	putative aspartic proteinase precursor				-2.10
XLOC_003971	FFC1_03704	FFUJ_14330	related to myo-inositol transport protein ITR1				-2.31
XLOC_008794	FFC1_08363	FFUJ_10000	related to dis1-suppressing protein kinase dsk1				-2.43